Sebastian Heinl | 2014

Sebastian Heinl
aus Windischeschenbach, geb. am 23.03.1984

Studium: Chemie, Universität Regensburg,
Abschluss Master of Science
Promotion: Prof. Dr. Manfred Scheer,
Institut für Anorganische Chemie

Diese Dissertation beschäftigt sich mit dem sterisch anspruchsvollen CpBIG-Liganden und dessen Verwendung in der Komplexchemie. Hierbei war die Darstellung und Charakterisierung von neuartigen Übergangsmetallkomplexen mit substituentenfreien Phosphorliganden (Pn-Liganden) und dessen Untersuchung bezüglich ihres Reaktionsverhaltens von zentralem Interesse.
Im Speziellen ist eindrucksvoll gezeigt, dass die kaum erforschte Substanzklasse der Pn-Ligandkomplexe des Mangans zugänglich gemacht werden konnte. Außerdem sind die selektiven Aktivierungen einer Reihe von Hauptgruppenverbindungen unter ausgesprochen milden Bedingungen durch CpBIG stabilisierte Radikale beschrieben. Weiterhin wurden einige der erhaltenen Verbindungen bezüglich ihrer Koordinationsfähigkeit gegenüber monovalenten Münzmetallsalzen untersucht. Hierbei ist es gelungen neben polymeren Architekturen auch neuartige sphärische Aggregate im nanoskaligen Bereich aufzubauen.
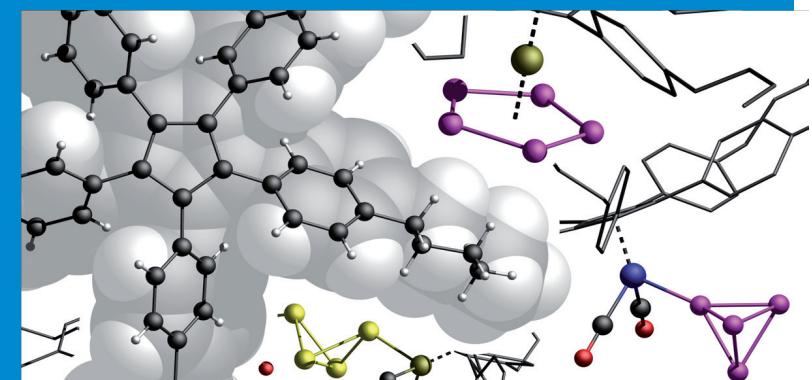
The Highly Sterically Demanding CpBIG

The Highly Sterically Demanding CpBIG

Sebastian Heinl
2014

Universität Regensburg

2

Sebastian Heinl

The Highly Sterically Demanding Cp$^{\text{BIG}}$

The Highly Sterically Demanding Cp^{BIG}

Dissertation zur Erlangung des Doktorgrades der Naturwissenschaften (Dr. rer. nat.)
der Fakultät für Chemie und Pharmazie der Universität Regensburg
vorgelegt von

Sebastian Heinl

Regensburg
2014

Die Arbeit wurde von Prof. Dr. Manfred Scheer angeleitet.
Das Promotionsgesuch wurde am 30.04.2014 eingereicht.
Das Kolloquium fand am 22.05.2014 statt.

Prüfungsausschuss: Vorsitzender: Prof. Dr. Arnd Vogler
                    1. Gutachter: Prof. Dr. Manfred Scheer
                    2. Gutachter: Prof. Dr. Henri Brunner
                    weiterer Prüfer: Prof. Dr. Frank-Michael Matysik

**Dissertationsreihe der Fakultät für Chemie und Pharmazie
der Universität Regensburg, Band 2**

The Highly Sterically Demanding Cp$^{\text{BIG}}$

Sebastian Heinl

Eidesstattliche Erklärung

Ich erkläre hiermit an Eides statt, dass ich die vorliegende Arbeit ohne unzulässige Hilfe Dritter und ohne Benutzung anderer als der angegebenen Hilfsmittel angefertigt habe; die aus anderen Quellen direkt oder indirekt übernommenen Daten und Konzepte sind unter Angabe des Literaturzitats gekennzeichnet.

_____

Sebastian Heinl

This thesis was elaborated within the period from Oktober 2010 till April 2014 in the Institute of Inorganic Chemistry at the University of Regensburg, under the supervision of Prof. Dr. Manfred Scheer.

Parts of this work have already been published or submitted:

❖ S. Heinl, E. V. Peresypkina, A. Y. Timoshkin, P. Mastrorilli, V. Gallo, M. Scheer, *Angew. Chem., Int. Ed.* **2013**, *52*, 10887-10891; *Angew. Chem.* **2013**, *125*, 11087-11091.

❖ S. Heinl, S. Reisinger, C. Schwarzmaier, M. Bodensteiner, M. Scheer, *Angew. Chem. Int. Ed.* **2014**, DOI: 10.1002/anie.201403295. *Angew. Chem.* **2014**, DOI: 10.1002/ange.201403295.

❖ C. Heindl, S. Heinl, D. Lüdeker, G. Brunklaus, W. Kremer and M. Scheer, *Inorg. Chim. Acta* **2014**, accepted.

❖ S. Heinl, M. Scheer, *Chem. Sci.* **2014**, DOI: 10.1039/c4sc01213e.

To Claudia and my family

for their enduring support

Preface

During the dissertation process some results have already been or are on the brink of being published. Among others, these results are also summarized in this thesis, often with literal citations and with the same pictures. To avoid accusations of plagiarism, in the beginning of each chapter a register gives the license number and demonstrates who was involved to which extent at a specific topic. Unfortunately, a strict separation of results is sometimes not possible. Therefore, it will be also listed if parts of appropriate chapters have already been discussed in other theses. Also on the first page of each chapter the 'table of content' (TOC)/'graphical abstract' is depicted and in case of unpublished results a proposal is given.

Since this work investigates different topics, each chapter includes an own short introduction about the current state of research. However, in the beginning of this thesis a comprehensive introduction is given. Some general aspects of the Cp^{BIG} ligand are also summarized to give a fundamental overview about its properties. At the end of this manuscript concluding statements about current work (English and German) are presented.

To ensure uniform design of this thesis, the unpublished results are also written in the style of publications. Furthermore, all chapters have the same text settings and the compound numeration begins anew.

Table of Contents

1.Introduction

1.1 White Phosphorus, Other Main Group Elements and Cage Compounds

Phosphorus is an essential element for life. With 4% (dry weight) it is a main substance in the body of mammals (like humans) and is mainly found as phosphates in the skeleton, ATP, DNA and RNA. Phosphates are also of high importance for human life as a fertilizer to increase crops production. However, it is mainly known in the broad public as a terrible weapon against humanity. The highly reactive molecular white phosphorus has been used in firebombs during the Second World War. To make things worse, unexploded bombs still provide headlines, because white phosphorus is still washed ashore on the coast of the Baltic Sea. Therefore, one might exaggerate and say, that white phosphorus it is now one of the native elements.

Phosphorus as an element is known in mainly three different allotropic modifications: red, black and white phosphorus (see Scheme 1.1).[1] The polymeric red modification can be further divided into some subgroups of crystalline (violet and fibrous) and amorphous phases, as Roth et al. demonstrated with a variety of analytical methods.[2] The violet and fibrous phosphorus both consist of P_2, P_8 and P_9 subunits forming tubes with $\{P_2-P_8-P_2-P_9\}$ repeating moieties.[3] While in the former case the tubes are linked in a perpendicular fashion, in the latter case parallel double-tubes are formed. The thermodynamically stable black phosphorus is the densest modification, which is why it is favored under high pressure. Hence, the first successful synthesis has been the heating of white phosphorus to 200 °C under 12000 bar pressure.[4] The crystal structure of P_{black} can be described as condensed layers of P_6 rings in chair conformation. Despite the thermodynamic preference of black phosphorus, the longest known modification is white phosphorus. Henning Brand discovered it in 1669 by concentrating of urine to dryness and roasting the residue in absence of air. The wax-like white phosphorus consists of discrete P_4 molecules forming perfect tetrahedra.[5] The slightly light sensitive material is highly flammable in air and has therefore to be handled under inert gas atmosphere. However, handled with the required expertise it is an excellent starting material for chemical processes: including industrial appliances and academic research.

Arsenic, as the heavier homologue of phosphorus, shows similar elemental modifications as like its lighter relative. The thermodynamically stable modification is grey (metallic) arsenic, containing double-layers of As_6 six-membered rings, which are connected by As–As edges. It

Scheme 1.1. Section of the structures of a) red phosphorus (Hittorf's), b) black phosphorus and c) black phosphorus (high pressure modification). d) Selected main group cage compounds.

is isostructural to the high pressure modification of black phosphorus. Also the labile yellow arsenic As_4[6] shows analogy to white phosphorus. As_4 can be easily obtained from As_{grey} by heating above ~600 °C. The high light sensitivity of yellow arsenic and its autocatalytical transformation into grey arsenic is a disadvantage for its use as starting material in chemistry.

Not only elemental phosphorus and arsenic can be obtained as discrete units, the heavier homologues of the 16th group S, Se and Te can also form molecular structures.[1] Probably the best known allotrope of this series is the crown shaped S_8 molecule. It represents the most stable modification of sulfur and can be found in huge amounts in the earth's crust. Other cyclic allotropes (up to S_{20}) can be obtained by extraction from melted sulfur. Direct synthetic routes are also known, especially by using $[Cp_2TiS_5]$ as a starting material.[7] In contrast to sulfur, the heavier homologues selenium and tellurium prefer a polymeric structure with 1D strains of spirals.[1] These modifications are in both cases called the grey or metallic ones. Cyclic allotropes are, however, also known for Se and Te. In analogy to S_8 crown shaped Se_8
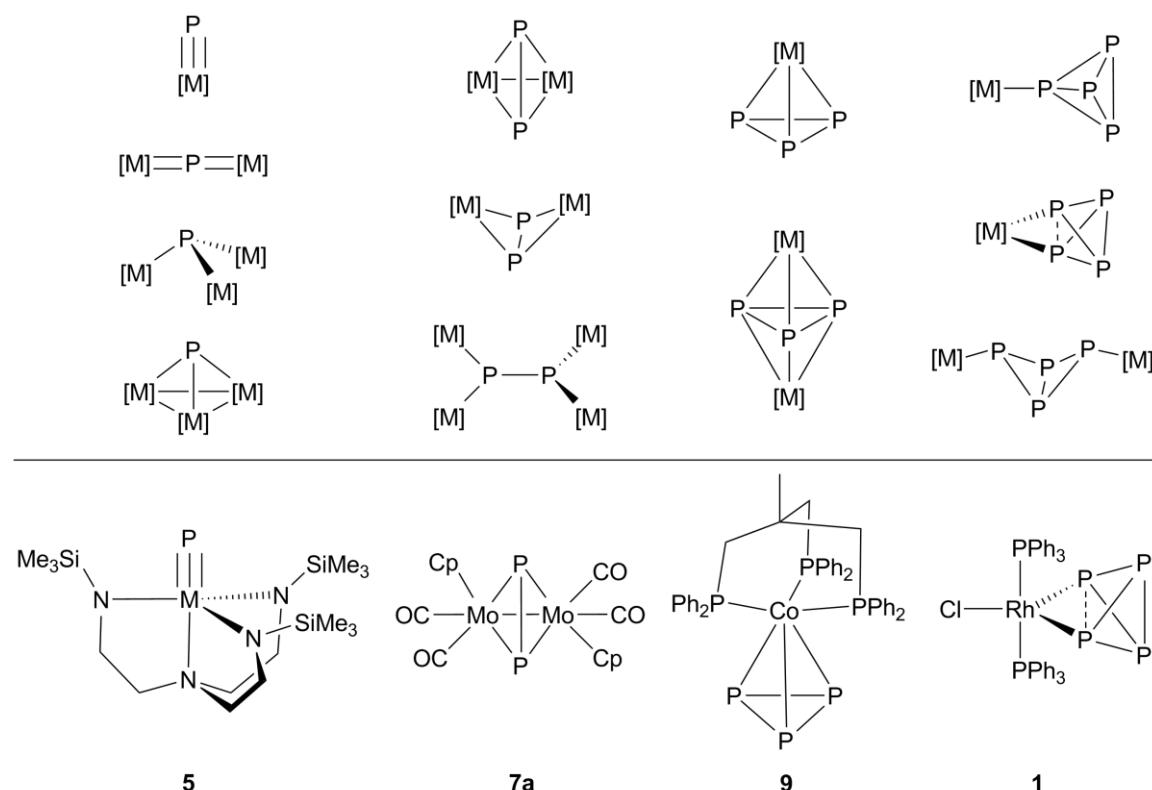
molecules are one of the main components of red selenium, which is metastable at ambient conditions. Other cyclic Se_n units can also be found there.

The combination of group 15 and group 16 elements opens a rich class of cage compounds (see Scheme 1.1 for selected examples). Many of the obtained cages exhibit structures, in which different amounts of Q atoms (Q = O, S, Se) are inserted into the E−E bonds of the E_4 tetrahedra (E = P, As). Probably three of the best known oxygen-free cages are the exceedingly stable molecules P_4S_3, P_4Se_3 and As_4S_4 (Realgar). The two isostructural cages P_4S_3 and P_4Se_3 show a nortricyclane structural motif with a *cyclo*-P_3 and a P_1 unit which are linked by three S or Se atoms, respectively. Of course, numerous other cage compounds are known, however these exceeds the volume of this work and will not be discussed here.

1.2 Substituent-Free P_n Ligand Complexes

Complexes with substituent-free phosphorus ligands are briefly called P_n ligand complexes. Here, the P atoms are only bound to the central metal and/or other P atoms. Due to the isolobal analogy of P atoms to CH fragments, many of the observed structural motifs of the P_n ligands can be associated to these of appropriate hydrocarbons $(CH)_n$. A high number of P_n ligand complexes are known so far, with numbers steadily increasing. Selected coordination modes of P_n ligands (n = 1-4) are shown in Scheme 1.2. Some review articles summarize the chemistry of this class of compounds, focusing either on transition metal complexes[8] or on main group element compounds.[9] In the following some particular examples are discussed.

From the beginning of this chemistry the direct activation of white phosphorus was the main synthetic strategy for the preparation of complexes with substituent-free phosphorus ligands. In 1971, Lindsell and Ginsberg reacted P_4 with [(PPh_3)_3RhCl] and obtained under elimination of PPh_3 the complex [(PPh_3)_2RhCl(η^2-P_4)] (**1**; also other phosphanes and arsanes can be used).[10] Later investigations proved an oxidative addition of the P_4 tetrahedron on the Rh(I) center, resulting in Rh(III) and a P_4^{2-} ligand.[11] An interesting series of different tetraphospha ligand complexes were reported by Scherer et al., demonstrating one possible reaction pathway for the degradation of the P_4 tetrahedra.[12] According to this, the first step in the reaction of [Cp''Fe(CO)_2]_2 with P_4 in thf under photolytical conditions leads to the formation of the tetraphospha*bicyclo*[1.1.0]butane (butterfly) complex [{Cp''Fe(CO)_2}_2($\mu,\eta^{1:1}$-P_4)] (**2**). CO elimination results first in a rearrangement retaining the butterfly motif of the P_4 ligand. This is followed by cleavage of the bond between the bridgehead P atoms forming [{Cp''Fe}Cp''Fe(CO)_2}($\mu,\eta^{4:1}$-P_4)] with a *cyclo*-P_4 ligand. Finally, when all CO groups are

Scheme 1.2. Top: selected coordination modes of P_n ligands with n = 1-4. Bottom: one selected representative of P_n ligand complexes with n = 1-4.

removed, the triple-decker complex $[(Cp''Fe)_2(\mu,\eta^{4:4}-P_4)]$ (**3**) is obtained, bearing a P_4 tetraphosphabutadiene chain as middle-deck.

The first compound with an intact P_4 tetrahedron as a ligand was reported by Sacconi et al. with the neutral nickel complex $[(np_3)Ni(\eta^1-P_4)]$ (**4a**; np_3 = tris(2-diphenylphosphinoethyl)amine).[13] This was soon followed by the analogue Pd derivative **4b**.[14] Unfortunately, **4a** and **4b** are totally insoluble in all solvents, which made investigations in solution impossible. Peruzzini et al. prepared a series of soluble cationic group 8 complexes with the general formula $[Cp^R M(L_2)(\eta^1-P_4)]$ (Cp^R = Cp, Cp*; M = group 8 metal; L = phosphane ligand). Today, several other η^1-P_4 complexes are known, the largest section being cationic species (Figure 1.1).[15] This can likely be explained by the higher Lewis acidity due to the positive charge on the metal atom in comparison to neutral compounds.

Most of the complexes, however, show degradation of the P_4 tetrahedron or aggregation to larger phosphorus frameworks. To date it was possible to characterize crystallographically P_n ligand complexes containing up to 24 P atoms.[16] The smallest possible P_n unit is a single P atom. These kinds of ligands are of special interest because of their capability of forming multiple bonds. Independently, in 1995 Schrock et al.[17] and Cummins et al.[18] published the

4a: M = Ni
4b: M = Pd

M = Mo, R = Cy
M = W, R = Cy, ^{i}Pr

M = Fe, Ru, Os
2 L = 2 PPh$_3$, C$_2$H$_4$(PPh$_2$)$_2$
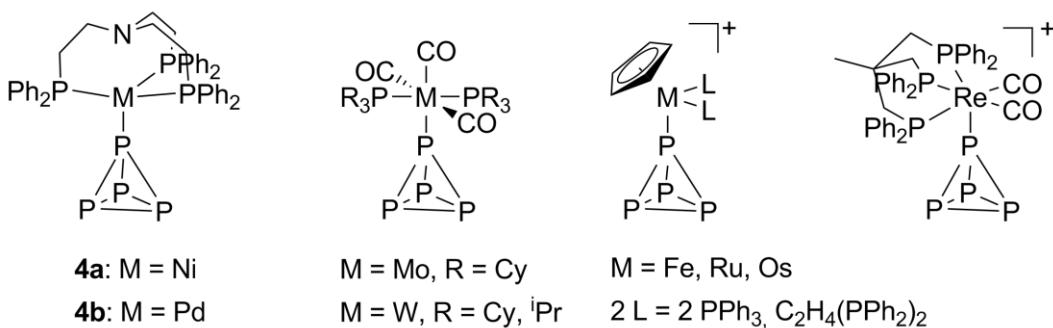
Figure 1.1. Transition metal complexes with η^1 bound P$_4$ tetrahedra as ligands.

first terminal P$_1$ complexes [(nn$_3$)W≡P] (**5**; nn$_3$ = (Me$_3$SiNCH$_2$CH$_2$)$_3$N) and [(NRAr)$_3$Mo≡P] (**6**; R = C(CH$_3$)$_3$CH$_3$, Ar = 3,5-C$_6$H$_3$Me$_2$) with a M≡P triple bond (Scheme 1.2). Since then a lot of effort has been put into the investigation of these kinds of complexes.[19]

Binuclear P$_2$ ligands can be obtained by the co-thermolysis of the carbonyl complexes [Cp^{R}Mo(CO)$_2$]$_2$ and [Cp^{R}Co(CO)$_2$] respectively, with white phosphorus in high boiling solvents. The obtained Mo complexes [{Cp^{R}Mo(CO)$_2$}$_2$(μ,η$^{2:2}$-P$_2$)] (**7a**: Cp^R = Cp;[20] **7b**: Cp^R = Cp*;[21] Scheme 1.2) exhibit tetrahedral structures with one P$_2$ moiety, whereas the Co complexes [(Cp^{R}Co)$_2$(μ,η$^{2:2}$-P$_2$)$_2$] (**8a**: Cp^R = Cp*;[22] **8b**: Cp^R = C$_5$H$_3$^{t}Bu$_2$, Cp'';[23] **8c**: Cp^R = C$_5$H$_2$^{t}Bu$_3$, Cp''';[24] **8d**: Cp^R = C$_5$H$_3$(SiMe$_3$)$_2$, Cp^{Si}) reveal triple-decker structures with two bridging P$_2$ units.[25]

The triphosphorus ligand generally shows a cyclic arrangement as first observed from Sacconi and co-workers in the complexes [(triphos)Co(η^3-P$_3$)] (**9**; triphos = CH$_3$C(CH$_2$PPh$_2$)$_3$; Scheme 1.2) and [(triphos)$_2$Ni$_2$(μ,η$^{3:3}$-P$_3$)] (**10**).[26]

As already mentioned, an aggregation to larger phosphorus scaffolds is possible depending on the complex fragments used (Figure 1.2). A milestone in the chemistry of P$_n$ ligand complexe was achieved by Scherer et al. with the preparation of the first pentaphosphaferrocene [Cp*Fe(η^5-P$_5$)] (**11**).[27] It bears a planar *cyclo*-P$_5$ ligand, which is isolobal to Cp. Ellis et al. even succeeded in the synthesis of the carbon-free metallocene [Ti(η^5-P$_5$)$_2$]$^{2-}$ (**12**) with two *cyclo*-P$_5$ ligands.[28] Hexaphosphabenzene can be stabilized as a middledeck in triple-decker complexes, with two possible conformations of the *cyclo*-P$_6$ ligand. In most cases a planar D_{6h} arrangement can be observed as in [Cp*$_2$Mo$_2$(μ,η$^{6:6}$-P$_6$)] (**13**),[20] [Cp*$_2$W$_2$(μ,η$^{6:6}$-P$_6$)] (**14**) and [Cp^{Et}$_2$V$_2$(μ,η$^{6:6}$-P$_6$)] (**15**)[29] but also, as in [Cp*$_2$Ti$_2$(μ,η$^{3:3}$-P$_6$)] (**16**),[30] P$_6$ rings in chair conformation could be obtained.

For the formation of larger phosphorus units, especially {Cp^{R}Co} fragments proved to be optimal. Here, also Scherer and co-workers rendered outstanding studies with the preparation of [(Cp'''Co)$_3$(μ$_3$,η$^{4:4:3}$-P$_{12}$)] (**17**) among other polyphosphorus ligand complexes.[24b] They used [Cp'''Co(CO)$_2$] as a starting material for the co-thermolysis reaction together with white phosphorus. However, the elevate temperatures which are needed for CO abstraction also

obviates the formation of even larger P_n ligands. Hence, in our own group the precursor complex [(Cp'''Co)$_2$toluene] was introduced because of its ability to form 14 VE {Cp'''Co} fragments in solution at ambient temperature.[31] Now reactions at very low temperatures were possible, which finally resulted in the formation and characterization of the P-richest complex [(Cp'''Co)$_5$(μ_5,$\eta^{4:4:3:3:3}$-P$_{24}$)] (**18**).[32] Mass spectrometric investigations of an isolated fraction even showed signals for [(Cp'''Co)$_6$(P$_{29}$)].
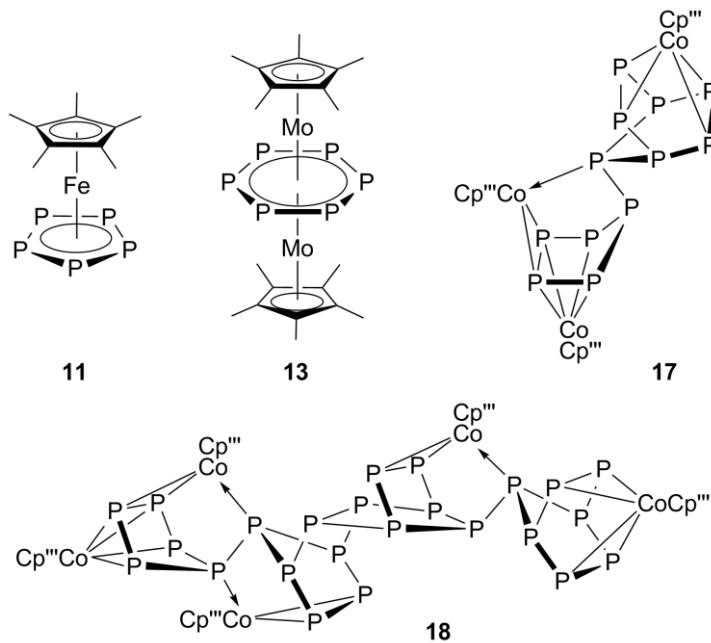
Figure 1.2. Selected P_n ligand complexes bearing polyphosphorus ligands with n > 4.

1.3 Reactivity of P_n Ligand Complexes

Compared to compounds bearing only organic ligands, P_n ligand complexes show significant differences in their reactivity. A good example for illustrating the differences is the redox behavior of the pentaphosphaferrocene **11** compared to its parent compound ferrocene. [Cp$_2$Fe] is well known for its reversible oxidation to [Cp$_2$Fe]$^+$, which is why it is used in cyclic voltammetry (CV) as an internal standard for referencing the electrochemical potential of target compounds. In the redox process the iron center is oxidized from Fe(II) to Fe(III). This, however, has not been observed by Winter et al. for **11**.[33] The initial oxidation product **11**$^+$ rapidly dimerizes to [Cp*Fe(P$_5$)]$_2^{2+}$ (**19**), which makes the process irreversible (Figure 1.3 top). An analogue observation can be made when **11** is reduced, finally resulting in the formation of [Cp*Fe(P$_5$)]$_2^{2-}$ (**20**). For both reactions the authors proposed a P–P bond formation and in case of **20** an envelope conformation of the two P$_5$ rings. Recently, our own
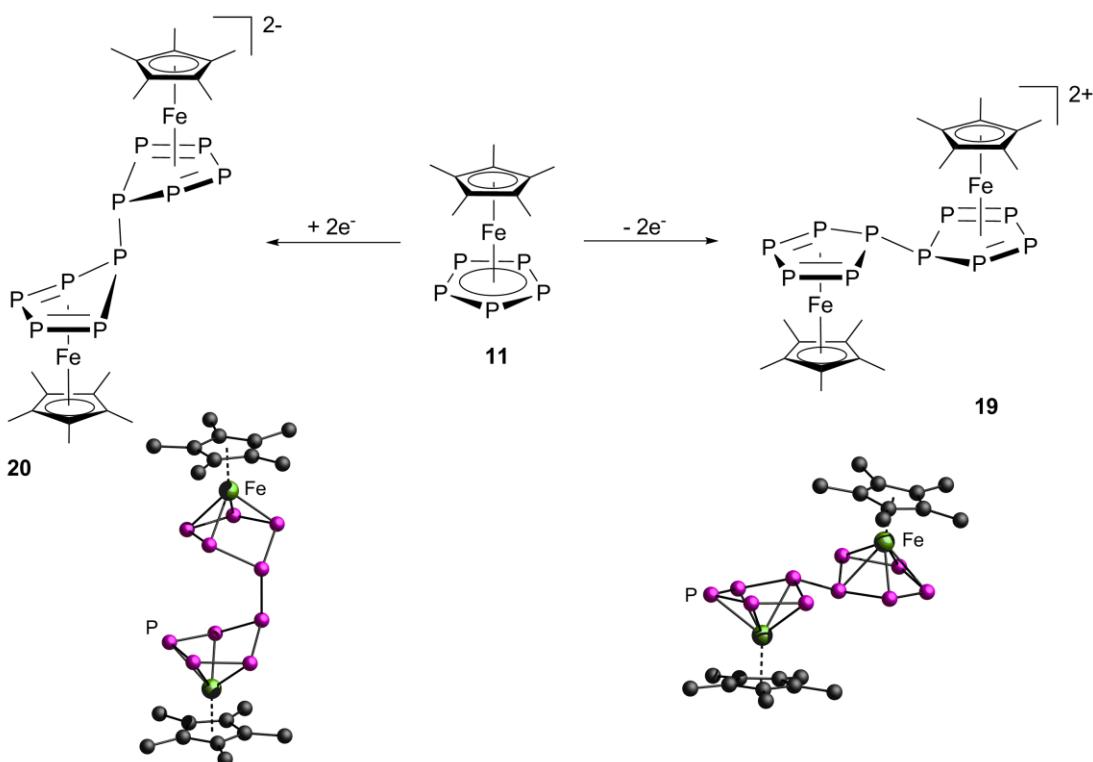
Figure 1.3. Top: electrochemical preparation of **19** and **20** from **11**. Bottom: structures of the two complex ions in the crystal;[34] counter ions, solvent molecules and H-atoms are omitted for clarity.

group has been able to prove these assumptions crystallographically by chemically oxidizing and reducing complex **11**, respectively (Figure 1.3 bottom).[34]

Another feature of P_n ligand complexes is the lone pair on each P atom, which in general is capable for coordination. Some of the first coordination compounds with P_n ligand complexes have been reported by Sacconi and co-workers, who reacted **9** with Lewis acids.[14] One remarkable result was obtained by the reaction of **9** with CuBr, forming [{(triphos)Co(η^3-P_3)}$_2$(CuBr)$_6$] (**21**) with a sandwich-like structure. Two molecules of **9** coordinate an almost planar Cu_6 ring on opposite sides (Figure 1.4).

Because of the multitopic nature of most P_n ligand complexes, not only small discrete units like **21** can be obtained, but also coordination polymers. In 2002, Scheer et al. reported on the synthesis of 1D polymers using **7a** together with AgNO$_3$ and CuBr, respectively.[35] Henceforward inspired by these results a variety of P_n ligand complexes were investigated in terms of their coordination behavior towards monovalent metal salts. Especially complex **11** shows a rich coordination chemistry. The reaction of **11** with CuCl leads to the formation of a 1D chain compound [{Cp*Fe($\eta^{5:1:1}$-P_5)}CuCl]$_n$ (**22**) in which the *cyclo*-P_5 rings bridge Cu_2Cl_2 four-membered rings (Figure 1.5).[36] In contrast, if CuBr or CuI are used, the compounds [{Cp*Fe($\eta^{5:1:1:1}$-P_5)}CuBr]$_n$ (**23**) and [{Cp*Fe($\eta^{5:1:1:1}$-P_5)}CuI]$_n$ (**24**) are obtained. In both cases, because of a further coordination of the P_5 ligand (1,2,4 coordination mode), 2D networks are
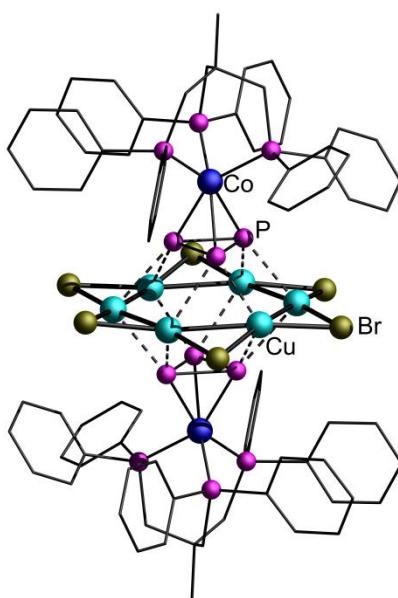
Figure 1.4. Molecular structure of **21** in the crystal.[14]

formed. In **23** and **24** each CuX (X = Br, I) unit is coordinated by three molecules of **11**, resulting in a tetrahedral coordination environment for copper (Figure 1.5).

These results were soon followed by the surprising appearance of supramolecules, also built by pentaphosphaferrocenes and copper(I)-chloride, but at different reaction conditions.[37] The obtained molecule [{Cp*Fe($\eta^{5:1:1:1:1:1}$-P$_5$)}$_{12}${CuCl}$_{10}${Cu$_2$Cl$_3$}$_5${Cu(CH$_3$CN)$_2$}$_5$] (**25**) has an overall scaffold of 90 inorganic atoms. The whole aggregate contains twelve molecules of **11** in a 1,2,3,4,5 coordination mode, 25 CuCl units and ten acetonitrile ligands, whose coordination saturates some of the copper ions. The ball-shaped cluster has a fullerene-like hollow structure and can be divided into two hemispherical parts with six molecules of **11** each and a linking belt of CuCl/CH$_3$CN. Once discovered, the formation of supramolecular aggregates derived from **11** could be expanded to CuBr[38] and the inside cavity of the clusters could be filled with a variety of templates.[39] One of the most remarkable result was achieved by the reaction of **11** with CuX (X = Cl, Br) and [(CpCr)$_2$(μ,$\eta^{5:5}$-As$_5$)] as a template.[39d]
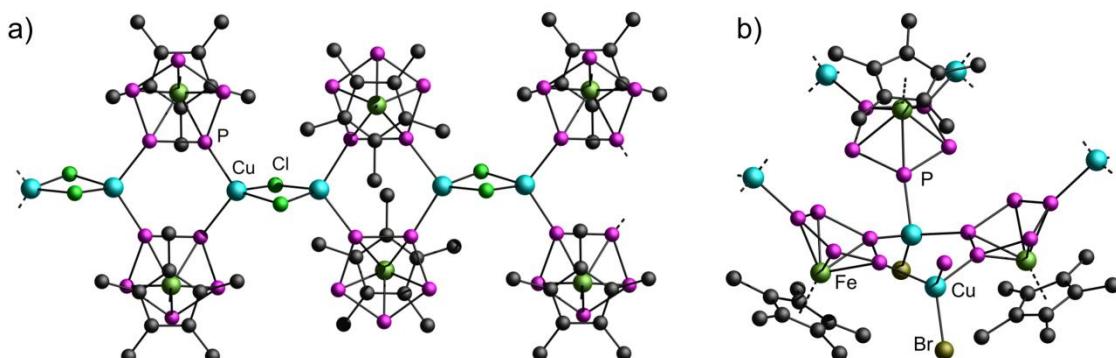
Figure 1.5. Sections of the polymer structures of a) **22** and b) **23**.[36]

Depending on the halide used, two aggregates, different in size and shape, [CpCr(η^5-As$_5$)]@[{Cp*Fe(η^5-P$_5$)}$_{12}${CuCl}$_{20}$] (**26**) and [(CpCr)$_2$(μ,$\eta^{5:5}$-As$_5$)]@[{Cp*Fe(η^5-P$_5$)}$_{12}${CuBr}$_{10}${Cu$_2$Br$_3$}$_5${Cu(CH$_3$CN)$_2$}$_5$] (**27**) with different encapsulated templates are obtained. If CuCl is used, the 80-vertex ball **26** is formed with I_h-C$_{80}$ fullerene topology and the 16 VE complex [CpCr(η^5-As$_5$)] as guest, which had not been known so far. However, changing to CuBr in **27**, the whole triple-decker complex [(CpCr)$_2$(μ,$\eta^{5:5}$-As$_5$)] is enclosed by a 90-vertex scaffold analogue to **25**. Due to this, the question arises whether supramolecular aggregates derived from pentaphosphaferrocene are generally able to stabilize reactive species or if they used as molecular vessels.[40]
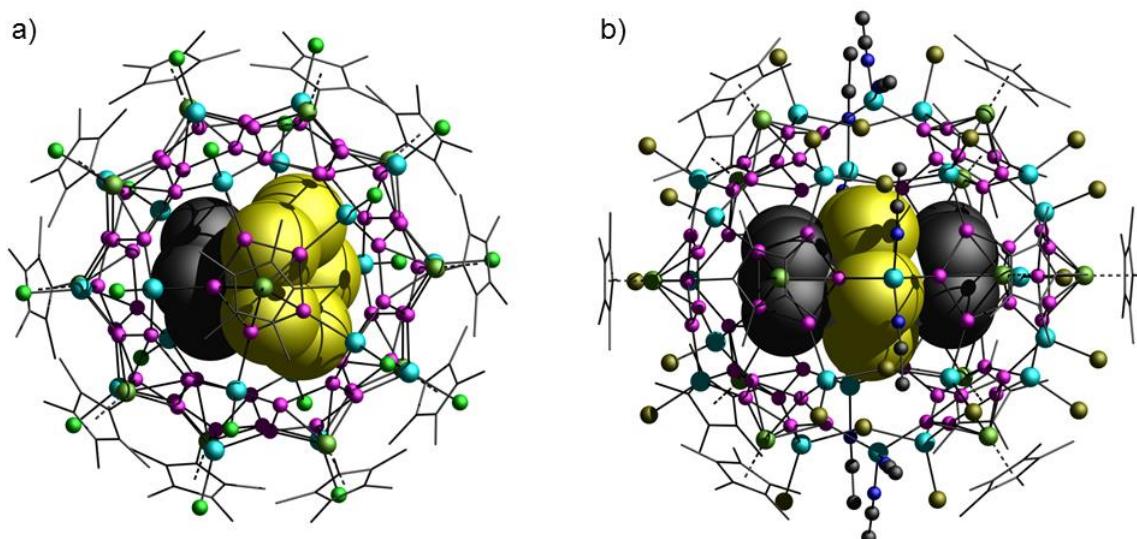
Figure 1.6. Molecular structures of the spherical clusters a) **26** and b) **27** in the solid state.[39d]

1.4 Cp^R Ligands with High Steric Demand

Since the discovery of the cyclopentadienide anion (C$_5$H$_5^-$, Cp$^-$) as a complex ligand in ferrocene, it has become one of the most important ligands in organometallic chemistry. The versatile coordination modes reach from η^1, η^3 and η^4 to a maximum of η^5, as observed in ferrocene.[41] Cp ligands can not only bind terminally, but can also act as a bridging moiety between two metal centers like in triple-decker complexes.[42]

The H atoms in the Cp ligand can easily be substituted, which enables the systematic and proper control of the properties of the Cp^R ligands in reference to its electronic structure and steric demand. Initially the pentamethylated derivative C$_5$Me$_5$ (Cp*) was well established in organometallic chemistry.[43] Since then, the sterical demand of the Cp^R ligands has been successively increased to investigate the properties of the obtained ligands. Not only the
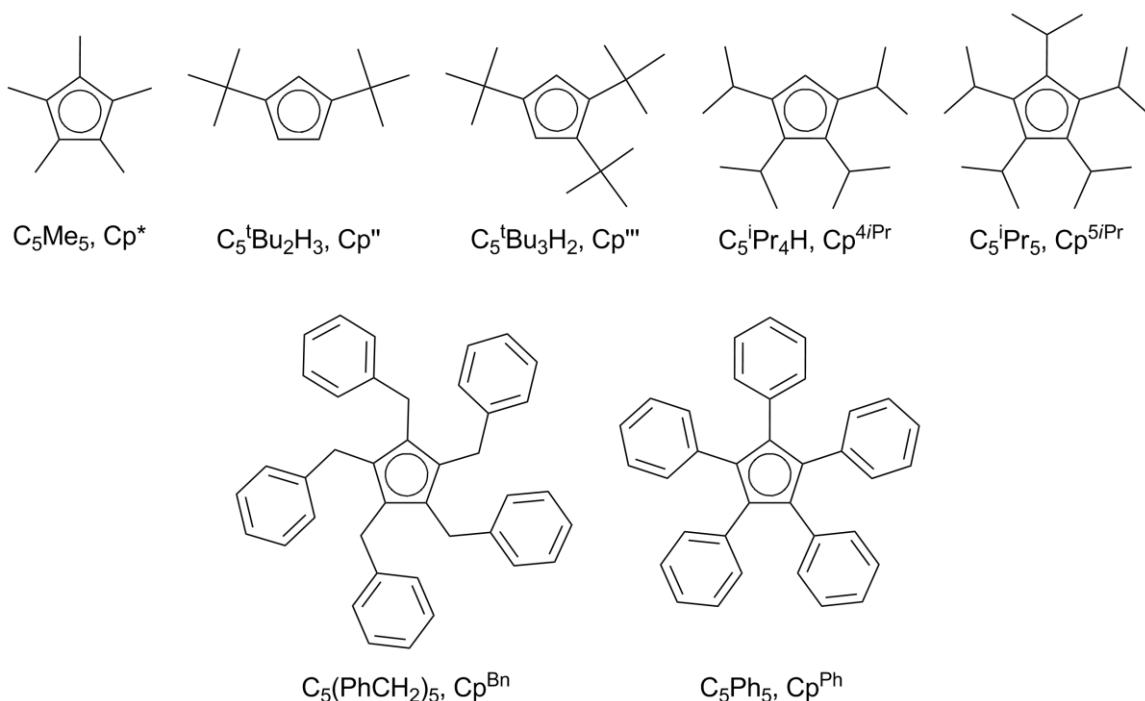
Figure 1.7. Selected Cp^R derivatives as neutral 5e$^-$ donors.

pentasubstituted C_5 symmetric Cp^R ligands were prepared, but also derivatives with a less number of substituents. Some rather frequently used Cp^R ligands are summarized in Figure 1.7.

The need to introduce larger Cp^R derivatives can be explained by four main reasons as argued by H. Schumann and C. Janiak: a) higher kinetic stability of complexes, b) novel structural motifs, c) facilitate possibility to study rotational dynamics and d) possible chirality of sandwich complexes.[44] In the following, the four aspects are briefly discussed with decreasing relevance for this thesis.

a) Higher Kinetic Stability of Complexes

In many cases 17 VE complexes with rather small Cp^R ligands are not stable. For instance, complex fragments of the general composition {Cp^{R}M(CO)$_n$} form dimers [Cp^{R}M(CO)$_n$]$_2$ (n = 1, M = Ni; n = 2, M = Fe; n = 3, M = Cr, Mo) to get the preferred 18 VE configuration.[42] However, with bigger Cp^R ligands the dimerization can be obviated and therefore the 17 VE species are stabilized. The complexes [Cp^{R}Fe(CO)$_2$]$_2$ (**28a**: Cp^R = Cp^{Ph} = C$_5$Ph$_5$; **28b**: Cp^R = Cp^{Tol} = C$_5$Ph$_4$(4-MeC$_6$H$_4$)),[45] [Cp*Cr(CO)$_3$]$_2$ (**29**)[46] and [Cp^{Ph}Mo(CO)$_3$]$_2$ (**30**) [47] e.g. show equilibria between monomeric and dimeric species. Using the sterically highly demanding Cp^{4iPr} and Cp^{5iPr} ligands, the radical recombination can be even be completely blocked, as the iron complex [Cp^{5iPr}Fe(CO)$_2$] (**28c**)[48] and the two cobalt compounds [Cp^{4iPr}Co(CH$_3$CN)$_2$][PF$_6$] (**31**) and [Cp^{4iPr}CoMe(PMe$_3$)] (**32**) show.[49]

Not only electron deficient compounds can be stabilized by sterical hindrance, but also complexes with a higher number of electrons. Using the penta-arylated ligand Cp^{Ph}, it is possible to synthesize 19 VE complexes.[44,47] The higher stability of the obtained complexes can not only be explained by the large volume of the ligand but also by the mesomeric effect of the phenyl groups. Because of that, the ligand can be considered as more Lewis acidic and is able to delocalize the electron density from the metal.[50]

In addition to the hindered radical coupling also a higher thermal stability is observed for some compounds. Janiak et. al. reported on group 14 metallocene complexes [Cp$^{Ph}_2$Z] (Z = Ge, Sn, Pb), which only start to decompose over 350 °C,[51] whereas the analogues with the less sterically demanding Cp^{Bn} (Cp^{Bn} = C$_5$(CH$_2$Ph)$_5$) ligand are only stable up to ~100 °C.[52]

b) Novel Structural Motifs

Sterically crowded Cp^R ligands can compulsory require the formation of unknown structural motifs. The use of Cp$^{Ph,[51,53]}$ and Cp$^{5iPr,[54]}$ give access to metallocene complexes with a parallel arrangement of the two Cp^R ligands. If smaller Cp^R ligands are used, often a bent structure is observed especially for metallocenes of the 14th group.[51,52,54,55]
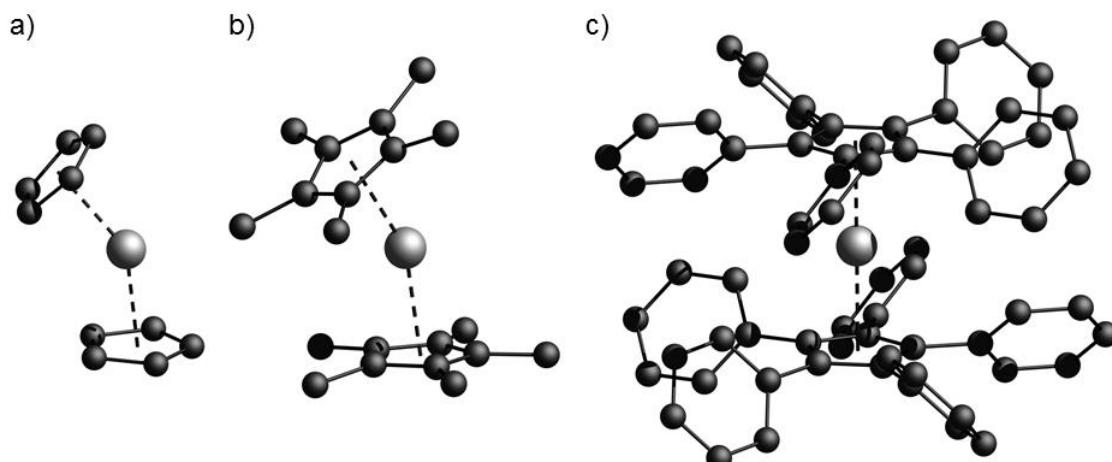
Figure 1.8. Molecular structures of stannocene derivatives a) **33a**, b) **33b** and c) **33c** with increasing steric demand. H atoms are omitted. C: black, Sn: grey.

This is obvious for the structures of the stannocene derivatives [Cp$_2$Sn] (**33a**),[56] [Cp*$_2$Sn] (**33b**)[57] and [Cp$^{Ph}_2$Sn] (**33c**)[51] in the solid state (**Figure 1.8**). The angle between the Cp rings decrease from **33a** to **33b** to **33c** from 33° to 25° and 0°.

Hanusa et al. and Sitzmann et al. synthesized [Cp^{R}MX]$_n$ (Cp^R = Cp''', Cp^{4iPr}, C$_5$(SiMe$_3$)$_3$H$_2$; M = alkaline earth metal; X = halide) with highly sterically demanding Cp ^{R} ligands.[58] This kind of complexes normally show Schlenk equilibria with [Cp$^R_2$M] and MX$_2$. However, with larger Cp^R ligands the rearrangement is blocked and the dimeric or polymeric compounds,

respectively, can be obtained. Naturally, this is also an example for the kinetic stabilization discussed above.

c) Facilitate Possibility to Study Rotational Dynamics

In $\{Cp^RM\}$ fragments in general two different dynamical movements can occur (Figure 1.9): rotation of the whole Cp^R ligand along the $Cp_{centroid}$–M axis (axial rotation) and rotation of the substituents R along the Cp–R bond (radial rotation).[44]
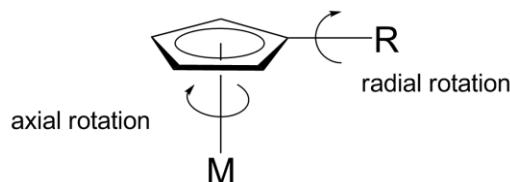
Figure 1.9. Possible rotations in $\{Cp^RM\}$ fragments.

By increasing the steric bulk and the number of substituents of the Cp^R ligands, a deceleration of both rotational modes can be expected. Dynamic processes could even be completely blocked with a sufficient size of the R moieties.

d) Possible Chirality of Sandwich Complexes

If the axial as well as the radial rotations are frozen, it is in principle possible to observe chiral sandwich complexes. Having a chiral Cp^R ligand itself would be another trivial possibility. In solution this would be less likely because of fast molecular dynamics. In the solid state it should be easier to observe this kind of chirality. Most promising are sandwich complexes with two highly sterically demanding Cp^R ligands like Cp^{5iPr} or Cp^{Ph}. Indeed, Sitzmann et al. were able to observe chirality in the complex $[Cp^{5iPr}_2Sn]$ in solid state and solution alike (mixture of sterioisomers).[54a] The isolation of enantiomerically pure compounds $[Cp^R_2M]$ has not been possible so far.

1.5 References

[1]   N. Wiberg, *Lehrbuch für Anorganische Chemie, Vol. 102*, de Gruyter, Berlin/New York, **2007**.

[2]   W. L. Roth, T. W. DeWitt, A. J. Smith, *J. Am. Chem. Soc.* **1947**, *69*, 2881-2885.

[3]   a) H. Thurn, H. Kerbs, *Angew. Chem., Int. Ed.* **1966**, *5*, 1047-1048. b) M. Ruck, D. Hoppe, B. Wahl, P. Simon, Y. Wang, G. Seifert, *Angew. Chem., Int. Ed.* **2005**, *44*, 7616-7619.

[4]   P. W. Bridgman, *J. Am. Chem. Soc.* **1914**, *36*, 1344-1363.

[5]   a) A. Simon, H. Borrmann, H. Craubner, *Phosphorus, Sulfur Silicon Relat. Elem.* **1987**, *30*, 507-510. b) H. Okudera, R. E. Dinnebier, A. Simon, *Z. Kristallogr.* **2005**, *220*, 259-264.

[6]   A. Bettendorff, *Justus Liebigs Ann. Chem.* **1867**, *144*, 110-114.

[7]   a) M. Schmidt, B. Block, H. D. Block, H. Köpf, E. Wilhelm, *Angew. Chem.* **1968**, *80*, 660-660. b) R. Steudel, R. Strauss, *J. Chem. Soc., Dalton Trans.* **1984**, 1775-1777. c) M. Draganjac, T. B. Rauchfuss, *Angew. Chem.* **1985**, *97*, 745-760.

[8]   a) B. M. Cossairt, N. A. Piro, C. C. Cummins, *Chem. Rev.* **2010**, *110*, 4164-4177. b) M. Caporali, L. Gonsalvi, A. Rossin, M. Peruzzini, *Chem. Rev.* **2010**, *110*, 4178-4235. d) M. Scheer, *Dalton Trans.* **2008**, 4372-4386.

[9]   a) M. Scheer, G. Balazs, A. Seitz, *Chem. Rev.* **2010**, *110*, 4236-4256. b) N. A. Giffin, J. D. Masuda, *Coord. Chem. Rev.* **2011**, *255*, 1342-1359.

[10]   A. P. Ginsberg, W. E. Lindsell, *J. Amer. Chem. Soc.* **1971**, *93*, 2082-2084.

[11]   a) A. P. Ginsberg, W. E. Lindsell, K. J. McCullough, C. R. Sprinkle, A. J. Welch, *J. Am. Chem. Soc.* **1986**, *108*, 403-416. b) I. Krossing, *J. Am. Chem. Soc.* **2001**, *123*, 4603-4604.

[12]   O. J. Scherer, G. Schwarz, G. Wolmershaeuser, *Z. Anorg. Allg. Chem.* **1996**, *622*, 951-957.

[13]   P. Dapporto, S. Midollini, L. Sacconi, *Angew. Chem., Int. Ed.* **1979**, *18*, 469-469.

[14]   M. D. Vaira, L. Sacconi, *Angew. Chem., Int. Ed.* **1982**, *21*, 330-342.

[15]   a) M. Peruzzini, L. Marvelli, A. Romerosa, R. Rossi, F. Vizza, F. Zanobini, *Eur. J. Inorg. Chem.* **1999**, 931-933. b) I. de los Rios, J.-R. Hamon, P. Hamon, C. Lapinte, L. Toupet, A. Romerosa, M. Peruzzini, *Angew. Chem., Int. Ed.* **2001**, *40*, 3910-3912. c) V. M. Di, M. Peruzzini, S. S. Costantini, P. Stoppioni, *J. Organomet. Chem.* **2006**, *691*, 3931-3937. d) M. Caporali, V. M. Di, M. Peruzzini, S. S. Costantini, P. Stoppioni, F. Zanobini, *Eur. J. Inorg. Chem.* **2010**, 152-158. e) V. Mirabello, M. Caporali, V. Gallo, L. Gonsalvi,

A. Ienco, M. Latronico, P. Mastrorilli, M. Peruzzini, *Dalton Trans.* **2011**, *40*, 9668-9671. f) V. Mirabello, M. Caporali, V. Gallo, L. Gonsalvi, D. Gudat, W. Frey, A. Ienco, M. Latronico, P. Mastrorilli, M. Peruzzini, *Chem. Eur. J.* **2012**, *18*, 11238-11250.

[16]   F. Dielmann, M. Sierka, A. V. Virovets, M. Scheer, *Angew. Chem., Int. Ed.* **2010**, *49*, 6860-6864.

[17]   a) N. C. Zanetti, R. R. Schrock, W. M. Davis, *Angew. Chem., Int. Ed.* **1995**, *34*, 2044-2046. b) N. C. Zanetti, R. R. Schrock, W. M. Davis, *Angew. Chem.* **1995**, *107*, 2184-2186.

[18]   C. E. Laplaza, W. M. Davis, C. C. Cummins, *Angew. Chem., Int. Ed.* **1995**, *34*, 2042-2044.

[19]   B. P. Johnson, G. Balazs, M. Scheer, *Coord. Chem. Rev.* **2006**, *250*, 1178-1195.

[20]   O. J. Scherer, H. Sitzmann, G. Wolmershaeuser, *J. Organomet. Chem.* **1984**, *268*, C9-C12.

[21]   O. J. Scherer, H. Sitzmann, G. Wolmershäuser, *Angew. Chem., Int. Ed.* **1985**, *24*, 351-353.

[22]   M. E. Barr, L. F. Dahl, *Organometallics* **1991**, *10*, 3991-3996.

[23]   M. Scheer, U. Becker, M. H. Chisholm, J. C. Huffman, F. Lemoigno, O. Eisenstein, *Inorg. Chem.* **1995**, *34*, 3117-3119.

[24]   a) O. J. Scherer, G. Berg, G. Wolmershäuser, *Chem. Ber.* **1995**, *128*, 635-639. b) O. J. Scherer, G. Berg, G. Wolmershäuser, *Chem. Ber.* **1996**, *129*, 53-58.

[25]   O. J. Scherer, T. Völmecke, G. Wolmershäuser, *Eur. J. Inorg. Chem.* **1999**, *1999*, 945-949.

[26]   M. D. Vaira, C. A. Ghilardi, S. Midollini, L. Sacconi, *J. Am. Chem. Soc.* **1978**, *100*, 2550-2551.

[27]   a) O. J. Scherer, T. Brück, *Angew. Chem., Int. Ed.* **1987**, *26*, 59-59. b) O. J. Scherer, T. Brück, *Angew. Chem.* **1987**, *99*, 59-59.

[28]   E. Urnezius, W. W. Brennessel, C. J. Cramer, J. E. Ellis, P. v. R. Schleyer, *Science* **2002**, *295*, 832-834.

[29]   O. J. Scherer, J. Schwalb, H. Swarowsky, G. Wolmershaeuser, W. Kaim, R. Gross, *Chem. Ber.* **1988**, *121*, 443-449.

[30]   O. J. Scherer, H. Swarowsky, G. Wolmershäuser, W. Kaim, S. Kohlmann, *Angew. Chem., Int. Ed.* **1987**, *26*, 1153-1155.

[31]   J. J. Schneider, D. Wolf, C. Janiak, O. Heinemann, J. Rust, C. Krüger, *Chem. Eur. J.* **1998**, *4*, 1982-1991.

[32]   F. Dielmann, M. Sierka, A. V. Virovets, M. Scheer, *Angew. Chem., Int. Ed.* **2010**, *49*,

6860-6864.

[33]   R. F. Winter, W. E. Geiger, *Organometallics* **1999**, *18*, 1827-1833.

[34]   M. V. Butovskiy, G. Balázs, M. Bodensteiner, E. V. Peresypkina, A. V. Virovets, J. Sutter, M. Scheer, *Angew. Chem.* **2013**, *125*, 3045-3049.

[35]   J. Bai, E. Leiner, M. Scheer, *Angew. Chem., Int. Ed.* **2002**, *41*, 783-786.

[36]   a) J. Bai, A. V. Virovets, M. Scheer, *Angew. Chem., Int. Ed.* **2002**, *41*, 1737-1740. b) J. Bai, A. V. Virovets, M. Scheer, *Angew. Chem.* **2002**, *114*, 1808-1811.

[37]   J. Bai, A. V. Virovets, M. Scheer, *Science* **2003**, *300*, 781-783.

[38]   M. Scheer, J. Bai, B. P. Johnson, R. Merkle, A. V. Virovets, C. E. Anson, *Eur. J. Inorg. Chem.* **2005**, 4023-4026.

[39]   a) M. Scheer, A. Schindler, R. Merkle, B. P. Johnson, M. Linseis, R. Winter, C. E. Anson, A. V. Virovets, *J. Am. Chem. Soc.* **2007**, *129*, 13386-13387. b) M. Scheer, A. Schindler, C. Groeger, A. V. Virovets, E. V. Peresypkina, *Angew. Chem., Int. Ed.* **2009**, *48*, 5046-5049. c) M. Scheer, A. Schindler, J. Bai, B. P. Johnson, R. Merkle, R. Winter, A. V. Virovets, E. V. Peresypkina, V. A. Blatov, M. Sierka, H. Eckert, *Chem. Eur. J.* **2010**, *16*, 2092-2107. d) A. Schindler, C. Heindl, G. Balázs, C. Gröger, A. V. Virovets, E. V. Peresypkina, M. Scheer, *Chem. Eur. J.* **2012**, *18*, 829-835. e) C. Schwarzmaier, A. Schindler, C. Heindl, S. Scheuermayer, E. V. Peresypkina, A. V. Virovets, M. Neumeier, R. Gschwind, M. Scheer, *Angew. Chem., Int. Ed.* **2013**, *52*, 10896-10899.

[40]   a) M. Yoshizawa, J. K. Klosterman, M. Fujita, *Angew. Chem., Int. Ed.* **2009**, *48*, 3418-3438. b) Y. Inokuma, M. Kawano, M. Fujita, *Nat. Chem.* **2011**, *3*, 349-358. c) S. Horiuchi, T. Murase, M. Fujita, *Angew. Chem., Int. Ed.* **2012**, *51*, 12029-12031.

[41]   a) T. J. Kealy, P. L. Pauson, *Nature* **1951**, *168*, 1039-1040. b) S. A. Miller, J. A. Tebboth, J. F. Tremaine, *J. Chem. Soc.* **1952**, 632-635.

[42]   C. Elschenbroich, *Organometallchemie, Vol. 6*, Teubner, Wiesbaden **2008**.

[43]   a) R. B. King, M. B. Bisnette, *J. Organomet. Chem.* **1967**, *8*, 287-297. b) R. B. King, A. Efraty, *J. Amer. Chem. Soc.* **1972**, *94*, 3773-3779.

[44]   C. Janiak, H. Schumann, *Adv. Organomet. Chem.* **1991**, *33*, 291-393.

[45]   a) I. Kuksis, M. C. Baird, *Organometallics* **1994**, *13*, 1551-1553. b) I. Kuksis, M. C. Baird, *Organometallics* **1996**, *15*, 4755-4762.

[46]   T. J. Jaeger, M. C. Baird, *Organometallics* **1988**, *7*, 2074-2076.

[47]   M. Fei, S. K. Sur, D. R. Tyler, *Organometallics* **1991**, *10*, 419-423.

[48]   a) H. Sitzmann, T. Dezember, W. Kaim, F. Baumann, D. Stalke, J. Kärcher, E. Dormann, H. Winter, C. Wachter, M. Kelemen, *Angew. Chem., Int. Ed.* **1996**, *35*, 2872-2875. b) H. Sitzmann, T. Dezember, W. Kaim, F. Baumann, D. Stalke, J. Kärcher, E. Dormann, H.

Winter, C. Wachter, M. Kelemen, *Angew. Chem.* **1996**, *108*, 3013-3016.

[49]   F. Baumann, E. Dormann, Y. Ehleiter, W. Kaim, J. Karcher, M. Kelemen, R. Krammer, D. Saurenz, D. Stalke, C. Wachter, G. Wolmershauser, H. Sitzmann, *J. Organomet. Chem.* **1999**, *587*, 267-283.

[50]   a) M. J. Heeg, C. Janiak, J. J. Zuckerman, *J. Am. Chem. Soc.* **1984**, *106*, 4259-4261. b) K. Broadley, G. A. Lane, N. G. Connelly, W. E. Geiger, *J. Am. Chem. Soc.* **1983**, *105*, 2486-2487.

[51]   C. Janiak, H. Schumann, C. Stader, B. Wrackmeyer, J. J. Zuckerman, *Chem. Ber.* **1988**, *121*, 1745-1751.

[52]   H. Schumann, C. Janiak, E. Hahn, C. Kolax, J. Loebel, M. D. Rausch, J. J. Zuckerman, M. J. Heeg, *Chem. Ber.* **1986**, *119*, 2656-2667.

[53]   G. B. Deacon, C. M. Forsyth, F. Jaroschik, P. C. Junk, D. L. Kay, T. Maschmeyer, A. F. Masters, J. Wang, L. D. Field, *Organometallics* **2008**, *27*, 4772-4778.

[54]   a) H. Sitzmann, R. Boese, P. Stellberg, *Z. Anorg. Allg. Chem.* **1996**, *622*, 751-755. b) H. Sitzmann, T. Dezember, O. Schmitt, F. Weber, G. Wolmershauser, M. Ruck, *Z. Anorg. Allg. Chem.* **2000**, *626*, 2241-2244.

[55]   T. K. Hollis, J. K. Burdett, B. Bosnich, *Organometallics* **1993**, *12*, 3385-3386.

[56]   J. L. Atwood, W. E. Hunter, A. H. Cowley, R. A. Jones, C. A. Stewart, *J. Chem. Soc., Chem. Commun.* **1981**, 925-927.

[57]   P. Jutzi, F. Kohl, P. Hofmann, C. Krüger, Y.-H. Tsay, *Chem. Ber.* **1980**, *113*, 757-769.

[58]   a) D. J. Burkey, E. K. Alexander, T. P. Hanusa, *Organometallics* **1994**, *13*, 2773-2786. b) M. J. Harvey, T. P. Hanusa, *Organometallics* **2000**, *19*, 1556-1566. c) H. Sitzmann, F. Weber, M. D. Walter, G. Wolmershaeuser, *Organometallics* **2003**, *22*, 1931-1936.

2. Research Objectives

The preparation of P_n ligand complexes has so far mostly been restricted to {$Cp^R M$} (M = transition metal) fragments bearing rather small Cp^R ligands. However, a trend for using larger Cp^R ligands can be observed without a doubt. To investigate the influence of sterically crowded Cp^R derivatives on the reaction behavior of transition metal fragments towards appropriate substrates, the pentaarylated ligand Cp^{BIG} ($C_5(4\text{-}n\text{BuC}_6H_4)$) has been chosen. On the one hand it meets the requested high steric demand and on the other hand its complexes show very good solubility in almost all solvents. The research objectives for this work therefore are:

❖ Preparation of transition metal precursors bearing the highly sterically demanding Cp^{BIG} ligand for the synthesis of P_n ligand complexes

❖ Comparison of the resulting reactivity and the obtained structural motifs with those of analogue complexes with rather small steric bulk on the Cp moiety

It was demonstrated in my master thesis that the Cp^{BIG} complex [$Cp^{BIG}Fe(CO)_2]_2$ can be prepared in good yields. The complex is subject to a monomer-dimer equilibrium as discussed in chapter 1.4a. Furthermore, the reaction of [$Cp^{BIG}Fe(CO)_2]_2$ with P_4 at r.t. was reported, but the product could not be identified with sufficient certainty. Initiating from these results some tasks arise:

❖ Studies of the reaction behavior at low temperatures of [$Cp^{BIG}Fe(CO)_2]_2$ with main group cage compounds (P_4, As_4, P_4S_3, P_4Se_3), group 16 allotropes (S_8, Se_{red}, α-Te) and other small molecules

❖ Investigation of the reactivity of the obtained complexes

It was also shown that the sterically crowded pentaphosphaferrocene [$Cp^{BIG}Fe(\eta^5\text{-}P_5)$] can be obtained in moderate to good yields. As discussed in chapter 1.3, this type of complexes represents a perfect starting material for the formation of supramolecular aggregates. Hence, we arrive at the following research objective:

❖ Reaction of [$Cp^{BIG}Fe(\eta^5\text{-}P_5)$] with monovalent coinage metal salts in terms of the formation of spherical macromolecules and polymeric compounds

❖ Comparative investigations on the reactivity of [$Cp^{BIG}Fe(\eta^5\text{-}P_5)$] with Cu(I) and Cu(II) halides

3. The Highly Sterically Demanding Cp^{BIG} Ligand

The intention of this chapter is to give a brief overview about the properties of the Cp^{BIG} ligand. Some general aspects will be spotlighted and discussed, but notice that this is not complete but rather an outline. The reviewed characteristics do not necessarily refer to specific compounds, but they can be seen as a summary of the observations made by working with this interesting ligand.

3.1 Solubility

Pentaarylated Cp^R derivatives and their compounds often show rare solubility properties.[1] Kuksis et al. reported on the dimeric complex [Cp^{Ph}Fe(CO)$_2$]$_2$ (**1a**) and its transformation into the better soluble analogue [Cp^{Tol}Fe(CO)$_2$]$_2$ (**1b**) by functionalization of one phenyl group with a methyl group in *para* position.[1b,c] This demonstrates that alkyl moieties can increase the solubility. Hence, Harder and co-workers used the same approach and first used the Cp^{BIG} ligand[2] in organometallic chemistry, which is substituted with five *n*-butyl groups.[3] The obtained pentaaryl metallocenes show very good solubility even in nonpolar solvents like pentane and hexane.

Complexes bearing Cp^{BIG} ligands, including the compounds discussed in this work, show very good solubility in THF, toluene, CH$_2$Cl$_2$ and in some cases even in hexane. Nevertheless, in a few examples (e.g. [Cp^{BIG}Fe(CO)$_2$]$_2$ and [Cp^{BIG}Fe(η^5-P$_5$)])[4] hexane pointed out to be a poor solvent. Neutral Cp^{BIG} complexes are solely insoluble in acetonitrile (CH$_3$CN). This is not too surprising considering the immiscibility of CH$_3$CN and hexane together with the relatedness of hexane with the *n*-butyl groups of the Cp^{BIG} ligand. However, this can be different for charged complexes, like it is observed for [Cp^{BIG}Fe(CO)$_2$]$^-$K$^+$. The insolubility of Cp^{BIG} compounds in CH$_3$CN can be used as an advantage for crystallization. For many of the described complexes crystals were obtained by slow diffusion of CH$_3$CN into CH$_2$Cl$_2$ solutions (layering experiments).

Due to the predominance of the Cp^{BIG} ligand in its complexes, most of them show very similar solubility properties (including the protonated ligand Cp^{BIG}H). This is a drawback in the separation and purification of the reaction mixtures and products. Therefore, column chromatography is often necessary. However, in some cases even this does not result in sufficient and satisfactory product purity, which can likely be explained by similar retention factors R$_f$.

3.2 Geometrical Considerations

The Cp^{BIG} ligand exhibits a high steric demand around the metal center. This can be demonstrated by the estimated angle between the outer substituents of a Cp^{R} ligand (considered as a disc) and the bound metal atom. It is illustrated in Figure 3.1 by the molecular structures of the cymantrene derivatives [Cp^{R}Mn(CO)$_3$] (Cp^{R} = Cp,[5] Cp*,[6] Cp^{BIG}). The cone angle increases dramatically with larger substituents (Cp: 105°; Cp*: 135°; Cp^{BIG}: 160°). The effective shielding of almost one complete hemisphere of the coordination sphere of metal centers results in higher kinetic stability of the formed complexes (cf. chapter 1.4a).
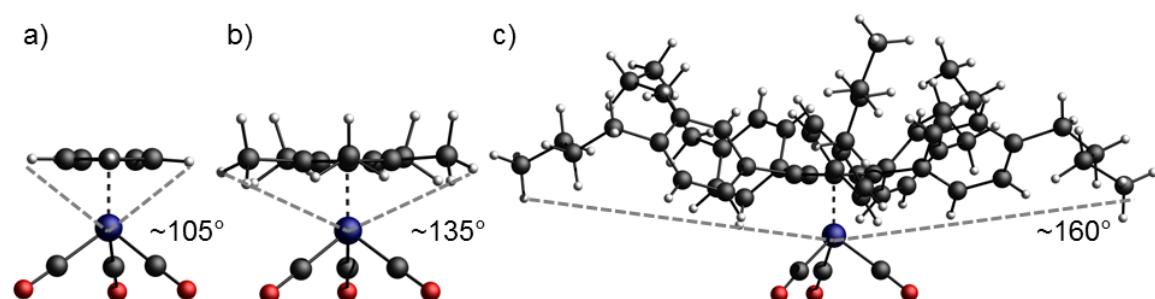
Figure 3.1. Molecular structures of cymantrene complexes [Cp^{R}Mn(CO)$_3$] with different Cp^{R} ligands: a) Cp, b) Cp* and c) Cp^{BIG}. The sterically shielding effect is demonstrated with the increasing cone angle between Cp^{R} ligand (considered as discs) and the Mn atom.

The different geometry of small Cp^{R} ligands compared to the bulky Cp^{BIG} ligand implicates that in some cases it is just impossible to form analogue complexes or compounds with the same ligand arrangement (cf. chapter 1.4b). It is trivial, that in a specific volume only a particular number of Cp^{R} ligands can be arranged (Figure 3.2). Increase of the steric bulk obviates at a specific point the formation of the compound. Hence, the system has to avoid steric repulsion by either a smaller number of Cp^{R} ligands or expansion of the structure. This concept is of special importance for this work and was applied to several topics.
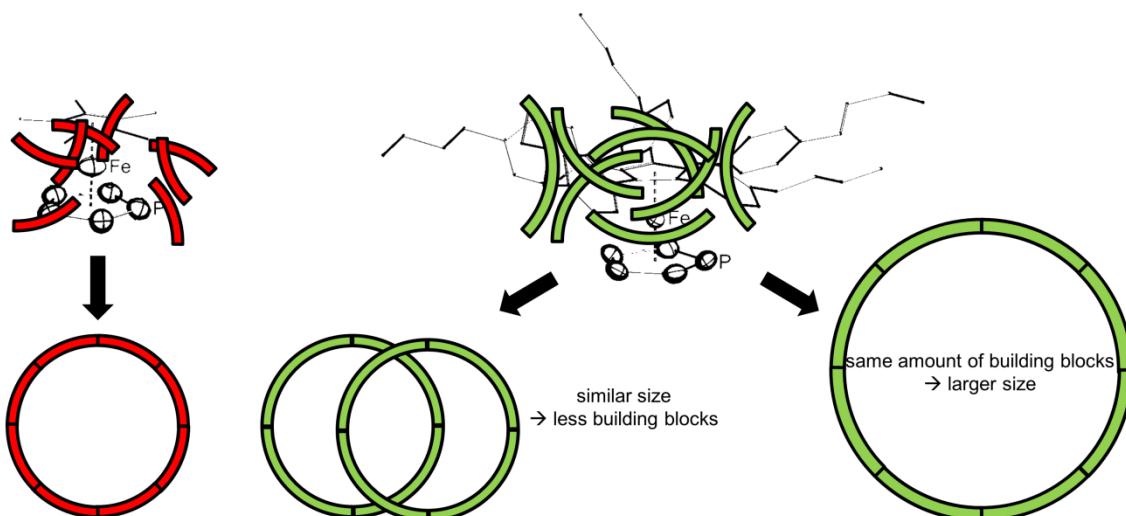
Figure 3.2. In a specific volume a particular amount of building blocks can be arranged (left). If the steric demand increases, the system has to avoid steric repulsion (right).

3.3 The Cp^{BIG} Ligand in Crystal Structures

Due to steric hindrance, it is not possible to arrange all of the aryl moieties in pentaarylated Cp^R derivatives (e.g. Cp^{Ph}, Cp^{BIG}) co-planar to the Cp plane. Therefore they generally exhibit propeller-like structures, in which the phenyl groups are twisted about 45°-60° from planarity (Figure 3.3a). This alignment results in close contacts between the *ortho*-H atoms and the *ipso*-C atoms of neighboring phenyl groups. The shortest observed intramolecular H⋯C$_{ipso}$ and H⋯Ph$_{centr}$ distances are about 2.6 Å and 2.9 Å, respectively (Figure 3.3b). Calculations with the pixel method show two minima structures for benzene dimers in the gas phase, face-to-face (parallel) and edge-to-face (perpendicular).[7] In the latter case a calculated distance H⋯Ph$_{centr}$ of 2.88 Å can be found.[7,8] Calculations for crystalline benzene even show further minima structures with orientations similar to that found in Cp^{BIG}. These results indicate multiple intramolecular H-π interactions for the Cp^{BIG} ligand.
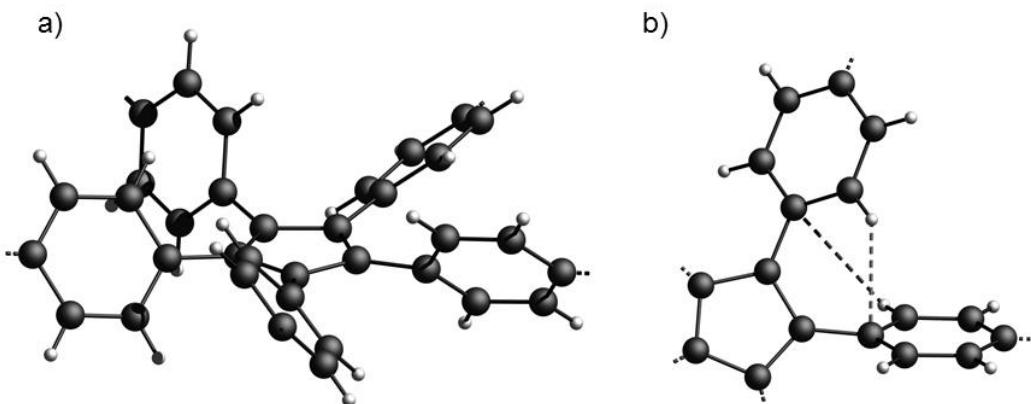
Figure 3.3. Arrangement of the Cp^{BIG} ligand in crystal structures: a) Orientation of the phenyl groups illustrating propeller-like structure; b) Section of the Cp^{BIG} ligand with H⋯C$_{ipso}$ interactions between two neighboring phenyl groups.

Not only intramolecular H-π interactions can be discussed, but also intermolecular ones. In over 90% of the measured crystal structures of Cp^{BIG} containing molecules two Cp^{BIG} ligands are stacked together (Figure 3.4; see also reference 4). On the one hand, this gearwheel-like arrangement results in very effective space filling packing. On the other hand, the phenyl H atoms are always orientated towards the π-system of the phenyl groups of the other Cp^{BIG} ring. The intermolecular H⋯Ph$_{centr}$ distances of about 3.0 Å - 3.5 Å are larger than the calculated values for benzene.[7] However, they are in a range where H-π interactions can be considered.
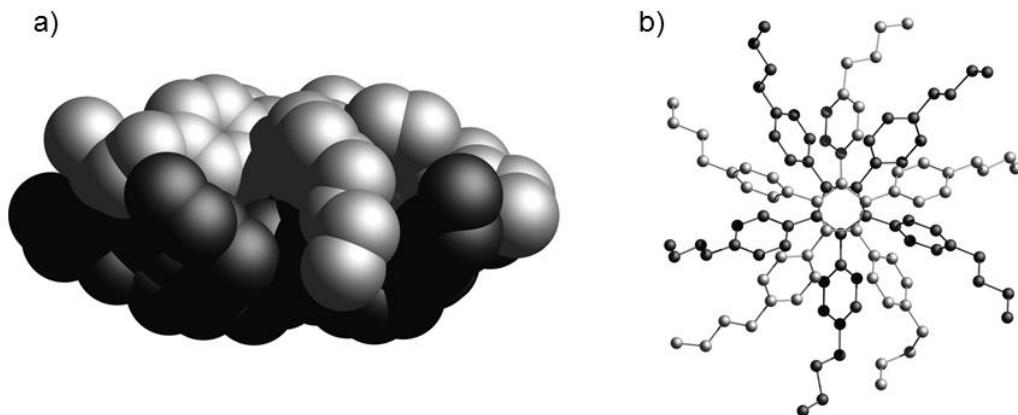
Figure 3.4. Predominant packing mode of Cp^BIG ligands relative to each other in the solid state. For clarity reasons only Cp^BIG ligands without H atoms are depicted. a) Side view, 'space-filling' model; b) top view, 'balls-and-stick' model.
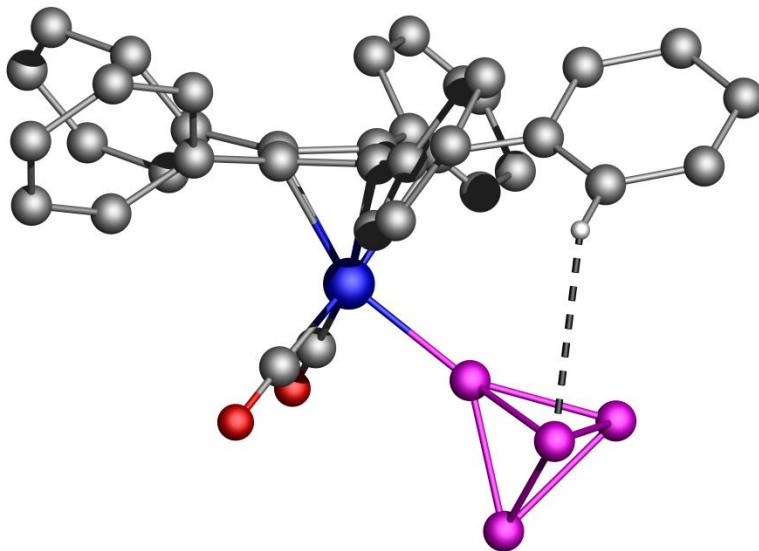
Crystal structure refinement of compounds bearing Cp^BIG ligands is often a meticulous exhausting job. In most compounds some of the nBu groups are disordered. In general, the nBu moieties can 'wobble', causing diffuse electron density. This hampers the localization of the C atoms in the chains and therefore sometimes irrelevant C–C distances are observed. In addition to this, they show large anisotropic displacement parameters. To obtain satisfactory refinement results, which are also consistent with chemical standpoints, the n-butyl groups have to be restrained. Frequently used commands in the SHELX 97[9] refinement program are SAME, SADI, DELU, SIMU and ISOR.

3.4 References

[1]   a) C. Janiak, H. Schumann, *Adv. Organomet. Chem.* **1991**, *33*, 291-393. b) I. Kuksis, M. C. Baird, *Organometallics* **1994**, *13*, 1551-1553. c) I. Kuksis, M. C. Baird, *Organometallics* **1996**, *15*, 4755-4762.

[2]   G. Dyker, J. Heiermann, M. Miura, J.-I. Inoh, S. Pivsa-Art, T. Satoh, M. Nomura, *Chem. Eur. J.* **2000**, *6*, 3426-3433.

[3]   a) L. Orzechowski, D. F. J. Piesik, C. Ruspic, S. Harder, *Dalton Trans.* **2008**, 4742-4746. b) C. Ruspic, J. R. Moss, M. Schuermann, S. Harder, *Angew. Chem., Int. Ed.* **2008**, *47*, 2121-2126. c) S. Harder, C. Ruspic, *J. Organomet. Chem.* **2009**, *694*, 1180-1184.

[4]   S. Heinl, Master Thesis, University of Regensburg (Regensburg, Germany), **2010**.

[5]   P. J. Fitzpatrick, Y. Le Page, J. Sedman, I. S. Butler, *Inorg. Chem.* **1981**, *20*, 2852-2861.

[6]   S. Fortier, M. C. Baird, K. F. Preston, J. R. Morton, T. Ziegler, T. J. Jaeger, W. C. Watkins, J. H. MacNeil, K. A. Watson, *J. Am. Chem. Soc.* **1991**, *113*, 542-551.

[7]   J. D. Dunitz, A. Gavezzotti, *Angew. Chem., Int. Ed.* **2005**, *44*, 1766-1787.

[8]   F. Dielmann, PhD Thesis, University of Regensburg (Regensburg, Germany), **2011**.

[9]   A. Altomare, M. C. Burla, M. Camalli, G.L. Cascarano, C. Giacovazzo, A. Guagliardi, A. G. G. Moliterni, Polidori, G., Spagna, R. *J. Appl. Cryst.* **1999**, *32*, 115-119

4. Intact P₄ Tetrahedra as Terminal and Bridging Ligands in Neutral Complexes of Manganese

Sebastian Heinl, Eugenia Peresypkina, Alexey Y. Timoshkin, Piero Mastrorilli, Vito Gallo and Manfred Scheer
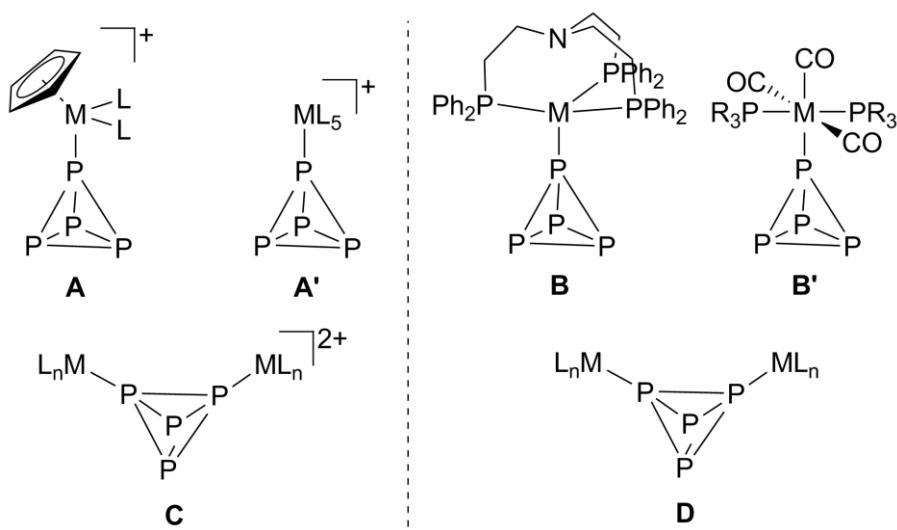
❖ **Reprinted with permission of 'John Wiley and Sons'. Copyright © 2013 WILEY-VCH Verlag GmbH & Co. KGaA, Weinheim. Licence Number: 3341310989491 (German Version), 3341310783971 (English Version)**

❖ **All syntheses and characterizations were performed by Sebastian Heinl, unless subsequently noted otherwise**

❖ **Manuscript was written by Sebastian Heinl except NMR discussions (Piero Mastrorilli and Vito Gallo) and DFT calculations (Alexey Y. Timoshkin)**

❖ **Figures were made by Sebastian Heinl except NMR pictures (Piero Mastrorilli and Vito Gallo)**

❖ **DFT calculations were performed by Alexey Y. Timoshkin**

❖ **EXSY and HOESY NMR were measured and interpreted by Piero Mastrorilli and Vito Gallo**

❖ **X-ray structure analyses and refinement were performed by Sebastian Heinl (3) and Eugenia Peresypkina (1a, 2)**

4.1 Introduction

The direct use of white phosphorus to generate organophosphorus compounds is still an unsolved problem,[1] although recently some progress has been achieved by the photolysis of P$_4$ with neat dienes.[2] A transition metal mediated conversion is one option for this goal,[3] a mode of activation that first requires coordination of a vertex or an edge of the P$_4$ tetrahedron at the metal. Looking into the existing compounds that feature end-on P$_4$ coordination, there are complexes of type **A**, which were synthesized by the Sacconi group.[4] However, these compounds are insoluble in all common solvents, and the other known neutral complexes of type **B** decompose in solution at temperatures above 0 °C.[5] So, complexes such as **A** and **B** do not represent useful starting materials for a subsequent P$_4$ activation. As Peruzzini et al. have shown, the use of cationic coordination compounds leads to the end-on coordinated P$_4$ complexes **C**, which are stable in the solid state and in solution.[6,7] An interesting and recently discovered feature is the dynamic process, experienced by a number of P$_4$ complexes,[6h,i] consisting of the P$_4$ tumbling of the cage while remaining chemically coordinated to the central metal moiety. In addition the P$_4$ ligand in mononuclear cationic complexes can bind a second metal fragment to give the binuclear dicationic species **D**. If P$_4$ bridges two Re, or Ru and Pt atoms, respectively, a dynamic behavior involving the coordinated P$_4$ has also been observed.[6h,i] In view of the activation of P$_4$, the second coordination seems to be decisive, since the hydrolysis of type **C** complexes leads to usual P$_4$ hydrolysis products. In contrast, the double fixation of P$_4$ in **D** leads via hydrolysis to novel triphosphines and thus to a change of the properties of P$_4$.[6j] Therefore, the question arises whether *neutral* complexes with a *tetrahedro*-P$_4$ ligand can be synthesized, which are stable at room temperature both in the solid state and in solution, and if the missing *neutral* type **E** complex with a bridging P$_4$ unit can be isolated.
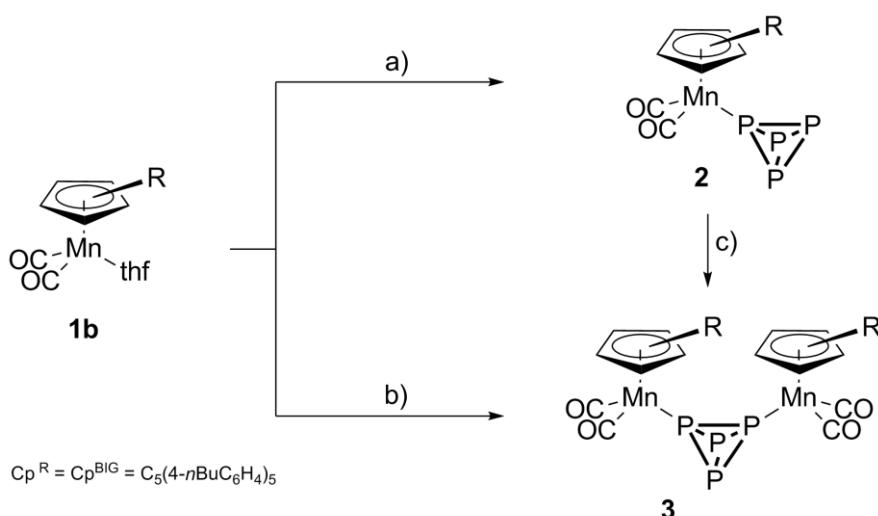
Both challenges motivated us to use manganese complexes such as [Cp^{R}Mn(CO)$_2$(thf)]. Interestingly, no unsubstituted E$_n$ ligand complexes of Manganese have been yet synthesized, which provides additional motivation for investigating this chemistry.[3,8] Intensive efforts to use common Cp and Cp* derivatives of cymantrene [Cp^{R}Mn(CO)$_3$] failed to coordinate P$_4$ or even to convert it under thermal or photolytic conditions. So, the design of a novel derivative with a high Lewis acidity was needed.

Herein we report on the synthesis and characterization of [Cp^{BIG}Mn(CO)$_3$] (**1a**) (Cp^{BIG} = pentakis(4-n-butylphenyl)cyclopentadienyl) and its conversion into neutral manganese complexes with a $tetrahedro$-P$_4$ ligand coordinating in a terminal and in a bridging fashion, and thus to result in the first example of a neutral type **E** complex.

4.2 Results and Discussion

The bulky substituted cymantrene complex **1a** is prepared by the reaction of Mn(CO)$_5$Br with one equivalent Cp^{BIG}Na under thermolytical conditions in THF.[9] Irradiation of a solution of **1a** in THF leads to the elimination of one carbonyl and the formation of [Cp^{BIG}Mn(CO)$_2$thf] (**1b**). Addition of a solution of **1b** to a solution of five equivalents white phosphorus yields in a quantitative conversion to [Cp^{BIG}Mn(CO)$_2$(η^1-P$_4$)] (**2**) (monitored by ^{31}P NMR spectroscopy; Scheme 4.1a). Only by using this stoichiometry the isolation of pure **2** is possible (33% yield). In contrast to the previously reported neutral η^1-P$_4$ complexes, **2** is stable not only in the solid state but also in solution, even in coordinating solvents like THF at room temperature. Due to the n-butyl groups of the Cp^{BIG} ligand, it has good solubility in all common organic solvents except acetonitrile.

Scheme 4.1. Synthesis of neutral $tetrahedro$-P$_4$ complexes **2** and **3** at r.t. in THF. a) + 5 equiv P$_4$; b) + 0.5 equiv P$_4$; c) + 1 equiv **1b**.
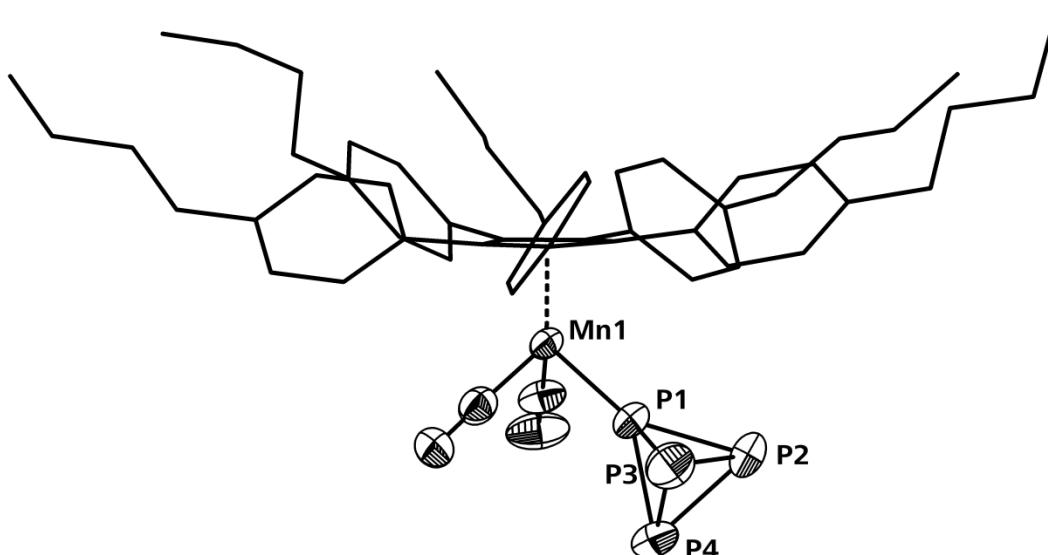
Figure 4.1.   Molecular structure of the neutral complex **2** in the crystal. For clarity reasons the Cp^{BIG} ligands are drawn in 'wire-or-stick' model, H atoms and solvent molecules are omitted; thermal ellipsoids drawn at 50% probability level.

The molecular structure of **2** (Figure 4.1) reveals the intact P₄ tetrahedron. The bonds between the apical and the basal P atoms (2.145(2) - 2.165(2) Å) are about 7 pm shorter than the basal bonds (2.211(4) - 2.232(2) Å). This behaviour was also observed for most of the P₄ units in the cationic complexes of group 8 elements[6a-f] and in the neutral tungsten complex of type **B**.[5] The ³¹P{¹H} NMR spectrum of **2** in toluene-d_8 at 253 K shows a quartet at 305.7 ppm and a doublet at 490.0 ppm with a $^1J_{PP}$ coupling constant of 224 Hz. At ambient temperature the signals broadened and the quartet splitting was no longer identifiable. The ¹³C{¹H} APT spectrum of **2** in toluene-d_8 at 298 K shows a broad signal of the carbonyls at 226.9, three signals in a ratio of 2:1:2 for the cyclopentadienyl carbon atoms (δ 104.6, δ 103.2, and δ 102.8, respectively) and several signals for each of the *n*-butylphenyl carbon atoms,[10] indicating the inequivalency of the five substituents of the ligand. Features of the ¹³C NMR (and of ¹H NMR, vide infra) suggest that the cyclopentadiene core does not freely rotate about the Cp-Mn axis, but each *n*-butylphenyl group freely rotate about the C_{ipso}-C_{Cp} bond. Based on the remarkable stability of **2** in solution, the question arises whether coordination of a second phosphorus atom is possible. Initial evidence of the existence of the neutral binuclear complex [{Cp^{BIG}Mn(CO)₂}₂(μ,η$^{1:1}$-P₄)] (**3**) appears if **1b** is reacted with an equimolar amount of white phosphorus at ambient temperatures (Scheme 4.1), which leads to a mixture of both complexes with **3** as the main component. The high stability of the products is also indicated by their successful chromatographic separation. Increasing the amount of P₄ shifts the ratio towards **2**, but the formation of the binuclear compound **3** is not totally suppressed until a fivefold excess of phosphorus is used. However, the reaction of **2**
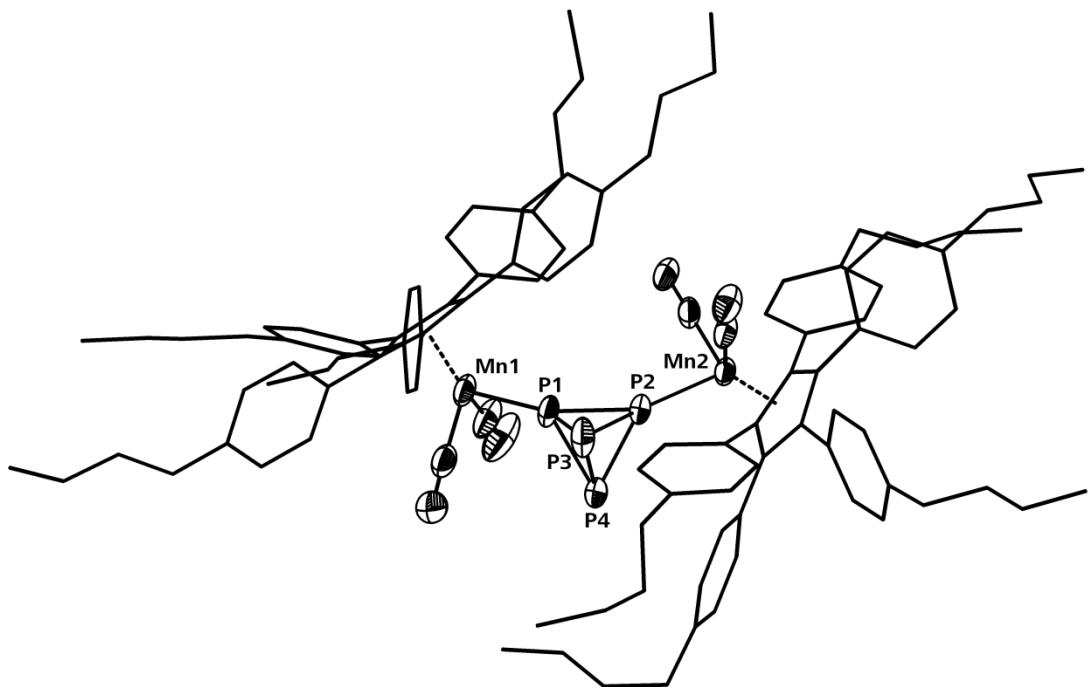
Figure 4.2. Molecular structure of the neutral complex 3 in the crystal. For clarity reasons the Cp^{BIG} ligands are drawn in 'wire-or-stick' model, H atoms are omitted and in case of disorder only the main part is shown; thermal ellipsoids drawn at 50% probability level.

with a second equivalent of **1b** leads to the formation of the bridging P$_4$ complex **3** in 44% isolated yield (Scheme 4.1c; Figure 4.2).

In comparison to the mononuclear complex **2** the formation of the binuclear complex **3** seems to be preferred. Caused by the 'encapsulation' of the reactive sites in **3** by the two Cp^{BIG} ligands a nucleophilic attack of a second P$_4$ tetrahedron at a manganese complex seems to be hindered.

In addition to the strong coordinative bonds of the P$_4$ ligand this moiety is encased by the two Cp^{BIG} ligands which enhance the stability of **3**. The Cp^{BIG} ligands are tilted against each other by an angle of 28.6(2)°.

In the molecular structure of **3** the P–P bond lengths show the same tendency as the cationic relatives.[6d-f] The shortest P–P bond is located between the coordinating P atoms (2.149(1) Å), the longest between the non-coordinating ones (2.247(3) Å). The other P–P distances lie between 2.187(2) and 2.200(2) Å. The Mn–P distances in **3** and **2** are identical within the experimental error, so one can assume that the second coordination of the P$_4$ tetrahedron is as strong as the first one.

The ^{31}P{^{1}H} NMR spectrum of **3** in toluene-d_8 at room temperature shows two broad signals with an integral ratio of 1:1. Upon cooling to 193 K the low field signal at −250.2 ppm sharpens into a triplet with a $^1J_{PP}$ coupling constant of 159 Hz. Though the signal at -478.7 ppm also gets sharper, it remains a broad triplet. The ^{1}H NMR spectrum of **3** in C$_6$D$_6$
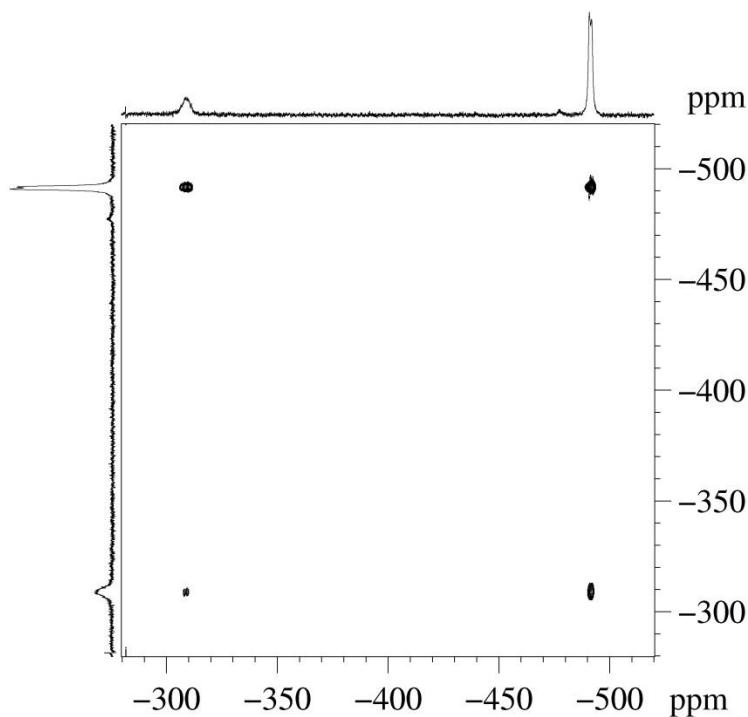
Figure 4.3. $^{31}P\{^1H\}$ EXSY spectrum of **2** (toluene-d_8, 298 K).

at 298 K shows several signals for each of the n-butylphenyl proton. Such a complex pattern seems to indicate that in this case only a limited number of the infinite possible rotamers are present. In fact, beside the conformers arising from hindered rotation about the Mn-Cp axis, the rotamers arising from hindered rotation about the Mn-P bond can be present in solution. In accordance with this view, the $^{13}C\{^1H\}$ APT spectrum of **2** in C_6D_6 at 298 K shows several signals not only for the cyclopentadienyl carbons, but also for the carbonyls.

In order to ascertain whether the P$_4$ ligand coordinated to Mn in **2** or **3** is subjected to a dynamic process like those observed for other P$_4$ complexes,[6h-i] the $^{31}P\{^1H\}$ EXSY and $^{31}P\{^1H\}$ NMR spectra were recorded in toluene-d_8 at various temperatures. The $^{31}P\{^1H\}$ EXSY spectrum of **2** at 298 K (Figure 4.3) shows intense cross peaks between the signals of the basal and coordinated P atoms, indicating that at this temperature the P$_4$ experiences the tumbling motion discussed above. At 183 K the same experiment did not show any exchange correlation, revealing that at this temperature the P$_4$ tumbling is slow on the NMR timescale. The $^{31}P\{^1H\}$ EXSY experiment carried out in the presence of free P$_4$ did not show any exchange peak between free and coordinated P$_4$, revealing that the mechanism responsible for P$_4$ motion is not dissociative.

An interesting feature observed recording VT $^{31}P\{^1H\}$ NMR spectra is that the signals are quite broad at 183 K, then they become sharper at 213 K, and then they progressively broaden again in the range between 233 and 313 K.[10] The broadening in the range between

233 and 313 K has been explained in terms of P$_4$ tumbling. A likely explanation for the broadening below 213 K can be a hindered rotation of the P$_4$ cage about the P-M axis. Activation parameters for the P$_4$ tumbling were calculated by line shape analysis in the range between 233 and 313 K. The values[10] are similar to those found for *trans*-[Ru(dppm)$_2$(H)(η^1-P$_4$)]BF$_4$ and *trans*-[Ru(dppe)$_2$(H)(η^1-P$_4$)]BF$_4$, and somehow different from those found for [CpRu(PPh$_3$)$_2$(η^1-P$_4$)]PF$_6$, [CpOs(PPh$_3$)$_2$(η^1-P$_4$)]PF$_6$, [Cp*Ru(dppe)(η^1-P$_4$)]PF$_6$, [(triphos)Re(CO)$_2$(η^1-P$_4$)]OTf.[6h-i]

Once the motions of the P$_4$ cage bonded to Mn were elucidated, we tried to gain insights about possible dynamics involving the Cp^{BIG} ligands. The ^{1}H NMR signals of **2**, which are broad already at 298 K, become even broader on lowering the temperature and, more interestingly, appear as the convolution of several quasi-isochronous signals. This evidence confirms that, in contrast to unsubstituted cyclopentadienyl ligands,[11] Cp^{BIG} does not freely rotate about the centroid of the Cp^{BIG}-Mn axis even at room temperature, and the ^{1}H NMR spectrum is the result of superimposition of all possible rotamers. Intrigued by this circumstance (*i.e.* the slow rotation, if any, of Cp^{BIG} at low T), we embarked on a heteronuclear Overhauser enhancement study recording ^{31}P-^{1}H HOESY spectra in toluene-*d$_8$* at various temperature. The detection of dipolar ^{31}P-^{1}H correlations[12] is a quite exhausting job, compared to the more common ^{1}H-^{1}H case, owing to the unfavourable γ_P/γ_H ratio.[13]
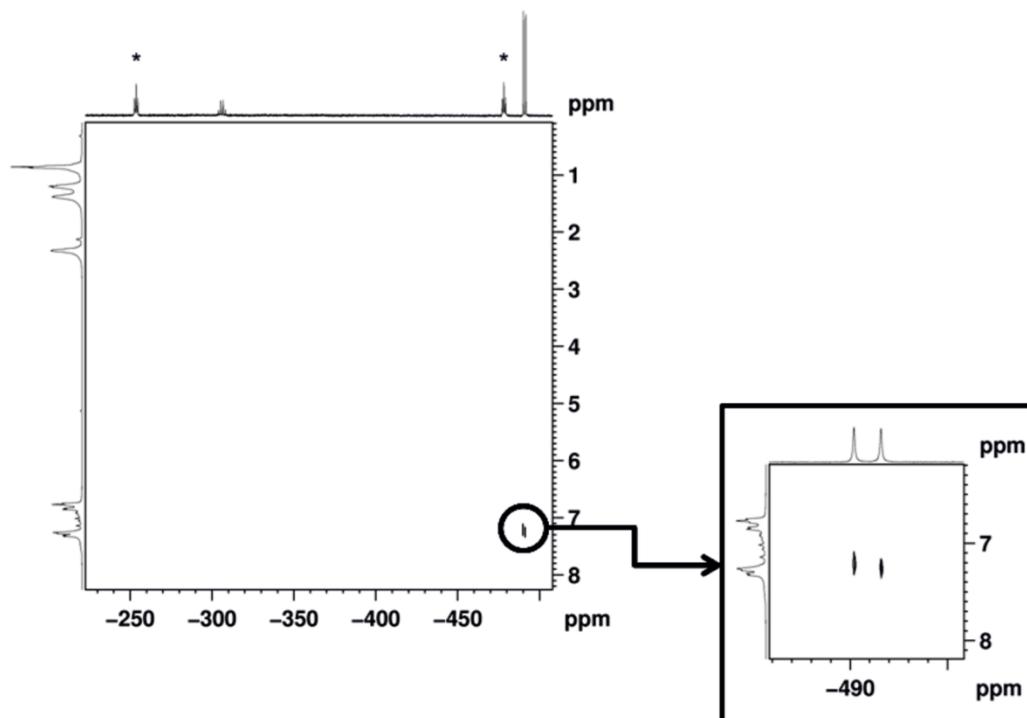
Figure 4.4. ^{31}P-^{1}H HOESY spectrum of **2** (in mixture with **3**) in toluene-*d$_8$* at 273 K showing the correlation between the basal P atoms of the P$_4$ cage and the *ortho* protons of Cp^{BIG}. With asterisks marked signals contain to **3**.

Despite these difficulties, the ^{31}P-^{1}H HOESY spectrum of **2** at 273 K in toluene-d_8 showed a heteronuclear NOE contact between the basal P atoms of the P$_4$ cage and the *ortho* H atoms of the Cp^{BIG} phenyls (Figure 4.4).[14] This result confirm that Cp^{BIG} is hindered in rotation while P$_4$ is rotating quickly and tumbling slowly (k = 80 s^{-1}). Moreover, these data indicate that the P$_4$ ligand does not exchange its position with that of the carbonyl ligands. The ^{31}P-^{1}H heteronuclear NOE contact was still observable at 283 K and vanished when the same experiment was carried out at 293 K.

As far as the dinuclear complex **3** is concerned, the ^{31}P{^{1}H} EXSY spectrum at 298 K[10] showed intense cross peaks between the signals of the coordinated and uncoordinated P atoms, indicating that at this temperature the cymantrene fragment hangs around the P$_4$ cage. The VT ^{31}P{^{1}H} NMR spectra showed the same trend observed for **2**, which means that the signals are quite broad at 183 K, become sharper until 253 K, and then progressively broaden again in the range 263-293 K,[10] suggesting that the same sequence of dynamic processes discussed for **2** occur, albeit at different temperatures.[10]

To get a better understanding on the surprising stability of complex **2**, DFT computations were carried out.[10] Thermodynamic characteristics for the gas phase complex formation for the three η^1-P$_4$ compounds **B$_w$** (tungsten complex of **B** with R = Cy) [CpMn(CO)$_2$(η^1-P$_4$)] (**4**) and **2** were obtained (Table 4.1, reactions 1-3). Complex formation enthalpy is only slightly exothermic in case of **B$_w$** (by -12 kJ mol^{-1}), but much more exothermic in case of **2** (by -69 kJ mol^{-1}) and **4** (by -93 kJ mol^{-1}), suggesting stronger Mn-P$_4$ bonding in the latter cases. The entropy disfavours the formation of all three complexes in the gas phase. Complexes **2** and **4** are predicted to be stable with respect to dissociation in solution, while for complexes **B$_w$** equilibrium dissociation is expected at room temperature. Processes of generation of **1b** via CO elimination and thf complex formation (reactions 4, 5) are highly endothermic (by about

Table 4.1. Theoretically predicted thermodynamic characteristics for the studied gaseous processes. Standard enthalpies $\Delta H°_{298}$ and Gibbs energies $\Delta G°_{298}$ are in kJ mol^{-1}, standard entropies $\Delta S°_{298}$ in J mol^{-1} K^{-1}.

Nr	Process	$\Delta H°_{298}$	$\Delta S°_{298}$	$\Delta G°_{298}$
1	[W(CO)$_3$(PCy$_3$)$_2$] + P$_4$ → **B$_w$**	-11.7	-184.2	43.2
2	[CpMn(CO)$_2$] + P$_4$ → **4**	-92.5	-140.9	-50.5
3	[Cp^{BIG}Mn(CO)$_2$] + P$_4$ → **2**	-69.1	-181.3	-15.0
4	[CpMn(CO)$_3$] + thf → [CpMn(CO)$_2$thf] + CO	133.2	-11.0	136.5
5	[Cp^{BIG}Mn(CO)$_3$] + thf → **1b** + CO	132.5	2.5	131.8
6	[CpMn(CO)$_2$thf] + P$_4$ → **4** + thf	3.0	21.8	-3.5
7	[Cp^{BIG}Mn(CO)$_2$thf] + P$_4$ → **2** + thf	2.1	16.1	-2.7

133 kJ mol^{-1}) and should proceed in non-equilibrium conditions (CO removal). Subsequent substitution of thf by P$_4$ (processes 6, 7) is almost thermoneutral and slightly favourable by entropy, making them exergonic by 3-4 kJ mol^{-1}. Note that both CO removal and thf substitution reactions do not depend on the bulkiness of the Cp^R ring (Cp vs Cp^{BIG}).

In summary, we have shown that the variation of the Cp^R substituents in the cymantrene complexes leads to a high Lewis acidity towards coordination of P$_4$ only in the case of [Cp^{BIG}Mn(CO)$_2$(thf)] (**1b**). The formed two neutral P$_4$ complexes **2** and **3** are remarkably stable in the solid state and especially in solution, a feature not observed yet for neutral P$_4$ complexes. Moreover, **3** is the first neutral complex with P$_4$ unit in a bridging η^1:η^1-coordination mode. The DFT calculations confirm the observed higher stability of the complexes in comparison to complexes of type **B**. Both **2** and **3** show fluxional behaviour in solution at room temperature due to the tumbling of the coordinated P$_4$. Moreover, at temperatures lower than 283 K the rotation of the Cp^{BIG} about the Mn-Cp axis is hindered and no position exchange between CO and P$_4$ occurs, as inferred by ^{31}P-^{1}H HOESY experiments. The introduction of the electronically and sterically special Cp^{BIG} ligand in main and transition metal chemistry opens up big perspectives for the stabilization of unprecedented compounds.

4.3 Experimental Part

General Remarks:

All experiments were carried out under an atmosphere of dry argon or nitrogen using glovebox and Schlenk techniques. Solvents were purified, dried and degassed prior to use. [(CO)$_5$MnBr] was available and Cp^{BIG}Na was prepared according to literature procedure.[15] The NMR spectra were measured on a Bruker Avance 300, 400 or 600 spectrometer. ESI-MS spectra were measured on a ThermoQuest Finnigan TSQ 7000 mass spectrometer and FD-MS spectra on a Finnigan MAT 95 mass spectrometer. The elemental analyses were determined on a Vario EL III apparatus. The IR spectra were measured on a VARIAN FTS-800 FT-IR spectrometer. For irradiations a TQ150-Z1 Hg lamp from Heraeus was used.

Synthesis of [Cp^{BIG}Mn(CO)$_3$] (1a):

A solution of 1.83 g (6.7 mmol) [(CO)$_5$MnBr] in 100 ml THF and 25 ml CH$_3$CN is heated to reflux for 2 h. To the reaction mixture a solution of 5.0 g (6.7 mmol) Cp^{BIG}Na in 50 ml THF is added and refluxed for further 16 h. After cooling the solution to room temperature the solvent is removed in vacuum. The residue is dissolved in CH$_2$Cl$_2$, filtered over celite and dried in vacuum. To remove [Mn$_2$(CO)$_{10}$] and Cp^{BIG}H impurities the solid is first cleaned by a column chromatography (silica gel, hexane/toluene 5:1) and subsequent reacted with 260 mg

(6.7 mmol) NaNH$_2$ in 50 ml THF. The suspension is dried in vacuum, triturated with hexane and filtered. Evaporation of the solvent gives pure **1a** (2.51 g, 43%).

1a: [C$_{58}$H$_{65}$MnO$_3$] calc.: C, 80.53; H, 7.57. Found: C, 80.27; H, 7.42. FD-MS (toluene): m/z (%) = 864 (100%, [M]$^+$), 727 (16%, Cp^{BIG}H$^+$). IR (toluene): ν$_{CO}$ [cm^{-1}] = 2011 (s), 1931 (s). ^{1}H NMR (C$_6$D$_6$): 0.78 (t, $^3J_{HH}$ = 7.3 Hz, 15H), 1.13 (m, 10H), 1.33 (m, 10H), 2.29 (t, $^3J_{HH}$ = 7.7 Hz, 10H), 6.76 (d, $^3J_{HH}$ = 8.2 Hz, 10H), 7.31 (d, $^3J_{HH}$ = 8.2 Hz, 10H).

Synthesis of [Cp^{BIG}Mn(CO)$_2$(η^1-P$_4$)] (2):

A solution of 120 mg (0.14 mmol) **1a** in 50 ml THF is irradiated for 10 min. The received red solution is added to a solution of 86 mg (0.69 mmol) P$_4$ in 25 ml THF and stirred for 1 h. The solvent is removed in vacuum. The crude product is purified by column chromatography (silica gel, hexane/toluene 5:1, -40 °C). Unreacted starting material **1a** is eluated first. Compound **2** can be collected as a second brown fraction (45 mg, 33%).[16]

2: IR (toluene): ν$_{CO}$ [cm^{-1}] = 1954 (s), 1901 (s). ^{1}H NMR (C$_6$D$_6$): 0.78 (br, 15H), 1.14 (br, 10H), 1.35 (br, 10H), 2.30 (br, 10H), 6.77 (br, 10H), 7.29 (br, 10H). ^{31}P{^{1}H} NMR (C$_6$D$_6$, 298 K): −490.3 (d-br, $^1J_{PP}$ = 209 Hz, 3P), −306.6 (m-br, 1P). ^{31}P{^{1}H} NMR (toluene-d$_8$, 253 K): −490.0 (d, $^1J_{PP}$ = 224 Hz, 3P), −305.7 (q, $^1J_{PP}$ = 224 Hz, 1P). ^{13}C{^{1}H} NMR (toluene-d$_8$, 298 K): see Table **S4.2** (Supplementary Information)

This reaction can also be monitored by IR spectroscopy. After about one hour reaction time the bands for **1b** (1921 and 1852 cm^{-1}) are completely vanished and two new CO stretch vibrations for **2** at 1954 and 1901 cm^{-1} can be observed.

Synthesis of [{Cp^{BIG}Mn(CO)$_2$}$_2$(μ-η^1:η^1-P$_4$)] (3):

A solution of 300 mg (0.35 mmol) **1a** in 50 ml THF is irradiated for 10 min. The received red solution is added to a solution of 17 mg (0.14 mmol) P$_4$ in 25 ml THF and stirred for 1 h. The solvent is removed in vacuum. The crude product is purified by column chromatography (silica gel, hexane/toluene 5:1, −40 °C). The first light yellow fraction is unreacted **1a** and the second brown fraction represents **3**. Evaporation of the solvent gives pure **3** (110 mg, 44%).

3: [C$_{114}$H$_{130}$Mn$_2$O$_4$P$_4$] calc.: C, 76.15; H, 7.29. Found: C, 76.26; H, 7.21. FD-MS (toluene): m/z (%) = 1798 (100%, [M]$^+$). IR (toluene): ν$_{CO}$ [cm^{-1}] = 1954 (s), 1901 (s). ^{1}H NMR (298 K, C$_6$D$_6$): 0.82 (t, $^3J_{HH}$ = 7.3 Hz, 30H), 1.19 (m, 20H), 1.39 (m, 20H), 2.33 (t, $^3J_{HH}$ = 7.9 Hz, 20H), 6.83 (d, $^3J_{HH}$ = 8.3 Hz, 20H), 7.27 (d, $^3J_{HH}$ = 8.3 Hz, 20H). ^{31}P{^{1}H} NMR (193 K, toluene-d_8): −478.6 (t, $^1J_{PP}$ = 159 Hz, 2P), −250.2 (t, $^1J_{PP}$ = 159 Hz, 2P). ^{13}C{^{1}H} NMR (193 K, toluene-d$_8$) 14.5, 23.1, 33.6, 35.7, 102.0, 129.9, 132.7, 142.0, 228.4.

4.4 Additional Notes

In multiple experiments for the synthesis of **1b** the irradiation step took significantly longer and often a quantitative transformation failed. Unfortunately, these observations were done after the results of chapter 4 were published.

By checking all variables of the reaction, we were able to empirically identify, that [Mn$_2$(CO)$_{10}$] catalyses the decarbonylation from **1a** to **1b**. However, this could not be proven for the unsubstituted cymantrene [CpMn(CO)$_3$] itself. The presence of [Mn$_2$(CO)$_{10}$] in the reaction mixture can be easily explained by unsuccessful column chromatographic workup of the preparation of **1a**. Because of the small amounts of [Mn$_2$(CO)$_{10}$], it was not detected or obscured by other signals in the IR spectra in solution. If pure solutions of **1a** are irradiated together with 5-10 mol% [Mn$_2$(CO)$_{10}$], a quantitative and fast (5-15 min) formation of **1b** is observed.

A possible mechanism might start with the photolytic cleavage of the Mn–Mn bond of [Mn$_2$(CO)$_{10}$] forming two 17 VE complex fragments {Mn(CO)$_5$}. One fragment could abstract a carbonyl moiety from **1a** resulting in the 16 VE fragment {Cp^{BIG}Mn(CO)$_2$} and the 19 VE fragment {Mn(CO)$_6$}. Complex **1b** is formed by addition of thf to {Cp^{BIG}Mn(CO)$_2$}. To complete the catalytic cycle one CO group is eliminated from {Mn(CO)$_6$}.
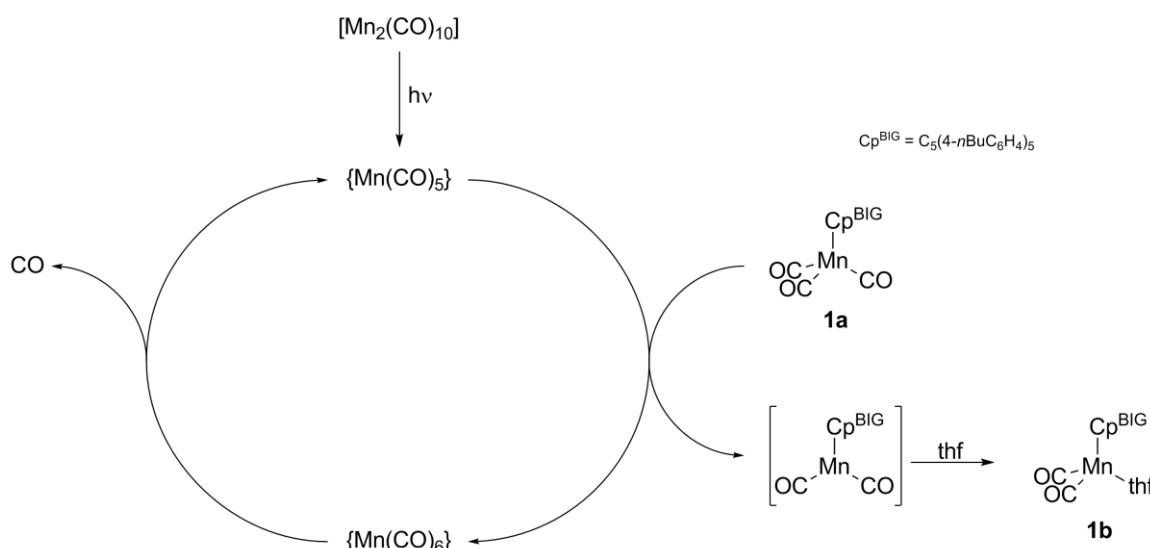
Figure 4.5. Proposed mechanism for the catalytical effect of [Mn$_2$(CO)$_{10}$] for the preparation of **1b**.

4.5 References

[1]   M. Scheer, G. Balazs, A. Seitz, *Chem. Rev.* **2010**, *110*, 4236-4256.

[2]   D. Tofan, C. C. Cummins, *Angew. Chem.* **2010**, *122*, 7678-7680; *Angew. Chem. Int. Ed.* **2010**, *49*, 7516–7518. For the reaction of P$_{red}$ with alkenes in alkaline media c.f.: a) A. V. Artem'ev, S. F. Malysheva, A. O. Korocheva, I. Y. Bagryanskaya, *Heteroat. Chem.* **2012**, *23*, 568-573. b) S. F. Malysheva, A. O. Korocheva, N. A. Belogorlova, A. V. Artem'ev, N. K. Gusarova, B. A. Trofimov, *Dokl. Chem.* **2012**, *445*, 164-165. c) S. F. Malysheva, V. A. Kuimov, A. V. Artem'ev, N. A. Belogorlova, A. I. Albanov, N. K. Gusarova, B. A. Trofimov, *Russ. Chem. Bull.* **2012**, *61*, 1787-1791.

[3]   a) B. M. Cossairt, N. A. Piro, C. C. Cummins, *Chem. Rev.* **2010**, *110*, 4164-4177; b) M. Caporali, L. Gonsalvi, A. Rossin, M. Peruzzini, *Chem. Rev.* **2010**, *110*, 4178-4235.

[4]   a) P. Dapporto, S. Midollini, L. Sacconi, *Angew. Chem.* **1979**, *91*, 510; *Angew. Chem. Int. Ed.* **1979**, *18*, 469.; b) P. Dapporto, L. Sacconi, P. Stoppioni, F. Zanobini, *Inorg. Chem.* **1981**, *20*, 3834-3839.

[5]   T. Groer, G. Baum, M. Scheer, *Organometallics* **1998**, *17*, 5916-5919.

[6]   a) I. de los Rios, J.-R. Hamon, P. Hamon, C. Lapinte, L. Toupet, A. Romerosa, M. Peruzzini, *Angew. Chem.* **2001**, *113*, 4028-4030; *Angew. Chem. Int. Ed.* **2001**, *40*, 3910-3912; b) M. Di Vaira, P. Frediani, S. S. Costantini, M. Peruzzini, P. Stoppioni, *Dalton Trans.* **2005**, 2234-2236; c) M. Di Vaira, M. Peruzzini, S. S. Costantini, P. Stoppioni, *J. Organomet. Chem.* **2006**, *691*, 3931-3937; d) P. Barbaro, V. M. Di, M. Peruzzini, S. S. Costantini, P. Stoppioni, *Chem. Eur. J.* **2007**, *13*, 6682-6690; e) M. Caporali, M. Di Vaira, M. Peruzzini, S. S. Costantini, P. Stoppioni, F. Zanobini, *Eur. J. Inorg. Chem.* **2010**, 152-158; f) M. Di Vaira, M. Peruzzini, S. S. Costantini, P. Stoppioni, *J. Organomet. Chem.* **2010**, *695*, 816-820; g) M. Peruzzini, L. Marvelli, A. Romerosa, R. Rossi, F. Vizza, F. Zanobini, *Eur. J. Inorg. Chem.* **1999**, 931-933; h) V. Mirabello, M. Caporali, V. Gallo, L. Gonsalvi, A. Ienco, M. Latronico, P. Mastrorilli, M. Peruzzini, *Dalton Trans.* **2011**, *40*, 9668-9671; i) V. Mirabello, M. Caporali, V. Gallo, L. Gonsalvi, D. Gudat, W. Frey, A. Ienco, M. Latronico, P. Mastrorilli, M. Peruzzini, *Chem. Eur. J.* **2012**, *18*, 11238–11250; j) P. Barbaro, M. Di Vaira, M. Peruzzini, S. S. Costantini, P. Stoppioni, *Chem. Eur. J.* **2007**, *13*, 6682-6690.

[7]   There is one neutral example described [Cl(PPh$_3$)$_2$Ru(μ-Cl)$_3$Ru(PPh$_3$)$_2$(η^1-P$_4$)] revealing high Lewis-acidity, based on the numerous Cl ligands cf.: M. Peruzzini, S. Manas, A. Romerosa, A. Vacca, *Mendeleev Commun.* **2000**, 134-135.

[8]   a) M. Scheer, E. Herrmann *Z. Chem.* **1990**, *30*, 41 – 55. b) O. J. Scherer, *Acc. Chem. Res.* **1999**, *32*, 751 – 762

[9]   L. D. Field, T. He, P. Humphrey, A. F. Masters, P. Turner, *Polyhedron* **2006**, *25*, 1498-1506.

[10]   Cf.: supplementary information for details on NMR investigations and computations.

[11]   J. Okuda, in Transition Metal Coordination Chemistry, Topics in Current Chemistry, Vol. 160, Ed. W. A. Herrmann **1992**, 97-145.

[12]   M. Latronico, F. Polini, V. Gallo, P. Mastrorilli, B. Calmuschi-Cula, U. Englert, N. Re, T. Repo, M. Räisänen, *Inorg. Chem.* **2008**, *47*, 9779-9796.

[13]   It is known that at a constant internuclear distance in H-X pairs, the heteronuclear dipolar coupling reduces proportionally to coefficient k, calculated via the equation $k = 0.44(v_X/v_H)^2 I_X(I_X+1)$ where v_X and v_H are the NMR frequencies of X and H nuclei, respectively, and I_X is the spin of X nuclei: V. I. Bakhmutov, Practical NMR relaxation for chemists, 2004, John Wiley & Sons Ldt, Chichester, England.

[14]   On the basis of the interatomic distances observed in the solid state a correlation between the apical P of the cage and the *ortho* H atoms of the Cp^{BIG} phenyls should be also expected to emerge in the ^{31}P-^{1}H HOESY spectrum of a toluene-d_8 solution of **2** at 273 K. However, the corresponding cross peak is missing, most likely due to the lower intensity of the signal of the apical P atom.

[15]   a) G. Dyker, J. Heiermann, M. Miura, J.I. Inoh, S. Pivsa-Art, T. Satoh, M. Nomura, *Chem. Eur. J.* **2000**,   *6*, 3426-3433. b) S. Harder, C. Ruspic, *J. Organomet. Chem.* **2009**, *694*, 1180-1184. c) R. Zhang, M.   Tsutsui, D. E. Bergbreiter, *J.Organomet. Chem.* **1982**, *229*, 109-112.

[16]   Sometimes the formation of **3** is not totally suppressed. Unfortunately, **2** and **3** elute together from the column chromatography.

4.6 Supplementary Information

Table S4.1. CO stretching frequencies of selected complexes for comparison

Compound	v_{CO} / cm^{-1}	Solvent	Ref.
[CpMn(CO)$_3$]	2028, 1947	*n*-Heptane	[1]
[CpMn(CO)$_2$(thf)]	1930, 1854	THF	[2]
[C$_5$Me$_5$Mn(CO)$_3$]	2017, 1928	*n*-Pentane/*n*-Hexane	[3]
[C$_5$Me$_5$Mn(CO)$_2$(thf)]	1910, 1836	THF	[2]
[C$_5$Cl$_5$Mn(CO)$_3$]	2048, 1982	*cyclo*-Hexane	[4]
[Cp^{BIG}Mn(CO)$_3$] (**1a**)	2011, 1931	THF	this work
[Cp^{BIG}Mn(CO)$_2$(thf)] (**1b**)	1921, 1852	THF	this work
[Cp^{BIG}Mn(CO)$_2$(η^1-P$_4$)] (**2**)	1954, 1901	THF	this work
[{Cp^{BIG}Mn(CO)$_2$}$_2$(μ-η^1:η^1-P$_4$)] (**3**)	1954, 1901	THF	this work

Crystallographic Details:

The crystal structure analyses were performed either on an Oxford Diffraction Gemini R Ultra CCD diffractometer (**1a**) or an Oxford Diffraction SuperNova diffractometer (**2**, **3**). For all compounds an analytical absorption correction was carried out.[5] The structures were solved by direct methods either of the program SIR-92[6] or SHELXS-97[7] and refined with the least square method on F^2 employing SHELXL-97[8] with anisotropic displacements for non-H atoms. Hydrogen atoms were located in idealized positions and refined isotropically according to the riding model.

CCDC-943752 (**1a**), CCDC-943753 (**2**) and CCDC-943754 (**3**) contain the supplementary crystallographic data for this paper. These data can be obtained free of charge at www.ccdc.cam.ac.uk/conts/retrieving.html (or from the Cambridge Crystallographic Data Centre, 12 Union Road, Cambridge CB2 1EZ, UK; Fax: + 44-1223-336-033; e-mail: deposit@ccdc.cam.ac.uk).

Crystal data for **1a**: C$_{58}$H$_{65}$MnO$_3$, M = 865.08 g/mol, space group $P2_1/c$ (no.14), a = 13.8586(2) Å, b = 17.1339(3) Å, c = 20.5198(4) Å, β = 98.730(2)°, V = 4816.0(2) Å^3, Z = 4, μ = 2.557 mm^{-1}, $F(000)$ = 1848, T = 123.0(1) K, 17715 reflections measured, 8643 unique (R_{int} = 0.0312), R_1 = 0.0590, wR_2 = 0.1218 for I > 2σ(I); CCDC-943752.

Crystal data for **2** · 0.125 C$_6$H$_{14}$: C$_{57.75}$H$_{66.75}$MnO$_2$P$_4$, M = 971.68 g/mol, space group $P\bar{1}$ (no.2), a = 13.687(1) Å, b = 14.373(1) Å, c = 16.140(1) Å, α = 65.544(7)°, β = 73.724(5)°, γ = 67.197(7)°, V = 2637.0(3) Å^3, Z = 2, μ = 3.486 mm^{-1}, F(000) = 1029, T = 123.0(2) K, 16526 reflections measured, 9974 unique (R_{int} = 0.0502), R_1 = 0.1062, wR_2 = 0.2444 for I > 2σ(I); CCDC-943753.

Crystal data for **3**: C$_{114}$H$_{130}$Mn$_2$O$_4$P$_4$, M = 1797.95 g/mol, space group $P2_1$/c (no.14), a = 26.4442(3) Å, b = 20.4404(4) Å, c = 19.6798(3) Å, β = 107.687(2)°, V = 10134.7(3) Å^3, Z = 4, μ = 3.010 mm^{-1}, F(000) = 3824, T = 123.0(1) K, 36724 reflections measured, 19629 unique (R_{int} = 0.0223), R_1 = 0.0744, wR_2 = 0.1879 for I > 2σ(I); CCDC-943754

NMR Investigations:

Table S4.2. ^{13}C NMR data of **2**.

	Chemical shift (ppm)
-CH$_2$CH$_2$CH$_2$**C**H$_3$	14.11
-CH$_2$CH$_2$**C**H$_2$CH$_3$	22.71
-CH$_2$CH$_2$**C**H$_2$CH$_3$	22.75
-CH$_2$**C**H$_2$CH$_2$CH$_3$	33.32
-CH$_2$**C**H$_2$CH$_2$CH$_3$	33.40
-**C**H$_2$CH$_2$CH$_2$CH$_3$	35.51
-**C**H$_2$CH$_2$CH$_2$CH$_3$	35.53
Cp	102.11
Cp	102.51
Cp	103.93
CH	127.90
CH	128.00
C	129.65
C	130.50
CH	132.80
CH	133.02
C	142.12
C	142.37
CO	226.24
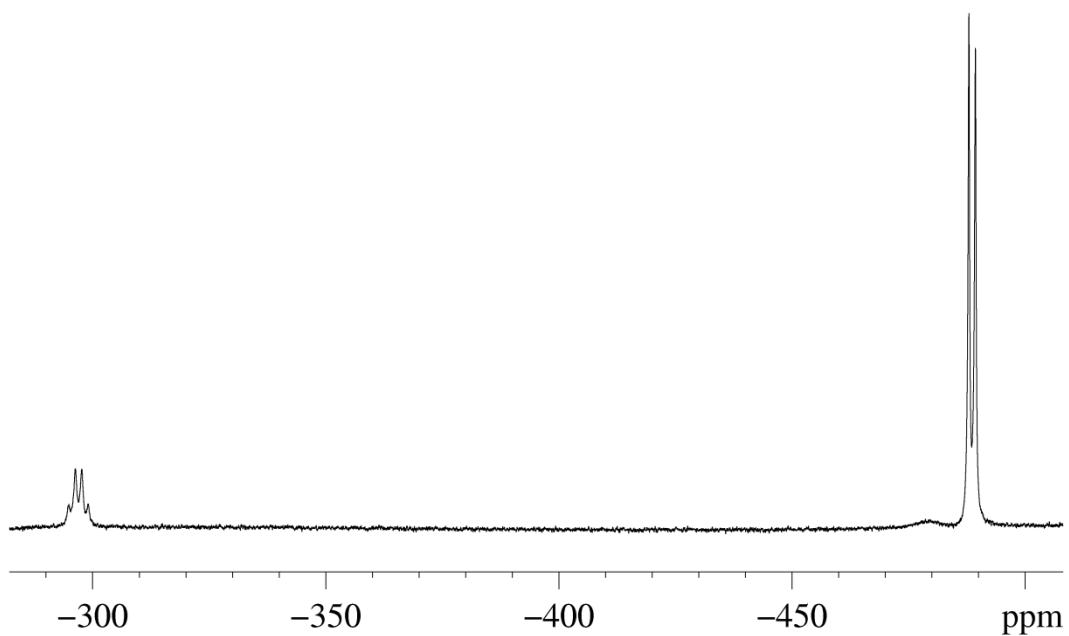
Figure S4.1. ^{31}P{^{1}H} NMR spectrum of **2** (Toluene-d_8, 183 K).
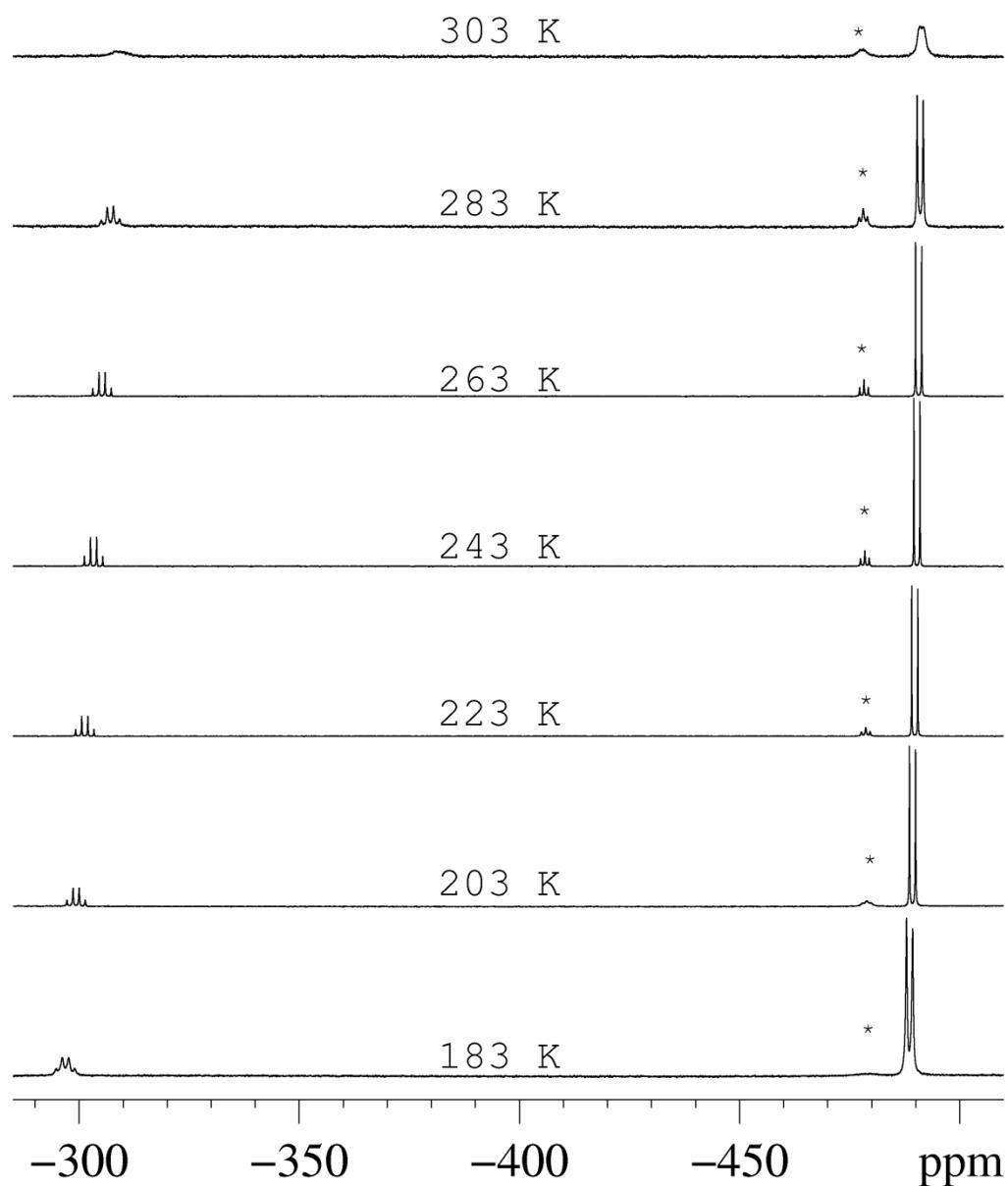
Figure S4.2. VT ^{31}P{^{1}H} NMR spectrum of **2** (toluene-d_8). Asterisked peaks are due to **3**.
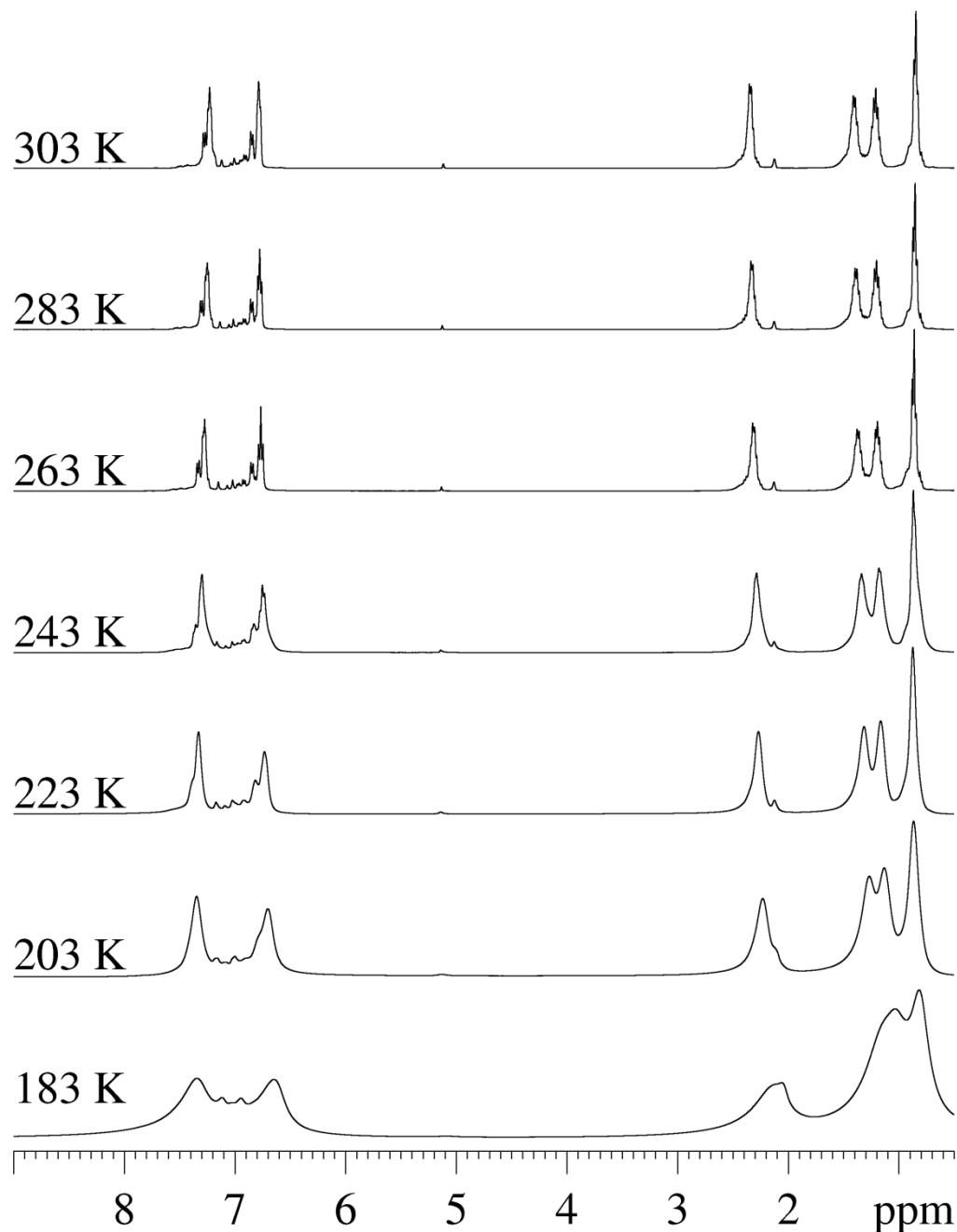
Figure S4.3. VT ^{1}H NMR spectrum of **2** (toluene-d_8). Asterisked peaks are due to **3**.
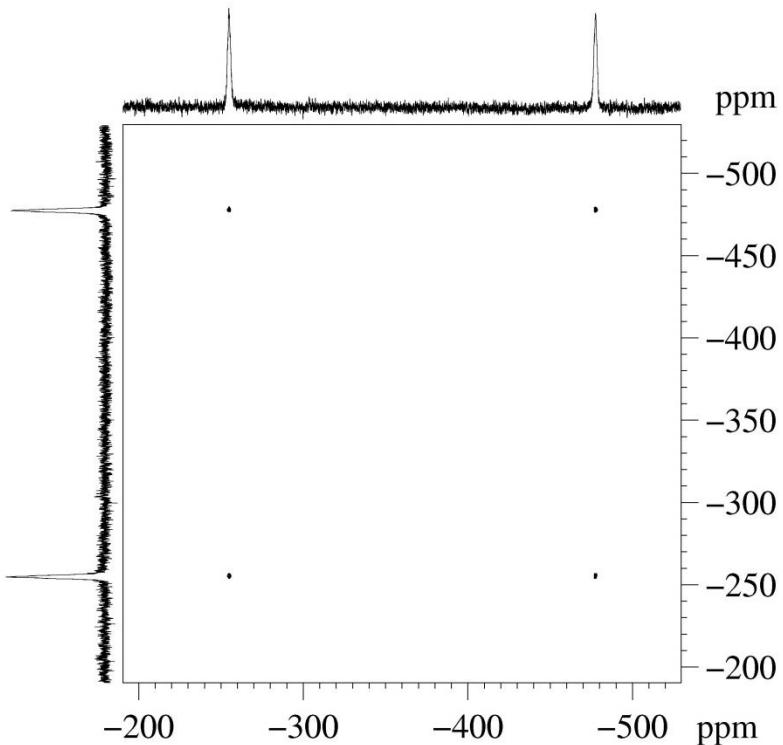
Figure S4.4. ^{31}P{^{1}H} EXSY spectrum of **3** (C$_6$D$_6$, 298 K).
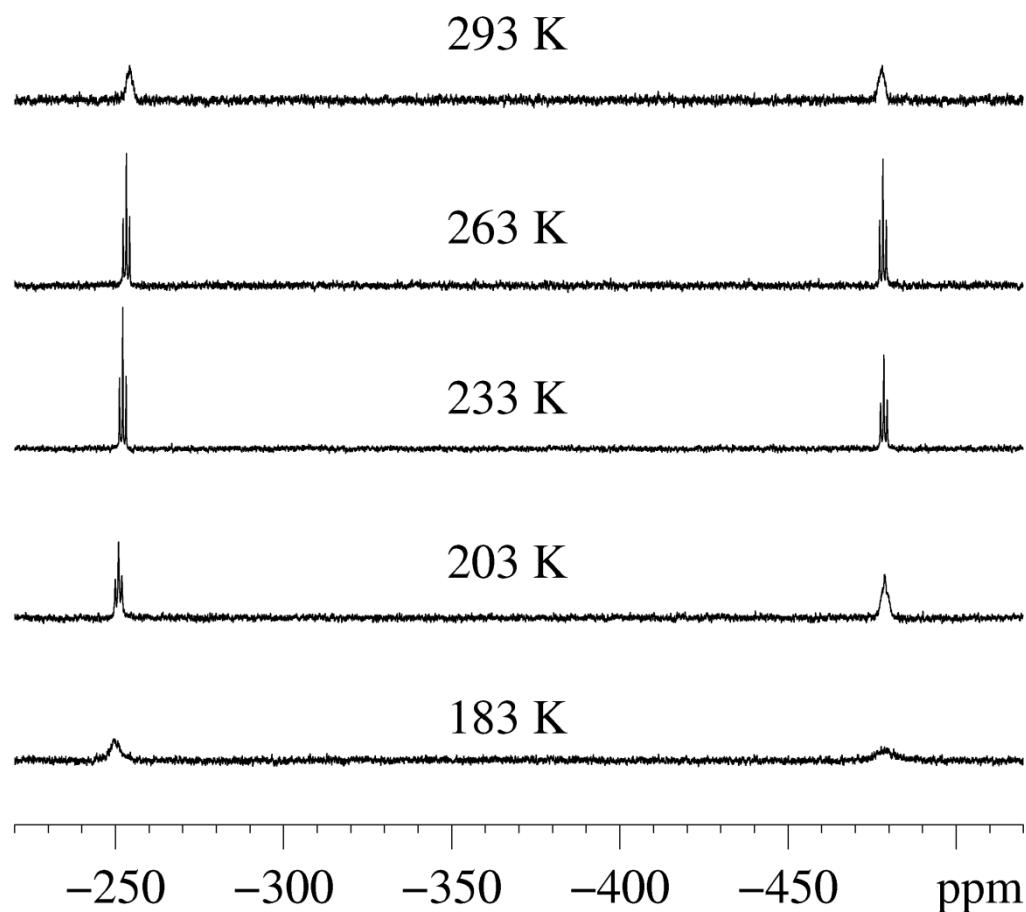
Figure S4.5. VT ^{31}P{^{1}H} NMR spectrum of **3** (toluene-d_8)

Computational details:

The DFT calculations have been performed by using the standard Gaussian 03 program suite[9]. B3LYP functional[10] has been used together with standard all electron 6-31G* basis set. Effective core potential basis set LANL2DZ[11] was used for W atoms. All structures were fully optimised with subsequent vibrational analysis and correspond to minima on their respective potential energy surfaces.

Table S4.3. Total energies E°$_0$, sum of electronic and thermal enthalpies H°$_{298}$ (Hartree) and standard entropies S°$_{298}$ (cal mol^{-1}K^{-1}) for studied compounds. B3LYP/6-31G* (ECP on W) level of theory.

Compound	E°$_0$	H°$_{298}$	S°$_{298}$
CO	-113.3069138	-113.298573	47.235
thf	-232.4456568	-232.322313	71.054
P$_4$	-1365.431338	-1365.419749	66.903
As$_4$	-8933.739612	-8933.729448	78.26
[W(CO)$_3$(PCy$_3$)$_2$)]	-2502.224171	-2501.173152	282.766
[W(CO)$_3$(PCy$_3$)$_2$)(η^1-P$_4$)]	-3867.663547	-3866.597368	305.652
[W(CO)$_3$(PCy$_3$)$_2$)(η^1-As$_4$)]	-11435.97423	-11434.90952	317.386
[CpMn(CO)$_3$]	-1684.493671	-1684.370119	106.697
[CpMn(CO)$_2$thf]	-1803.581457	-1803.343107	127.897
[CpMn(CO)$_2$]	-1571.096354	-1570.984429	95.721
[CpMn(CO)$_2$(η^1-P$_4$)]	-2936.565579	-2936.439407	128.946
[CpMn(CO)$_2$(η^1-As$_4$)]	-10504.87413	-10504.74954	141.712
[Cp^{BIG}Mn(CO)$_3$]	-3626.013107	-3624.863168	370.185
[Cp^{BIG}Mn(CO)$_2$thf]	-3745.100731	-3743.836438	394.595
[Cp^{BIG}Mn(CO)$_2$]	-3512.625035	-3511.487011	370.713
[Cp^{BIG}Mn(CO)$_2$(η^1-P$_4$)]	-4878.085295	-4876.933076	394.284
[Cp^{BIG}Mn(CO)$_2$(η^1-As$_4$)]	-12446.39556	-12445.24486	407.797

Table S4.4. Optimized geometries (xyz coordinates in Å) for studied compounds at the B3LYP/6-31G* (ECP on W) level of theory.

[CpMn(CO)$_2$]

Atom	x	y	z	Atom	x	y	z
Mn	-0.9069410171	-0.0126875229	0.9930187031	C	-2.2499476813	-0.7651736329	1.8947991126
O	-3.1942296305	-1.2303250469	2.3850628223	C	-0.6184364044	1.3062033399	2.1593711387
O	-0.4594802824	2.2417702675	2.8285795958	C	0.1004313457	0.8882591991	-0.6838787329
H	0.9978581358	1.4906783259	-0.6473816005	C	-1.2504421331	1.3664185131	-0.5733702615
H	0.8892932578	-1.1776416547	-0.973666318	C	-2.1248888615	0.2572364982	-0.7149688966
H	-1.548771992	2.396014042	-0.4275323473	C	-1.3253107337	-0.9202562338	-0.9148113346
H	-3.2059147448	0.2939911166	-0.695917302	C	0.0348023151	-0.5147236616	-0.8896890954
H	-1.6933770745	-1.9231397214	-1.0832436078				

[CpMn(CO)$_3$]

Atom	x	y	z	Atom	x	y	z
C	-1.054562699	-1.033076364	-1.093554731	C	1.69739633	-1.217660873	0.16914072
C	-1.036098038	1.477726925	-0.357389749	H	1.70252371	-2.28977293	0.30983504
H	1.730545641	2.001696116	1.111547704	C	1.7043426	-0.232335787	1.19740245
C	1.714397131	1.052512072	0.593411963	O	-1.62147733	-1.731889672	-1.82114117
C	1.724252258	0.864368094	-0.825880286	O	-1.59007387	2.466198523	-0.59272919

				Atom	x	y	z
H	1.69308293	-0.429921946	2.261465508	Mn	-0.08393567	0.003020335	-0.00246995
H	1.742138444	1.648423797	-1.571052958	C	-1.06958777	-0.420338992	1.43082083
C	1.715919654	-0.529205913	-1.082750142	O	-1.64665828	-0.707407669	2.3917618
H	1.719419952	-0.993077821	-2.060384296				

[CpMn(CO)$_2$thf]

Atom	x	y	z	Atom	x	y	z
C	-0.600527461	0.559665988	2.405435162	Mn	-1.18440638	-0.220219282	0.92426446
H	0.731489798	-0.333873233	-1.217097727	C	-0.22394541	-1.688249519	1.1680221
C	-0.204191874	0.130084462	-0.933791691	O	0.47676494	-2.618690237	1.2365175
C	-0.347681273	1.359091226	-0.240975249	O	-2.93210752	-1.008717066	1.79435292
H	-1.742897637	-1.279271363	-1.774519286	C	-3.53296774	-2.168902249	1.17707288
H	0.458563632	1.997170841	0.096129886	C	-4.72006829	-2.534485104	2.08267857
C	-1.750899477	1.627486353	-0.096478714	C	-4.36747354	-1.880703215	3.44913817
H	-2.191641621	2.497435841	0.371199038	C	-2.98326164	-1.264047199	3.21667261
C	-2.449529336	0.556735619	-0.703011722	H	-2.78425929	-2.970413102	1.13559698
H	-3.52756295	0.450138286	-0.723636656	H	-3.81000843	-1.889981346	0.16025604
C	-1.514978193	-0.376986853	-1.223077144	H	-5.65539814	-2.127974867	1.68794999
O	-0.152831506	1.153084379	3.304196628	H	-4.83550808	-3.619538794	2.1563942
H	-2.17380706	-1.958323881	3.478682618	H	-4.34756424	-2.604231893	4.26891741
H	-2.813998747	-0.312879141	3.721084462	H	-5.09615342	-1.10653725	3.70552064

[CpMn(CO)$_2$(η^1-P$_4$)]

Atom	x	y	z	Atom	x	y	z
Mn	-0.813635677	-0.298134342	0.860692574	H	0.40272148	2.121731331	-0.25728912
P	1.06359138	1.339286858	1.43055117	H	-2.25627908	2.124661716	0.24530094
P	3.228083012	-1.060910376	1.62472926	H	-3.27542277	-0.198338518	-0.64248145
P	2.374448441	-3.006824302	0.881743608	C	-1.86937047	-1.584820533	1.50073581
P	2.10295419	-2.405260497	3.028236276	C	-0.8829518	0.664243617	2.36029635
O	-2.626857325	-2.395173815	1.841312781	C	0.02288538	0.089445803	-1.11375007
O	-0.976916102	1.366719841	3.279071899	C	-0.29058842	1.322639654	-0.48136981
H	1.008534632	-0.218518972	-1.439393588	C	-1.69715555	1.323413285	-0.21959854
H	-1.253285302	-1.652932686	-1.699839469	C	-2.23539276	0.096573225	-0.68845349
C	-1.16724401	-0.675596368	-1.245033816				

CpMn(CO)$_2$(η^1-As$_4$)]

Atom	x	y	z	Atom	x	y	z
Mn	-0.713521439	-0.067200787	0.889228778	C	-1.71287033	-0.553866713	-0.97265051
C	-1.965053676	-0.702415512	1.989509223	H	-2.27130266	-1.459467692	-1.16629723
C	-0.023662064	1.032182846	2.112280323	C	-0.334284	-0.341568379	-1.24185603
H	0.982780566	1.445691627	-0.961111999	O	-2.85233936	-1.073640304	2.63915711
C	0.009720055	0.983973864	-0.864029605	O	0.39622294	1.828837614	2.84451396
C	-1.175562773	1.604979125	-0.355876852	As	0.78726491	-1.780648219	1.36683264
H	0.345801452	-1.074037552	-1.657976206	As	3.10207098	-2.474783279	1.06497178
H	-1.255160053	2.621950317	0.004890852	As	1.24260027	-4.136155642	0.94739596
C	-2.233148375	0.660833783	-0.422520734	As	1.83664175	-3.079713472	3.12470414
H	-3.257842149	0.83405507	-0.121333303				

[W(CO)$_3$(PCy$_3$)$_2$]

Atom	x	y	z	Atom	x	y	z
W	0.1027850359	0.1452010823	0.1906058759	H	5.6168636559	4.3059887354	-2.4881360409
P	-2.436857313	0.1374616756	0.0064123226	H	5.2406192327	0.0973563752	-1.6013934778
P	2.597948435	-0.092698923	-0.0625416688	H	2.1622751018	2.8823529966	-0.3103635465
O	0.1958143444	2.0431853854	2.6472286794	H	6.023640136	0.0344325391	2.9697283853
O	0.0613927568	2.5315013603	-1.9336422953	H	5.023797911	-2.4288976	3.027434197
O	-0.0822152863	-2.5253310559	1.9448391435	H	3.6142841467	-0.3774537233	4.8194402337
H	-4.2929756445	-1.8579843919	-3.6724146959	H	2.2217009832	-1.2051233341	2.773853904

Atom	x	y	z	Atom	x	y	z
H	-4.2924769214	-3.6661093652	-1.7149896979	H	3.1813666248	1.1541105965	2.649129177
H	-1.6959102874	-3.4529444835	-3.3341008086	H	4.6635972193	-0.9214193619	0.9468484451
H	-1.5415550191	-2.6405139245	-0.8259347428	H	5.2701686298	1.2626360132	3.9821393858
H	-1.5590011351	-0.8412807573	-2.7177154493	H	3.6587653455	-2.7442656832	4.0956035685
H	-4.1827460212	-1.1365571936	-1.171343226	H	5.2371656984	-1.0212081943	5.0634439384
H	-2.8432869871	-1.6991405079	-4.6579828876	H	2.8550350945	-2.5012639388	1.7818204507
H	-2.8454366318	-4.6443614936	-1.4909663403	H	4.5729533524	1.4844480035	1.6271912066
H	-3.232927322	-4.0803296358	-3.9208814371	C	-0.000254771	-1.529853679	1.3392351727
H	-2.9427044891	-2.8311230437	0.2082306255	C	0.0939453119	1.6798714201	-1.1327226602
H	-3.0034758522	0.1241379451	-2.9752794464	C	0.1453512903	1.3235573694	1.7126787404
H	-5.9920603065	0.3368955095	2.8489918437	C	-3.1377686672	1.7508756788	-0.7150587564
H	-3.7808400413	0.4477469805	4.3258757522	C	-3.5165198794	-0.0735718471	1.5725052844
H	-4.8432912755	-2.3672260856	3.7286877997	C	-3.0865017769	-1.166243357	-1.2088016278
H	-2.5295800711	-1.7337880162	2.5732771704	C	3.5024507421	1.2988502719	-0.9948104825
H	-4.6975197877	-1.8486772294	1.1375048768	C	2.8228386106	-1.476121213	-1.3556061175
H	-3.7393981147	0.9694461862	1.8392403088	C	3.737658749	-0.5271686349	1.3939359053
H	-6.6774559237	-1.2461967184	2.4935877127	C	-3.1952282041	-1.9239170329	-3.6427885899
H	-3.0826607808	-1.0664079293	4.8900574334	C	-3.1949034924	-3.6471767301	-1.787857122
H	-5.6045576802	-1.1730037643	4.7766178145	C	-2.7870802362	-3.3467582075	-3.237108283
H	-1.8259461997	-0.1651348038	2.9356367635	C	-2.6392504083	-2.5914015259	-0.8170924701
H	-5.4332207386	-0.3677541688	0.5398851241	C	-2.6574475463	-0.8667432273	-2.6617334136
H	-4.4856406404	3.1102963356	-2.7647830852	C	-5.7306654113	-0.7140227476	2.6548683108
H	-2.5311881781	4.3955378881	-1.4602714168	C	-3.6287464211	-0.6079592675	4.0558195004
H	-5.2674715525	4.3478546326	-0.0700981524	C	-4.9926992607	-1.2866468504	3.872490197
H	-3.343822953	2.9325698322	1.1032268595	C	-2.7748284401	-0.6839341815	2.7783822203
H	-5.2370506804	1.7107634062	-0.1459019497	C	-4.8722065342	-0.7917176537	1.3782791259
H	-2.5774130128	1.861217302	-1.6529961683	C	-5.0134856398	3.0783344663	-1.800230364
H	-6.0869180503	3.0791773584	-2.0310227756	C	-3.1625796	4.2905666295	-0.5664623008
H	-2.9306437802	5.1450383687	0.082067921	C	-4.6421851954	4.3182833208	-0.9750691951
H	-4.8671767518	5.2324174029	-1.5394261199	C	-2.7919668425	2.9818185515	0.1535251433
H	-1.7296386357	2.9856725454	0.4108312698	C	-4.6408457934	1.7761849252	-1.0660199325
H	-4.9216954833	0.9171756239	-1.6865691451	C	3.0285880373	-3.9448568006	-1.948774596
H	3.9537440494	-3.7780392072	-2.5202658062	C	1.6727661536	-2.4262997369	-3.4482871387
H	2.52728446	-2.1950463397	-4.1009885849	C	1.8245019863	-3.8490160529	-2.8950933119
H	0.9109628479	-4.1268860081	-2.34840735	C	1.6206168553	-1.3772022917	-2.3241332511
H	0.6894205097	-1.5405444947	-1.7411988011	C	2.9408979713	-2.9122116009	-0.8098178244
H	2.0677565311	-3.1448605127	-0.1856030761	C	3.7658351556	3.7767492181	-1.4700068176
H	3.7371572354	-1.2662229337	-1.9272711591	C	5.5697305346	2.1518093111	-2.2039951699
H	3.1010261655	-4.9541896589	-1.5243917827	C	5.2653100844	3.5836419071	-1.7402682079
H	0.7738398471	-2.3470838606	-4.0729911966	C	5.0185192951	1.1015406509	-1.220526828
H	1.9259040323	-4.5668517397	-3.7187267018	C	3.2303575044	2.7300459761	-0.4778155181
H	1.5500512548	-0.3754227967	-2.7613783848	C	5.0614076537	0.360201143	3.3933372752
H	3.8242315344	-3.0039629148	-0.1685516464	C	4.1175207179	-1.9772081949	3.4588675112
H	3.2073396343	3.6971330813	-2.4141370434	C	4.5045612513	-0.7499193482	4.2924314186
H	5.1187434711	1.9869986495	-3.193846886	C	3.1417235974	-1.6019259171	2.3300199752
H	5.8277447257	3.7909167489	-0.8175406593	C	4.1022184343	0.714644545	2.2420165995
H	5.5523673483	1.195038667	-0.2658651299	H	3.5765506268	4.7851062929	-1.0805630443
H	3.7187539917	2.8826573651	0.4915280729	H	6.6516622259	2.0115126138	-2.3270559777
H	3.0177225367	1.2340630091	-1.9821258585				

[W(CO)$_3$(PCy$_3$)$_2$(η^1-P$_4$)]

Atom	x	y	z	Atom	x	y	z
W	-0.42606	0.01931	1.22202	H	-1.84365	-4.41153	6.19968
P	-0.26361	0.19457	-1.37031	H	1.82092	-4.76486	3.9319
P	-0.19228	-0.15485	3.81549	H	0.2261	-5.73265	5.63318
P	-1.76352	-2.11928	1.09901	H	1.81014	-2.31685	3.52489
P	-1.85488	-4.32786	1.19229	H	-1.84569	-1.9608	5.82683
P	-3.25827	-3.1936	-0.12638	H	4.20734	1.0025	4.22658
P	-3.48354	-3.08332	2.09121	H	3.38347	0.12018	6.59017
O	0.57539	2.99067	1.42398	H	3.02187	3.1257	6.0955
O	2.61049	-0.99289	1.26766	H	0.80144	1.72854	6.24252
O	-3.20415	1.59504	1.21393	H	1.59681	2.57236	3.8838
H	2.59287	-2.44886	-3.68303	H	2.10537	-0.37944	4.45293
H	0.14201	-3.03451	-4.58165	H	4.05988	2.72211	3.87871
H	1.08008	-4.61756	-2.12929	H	2.72386	1.28816	7.73229
H	-0.90468	-2.87881	-1.70434	H	4.55739	2.29053	6.31594
H	1.42622	-2.3579	-0.84856	H	0.90153	0.02175	6.64308
H	0.62307	-0.83636	-3.37487	H	2.27544	1.40286	2.76686
H	3.19249	-3.34366	-2.28924	H	-2.19902	2.87971	6.55036

Atom	x	y	z	Atom	x	y	z
H	-0.76818	-4.28511	-3.74087	H	-3.79334	0.7439	6.48856
H	1.71095	-4.76643	-3.76713	H	-4.20882	2.7831	4.23628
H	-1.55332	-2.02937	-3.09874	H	-3.21554	0.47132	3.49135
H	2.41051	-1.10638	-1.57696	H	-1.66155	2.5002	3.5538
H	-2.92327	2.66213	-4.09684	H	-1.30181	0.53709	5.87958
H	-4.42982	1.77375	-2.07847	H	-2.3999	4.10014	5.29596
H	-4.25349	-0.06658	-4.52888	H	-4.99598	0.64646	5.2051
H	-3.09687	-0.96831	-2.3369	H	-4.59539	3.02835	5.93918
H	-1.59609	-0.09454	-4.27772	H	-3.07094	-0.80777	4.6768
H	-1.92069	1.81188	-1.90177	H	-0.44678	2.65875	4.80778
H	-2.79713	1.66175	-5.54065	C	-2.21983	0.96682	1.23221
H	-5.25495	0.2321	-2.28314	C	1.48549	-0.68844	1.22419
H	-5.07295	1.49106	-4.46403	C	0.25264	1.86521	1.34824
H	-3.2319	-0.02485	-0.86371	C	1.03297	1.55331	-1.79409
H	-0.77233	1.44872	-4.1197	C	-1.81051	0.79415	-2.30101
H	3.69528	2.30881	-2.22821	C	0.37816	-1.27323	-2.39774
H	2.09787	3.9877	-0.87973	C	1.4596	0.5035	4.56624
H	1.8795	4.08819	-3.94185	C	-0.00115	-1.87129	4.6708
H	-0.20946	3.10325	-2.68189	C	-1.52477	0.7459	4.82309
H	1.31136	1.47635	-3.96344	C	2.28289	-2.93119	-2.74387
H	1.70382	1.49154	-0.92785	C	-0.03507	-3.48188	-3.59214
H	3.63092	2.33958	-3.98767	C	1.28227	-4.05325	-3.05152
H	1.05305	5.04771	-1.81816	C	-0.62922	-2.41117	-2.65756
H	3.25773	4.62508	-2.98546	C	1.6689	-1.87873	-1.80465
H	-0.22364	3.12644	-0.92188	C	-2.90308	1.62004	-4.44871
H	2.39299	0.4063	-3.08396	C	-4.33969	0.78019	-2.54097
H	-0.38666	-3.65071	6.83049	C	-4.21867	0.93014	-4.06391
H	1.85437	-3.86943	5.44773	C	-3.11958	0.0558	-1.94628
H	-0.61221	-5.18454	4.18434	C	-1.68074	0.90834	-3.83741
H	0.35908	-3.06429	2.89317	C	3.02159	2.46651	-3.08329
H	-1.92072	-2.8416	4.30512	C	1.51699	4.05307	-1.80971
H	0.56745	-1.63715	5.5802	C	2.44601	3.88711	-3.02008
C	2.80338	1.05202	6.66302	C	0.42022	2.97472	-1.79131
C	3.54122	2.17218	5.91838	C	1.91816	1.39064	-3.05218
C	1.39682	0.82166	6.08041	C	-0.91778	-3.90364	5.90045
C	2.17956	1.64559	3.82595	C	1.22309	-4.11065	4.57927
C	-2.46645	3.02236	5.49233	C	-0.04042	-4.83699	5.05754
C	-3.98336	1.00161	5.43551	C	0.88156	-2.81434	3.82435
C	-3.89829	2.52311	5.25824	C	-1.26822	-2.60217	5.15407
C	-2.96808	0.2701	4.53739	C	3.58311	1.88945	4.41126
C	-1.45193	2.27673	4.60677				

[W(CO)$_3$(PCy$_3$)$_2$(η^1-As$_4$)]

Atom	x	y	z	Atom	x	y	z
P	-2.531548519	0.950051187	-0.133988046	H	-5.25869927	5.2832393	0.31045033
W	0.054826135	0.796182875	0.0781644	H	-4.00597718	3.28242425	1.47349278
P	2.656887063	0.819958115	-0.013642485	H	-5.16023164	2.84041156	-0.77992029
C	-0.092309068	0.592705717	2.092536209	H	-2.12128663	3.17534362	-0.92632021
C	0.209624461	1.254691487	-1.899849435	H	-5.16824544	4.91051567	-2.13527065
C	0.099377609	2.70573849	0.516194621	H	-3.21082616	5.61869097	1.65334217
As	-0.017266701	-1.859306658	0.022181701	H	-4.29389399	6.55498675	-0.43356053
O	0.115710092	3.831918614	0.849871022	H	-2.24886289	3.33842751	1.59015552
O	0.345200298	1.620998376	-2.999183998	H	-4.19789485	2.64253526	-2.23658158
O	-0.211066299	0.572937736	3.254084144	C	4.86834016	-2.70541867	-1.26311455
C	-3.0045756	2.796746843	-0.396468991	C	3.7281444	-1.70680914	-3.28355391
C	-3.561420008	0.482757379	1.398550434	C	4.14871212	-3.00534886	-2.58358659
C	-3.428064531	0.115353411	-1.586772813	C	2.88167575	-0.81366463	-2.36020658
C	3.456466114	2.285527672	-0.98333247	C	4.0299991	-1.8080948	-0.33240351
C	3.612340337	-0.502667534	-1.035522019	H	5.82298848	-2.20263946	-1.47927012
C	3.546600784	0.866136211	1.660726324	H	4.62672448	-1.15568088	-3.59911941
As	0.360785435	-3.961070223	-1.185812945	H	3.25440257	-3.61284455	-2.37988541
As	-1.418842758	-3.807613313	0.533554914	H	1.93407022	-1.31858139	-2.13819626
As	0.962435568	-3.758662334	1.215187145	H	3.14166357	-2.36072768	-0.00223884
C	-3.613526944	-0.080695545	-4.118723253	H	4.5484878	0.00677942	-1.29902903
C	-4.44259384	-1.963995724	-2.646633969	H	5.11906577	-3.63799774	-0.74135883
C	-3.842710313	-1.59430368	-4.009703382	H	3.16279762	-1.92929747	-4.19767022
C	-3.606340702	-1.412466545	-1.476588534	H	4.791143	-3.60577291	-3.24043736
C	-2.767731431	0.439405347	-2.944047455	H	2.61942645	0.10759679	-2.8908539
H	-4.584101569	0.437732257	-4.130335498	H	4.62091523	-1.58834726	0.56201981

H	-5.463977263	-1.560274762	-2.577638931	C	3.33795744	4.60358636	-2.01574032
H	-2.880151022	-2.112210887	-4.133254588	C	5.58641534	3.50372484	-1.67738479
H	-2.621129477	-1.895348309	-1.475980211	C	4.82783644	4.83607431	-1.73497172
H	-1.782765365	-0.039688517	-2.978089184	C	4.94974863	2.53880424	-0.66012068
H	-4.433164948	0.557922165	-1.580579592	C	2.69999058	3.62701603	-1.01006846
H	-3.117303835	0.163385651	-5.066562562	H	3.21964566	4.19813399	-3.03167313
H	-4.532110327	-3.053849162	-2.551117568	H	5.58082572	3.03629269	-2.67317549
H	-4.493606163	-1.945087754	-4.820754306	H	4.94010606	5.35675156	-0.77232274
H	-4.090507643	-1.686187937	-0.535233207	H	5.04201662	2.98001375	0.33985041
H	-2.587509212	1.513056547	-3.060709942	H	2.69070762	4.08595338	-0.01433048
C	-5.811569125	0.426427089	2.591127445	H	3.41574204	1.89916738	-2.0120838
C	-3.90041774	-1.006772596	3.426990051	H	2.79187137	5.55524731	-1.99499563
C	-5.424501435	-0.881297783	3.294677514	H	6.63955547	3.67111477	-1.41597867
C	-3.200266149	-0.862175244	2.064798881	H	5.26526252	5.49221242	-2.49845215
C	-5.09501163	0.584574173	1.236639143	H	5.52539616	1.60612582	-0.64097879
H	-5.547455265	1.277203577	3.236524982	H	1.65788104	3.46707433	-1.28773543
H	-3.52435386	-0.230067815	4.108485349	C	4.08466409	2.28316398	3.71276475
H	-5.808241878	-1.732678719	2.712614636	C	4.03276544	-0.23908074	3.89963086
H	-3.505157965	-1.697628061	1.423440988	C	3.8109333	1.08859397	4.63663984
H	-5.448548045	-0.198860536	0.552317829	C	3.20372448	-0.31038566	2.60390535
H	-3.253249835	1.260823766	2.110609751	C	3.27298265	2.19319714	2.40825379
H	-6.898138057	0.474238514	2.441462893	H	5.15769126	2.31813206	3.47035318
H	-3.634336303	-1.971853117	3.876922855	H	5.10076899	-0.35138986	3.65834772
H	-5.901828932	-0.937467874	4.281346439	H	2.76961678	1.13431208	4.98614963
H	-2.120090333	-0.947084716	2.1965561	H	2.1424782	-0.2674814	2.86336987
H	-5.381877527	1.540209844	0.788852345	H	2.20350657	2.25815153	2.64276191
C	-4.287816097	4.674695159	-1.523199731	H	4.6214535	0.81599126	1.43274451
C	-3.138205581	5.093660207	0.692206826	H	3.85008858	3.22457521	4.22602683
C	-4.312809291	5.479168719	-0.216872059	H	3.76925558	-1.08373539	4.54918756
C	-3.093131757	3.575924716	0.937900863	H	4.44668448	1.14264019	5.52989686
C	-4.229760432	3.154791094	-1.270898425	H	3.36284288	-1.27619384	2.11996463
H	-3.40842244	4.969863308	-2.11430883	H	3.50199029	3.05851936	1.77988897
H	-2.190533127	5.40858035	0.23527042				

[Cp^BIG Mn(CO)₂]

Atom	x	y	z	Atom	x	y	z
Mn	-0.232938	-0.061898	2.128779	H	-9.616141	-2.138354	-2.062183
O	0.408809	2.119243	4.001772	H	-2.370149	7.150269	0.394095
O	0.773477	-2.183135	3.905028	H	-1.345801	7.223889	-1.035016
H	-3.01832	1.426374	-1.254866	H	-4.206548	6.116847	-0.977574
H	-2.792936	-1.484337	1.904472	H	-3.183995	6.189063	-2.403737
H	-5.246934	-1.439837	2.121047	H	-4.109393	8.625119	-0.778977
H	-5.477274	1.419996	-1.075436	H	-3.082773	8.69908	-2.202309
H	-2.019015	-2.005305	-1.683462	H	-5.463075	9.196271	-2.808353
H	0.144038	-3.531238	1.703224	H	-5.973574	7.626001	-2.168772
H	-0.617067	-5.79955	1.164986	H	-4.938626	7.702831	-3.602194
H	-2.788751	-4.282211	-2.214705	C	0.142678	1.247898	3.279455
H	3.043275	-0.822774	2.252839	C	0.343161	-1.33842	3.232109
H	1.586578	-2.628806	-1.363251	C	-0.877485	-2.585797	0.051575
H	3.609707	-4.029361	-1.477427	C	-0.41557	-1.1975	0.316156
H	5.061918	-2.226472	2.139869	C	-1.237225	-0.019744	0.2514
H	3.05955	0.374442	-1.173944	C	2.161587	-1.617473	0.453672
H	1.586682	2.976753	1.914819	C	-2.719742	-0.020742	0.315644
H	3.544966	4.421352	1.629652	C	-0.408527	1.145028	0.357702
H	5.022356	1.827931	-1.457112	C	-0.840378	2.558083	0.176563
H	0.28564	2.791949	-1.646763	C	0.962903	0.686499	0.489059
H	-2.0579	2.689763	1.951317	C	2.167453	1.555035	0.396477
H	-2.779925	5.006609	1.547728	C	0.955049	-0.748732	0.474905
H	-0.432366	5.116326	-2.046522	C	-5.549273	-0.009405	0.535922
H	5.536777	-5.016974	-0.26686	C	-3.502188	0.789707	-0.521248
H	6.110984	-4.307049	1.237684	C	-3.376074	-0.827384	1.262481
H	7.108926	-2.390997	-0.049115	C	-4.764999	-0.813219	1.373821
H	6.540008	-3.101746	-1.550815	C	-4.891169	0.786052	-0.413448
H	7.951959	-5.142016	-1.122182	C	-7.059517	-0.032895	0.624769
H	8.516118	-4.43638	0.384196	C	-1.758613	-5.219561	-0.568906
H	9.571146	-2.527518	-0.896276	C	-1.707889	-2.83443	-1.054724
H	9.00286	-3.236829	-2.414648	C	-0.492503	-3.683149	0.838763
H	10.205424	-4.090808	-1.434616	C	-0.926193	-4.971248	0.530759
H	-3.203537	-6.599584	-1.358283	C	-2.140645	-4.124701	-1.354829

Atom	x	y	z	Atom	x	y	z
H	-2.271091	-7.227387	-0.004407	C	-2.196707	-6.624901	-0.919643
H	-1.158644	-6.723876	-2.818972	C	4.494668	-3.231622	0.31885
H	-0.232788	-7.357542	-1.467908	C	3.16327	-1.522042	1.431576
H	-2.696895	-8.714756	-2.699851	C	2.346969	-2.533626	-0.594078
H	-1.771735	-9.349239	-1.348291	C	3.493759	-3.324438	-0.656678
H	-0.657306	-8.891602	-4.186814	C	4.305787	-2.315443	1.362693
H	-1.08077	-10.461202	-3.484735	C	4.434896	3.239966	0.062173
H	0.274052	-9.531227	-2.824967	C	3.159081	1.260203	-0.555191
H	6.498831	3.567956	-0.436814	C	2.329304	2.714363	1.171314
H	5.877181	4.647008	0.806694	C	3.443136	3.5354	1.006393
H	4.483269	5.829802	-0.921085	C	4.269513	2.086488	-0.715129
H	5.105662	4.752988	-2.161094	C	5.620325	4.158092	-0.142579
H	7.442534	5.581138	-1.703901	C	-1.671749	5.236222	-0.286285
H	6.815605	6.66301	-0.470302	C	-0.39384	3.271474	-0.948012
H	5.452881	7.879509	-2.220968	C	-1.705275	3.211001	1.066602
H	6.084546	6.789291	-3.463385	C	-2.113486	4.523892	0.836038
H	7.177972	7.898125	-2.62033	C	-0.801199	4.585504	-1.171187
H	-7.462062	0.94072	0.315112	C	-2.148699	6.646972	-0.556431
H	-7.364868	-0.178351	1.669721	C	6.891268	-3.350294	-0.539283
H	-7.29221	-2.11293	0.063412	C	8.175321	-4.184518	-0.630289
H	-7.396123	-0.995743	-1.287601	C	9.30225	-3.471705	-1.385709
H	-9.630378	-0.18906	-0.449376	C	-1.240905	-7.328742	-1.904801
H	-9.52464	-1.302668	0.904797	C	-1.686969	-8.750918	-2.266747
H	-10.956945	-2.263212	-0.912395	C	-0.735951	-9.448766	-3.245068
H	-9.5095	-3.26035	-0.697905	C	5.365011	5.241027	-1.210882
C	-9.229808	-1.166772	-0.145551	C	6.562039	6.176717	-1.423124
C	-9.864609	-2.267884	-1.001609	C	6.306701	7.245813	-2.490901
C	-3.402734	6.696366	-1.453338	C	-7.699073	-1.138259	-0.240714
C	-3.892653	8.12276	-1.732573				
C	-5.135968	8.165935	-2.627502				

[Cp^BIG^Mn(CO)₃]

Atom	x	y	z	Atom	x	y	z
Mn	1.748120807	7.995639936	16.51726643	H	8.27372642	8.40063801	17.4475168
C	0.427016185	8.987590105	15.83560835	H	4.86996359	13.4814779	18.7212828
C	0.841760485	6.499639477	16.15761215	C	3.03746425	13.8475465	17.6445202
C	2.57719061	7.884305598	14.93763587	H	1.17240838	13.8298743	16.5656286
C	1.556805459	8.832690464	18.52252068	C	-3.10578722	11.2073825	21.1206501
C	1.950682635	7.458960681	18.64263312	C	-0.53960351	3.48928463	22.1425494
C	3.214577524	7.291888099	17.96108746	C	6.57072915	2.50907769	18.0670384
C	3.628881666	8.588462228	17.48505811	C	8.85628545	9.96684029	15.2599573
C	2.605305383	9.539286546	17.81327864	C	3.17600441	15.3543949	17.6546276
O	-0.441339552	9.628380492	15.41271923	H	-3.99594976	11.0976397	20.4863315
O	0.254695162	5.52965919	15.91874248	H	-2.95038371	12.2843939	21.2580981
O	3.136069586	7.794587111	13.92704159	C	-3.38482794	10.5448697	22.4870768
C	0.356459174	9.453348247	19.14569327	H	-0.46150906	3.81909834	23.1870038
C	1.281272147	6.43353563	19.49063606	H	0.01176648	2.54228239	22.0727066
C	4.042502479	6.054138745	17.95806025	C	-2.02437923	3.21490576	21.8109593
C	4.948858574	8.917408345	16.8101133	H	6.3616656	1.87301772	17.1964292
C	2.735946096	11.0195473	17.69769224	H	6.33732046	1.90704758	18.9554616
C	0.49515171	10.55714767	20.00210973	C	8.07292233	2.85943839	18.0803437
C	-0.933055941	8.938680179	18.93926363	H	9.63963295	9.76329854	16.0020185
C	0.890548085	6.778469913	20.79525906	H	8.89027436	11.0462976	15.0603389
C	1.097322361	5.101177699	19.0852807	C	9.19392633	9.21790333	13.9512733
C	4.492982711	5.450345771	16.77456641	H	2.66584267	15.7778148	16.7793707
C	4.426263249	5.475182213	19.17909856	H	4.23546507	15.6293176	17.5617739
C	5.072635278	9.761996404	15.76491472	C	2.60197888	16.0018866	18.9317412
C	6.127127939	8.4397446	17.47543999	H	-3.50180209	9.46405577	22.3316306
C	3.847993382	11.64422669	18.28912048	H	-2.5017256	10.6662404	23.1306653
C	1.777345093	11.8373893	17.0823181	C	-4.62759472	11.0881329	23.2112133
H	1.479508345	10.97764506	20.18145146	H	-2.1046102	2.89874112	20.761268
C	-0.617441627	11.12355272	20.62338902	H	-2.36264146	2.36193873	22.4163855
C	-2.039247836	9.508066748	19.56459004	C	-2.95741543	4.40730646	22.0556448
H	-1.06943462	8.085351257	18.28218879	H	8.28581208	3.49713819	18.9500579
H	1.03917649	7.793266022	21.14858523	H	8.30799833	3.46562538	17.1941512
C	0.319418408	5.835229761	21.64866865	C	8.98010875	1.6230028	18.1141845
C	0.521227317	4.16635371	19.94139896	H	10.1147497	9.64860189	13.5327807
H	1.408717409	4.785302601	18.09749139	H	8.40174366	9.40965134	13.2137683
H	4.216467719	5.872623855	15.81382666	C	9.37650751	7.70420851	14.1187976

Atom	x	y	z	Atom	x	y	z
C	5.295294546	4.311321191	16.81430952	H	10.1811949	7.51674743	14.8448385
C	5.226643656	4.334407961	19.21136147	H	3.10897621	15.575325	19.8089297
H	4.087544472	5.919192192	20.11054685	H	1.54265638	15.7253008	19.0287619
H	4.182890675	10.16384385	15.29217161	C	2.73943381	17.5294292	18.9508226
C	6.323883243	10.09820968	15.2581378	H	-4.81813804	10.4598559	24.0917634
C	7.378404046	8.783487341	16.96288058	H	-5.50576579	10.9718949	22.5597981
H	6.067138396	7.798629967	18.34846685	C	-4.51423491	12.5503203	23.6602546
H	4.606888321	11.0361147	18.77205506	H	-2.61671383	5.26614805	21.4633897
C	3.994358764	13.02930621	18.25989235	H	-2.88249218	4.71282205	23.1095985
C	1.929990272	13.22331834	17.05731347	C	-4.41967761	4.09837308	21.7164722
H	0.904880554	11.39613454	16.61580045	H	8.75724961	0.98635357	17.2460887
H	-0.480539799	11.98268589	21.27689725	C	10.4721522	1.97258305	18.1218965
C	-1.905056347	10.61243369	20.41742096	H	8.73970783	1.02098189	19.0021426
H	-3.027338486	9.093033605	19.37769432	H	8.46587023	7.27218429	14.5531075
H	0.031302801	6.134575739	22.65386697	C	9.70220402	6.99480942	12.8001939
C	0.113569039	4.51281707	21.23748935	H	3.79985614	17.7997021	18.8448069
H	0.390067807	3.143678515	19.59416676	H	2.22930397	17.9505933	18.0727416
H	5.622805905	3.860746468	15.87978828	C	2.17472977	18.1666517	20.2250243
C	5.676099237	3.728987869	18.03060061	H	-4.40433431	13.233607	22.8104981
H	5.500747557	3.90381356	20.1722472	H	-3.6468298	12.6945979	24.3168463
H	6.385349425	10.75376822	14.39214017	H	-5.40642866	12.8609425	24.2159402
C	7.503493511	9.612054393	15.84176599	H	-5.06491374	4.96417726	21.9049275
H	9.835183361	5.917004208	12.94879129	H	-4.80028226	3.2624764	22.3167971
H	8.897177307	7.132717017	12.06793452	H	-4.53125423	3.82400872	20.6602114
H	2.28610057	19.25690441	20.21006561	H	11.0941898	1.07052578	18.1473121
H	2.690206886	17.79102893	21.11756279	H	10.732141	2.58163271	18.996537
H	1.107241458	17.94216529	20.34101852	H	10.7495776	2.54380024	17.2274156
H	10.62534769	7.385882059	12.3541921				

[Cp^{BIG}Mn(CO)$_2$thf]

Atom	x	y	z	Atom	x	y	z
Mn	-0.21482	-0.08869	1.81704	H	7.302	-0.46617	-0.11114
O	1.53149	-0.60866	2.90486	H	7.15657	0.97326	-1.11356
C	-1.18267	-1.24515	2.74121	C	7.12167	-0.89433	-2.22462
C	-0.5949	1.21095	2.9559	H	2.00768	-6.6566	-2.42252
C	0.99819	0.05307	-0.05805	H	0.82874	-7.25559	-1.26284
C	0.14143	-1.10809	-0.07727	C	2.84021	-7.15503	-0.48459
C	-1.22622	-0.6362	-0.01097	H	-6.57771	-3.99031	-0.09391
C	-1.20621	0.79168	0.09686	H	-5.82509	-4.68023	-1.52735
C	0.18036	1.21821	0.08142	C	-7.06501	-2.95226	-1.92856
O	-1.85059	-2.00721	3.31924	H	-6.08003	4.30384	-1.8098
O	-0.85705	2.07693	3.69378	H	-5.46714	5.3876	-0.56676
C	2.47478	0.04257	-0.23755	C	-6.99058	4.02845	0.13783
C	0.55407	-2.50643	-0.37333	H	2.13343	7.20534	0.61744
C	-2.44963	-1.45863	-0.21936	H	1.16275	7.38206	-0.8395
C	-2.38371	1.691	-0.06476	C	3.23603	6.89152	-1.21802
C	0.62132	2.63925	0.01519	H	6.68716	-1.89455	-2.09504
C	3.09494	0.99568	-1.06545	H	6.62469	-0.45822	-3.10282
C	3.2975	-0.94241	0.33374	C	8.62784	-1.03202	-2.50028
C	1.33456	-2.78536	-1.5075	H	2.54047	-7.08565	0.57097
C	0.14355	-3.59493	0.41626	H	2.95676	-8.22654	-0.7012
C	-3.58591	-1.32981	0.59512	C	4.1904	-6.45347	-0.67687
C	-2.51963	-2.34645	-1.30544	H	-6.56677	-2.69005	-2.87265
C	-2.66565	2.75469	0.80678	H	-7.31368	-1.99879	-1.44162
C	-3.21689	1.52693	-1.18406	C	-8.35307	-3.73064	-2.22489
C	0.19524	3.44199	-1.05676	H	-7.73274	4.83046	0.0151
C	1.47238	3.22109	0.96553	H	-6.67858	4.05567	1.19153
H	2.49441	1.75907	-1.54634	C	-7.65475	2.67876	-0.16086
C	4.47094	0.97461	-1.28737	H	-7.97024	2.65858	-1.21438
C	4.67254	-0.95751	0.11209	H	3.05505	6.45321	-2.21234
H	2.85508	-1.71008	0.95855	H	4.02392	6.27778	-0.75877
H	1.65483	-1.96773	-2.14619	C	3.72991	8.33607	-1.36729
C	1.69906	-4.09298	-1.82953	H	8.76517	-1.75112	-3.3191
C	0.50735	-4.8992	0.08657	H	9.11717	-1.47643	-1.62139
H	-0.48398	-3.42151	1.28483	C	9.33253	0.27952	-2.86818
H	-3.5655	-0.64908	1.43909	H	4.07699	-5.38055	-0.47463
C	-4.7387	-2.06734	0.33774	H	4.49141	-6.53508	-1.73149
C	-3.6772	-3.08197	-1.55741	C	5.29493	-7.0311	0.21477
H	-1.66105	-2.4631	-1.95879	H	-8.84293	-3.99524	-1.27685

H	-2.03907	2.92286	1.67393	C	-9.33538	-2.95379	-3.10819
C	-3.74481	3.60464	0.57324	H	-8.09758	-4.68332	-2.71073
C	-4.29516	2.38125	-1.41209	H	-6.91681	1.87448	-0.04736
H	-3.0167	0.72134	-1.88362	C	-8.86309	2.39759	0.73891
H	-0.47315	3.02278	-1.80275	H	2.9358	8.94559	-1.82178
C	0.61125	4.76727	-1.17237	H	3.90729	8.76322	-0.36995
C	1.88775	4.54611	0.84454	C	5.00652	8.4513	-2.20724
H	1.80654	2.63314	1.8135	H	9.30548	1.00521	-2.0473
H	4.91467	1.73031	-1.93247	H	8.86189	0.74865	-3.74152
C	5.29009	0.00138	-0.70201	H	10.38613	0.10351	-3.11368
H	5.27851	-1.73456	0.57477	H	6.24952	-6.51681	0.05361
H	2.29957	-4.27363	-2.71862	H	5.45345	-8.0977	0.01219
C	1.29769	-5.17658	-1.03829	H	5.03869	-6.93254	1.27713
H	0.16247	-5.71925	0.71355	H	-10.24385	-3.53501	-3.30425
H	-5.59853	-1.95416	0.99486	H	-8.88452	-2.70296	-4.07637
C	-4.80839	-2.95895	-0.74141	H	-9.63773	-2.01311	-2.63159
H	-3.69888	-3.76642	-2.40322	H	-9.32364	1.432	0.49981
H	-3.93558	4.41993	1.26839	H	-8.5721	2.37427	1.79644
C	-4.58532	3.43414	-0.53559	H	5.33473	9.49331	-2.29596
H	-4.91965	2.22806	-2.28967	H	4.84964	8.06369	-3.22152
H	0.25772	5.36454	-2.01051	H	5.82879	7.87977	-1.75909
C	1.46765	5.34568	-0.22619	H	-9.63304	3.1712	0.62543
H	2.54224	4.97015	1.60356	C	2.42561	0.36576	3.51107
C	6.77671	-0.04714	-0.98059	C	3.16262	-0.38106	4.62718
C	1.70207	-6.59843	-1.36938	C	1.71793	-1.91024	3.51629
C	-6.07636	-3.73046	-1.03613	C	3.09865	-1.84412	4.15975
C	-5.77174	4.34973	-0.75661	H	3.10054	0.71775	2.72506
C	1.94969	6.77247	-0.37514	H	1.82628	1.20171	3.87819
H	1.62079	-2.65995	2.72796	H	2.63443	-0.2639	5.58011
H	3.87787	-2.04541	3.41625	H	4.185	-0.0157	4.75972
H	3.20883	-2.56222	4.97764	H	0.92504	-2.07009	4.25664

[Cp^{BIG}Mn(CO)$_2$(η^1-P$_4$)]

Atom	x	y	z	Atom	x	y	z
Mn	-0.1259337237	-0.3542448182	0.9149432132	H	6.9899548082	-2.9083109928	-1.823842982
P	0.6793205916	0.6637447754	2.739210923	H	7.7505340061	-0.2492918981	-0.4948224518
P	2.4560744078	1.4161442559	3.7676244208	H	7.5561994237	-0.4906440408	-2.2236357043
P	0.8891490381	0.2523558286	4.8791844661	H	9.6113964887	-1.9484623112	-0.4681325748
P	0.4346244307	2.3243991764	4.1458510911	H	9.4176772599	-2.1863239498	-2.1976268739
O	0.4965003495	-2.9634809432	2.1162332943	H	11.3186702978	-0.6207980072	-1.7345183706
O	-2.8270778129	-0.4144347134	2.0737128351	H	10.2316324586	0.4713156031	-0.8620296007
H	3.3571131752	1.5409109736	-1.5586877399	H	10.0351346683	0.2343435588	-2.6046601836
H	0.4341010869	3.2037258705	1.1194095679	C	0.2614325813	-1.9252784267	1.6503109904
H	1.8764132627	5.1523174942	1.4814464532	C	-1.7482905345	-0.3797200534	1.6428475536
H	4.7895650777	3.4977557993	-1.2039267561	C	-1.3285656747	2.3240485886	-0.7791516628
H	-0.0724699573	3.1695582733	-2.3150017228	C	-0.510706481	1.0811285059	-0.6930616087
H	-2.7980654448	1.8009519223	0.7133550486	C	0.9112555303	1.022945921	-0.4890436852
H	-4.12404469	3.8469723277	0.4427423259	C	-2.3246193055	-0.6116610463	-1.5261469662
H	-1.4105653915	5.2190819342	-2.5896369446	C	1.7885879989	2.1966245711	-0.2273226646
H	-2.4967809634	-2.371260012	-0.2921884754	C	1.3449897086	-0.3326589277	-0.6984957276
H	-2.4964326374	1.0459916734	-2.8977849979	C	2.75067798	-0.8248209133	-0.7406044107
H	-4.7229492007	0.4118870085	-3.7267094822	C	0.1906105495	-1.1075699774	-1.1009950481
H	-4.7241478492	-3.0010094291	-1.1198504869	C	0.2387567764	-2.4745024108	-1.6917088712
H	-0.9210193436	-1.8945299458	-3.4175097842	C	-0.9549697451	-0.2438086058	-1.0740091112
H	1.4491915667	-3.4068611742	-0.1636817863	C	3.4500342818	4.4770877585	0.1706380846
H	1.5676931081	-5.5865688952	-1.2654742337	C	3.0249612923	2.3207738805	-0.883611576
H	-0.7894355848	-4.0824296062	-4.5241014147	C	1.3940126182	3.2495408098	0.6170444866
H	2.6741693497	-1.2297171552	-2.8573445275	C	2.2101503142	4.3611805232	0.8134709247
H	3.1781637475	-0.5639993231	1.3542827906	C	3.8355588754	3.4372958145	-0.6842213561
H	5.5089057762	-1.3412222843	1.1987089651	C	4.318356953	5.7017864684	0.3575112874
H	5.0076944037	-2.0080987545	-3.0132456144	C	-2.8749741412	4.6897936542	-1.0976582096
H	-6.8198043447	-0.8677570172	-3.3172608175	C	-0.9636078433	3.3119885019	-1.7104897293
H	-6.821867718	-2.2600081627	-2.241211551	C	-2.48227969	2.5419084107	-0.0121121173
H	-5.5670055095	-3.5919662959	-3.9675902975	C	-3.2372375674	3.703972988	-0.1711304234
H	-5.5727359844	-2.2036173222	-5.0431541331	C	-1.722122992	4.470456239	-1.863965654
H	-8.092497046	-2.2351464277	-5.0689572661	C	-3.7207993404	5.9286365696	-1.2970164623
H	-8.0848858619	-3.6252847109	-3.9954852735	C	-4.8947450937	-1.346174434	-2.4917522043
H	-6.8714782064	-4.9830143698	-5.7526446129	C	-2.979141302	-1.7565428141	-1.045114631
H	-6.8804291155	-3.5822654857	-6.8339823404	C	-2.9775545111	0.157280504	-2.5027333249
H	-8.4062414444	-4.3529030429	-6.3716077284	C	-4.2390159295	-0.2063179168	-2.9733128291

H	-3.0760750357	6.7772322631	-1.5631795043	C	-4.2383932668	-2.1134145201	-1.519422705
H	-4.2138920112	6.1958003249	-0.3528652827	C	-6.2464113045	-1.7599138858	-3.0317420824
H	-4.3038151208	5.4768186424	-3.3343222947	C	0.3981769536	-5.0075076095	-2.9806260941
H	-5.4442153994	4.9096446031	-2.1251499506	C	-0.3751000741	-2.6993231497	-2.9367643777
H	-4.9891922769	7.8554242996	-2.8649003366	C	0.9494663093	-3.5388614443	-1.1147358967
H	-6.1341430461	7.287146712	-1.6601297761	C	1.0200697995	-4.7789953983	-1.7466838424
H	-6.2462660518	6.5958313832	-4.6631807771	C	-0.2969716048	-3.9406206319	-3.5642190445
H	-7.2978394527	7.7528277087	-3.8314950926	C	0.5092406517	-6.344750477	-3.6795740684
H	-7.4021880947	6.0267783327	-3.4500979558	C	5.4414428077	-1.7245284809	-0.9209044594
H	-0.4065282847	-6.537736746	-4.2545852931	C	3.2951583256	-1.2436761329	-1.9663312454
H	0.5829818931	-7.1465555321	-2.9327481569	C	3.5753512893	-0.8707878891	0.3921216037
H	2.6405013841	-6.2380655425	-4.0568228945	C	4.8950037018	-1.31077228	0.3009934498
H	1.6530913877	-5.6281909184	-5.3749747565	C	4.6148898713	-1.6838516763	-2.0517757952
H	0.9110279382	-7.9769292751	-5.9050908778	C	6.8856965417	-2.1648948979	-1.0221853657
H	1.901662516	-8.5865557384	-4.5890880265	C	-6.1470979307	-2.7018711594	-4.2492573278
H	3.9795337962	-7.7177199668	-5.7426987197	C	-7.5153272213	-3.1298806484	-4.7947631111
H	2.980848442	-7.105263519	-7.0689467677	C	-7.4413753213	-4.0639094134	-6.0054690795
H	3.0929145874	-8.8484356079	-6.7775982554	C	-4.7945524567	5.7553707776	-2.3909981519
H	5.377050088	5.4158591243	0.295450348	C	-5.6463404515	7.0127126521	-2.606338882
H	4.164752128	6.1121114921	1.3644921337	C	-6.7077224946	6.8389058216	-3.6980959549
H	2.976584499	7.0913598899	-0.6247851898	C	1.7222554606	-6.4324251468	-4.6287205877
H	4.187927219	6.3977386318	-1.6905832373	C	1.8348236106	-7.7865346794	-5.3402336997
H	5.9731249139	7.7585665336	-0.5459820771	C	3.0383802877	-7.8707307588	-6.2851937586
H	4.7606409006	8.452634632	0.518577829	C	4.0366923384	6.8066875848	-0.6815434873
H	5.2732816601	10.0212837068	-1.3657519194	C	4.9145165203	8.0504305164	-0.4929526672
H	3.5903459873	9.4814628066	-1.4750649758	C	4.6335549185	9.1460516898	-1.5268591815
H	4.8139011619	8.784396828	-2.5467032707	C	7.8550632496	-0.9962211465	-1.2943914676
H	7.1848867206	-2.6660127916	-0.0918195919	C	9.3203719362	-1.4385514163	-1.3975708014
C	10.281043894	-0.274879484	-1.6645817633				

[Cp^{BIG}Mn(CO)$_2$(η^1-As$_4$)]

Atom	x	y	z	Atom	x	y	z
Mn	-0.1817128221	-0.3871024713	0.8624186808	H	9.4328515959	-2.2354147208	-1.9697367012
O	0.4046462919	-3.0146828432	2.0448291832	H	11.3273317138	-0.678985619	-1.4552392241
O	-2.9016717193	-0.4279331084	1.9811823761	H	10.2198319247	0.4262080146	-0.6261472006
H	3.3350971334	1.532645727	-1.5564322223	H	10.0790820708	0.1786482677	-2.3727407367
H	0.401352625	3.1608663788	1.1322544103	C	0.183593977	-1.9685830464	1.5895087494
H	1.8447665944	5.1001435628	1.530303644	C	-1.8153899399	-0.4016986094	1.5685767343
H	4.7682066385	3.4829716028	-1.1672588438	C	-1.3410356282	2.3159475864	-0.8250081892
H	-0.0515802903	3.1680708447	-2.3287831865	C	-0.5323040168	1.0673789854	-0.7366134603
H	-2.8391556141	1.7889578712	0.6371299645	C	0.8846598275	1.0031081141	-0.5092638877
H	-4.1434810807	3.8496291944	0.3670287465	C	-2.3373465635	-0.6118805566	-1.6121824652
H	-1.3650129773	5.2341127013	-2.5999374363	C	1.7604845681	2.1721666975	-0.2244732595
H	-2.5411455884	-2.3766643512	-0.3908512414	C	1.3193316238	-0.3520002482	-0.7192496528
H	-2.4751275448	1.055112364	-2.9760283457	C	2.7255633266	-0.8436525711	-0.7241016645
H	-4.6917121724	0.4393230019	-3.8469632581	C	0.1699724728	-1.1210683834	-1.1487927484
H	-4.7589942355	-2.9876087026	-1.259647514	C	0.2225654639	-2.4852032049	-1.7456744712
H	-0.9161775259	-1.8960284115	-3.4824401693	C	-0.9742115908	-0.2542693095	-1.1336661446
H	1.4150055435	-3.4268484166	-0.2089980182	C	3.4234522704	4.4432215645	0.2160177476
H	1.5398880057	-5.6022303166	-1.317779222	C	3.0004889859	2.3036717212	-0.872120679
H	-0.7792707368	-4.0799375999	-4.5951455828	C	1.3629067528	3.2124453327	0.6337080745
H	2.6975496072	-1.3029863453	-2.8307794192	C	2.1803087386	4.3190822017	0.8513134947
H	3.1098704775	-0.5183263629	1.3716189948	C	3.8118202195	3.4160610604	-0.6527081552
H	5.4399471253	-1.3037868847	1.2897428453	C	4.2921237126	5.6637855163	0.4268855964
H	5.0334195172	-2.0844334234	-2.9129802619	C	-2.8597072153	4.7000834269	-1.1398394683
H	-6.7977053179	-0.8287554502	-3.4905533271	C	-0.9517522842	3.3114989637	-1.7381227298
H	-6.8363857958	-2.2151946984	-2.4074369956	C	-2.5059170352	2.534803032	-0.0754103546
H	-5.567868335	-3.5723251566	-4.1027088489	C	-3.2474343937	3.7057289858	-0.2331057134
H	-5.5321089913	-2.1892929807	-5.1845919136	C	-1.6962688949	4.4792701102	-1.8895614284
H	-8.0504196758	-2.1854915405	-5.2621406709	C	-3.6891166967	5.9509992517	-1.3339943586
H	-8.0851768369	-3.5696105948	-4.1813011885	C	-4.8947652723	-1.3246132905	-2.6256201575
H	-6.8543410897	-4.9538818349	-5.9060656098	C	-3.0070413869	-1.7552820098	-1.1486671291
H	-6.8237146107	-3.5596149893	-6.9952603075	C	-2.9686366468	0.1669883154	-2.5950322184
H	-8.3683226896	-4.3074967257	-6.5586006604	C	-4.2239859207	-0.186240827	-3.0894076449
H	-3.0300877511	6.8002218642	-1.5602534356	C	-4.2602271496	-2.1014668395	-1.6463736231
H	-4.2064404233	6.1988918337	-0.3975179786	C	-6.2403976501	-1.7260250089	-3.1896151162
H	-4.2174933953	5.5653505553	-3.3998181188	C	0.389374815	-5.0140331205	-3.042717047
H	-5.3911446354	4.9630842057	-2.240403519	C	-0.3784351896	-2.7040266327	-2.9979926834
H	-4.9122132621	7.9300949262	-2.8724546252	C	0.924854729	-3.553794822	-1.1655718244

H	-6.0903382517	7.3247428566	-1.7188011212	C	0.9991725294	-4.7914677354	-1.8015050605
H	-6.1219238609	6.7350213147	-4.7453016027	C	-0.2971961035	-3.9434146992	-3.6292238789
H	-7.1960348921	7.8622997333	-3.9019292384	C	0.5073694739	-6.3486774211	-3.7456253651
H	-7.3085541573	6.1241188682	-3.583277563	C	5.4199732175	-1.7458403266	-0.8195271431
H	-0.387455571	-6.523832388	-4.3579205179	C	3.2977756725	-1.2934510183	-1.9257123872
H	0.539179651	-7.15631707	-3.0019557696	C	3.525358725	-0.8568743029	0.4279043037
H	2.6535641522	-6.2737217435	-4.0354117404	C	4.8463031371	-1.2982082752	0.3779329115
H	1.7299843804	-5.6375816443	-5.3870594516	C	4.6194388472	-1.7350164594	-1.9693843436
H	0.9757729485	-7.968668823	-5.9701651995	C	6.8651559421	-2.1917579311	-0.8740557495
H	1.8973418964	-8.6058708561	-4.6175038373	C	-6.1293533404	-2.6755071961	-4.4001902476
H	4.037983183	-7.7639541182	-5.6707090346	C	-7.4922655463	-3.0869821143	-4.9713570945
H	3.1097271178	-7.1228640364	-7.0340631379	C	-7.3801029322	-4.0292855772	-6.1746530017
H	3.1787615119	-8.8701300846	-6.7542458295	C	-4.7329344742	5.8150162668	-2.4615543467
H	5.3502233892	5.3824204567	0.3406239856	C	-5.5769219397	7.0805219926	-2.6597277262
H	4.1528178127	6.043419132	1.447976149	C	-6.6086135777	6.9444129089	-3.7846978889
H	2.93416293	7.0806959974	-0.4927478801	C	1.7562473815	-6.4487213362	-4.6456248009
H	4.1310294157	6.4226851923	-1.5967577838	C	1.8769546462	-7.7987832904	-5.3637520207
H	5.9309837664	7.7485977057	-0.434315491	C	3.119342353	-7.8958600206	-6.2556661877
H	4.7328571092	8.4075513544	0.6679511804	C	3.9936946533	6.7996561402	-0.5734191176
H	5.2221817029	10.0342197783	-1.1747827148	C	4.8730219964	8.0378898391	-0.357927377
H	3.5365819703	9.5012861824	-1.2740313232	C	4.5779480029	9.1655560009	-1.3527342169
H	4.7413462964	8.8353092121	-2.3859679496	C	7.8483168847	-1.0302677202	-1.1267805199
H	7.1343611662	-2.685417811	0.0695299975	C	9.3135261255	-1.4813250801	-1.1786262278
H	6.9903881111	-2.9431523384	-1.6650431422	C	10.2903116846	-0.3257757806	-1.4216882869
H	7.7222862661	-0.2751805082	-0.3379653824	As	0.6563575921	0.6549349857	2.7884025327
H	7.5818013896	-0.5323752252	-2.069823223	As	2.5920532685	1.5948815272	3.9039591387
H	9.5703297857	-1.9863742004	-0.2364952449	As	0.9648836799	0.1757937352	5.1532685728
As	0.3007950631	2.4524365482	4.3907460143				
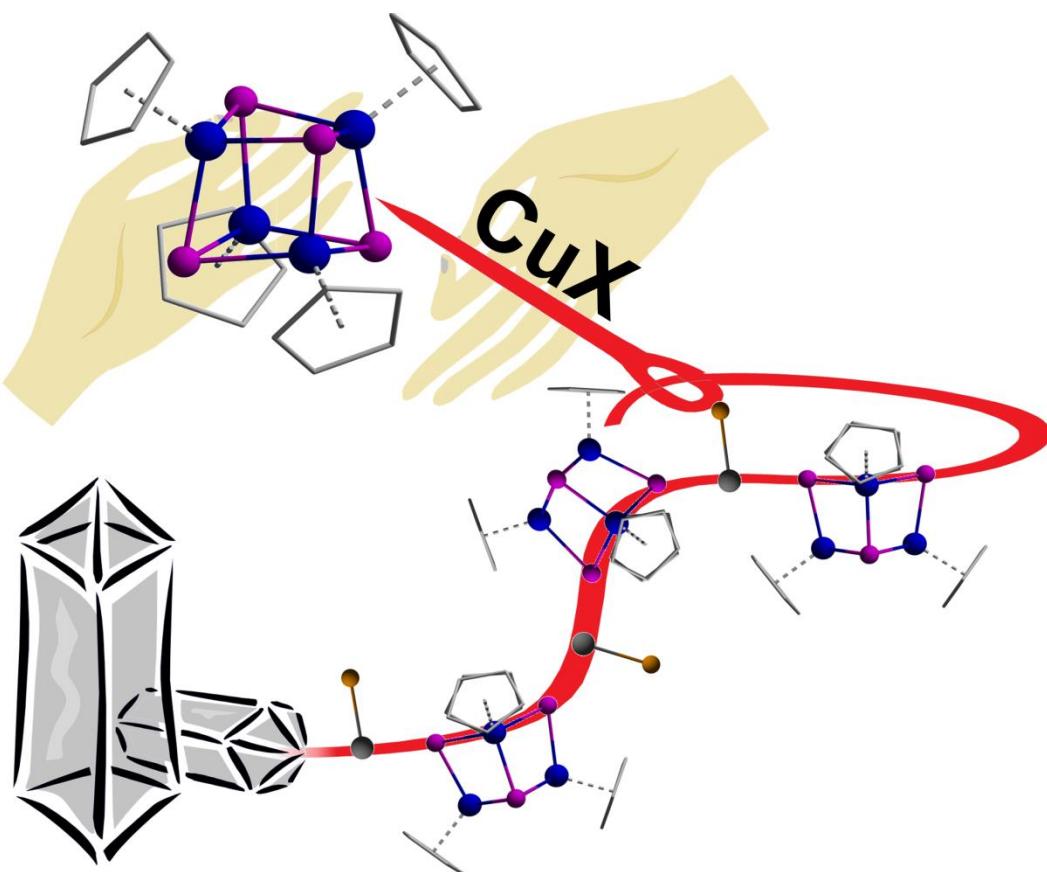
References for Supplementary Information:

[1]   B. S. Creaven, M. W. George, A. G. Ginzburg, C. Hughes, J. M. Kelly, C. Long, I. M. McGrath and M. T. Pryce, *Organometallics*, 1993, **12**, 3127.

[2]   W. A. Herrmann, R. Serrano, J. Weichmann, *J. Organomet. Chem.* **1983**, *246*, c57-c60.

[3]   R. B. King, A. Efraty, *J. Amer. Chem. Soc.* **1972**, *94*, 3773-3779.

[4]   K. J. Reimer, A. Shaver, *Inorg. Chem.* **1975**, *14*, 2707-2716.

[5]   R. C. Clark, J. S. Reid, *Acta Cryst.* **1995**, A51, 887-897.

[6]   A. Altomare, M. C. Burla, M. Camalli, G.L. Cascarano, C. Giacovazzo, A. Guagliardi, A. G. G. Moliterni, G. Polidori, R. Spagna, *J. Appl. Cryst.* **1999**, 32, 115-119.

[7]   G. M. Sheldrick, *Acta Cryst.* **2008**, A64, 112-122.

[8]   A. Altomare, M. C. Burla, M. Camalli, G.L. Cascarano, C. Giacovazzo, A. Guagliardi, A. G. G. Moliterni, G. Polidori, R. Spagna, *J. Appl. Cryst.* **1999**, *32*, 115-119.

[9]   M. J. Frisch, G. W. Trucks, H. B. Schlegel, G. E. Scuseria, M. A. Robb, J. R. Cheeseman, J. A. Montgomery, Jr., T. Vreven, K. N. Kudin, J. C. Burant, J. M. Millam, S. S. Iyengar, J. Tomasi, V. Barone, B. Mennucci, M. Cossi, G. Scalmani, N. Rega, G. A. Petersson, H. Nakatsuji, M. Hada, M. Ehara, K. Toyota, R. Fukuda, J. Hasegawa, M. Ishida, T. Nakajima, Y. Honda, O. Kitao, H. Nakai, M. Klene, X. Li, J. E. Knox, H. P. Hratchian, J. B. Cross, V. Bakken, C. Adamo, J. Jaramillo, R. Gomperts, R. E. Stratmann, O. Yazyev, A. J. Austin, R. Cammi, C. Pomelli, J. W. Ochterski, P. Y. Ayala, K. Morokuma, G. A.

Voth, P. Salvador, J. J. Dannenberg, V. G. Zakrzewski, S. Dapprich, A. D. Daniels, M. C. Strain, O. Farkas, D. K. Malick, A. D. Rabuck, K. Raghavachari, J. B. Foresman, J. V. Ortiz, Q. Cui, A. G. Baboul, S. Clifford, J. Cioslowski, B. B. Stefanov, G. Liu, A. Liashenko, P. Piskorz, I. Komaromi, R. L. Martin, D. J. Fox, T. Keith, M. A. Al-Laham, C. Y. Peng, A. Nanayakkara, M. Challacombe, P. M. W. Gill, B. Johnson, W. Chen, M. W. Wong, C. Gonzalez, and J. A. Pople, Gaussian 03 (Revision D.01): Gaussian, Inc., Wallingford CT, 2004.

[10]   a) A. D. Becke, *J. Chem. Phys.* **1993**, *98*, 5648; b) C. Lee, W. Yang, R. G. Parr, *Phys. Rev. B*. **1988**, *37*, 785.

[11]   a) P. J. Hay, W. R. Wadt, *J. Chem. Phys.* **1985**, *82*, 270. b) W.R. Wadt, P.J. Hay, J. *Chem. Phys.* **1985**, *82*, 284. c) P.J. Hay, W.R. Wadt, *J. Chem. Phys.* **1985**, *82*, 299.

5. Synthesis of the Heterocubane Cluster [{CpMn}₄(μ₃-P)₄] as a Starting Material for the Formation of Polymeric Coordination Compounds

Sebastian Heinl, Gabor Balázs and Manfred Scheer

unpublished results

- ❖ **All syntheses and characterizations were performed by Sebastian Heinl, unless subsequently noted otherwise**
- ❖ **Manuscript was written by Sebastian Heinl except part for DFT calculations (Gabor Balázs)**
- ❖ **Figures were made by Sebastian Heinl except pictures corresponding to DFT calculations**
- ❖ **DFT calculations were performed and interpreted by Gabor Balázs**
- ❖ **X-ray structure analyses and refinement were performed by Sebastian Heinl**

5.1 Introduction
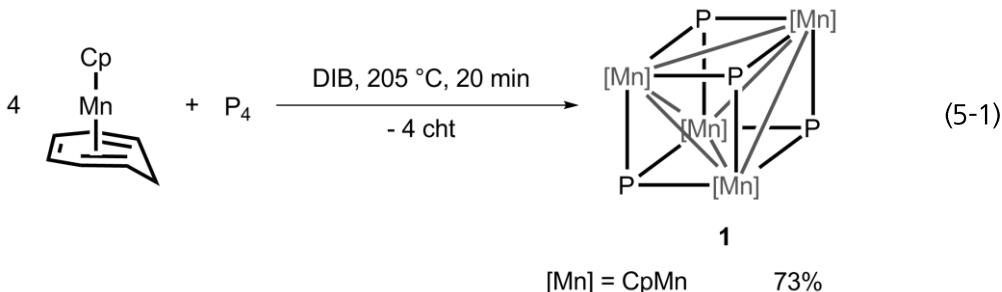
The preparation of porous compounds is of great interest in current research. The most famous representatives are zeolites, built by covalently connected AlO_4 and SiO_4 tetrahedra. They are used in a wide range of applications, not only in commercial detergents but also for catalytical processes.[1] The so called MOFs (Metal-Organic-Frameworks) represent another well-known class of porous compounds, consisting of metal centers linked by multitopic organic linkers (e.g. pyridines, carboxylates). Undoubtable, one big advantage of MOFs is the possible rational structural design, where different pore-sizes can be realized by the right choice of the metal and the linkers. First studies in this field were done by Yaghi et al.,[2] Robson et. al.,[3] Kitagawa et al.[4] and others. Even though a lot of effort was put into the exploration of this field, almost exclusively organic substrates with N, O and S donor atoms are used as linking units. In contrast, the groups of Stang, Hahn and Severin published some examples using organometallic building blocks for the formation of similar compounds, resulting in discrete (macro-) molecules.[5]

In the last decade, we demonstrated that P$_n$ ligand complexes[6] in combination with monovalent coinage metal salts are perfect starting materials to buildup supramolecular assemblies. Especially with [{CpMo(CO)$_2$}$_2$($\mu,\eta^{2:2}$-P$_2$)] and [Cp*Fe(η^5-P$_5$)] (Cp* = C$_5$Me$_5$) together with CuX (X = Cl, Br, I), a wide spectrum of *pseudo*-0D,[7] 1D[8] or 2D[8a,d] frameworks could be realized. For the formation of 3D architectures, multitopic linkers with an appropriate symmetry (e.g. T$_d$, O$_h$) would be needed. All attempts to construct 3D scaffolds by the P$_n$ ligand approach failed so far.

Herein we report on the synthesis and characterization of the heterocubane cluster [(CpMn)$_4$(μ_3-P)$_4$] (**1**) and the first coordination studies of **1** with CuX (X = Cl, Br) resulting in 1D coordination polymers. It is also shown that the coordination of all four P atoms in **1** can be generally achieved.

5.2 Results and Discussion

The restricted number of clusters and complexes of manganese with substituent-free P atoms motivated us to prepare such compounds. The co-thermolysis (20 min) of [CpMn(η^6-cht)] (cht = cycloheptatriene) and P$_4$ in 1,3-diisopropylbenzene (DIB) results in the formation of [Cp$_4$Mn$_4$P$_4$] (**1**) (Equation 5-1). After solvent removal, extraction with CH$_2$Cl$_2$ and cooling to -35 °C, **1** is obtained as dark red to brown needle shaped crystals in yields up to 73%. Decomposition is observed at longer reaction times (metal mirror).

$$4 \quad \underset{\text{Mn}}{\overset{\text{Cp}}{|}} \quad + \quad P_4 \quad \xrightarrow[- 4 \text{ cht}]{\text{DIB, 205 °C, 20 min}} \quad \mathbf{1} \qquad (5\text{-}1)$$

[Mn] = CpMn   73%

Heterocubanes M_4E_4 (M = metal fragment; E = 'naked' element of 15th or 16th group) have been well known in chemistry for decades. Especially O, S and N atoms show a high tendency to form this structural motif; that is why hundreds of compounds could be characterized up to now. Additionally, a very large number of Se and Te heterocubanes have been published. However, only very few phosphorus derivatives are known. Structural characterization was possible for three analogue cobalt compounds $[(Cp^R Co)_4(µ_3\text{-}P)_4]$ (**A**: $Cp^R = C_5H_5$; **B**: $Cp^R = C_5H_4{}^tBu$; **C**: $Cp^R = C_5H_3{}^tBu_2)^{[9]}$ and the tungsten cluster $[\{W(CO)_3Cp^*W\}_2(µ_3\text{-}P)_2\{µ_3\text{-}PW(CO)_5\}_2]$ (**D**).[10] Schumann et al. also proposed a heterocubane structure for $(PhSnP)_4$.[11] Structural similarities can also be found for $[(CpFe)_4(P_2)_2]$,[12] $[(Cp^*Ni)_3(µ_3\text{-}P)(P_4)]$[13] and $[(CpV)_4(P_2)_2]$.[14] Heterocubane clusters with substituent-free As units are also known, but very rare.[12,15]
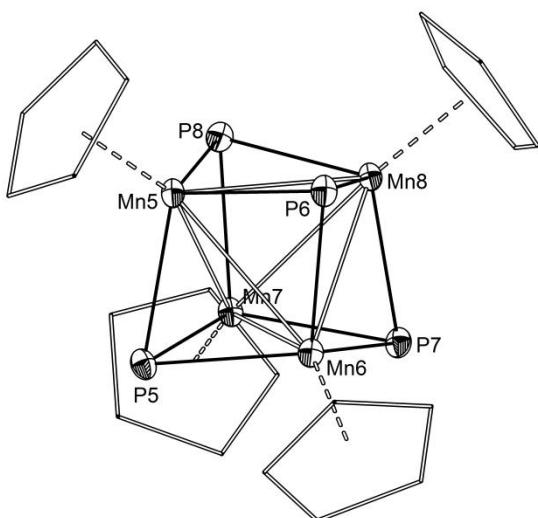
Figure 5.1. Molecular structure of **1** in the crystal. For clarity only one molecule of the asymmetric unit is depicted, C atoms are shown in 'wire-or-stick' model and H atoms and solvent molecules are omitted. Ellipsoids are drawn at 50% probability level. Selected bond lengths [Å] and angles [°]: Mn1-P1 2.2381(8), Mn1-P2 2.2251(9), Mn1-P3 2.2628(10), Mn2-P1 2.2365(9), Mn2-P2 2.2284(9), Mn2-P4 2.2374(10), Mn3-P1 2.2411(10), Mn3-P3 2.2353(9), Mn3-P4 2.2249(9), Mn4-P2 2.2398(10), Mn4-P3 2.2337(9), Mn4-P4 2.2299(9), Mn5-P5 2.2373(9), Mn5-P6 2.2392(8), Mn5-P8 2.2336(10), Mn6-P5 2.2311(8), Mn6-P6 2.2299(9), Mn6-P7 2.2352(10), Mn7-P5 2.2377(10), Mn7-P7 2.2367(9), Mn7-P8 2.2395(9), Mn8-P6 2.2336(10), Mn8-P7 2.2285(9), Mn8-P8 2.2343(9), Mn1-Mn2 2.7320(6), Mn1-Mn3 2.6992(5), Mn1-Mn4 2.6948(8), Mn2-Mn3 2.6997(6), Mn2-Mn4 2.6914(8), Mn3-Mn4 2.7227(7), Mn5-Mn6 2.7095(6), Mn5-Mn7 2.7282(7), Mn5-Mn8 2.7170(5), Mn6-Mn7 2.7182(8), Mn6-Mn8 2.7150(6), Mn7-Mn8 2.7273(8), av. Mn-P 2.235, av. Mn-Mn 2.713.

Synthesis of the Heterocubane Cluster [{CpMn}$_4$(μ_3-P)$_4$] as a Starting Material for the Formation of Polymeric Coordination Compounds

57

Both the ^{1}H NMR and the ^{13}C{^{1}H} NMR spectra (CD$_2$Cl$_2$) show singlets at 4.58 ppm and 82.7 ppm respectively in the expected regions. In contrast, the ^{31}P{^{1}H} NMR spectrum shows an extremely low-field shifted singlet at 1079.8 ppm (slightly broadened, $\omega_{1/2}$ = 31.3 Hz). The signal is about 230 ppm to 600 ppm low field shifted compared to **A-D**, respectively.

The NMR data indicate a highly symmetric molecule, which is confirmed by single crystal X-ray diffraction (Figure 5.1). Compound **1** crystallizes with one solvent molecule CH$_2$Cl$_2$ from concentrated CH$_2$Cl$_2$ solutions in the monoclinic space group $C_{2/c}$. The core of **1** can be described as a Mn$_4$ tetrahedron, wherein the faces are capped by P atoms, resulting in a heterocubane structure. In comparison, the central cores of the structures of **A**, **C** and **D** are much more distorted from a perfect cube structure than **1** is. The four Mn atoms in **1** are coordinatively saturated by Cp ligands. The Mn–Mn and Mn–P bond lengths vary from 2.6914(8) Å to 2.7320(6) Å and from 2.2249(9) Å to 2.2411(10) Å, respectively.

The number of valence electrons of the Mn atoms can be calculated classically as 18 and the Mn centers have a formal oxidation state of +4. To gain more insight into the electronic structure of **1** DFT calculations have been performed. The geometry of **1** has been optimized in different spin states. Their relative energies are listed in Table S5.1. According to the calculations **1** has a singlet ground state. The triplet spin state is with 70.27 kJ·mol^{-1} higher in energy. All other spin states are more than 100 kJ·mol^{-1} higher in energy. Interestingly, the spin state of **1** has a strong influence on the geometry. In the singlet spin state the optimized geometry is very close to the observed experimental one, having short Mn–Mn distances (2.705 Å) which are very similar to the experimentally determined distance of 2.713 Å (average). By stepwise increasing the spin multiplicity the stepwise elongation of one Mn–Mn distance is observed. For example in the triplet spin state there are one longer Mn–Mn distance of 3.189 Å and five shorter ones of 2.714 Å (average). In comparison with the experimental found parameters it is indicative that **1** has a singlet spin state. The molecular orbitals (MO) as well as the localized molecular orbitals (LMO) of **1** show the presence of Mn$_2$P$_2$ four center bonds (2e$^-$) and the presence of lone pairs on the phosphorus atoms (Figure S5.18 and Figure S5.19). The Wiberg bond index indicates a Mn–Mn bond order of 0.33, while the Mn–P bond order is close to unity (0.92).

The four P atoms in **1** are tetrahedral orientated and bear a lone pair each. This should be a perfect building block for the formation of three-dimensional networks. By slow diffusion of CH$_3$CN solutions of CuX (X = Cl, Br) into CH$_2$Cl$_2$ solutions of **1**, some black needle-shaped crystals and plenty of off-white to brown voluminous, amorphous powder were obtained. The reaction with a 1:1 stoichiometry of **1** and CuX results in a still colored surnatant solution and a larger amount of crystals. In contrast, a 1:5 stoichiometry results in a colorless solution and more powder. The crystals as well as the powder are totally insoluble in all common solvents.
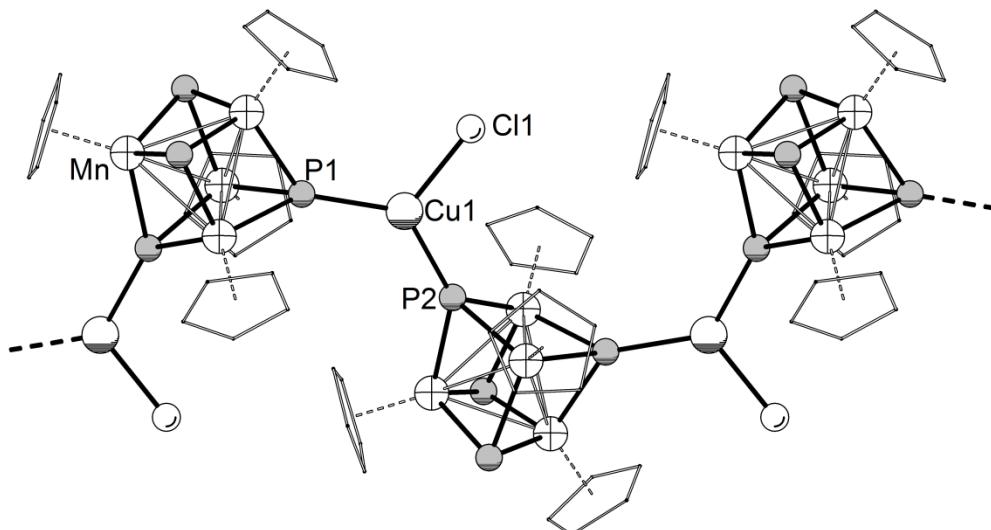
Figure 5.2. Section of the 1D zigzag chain [{(CpMn)$_4$(μ^3-P)$_4$}(CuCl)]$_n$ (**2-Cl**) in the crystal. View along crystallographic c-axis. For clarity reasons the C atoms are shown in 'wire-or-stick' model and H atoms and solvent molecules are omitted. Because of the isostructural constitution of **2-Br**, its structure is not depicted. Selected bond lengths [Å] and angles [°] of **2-Cl**: P1-Cu1 2.248(1), P2-Cu1 2.252(1), Cu1-Cl1 2.245(2), P1-Cu1-P2 129.64(5), P1-Cu1-Cl1 117.26(5), P2-Cu1-Cl1 112.85(5), av. Mn-P 2.228, av. Mn-Mn 2.720. Selected bond lengths [Å] and angles [°] of **2-Br** (for labeling see Supporting Information): P1-Cu1 2.248(3), P4-Cu1 2.252(3), Cu1-Br1 2.372(8), Cu1-Br2 2.324(5), P1-Cu1-P4 129.0(1), P1-Cu1-Br1 119.8(2), P1-Cu1-Br2 115.1(1), P4-Cu1-Br1 108.0(2), P4-Cu1-Br2 115.9(1), av. Mn-P 2.231, av. Mn-Mn 2.718.

The crystals were characterized by single crystal X-ray diffraction. The crystal structures illustrate zigzag like 1D coordination polymers with the sum formulas [{(CpMn)$_4$(μ_3-P)$_4$}(CuX)]$_n$ (**2-Cl**: X = Cl; **2-Br**: X = Br) (Figure 5.2).[16] However, in case of **2-Cl**, one molecule CH$_2$Cl$_2$ co-crystallizes per formula unit, which is not the case for **2-Br**. Two of the P atoms in **2-Cl** and **2-Br** coordinate to CuX units resulting in a trigonal planar coordination of the Cu atoms. In **2-Br** a disorder of the Br atom over two positions can be observed. With angular sums around the Cu centers of 359.8° for **2-Cl** and 356.8° and 360.0° respectively for **2-Br** this is an indication for almost perfect planarity. The polymeric strands are orientated parallel to each other.

The off-white powder was found to be amorphous, as indicated by X-ray powder diffraction. Also ^{31}P{^{1}H} MAS NMR did not show any signals. To further analyze the amorphous powders, it has been washed several times with CH$_3$CN and dried carefully in vacuum. To get a hint towards the composition, elemental analyses were carried out. With the assumption of complete removal of the solvent and excesses of CuX, the result fits best for a **1**:CuX ratio of roughly 1:3. This might be a hint for the coordination of more than two of the P atoms to CuX. Unfortunately, a definite structural statement on this cannot be made.

For the formation of three-dimensional networks, the coordination of all four P atoms in **1** is necessary. To check whether this is possible at all, **1** was reacted with [CpMn(CO)$_2$(thf)], and in fact, the coordination of only one to all four P atoms can be achieved, resulting in [{(CpMn)$_4$(μ_3-P)$_4${CpMn(CO)$_2$}$_n$] (**3a**: n = 1; **3b**: n = 2; **3c**: n = 3; **3d**: n = 4).[17] In a 1:1

stoichiometry the mono- and di-coordination is obtained and in a 1:4 stoichiometry the tri- and tetra-coordination. Compounds **3a-d** can be separated by column chromatography. However, complex **3a** elutes simultaneously with unreacted cluster **1**.

All four compounds were crystallized as solvates from concentrated CH_2Cl_2 solutions. The molecular structures are depicted in Figure 5.3. The average bond lengths between the P atoms and the {CpMn(CO)₂} fragments increase with the degree of coordination (**3a**: 2.260 Å; **3b**: 2.262 Å; **3c**: 2.272 Å; **3d**: 2.287 Å). The sterical parameters of the heterocubane cores are also affected by the coordination. While the average Mn–Mn and Mn–P bond lengths in **3a** are almost identical in comparison to **1**, they increase steadily from **3b** to **3d** (**1**: av. Mn-P 2.235 Å, av. Mn-Mn 2.713 Å; **3d**: av. Mn-P 2.258 Å, av. Mn-Mn 2.757 Å). The raise of the Mn–Mn and Mn–P bond lengths effectively result in an expansion of the heterocubane cages. The volumes of the Mn_4P_4 cages vary in the same way like the bond lengths. With just one
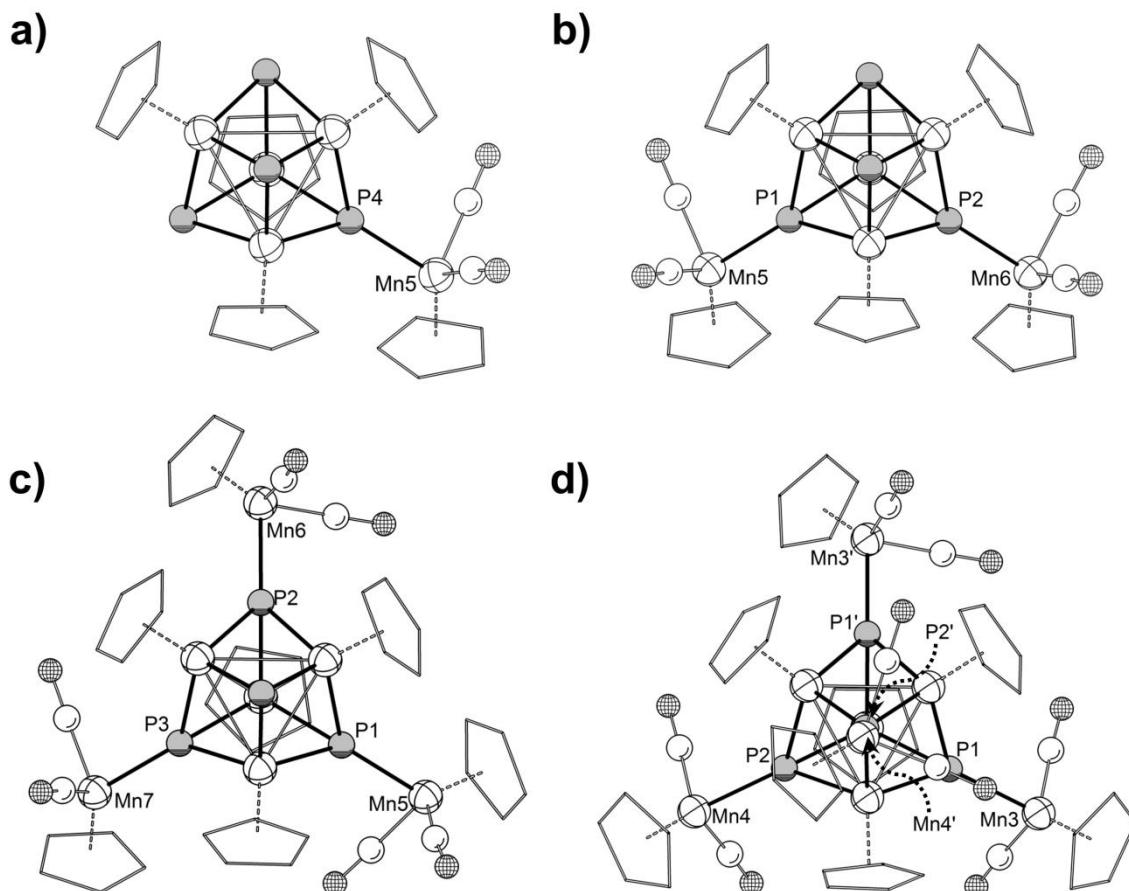
Figure 5.3. Molecular structures in the crystals: a) **3a**, b) **3b**, c) **3c**, d) **3d**. For clarity C atoms are shown in 'wire-or-stick' model and H atoms and solvent molecules are omitted. In case of the disordered molecule **3b** only the main part is depicted. Selected Mn–P bond lengths [Å] in **3a**: Mn5-P4 2.2603(8), av. Mn-P 2.234, av. Mn-Mn 2.719; in **3b**: Mn5-P1 2.2576(10), Mn6-P2 2.2672(8), av. Mn-P 2.246, av. Mn-Mn 2.740; in **3c**: Mn5-P1 2.2779(8), Mn6-P2 2.2778(7), Mn7-P3 2.2616(9) av. Mn-P 2.245, av. Mn-Mn 2.748; in **3d**: Mn3-P1 2.2928(7), Mn4-P2 2.2818(11), av. Mn-P 2.258, av. Mn-Mn 2.757. Average values are calculated only from the heterocubane cores.

coordination it remains almost unaffected, but starting from the second coordination in **3b** the volume increases constantly ($V(\mathbf{1})$ = 9.159 Å^3; $V(\mathbf{3a})$ = 9.151 Å^3; $V(\mathbf{3b})$ = 9.333 Å^3; $V(\mathbf{3c})$ = 9.372 Å^3; $V(\mathbf{3d})$ = 9.490 Å^3).[18] The core overall expands by 3.5%. This observation might be explained by an electron withdrawing effect of the {CpMn(CO)₂} fragments.

In conclusion, we have reported on the synthesis of the novel cluster [Cp₄Mn₄P₄] (**1**) with a central heterocubane structure in good yields. Compound **1** was characterized by X-ray diffraction, spectroscopic measurements and DFT calculations. Reaction with CuX (X = Cl, Br) leads to the formation of 1D coordination polymers with zigzag-like structures. As a proof of concept it is also demonstrated that all four P atoms in **1** can be addressed for coordination, which was exemplified by the coordination of {CpMn(CO)₂} moieties. An interesting cluster volume expansion is observed, correlating with the degree of coordination. The formation of 3D networks starting from **1** will be in focus for future work.

5.3 Experimental Part

General Remarks:

All experiments were carried out under an atmosphere of dry argon or nitrogen using glovebox and schlenk techniques. Solvents were purified, dried and degassed prior to use. P₄, CuCl and CuBr were available, [CpMn(cht)][19] and [CpMn(CO)₂(thf)][20] were prepared according to literature procedures. The NMR spectra were measured on a Bruker Avance 300, 400 or 600 spectrometer. EI-MS spectra were measured on a Finnigan MAT SSQ 710A mass spectrometer and FD-MS spectra on a Finnigan MAT 95 mass spectrometer. The elemental analyses were determined on a Vario EL III apparatus.

Synthesis of [Cp₄Mn₄P₄] (1):

[CpMn(cht)] (0.93 g, 4.4 mmol) and P₄ (1.8 g, 14.5 mmol) are dissolved 50 mL 1,3-diisopropylbenzene and refluxed for 20 min. The solution becomes dark brown and sometimes a metal mirror is observed. The solvent and unreacted P₄ are removed in vacuum at 60 °C. The residue is triturated with 25 mL CH₂Cl₂ and filtered through Celite. This is repeated with a further portion of 10 mL CH₂Cl₂. The collected filtrates are condensed to 15 mL and cooled to -35 °C. The obtained crystals are decanted and dried in vacuum. Another portion of crystals is obtained from the mother liquor (485 mg, 73%).

1: [C₂₀H₂₀Mn₄P₄] calc.: C, 39.77; H, 3.34. found: C, 39.48; H, 3.49. ESI-MS (CH₂Cl₂): *m/z* (%) = 603.9 (51%, [M]$^+$) , 422.0 (78%, [Cp₃Mn₃P₂]$^+$), 185.1 (48%, [Cp₂Mn]$^+$), 66.1 (100%, [CpH]$^+$). ^{1}H NMR (CD₂Cl₂): δ [ppm] = 4.58 (s, C₅H₅). ^{31}P{^{1}H} NMR (CD₂Cl₂): δ [ppm] = 1079.8 (s, ω$_{1/2}$ = 31 Hz, P). ^{13}C{^{1}H} NMR (CD₂Cl₂): δ [ppm] = 82.7 (C₅H₅).

Synthesis of [{Cp₄Mn₄P₄}{CuX}]ₙ (2-Cl: X = Cl; 2-Br: X = Br):

A solution of CuX (83 μmol) in 10 mL CH₃CN is layered over a solution of [Cp₄Mn₄P₄] (50 mg, 83 μmol) in 10 mL CH₂Cl₂. After complete diffusion, black crystals of **2-Cl** and **2-Br**, respectively, and an off-white powder is obtained. The heterogeneous mixture is shaken carefully, the crystals are allowed to settle down and the surnatant suspension is decanted via cannula. The crystals are washed twice with 15 mL CH₃CN in the same manner as before and dried in vacuum. The collected liquids are filtrated, washed with 15 mL CH₃CN three-times and dried in vacuum.

2-Cl: Crystalline yield of **2-Cl**: 42 mg (72%); Yield (Powder): 5 mg.

[$C_{20}H_{20}Mn_4P_4CuCl$] calc.: C, 34.17; H, 2.87. found: C, 39.94; H, 2.92. Powder found: C, 24.64; H, 2.55; N, 2.25.

2-Br: Crystalline yield of **2-Br**: 11 mg (18%); Yield (Powder): 5 mg.

[$C_{20}H_{20}Mn_4P_4CuBr$] calc.: C, 32.14; H, 2.70. found: C, 31.86; H, 2.79. Powder found: C, 26.21; H, 2.77; N, traces.

Synthesis of [{(CpMn)₄(μ₃-P)₄}{CpMn(CO)₂}ₙ] (3a: n = 1; 3b: n = 2):

A solution of [CpMn(CO)₃] (2.04 g, 10 mmol) and cycloheptatriene (3.0 g, 3.4 mL, 32.6 mmol) in 150 mL 1,3-diisopropylbenzene is irradiated for 20 h (CO bands have not completely vanished). After P_4 (3.72 g, 30 mmol) was added, the reaction mixture is refluxed for 60 min. The solvent and unreacted P_4 are removed in vacuum at 60 °C. The residue is triturated with 25 mL CH₂Cl₂ and filtered through Celite. This is repeated with a further portion of 10 mL CH₂Cl₂. A column chromatography (silica, 20x4 cm, CH₂Cl₂) affords a small brown fraction of **3b**. With THF another brown band is collected which is composed of a 3:1 mixture of **3a** and **1**, as indicated by NMR spectroscopy and elemental analysis. An analytically pure sample of **3b** can be obtained from concentrated CH₂Cl₂ solution. A crystalline mixture of **3a** and **1** is also obtained from concentrated CH₂Cl₂ solution.

3a (as 3:1 mixture with **1**): Yield: 215 mg → 180 mg pure **3a** (9%).

3[$C_{27}H_{25}Mn_5O_2P_4$] * **1** calc.: C, 40.79; H, 3.28. found: C, 41.22; H, 3.32. ESI-MS (CH₂Cl₂): *m/z* (%) = 779.7 (12%, [M]⁺), 723.7 (9%, [Cp₅Mn₅P₄]⁺), 603.7 (61%, [Cp₄Mn₄P₄]⁺), 510.8 (30%, [Cp₄Mn₄P]⁺), 421.9 (100%, [Cp₃Mn₃P₂]⁺), 301.9 (16%, [Cp₂Mn₂P₂]⁺), 185.0 (91%, [Cp₂Mn]⁺), 120.0 (65%, [CpMn]⁺). IR (CH₂Cl₂): ν_{CO} [cm⁻¹] = 1917 (s), 1858 (s). ¹H NMR (CD₂Cl₂): δ [ppm] = 4.59 (s-br, ω₁/₂ = 10 Hz, 5H, C₅H₅), 4.62 (s-br, ω₁/₂ = 5 Hz, 15H, C₅H₅), 4.68 (d, ³J_PH = 1.3 Hz, 5H, C₅H₅); 4.53 (s, 6.8H, C₅H₅ from **1**). ³¹P{¹H} NMR (CD₂Cl₂): δ [ppm] = 915.0 (s, 1P), 1091.8 (s-br, ω₁/₂ = 107 Hz, 3P); 1079.7 (s, 1P from **1**). ¹³C{¹H} NMR (CD₂Cl₂): δ [ppm] = 82.6 (s, C₅H₅, superimposed with signal of **1**) 83.1 (q, ³J_PC = 4 Hz, C₅H₅), 85.3 (m, C₅H₅), 234.8 (d, ²J_PC = 19 Hz, CO).

3b: Yield: 13 mg (<1%).

ESI-MS (CH$_2$Cl$_2$): *m/z* (%) = 955.5 (10%, [M]$^+$), 899.6 (2%, [Cp$_6$Mn$_6$P$_4$(CO)$_2$]$^+$), 779.6 (17%, [Cp$_5$Mn$_5$P$_4$(CO)$_2$]$^+$), 723.6 (5%, [Cp$_5$Mn$_5$P$_4$]$^+$), 658.6 (10%, [Cp$_4$Mn$_5$P$_4$]$^+$), 603.7 (33%, [Cp$_4$Mn$_4$P$_4$]$^+$), 510.8 (71%, [Cp$_4$Mn$_4$P]$^+$), 421.9 (16%, [Cp$_3$Mn$_3$P$_2$]$^+$), 325.9 (21%, [Cp$_2$Mn$_3$P]$^+$), 301.9 (19%, [Cp$_2$Mn$_2$P$_2$]$^+$), 207.0 (44%, [CpMn(CO)$_2$P]$^+$), 185.0 (77%, [Cp$_2$Mn]$^+$), 181.1 (48%, [CpMnP$_2$]$^+$), 119.9 (83%, [CpMn]$^+$). IR (CH$_2$Cl$_2$): ν_{CO} [cm^{-1}] = 1917 (s), 1858 (s). ^{1}H NMR (CD$_2$Cl$_2$): δ [ppm] = 4.77 (d, $^3J_{PH}$ = 1.1 Hz, 10H, C$_5$H$_5$), 4.81 (s-br, $\omega_{1/2}$ = 11 Hz, 20H, C$_5$H$_5$). ^{31}P{^{1}H} NMR (CD$_2$Cl$_2$): δ [ppm] = 922 (s-br, $\omega_{1/2}$ ≈ 310 Hz, 1P), δ 925 (s-br, $\omega_{1/2}$ ≈ 730 Hz, 1P), 1100 (s-br, $\omega_{1/2}$ ≈ 560 Hz, 1P), 1105 (s-br, $\omega_{1/2}$ ≈ 420 Hz, 1P). ^{13}C{^{1}H} NMR (CD$_2$Cl$_2$): δ [ppm] = 82.9 (C$_5$H$_5$), 85.9 (C$_5$H$_5$), 88.9 (C$_5$H$_5$); CO signal is not observed.

As expected, the ^{1}H and ^{13}C{^{1}H} NMR spectra show only one set of signals. However, the ^{31}P{^{1}H} NMR show two sets of signals. This may likely be explained by two different rotamers.

Synthesis of [{(CpMn)$_4$(μ_3-P)$_4${CpMn(CO)$_2$}$_n$] (3c: n = 3; 3d: n = 4):

According to literature procedure a solution of [CpMn(CO)$_2$(thf)] in 50 mL is prepared from [CpMn(CO)$_3$] (200 mg, 0.99 µmol). The solution is added to a solution of [Cp$_4$Mn$_4$P$_4$] (100 mg, 0.16 µmol) in 10 mL THF. The mixture is dried under vacuum, the residue is dissolved in 15 mL toluene and refluxed for 3 h. The solvent is removed again and the residue is washed with hexane. A column chromatography (silica, 15x4 cm, CH$_2$Cl$_2$) first affords a brown fraction of **3d** followed by another brown band of **3c**. Analytically pure samples can be obtained from concentrated CH$_2$Cl$_2$ solutions.

3c: Yield: 51 mg (28%).

[C$_{41}$H$_{35}$Mn$_7$O$_6$P$_4$] * 1.5 CH$_2$Cl$_2$ calc.: C, 40.53; H, 3.04. found: C, 41.08; H, 3.38. ESI-MS (CH$_2$Cl$_2$): *m/z* (%) = 1131.4 (< 1%, [M]$^+$), 955.5 (4%, [Cp$_6$Mn$_6$P$_4$(CO)$_4$]$^+$), 723.6 (5%, [Cp$_5$Mn$_5$P$_4$]$^+$), 421.8 (16%, [Cp$_3$Mn$_3$P$_2$]$^+$), 207.0 (100%, [CpMn(CO)$_2$P]$^+$), 185.0 (42%, [Cp$_2$Mn]$^+$), 119.9 (57%, [CpMn]$^+$). IR (CH$_2$Cl$_2$): ν_{CO} [cm^{-1}] = 1918 (s), 1860 (s). ^{1}H NMR (CD$_2$Cl$_2$): δ [ppm] = 4.75 (d, $^3J_{PH}$ = 1.2 Hz, 15H, C$_5$H$_5$), 4.86 (q, $^3J_{PH}$ = 1.6 Hz, 5H, C$_5$H$_5$), 4.91 (s-br, $\omega_{1/2}$ = 9 Hz, 15H, C$_5$H$_5$). ^{31}P{^{1}H} NMR (CD$_2$Cl$_2$): δ [ppm] = 932.1 (s-br, $\omega_{1/2}$ = 288 Hz, 3P), 1103.5 (s-br, $\omega_{1/2}$ = 348 Hz, 1P). ^{13}C{^{1}H} NMR (CD$_2$Cl$_2$): δ [ppm] = 81.8 (C$_5$H$_5$); CO signal is not observed.

3d: Yield: 39 mg (19%).

[C$_{48}$H$_{40}$Mn$_8$O$_8$P$_4$] calc.: C, 44.07; H, 3.08. found: C, 43.68; H, 3.38. ESI-MS (CH$_2$Cl$_2$): *m/z* (%) = 1308.3 (< 1%, [M]$^+$), 1131.4 (< 1%, [M]$^+$), 955.5 (2%, [Cp$_6$Mn$_6$P$_4$(CO)$_4$]$^+$), 421.8 (8%, [Cp$_3$Mn$_3$P$_2$]$^+$), 207.0 (37%, [CpMn(CO)$_2$P]$^+$), 185.0 (86%, [Cp$_2$Mn]$^+$), 119.9 (100%, [CpMn]$^+$). IR (CH$_2$Cl$_2$): ν_{CO} [cm^{-1}] = 1921 (s), 1862 (s). ^{1}H NMR (CD$_2$Cl$_2$): δ [ppm] = 4.77 (d, $^3J_{PH}$ = 1.1 Hz, 20H, C$_5$H$_5$), 5.0 (s-br, $\omega_{1/2}$ = 13 Hz, 20H, C$_5$H$_5$). ^{31}P{^{1}H} NMR (CD$_2$Cl$_2$): δ [ppm] = 940 (very broad,

$\omega_{1/2} \approx 2000$ Hz). ^{13}C{^{1}H} NMR (CD$_2$Cl$_2$): δ [ppm] = 81.9 (C$_5$H$_5$), 82.2 (C$_5$H$_5$); CO signal is not observed.

5.4 References

[1] a) A. Corma, *Chem. Rev.* **1997**, *97*, 2373-2420. b) J. Čejka, G. Centi, J. Perez-Pariente, W. J. Roth, *Catal. Today* **2012**, *179*, 2-15.

[2] a) O. M. Yaghi, G. Li, *Angew. Chem., Int. Ed.* **1995**, *34*, 207-209. b) O. M. Yaghi, H. Li, *J. Am. Chem. Soc.* **1995**, *117*, 10401-10402.

[3] a) B. F. Hoskins, R. Robson, *J. Am. Chem. Soc.* **1990**, *112*, 1546-1554. b) S. R. Batten, B. F. Hoskins, R. Robson, *J. Am. Chem. Soc.* **1995**, *117*, 5385-5386.

[4] a) S. Kitagawa, S. Matsuyama, M. Munakata, T. Emori, *J. Chem. Soc., Dalton Trans.* **1991**, 2869-2874. b) S. Kitagawa, S. Kawata, Y. Nozaka, M. Munakata, *J. Chem. Soc., Dalton Trans.* **1993**, 1399-1404.

[5] a) B. Olenyuk, J. A. Whiteford, A. Fechtenkotter, P. J. Stang, *Nature* **1999**, *398*, 796-799. b) S. Leininger, B. Olenyuk, P. J. Stang, *Chem. Rev.* **2000**, *100*, 853-908. c) K. Severin, *Coord. Chem. Rev.* **2003**, *245*, 3-10. d) K. Severin, *Chem. Commun.* **2006**, 3859-3867. e) M. Schmidtendorf, T. Pape, F. E. Hahn, *Angew. Chem., Int. Ed.* **2012**, *51*, 2195-2198.

[6] Complexes, mainly of transition metals, with unsubstituted P_n ligands. P atoms are only bound to the metal atoms and/or other P atoms.

[7] a) J. Bai, A. V. Virovets, M. Scheer, *Science* **2003**, *300*, 781-783. b) M. Scheer, J. Bai, B. P. Johnson, R. Merkle, A. V. Virovets, C. E. Anson, *Eur. J. Inorg. Chem.* **2005**, 4023-4026. c) M. Scheer, A. Schindler, R. Merkle, B. P. Johnson, M. Linseis, R. Winter, C. E. Anson, A. V. Virovets, *J. Am. Chem. Soc.* **2007**, *129*, 13386-13387.

[8] a) J. Bai, A. V. Virovets, M. Scheer, *Angew. Chem., Int. Ed.* **2002**, *41*, 1737-1740. b) M. Scheer, L. J. Gregoriades, A. V. Virovets, W. Kunz, R. Neueder, I. Krossing, *Angew. Chem., Int. Ed.* **2006**, *45*, 5689-5693. c) S. Welsch, L. J. Gregoriades, M. Sierka, M. Zabel, A. V. Virovets, M. Scheer, *Angew. Chem., Int. Ed.* **2007**, *46*, 9323-9326. d) F. Dielmann, A. Schindler, S. Scheuermayer, J. Bai, R. Merkle, M. Zabel, A. V. Virovets, E. V. Peresypkina, G. Brunklaus, H. Eckert, M. Scheer, *Chem. Eur. J.* **2012**, *18*, 1168-1179. e) M. Scheer, L. Gregoriades, J. Bai, M. Sierka, G. Brunklaus, H. Eckert, *Chem. Eur. J.* **2005**, *11*, 2163-2169. f) B. Attenberger, S. Welsch, M. Zabel, E. Peresypkina, M. Scheer, *Angew. Chem., Int. Ed.* **2011**, *50*, 11516-11519. g) J. Bai, E. Leiner, M. Scheer, *Angew. Chem., Int. Ed.* **2002**, *41*, 783-786.

[9] a) G. L. Simon, L. F. Dahl, *J. Am. Chem. Soc.* **1973**, *95*, 2175-2183. b) O. J. Scherer, S. Weigel, G. Wolmershäuser, *Chem. Eur. J.* **1998**, *4*, 1910-1916.

[10] M. Scheer, E. Leiner, P. Kramkowski, M. Schiffer, G. Baum, *Chem. Eur. J.* **1998**, *4*,

Synthesis of the Heterocubane Cluster [{CpMn}$_4$(μ$_3$-P)$_4$] as a Starting Material for the Formation of Polymeric Coordination Compounds

65

1917-1923.

[11]   H. Schumann, H. Benda, *Angew. Chem., Int. Ed.* **1968**, *7*, 813-813.

[12]   O. J. Scherer, G. Kemény, G. Wolmershäuser, *Chem. Ber.* **1995**, *128*, 1145-1148.

[13]   O. J. Scherer, J. Braun, G. Wolmershäuser, *Chem. Ber.* **1990**, *123*, 471-475.

[14]   M. Herberhold, G. Frohmader, W. Milius, *J. Organomet. Chem.* **1996**, *522*, 185-196.

[15]   a) B. P. Johnson, M. Schiffer, M. Scheer, *Organometallics* **2000**, *19*, 3404-3409.

[16]   The obtained crystals of the reactions with a different stoichiometry show the same crystal structures.

[17]   Compounds **3a** and **3b** were not obtained by the direct reaction of **1** with [CpMn(CO)$_2$(thf)], but incidentally by the co-thermolysis of [CpMn(cht)], [CpMn(CO)$_2$(thf)] and P$_4$. The reason for this was a failed upscaling experiment for the preparation of [CpMn(cht)]. Because the high concentration of [CpMn(CO)$_3$] has been too high, the irradiation could not be achieved quantitatively.

[18]   The heterocubane scaffold is broken up into one Mn$_4$ pyramid and four Mn$_3$P pyramids for the volume calculations (Heron's formula and V = 1/3*b*h).

[19]   a) P. L. Pauson, J. A. Segal, *J. Organomet. Chem.* **1973**, *63*, C13-C14. b) P. L. Pauson, J. A. Segal, *J. Chem. Soc., Dalton Trans.* **1975**, 2387-2392.

[20]   W. A. Herrmann, R. Serrano, J. Weichmann, *J. Organomet. Chem.* **1983**, *246*, c57-c60.

5.5 Supplementary Information

NMR Investigations:
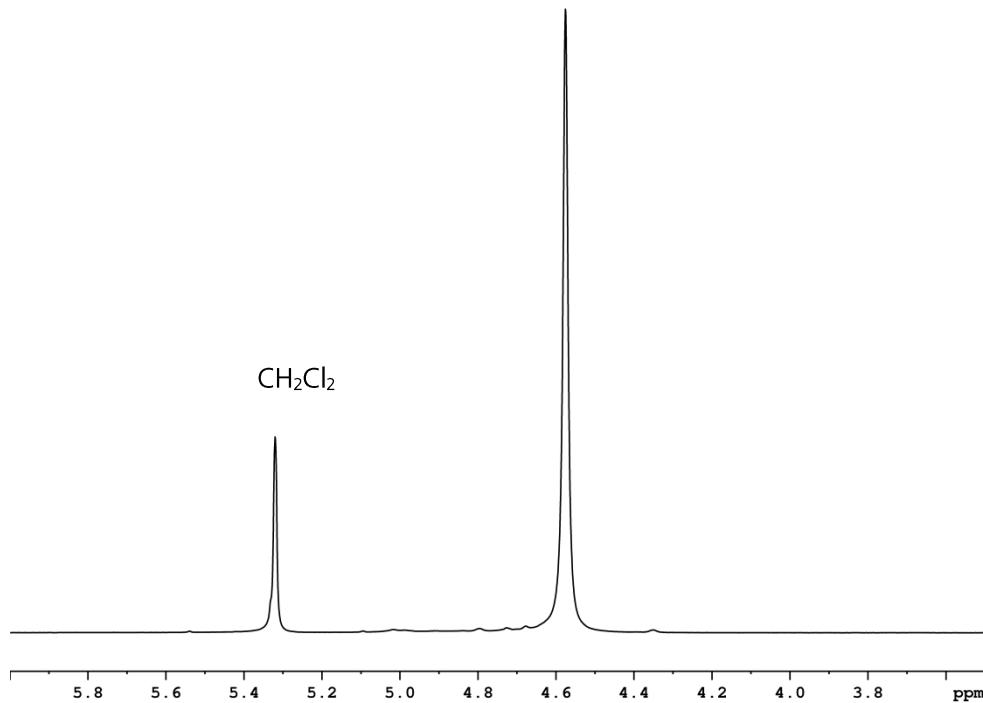
Figure S5.1. ^{1}H NMR spectrum of **1** in CD$_2$Cl$_2$ at 298 K.
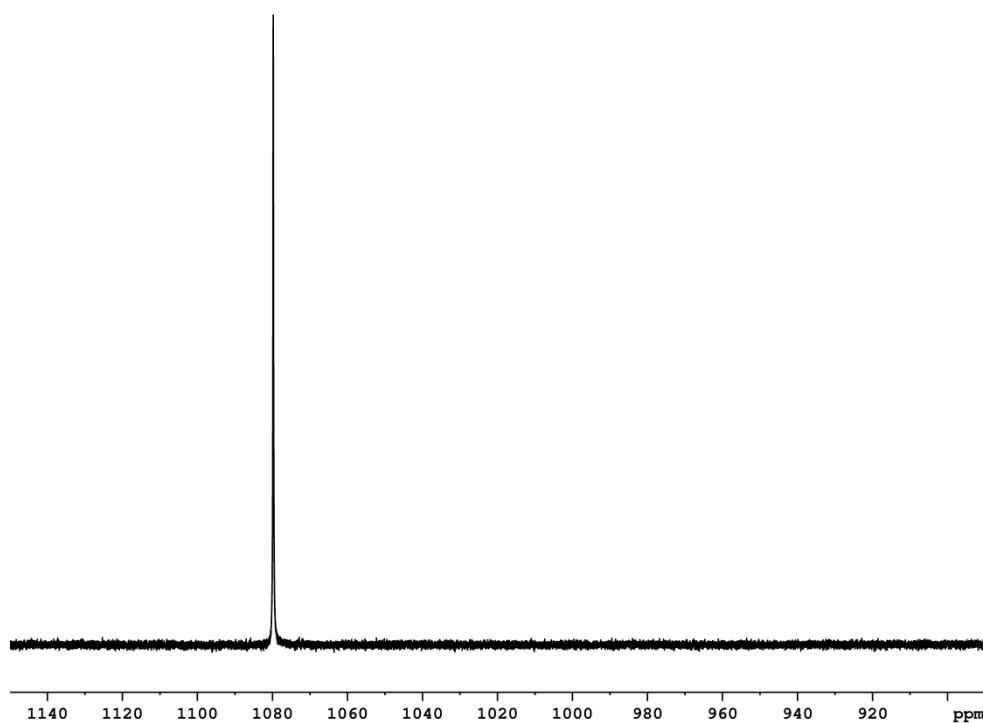
Figure S5.2. ^{31}P{^{1}H} NMR spectrum of **1** in CD$_2$Cl$_2$ at 298 K.

Synthesis of the Heterocubane Cluster [{CpMn}$_4$(μ_3-P)$_4$] as a Starting Material for the Formation of Polymeric Coordination Compounds

67
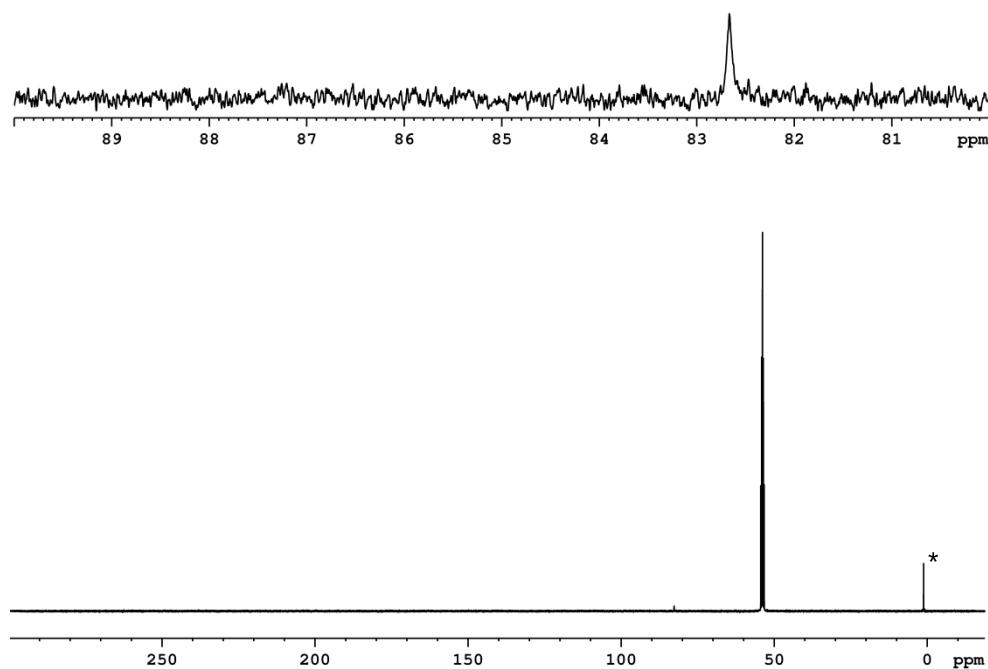
Figure S5.3. ^{13}C{^{1}H} NMR spectrum of **1** in CD$_2$Cl$_2$ at 298 K. Signal marked with an asterisk arises from silicon grease.
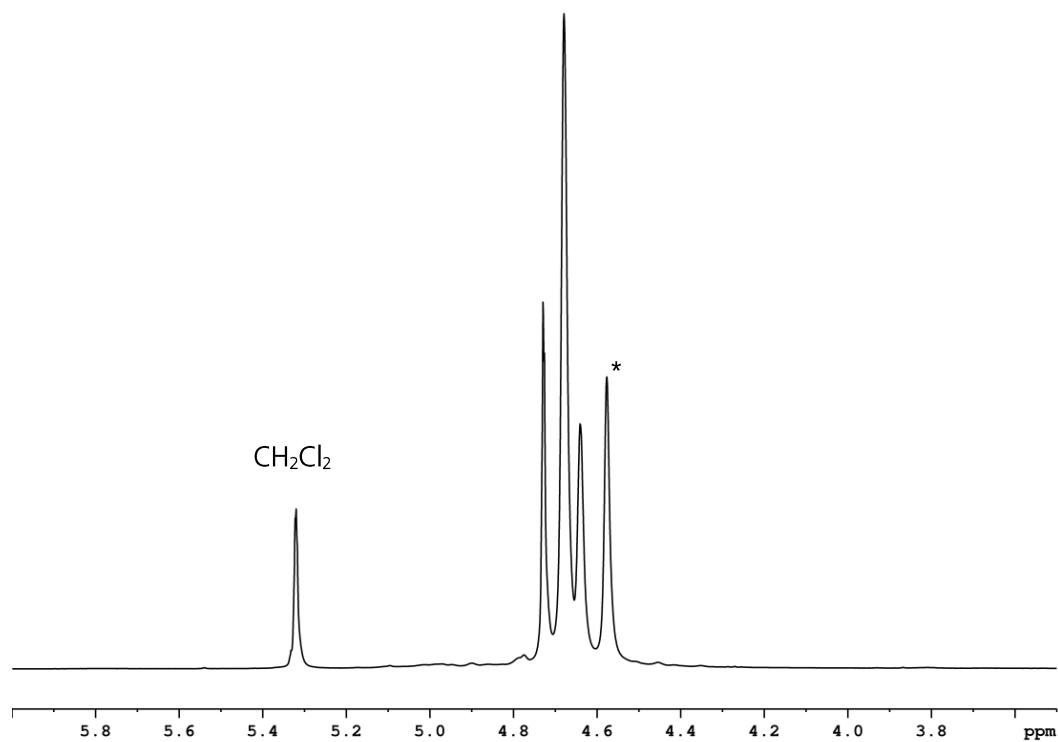

**Figure S5.4.** ^{1}H NMR spectrum of **3a** in CD$_2$Cl$_2$ at 298 K. Signal marked with an asterisk arises from impurities of **1**.
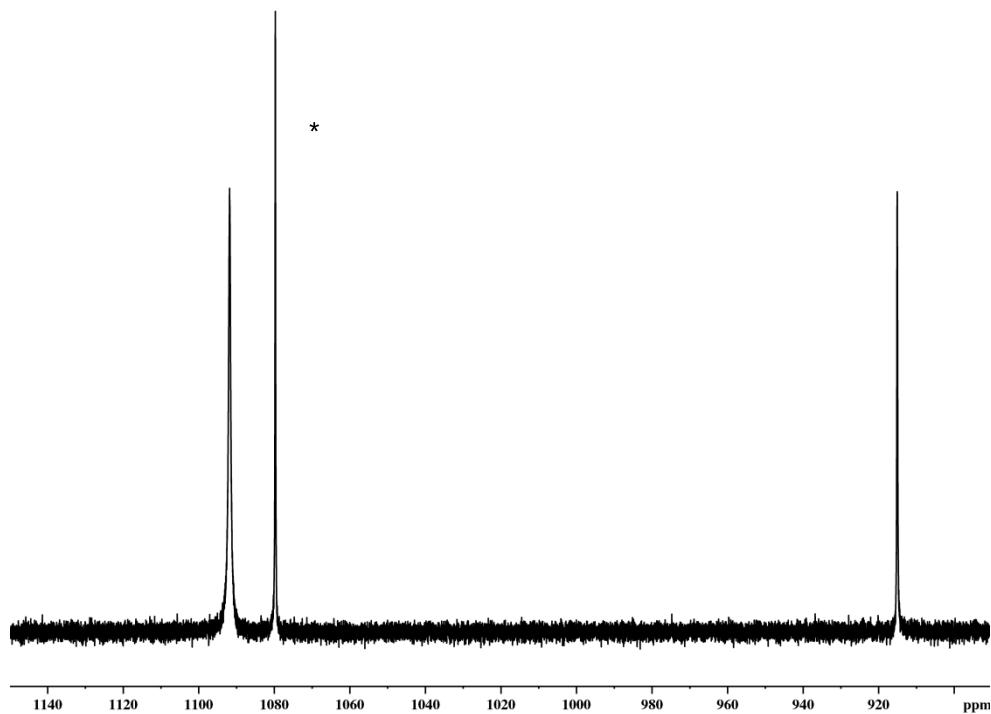
Figure S5.5. ^{31}P{^{1}H} NMR spectrum of **3a** in CD$_2$Cl$_2$ at 298 K. Signal marked with an asterisk arises from impurities of **1**.
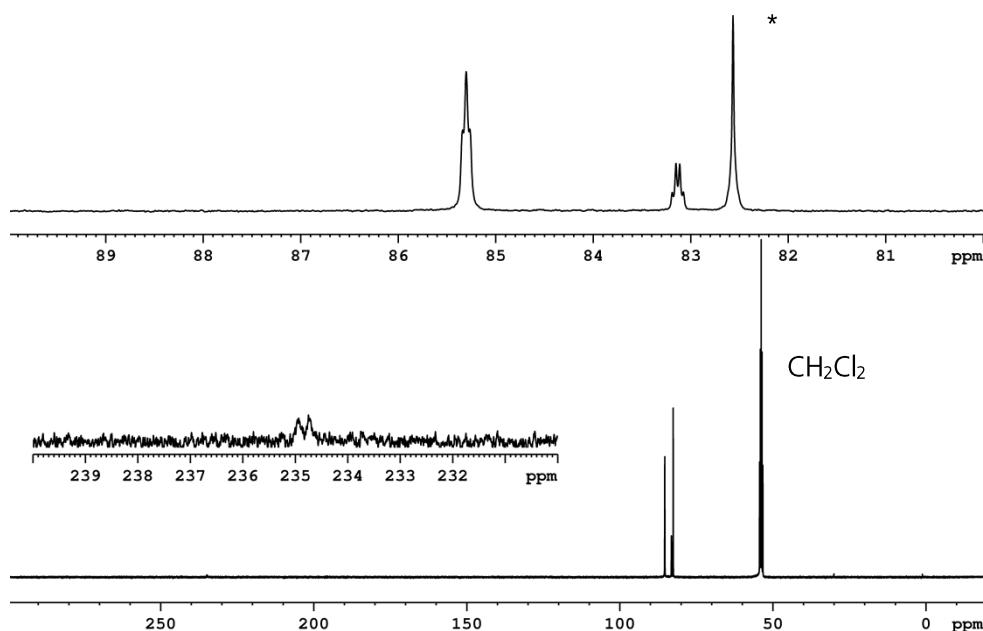
Figure S5.6. ^{13}C{^{1}H} NMR spectrum of **3a** in CD$_2$Cl$_2$ at 298 K. Signal marked with an asterisk is superimposed with signal of **1**.

Synthesis of the Heterocubane Cluster [{CpMn}$_4$(μ_3-P)$_4$] as a Starting Material for the Formation of Polymeric Coordination Compounds

69

CH$_2$Cl$_2$
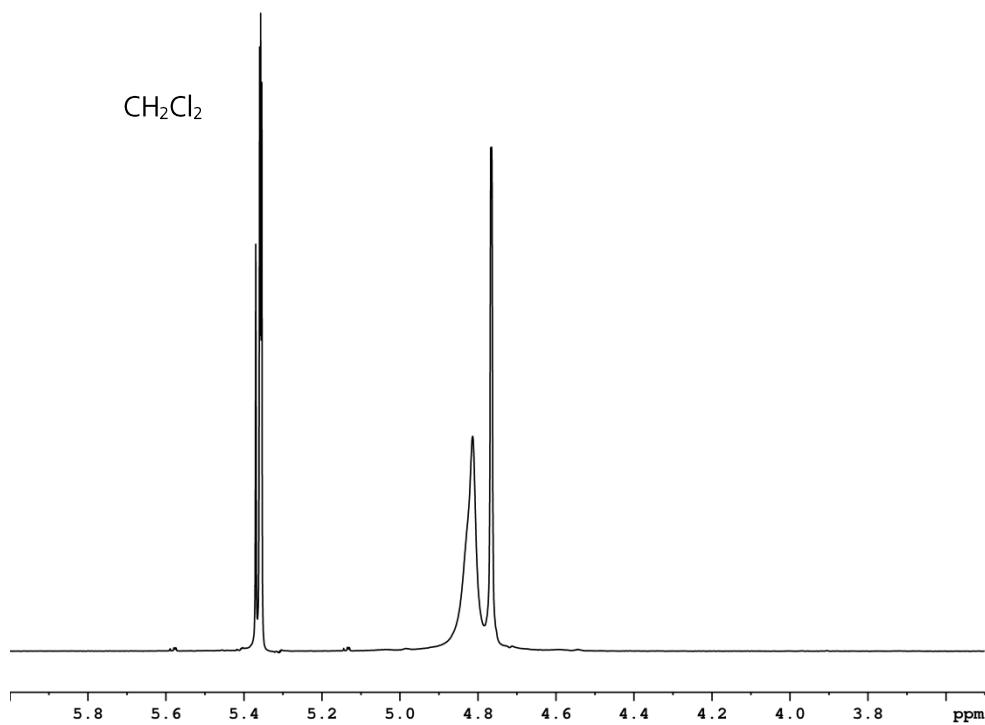
Figure S5.7. ^{1}H NMR spectrum of **3b** in CD$_2$Cl$_2$ at 298 K.
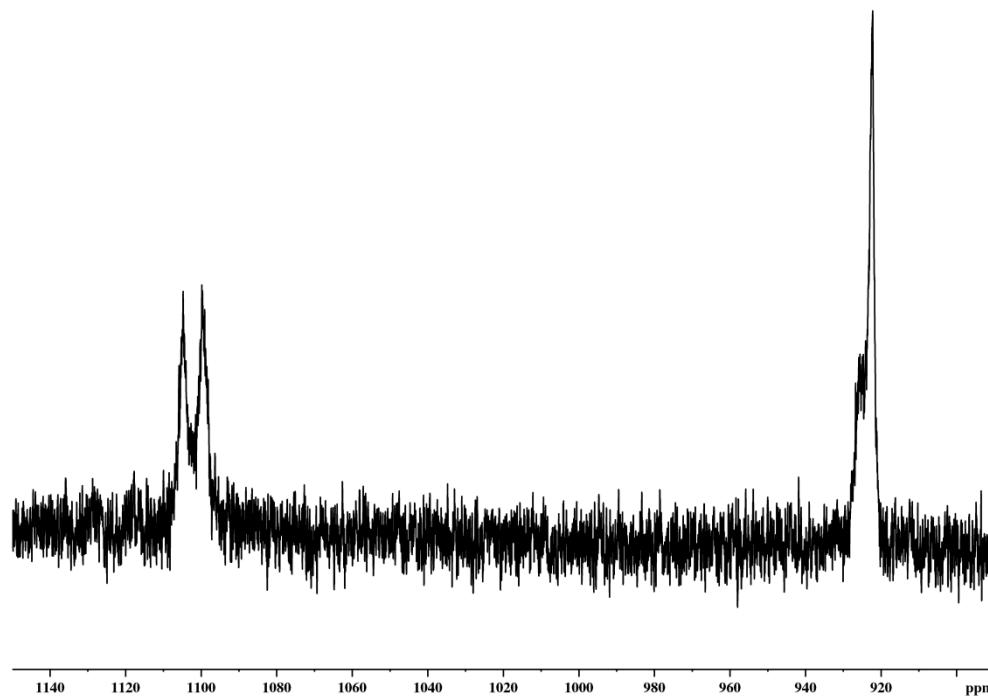
Figure S5.8. ^{31}P{^{1}H} NMR spectrum of **3b** in CD$_2$Cl$_2$ at 298 K.
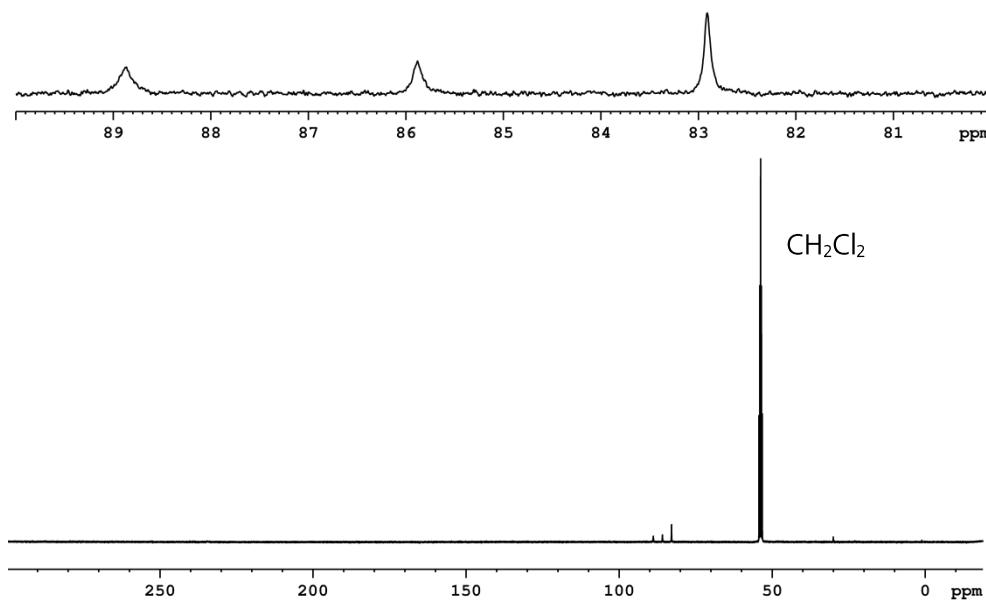
Figure S5.9. ^{13}C{^{1}H} NMR spectrum of **3b** in CD$_2$Cl$_2$ at 298 K.
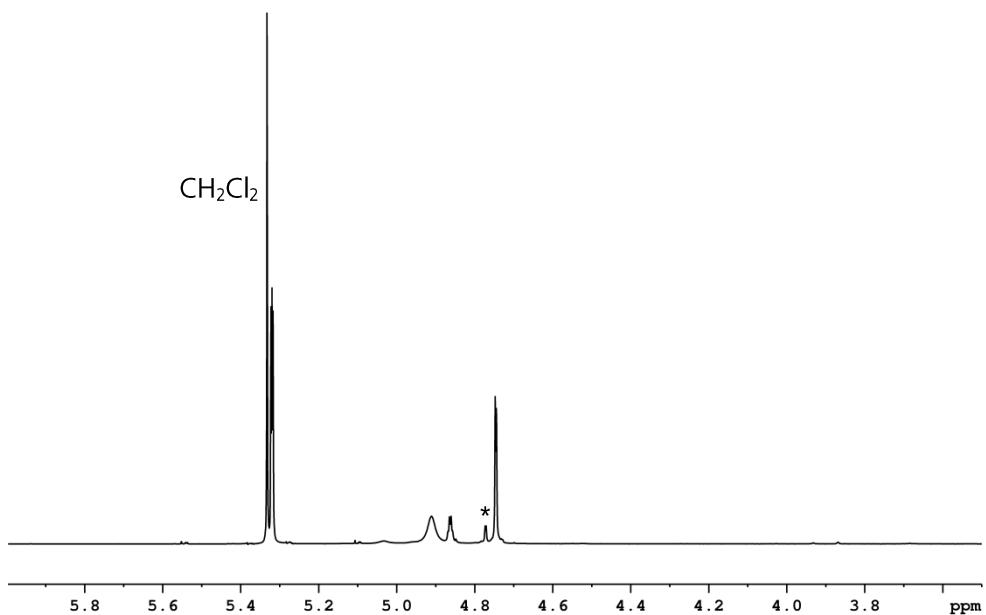
Figure S5.10. ^{1}H NMR spectrum of **3c** in CD$_2$Cl$_2$ at 298 K. Signal marked with an asterisk arises from impurities.
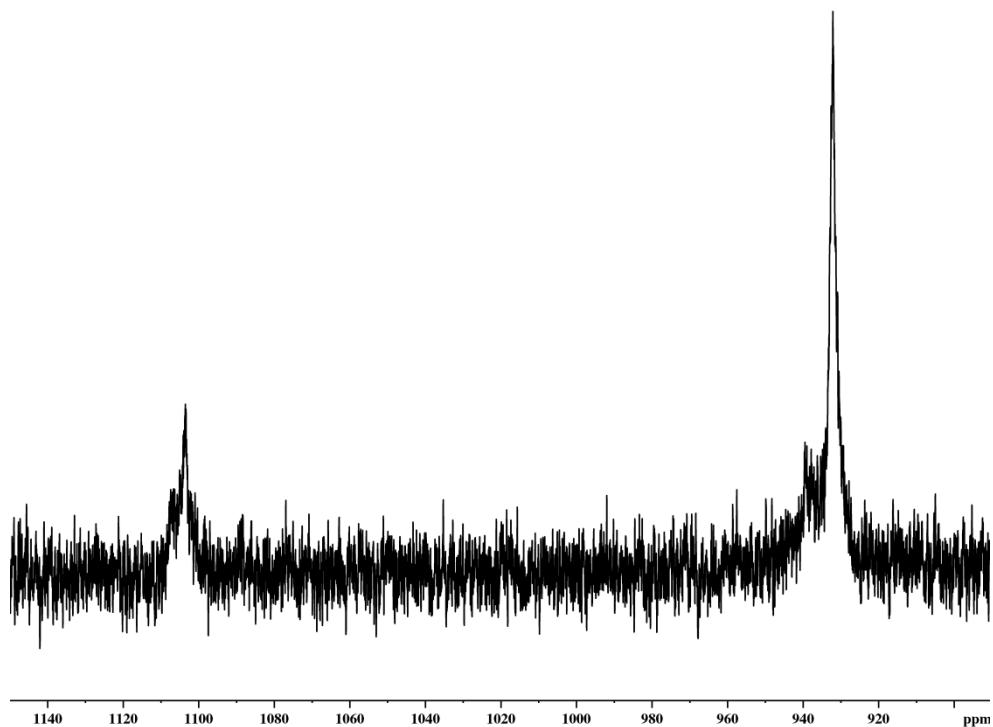
Figure S5.11. ^{31}P{^{1}H} NMR spectrum of **3c** in CD$_2$Cl$_2$ at 298 K.
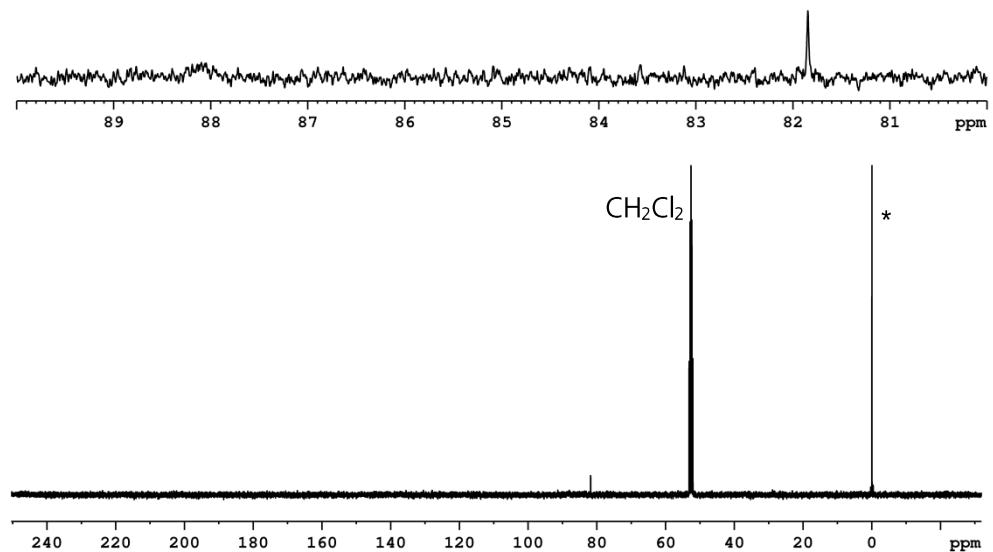
Figure S5.12. ^{13}C{^{1}H} NMR spectrum of **3c** in CD$_2$Cl$_2$ at 298 K. Signal marked with an asterisk arises from silicon grease.
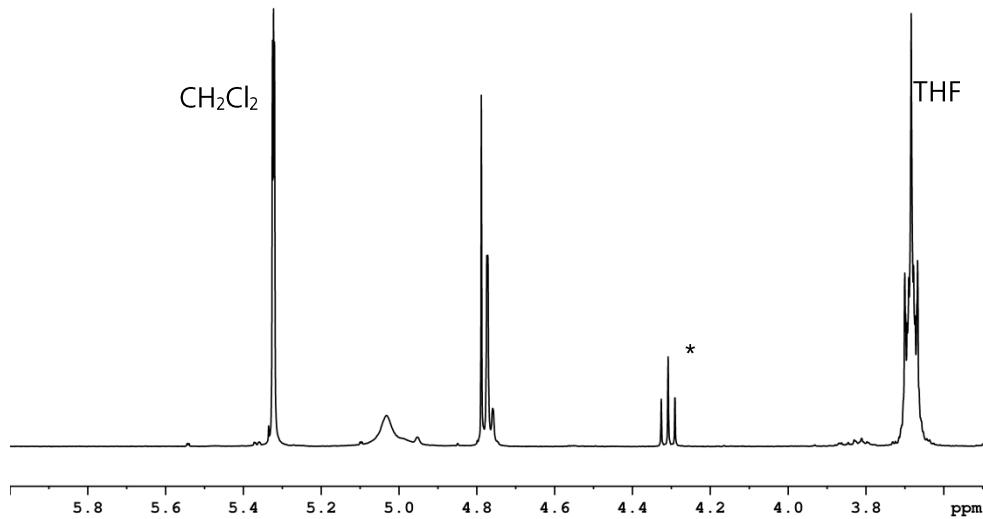
Figure S5.13. ^{1}H NMR spectrum of **3d** in CD$_2$Cl$_2$ at 298 K. Signal marked with an asterisk arises from impurities.
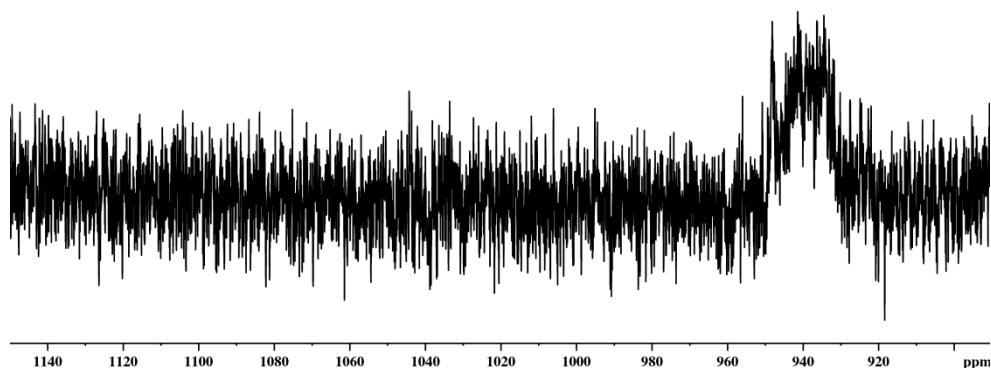
Figure S5.14. ^{31}P{^{1}H} NMR spectrum of **3d** in CD$_2$Cl$_2$ at 298 K.
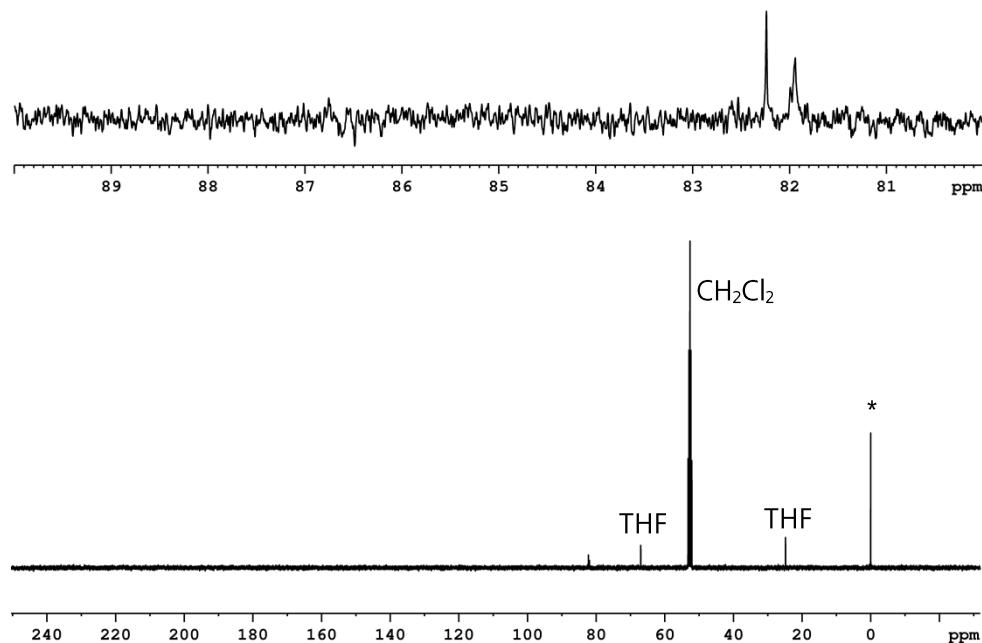
Figure S5.15. ^{13}C{^{1}H} NMR spectrum of **3d** in CD$_2$Cl$_2$ at 298 K. Signal marked with an asterisk arises from silicon grease.

Crystallographic Details:

The crystal structure analyses were performed on an Oxford Diffraction Gemini R Ultra CCD diffractometer (**1**, **2-Cl**, **2-Br**, **3a**) or an Oxford Diffraction SuperNova diffractometer (**3b**, **3c**, **3d**). For all compounds an analytical absorption correction was carried out.[1] The structures were solved by direct methods of the program SIR-92[2] and refined with least the square method on F^2 employing SHELXL-97[3] with anisotropic displacements for non-H atoms. Hydrogen atoms were located in idealized positions and refined isotropically according to the riding model.

	Crystal Data for **1***CH$_2$Cl$_2$	Crystal Data for **2-Cl***2CH$_2$Cl$_2$
Empirical Formula	C$_{21}$H$_{22}$Cl$_2$Mn$_4$P$_4$	C$_{22}$H$_{24}$Cl$_5$CuMn$_4$P$_4$
Formula Weight	688.93	872.85
Temperature [K]	123.0(6)	123.0(4)
Crystal System	monoclinic	monoclinic
Space Group	C2/c	C2/c
a [Å]	40.9164(6)	23.8316(6)
b [Å]	9.3302(1)	12.8659(3)
c [Å]	27.2353(4)	18.4127(4)
α [°]	90	90
β [°]	116.922(2)	93.404(2)
γ [°]	90	90
Volume [Å^3]	9270.5(3)	5635.7(2)
Z	16	8
ρ_{calc} [mg/mm^3]	1.974	2.057
μ [mm^{-1}]	22.144	21.660
F(000)	5472.0	3440.0
Crystal Size [mm^3]	0.5337 × 0.1091 × 0.0262	0.2249 × 0.0817 × 0.0446
Radiation	Cu-K$_\alpha$ (λ = 1.54178)	Cu-K$_\alpha$ (λ = 1.54178)
2Θ Range	7.28 to 133.08°	7.44 to 133.38°
Index Ranges	-39 ≤ h ≤ 48	-26 ≤ h ≤ 28
	-9 ≤ k ≤ 10	-14 ≤ k ≤ 15
	-32 ≤ l ≤ 31	-21 ≤ l ≤ 16
Reflections Collected	25380	18021
Independent Reflections	8019	4948
	[R_{int} = 0.0490, R_{sigma} = 0.0385]	[R_{int} = 0.0260, R_{sigma} =0.0234]
Data/Restraints/Parameters	8019/24/559	4948/0/325
Goodness-of-Fit on F^2	0.975	1.096
Final R Indexes [I > 2σ(I)]	R_1 = 0.0390, wR_2 = 0.1010	R_1 = 0.0414, wR_2 = 0.1276
Final R Indexes [All Data]	R_1 = 0.0425, wR_2 = 0.1021	R_1 = 0.0451, wR_2 = 0.1294
Largest Diff. Peak/Hole [e·Å^{-3}]	0.96/-1.00	2.21/-1.54
Flack Parameter	-	-

	Crystal Data for **2-Br**	Crystal Data for **3a***CH$_2$Cl$_2$
Empirical Formula	C$_{20}$H$_{20}$BrCuMn$_4$P$_4$	C$_{28}$H$_{27}$Cl$_2$Mn$_5$O$_2$P$_4$
Formula Weight	747.45	864.98
Temperature [K]	123.0(2)	123.10(10)
Crystal System	monoclinic	monoclinic
Space Group	*Cc*	*P2$_1$/n*
a [Å]	14.1032(6)	11.9099(1)
b [Å]	12.6047(5)	14.8210(1)
c [Å]	12.7139(4)	17.9552(2)
α [°]	90	90
β [°]	101.172(3)	106.097(1)
γ [°]	90	90
Volume [Å^3]	2217.28(15)	3045.13(5)
Z	4	4
ρ_{calc} [mg/mm^3]	2.239	1.887
μ [mm^{-1}]	23.994	20.248
F(000)	1456.0	1720.0
Crystal Size [mm^3]	0.078 × 0.0436 × 0.0287	0.1889 × 0.1035 × 0.1005
Radiation	Cu-K$_\alpha$ (λ = 1.54178)	Cu-K$_\alpha$ (λ = 1.54178)
2Θ Range	9.5 to 132.96°	7.86 to 133.1258°
Index Ranges	-16 ≤ h ≤ 16	-13 ≤ h ≤ 13
	-10 ≤ k ≤ 14	-17 ≤ k ≤ 16
	-14 ≤ l ≤ 15	-21 ≤ l ≤ 14
Reflections Collected	3838	13200
Independent Reflections	2437	5258
	[R_{int} = 0.0229, R_{sigma} = 0.0264]	[R_{int} = 0.0311, R_{sigma} = 0.0419]
Data/Restraints/Parameters	2437/8/280	5258/0/370
Goodness-of-Fit on *F^2*	1.071	0.867
Final *R* Indexes [I > 2σ(I)]	*R$_1$* = 0.0402, *wR$_2$* = 0.1244	*R$_1$* = 0.0255, *wR$_2$* = 0.0561
Final *R* Indexes [All Data]	*R$_1$* = 0.0409, *wR$_2$* = 0.1248	*R$_1$* = 0.0329, *wR$_2$* = 0.0572
Largest Diff. Peak/Hole [e·Å^{-3}]	1.35/-1.12	0.48/-0.30
Flack Parameter	0.013(7)	-

	Crystal Data for **3b***2CH₂Cl₂	Crystal Data for **3c***3CH₂Cl₂
Empirical Formula	$C_{36}H_{34}Cl_4Mn_6O_4P_4$	$C_{85}H_{76}Cl_6Mn_{14}O_{12}P_8$
Formula Weight	1125.95	2519.08
Temperature [K]	123.00(10)	123.00(10)
Crystal System	triclinic	triclinic
Space Group	$P\bar{1}$	$P\bar{1}$
a [Å]	10.5319(4)	10.3548(2)
b [Å]	10.8158(6)	10.5563(1)
c [Å]	18.0191(8)	20.4728(3)
α [°]	77.832(4)	79.072(1)
β [°]	80.265(4)	82.668(1)
γ [°]	85.858(4)	83.529(1)
Volume [Å³]	1976.14(16)	2170.28(6)
Z	2	1
ρ_{calc} [mg/mm³]	1.892	1.927
μ [mm⁻¹]	19.488	19.547
F(000)	1120.0	1254.0
Crystal Size [mm³]	0.1852 × 0.1225 × 0.0656	0.3779 × 0.0484 × 0.0379
Radiation	Cu-K$_\alpha$ (λ = 1.54178)	Cu-K$_\alpha$ (λ = 1.54178)
2Θ Range	8.36 to 147.0416°	8.56 to 147.0034°
Index Ranges	-10 ≤ h ≤ 13	-12 ≤ h ≤ 12
	-12 ≤ k ≤ 13	-11 ≤ k ≤ 12
	-19 ≤ l ≤ 22	-25 ≤ l ≤ 25
Reflections Collected	14154	26928
Independent Reflections	7594	8389
	[R_{int} = 0.0351, R_{sigma} = 0.0436]	[R_{int} = 0.0413, R_{sigma} = 0.0290]
Data/Restraints/Parameters	7594/132/706	8389/0/568
Goodness-of-Fit on F^2	0.948	1.077
Final R Indexes [I > 2σ(I)]	R_1 = 0.0364, wR_2 = 0.0886	R_1 = 0.0363, wR_2 = 0.1004
Final R Indexes [All Data]	R_1 = 0.0448, wR_2 = 0.0907	R_1 = 0.0398, wR_2 = 0.1019
Largest Diff. Peak/Hole [e·Å⁻³]	0.97/-0.62	0.90/-1.02
Flack Parameter	-	-

	Crystal Data for **3d***2CH₂Cl₂
Empirical Formula	$C_{50}H_{44}Cl_4Mn_8O_8P_4$
Formula Weight	1478.05
Temperature [K]	123.00(10)
Crystal System	monoclinic
Space Group	$C2/c$
a [Å]	29.4777(8)
b [Å]	11.0635(3)
c [Å]	21.2608(6)
$α$ [°]	90
$β$ [°]	132.060(4)
$γ$ [°]	90
Volume [Å³]	5147.9(4)
Z	4
$ρ_{calc}$ [mg/mm³]	1.907
$μ$ [mm⁻¹]	18.978
F(000)	2944.0
Crystal Size [mm³]	0.067 × 0.0411 × 0.0365
Radiation	$Cu-K_α$ ($λ$ = 1.54178)
$2Θ$ Range	8.08 to 147.1652°
Index Ranges	-36 ≤ h ≤ 35
	-12 ≤ k ≤ 13
	-23 ≤ l ≤ 26
Reflections Collected	13730
Independent Reflections	4948
	[R_{int} = 0.0269, R_{sigma} = 0.0312]
Data/Restraints/Parameters	4948/0/334
Goodness-of-Fit on F^2	0.988
Final R Indexes [I > 2σ(I)]	R_1 = 0.0267, wR_2 = 0.0652
Final R Indexes [All Data]	R_1 = 0.0343, wR_2 = 0.0667
Largest Diff. Peak/Hole [e·Å⁻³]	1.17/-1.07
Flack Parameter	-
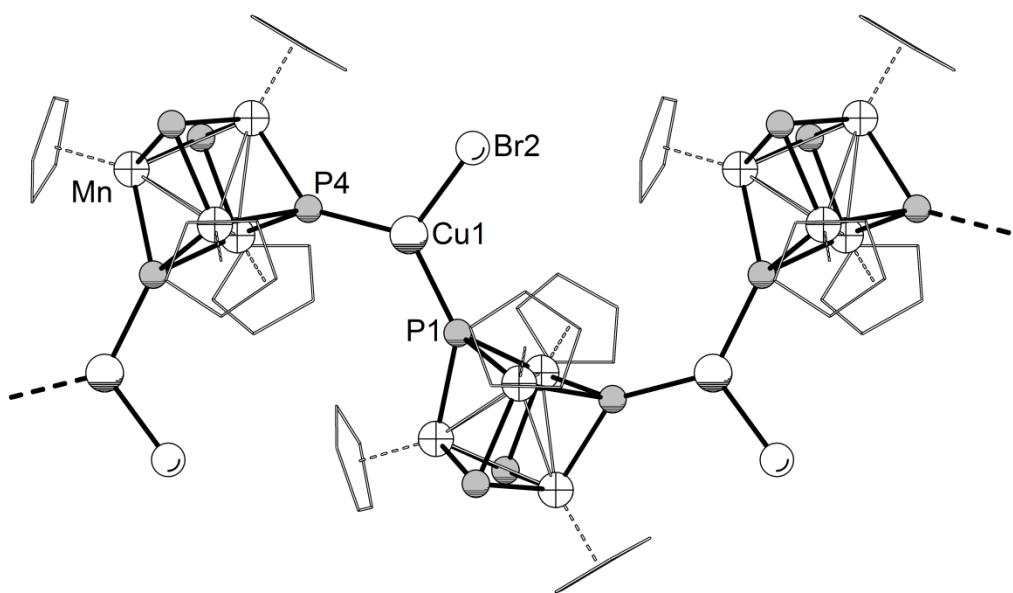
Figure S5.16. Section of 1D zigzag chain [{(CpMn)₄(µ₃-P)₄}(CuBr)]ₙ (**2-Br**) in the crystal. View along crystallographic a-axis. For clarity reasons the C atoms are shown in 'wire-or-stick' model and H atoms and solvent molecules are omitted. Br atom is disordered over two positions with occupancies of 0.57 and 0.43, only main part is shown. Selected bond lengths [Å] and angles [°]: P1-Cu1 2.248(3), P4-Cu1 2.252(3), Cu1-Br1 2.372(8), Cu1-Br2 2.324(5), P1-Cu1-P4 129.0(1), P1-Cu1-Br1 119.8(2), P1-Cu1-Br2 115.1(1), P4-Cu1-Br1 108.0(2), P4-Cu1-Br2 115.9(1), av. Mn-P 2.231, av. Mn-Mn 2.718.
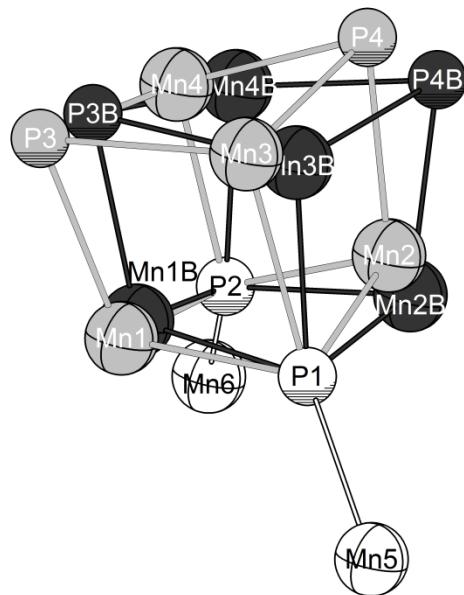
Figure S5.17. Disordered core of compound **3b**. Cp and CO ligands as well as Mn–Mn bonds are omitted for clarity. Parts 1 and 2 are colored differently. White colored atoms belong to both parts and therefore are not disordered.

Synthesis of the Heterocubane Cluster [{CpMn}$_4$(μ$_3$-P)$_4$] as a Starting Material for the Formation of Polymeric Coordination Compounds

79

DFT Calculations:

All calculations were carried out using the TURBOMOLE program package package.[4] The geometries were optimized using the RI-[5]BP86[6] functional together with the def2-TZVP[7] basis set for all atoms. The Multipole Accelerated Resolution of Identity (MARI-J)[8] approximation was used in the geometry optimizations. The final energy of the molecules has been determined by single point calculations without using the RI formalism. The relative energies were calculated by using the SCF energies.

Table S5.1. Relative energies of [(CpMn)$_4$(P)$_4$] (**1**) in different spin states. Calculated at the BP86/def2-TZVP level of theory.

S (spin multiplicity)	1	3	5	7	9	11	13
Rel. Energ. (kJ mol^{-1})	0	70.27	127.92	163.67	214.09	n.c.	n.c.

n.c. = SCF not converged

HOMO-12
-5.989 eV

HOMO-13
-5.992 eV
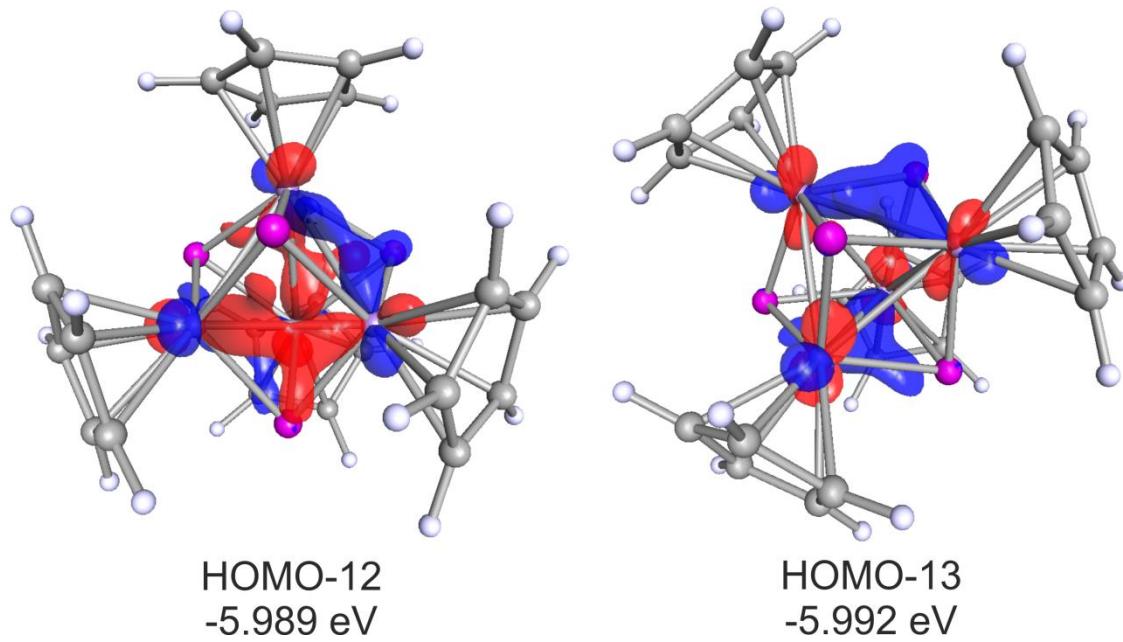
Figure S5.18. Selected molecular orbitals representing the Mn–P bonding in [(CpMn)$_4$(P)$_4$] (**1**) in singlet spin state. Calculated at the BP86/def2-TZVP level of theory.
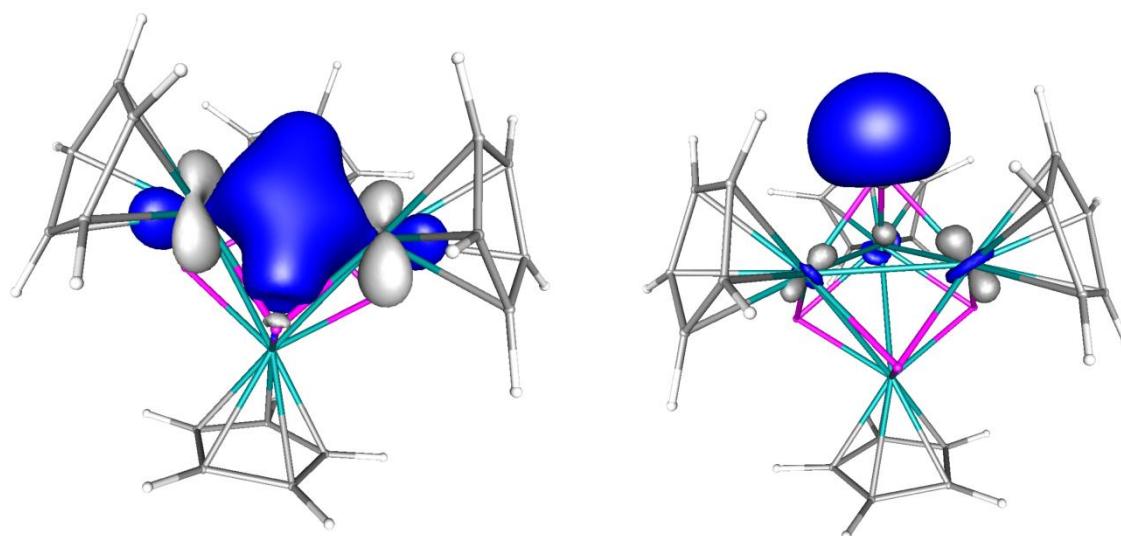
Figure S5.19. Selected localized molecular orbitals representing the Mn–P bonding (left) and the lone pair of the phosphorus atoms (right) in [(CpMn)₄(P)₄] (**1**) in singlet spin state. Calculated at the BP86/def2-TZVP level of theory.

Table S5.2. Cartesian coordinates of the optimized geometry of [(CpMn)₄(P)₄] (**1**; S = 1) at the BP86/def2-SVP level of theory.

Atom	x	z	y	Atom	x	z	y
Mn	5.5725756	-3.0634705	16.7212452	C	3.07046	-1.23439	19.78121
Mn	4.4295672	-0.780238	15.828574	C	1.901976	-0.96697	19.01673
Mn	3.2767684	-3.1683163	15.295251	C	1.269736	-2.21751	18.72319
Mn	3.2587448	-2.1899478	17.817917	C	2.050283	-3.25219	19.30629
P	5.2565477	-2.4400967	14.6078313	H	8.273309	-1.95713	16.58867
P	5.2413819	-1.1816545	17.8549663	H	7.665807	-3.90772	14.81939
P	3.7592589	-4.2584852	17.1741544	H	6.303916	-5.83436	16.14081
P	2.2793741	-1.3224908	16.0272746	H	6.146716	-5.11517	18.73696
C	7.7470084	-2.8801391	16.8106809	H	7.381371	-2.72568	19.01929
C	7.4122899	-3.9027522	15.874507	H	6.588404	1.072342	16.56285
C	6.7074606	-4.9235299	16.5717124	H	4.059358	1.78271	17.18297
C	6.6204181	-4.5396379	17.9480624	H	2.503126	1.307666	15.0236
C	7.2646951	-3.2823474	18.0950039	H	4.057655	0.209622	13.10423
C	5.7262542	0.9805842	15.9099766	H	6.588414	0.100508	14.03894
C	4.3872114	1.3649001	16.2363589	H	0.548504	-4.19416	15.49668
C	3.5651945	1.0999081	15.1035968	H	1.009164	-2.29246	13.63404
C	4.3868254	0.5352782	14.0858768	H	3.323527	-2.903	12.37527
C	5.7261218	0.4699881	14.5847377	H	4.271524	-5.19567	13.43602
C	1.3922883	-4.1618776	14.8146396	H	2.530091	-6.02344	15.33232
C	1.6426191	-3.1500011	13.8366192	H	3.964267	-3.17233	20.47732
C	2.8554954	-3.4731431	13.1714595	H	3.758438	-0.49521	20.17857
C	3.3565688	-4.6917494	13.7311885	H	1.546295	0.010662	18.70727
C	2.4466874	-5.1196405	14.7374808	H	0.353671	-2.3456	18.15533
C	3.1721966	-2.6482725	19.9517225	H	1.829074	-4.3143	19.27877

Table S5.3. Cartesian coordinates of the optimized geometry of [(CpMn)₄(P)₄] (**1**; S = 3) at the BP86/def2-SVP level of theory.

Atom	x	z	y	Atom	x	z	y
Mn	5.5157269	-3.0253051	16.8091735	C	2.6371031	-1.395784	19.804361
Mn	4.6290623	-0.7375794	15.6422317	C	1.4622202	-1.451054	19.003502
Mn	3.2850243	-3.0710769	15.2843875	C	1.1352834	-2.828424	18.797743
Mn	3.1144965	-2.3912554	17.9093481	C	2.1013928	-3.622035	19.479391
P	5.3609971	-2.5546379	14.6271973	H	8.221419	-2.144034	16.168051
P	4.9693622	-1.1122162	17.8389117	H	7.4377784	-4.51897	15.148126
P	3.7244339	-4.3403551	17.0746532	H	6.1664419	-5.88693	17.100366

Atom	x	z	y	Atom	x	z	y
P	2.4699369	-1.1639139	16.1310632	H	6.1604838	-4.354261	19.324663
C	7.688959	-2.9212022	16.7066911	H	7.4817765	-2.062344	18.767655
C	7.2657471	-4.1767718	16.1634721	H	7.2479494	0.5993296	15.664201
C	6.5971343	-4.8947894	17.1886465	H	5.2349254	1.7705852	17.033457
C	6.6027146	-4.0867333	18.3704189	H	3.0243399	1.7107792	15.475774
C	7.2898679	-2.8742142	18.0733341	H	3.679824	0.5034717	13.149146
C	6.2348005	0.7467601	15.3026008	H	6.3045822	-0.12682	13.239383
C	5.1654026	1.3523838	16.0350373	H	0.765221	-4.499854	15.629865
C	4.0025491	1.3208852	15.2155214	H	0.7012471	-2.222958	14.172974
C	4.354388	0.6955719	13.9779611	H	2.8444657	-2.23456	12.524838
C	5.7349226	0.3505554	14.029896	H	4.1759716	-4.554792	12.897694
C	1.4765993	-4.2106578	14.8631472	H	2.890335	-5.955322	14.817297
C	1.4493911	-3.0060621	14.1027787	H	3.9077634	-3.033255	20.667805
C	2.572732	-3.0165659	13.2264806	H	3.1381329	-0.496574	20.146576
C	3.2838163	-4.2424378	13.43079	H	0.9048766	-0.601365	18.624005
C	2.6085927	-4.9779438	14.4390396	H	0.3030187	-3.202737	18.209424
C	3.0342743	-2.7394491	20.0935529	H	2.121101	-4.705952	19.524689

Table S5.4. Cartesian coordinates of the optimized geometry of [(CpMn)₄(P)₄] (**1**; S = 5) at the BP86/def2-SVP level of theory.

Atom	x	z	y	Atom	x	z	y
Mn	5.7403328	-3.0005743	16.6385054	C	2.5867844	-1.5294436	19.9850084
Mn	4.5859699	-0.7715821	15.6566187	C	1.5111141	-1.0356547	19.1867783
Mn	3.3523784	-3.1741039	15.353298	C	0.739567	-2.1560303	18.754885
Mn	2.9004949	-2.2698718	17.9255581	C	1.3396494	-3.3323808	19.2690535
P	5.3410689	-2.513508	14.5144913	H	8.3905361	-1.7390826	16.4169772
P	4.9636355	-1.2527083	17.8209838	H	7.9416687	-3.8585699	14.8046727
P	3.9169676	-4.1706045	17.2851866	H	6.6838986	-5.754322	16.2606482
P	2.3997669	-1.2426354	15.9891152	H	6.4540538	-4.8522473	18.7970171
C	7.9253858	-2.6749156	16.7100631	H	7.5096662	-2.3644581	18.8945906
C	7.6797382	-3.7905877	15.8553527	H	7.222645	0.520436	15.4726204
C	7.0352308	-4.7944454	16.6266916	H	5.4120121	1.6150137	17.1538293
C	6.8937829	-4.3093069	17.967207	H	3.034971	1.708532	15.8674639
C	7.4502886	-3.0016838	18.0185331	H	3.3842289	0.6688642	13.3980417
C	6.1770969	0.7063007	15.2484478	H	5.9865764	-0.0013484	13.1284542
C	5.2167401	1.2758045	16.1420783	H	0.7034084	-4.3150159	15.7486653
C	3.9663645	1.3232674	15.4664864	H	0.9497907	-2.4289564	13.8298699
C	4.1577062	0.7914971	14.1500629	H	3.2038933	-2.9532632	12.4329868
C	5.5224988	0.4211039	14.0135019	H	4.3225678	-5.1880628	13.4589765
C	1.4969344	-4.2570219	15.0108279	H	2.756977	-6.0517244	15.4868409
C	1.6339913	-3.2536448	14.002895	H	3.1581095	-3.6284162	20.5494962
C	2.8161707	-3.5316448	13.2655087	H	3.3458061	-0.9281791	20.4746162
C	3.40908	-4.7181097	13.8092662	H	1.3040661	0.0056531	18.9609868
C	2.5892687	-5.1679541	14.8794384	H	-0.1337362	-2.1104894	18.1106452
C	2.4895458	-2.9532558	20.0248108	H	1.0099471	-4.3515684	19.0894866

Table S5.5. Cartesian coordinates of the optimized geometry of [(CpMn)₄(P)₄] (**1**; S = 7) at the BP86/def2-SVP level of theory.

Atom	x	z	y	Atom	x	z	y
Mn	5.7553035	-3.2130165	16.7876934	C	2.6729504	-1.5049534	19.9393966
Mn	4.4017806	-0.5935081	15.6338052	C	1.5810929	-1.0134058	19.1627546
Mn	3.403398	-3.1782646	15.2826075	C	0.7840769	-2.1326567	18.7723004
Mn	2.914955	-2.2873878	17.8766625	C	1.3866983	-3.3061161	19.2871445
P	5.4306488	-2.378698	14.7183527	H	8.5137625	-2.3377435	16.1255933
P	4.9750405	-1.2800627	17.7450771	H	7.7885509	-4.7317523	15.1157365
P	3.8041297	-4.2521186	17.2224667	H	6.5601923	-6.129596	17.0692072
P	2.2935184	-1.3287525	15.9338926	H	6.5183554	-4.6028	19.2934518
C	7.9979606	-3.1254254	16.6654403	H	7.7373628	-2.2561588	18.7174893
C	7.6313785	-4.4018625	16.1382912	H	6.9799204	0.6487621	14.8445545
C	6.987068	-5.1356428	17.1637887	H	5.7022731	1.6339352	17.0176628
C	6.9459161	-4.3211156	18.3364029	H	3.0954324	1.9646396	16.3695672
C	7.5884374	-3.0834328	18.0314008	H	2.7739167	1.2014317	13.8014946
C	5.9246483	0.8935912	14.9113504	H	5.1691	0.3899674	12.8617069

Atom	x	z	y	Atom	x	z	y
C	5.2502446	1.4129494	16.0563931	H	0.7684698	-4.4306239	15.3877916
C	3.8753093	1.5880227	15.7154285	H	1.1108377	-2.4487835	13.5838834
C	3.7112971	1.2031411	14.3495797	H	3.501937	-2.8235335	12.3787797
C	4.9681687	0.7762582	13.856503	H	4.6095721	-5.0643368	13.399781
C	1.6202983	-4.311209	14.7259005	H	2.9021974	-6.0805798	15.2330305
C	1.808856	-3.2559032	13.7825504	H	3.2406886	-3.6000726	20.5179359
C	3.0621525	-3.4574151	13.1421822	H	3.4501812	-0.9038765	20.3996621
C	3.649	-4.6457273	13.6827646	H	1.3790375	0.0263202	18.9258124
C	2.7549862	-5.1742198	14.6543568	H	-0.107077	-2.0884379	18.1532671
C	2.5633764	-2.9265588	20.0025441	H	1.0412385	-4.3241706	19.1341013

Table S 5.6. Cartesian coordinates of the optimized geometry of [(CpMn)₄(P)₄] (**1**; S = 9) at the BP86/def2-SVP level of theory.

Atom	x	z	y	Atom	x	z	y
Mn	5.8004432	-3.0323588	16.2536918	C	2.0540377	-0.898801	19.8474125
Mn	4.8824877	-0.525285	15.996755	C	1.3279096	-0.3511964	18.7576281
Mn	3.3919833	-3.8070325	15.3718385	C	0.5445291	-1.3988551	18.1761412
Mn	2.7363979	-1.9433513	17.8791211	C	0.7830631	-2.588644	18.9225037
P	4.7121362	-2.1988415	14.4887504	H	8.3409934	-1.6670871	15.812135
P	5.0645228	-1.6686014	17.9256618	H	7.4816609	-3.3537843	13.8803423
P	4.0766289	-3.8313151	17.5162959	H	6.5579306	-5.5945002	15.0795994
P	2.7234509	-1.5109147	15.603213	H	6.8579634	-5.2972345	17.7512656
C	7.9225941	-2.6557894	15.9699113	H	7.9606995	-2.8719846	18.2035199
C	7.4573419	-3.5418673	14.949191	H	7.2713668	0.912841	17.0458645
C	6.9800321	-4.7307977	15.582924	H	4.8572608	1.573297	18.0537441
C	7.1383128	-4.5743996	16.9920598	H	3.1226311	1.7944579	15.9770588
C	7.7216322	-3.2907909	17.2314395	H	4.4874666	1.2938034	13.6996625
C	6.3702173	1.0903383	16.466679	H	7.048025	0.7637951	14.3566026
C	5.0880909	1.431524	17.0028216	H	1.6360072	-5.7648103	16.6785982
C	4.1782271	1.5502276	15.9112834	H	0.5108381	-3.9715714	14.9779047
C	4.9032602	1.2976217	14.7023521	H	2.0294914	-3.8829332	12.7444888
C	6.2548575	1.0283485	15.0504342	H	4.0797144	-5.6034988	13.0555164
C	2.0029154	-5.490608	15.694844	H	3.8521064	-6.7474143	15.4937333
C	1.4097582	-4.5530559	14.7986574	H	2.1417246	-2.9871149	20.6609788
C	2.205574	-4.5155703	13.6089165	H	2.7591111	-0.3670409	20.4798206
C	3.2807359	-5.4301936	13.7711635	H	1.3598623	0.6797343	18.4166162
C	3.1725937	-6.0192463	15.0611078	H	-0.1313125	-1.2926697	17.3329821
C	1.7307814	-2.2851918	19.9411377	H	0.3405838	-3.562548	18.7331704

Calculation of Core Volumes:

Table S5.7. Volumes V of cluster cores of **1** and **3a-d**. The heterocubane scaffold is broken up into one Mn₄ pyramid and four Mn₃P pyramids for the volume calculations (Heron's formula and $V = 1/3*b*h$). ΔV and the percentage increases are calculated compared to compound **1**.

		V [Å³]	ΔV [Å³]	percentage
1	unsubstituted	9.159		
3a	mono-coordinated	9.151	-0.008	-0.1%
3b	di-coordinated	9.333	0.173	1.9%
3c	tri-coordinated	9.372	0.213	2.3%
3d	tetra-coordinated	9.490	0.331	3.5%

Synthesis of the Heterocubane Cluster [{CpMn}₄(µ₃-P)₄] as a Starting Material for the Formation of Polymeric Coordination Compounds

83
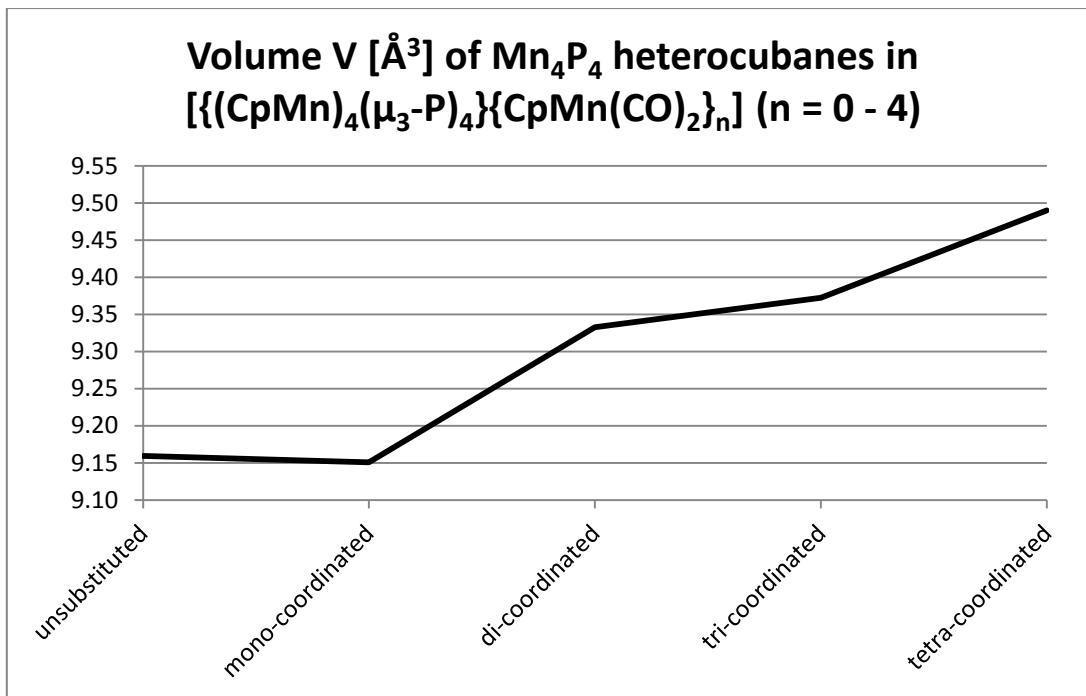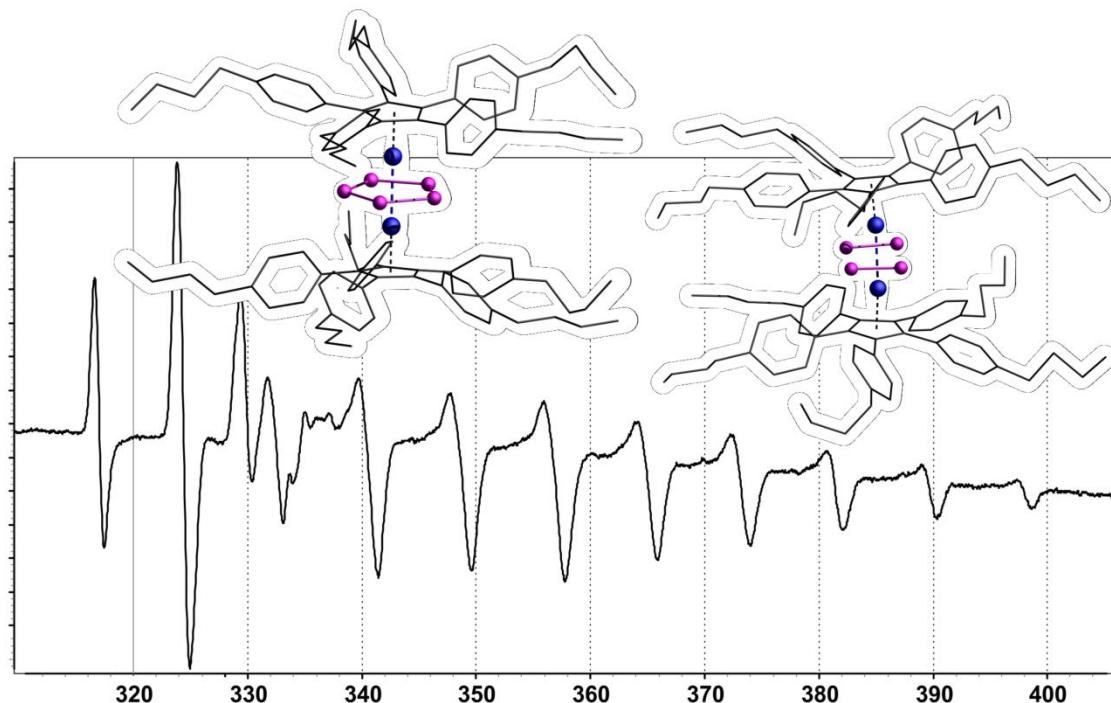
Figure S5.20. Graphical display of volumes V [Å³] of cluster cores of **1** and **3a-d**.

References for Supplementary Information:

[1]   R. C. Clark, J. S. Reid, *Acta Cryst.* **1995**, A51, 887-897.

[2]   A. Altomare, M. C. Burla, M. Camalli, G.L. Cascarano, C. Giacovazzo, A. Guagliardi, A. G. G. Moliterni, G. Polidori, R. Spagna, *J. Appl. Cryst.* **1999**, 32, 115-119.

[3]   G. M. Sheldrick, *Acta Cryst.* **2008**, A64, 112-122.

[4]   a) R. Ahlrichs, M. Bär, M. Häser, H. Horn, C. Kölmel, *Chem. Phys. Lett.***1989**, *162*, 165–169; b) O. Treutler, R. Ahlrichs, *J. Chem. Phys.***1995**, *102*, 346–354.

[5]   a) K. Eichkorn, O. Treutler, H. Oehm, M. Häser, R. Ahlrichs, *Chem. Phys. Lett.***1995**, *242*, 652–660; b) K. Eichkorn, F. Weigend, O. Treutler, R. Ahlrichs, *Theor. Chem. Acc.***1997**, *97*, 119.

[6]   a) P. A. M. Dirac, *Proc. Royal Soc. A*, **1929**, *123*, 714-733. b) J. C. Slater, *Phys. Rev.***1951**, *81*, 385-390. c) S. H. Vosko, L. Wilk, M. Nusair, *Can. J. Phys.* **1980**, *58*, 1200-1211. d). A. D. Becke, *Phys. Rev. A*, **1988**, *38*, 3098. e) J. P. Perdew, *Phys. Rev. B* **1986**, *33*, 8822-8824.

[7]   a) F. Weigend, M. Häser, H. Patzelt, R. Ahlrichs, *Chem. Phys. Letters* **1998**, *294*, 143; b) F. Weigend, R. Ahlrichs, *Phys. Chem. Chem. Phys.* **2005**, *7*, 3297; c) F. Weigend, *Phys. Chem. Chem. Phys.* **2006**, *8*, 1057.

[8]   M. Sierka, A. Hogekamp, R. Ahlrichs, *J. Chem. Phys.***2003**, *118*, 9136.

6. Synthesis and Characterization of Manganese Triple-Decker Complexes

Sebastian Heinl, Gabor Balázs and Manfred Scheer
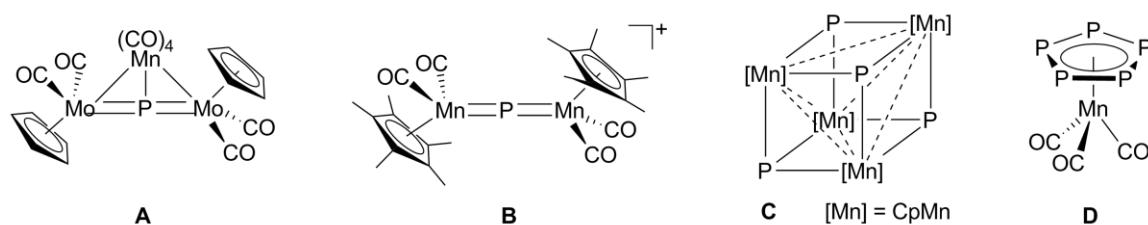
unpublished results

- ❖ **All syntheses and characterizations were performed by Sebastian Heinl, unless subsequently noted otherwise**
- ❖ **Manuscript was written by Sebastian Heinl**
- ❖ **Figures were made by Sebastian Heinl, unless subsequently noted otherwise**
- ❖ **X-ray structure analyses and refinement were performed by Sebastian Heinl**
- ❖ **DFT calculations, EPR simulation and corresponding figures were performed/made by Gabor Balázs**

6.1 Introduction

Since Ginsberg and Lindsell[1] first reported on the synthesis of complexes with substituent-free phosphorus ligands, numerous so called P_n ligand complexes were prepared and described in literature. In most cases the tetrahedral molecule P_4 is the starting material of choice.[2] Up to now, P_n ligand complexes are known for almost all transition metals[3] and a large number of main group elements.[4] However, there are some unexplored spots within the d-block elements, where no or only very few compounds with substituent-free P_n ligands are known. The 7th group might be seen as a border between the early and the late transition metals, where in both latter cases a large number of substances with P_n units are known. The absence of technetium derivatives can most likely be explained by its artificial and radioactive nature. However, while for rhenium several compounds are known, for manganese only very few examples exist.[3] To the best of our knowledge, the only crystallographically characterized P_n ligand complex of manganese is [{CpMo(CO)$_2$}$_2${Mn(CO)$_4$}(μ_3-P)}] (**A**) with a P_1 unit, reported by Mays and co-workers (Scheme 6.1).[5] Huttner et al. also reported on Mn containing dimetallaphosphacumulenes **B** containing P_1 units.[6] Recently we obtained the heterocubane cluster [Cp$_4$Mn$_4$P$_4$] (**C**), also bearing P_1 moieties that are bridging {CpMn} fragments.[7] The only Mn complex with a P_n moiety with $n > 1$ was described by Baudler et al. in 1991 with [(CO)$_3$Mn(η^5-P$_5$)] (**D**). [8] Unfortunately, the only analytical proof of **D** is an IR spectrum. There are also several other examples of P_n ligand complexes with direct Mn–P bonds. However, they are based on the coordination of the phosphorus lone pair towards 16 VE {CpMn(CO)$_2$} fragments.[3]

The lack of manganese complexes with substituent-free P_n ligands prompted us to investigate this class of compounds. Furthermore, the question arises what will happen if the Cp ligand in preparation of **C** is substituted by the superbulky Cp^{BIG} ligand (Cp^{BIG} = C$_5$(4-nBuC$_6$H$_4$)$_5$)?

Herein, we report on the synthesis of the precursor complex [Cp^{BIG}Mn(cht)] (**1**; cht = cycloheptatriene) and its reaction with P_4 forming the triple-decker complexes [{Cp^{BIG}Mn}$_2$(μ,$\eta^{5:5}$-P$_5$)] (**2**) and [{Cp^{BIG}Mn}$_2$(μ,$\eta^{2:2}$-P$_2$)$_2$] (**3**). The compounds are characterized by NMR and EPR spectroscopy, mass spectrometry as well as by single crystal X-ray diffraction.

Scheme 6.1. P_n ligand complexes of manganese.

6.2 Results and Discussion

The UV irradiation of the sterically crowded cymantrene complex [Cp^{BIG}Mn(CO)$_3$][9] in toluene with an excess of cycloheptatriene (cht) results in the substitution of all three carbonyl groups by one cht ligand (Equation 6-1). After filtration over Celite, [Cp^{BIG}Mn(cht)] (**1**) is obtained pure as a brown powder in 90% yield. If silica gel is used instead of Celite, decomposition is observed. As expected, complex **1** exhibits a sandwich structure with a η^6 bound cht ligand and the methylene group pointing away from the {Cp^{BIG}Mn} fragment (Figure 6.1). The structural parameters compare rather well with the only other known cht-Mn complex [(C$_5$H$_4$Me)Mn(cht')] (cht' = 1-phenylcycloheptatriene).[10] In both cases no alternating bond lengths in the triene moiety is observed, which is normal for η^6-cht complexes.
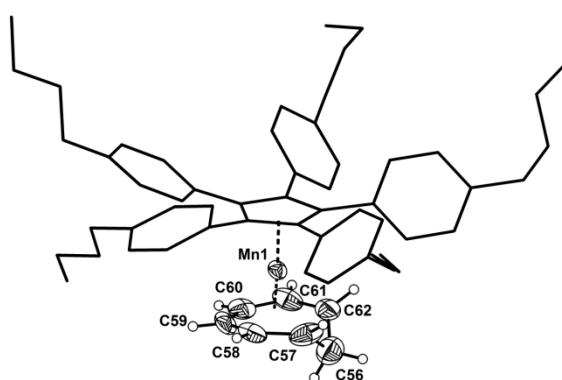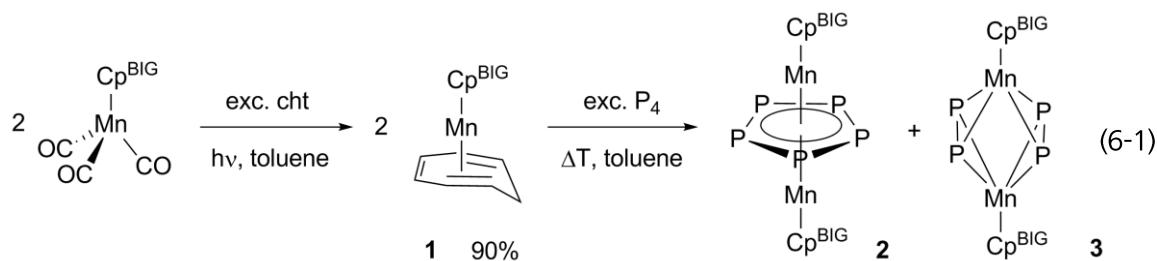
Figure 6.1. Molecular structure of **1** in the crystal. Thermal ellipsoids are drawn at 50% probability level. For clarity reasons H atoms on the Cp^{BIG} ligand are omitted and it is drawn in 'wire-or-stick' model. Selected bond lengths [Å] and angles [°]: Mn1···C56 2.737(5), Mn1-C57 2.176(4), Mn1-C58 2.106(3), Mn1-C59 2.109(3), Mn1-C60 2.113(3), Mn1-C61 2.084(3), Mn1-C62 2.145(5), C56-C57 1.415(7), C57-C58 1.520(6), C58-C59 1.400(4), C59-C60 1.397(4), C60-C61 1.383(5), C56-C62 1.457(4), C56-(C57-C62)$_{Plane}$ 115.5(3).

The precursor complex **1** reacts with P$_4$ in toluene in a co-thermolysis reaction under cht elimination. Chromatographic workup affords one single brown fraction of a mixture of [{Cp^{BIG}Mn}$_2$(μ,η$^{5:5}$-P$_5$)] (**2**) and [{Cp^{BIG}Mn}$_2$(μ,η$^{2:2}$-P$_2$)$_2$] (**3**), which could not be separated from each other (Equation 6-1). Single crystals suitable for X-ray diffraction were obtained from a concentrated toluene solution as solvate with six toluene molecules per formula unit. Both compounds co-crystallize on the same position. Therefore, effectively a triple-decker complex with a disordered middledeck is observed. Accordingly to the occupancies of the *cyclo*-P$_5$

ligand (70%) and that of the two P_2 ligands (30%), a 7:3 mixture of **2** and **3** is obtained. The P1 and P2 atoms belong to both complexes. This composition is also confirmed by the elemental analysis. The molecular structures of **2** and **3** are depicted in Figure 6.2. The P–P bond lengths in **2** are with an average value of 2.20 Å in good agreement with other known triple-decker complexes with a *cyclo*-P_5 middledeck (2.15 Å - 2.28 Å).[11] Binuclear compounds with two bridging P_2 units are rather rare. Only [(Cp^{R}Co)$_2$(μ,$\eta^{2:2}$-P_2)$_2$] (Cp^R = Cp′′′,[12] Cp*)[13] and [(Cp*Fe)$_2$(μ,$\eta^{2:2}$-P_2)$_2$][13] are known. In complex **3** the bond lengths P1–P2 and P6–P7 are in between a single and a double bond with 2.152(2) Å and 2.094(8) Å and roughly 0.1 Å longer than in the previously described cobalt and iron examples. The Cp^{BIG} ligands in **2** and **3** are not co-planar but 8.70(9)° tilted against each other and 4.35(6)° against the phosphorus middledecks. In complex **2**, the Cp^{BIG} moieties and the P_5 ring are almost ecliptic (~10°),
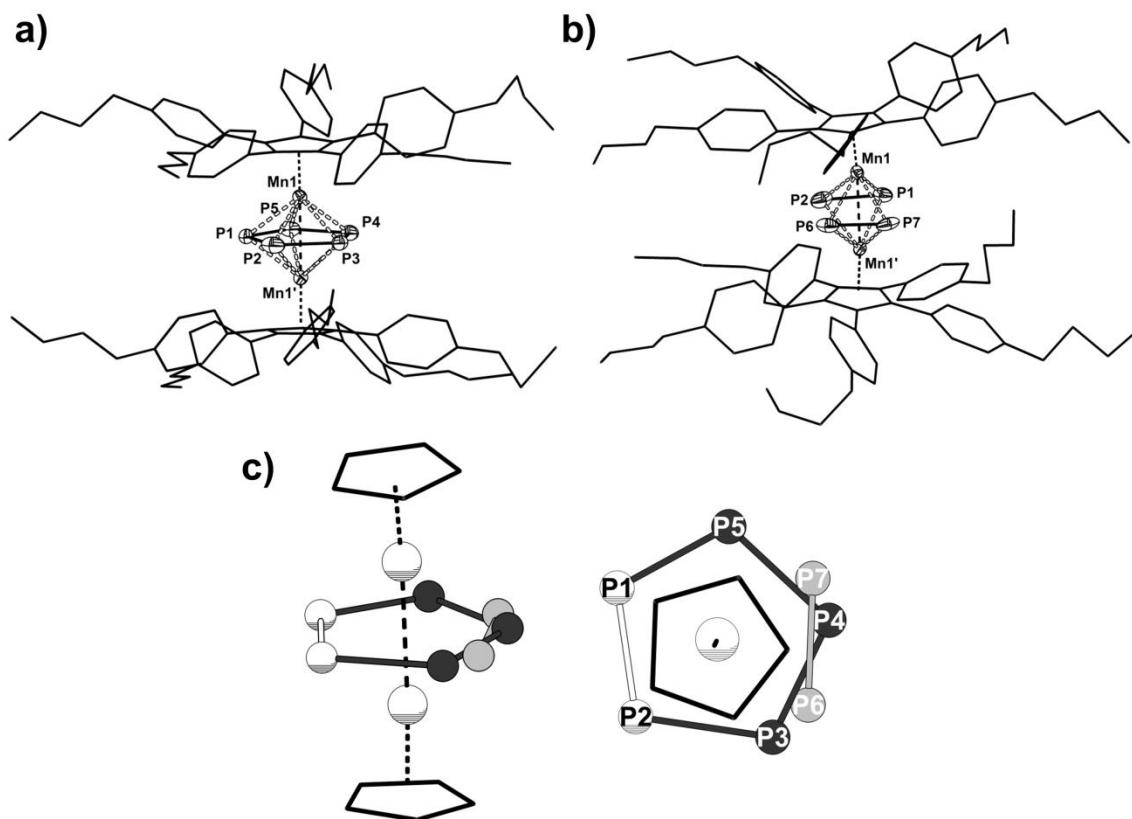
Figure 6.2. Molecular structures of a) **2** and b) **3** in the crystal. For clarity C atoms are shown in 'wire-or-stick' model and H atoms and solvent molecules are omitted. Ellipsoids are drawn at 50% probability level. c) Schematic illustration of the disorder of **2** and **3** in the crystal (left: side view; right: top view). Different parts are colored differently; hashed globes belong to both parts. Selected bond lengths [Å] and angles [°] of **2**: Mn1-Mn1′ 2.7951(3), P1-P2 2.151(2), P2-P3 2.296(2), P3-P4 2.147(3), P4-P5 2.268(2), P1-P5 2.112(2), Mn1-P1 2.3301(6), Mn1-P2 2.327(1), Mn1-P3 2.3280(12), Mn1-P4 2.3414(12), Mn1-P5 2.3375, P_5-Cp 4.35(6), Cp-Cp 8.70(9). Selected bond lengths [Å] and angles [°] of **3**: Mn1-Mn1′ 2.7951(3), P1-P2 2.151(2), P6-P7 2.094(8), P1···P7 3.248(4), P2···P6 2.863(4), Mn1-P1 2.3301(6), Mn1-P2 2.327(1), Mn1-P6 2.324(3), Mn1-P7 2.341(1), (P_2)$_2$-Cp 4.35(6), Cp-Cp 8.70(9), P_2-P_2 10.4(1).

which results in a staggered conformation of the P_5 ring and the downwardly orientated Ph groups. This is also the case for the pentaphosphaferrocene $[Cp^{BIG}Fe(\eta^5\text{-}P_5)]$.[14] Also an interesting feature in the molecular structures of **2** and **3** is the Mn1–Mn1' distance of 2.7951(3) Å, which is in a normal range for Mn–Mn single bonds (CCDC search: 2.5 – 3.1 Å).

In the $^{31}P\{^1H\}$ NMR spectrum of the mixture, only one broadened singlet is observed. Therefore, the signal of one of the two compounds is not observed or **2** and **3** have incidentally the same chemical shifts. By cooling, the signal steadily sharpens, accompanied with an intensity decrease. At 213 K the signal is not observed anymore. Heating up to temperatures up to 373 K results in a further broadening. The ^1H NMR spectrum shows several superimposed signals, which cannot further be assigned to a particular product (see supporting information for the spectrum). The broadening might be explained by the odd number of valence electrons in complex **2**, making it paramagnetic. An unpaired electron also explains the mismatched integrals in the ^1H NMR spectrum.

EPR measurements at room temperature in toluene do not show an EPR signal, as would be expected for the 29 VE triple-decker complex **2**. However, the spectrum at 77 K shows a well resolved anisotropic multiplet (Figure 6.3). The splitting can be explained by coupling of the electron with two Mn centers with a spin of 5/2 each. The g_{iso} value is identified to 1.891035 G. This is slightly smaller than the value of 1.9571398 G we obtained by DFT calculations.[15] The absence of an EPR signal at room temperature might be explained with high spin states for the manganese centers. Upon cooling, the Mn nuclei could alter to low spin states resulting in one single unpaired electron.
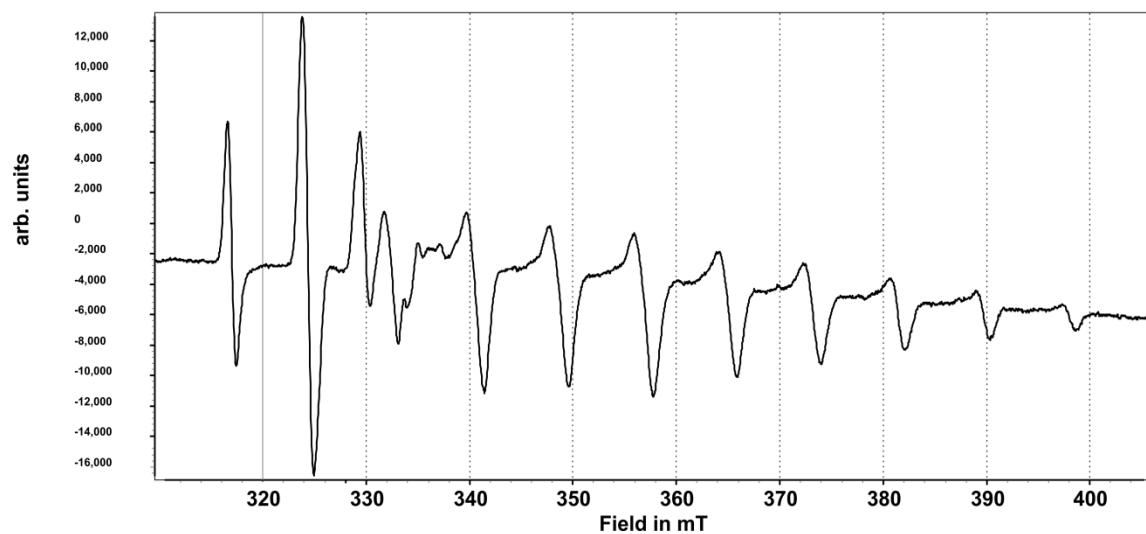
Figure 6.3. EPR spectrum of a mixture of **2** and **3** in toluene at 77 K.

LUMO   HOMO   HOMO-4
              (SOMO)
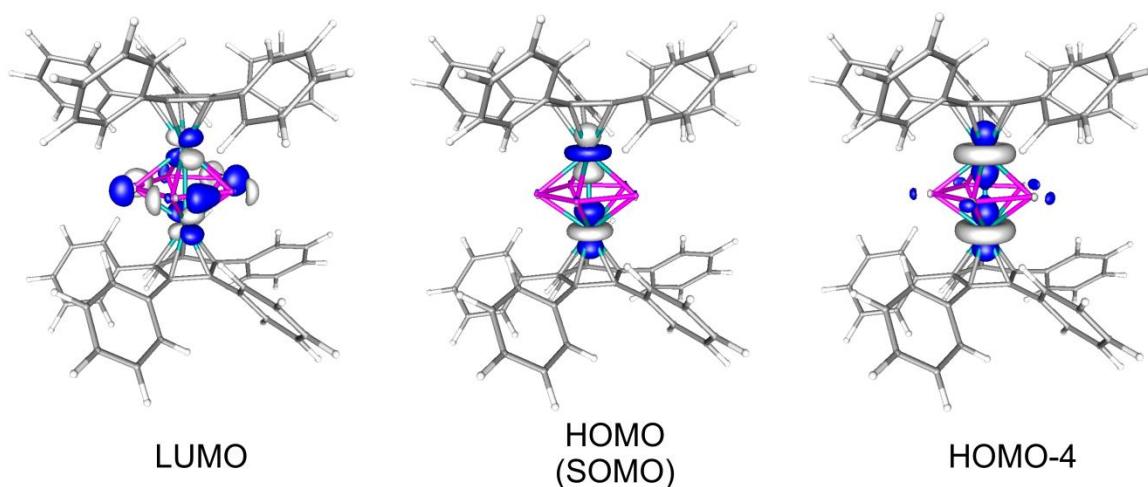
Figure 6.4. Selected α-spin molecular orbitals of [(C$_5$Ph$_5$)Mn(μ,η$^{5:5}$-P$_5$)] (**2b**), calculated at the BP86/def2-SVP level of theory.

The FD mass spectrum exhibits the basic peak at m/z = 1716.5 corresponding to **2**. The two other strong peaks belong to [Cp$^{BIG}_2$Mn] and Cp^{BIG}H, each with relative intensities of 10%. The molecular ion peak of **3** is only observed with an intensity of <1%. The question remains, if in comparison compound **3** is more difficult to be vaporized and ionized than **2**.

To gain more insight into the electronic structure of **2**, DFT calculations have been performed on the model compound [(C$_5$Ph$_5$)Mn(μ,η$^{5:5}$-P$_5$)] (**2′**).[15] The geometric parameters of the optimized structure of **2′** in the doublet spin state are in agreement with the experimental values determined by X-ray diffractions. The calculated Mn–Mn distance in **2′** is 2.878 Å, which is slightly longer than the experimentally determined value of 2.7951(3) Å for **2**. Interestingly, the optimized geometry of **2′** in the excited, quartet spin state differs considerably from the experimental geometry, and is 67.31 kJ mol^{-1} higher in energy. In the quartet spin state the P$_5$ middle deck adopts an envelope conformation with a μ,η$^{4:3}$
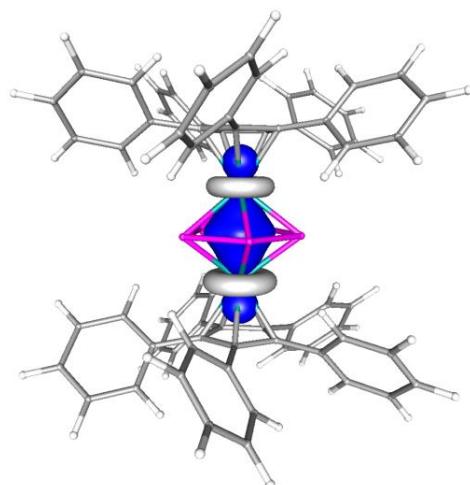
Figure 6.5. Localized molecular orbital representing the Mn–Mn bond in [(C$_5$Ph$_5$)Mn(μ,η$^{5:5}$-P$_5$)] (**2′**). Calculated at the BP86/def2-SVP level of theory.

coordination mode. The Mn–Mn distance is 3.164 Å, considerably longer than the corresponding distance in the doublet spin state. All these results suggest that the ground spin state of **2′** is a doublet, which could be definitely proven by the simulation of the EPR spectrum. According to the calculations, the unpaired electron is equally localized on both manganese atoms. The single occupied molecular orbital (SOMO) is the highest occupied molecular orbital (Figure 6.4). It represents an out-of-phase combination of the dz^2 orbitals of the two manganese atoms. Since the in-phase combination is doubly occupied, results a Mn–Mn bond order of 0.5. This is also confirmed by the calculated Wiberg bond index of 0.6. The localized molecular orbital representing the Mn–Mn bond is depicted in Figure 6.5.

The geometry of the model compound $[(C_5Ph_5)Mn(\mu,\eta^{2:2}-P_2)_2]$ (**3′**) has been optimizes using the same functional and basis set as for **2′**. The optimized geometry shows a short Mn–Mn distance of 2.597 Å which is shorter than the corresponding distance in **2′** (Mn–Mn 2.878 Å) as well as the experimentally determined distance (2.7951(3) Å). This is probably a result of the overestimation of the Mn–Mn interaction in **3′**. The presence of a Mn-Mn bond is clearly indicated by the Localized Molecular Orbitals (Figure 6.6). Furthermore, the Wiberg Bond Index for the Mn-Mn bond is high (1.18) and indicates a very strong bond. Similarly high bond orders were obtained for the Mn–P (0.97) and P–P (0.84 and 0.86) bonds. The Natural Population Analysis shows a moderate charge separation. The two Mn atoms carry a partial positive charge of 0.45 e$^-$ each, while the negative partial charge is delocalized over the Cp ligands. Calculations on **3′** in higher spin states are in progress.

Summing up, we reported on the synthesis of two triple-decker complexes $[\{Cp^{BIG}Mn\}_2(\mu,\eta^{5:5}-P_5)]$ (**2**) and $[\{Cp^{BIG}Mn\}_2(\mu,\eta^{2:2}-P_2)_2]$ (**3**). Unfortunately, a separation of the two compounds was not possible. They represent two new derivatives of the rare P_n ligand

LMO 289   LMO 288   LMO 280
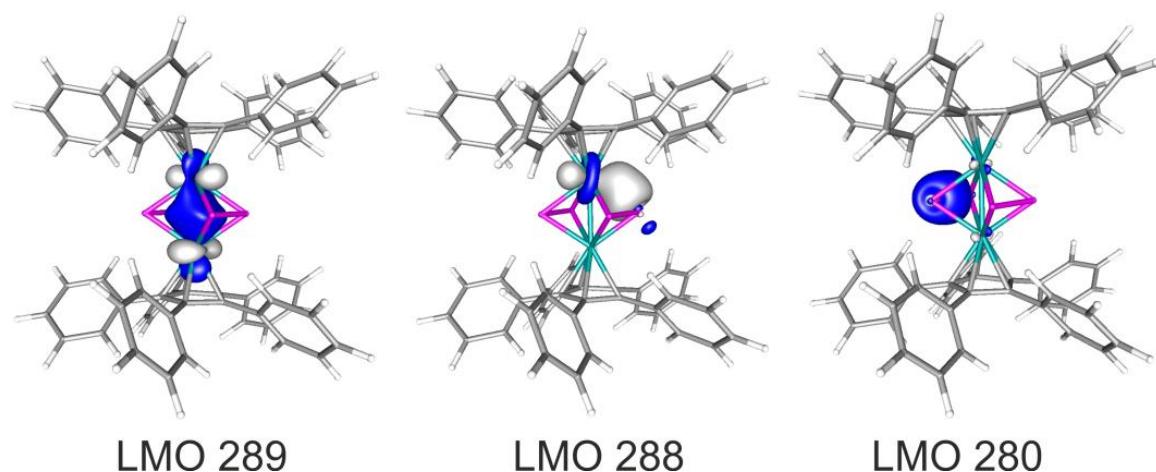
Figure 6.6. Selected localized molecular orbitals representing the Mn–Mn, Mn–P and P–P bond in $[(C_5Ph_5)Mn(\mu,\eta^{2:2}-P_2)_2]$. Calculated at the BP86/def2-SVP level of theory.

complexes of manganese. The compounds were characterized by single crystal X-ray diffraction, mass spectrometry, VT NMR and EPR spectroscopy and elemental analysis. DFT calculations confirmed a doublet ground state for **2** with a Mn–Mn bond through the *cyclo*-P_5 ligand with calculated Wiberg bond index of 0.6.

6.3 Experimental Part

General Remarks:

All experiments were carried out under an atmosphere of dry argon or nitrogen using glovebox and Schlenk techniques. Solvents were purified, dried and degassed prior to use. P_4 was available, cht was used as obtained from commercial suppliers and [$Cp^{BIG}Mn(CO)_3$] was prepared according to literature procedure.[9] The NMR spectra were measured on a Bruker Avance 300, 400 or 600 spectrometer. FD-MS spectra were measured on a Finnigan MAT 95 mass spectrometer. The elemental analyses were determined on a Vario EL III apparatus. The IR spectra were measured on a VARIAN FTS-800 FT-IR spectrometer. For irradiations a TQ150-Z1 Hg lamp from Heraeus was used. The X-Band EPR measurements were carried out with a MiniScope MS400 device with a frequency of 9.5 GHz and rechtangular resonator TE102 of the company Magnettech GmbH.

Synthesis of [$Cp^{BIG}Mn(cht)$] (1):

A solution of [$Cp^{BIG}Mn(CO)_3$] (1.0 g, 1.16 mmol) in 50 mL toluene is irradiated together with cht (0.32g, 0.36 mL, 3.46 mmol) for 30 min. The brown reaction mixture is filtered through Celite and carefully dried in vacuum. Compound **1** is obtained as a brown powder (914 mg, 90%).

1: [$C_{62}H_{73}Mn$] calc.: C, 85.28; H, 8.43. found: C, 84.90; H, 8.37. FD-MS (toluene): *m/z* (%) = 872.7 (100%, [M]+), 818.9 (30%, [$Cp^{BIG}H+cht$]+, Diels-Alder product). IR (CH_2Cl_2, cm-1): ν_{CO} 1917 (s), 1858 (s). ^1H NMR (C_6D_6): δ [ppm] = 0.10 (d, $^3J_{HH}$ = 12.1 Hz, 1H, CH_2-cht), 0.82 (t, $^3J_{HH}$ = 6.8 Hz, 30H, nBu), 1.22 (m, 20H, nBu), 1.47 (m, 20H, nBu), 2.42 (t, $^3J_{HH}$ = 7.3 Hz, 20H, nBu), 2.79 (q, $^3J_{HH}$ = 10.0 Hz, 1H, CH_2-cht), 3.06 (s, 2H, CH-cht), 5.03 (s, 2H, CH-cht), 5.97 (s, 2H, CH-cht), 6.88 (d, $^3J_{HH}$ = 7.0 Hz, 20H, Ph), 7.24 (d, $^3J_{HH}$ = 7.0 Hz, 20H, Ph); see also supplementary information. $^{13}C\{^1H\}$ NMR (CD_2Cl_2): δ [ppm] = 14.1 (*n*Bu), 22.2 (CH_2-cht), 22.7 (*n*Bu), 33.5 (*n*Bu), 35.6 (*n*Bu), 91.0 (CH-cht), 91.4 (CH-cht), 92.5 (CH-cht), 132.7 (Ph), 134.1 (Ph), 140.7 (Ph); one Ph signal is obscured by C_6D_6 signal.

Synthesis of [{Cp^{BIG}Mn}$_2$(μ,$\eta^{5:5}$-P$_5$)] (2) and [{Cp^{BIG}Mn}$_2$(μ,$\eta^{2:2}$-P$_2$)$_2$] (3):

A solution of [Cp^{BIG}Mn(cht)] (400 mg, 0.46 mmol) and P$_4$ (284 mg, 2.3 mmol) in 100 mL toluene is refluxed for 16 h. The brown reaction mixture is dried in vacuum. Column chromatography (25x3 cm, hexane/toluene 2:1, silica) of the residue affords one brown fraction of a mixture of **2** and **3**. A co-crystallized product mixture is obtained from a concentrated toluene solution (310 mg).

Mixture of **2** and **3**: [70% **2** / 30% **3**] calc.: C, 77.37; H, 7.67. found: C, 77.76; H, 7.64. FD-MS (toluene): *m/z* (%) = 1716.5 (100%, [**2**]$^+$), 1686.3 (<1%, [**3**]$^+$), 1506.7 (10%, [Cp$^{BIG}_2$Mn]$^+$), 727.0 (10%, [Cp^{BIG}H]$^+$). ^{1}H NMR (C$_6$D$_6$): δ [ppm] = 0.73 (s-br, 30H, ^{n}Bu), 1.09 (s-br, 20H, ^{n}Bu), 1.29 (s-br, 10H, ^{n}Bu), 1.41 (s, 10H, ^{n}Bu), 2.18 (s-br, 10H, ^{n}Bu), 6.2 (very broad, $\omega_{1/2}$ = 236 Hz, 5H), 6.67 (s-br, 10H, Ph), 7.31 (s-br, 10H). ^{31}P{^{1}H} NMR (C$_6$D$_6$): δ [ppm] = 396.9 (s-br, $\omega_{1/2}$ = 467 Hz).

6.4 References

[1]   A. P. Ginsberg, W. E. Lindsell, *J. Amer. Chem. Soc.* **1971**, *93*, 2082-2084.

[2]   B. M. Cossairt, N. A. Piro, C. C. Cummins, *Chem. Rev.* **2010**, *110*, 4164-4177.

[3]   M. Caporali, L. Gonsalvi, A. Rossin, M. Peruzzini, *Chem. Rev.* **2010**, *110*, 4178-4235.

[4]   a) M. Scheer, G. Balazs, A. Seitz, *Chem. Rev.* **2010**, *110*, 4236-4256. b) N. A. Giffin, J. D. Masuda, *Coord. Chem. Rev.* **2011**, *255*, 1342-1359.

[5]   A. J. Bridgeman, M. J. Mays, A. D. Woods, *Organometallics* **2001**, *20*, 2932-2935.

[6]   A. Strube, J. Heuser, G. Huttner, H. Lang, *J. Organomet. Chem.* **1988**, *356*, C9-C11.

[7]   See chapter 5.

[8]   M. Baudler, T. Etzbach, *Angew. Chem., Int. Ed.* **1991**, *30*, 580-582.

[9]   a) S. Heinl, E. V. Peresypkina, A. Y. Timoshkin, P. Mastrorilli, V. Gallo, M. Scheer, *Angew. Chem., Int. Ed.* **2013**, *52*, 10887-10891. b) S. Heinl, E. V. Peresypkina, A. Y. Timoshkin, P. Mastrorilli, V. Gallo, M. Scheer, *Angew. Chem.* **2013**, *125*, 11087-11091.

[10]   J. A. D. Jeffreys, J. MacFie, *J. Chem. Soc., Dalton Trans.* **1978**, 144-147.

[11]   a) O. J. Scherer, J. Schwalb, G. Wolmershäuser, W. Kaim, R. Gross, *Angew. Chem., Int. Ed.* **1986**, *25*, 363-364. b) Alexander R. Kudinov, Dmitry A. Loginov, Zoya A. Starikova, Pavel V. Petrovskii, M. Corsini, P. Zanello, *Eur. J. Inorg. Chem.* **2002**, *2002*, 3018-3027. c) O. J. Scherer, T. Brueck, G. Wolmershaeuser, *Chem. Ber.* **1989**, *122*, 2049-2054. d) L. Y. Goh, R. C. S. Wong, C. K. Chu, T. W. Hambley, *J. Chem. Soc., Dalton Trans.* **1990**, *0*, 977-982.

[12]   O. J. Scherer, G. Berg, G. Wolmershäuser, *Chem. Ber.* **1995**, *128*, 635-639.

[13]   M. E. Barr, L. F. Dahl, *Organometallics* **1991**, *10*, 3991-3996.

[14]   S. Heinl, G. Balázs, M. Scheer, *Phosphorus, Sulfur Silicon Relat. Elem.* **2014**, DOI: 10.1080/10426507.2014.903489.

[15]   For details on DFT calculations and EPR simulation see supporting information.

6.5 Supplementary Information

NMR Investigations:
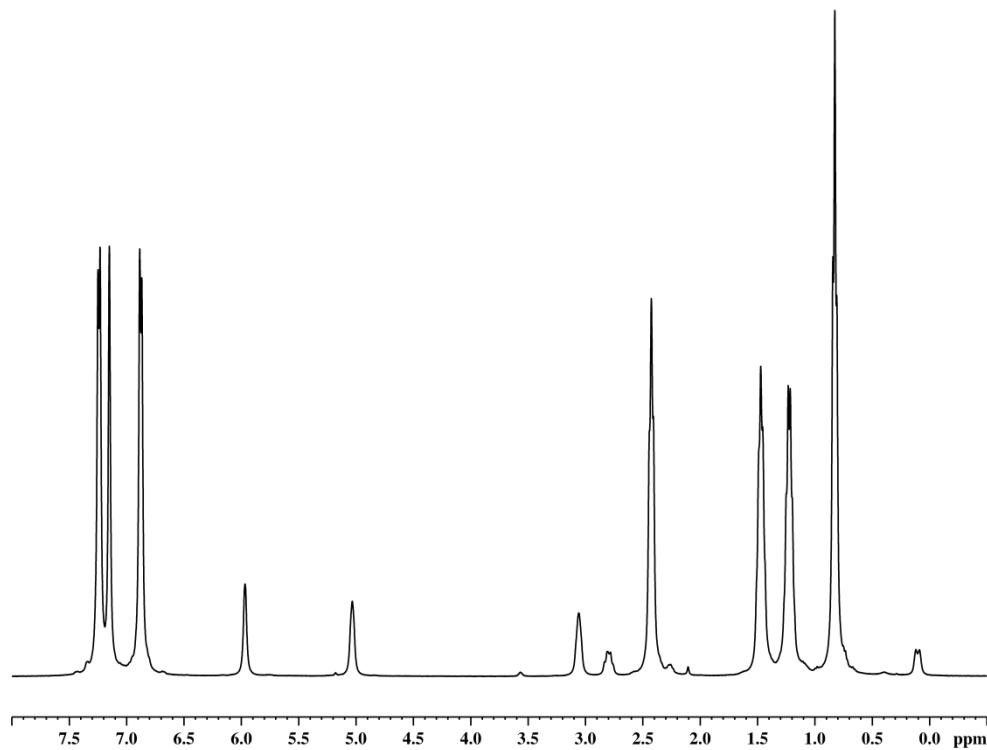
Figure S6.1. ^{1}H NMR spectrum of **1** in C_6D_6 at 298 K.
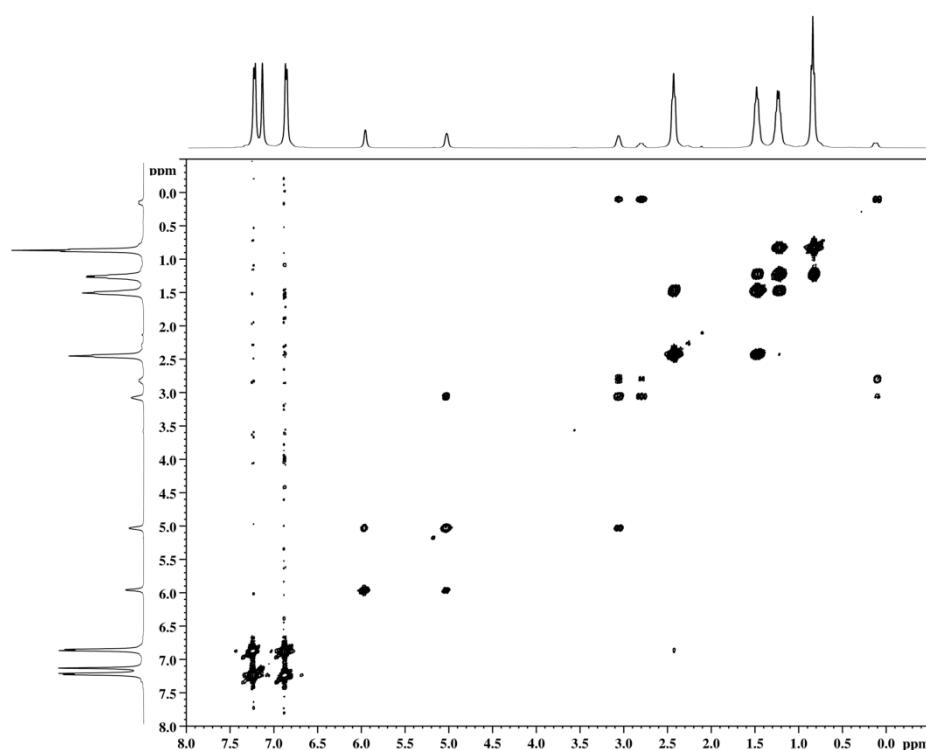
Figure S6.2. ^{1}H COSY NMR of **1** in C_6D_6 at 298 K.
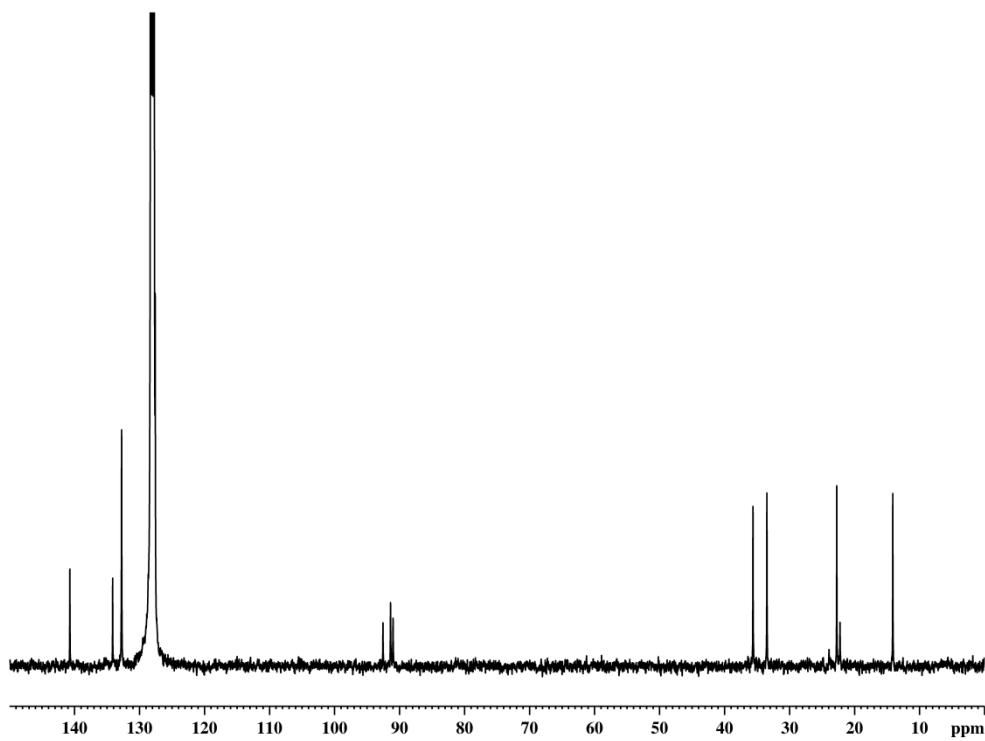
Figure S6.3. $^{13}\{^1H\}$ NMR spectrum of **1** in C_6D_6 at 298 K.
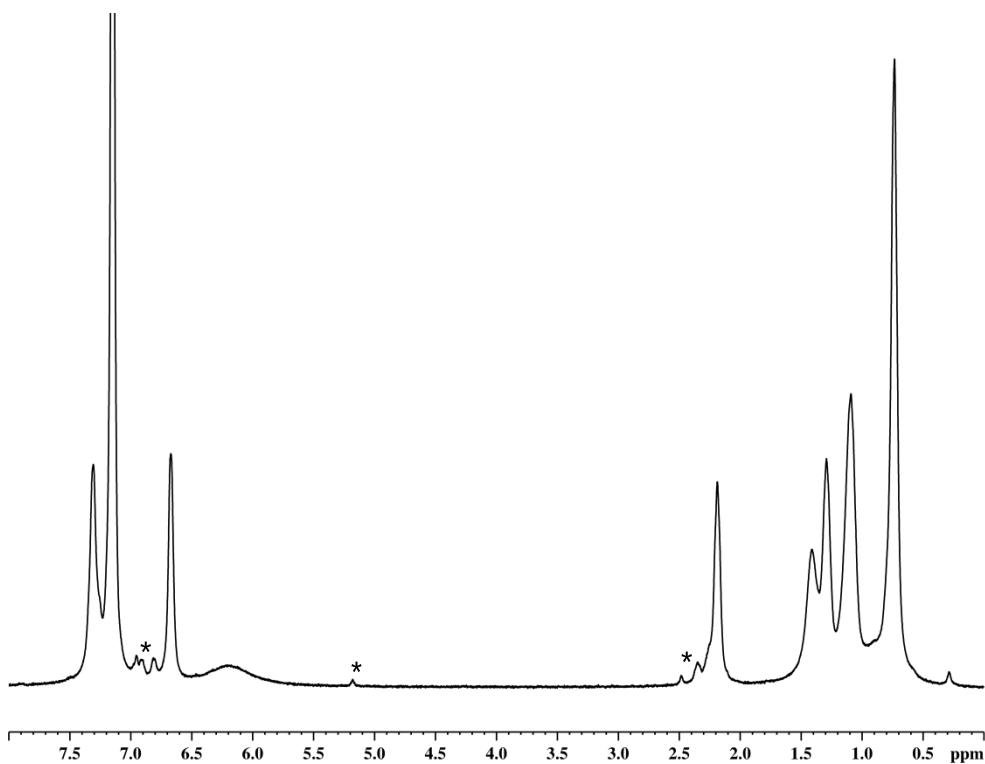
Figure S6.4. ^1H NMR spectrum of a mixture of **2** and **3** in C_6D_6 at 298 K. Signals marked with an asterisk are due to Cp^{BIG}H impurities.
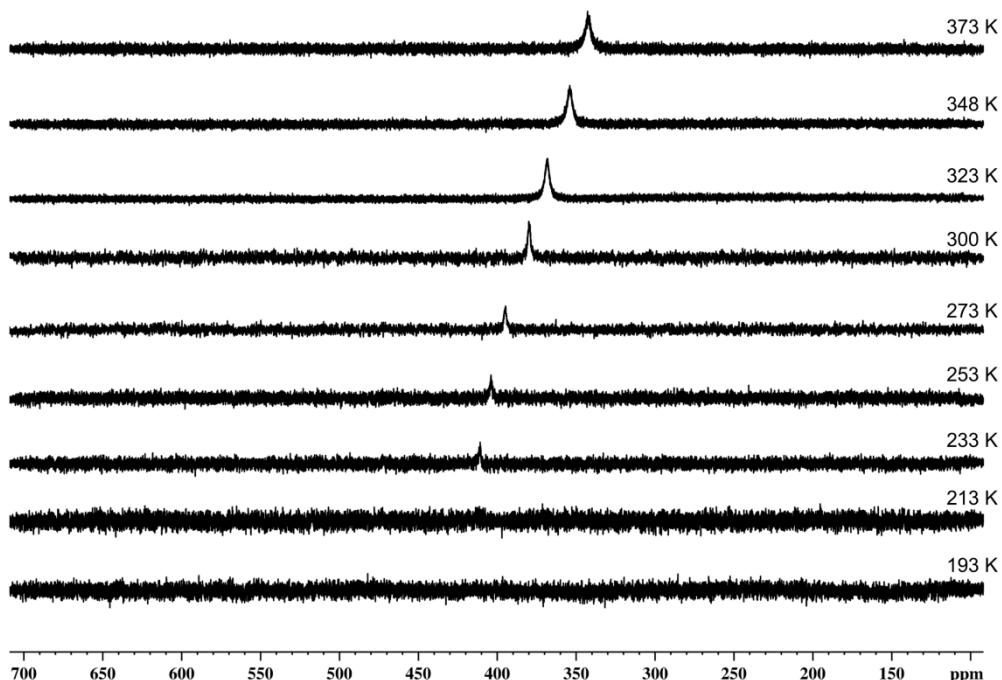
Figure S6.5. ^{31}P{^{1}H} NMR spectrum of a mixture of **2** and **3** at various temperatures. Spectra from 193 K to 300 K have been collected in CD_2Cl_2 and spectra from 323 K to 373 K in d_8-toluene.

Table S6.1. ^{31}P{^{1}H} NMR parameters of a mixture of **2** and **3** at various temperatures. Decrease of temperature results in a signal sharpening effect.

T [K]	Solvent	δ [ppm]	ω$_{1/2}$ [Hz]
373	d_8-toluene	342.9	717
348		354.1	684
323		368.2	559
300		385.2	460
300	CD_2Cl_2	380.1	379
273		394.8	329
253		404.1	375
233		410.9	293

Crystallographic Details:

The crystal structure analyses were performed on an Oxford Diffraction SuperNova diffractometer. For both compounds an analytical absorption correction was carried out.[1] The structures were solved by direct methods of the program SIR-92[2] and refined with the least square method on F^2 employing SHELXL-97[3] with anisotropic displacements for non-H atoms. Hydrogen atoms were located in idealized positions and refined isotropically according to the riding model.

	Crystal Data for **1**	Crystal Data for **2/3**
Empirical Formula	$C_{62}H_{73}Mn$	$C_{110}H_{130}Mn_2P_{4.5}$
Formula Weight	873.14	1707.70
Temperature [K]	123.00(10)	123.0(2)
Crystal System	triclinic	monoclinic
Space Group	$P\bar{1}$	$P2_1/m$
a [Å]	14.1067(7)	17.1190(2)
b [Å]	14.5710(5)	23.5711(3)
c [Å]	14.6081(5)	17.2257(2)
α [°]	105.957(3)	90
β [°]	94.745(3)	110.986(1)
γ [°]	118.726(4)	90
Volume [Å^3]	2448.1(2)	6489.74(14)
Z	2	2
ρ_{calc} [mg/mm^3]	1.184	0.874
μ [mm^{-1}]	2.469	2.386
F(000)	940.0	1821.0
Crystal Size [mm^3]	0.1544 × 0.0909 × 0.0246	0.3349 × 0.1496 × 0.1079
Radiation	Cu-K$_\alpha$ (λ = 1.54178)	Cu-K$_\alpha$ (λ = 1.54178)
2Θ Range	6.5 to 141.76°	6.24 to 147.34°
Index Ranges	-17 ≤ h ≤ 16	-21 ≤ h ≤ 19
	-17 ≤ k ≤ 12	0 ≤ k ≤ 29
	-17 ≤ l ≤ 17	0 ≤ l ≤ 21
Reflections Collected	20575	13256
Independent Reflections	9066	13256
	[R_{int} = 0.0244, R_{sigma} = 0.0291]	[R_{int} = 0.0000, R_{sigma} = 0.0235]
Data/Restraints/Parameters	9066/0/568	13256/228/655
Goodness-of-Fit on F^2	1.034	1.089
Final R Indexes [I > 2σ(I)]	R_1 = 0.0491, wR_2 = 0.1336	R_1 = 0.0654, wR_2 = 0.1955
Final R Indexes [All Data]	R_1 = 0.0558, wR_2 = 0.1400	R_1 = 0.0703, wR_2 = 0.2008
Largest Diff. Peak/Hole [e·Å^{-3}]	1.43/-0.35	1.74/-1.23
Flack Parameter	-	-

With the aid of PLATON,[4] two solvent accessible areas were found in the crystal structure of **2/3**, but it was impossible to refine any reasonable molecules from difference Fourier peaks. Therefore the midpoints, the sizes and the numbers of electrons in the voids were refined and the contribution to the calculated structure factors of the disordered solvent is taken into account by back-Fourier transformation with the program SQUEEZE[5] (Sluis and Spek, 1990). The voids are found around (0.007 0.250 -0.011), and (-0.046 0.750 -0.004) and the sizes are 1052 Å^3 and 298 e$^-$ were detected (whole cell). The number of electrons corresponds each to six toluene molecules.

DFT Calculations:

All calculations were carried out using the TURBOMOLE program package package.[6] The geometries were optimized using the RI-[7]BP86[8] functional together with the def2-SVP[9] basis set for all atoms. The Multipole Accelerated Resolution of Identity (MARI-J)[10] approximation was used in the geometry optimizations. The final energy of the molecules has been determined by single point calculations without using the RI formalism. The EPR g tensors for the model compound [(C$_5$Ph$_5$)Mn(μ,$\eta^{5:5}$-P$_5$)] (**2'**) have been computed using the Orca[11] program package. The EPR spectrum has been simulated with the EasySpin program.[12]

Table S6.2. Calculated g-matrix of [(C$_5$Ph$_5$)Mn(μ,$\eta^{5:5}$-P$_5$)] (**2'**) at the BP86/def2-SVP level of theory.

1.9332035	-0.0026597	0.0000001
0.0026241	1.9332197	0.0000001
0.0000002	0.0000001	2.0049926

Table S6.3. Calculated hyperfine coupling (all values in MHz) for [(C$_5$Ph$_5$)Mn(μ,$\eta^{5:5}$-P$_5$)] (**2'**) at the BP86/def2-SVP level of theory.

Mn 0			
A(FC)	88.1149	88.1149	88.1149
A(SD)	-65.9072	-65.8556	131.7628
A(tot)	22.2077	22.2593	219.8776
A(iso)	88.1149		

Mn 1			
A(FC)	88.1147	88.1147	88.1147
A(SD)	-65.9071	-65.8571	131.7642
A(tot)	22.2076	22.2575	219.8789
A(iso)	88.1147		
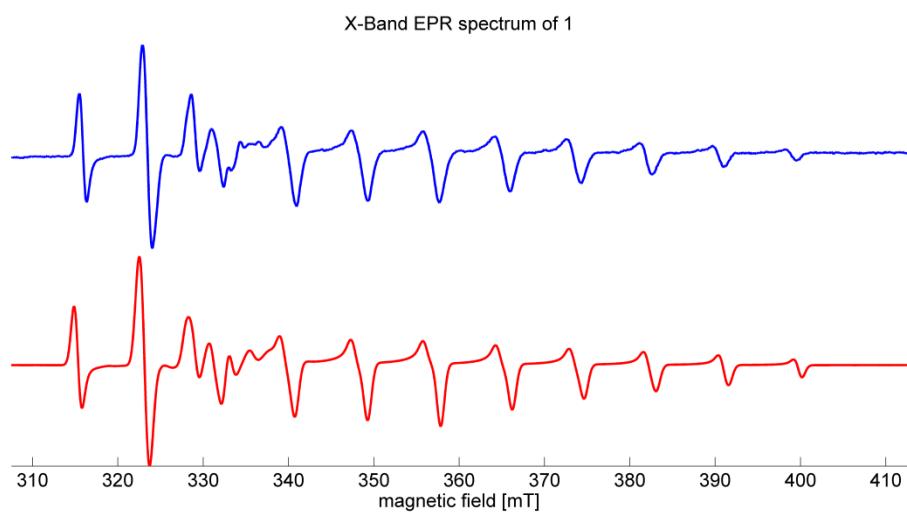
Figure S6.6. Experimental (top) and fitted (bottom) X-Band EPR spectrum of **2** in toluene at 77 K. Parameters used for the fitting: $g_x = g_y = 1.8850$, $g_z = 2.0012$; $A_x = A_y = 30.25$, $A_z = 223.58$ MHz.
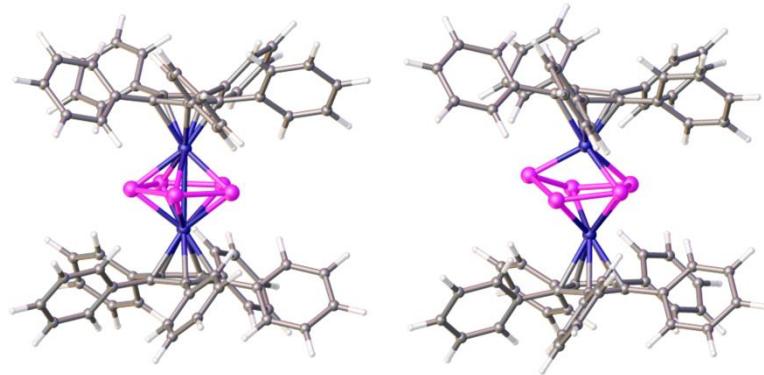
Figure S6.7. Calculated minimum structures of **2'** in doublet (left) and quartet (right) spin state.

Table S6.4. Cartesian coordinates of the optimized geometry of $[(C_5Ph_5)Mn(\mu,\eta^{5:5}-P_5)]$ (**2'**) in the doublet spin state at the BP86/def2-SVP level of theory.

Atom	x	y	z	Atom	x	y	z
Mn	0.001052	-0.0008043	1.438787	C	5.310225	-1.43749	3.944381
Mn	0.0010462	-0.0008075	-1.4387371	H	5.804816	-0.08309	2.313421
P	-1.8824285	-0.1772805	0.0000291	C	0.965445	-3.54151	-2.65858
P	-0.4134781	-1.8469821	0.0000282	C	-0.65845	-3.30378	-4.44699
P	1.6286256	-0.9659119	0.0000229	C	-3.06926	-2.01278	-2.65655
P	1.4219527	1.2486721	0.0000212	C	-3.34617	-0.39465	-4.44452
P	-0.7480431	1.7362972	0.0000249	C	-2.8618	2.298489	-2.6556
C	0.0454834	-1.2351883	3.2128637	C	-1.40909	3.060238	-4.44485
C	-1.160607	-0.424958	3.2119433	C	1.301008	3.431885	-2.65549
C	1.1887648	-0.3385772	3.2130098	C	2.474369	2.286809	-4.44549
C	0.1058738	-2.709742	3.413599	C	2.936989	-1.64438	-4.45176
C	-0.7626528	0.9725086	3.211654	C	3.666855	-0.18005	-2.65862
C	-2.544442	-0.9379756	3.4116304	H	-4.64924	3.474777	2.308724
C	0.6893918	1.0258883	3.2120231	C	-3.45176	4.285365	3.936044
C	2.6095139	-0.7371777	3.4150733	H	-2.05515	4.83353	5.513972
C	0.9654743	-3.5414995	2.6586674	H	1.866291	5.495744	2.308534
C	-0.6584083	-3.3037539	4.4470806	C	3.006982	4.60832	3.936493
C	-1.6779281	2.1304483	3.411376	H	3.959646	3.450542	5.515355
C	-3.0692723	-2.0127205	2.6565411	H	1.581363	-3.10221	-1.86134
C	-3.3461974	-0.3945948	4.4445184	C	1.046734	-4.91789	-2.91747
C	1.5073283	2.2545014	3.4117376	H	-1.31746	-2.67534	-5.06282
C	2.937019	-1.6444451	4.4517102	C	-0.57433	-4.68066	-4.70611
C	3.6668521	-0.1801128	2.6585636	H	-2.46078	-2.46272	-1.85956

Atom	x	y	z	Atom	x	y	z
H	1.5813209	-3.102226	1.8613621	C	-4.35305	-2.5158	-2.91516
C	1.0468584	-4.9178632	2.9176511	H	-2.95269	0.426755	-5.06014
H	-1.3174921	-2.6753184	5.0628524	C	-4.6295	-0.90066	-4.70345
C	-0.5741985	-4.6806066	4.7063058	H	-3.10173	1.581227	-1.85818
C	0.0454727	-1.2351952	-3.2128125	C	-3.73642	3.364481	-2.91401
C	-1.1606183	-0.4249663	-3.2118902	H	-0.50679	2.938892	-5.06097
C	-0.762667	0.9725011	-3.2116053	C	-2.28629	4.124992	-4.70354
C	0.6893773	1.0258826	-3.2119793	H	0.544887	3.437461	-1.858
C	1.1887519	-0.338582	-3.2129666	C	2.043895	4.59355	-2.91381
C	-2.8617778	2.2985091	2.6556365	H	2.637955	1.391454	-5.06197
C	-1.4090588	3.0602636	4.4448759	C	3.21516	3.450594	-4.70419
H	-2.4607215	-2.4627776	1.8596759	H	2.134879	-2.07409	-5.06859
C	-4.3531715	-2.5155748	2.9149788	C	4.272106	-1.9898	-4.71287
H	-2.9526482	0.4266905	5.0602511	H	3.440042	0.538428	-1.85848
C	-4.6296296	-0.900434	4.7032674	C	5.000659	-0.52792	-2.91955
C	1.3009978	3.4319027	2.6555624	H	1.721057	-5.54368	-2.31283
C	2.4743602	2.2868215	4.4455559	C	0.274887	-5.49547	-3.9393
H	2.1349396	-2.0739847	5.0686999	H	-1.1778	-5.11782	-5.51662
C	4.2721178	-1.9901103	4.7125921	H	-4.73936	-3.35075	-2.31053
H	3.4400418	0.538532	1.8585675	C	-5.14133	-1.96049	-3.93675
C	5.0006382	-0.5282237	2.9192593	H	-5.23211	-0.46199	-5.51379
H	1.7212326	-5.5436413	2.3130694	H	-4.64933	3.474693	-2.30877
C	0.2750584	-5.4954155	3.9395309	C	-3.45184	4.285281	-3.93609
H	-1.1776008	-5.1177529	5.5168691	H	-2.05524	4.833435	-5.51402
C	0.1058611	-2.709751	-3.413533	H	1.866456	5.495659	-2.30831
C	-2.5444477	-0.9379925	-3.4115932	C	3.00713	4.608246	-3.93629
C	-1.677946	2.1304368	-3.4113338	H	3.959809	3.450467	-5.51514
C	1.5073161	2.254495	-3.4116883	H	4.500564	-2.69616	-5.52593
C	2.6094992	-0.7371703	-3.4150663	C	5.310238	-1.43708	-3.94477
H	-3.1017312	1.5812167	1.8582506	H	5.80486	-0.08265	-2.31384
C	-3.7363529	3.3645439	2.913995	H	0.338207	-6.57606	4.140297
H	-0.5067875	2.9388926	5.0610236	H	-6.14965	-2.35459	4.136944
C	-2.2862281	4.1250606	4.7035159	H	-4.13793	5.122717	4.136316
H	-4.7395321	-3.3504262	2.3102488	H	3.590562	5.520123	4.13688
C	-5.1414941	-1.9601952	3.9364967	H	6.3572104	-1.711444	4.1465517
H	-5.232297	-0.4616639	5.513506	H	0.3379799	-6.576126	-4.140007
H	0.5449438	3.4374513	1.8580119	H	6.3572332	-1.71089	-4.14708
C	2.0437875	4.5936094	2.9139737	H	-6.149424	-2.354984	-4.137303
H	2.6380155	1.3914319	5.0619742	H	-4.138034	5.1226063	-4.136389
C	3.2150535	3.4506475	4.7043511	H	3.5907646	5.520026	-4.136622
H	4.5005798	-2.6966028	5.5255272				

Table S6.5. Cartesian coordinates of the optimized geometry of $[(C_5Ph_5)Mn(\mu,\eta^{4:3}-P_5)]$ (**2′**) in the quartet spin state at the BP86/def2-SVP level of theory.

Atom	x	y	z	Atom	x	y	z
Mn	-0.0624735	-0.1911833	1.6008121	C	5.2539884	-1.621206	4.1176793
Mn	-0.0257799	-0.0714212	-1.5606218	H	5.7487031	-0.566309	2.2789972
P	-1.9085371	-0.4435226	-0.1426019	C	1.0522828	-3.508108	-3.032862
P	-0.6372244	-2.1223567	0.5123983	C	-0.528837	-3.223461	-4.853048
P	1.3483396	-1.4168045	-0.1385719	C	-2.963619	-2.112009	-2.933343
P	1.430057	0.8257953	0.1013866	C	-3.342833	-0.426089	-4.640114
P	-0.7378658	1.4757771	0.096471	C	-2.898113	2.1972079	-2.700549
C	-0.0004119	-1.2717109	3.4737666	C	-1.517123	3.118368	-4.472762
C	-1.1877332	-0.434881	3.4225062	C	1.2014715	3.423014	-2.610034
C	1.1663902	-0.416371	3.3708429	C	2.4616186	2.49463	-4.468726
C	0.0374511	-2.7296277	3.7739988	C	3.0437191	-1.440561	-4.68631
C	-0.7541651	0.9437676	3.2949111	C	3.6379006	-0.095824	-2.75185
C	-2.5847755	-0.8801762	3.6880728	H	-4.592207	3.4413054	2.2157008
C	0.7007725	0.9537359	3.2703191	C	-3.369361	4.3557212	3.7672858
C	2.5760014	-0.8514958	3.5791614	H	-1.952119	5.00502	5.2873301
C	0.8838331	-3.6164714	3.0672101	H	1.9421025	5.3038769	1.9587145
C	-0.7336431	-3.2478924	4.8408711	C	3.1473016	4.5101777	3.5887914
C	-1.6419921	2.1332061	3.4114919	H	4.1552677	3.4481055	5.1999582
C	-3.1844826	-1.9610357	3.0026157	H	1.6314191	-3.09297	-2.19479
C	-3.3259117	-0.2498269	4.7172013	C	1.1649421	-4.871	-3.346503
C	1.5591297	2.169398	3.3308897	H	-1.184708	-2.580045	-5.45715
C	2.8973514	-1.6118412	4.7298206	C	-0.413511	-4.586198	-5.166395
C	3.6254535	-0.4809904	2.7084078	H	-2.319287	-2.566582	-2.16698

H	1.5049793	-3.2326579	2.2446259	C	-4.233082	-2.652206	-3.185859
C	0.9474916	-4.9753444	3.4084645	H	-2.995206	0.4381035	-5.224126
H	-1.3845654	-2.5745059	5.4166392	C	-4.612651	-0.969163	-4.892187
C	-0.6676278	-4.6084997	5.1816453	H	-3.091589	1.4253844	-1.941448
C	0.0945302	-1.1986888	-3.5136846	C	-3.809945	3.2501083	-2.86646
C	-1.1294579	-0.4366745	-3.4483193	H	-0.626851	3.0645117	-5.115969
C	-0.7732273	0.9835636	-3.3823202	C	-2.431487	4.1699023	-4.638393
C	0.6659171	1.083259	-3.4245666	H	0.4268735	3.3200349	-1.836186
C	1.2032512	-0.2595214	-3.4571923	C	1.9298902	4.6168708	-2.715503
C	-2.8254013	2.2615001	2.6476864	H	2.6654124	1.6707277	-5.167936
C	-1.3466489	3.1373691	4.3639468	C	3.1881532	3.6907388	-4.57279
H	-2.6238274	-2.4781566	2.2095426	H	2.2854144	-1.841091	-5.37449
C	-4.4812622	-2.38895	3.3240917	C	4.3986301	-1.743398	-4.891322
H	-2.8740884	0.581502	5.2772614	H	3.3455238	0.5511856	-1.911626
C	-4.6222386	-0.6798981	5.0399475	C	4.991219	-0.403894	-2.956092
C	1.3431573	3.2913556	2.4966084	H	1.8319361	-5.510665	-2.748197
C	2.5826121	2.2519192	4.3056686	C	0.4315302	-5.41786	-4.412497
H	2.0979041	-1.8995387	5.4281366	H	-0.988591	-4.999572	-6.009401
C	4.2219688	-1.991513	4.9959039	H	-4.574847	-3.525839	-2.609745
H	3.3983191	0.1110899	1.810272	C	-5.064899	-2.082201	-4.164499
C	4.9489062	-0.8633403	2.9747592	H	-5.252033	-0.517116	-5.666177
H	1.6111381	-5.6461195	2.841454	H	-4.708129	3.29371	-2.23144
C	0.1696611	-5.4788665	4.4649564	C	-3.580635	4.2430459	-3.833645
H	-1.2766829	-4.9886965	6.0163255	H	-2.243421	4.9366684	-5.405813
C	0.1997158	-2.659868	-3.776593	H	1.716958	5.4450133	-2.022088
C	-2.497803	-0.9865603	-3.6527642	C	2.9272438	4.7567055	-3.695626
C	-1.7316599	2.1158862	-3.4961122	H	3.963104	3.7895582	-5.348597
C	1.4560856	2.3397726	-3.4839782	H	4.6893401	-2.386959	-5.735953
C	2.6410582	-0.6117216	-3.6116251	C	5.3780307	-1.229164	-4.025321
H	-3.077799	1.4867717	1.9097398	H	5.7495675	0.0053978	-2.271065
C	-3.6780833	3.3614223	2.823887	H	0.2183371	-6.546231	4.7303436
H	-0.4414446	3.0483171	4.9819499	H	-6.226571	-2.083896	4.5917356
C	-2.2016428	4.2368575	4.5390606	H	-4.038355	5.2196094	3.9025453
H	-4.9265635	-3.2305837	2.7716103	H	3.7650386	5.4163179	3.6854423
C	-5.208033	-1.748889	4.3418419	H	6.2928999	-1.92165	4.3238543
H	-5.1771765	-0.1739446	5.8450477	H	0.5192853	-6.487908	-4.656145
H	0.54373	3.2617441	1.7418921	H	6.4404407	-1.470508	-4.183892
C	2.1289008	4.4462689	2.6230298	H	-6.06225	-2.50533	-4.360279
H	2.7566372	1.4026638	4.9812944	H	-4.29682	5.0692855	-3.962029
C	3.3668938	3.4091148	4.4324653	H	3.4989178	5.6941387	-3.776016
H	4.4472083	-2.5813435	5.8978903				

LUMO+1
-2.851 eV

LUMO
-3.847 eV

HOMO
-4.574 eV

HOMO-3
-5.100 eV

HOMO-1
-4.789 eV
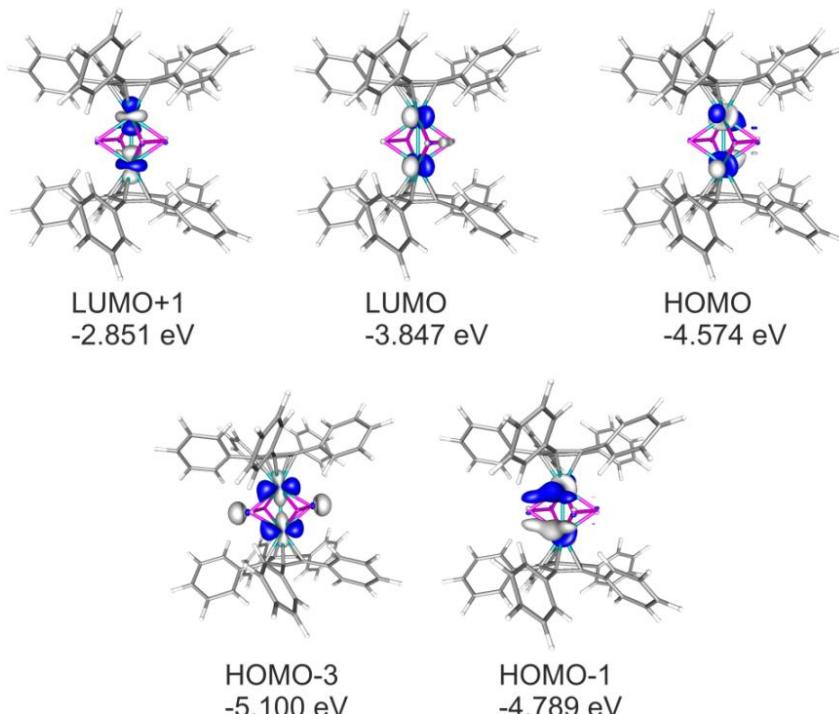
Figure S6.8. Selected molecular orbitals in [(C$_5$Ph$_5$)Mn(μ,$\eta^{2:2}$-P$_2$)$_2$] (**3′**). Calculated at the BP86/def2-SVP level of theory.

Table S6.6. Cartesian coordinates of the optimized geometry of [(C₅Ph₅)Mn(μ,η$^{4:3}$-P₅)] (**3′**) in the singlet spin state at the BP86/def2-SVP level of theory.
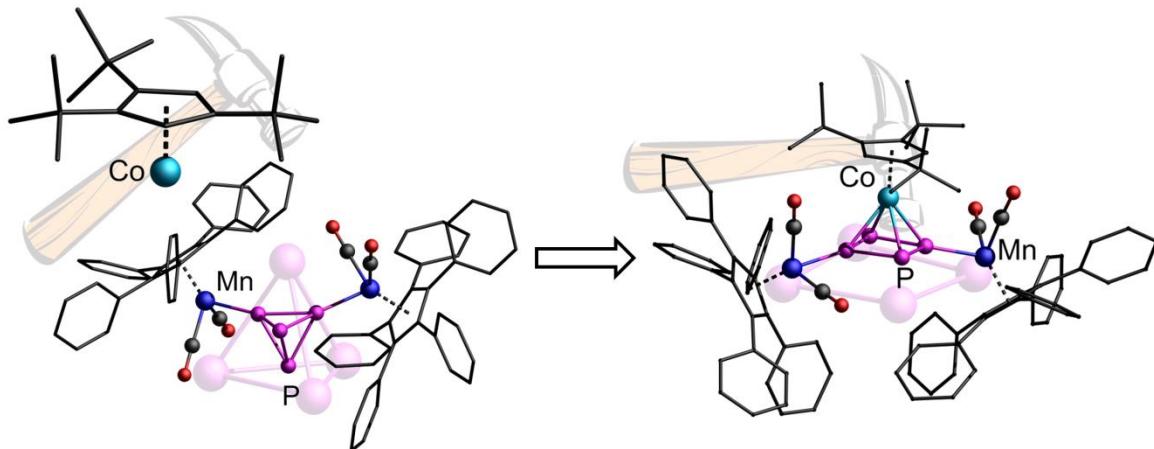
Atom	x	y	z	Atom	x	y	z
Mn	-0.1195806	0.0991271	0.0835406	C	3.749817	6.127878	2.6798709
Mn	-0.1195849	2.6959809	0.0835199	C	3.4836867	6.3724826	-2.6965108
P	-0.5156862	1.3975386	-1.7461554	C	4.5881455	4.4336897	-1.7465684
P	-1.9719006	1.3975484	-0.1397941	C	-0.9833635	-2.6853589	-5.3150265
P	0.1636388	1.3975689	1.9232613	C	-5.5862202	-2.3787811	-0.7285272
P	1.716637	1.397558	0.4154819	C	-2.5918863	-2.2360847	5.0220311
C	-0.3532298	-1.7448837	-1.1384484	C	3.8015714	-2.6165852	3.8866637
C	-1.3579812	-1.7152952	-0.0856847	C	4.6371798	-2.7888649	-2.5511169
C	-0.6624749	-1.7035135	1.1890557	C	-0.9831866	5.4804695	-5.3150965
C	0.7647095	-1.7589714	0.9230306	C	-5.5862838	5.1737018	-0.7284805
C	0.9536436	-1.764825	-0.5158657	C	-2.591824	5.0311435	5.0220346
C	-0.3532358	4.5399688	-1.1384985	C	3.8017637	5.4113868	3.8865107
C	-1.3579929	4.5103965	-0.0857389	C	4.6371791	5.5841579	-2.5510509
C	-0.6624929	4.498638	1.1890059	H	0.7811527	-0.5084434	-3.3383807
C	0.7646937	4.5540951	0.9229875	H	-1.9983119	-3.6305904	-2.1804242
C	0.9536347	4.5599314	-0.5159083	H	-2.9929843	-0.4998946	-1.9514015
C	-0.5999992	-2.0087433	-2.5846524	H	-3.0060353	-3.3945328	1.285119
C	-2.8214632	-1.8985348	-0.2892797	H	-2.5702492	-0.0894684	2.3407912
C	-1.307794	-1.8444305	2.5253956	H	-0.208423	-3.6610605	3.008723
C	1.8288414	-1.9979961	1.9373541	H	1.1588319	-0.4961137	3.364664
C	2.2292033	-2.0548895	-1.2368702	H	2.7420811	-3.6076172	0.7834851
C	-0.599998	4.803792	-2.5847117	H	1.3993341	-3.8448813	-2.1627033
C	-2.8214768	4.6936281	-0.2893457	H	3.3679981	-0.3721382	-0.4702731
C	-1.3078045	4.6395487	2.5253514	H	0.7810194	3.3033475	-3.3383996
C	1.8288318	4.7930829	1.9373143	H	-1.9982688	6.4256885	-2.1805338
C	2.2291914	4.8500391	-1.2369022	H	-2.9929602	3.2950419	-1.9515177
C	0.0882389	-1.317604	-3.6079378	H	-3.0060568	6.1896864	1.2849954
C	-1.4721659	-3.0594927	-2.9586053	H	-2.5702448	2.8845737	2.3407563
C	-3.5248021	-1.2196945	-1.313722	H	-0.2084175	6.4561668	3.0086914
C	-3.5323903	-2.8345258	0.4997858	H	1.1587823	3.2911949	3.3645993
C	-2.3014247	-0.9469886	2.9758665	H	2.7420942	6.4027247	0.7834895
C	-0.9714492	-2.9449914	3.3478698	H	1.3992685	6.6400103	-2.1627281
C	1.8853675	-1.2970289	3.1642123	H	3.3680482	3.1673394	-0.470281
C	2.7765493	-3.0276513	1.7160067	H	0.4401277	-1.0927264	-5.7352673
C	2.2933165	-3.2148898	-2.0477639	H	-2.3459809	-4.2135516	-4.5739004
C	3.3986692	-1.2768855	-1.0955676	H	-5.4151313	-0.9104827	-2.3270554
C	0.0882629	4.1126377	-3.6079727	H	-5.4283254	-3.8046395	0.9092225
C	-1.4721522	5.8545401	-2.9586983	H	-3.7097383	-0.4305432	4.5419357
C	-3.5248085	4.014771	-1.3137832	H	-1.3275491	-3.9981493	5.2119255
C	-3.5324198	5.6296126	0.4997149	H	2.8885126	-1.0306417	5.0661491
C	-2.301401	3.7420791	2.9758443	H	4.4721039	-4.1400781	2.4829795
C	-0.9714509	5.7401022	3.3478326	H	3.5072221	-4.4838838	-3.3207261
C	1.885375	4.0920562	3.1641379	H	5.484662	-1.0115378	-1.6228877
C	2.7765954	5.8226875	1.7159659	H	0.440505	3.8879977	-5.7352687
C	2.2932744	6.0100531	-2.0477796	H	-2.3461401	7.0083984	-4.5740444
C	3.3986914	4.0720899	-1.0955726	H	-5.4151637	3.7054298	-2.3270295
C	-0.1037669	-1.6500278	-4.9571965	H	-5.428388	6.5996451	0.9091952
C	-1.6621643	-3.3924196	-4.308921	H	-3.7095799	3.225526	4.5419992
C	-4.8906946	-1.455642	-1.5273366	H	-1.327556	6.793263	5.2118859
C	-4.8990418	-3.0705346	0.2822605	H	2.8886137	3.825499	5.0660017
C	-2.9384355	-1.1422472	4.2098505	H	4.4723104	6.9349165	2.4828726
C	-1.6065922	-3.1367229	4.5856805	H	3.5071493	7.2791043	-3.3207147
C	2.8625642	-1.5990566	4.1237263	H	5.4847095	3.8068417	-1.6228442
C	3.7496638	-3.3329907	2.6799719	H	-6.6589966	5.3562885	-0.8961242
C	3.4837274	-3.5772563	-2.6965322	H	5.5705697	5.8656533	-3.0626033
C	4.5881201	-1.6384185	-1.7466054	H	5.5705609	-3.0702942	-3.0627227
C	-0.103566	4.4451713	-4.9572295	H	-1.1362354	-2.9430266	-6.374441
C	-1.6621529	6.187421	-4.3090256	H	-6.658894	-2.5615014	-0.8962739
C	-4.8907285	4.2506209	-1.5273313	H	-1.1359348	5.7382089	-6.3745116
C	-4.8990949	5.8655379	0.2822436	H	-3.0882056	-2.3847907	5.9934161
C	-2.9383514	3.9372888	4.2098673	H	4.5684116	-2.8523347	4.6407182
C	-1.606575	5.9318179	4.5856559	H	-3.0881563	5.179859	5.9934118
C	2.8626654	4.3939478	4.1235993	H	4.5687036	5.6470019	4.6405061

References for Supplementary Information:

[1]   R. C. Clark, J. S. Reid, *Acta Cryst.* **1995**, A51, 887-897.

[2]   A. Altomare, M. C. Burla, M. Camalli, G.L. Cascarano, C. Giacovazzo, A. Guagliardi, A. G. G. Moliterni, G. Polidori, R. Spagna, *J. Appl. Cryst.* **1999**, 32, 115-119.

[3]   G. M. Sheldrick, *Acta Cryst.* **2008**, A64, 112-122.

[4]   Spek, A.L. *J. Appl. Cryst.* **2003**, 36, 7-13.

[5]   Sluis, P. van der & Spek, A.L. *Acta Cryst.* **1990**, A46, 194-201.

[6]   a) R. Ahlrichs, M. Bär, M. Häser, H. Horn, C. Kölmel, *Chem. Phys. Lett.* **1989**, *162*, 165–169; b) O. Treutler, R. Ahlrichs, *J. Chem. Phys.* **1995**, *102*, 346–354.

[7]   a) K. Eichkorn, O. Treutler, H. Oehm, M. Häser, R. Ahlrichs, *Chem. Phys. Lett.* **1995**, *242*, 652–660; b) K. Eichkorn, F. Weigend, O. Treutler, R. Ahlrichs, *Theor. Chem. Acc.* **1997**, *97*, 119.

[8]   a) P. A. M. Dirac, *Proc. Royal Soc. A*, **1929**, *123*, 714-733. b) J. C. Slater, *Phys. Rev.* **1951**, *81*, 385-390. c) S. H. Vosko, L. Wilk, M. Nusair, *Can. J. Phys.* **1980**, *58*, 1200-1211. d). A. D. Becke, *Phys. Rev. A*, **1988**, *38*, 3098. e) J. P. Perdew, *Phys. Rev. B* **1986**, *33*, 8822-8824.

[9]   a) A. Schäfer, H. Horn, R. Ahlrichs; *J. Chem. Phys.* **1992**, *97*, 2571; b) F. Weigend *Phys. Chem. Chem. Phys.* **2006**, *8*, 1057.

[10]   M. Sierka, A. Hogekamp, R. Ahlrichs, *J. Chem. Phys.* **2003**, *118*, 9136.

[11]   F. Neese, *WIREs Comput. Mol. Sci.,* **2012**, *2*, 73-78.

[12]   S. Stoll, A. Schweiger, *J. Magn. Reson.* **2006**, *178*, 42-55.

7. Activation of Coordinated P$_4$ Tetrahedra with 14 Valence Electron {Cp'''Co} Fragments

Sebastian Heinl, Maria Caporali, Fuencisla Delgado, Maurizio Peruzzini and Manfred Scheer
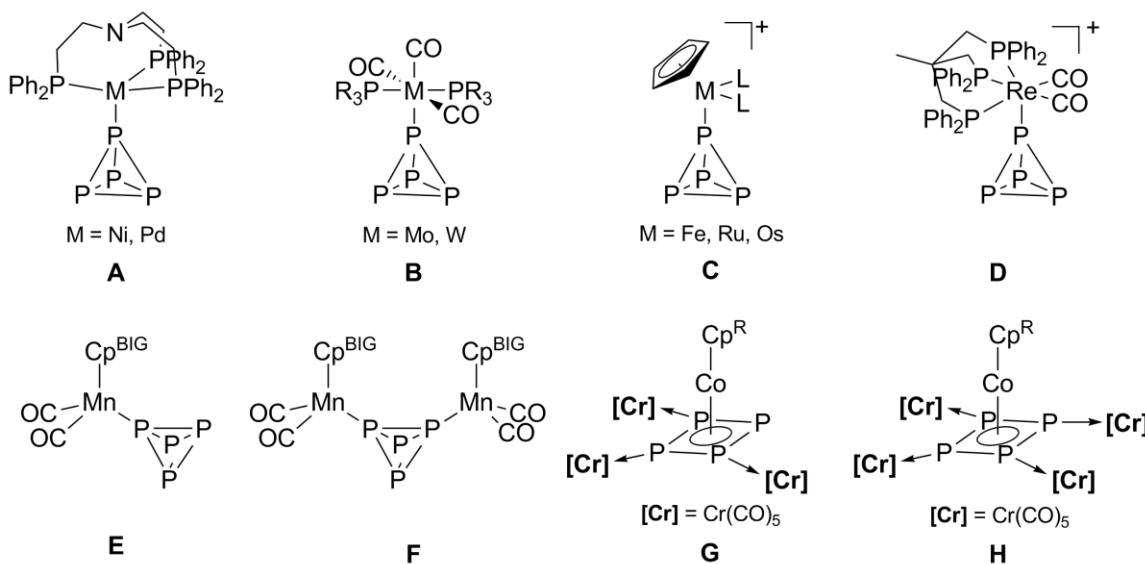
unpublished results

- ❖ **All syntheses and characterizations were performed by Sebastian Heinl with the aid of Dr. Maria Caporali, Fuencisla Delgado and Dr. Maurizio Peruzzini in the course of a short term scientific mission (STSM; COST Action CM0802)**
- ❖ **Manuscript was written by Sebastian Heinl**
- ❖ **Figures were made by Sebastian Heinl**
- ❖ **X-ray structure analyses and refinement were performed by Sebastian Heinl**
- ❖ **NMR simulation was performed by Sebastian Heinl**

7.1 Introduction

Compounds with substituent-free phosphorus P$_n$ units are known for almost all transition metals[1] and for a large number of main group elements.[2] The starting material of choice is white phosphorus. For the metal mediated activation of P$_4$ coordinative unsaturated metal fragments are needed. To generate such fragments, normally elevate temperatures are used. During the thermodynamic controlled reactions usually a degradation of the P$_4$ molecule is observed, but aggregation to larger phosphorus scaffolds is also known. To be able to obtain and characterize intermediates, milder reaction conditions should be applied. The triple-decker complex [(Cp′′′Co)$_2$(μ-toluene)] (1) for example is known to partially dissociate into the electron deficient 14 valence electron fragment {Cp′′′Co} in solution.[3] This enables the activation of white phosphorus under exceedingly mild conditions, inter alia resulting in P$_n$ ligand complexes with very large number of P atoms (n ≤ 29).[4]

Among P$_n$ ligand complexes, compounds with white phosphorus as ligand are rather rare (Scheme 7.1). In the late 1970s, Sacconi and co-workers reported on the first complexes of type **A** bearing intact P$_4$ tetrahedra.[5] Some further neutral complexes **B**, **E** and **F** were published by Scheer et al.[6] Furthermore, the group of Peruzzini et al. synthesized a large number of cationic complexes of the 8th group from the type **C** and the Re complex **D**.[7] Several of the cationic derivatives show an interesting reaction behavior towards water. Treatment with H$_2$O results in the hydrolysis of the P$_4$ ligand and formation of PH$_3$, P$_2$H$_4$ and other phosphorus containing products PO$_n$H$_m$.[7b-e,8] This is surprising, considering that free P$_4$ is inert against water, the reason why white phosphorus is stored under it.
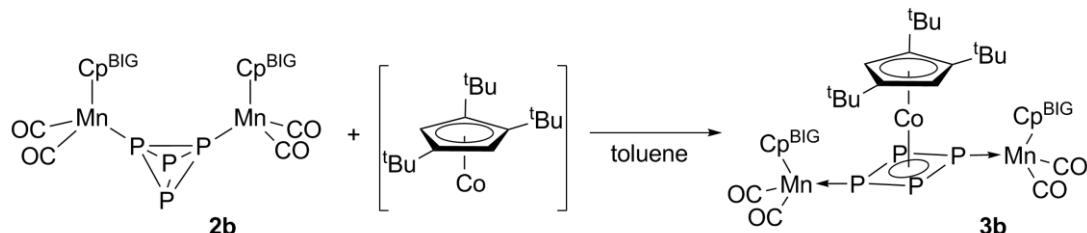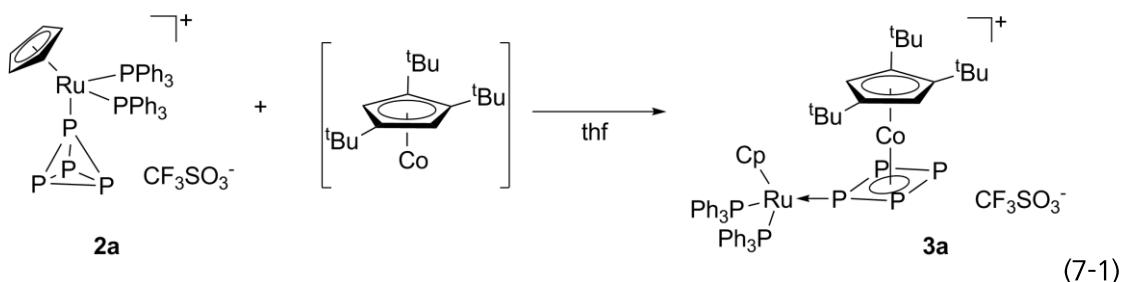
Scheme 7.1. Selected complexes with P$_4$ tetrahedra as ligands.

It was of special interest whether a pre-coordinated P_4 tetrahedron shows different reactivity in comparison to free P_4. Herein we report on the reactions of [(Cp'''Co)$_2$(μ-toluene)] (**1**) with the cationic mononuclear complex [CpRu(PPh$_3$)$_2$(η^1-P$_4$)][CF$_3$SO$_3$] (**2a**; type C) and the neutral binuclear complex [{Cp^{BIG}Mn(CO)$_2$}$_2$(μ,η$^{1:1}$-P$_4$)] (**2b**; type B), both bearing an intact P_4 tetrahedron as a ligand.

7.2 Results and Discussion

The P_4 ligand complexes **2a** and **2b** readily react with the triple-decker **1** in toluene at room temperature. In both cases a degradation of the P_4 tetrahedron to planar *cyclo*-P_4 units is observed. The obtained binuclear and trinuclear compounds [{CpRu(PPh$_3$)$_2$}{CoCp'''}(μ,η$^{1:4}$-P$_4$)][CF$_3$SO$_3$] (**3a**) and [{Cp^{BIG}Mn(CO)$_2$}$_2${CoCp'''}(μ,η$^{1:1:4}$-P$_4$)] (**3b**), respectively, show *cyclo*-P_4 units bridging the metal atoms (Equation 7-1). They can be described as a [Cp'''Co(η^4-P$_4$)] complex coordinating to 16 VE complex fragments {CpRu(PPh$_3$)$_2$} and {Cp^{BIG}Mn(CO)$_2$}, respectively. This is in contrast to the reaction of **1** with P_4, where the binuclear derivative [(Cp'''Co)$_2$(μ,η$^{2:2}$-P$_2$)$_2$] and larger aggregates are formed.[4] However, [Cp'''Co(η^4-P$_4$)] (**3**) is assumed to be the initial product, which subsequently reacts to the observed final products. Up to now, the free complexes [Cp^{R}Co(η^4-P$_4$)] are not known in literature. However, similar results were obtained by Scheer et al. by three component reactions. Irradiation of [Cp^{R}Co(CO)]$_2$ together with P_4 in the presence of [Cr(CO)$_5$(thf)] resulted in the formation of complexes of the type [Cp^{R}Co(η^4-P$_4$){Cr(CO)$_5$}$_3$] (**G**; Cp^R = Cp'', Cp''', Cp^{Ph}) and [Cp^{R}Co(η^4-P$_4$){Cr(CO)$_5$}$_4$] (**H**; Cp^R = Cp, Cp').[9]

From both products, **3a** and **3b**, crystals suitable for single crystal X-ray diffraction could be obtained by cooling concentrated CH$_2$Cl$_2$ solutions to -30 °C (**3a**: Figure 7.1, **3b**: Figure 7.2). The average P–P bond length in the *cyclo*-P_4 ligand in **3a** and **3b** is 2.15 Å and lies in

(7-1)
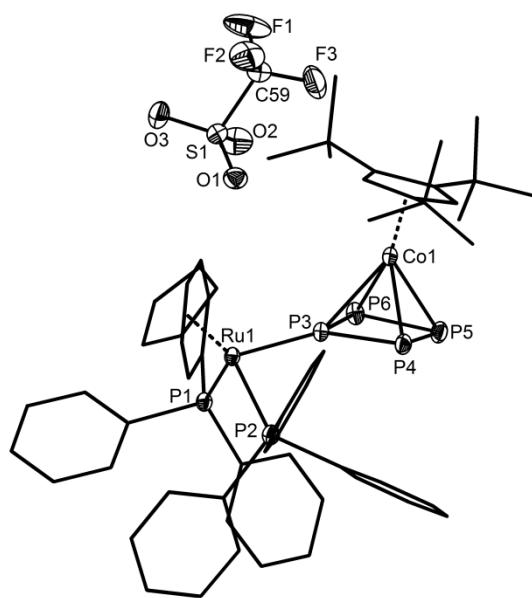
Figure 7.1. Molecular structure of **3a** in the crystal. Thermal ellipsoids are set at 50% probability. For clarity reasons solvent molecules are omitted and C atoms are depicted in 'wire-or-stick' model. Selected bond lengths [Å] and angles [°]: Ru1-P1 2.3548(8), Ru1-P2 2.3681(7), Ru1-P3 2.2945(6), P3-P4 2.1243(9), P4-P5 2.1549(8), P5-P6 2.1722(9), P3-P6 2.1481(8), Co1-P3 2.3927(10), Co1-P4 2.3412(9), Co1-P5 2.2825(9), Co1-P6 2.3247(10), Cp'''$_{cent}$-Co1-P$_{4,cent}$ 172.61(3), Ru1-P3-P4 129.23(4), Ru1-P3-P6 135.05(3), P4-P3-P6 93.58(4), P3-P4-P5 87.57(4), P4-P5-P6 92.05(4), P3-P6-P5 86.53(4).

Figure 7.2. Molecular structure of **3b** in the crystal. Thermal ellipsoids are set at 50% probability. For clarity reasons solvent molecules are omitted, in case of disorder only the main part is shown and C atoms are depicted in 'wire-or-stick' model. Selected bond lengths [Å] and angles [°]: Mn1-P1 2.222(1), Mn2-P3 2.203(1), P1-P2 2.161(2), P2-P3 2.168(1), P3-P4 2.131(2), P1-P4 2.143(1), Co1-P1 2.338(1), 2.339(1), 2.297(1), 2.359(1), Cp'''$_{cent}$-Co1-P$_{4,cent}$ 175.21(5), P1-P2-P3 85.19(6), P2-P3-P4 94.16(6), P1-P4-P3 86.58(6), P2-P1-P4 93.97(6).

between a P–P single bond (2.22 Å)[10] and a P=P double bond (2.04 Å).[11] The sum of P-P-P bond angles of 359.7° and 359.9°, respectively, indicates almost perfectly planar P$_4$ cycles. The ^{t}Bu groups are orientated along the non-coordinating P atoms to minimize steric repulsion. A distortion of the co-planar orientation of the Cp''' rings and the *cyclo*-P$_4$ ligands by 11.05(8)° in **3a** and 4.7(1)° in **3b** is observed. Nevertheless, the structural parameters do not show significant discrepancies to that of the complexes **G** and **H**.

The ^{31}P{^{1}H} NMR spectrum of **3a** shows an AM$_2$XY$_2$ spin system, however at room temperature, three of the four signals are strongly broadened. Therefore, NMR investigations at variable temperatures were carried out (Figure 7.3). While by cooling signals A and X steadily get sharper, signal M first gets sharper until it reaches a maximum at 233 K and then progressively broadens again (cf. Figure 7.3 for labeling). At 233 K, a spectrum of first order is obtained, where the coupling constants can be figured out. It can be expected that further cooling would result in a splitting of signal M into two sets of signals. However, this was not possible due to limitation of the used solvent. At the lowest temperature achieved (193 K), signal M is nearby at coalescence. Furthermore, in the ^{1}H NMR at various temperatures the
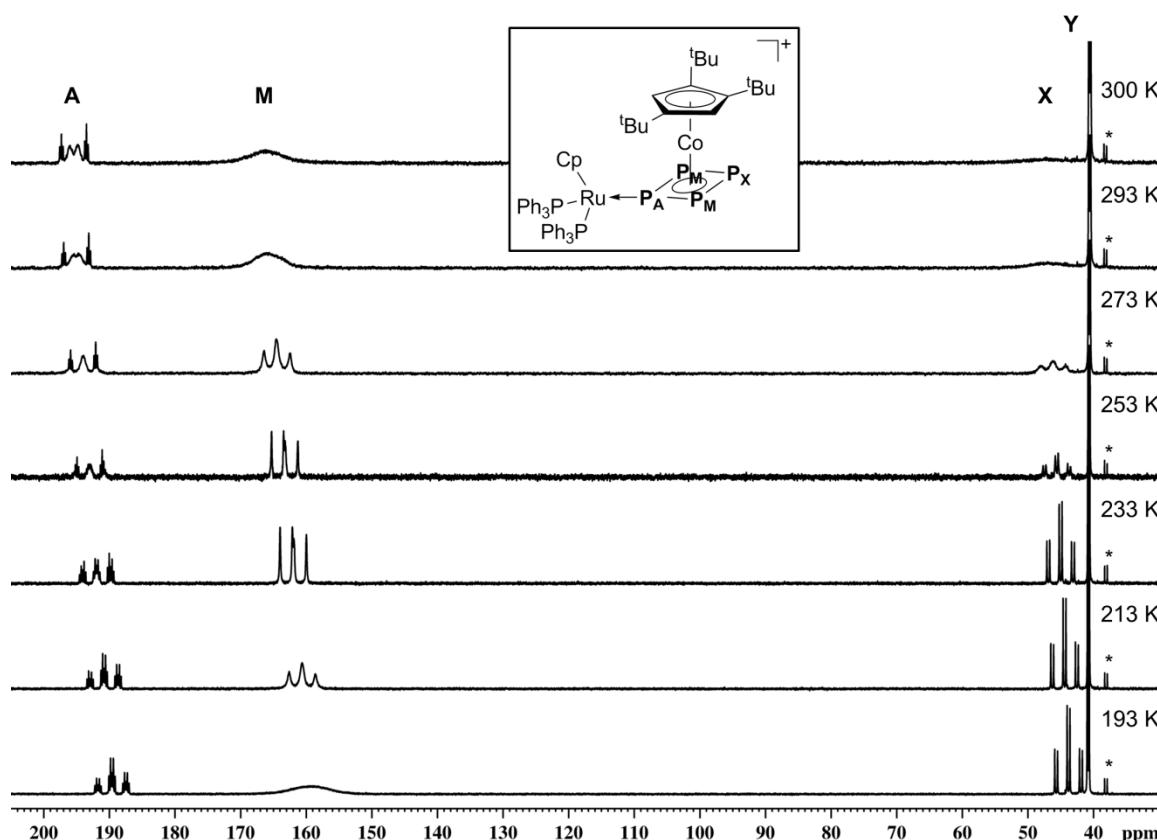
Figure 7.3. ^{31}P{^{1}H} NMR spectra of **3a** in CD$_2$Cl$_2$ at various temperatures. ^{31}P{^{1}H} (233 K, CD$_2$Cl$_2$) δ [ppm] = 191.9 (tdt, $^1J_{PP}$ = 345 Hz, $^2J_{PP}$ = 71 Hz, $^2J_{PP}$ = 42 Hz, 1P$_A$), 162.0 (dd, $^1J_{PP}$ = 345 Hz, $^1J_{PP}$ = 303 Hz, 1P$_M$), 45.0 (td, $^1J_{PP}$ = 303 Hz, $^2J_{PP}$ = 71 Hz, 1P$_X$), 40.7 (d, $^2J_{PP}$ = 42 Hz, 2P$_Y$). Signal marked with an asterisk are due to small impurities.
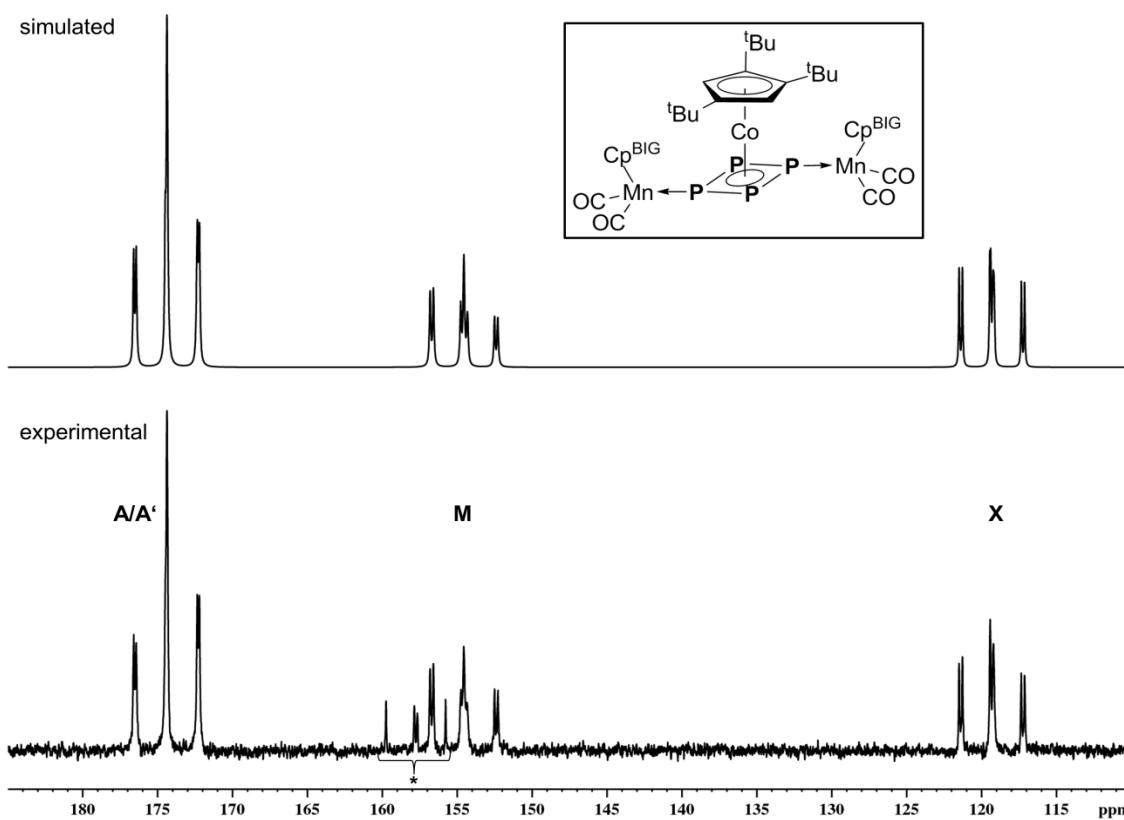
Figure 7.4. ³¹P{¹H} NMR spectra of **3b** in C_6D_6 (bottom) at 298 K and simulated spectrum (top). Parameters from simulated ³¹P{¹H} NMR spectrum: δ [ppm] = 174.34 (P_A), 174.31 ($P_{A'}$), 154.68 (P_M), 119.35 (P_X); $^2J(P_AP_{A'})$ = -25.2 Hz, $^1J(P_AP_M)$ = 347.6 Hz, $^1J(P_AP_X)$ = 336.0 Hz, $^1J(P_{A'}P_M)$ = 351.2 Hz, $^1J(P_{A'}P_X)$ = 339.7 Hz, $^2J(P_MP_X)$ = 33.3 Hz.[12] Signal marked with an asterisk is due to small impurities.

signals for the phenyl protons steadily get broader. Finally, at 213 K the signals split into several new resonances combined with a broadening of the signals of the Cp''' ligand. Further cooling again results in a sharpening of the phenyl signals in contrast to that of the Cp''' moiety. These observations in the ¹H and ³¹P{¹H} NMR spectra might be explained by a hindered rotation at room temperature of the Cp''' ligand. In addition to this, starting from 213 K the rotation of the {CpRu(PPh₃)₂} fragment around the Ru-P_A bond could also be hampered.

The ³¹P{¹H} NMR spectrum of **3b** does not show broadened signals. Surprisingly, instead of the expected two sets of signals three are observed in an integral ratio of 2:1:1. The spectrum is of higher order and was simulated to determine the coupling constants (Figure 7.4).[12] The fit was successful with an AA'MX spin system. This indicates magnetically non-equivalent P atoms in **3b**. However, in the ¹H NMR spectrum only one set of sharp signals can be observed, which is consistent with freely rotating Cp^BIG and Cp''' ligands. Because of the expected C_v-symmetry and the close chemical shifts, it was not possible to definitely assign the signals to the related P atoms in the P₄ ring.

Summing up, it was shown that pre-coordinated P$_4$ tetrahedra react with **1** in a way similar to white phosphorus. However, the otherwise unstable *cyclo*-P$_4$ ligand complex **3** is stabilized by the coordination to 16 VE complex fragments. Therefore, by using coordinated P$_4$ as P source it should be also possible to capture labile intermediates in other reactions.

7.3 Experimental Part

General Remarks:

All experiments were carried out under an atmosphere of dry argon or nitrogen using glovebox and schlenk techniques. Solvents were purified, dried and degassed prior to use. [(Cp'''Co)$_2$(μ-toluene)] (**1**),[3] [CpRu(PPh$_3$)$_2$(η^1-P$_4$)][CF$_3$SO$_3$] (**2a**)[7b] and [{Cp^{BIG}Mn(CO)$_2$}$_2$(μ,η$^{1:1}$-P$_4$)] (**2b**)[6b,c] were prepared according to literature procedures. The NMR spectra were measured on a Bruker Avance 300, 400 or 600 spectrometer. ESI-MS spectra were measured on a ThermoQuest Finnigan TSG 7000 mass spectrometer and FD-MS spectra on a Finnigan MAT 95 mass spectrometer. The elemental analyses were determined on a Vario EL III apparatus. The IR spectra were measured on a VARIAN FTS-800 FT-IR spectrometer.

Synthesis of [{CpRu(PPh$_3$)$_2$}{CoCp'''}(μ,η$^{1:4}$-P$_4$)][CF$_3$SO$_3$] (3a)

An orange solution of [CpRu(PPh$_3$)$_2$(η^1-P$_4$)][CF$_3$SO$_3$] (285 mg, 0.3 mmol) in 10 mL THF is cooled to -50 °C and a solution of [(Cp'''Co)$_2$toluene] (100 mg, 0.15 mmol) in 10 mL THF is added drop wise. The solution is stirred for 16 h while warming up to room temperature. A red precipitate of **3a** is formed, which is filtered, washed with cold THF and dried in vacuum to give pure **3a** (305 mg, 82%). Crystals can be obtained from CH$_2$Cl$_2$ solutions as solvate.

3a: [C$_{59}$H$_{64}$F$_3$CoO$_3$P$_6$RuS] * 2 CH$_2$Cl$_2$ (solvent molecules were found in the crystal structure) calc: C, 51.38; H, 4.81; S, 2.25. found: C, 51.82; H, 4.93; S, 2.25. ESI-MS (CH$_2$Cl$_2$, cation): *m/z* (%) = 1107.4 (100%, [{CpRu(PPh$_3$)$_2$}{CoCp'''}(μ,η$^{1:4}$-P$_4$)]$^+$). ^{1}H NMR (CD$_2$Cl$_2$): δ [ppm] = 1.43 (s, 9H, ^{t}Bu), 1.54 (s, 18H, ^{t}Bu), 4.58 (s, 5H, Cp), 5.86 (s, 2H, Cp'''), 7.00 (m, 12H, Ph), 7.31 (t, $^3J_{HH}$ = 7.1 Hz, 12H, Ph), 7.46 (t, $^3J_{HH}$ = 7.3 Hz, 6H, Ph). ^{31}P{^{1}H} (233 K, CD$_2$Cl$_2$) δ [ppm] =   40.7 (d, $^2J_{PP}$ = 42 Hz, 2P$_Y$), 45.0 (td, $^1J_{PP}$ = 303 Hz, $^2J_{PP}$ = 71 Hz, 1P$_X$), 162.0 (dd, $^1J_{PP}$ = 345 Hz, $^1J_{PP}$ = 303 Hz, 1P$_M$), 191.9 (tdt, $^1J_{PP}$ = 345 Hz, $^2J_{PP}$ = 71 Hz, $^2J_{PP}$ = 42 Hz, 1P$_A$). ^{31}P{^{1}H} (298 K, CD$_2$Cl$_2$) δ [ppm] = 40.5 (d, $^2J_{PP}$ = 40 Hz, 2P), 42 - 55 (br, too broad to assign ω$_{1/2}$, 1P), 166 (s-br, ω$_{1/2}$ = 1060 Hz, 2P), 195.4 (m, 1P). For more details on ^{31}P{^{1}H} NMR investigations see text. ^{19}F NMR (CD$_2$Cl$_2$) δ [ppm] = -78.8. ^{13}C{^{1}H} NMR (CD$_2$Cl$_2$): δ [ppm] = 31.7 (^{t}Bu), 32.0 (^{t}Bu), 33.8 (^{t}Bu), 34.3 (^{t}Bu), 80.5 (Cp'''), 86.7 (Cp), 116.5 (Cp'''), 118.4 (Cp'''), 128.9 (Ph), 131.0 (Ph), 134.5 (Ph), 135.7 (Ph).

Synthesis of [{Cp^{BIG}Mn(CO)$_2$}$_2${CoCp'''}(μ,η$^{1:1:4}$-P$_4$)] (3b)

To a brown solution of [{Cp^{BIG}Mn(CO)$_2$}$_2$(η$^{1:1}$-P$_4$)] (100 mg, 56 μmol) in 5 mL toluene a solution of [(Cp'''Co)$_2$toluene] (19 mg, 28 μmol) in 5 mL toluene is added. The solution is stirred for 16 h and the solvent is removed in vacuum. The residue is dissolved in 5 mL CH$_2$Cl$_2$ and cooled to -35 °C. Product **3b** is obtained as solvate with CH$_2$Cl$_2$ as brown bar-shaped crystals (30 mg, 25%).

3b: [C$_{131}$H$_{159}$CoMn$_2$O$_4$P$_4$] * 4 CH$_2$Cl$_2$ (solvent molecules were found in the crystal structure) calc: C, 66.72; H, 6.93. found: C, 66.47; H, 7.15. FD-MS (toluene): *m/z* (%) = 2089.7 (100%, [M]$^+$), 1253.5 (6%, [M - {Cp^{BIG}Mn(CO)$_2$}]$^+$). IR (toluene): ν$_{CO}$ [cm^{-1}] = 1937 (s), 1887 (s). ^{1}H NMR (C$_6$D$_6$): δ [ppm] = 0.83 (t, $^3J_{HH}$ = 7.3 Hz, 30H, ^{n}Bu), 1.21 (m, 20H, ^{n}Bu), 1.45 (m, 29H, ^{n}Bu and ^{t}Bu), 1.66 (s, 18H, ^{t}Bu), 2.39 (t, $^3J_{HH}$ = 7.7 Hz, 20H, ^{n}Bu), 6.66 (s, 2H, Cp'''), 6.83 (d, $^3J_{HH}$ = 8.1 Hz, 20H, Ph), 7.36 (d, $^3J_{HH}$ = 8.1 Hz, 20H, Ph). For details on ^{31}P{^{1}H} NMR investigations see text and supporting information. ^{13}C{^{1}H} NMR (C$_6$D$_6$): δ [ppm] = 14.1 (^{n}Bu), 22.6 (^{n}Bu), 31.7 (^{t}Bu), 33.4 (^{n}Bu), 33.6 (^{t}Bu), 35.5 (^{n}Bu), 102.3 (C$_5$/Cp^{BIG}), 119.6 (C$_5$/Cp'''), 130.6 (Ph), 133.4 (Ph), 141.7(Ph), 231.6 (CO, low certainty); some quaternary C atoms are either obscured by other signals or not observed.

7.4 References

[1]   a) B. M. Cossairt, N. A. Piro, C. C. Cummins, *Chem. Rev.* **2010**, *110*, 4164-4177. b) M. Caporali, L. Gonsalvi, A. Rossin, M. Peruzzini, *Chem. Rev.* **2010**, *110*, 4178-4235.

[2]   a) M. Scheer, G. Balazs, A. Seitz, *Chem. Rev.* **2010**, *110*, 4236-4256. b) N. A. Giffin, J. D. Masuda, *Coord. Chem. Rev.* **2011**, *255*, 1342-1359.

[3]   J. J. Schneider, D. Wolf, C. Janiak, O. Heinemann, J. Rust, C. Krüger, *Chem. Eur. J.* **1998**, *4*, 1982-1991.

[4]   F. Dielmann, M. Sierka, A. V. Virovets, M. Scheer, *Angew. Chem., Int. Ed.* **2010**, *49*, 6860-6864.

[5]   a) P. Dapporto, S. Midollini, L. Sacconi, *Angew. Chem. Int. Ed.* **1979**, *18*, 469-469.; b) P. Dapporto, L. Sacconi, P. Stoppioni, F. Zanobini, *Inorg. Chem.* **1981**, *20*, 3834-3839.

[6]   a) T. Groer, G. Baum, M. Scheer, *Organometallics* **1998**, *17*, 5916-5919. b) S. Heinl, E. V. Peresypkina, A. Y. Timoshkin, P. Mastrorilli, V. Gallo, M. Scheer, *Angew. Chem., Int. Ed.* **2013**, *52*, 10887-10891. c) S. Heinl, E. V. Peresypkina, A. Y. Timoshkin, P. Mastrorilli, V. Gallo, M. Scheer, *Angew. Chem.* **2013**, *125*, 11087-11091.

[7]   a) I. de los Rios, J.-R. Hamon, P. Hamon, C. Lapinte, L. Toupet, A. Romerosa, M. Peruzzini, *Angew. Chem. Int. Ed.* **2001**, *40*, 3910-3912; b) M. Di Vaira, P. Frediani, S. S. Costantini, M. Peruzzini, P. Stoppioni, *Dalton Trans.* **2005**, 2234-2236; c) M. Di Vaira, M. Peruzzini, S. S. Costantini, P. Stoppioni, *J. Organomet. Chem.* **2006**, *691*, 3931-3937; d) P. Barbaro, V. M. Di, M. Peruzzini, S. S. Costantini, P. Stoppioni, *Chem. Eur. J.* **2007**, *13*, 6682-6690; e) M. Caporali, M. Di Vaira, M. Peruzzini, S. S. Costantini, P. Stoppioni, F. Zanobini, *Eur. J. Inorg. Chem.* **2010**, 152-158; f) M. Di Vaira, M. Peruzzini, S. S. Costantini, P. Stoppioni, *J. Organomet. Chem.* **2010**, *695*, 816-820; g) M. Peruzzini, L. Marvelli, A. Romerosa, R. Rossi, F. Vizza, F. Zanobini, *Eur. J. Inorg. Chem.* **1999**, 931-933; h) V. Mirabello, M. Caporali, V. Gallo, L. Gonsalvi, A. Ienco, M. Latronico, P. Mastrorilli, M. Peruzzini, *Dalton Trans.* **2011**, *40*, 9668-9671; i) V. Mirabello, M. Caporali, V. Gallo, L. Gonsalvi, D. Gudat, W. Frey, A. Ienco, M. Latronico, P. Mastrorilli, M. Peruzzini, *Chem. Eur. J.* **2012**, *18*, 11238–11250.

[8]   a) P. Barbaro, V. M. Di, M. Peruzzini, C. S. Seniori, P. Stoppioni, *Angew. Chem., Int. Ed.* **2008**, *47*, 4425-4427. b) P. Barbaro, V. M. Di, M. Peruzzini, C. S. Seniori, P. Stoppioni, *Inorg. Chem.* **2009**, *48*, 1091-1096. c) M. Di Vaira, M. Peruzzini, P. Stoppioni, *C. R. Chim.* **2010**, *13*, 935-942.

[9]   M. Scheer, U. Becker, *J. Organomet. Chem.* **1997**, *545–546*, 451-460.

[10] P. Pyykkö, M. Atsumi, *Chem. Eur. J.* **2009**, *15*, 186-197.

[11] P. Pyykkö, M. Atsumi, *Chem. Eur. J.* **2009**, *15*, 12770-12779.

[12] Full details on NMR simulation can be found in the Supplementary Information.

7.5 Supplementary Information

NMR Investigations:
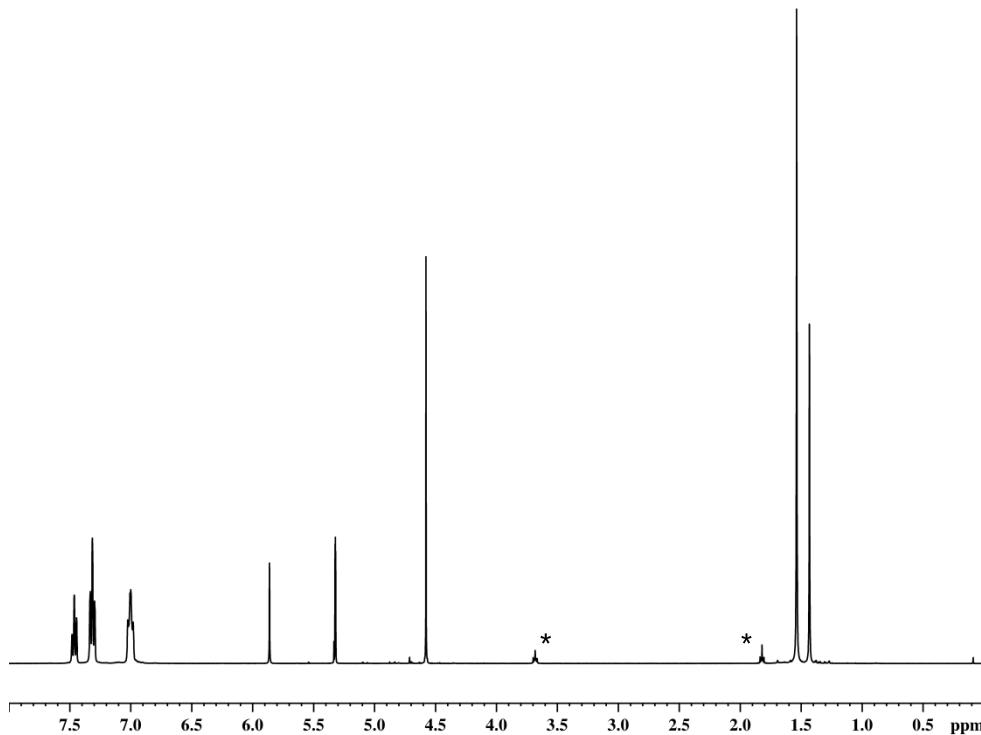
Figure S7.1. ^{1}H NMR spectrum of **3a** in CD$_2$Cl$_2$ at 298 K. Signals marked with asterisks are due to THF.
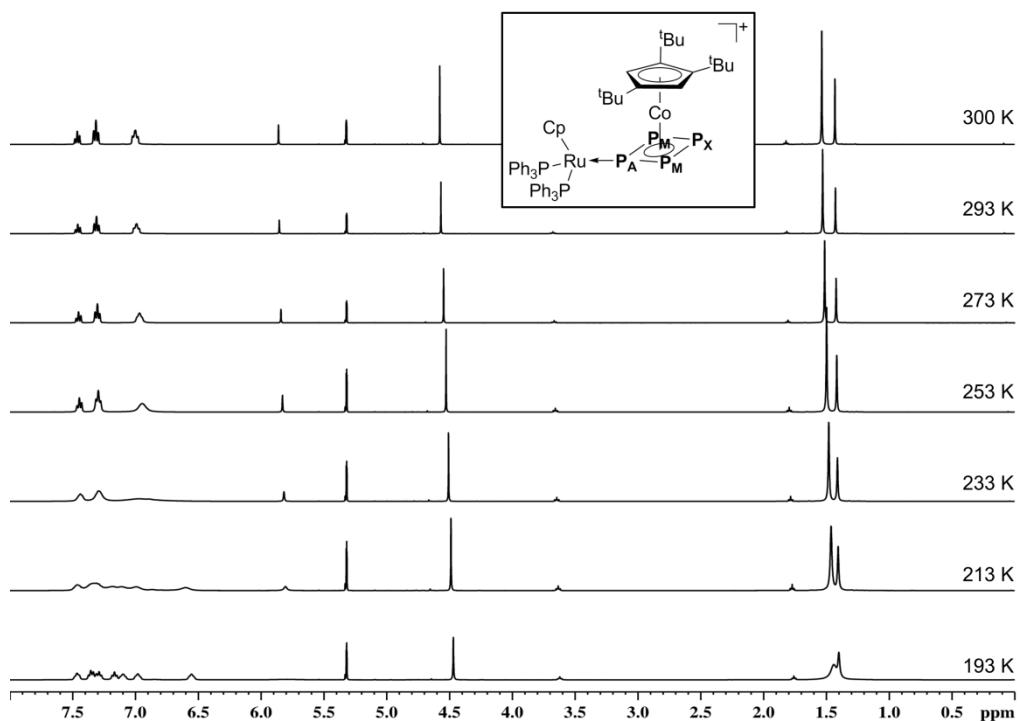
Figure S7.2. ^{1}H NMR spectra of **3a** in CD$_2$Cl$_2$ at various temperatures.
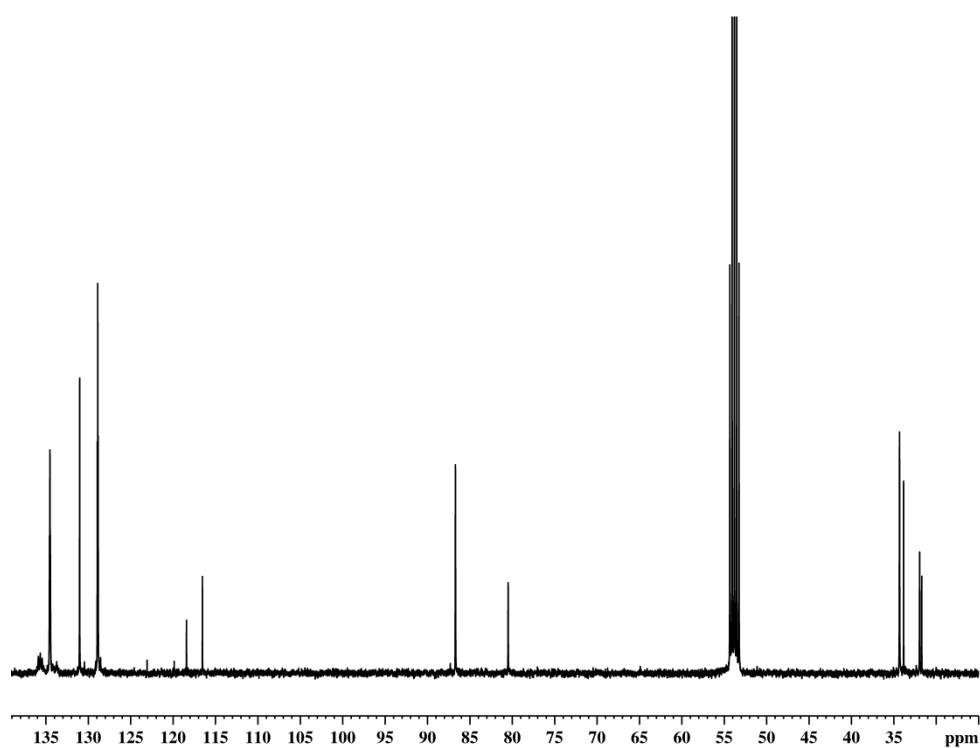
Figure S7.3. ¹³C{¹H} NMR spectrum of **3a** in CD₂Cl₂ at 298 K.
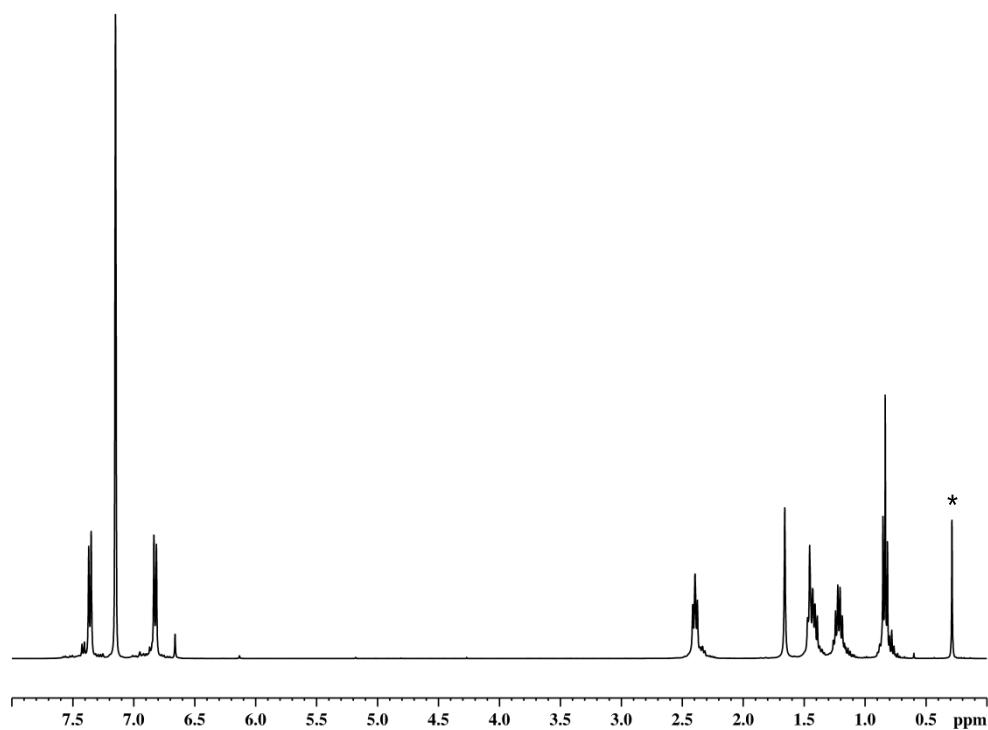
Figure S7.4. ¹H NMR spectrum of **3b** in C₆D₆ at 298 K. Signal marked with an asterisk is due to silicon grease.
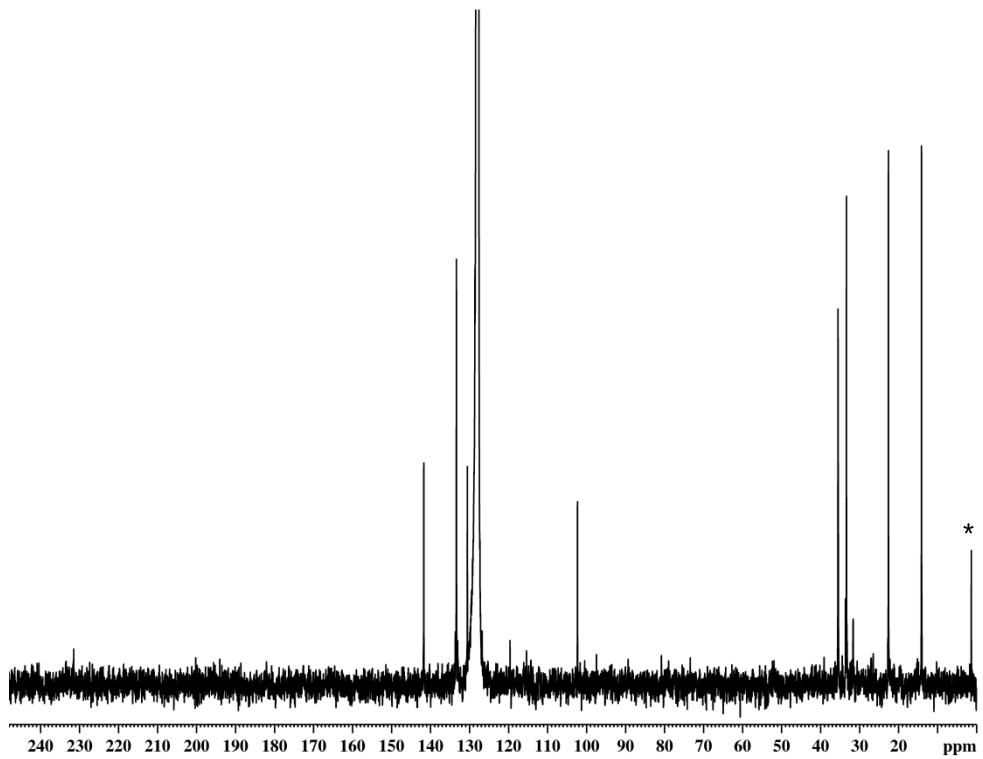
Figure S7.5. $^{13}C\{^1H\}$ NMR spectrum of **3b** in C_6D_6 at 298 K. Signal marked with an asterisk is due to silicon grease.

Details on ^{31}P{^{1}H} NMR Simulation of compound 3b (whole LOC-file):

```
Constants defining experimental spectrum :
First frequency point of region  1  :      29458.38078
Last  frequency point of region  1  :      27035.24810
Number of points in region          :          1589
First frequency point of region  2  :      25509.34591
Last  frequency point of region  2  :      24517.50949
Number of points in region          :           651
First frequency point of region  3  :      19779.58319
Last  frequency point of region  3  :      18865.56778
Number of points in region          :           600
Hz/Point                 :        1.52590
Number of spectral points     :         2840

ITERATION
MAXIMUM NUMBER OF ITERATIONS =          100
CONVERGENCE CRITERIUM       =      0.05000
TOTAL NUMBER OF CYCLES      =         10
BROADENING FACTOR           =          8
MULTIPLIER          =       0.80000
SWITCH-OVER ERROR       =      10.00000
TRADITIONAL TARGET FUNCTION
ITERATION OF LINESHAPE STARTING IN THE
Parameters to be iterated

Fragment   Type    starting value   lower limit   upper limit
------------------------------------------------------------------
  1   F( 1)      28234.3221     25029.7910     28245.5674
  1   F( 2)      25054.0666     19320.1550     26684.1237
  1   F( 3)      19332.0901     19328.5352     19345.0142
  1   F( 4)      28238.4734        -4.0494     28245.5674
  1   J( 1, 2)     351.22000        -2.00000      382.00000
  1   J( 1, 3)     338.99000         0.00000      381.47000
  1   J( 1, 4)     -25.17000       -27.17000      -23.17000
  1   J( 2, 3)      33.23000       -35.20000       37.10000
  1   J( 2, 4)     347.77000         0.00000      351.46000
  1   J( 3, 4)     335.81000         0.00000      339.72000
  1   H( 1)        13.53340         0.00100       40.00000
  1   H( 2)        16.75280         0.00100       40.00000
  1   H( 3)        10.99640         0.00100       11.00000
  1   H( 4)        17.45810         0.00100       30.00000


CYCLE 1 - SMOOTHING FACTOR =     6 ( 10 PARAMETERS )
OLD TARGET FUNCTION AND COMBINED GRADIENTS
ITERATION
ITERATION NO. :      1

CYCLE 2 - SMOOTHING FACTOR =     4 ( 10 PARAMETERS )
OLD TARGET FUNCTION AND COMBINED GRADIENTS
ITERATION
ITERATION NO. :      2
ITERATION   2 NO FURTHER ERROR REDUCTION

CYCLE 3 - SMOOTHING FACTOR =     3 ( 10 PARAMETERS )
OLD TARGET FUNCTION AND COMBINED GRADIENTS
ITERATION
ITERATION NO. :      3
ITERATION   3 NO FURTHER ERROR REDUCTION

CYCLE 4 - SMOOTHING FACTOR =     2 ( 10 PARAMETERS )
OLD TARGET FUNCTION AND COMBINED GRADIENTS
ITERATION
ITERATION NO. :      4
ITERATION   4 NO FURTHER ERROR REDUCTION


CYCLE 5 - SMOOTHING FACTOR =     1 ( 10 PARAMETERS )
OLD TARGET FUNCTION AND COMBINED GRADIENTS
ITERATION
ITERATION NO. :      5
ITERATION   5 NO FURTHER ERROR REDUCTION

CYCLE 6 - SMOOTHING FACTOR =     6 ( 10 PARAMETERS )
OLD TARGET FUNCTION AND NEWTON METHOD ITERATION
TYPE
ITERATION NO. :      6

CYCLE 7 - SMOOTHING FACTOR =     4 ( 10 PARAMETERS )
OLD TARGET FUNCTION AND NEWTON METHOD ITERATION
TYPE
ITERATION NO. :      7

CYCLE 8 - SMOOTHING FACTOR =     3 ( 10 PARAMETERS )
OLD TARGET FUNCTION AND NEWTON METHOD ITERATION
TYPE
ITERATION NO. :      8

CYCLE 9 - SMOOTHING FACTOR =     2 ( 10 PARAMETERS )
OLD TARGET FUNCTION AND NEWTON METHOD ITERATION
TYPE
ITERATION NO. :      9
ITERATION   9 NO FURTHER ERROR REDUCTION

CYCLE 10 - SMOOTHING FACTOR =     1 ( 10 PARAMETERS )
OLD TARGET FUNCTION AND NEWTON METHOD ITERATION
TYPE
ITERATION NO. :     10
ITERATION  10 NO FURTHER ERROR REDUCTION

Statistical Information :
Final sum of squares           = 49.967173
Number of spectral points      =     2840
Degrees of Freedom             =     2830
Standard Deviation of Measurements =  0.132877
R-Factor ( % )                 =  1.928709


Fragm. Parameter type  Initial Parameter  Best Parameter  Standard
 No.                Vector          Vector      Deviation
------------------------------------------------------------------
  1   F( 1)        28234.32210     28234.28464     0.34696
  1   F( 2)        25054.06660     25054.03585     0.11395
  1   F( 3)        19332.09010     19332.11656     0.07015
  1   F( 4)        28238.47340     28238.48943     0.37115
  1   J( 1, 2)       351.22000       351.19027     0.78675
  1   J( 1, 3)       338.99000       338.71950     0.31808
  1   J( 1, 4)       -25.17000       -25.15142     0.32335
  1   J( 2, 3)        33.23000        33.32225     0.11570
  1   J( 2, 4)       347.77000       347.63669     0.73462
  1   J( 3, 4)       335.81000       336.04220     0.31522

 1 sec
   0.09
```

Crystallographic Details:

The crystal structure analyses were performed either on an Oxford Diffraction Gemini R Ultra CCD diffractometer (**3a**) or an Oxford Diffraction SuperNova diffractometer (**3b**). For both compounds an analytical absorption correction was carried out.[1] The structures were solved by direct methods of the program SIR-92[2] and refined with the least square method on F^2 employing SHELXL-97[3] with anisotropic displacements for non-H atoms. Hydrogen atoms were located in idealized positions and refined isotropically according to the riding model.

	Crystal Data for **3a***2CH$_2$Cl$_2$	Crystal Data for **3b***4.8CH$_2$Cl$_2$
Empirical Formula	$C_{61}H_{68}Cl_4CoF_3O_3P_6RuS$	$C_{543.2}H_{672.4}Cl_{38.4}Co_4Mn_8O_{16}P_{16}$
Formula Weight	1425.85	9989.69
Temperature [K]	123.0(3)	123.00(10)
Crystal System	triclinic	monoclinic
Space Group	$P\bar{1}$	$P2_1/n$
a [Å]	13.8494(5)	18.5451(4)
b [Å]	15.8930(6)	24.9628(5)
c [Å]	16.3566(6)	28.8243(6)
α [°]	69.257(3)	90
β [°]	75.544(3)	92.132(2)
γ [°]	70.679(3)	90
Volume [Å^3]	3141.2(2)	13334.6(5)
Z	2	1
ρ_{calc} [mg/mm^3]	1.508	1.244
μ [mm^{-1}]	7.771	5.086
F(000)	1460.0	5260.4
Crystal Size [mm^3]	0.1604 × 0.1358 × 0.0682	0.2964 × 0.142 × 0.1109
Radiation	Cu-K$_\alpha$ (λ = 1.54178)	Cu-K$_\alpha$ (λ = 1.54178)
2Θ Range	5.84 to 133.22°	6.14 to 147.742°
Index Ranges	-16 ≤ h ≤ 15	-20 ≤ h ≤ 22
	-18 ≤ k ≤ 18	-29 ≤ k ≤ 28
	-17 ≤ l ≤ 19	-35 ≤ l ≤ 35
Reflections Collected	35981	68456
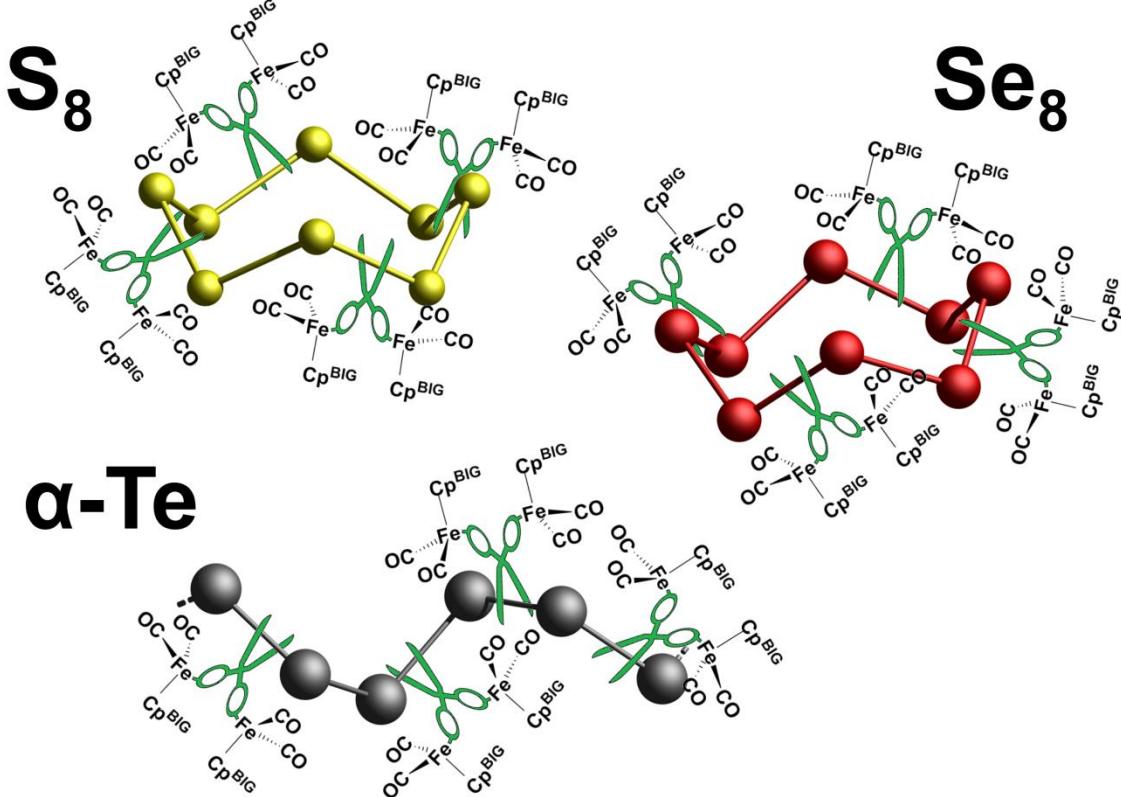
Independent Reflections	11025	25963
	[R_{int} = 0.0323, R_{sigma} = 0.0326]	[R_{int} = 0.0526, R_{sigma} = 0.0542]
Data/Restraints/Parameters	11025/45/757	25963/119/1504
Goodness-of-Fit on F^2	1.032	1.055
Final R Indexes [I > 2σ(I)]	R_1 = 0.0318, wR_2 = 0.0851	R_1 = 0.0764, wR_2 = 0.2401
Final R Indexes [All Data]	R_1 = 0.0333, wR_2 = 0.0865	R_1 = 0.0957, wR_2 = 0.2506
Largest Diff. Peak/Hole [e·Å^{-3}]	1.64/-0.93	1.41/-1.30
Flack Parameter	-	-

References for Supplementary Information:

[1]   R. C. Clark, J. S. Reid, *Acta Cryst.* **1995**, A51, 887-897.

[2]   A. Altomare, M. C. Burla, M. Camalli, G.L. Cascarano, C. Giacovazzo, A. Guagliardi, A. G. G. Moliterni, G. Polidori, R. Spagna, *J. Appl. Cryst.* **1999**, 32, 115-119.

[3]   G. M. Sheldrick, *Acta Cryst.* **2008**, A64, 112-122.

8. Low Temperature Activation of S$_8$, Se$_{red}$ and α-Te with [Cp^{BIG}Fe(CO)$_2$] Radicals
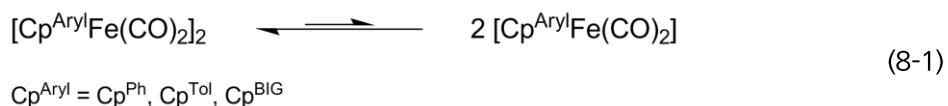
Sebastian Heinl and Manfred Scheer

unpublished results.

- ❖ **All syntheses and characterizations were performed by Sebastian Heinl**
- ❖ **Manuscript was written by Sebastian Heinl**
- ❖ **Figures were made by Sebastian Heinl**
- ❖ **X-ray structure analyses and refinement were performed by Sebastian Heinl**

8.1 Introduction

Transition metal complexes bearing chalcogenide ligands exhibit a long history in chemical research.[1] The countless number of structural motifs with a great variety of electronic configurations opens a rich chemistry with a wide range of applications. Investigations reach from cluster expansion reactions[2] and synthesis of new (binary) chalcogen phases[3] to reactivity studies with organic substrates.[4] A renaissance of this chemistry took place, following the discovery that proteins can contain metal-sulfur clusters as co-factors, especially in nitrogenases.[5] The preparation methods of such complexes mostly start from elemental chalcogenes under thermal or photolysis conditions. However, reactions under mild conditions are rather rare.[4a,6] The harsh conditions (boiling toluene) in the reaction of [$Cp^RFe(CO)_2$]$_2$ with chalcogenes lead to a total decarbonylation and the formation of [($Cp^RFe)_2(S_2)_2$] (Cp^R = Cp, Cp*, $C_5H_3(SiMe_3)_2$) and [($Cp^RFe)_3(Se_2)_2(Se)$] (Cp^R = Cp*), respectively.[1d,7] The elevate temperature in the reactions favors the thermodynamic products, therefore the intermediate products are not obtained.

We are interested in complexes with bulky Cp^R ligands because they are capable to kinetically stabilize reactive species. Our attention was attracted by the dimeric compounds [($Cp^{Aryl})Fe(CO)_2$]$_2$ (Cp^{Aryl} = Cp^{Ph}, Cp^{Tol}), which partially dissociate in solution resulting in 17 VE radical fragments (Equation 8-1).[8] Unfortunately, compounds with these two Cp^{Aryl} ligands tend to have poor solubility, which impedes subsequent reactions and spectroscopic studies. Hence, to obtain a soluble analogue which similar properties, we synthesized [$Cp^{BIG}Fe(CO)_2$]$_2$ (**1**) (Cp^{BIG} = $C_5(4\text{-}n\text{Bu}C_6H_4)_5$).[9]

$$[Cp^{Aryl}Fe(CO)_2]_2 \quad \rightleftharpoons \quad 2\,[Cp^{Aryl}Fe(CO)_2]$$

$$Cp^{Aryl} = Cp^{Ph},\ Cp^{Tol},\ Cp^{BIG}$$

(8-1)

Herein we report the reactions of **1** with elemental chalcogenes sulfur, selenium and tellurium, respectively, which, at room temperature, result in the formation of five binuclear iron-chalcogen complexes. Furthermore, the reactions of **1** with S or Se were also investigated at elevated temperatures.

8.2 Results and Discussion

The reactions of **1** with S_8 and Se_{red} in toluene at room temperature result in immediate change of color from dark green to purple/red. The fast reactions can easily be monitored via IR spectroscopy by the extinction of the four bands of **1** (1986, 1954, 1918 and
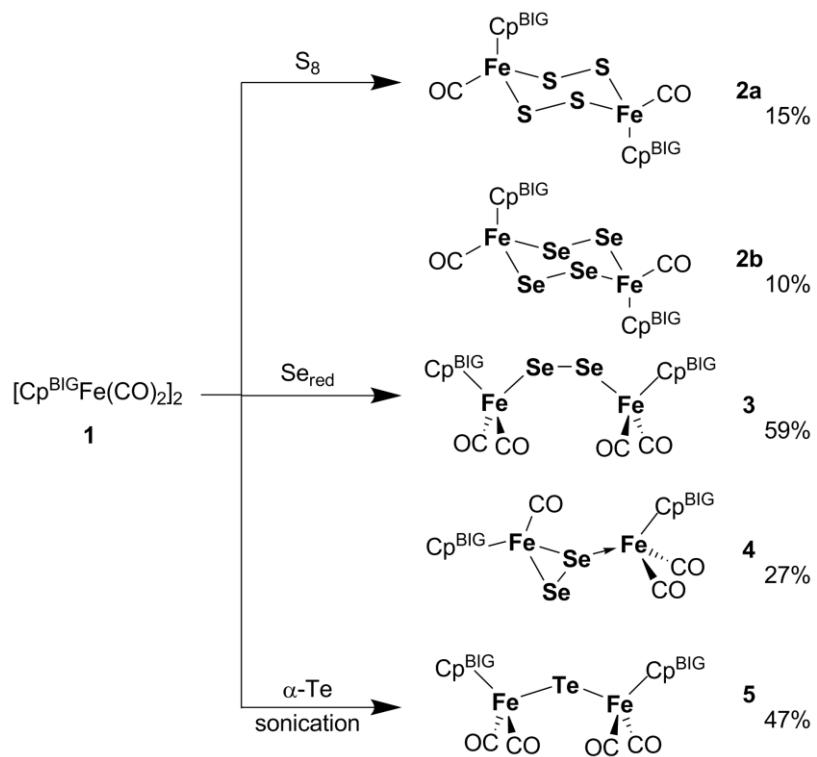
Figure 8.1. Preparation of chalcogenide iron complexes by reaction of [$Cp^{BIG}Fe(CO)_2$]$_2$ (**1**) with the elemental phases S_8, Se_{red} and α-Te in toluene at room temperature. For tellurium it was necessary to use ultrasonic activation.
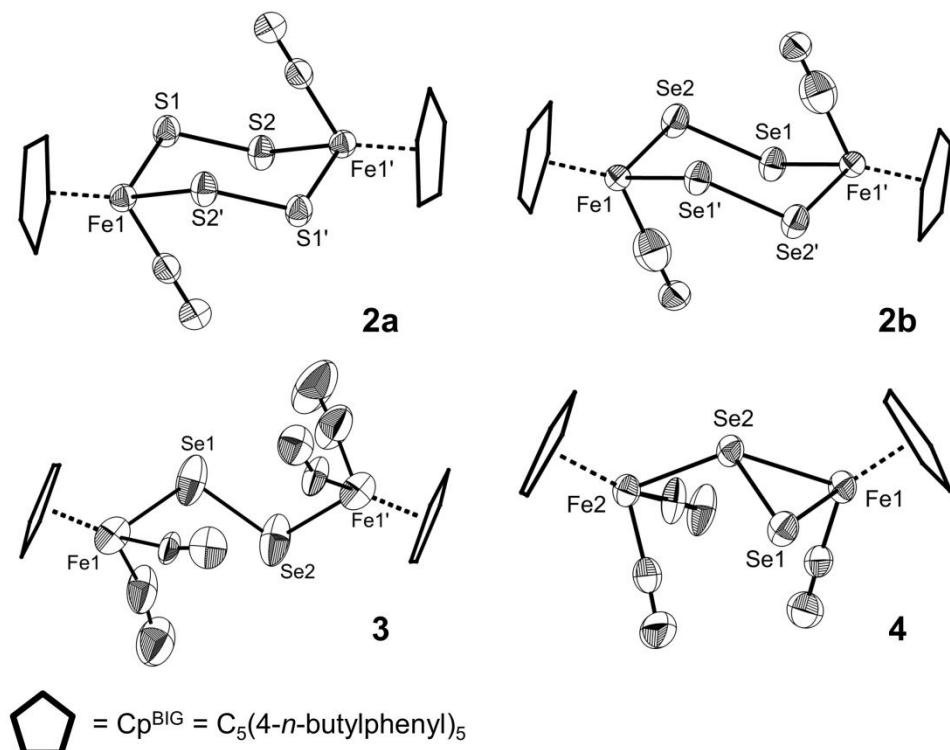
Figure 8.2. Central cores of the molecular structures in the crystal with selected labels of **2a-4**. Ellipsoids are drawn at 50% probability level. For clarity reasons the main part of disordered atoms and only one molecule of the asymmetric unit are depicted (if more present).[10]

1779 cm^{-1}) and the appearance of new CO absorption bands. While with sulfur only [{$Cp^{BIG}Fe(CO)$}$_2$(μ-S_2)$_2$] (**2a**) is isolated, with selenium three different compounds are obtained: [{$Cp^{BIG}Fe(CO)$}$_2$(μ-Se_2)$_2$] (**2b**), [{$Cp^{BIG}Fe(CO)_2$}$_2$(μ-Se_2)] (**3**) and [{$Cp^{BIG}Fe(CO)$}{$Cp^{BIG}Fe(CO)_2$}(μ,$η^{2:1}$-Se_2)] (**4**) (Figure 8.1). Unfortunately, it was not possible to discern the exact reaction conditions to selectively address one certain Se complex.

The ^{1}H NMR spectra of **2a**, **2b** and **4** at room temperature do not show the expected two doublets for the phenyl protons, but numerous signals in the area for aromatic protons. This can be explained by hindered or even halted rotation of the Cp^{BIG} ligand (along Cp-Fe and/or Cp-Ph axis) and thus, the NMR spectra arise from superimposition of different rotamers.[10] The same observations were made for the complexes [{$Cp^{BIG}Mn(CO)_2$}$_n$P$_4$] (n = 1, 2) at low temperatures.[11] In contrast, **3** does not show this behavior and remains dynamic on the NMR timescale. This might be due to its more flexible chain-like central structure.

Crystals of all compounds can be grown by the diffusion of CH_3CN into CH_2Cl_2 solutions. The molecular structures of **2a-4** contain Q_2^{2-} ligands (Q = S,Se), which is a common unit among poly-chalcogenide complexes (Figure 8.2). The structural parameters of **2a-4** are similar to those complexes with comparable structures. Selected bond lengths and angles are summarized in Table 8.1. The complex cores of **3** and **4** show a disorder over two positions, while the Cp^{BIG} ligands remain unaffected.[10] This is in accordance with an empirical observation that Cp^{BIG} ligands mainly dominate the crystal packing.

Table 8.1. Selected bond lengths [Å], angles [°] and CO stretching frequencies [cm^{-1}] (toluene) of complexes **2a-6b**. If different molecular units are present, a range of structure parameters is given. For bond angles only $η^1$ bound Q_2 units are considered.

	Q	Q-Q	Fe-Q	Fe-Q-Q Fe-Te-Fe	Fe-Q-Q-Fe	$ν_{CO}$[a]
2a	S	1.997(1)	2.2217(6)	116.30(4)	62.79(5)	2020
			2.2220(9)	116.51(4)		1980
2b	Se	2.2836(6)	2.3570(8)	115.18(2)	65.28(4)	2016
			2.3615(6)	115.65(3)		1973
3	Se	2.325(3)	2.318(2)	109.18(6)	122.04(7)	2016
			2.579(1)	109.76(7)		2002
						1969
4	Se	2.2902(1)	2.2534(1)	111.392(2)	-	2023
		2.3096(1)	2.5986(1)	115.999(2)		1979
						1971
5	Te	-	2.616(1)	118.00(3)	-	2009
			2.6226(8)	118.02(3)		1977
						1956
6a	S	2.0018(5)	2.1207(5)	111.32(3)	2.01(3)	-
		2.0396(5)	2.3123(4)	111.78(2)		
6b	Se	2.2814(6)	2.2463(9)	108.31(3)	0.44(4)	-
		2.3295(6)	2.4385(8)	109.21(3)	4.62(4)	

a) $ν_{CO}$ of **1** in toluene: 1986, 1954, 1918, 1779 cm^{-1}.
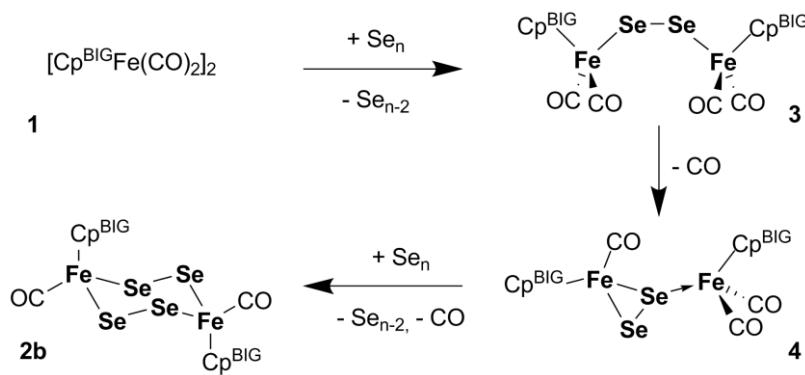
Figure 8.3. Proposed reaction pathway of **1** with red selenium resulting in the stepwise formation of **2b**.

Interestingly, the selenium complexes **2b**, **3** and **4** show a different number of carbonyl ligands. Starting from two CO groups per iron atom in **3**, an average of 1.5 is found in **4** and only one equivalent in **2b**. This enables a proposal for a possible reaction pathway (Figure 8.3). At first, one molecule of **1** reacts with selenium by a radical mechanism forming **3** with one Se_2 unit. A Se atom of the Se_2 unit intramolecular attacks an iron center under CO elimination, resulting in the non-symmetrical compound **4**. Complex **4** subsequently reacts with one molecule of Se_n under loss of a further CO molecule, which finally results in the formation of **2b**.

In contrast, even at -50 °C none of the possible intermediates could be isolated by the reaction of **1** with S_8. In all reactions, **2a** was the only product which could be observed. This discrepancy between sulfur and selenium is not too surprising. S has better donor ability than Se, which supports the faster substitution of CO groups and therefore the formation of **2a** as the final stage of the proposed reaction pathway.

While S_8 and Se_{red} are soluble in organic solvents, α-Te is totally insoluble, which reduces its utility in direct activation. Hence, stirring a solution of **1** with α-Te powder does not lead to any observable reaction. However, if the reaction mixture is sonicated for 16h, a complete conversion of **1** takes place, accompanied with a change of color from green to brown. The X-ray structure analysis exhibits the composition $[\{Cp^{BIG}Fe(CO)_2\}_2(\mu\text{-Te})]$ (**5**) with a bridging mononuclear Te^{2-} ligand (Figure 8.4). The ^1H NMR spectra of **5** do not show multiple signals for the phenyl protons, but all the signals are significantly broader. A hindered rotation would explain this, although it is not as much hampered as in case of **2a**, **2b** and **4**.

All reactions mentioned up to now were carried out at room temperature. If the elemental chalcogenes S_8 and Se_{red} are co-thermolyzed with the dimer complex **1** in toluene, a complete decarbonylation takes place. The obtained cage compounds $[(Cp^{BIG}Fe)_2(\mu,\eta^{1:1}\text{-}Q_2)(\mu,\eta^{2:2}\text{-}Q_2)]$ (Q = S (**6a**), Se (**6b**)) were characterized by single crystal X-ray diffraction. The molecules are isostructural and exhibit two Q_2^{2-} ligands. Albeit both ligands bridge two iron centers, one
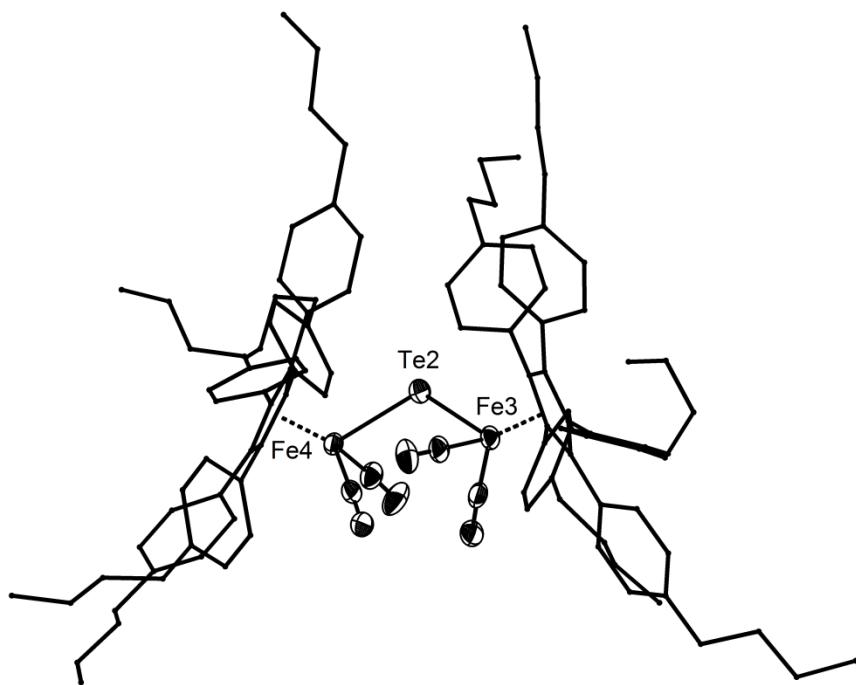
Figure 8.4. Molecular structure of **5** in the crystal. Ellipsoids are drawn at 50% probability level. Only one of the two molecules in the asymmetric unit is depicted. From disordered groups only the main part is shown.

binds $\eta^{1:1}$ and the other $\eta^{2:2}$ (Figure 8.5). This difference in the coordination mode results in an almost perpendicular orientation towards each other. The same compounds are obtained when solutions of **2a** and **2b** are filtered over silica or if the solutions are stored
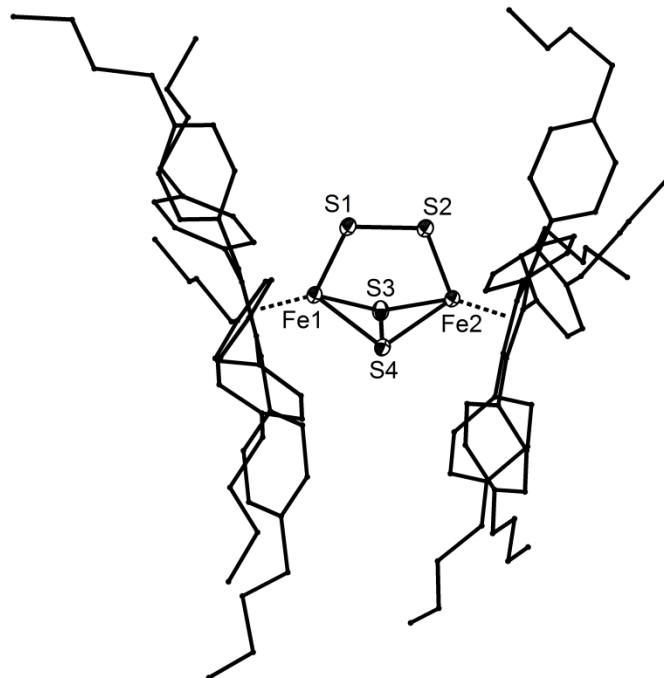
Figure 8.5. Molecular structure of **6a** in the crystal. Ellipsoids are drawn at 50% probability level. In case of disorder, only the main part is shown.

over a long period of time (several weeks). The related complexes with other Cp^R ligands are formed when the reaction is performed at high temperatures.[1d]

As discussed above, **6a** also shows rotational hindrance in the ^1H NMR spectrum. However, this cannot be observed for **6b**. The longer bond lengths in the selenium complex seem to allow sufficient distance between the two Cp^{BIG} ligands enabling them for free rotation.

We have shown that use of sterically crowded $[Cp^{BIG}Fe(CO)_2]_2$ (**1**) directly activates elemental chalcogenes not only at elevate temperatures but also below room temperature. This enables the isolation of products **2-5** along the reaction coordinate to the final products **6a** and **6b**, which are obtained in the corresponding co-thermolysis reaction. Three different selenium complexes were obtained, giving defined hints of a stepwise reaction pathway. In all complexes **2-5** exclusively Q_2^{2-} ligands (Q = S, Se) were found. The radicals, formed by dissociation of **1**, are also capable to react with α-Te at ambient temperature if ultrasonic activation is used. Complex **5** contains a Te^{2-} ligand, bridging two iron centers.

8.3 Experimental Part

General Remarks:

All experiments were carried out under an atmosphere of dry argon or nitrogen using glovebox and schlenk techniques. Solvents were purified, dried and degassed prior to use. S_8, Se_{red} and α-Te were available and $[Cp^{BIG}Fe(CO)_2]_2$ was prepared according to literature procedure.[9] The NMR spectra were measured on a Bruker Avance 300, 400 or 600 spectrometer. FD-MS spectra were measured on a Finnigan MAT 95 mass spectrometer. The elemental analyses were determined on a Vario EL III apparatus. The IR spectra were measured on a VARIAN FTS-800 FT-IR spectrometer.

Synthesis of $[(Cp^{BIG}FeCO)_2(μ-S_2)_2]$ (2a)

A solution of $[Cp^{BIG}Fe(CO)_2]_2$ (**1**) (100 mg, 55 μmol) in 5 mL toluene is added to a solution of S_8 (14 mg, 55 μmol) in 5 mL toluene and stirred for 30 min. The mixture turns into dark red. After removal of the solvent in vacuum, the residue is resolved in 3 mL CH_2Cl_2 and filtered via cannula. In a thin Schlenk-tube, 5 mL CH_3CN are layered over the solution. After full diffusion the product **2a** crystalizes as red blocks (15 mg, 15%).

2a: $[C_{112}H_{130}Fe_2O_2S_4]$ calc.: C, 76.95; H, 7.50; S, 7.34. Found: C, 77.23; H, 7.28; S, 8.48. FD-MS (toluene): m/z (%) = 1691.7 (100%, $[M - 2\ CO]^+$), 1627.8 (40%, $[M - 2\ CO - S_2]^+$). IR (toluene): v_{CO} [cm^{-1}] = 2020 (s), 1980 (s). ^1H NMR (CD_2Cl_2): δ [ppm] = 0.90 (t, $^3J_{HH}$ = 7.2 Hz, 30H, ^nBu), 1.30 (m, 20H, ^nBu), 1.54 (m, 20H, ^nBu), 2.52 (t, $^3J_{HH}$ = 7.3 Hz, 20H, ^nBu), 6.44 (d, $^3J_{HH}$

= 8.4 Hz, 1H, Ph), 6.53 (d, $^3J_{HH}$ = 7.7 Hz, 1H, Ph), 6.64 (d, $^3J_{HH}$ = 7.7 Hz, 1H, Ph), 6.71 (d, $^3J_{HH}$ = 7.3 Hz, 2H, Ph), 6.88 (m, 35H, Ph). $^{13}C\{^1H\}$ NMR (CD_2Cl_2): δ [ppm] = 14.1 (^nBu), 22.7 (^nBu), 33.6 (^nBu), 35.6 (^nBu), 107.2 (Cp), 127.8 (Ph), 128.5 (Ph), 132.8 (Ph), 143.0 (Ph), 210.9 (CO). (Carbonyl C atom is not detected reliably)

Synthesis of [{$Cp^{BIG}FeCO$)}$_2$(μ-Se_2)$_2$] (2b), [{$Cp^{BIG}Fe(CO)_2$}$_2$(μ-Se_2)] (3) and [{$Cp^{BIG}FeCO$}{$Cp^{BIG}Fe(CO)_2$}(μ,η$^{2:1}$-Se_2)] (4)

A solution of [$Cp^{BIG}Fe(CO)_2$]$_2$ (1) (100 mg, 55 μmol) in 5 mL toluene is added to a solution of red selenium (38 mg, 55 μmol) in 5 mL toluene and stirred 30 min. The mixture turns into red/purple. After removal of the solvent in vacuum, the residue is solved in 3 mL CH_2Cl_2 and filtered via a cannula. In a thin Schlenk-tube 5 mL CH_3CN are layered over the solution. After full diffusion the product crystalizes. Sometimes only one distinct, but in other cases multiple compounds are obtained simultaneously.

2b: [($Cp^{BIG}FeCO$)$_2$(μ-Se_2)$_2$]: Yield: up to 11 mg (10%). IR (toluene): v_{CO} [cm^{-1}] = 2016 (s), 1973 (s). ^1H NMR (CD_2Cl_2): δ [ppm] = 0.90 (br-s, 30H, ^nBu), 1.31 (br-s, 20H, ^nBu), 1.54 (br-s, 20H, ^nBu), 2.52 (br-s, 20H, ^nBu), 6.40 (br-s, 1H, Ph), 6.54 (br-s, 1H, Ph), 6.62 (br-s, 1H, Ph), 6.71 (br-s, 2H, Ph), 6.90 (m, 35H, Ph). $^{13}C\{^1H\}$ NMR (CD_2Cl_2): δ [ppm] = 14.1 (^nBu), 22.8 (^nBu), 33.6 (^nBu), 35.6 (^nBu), 106.7 (Cp), 127.9 (Ph), 128.7 (Ph), 132.8 (Ph), 143.1 (Ph), 214.0 (CO). $^{77}Se\{^1H\}$ NMR (CD_2Cl_2): δ [ppm] = 1453 (s).

3: [{$Cp^{BIG}Fe(CO)_2$}$_2$(μ-Se_2)]: Yield: up to 60 mg (59%). [$C_{114}H_{130}Fe_2O_4Se_4$] calc.: C, 74.66; H, 7.14. Found: C, 73.89; H, 7.02. FD-MS (toluene): m/z (%) = 1835.0 (100%, [M]$^+$). IR (toluene): v_{CO} [cm^{-1}] = 2016 (s), 2003(s), 1969 (s). ^1H NMR (C_6D_6): δ [ppm] = 0.79 (t, $^3J_{HH}$ = 7.3 Hz, 30H, ^nBu), 1.14 (m, 20H, ^nBu), 1.34 (m, 20H, ^nBu), 2.28 (t, $^3J_{HH}$ = 7.8 Hz, 20H, ^nBu), 6.76 (d, $^3J_{HH}$ = 8.2 Hz, 20H, Ph), 7.44 (d, $^3J_{HH}$ = 8.2 Hz, 20H, Ph). $^{13}C\{^1H\}$ NMR (C_6D_6): δ [ppm] = 14.1 (^nBu), 22.7 (^nBu), 33.1 (^nBu), 35.5 (^nBu), 101.9 (Cp), 129.2 (Ph), 132.8 (Ph), 142.4 (Ph), 217.7 (CO), one phenyl C atom is overlaid by the solvent signal.

4: [{$Cp^{BIG}FeCO$}{$Cp^{BIG}Fe(CO)_2$}(μ,η$^{2:1}$-Se_2)]: Yield: up to 29 mg (27%). [$C_{113}H_{130}Fe_2O_3Se_2$*$CH_2Cl_2$] calc.: C, 72.42; H, 7.04. Found: C, 72.35; H, 7.12. FD-MS (toluene): m/z (%) = 1804.6 (100%, [M]$^+$). IR (toluene): v_{CO} [cm^{-1}] = 2023 (s), 1979 (s), 1971 (s). ^1H NMR (CD_2Cl_2): δ [ppm] = 0.91 (br-s, 30H, ^nBu), 1.31 (br-s, 20H, ^nBu), 1.53 (br-s, 20H, ^nBu), 2.52 (br-m, 20H, ^nBu), 6.88 (br-m, 40H, Ph).

Synthesis of [{$Cp^{BIG}Fe(CO)_2$}$_2$(μ-Te)] (5)

A solution of [$Cp^{BIG}Fe(CO)_2$]$_2$ (1) (50 mg, 28 μmol) in 5 mL toluene is added powdery tellurium (50 mg, 392 μmol). The mixture is put into an ultrasonic bath for 16 h. The

remaining Te powder is filtered off via a cannula. The solvent is removed in vacuum and the residue is dissolved in 3 mL CH_2Cl_2. In a thin Schlenk-tube 5 mL CH_3CN are layered over the solution. After full diffusion the product crystalizes in dark purple blocks (25 mg, 47%).

5: [$C_{114}H_{130}Fe_2O_4Te$]: calc.: C, 75.92; H, 7.26. Found: C, 75.71; H, 7.28. FD-MS (toluene): *m/z* (%) = 1804.4 (100%, [M]$^+$). IR (toluene): v_{CO} [cm^{-1}] = 2009 (s), 1977 (s), 1956 (s). ^{1}H NMR (CD_2Cl_2): δ [ppm] = 0.91 (br-s, 30H, ^{n}Bu), 1.32 (br-s, 20H, ^{n}Bu), 1.55 (br-s, 20H, ^{n}Bu), 2.53 (br-s, 20H, ^{n}Bu), 6.87 (br-s, 20H, Ph), 7.06 (br-s, 20H, Ph). ^{13}C{^{1}H} NMR (CD_2Cl_2): δ [ppm] = 14.1 (^{n}Bu), 22.7 (^{n}Bu), 33.6 (^{n}Bu), 35.6 (^{n}Bu), 101.7 (Cp), 127.6 (Ph), 129.2 (Ph), 132.8 (Ph), 142.5 (Ph), 221.8 (CO).

Synthesis of [($Cp^{BIG}Fe)_2(μ,η^{1:1}$-$Q_2)(μ,η^{2:2}$-$Q_2)$] (Q = S (6a), Se (6b))

A solution of [$Cp^{BIG}Fe(CO)_2$]$_2$ (200 mg, 119 μmol) and Q_n (Q_n = S_8: 61 mg, 239 μmol; Q_n = Se_{red}: 151 mg, 239 μmol) in 30 mL toluene is refluxed for 1 h. The solvent is removed in vacuum. The residue is purified by column chromatography (10x3 cm, silica, hexane/toluene 3/1). The product is eluted as red band. The solvent is again removed and the product is dissolved in 5 mL CH_2Cl_2. In a thin Schlenk-tube, 10 mL CH_3CN are layered over the solution. After full diffusion the product crystallizes in red blocks.

6a: [($Cp^{BIG}Fe)_2(μ,η^{1:1}$-$S_2)(μ,η^{2:2}$-$S_2)$]: Yield: 160 mg (80%). [$C_{110}H_{130}Fe_2S_4$] calc.: C, 78.08; H, 7.74; S, 7.58. Found: C, 78.26; H, 7.72; S, 7.74. FD-MS (toluene): *m/z* (%) = 1691.5 (100%, [M]$^+$), 1627.5 (40%, [M - S_2]$^+$). ^{1}H NMR (CD_2Cl_2): δ [ppm] = 0.92 (t, $^3J_{HH}$ = 7.3 Hz, 30H, ^{n}Bu), 1.32 (sextet, $^3J_{HH}$ = 7.3 Hz, 20H, ^{n}Bu), 1.55 (m, 20H, ^{n}Bu), 2.53 (t, $^3J_{HH}$ = 7.7 Hz, ^{n}Bu), 6.85 (m, 40H, Ph). ^{13}C{^{1}H} NMR (CD_2Cl_2): δ [ppm] = 14.1 (^{n}Bu), 22.7 (^{n}Bu), 33.6 (^{n}Bu), 35.6 (^{n}Bu), 99.0 (Cp), 127.5 (Ph), 130.2 (Ph), 133.1 (Ph), 142.1 (Ph).

6b: [($Cp^{BIG}Fe)_2(μ,η^{1:1}$-$Se_2)(μ,η^{2:2}$-$Se_2)$]: Yield: 160 mg (72%). [$C_{110}H_{130}Fe_2Se_4$] calc.: C, 70.29; H, 6.97. Found: C, 69.74; H, 6.56. FD-MS (toluene): *m/z* (%) = 1880.0 (100%, [M]$^+$), 1722.6 (85%, [M - Se_2]$^+$). ^{1}H NMR (C_6D_6): δ [ppm] = 0.78 (br-t, $^3J_{HH}$ = 7.2 Hz, 30H, ^{n}Bu), 1.14 (m, 20H, ^{n}Bu), 1.34 (m, 20H, ^{n}Bu), 2.53 (br-t, $^3J_{HH}$ = 7.3 Hz, 20H, ^{n}Bu), 6.70 (d, $^3J_{HH}$ = 7.3 Hz, 20H, Ph), 7.38 (d, $^3J_{HH}$ = 7.3 Hz, 20H, Ph). ^{13}C{^{1}H} NMR (CD_2Cl_2): δ [ppm] = 14.1 (^{n}Bu), 22.7 (^{n}Bu), 33.1 (^{n}Bu), 35.6 (^{n}Bu), 98.6 (Cp), 130.9 (Ph), 133.7 (Ph), 141.8 (Ph), signal of one phenyl C atom is obscured by the solvent signal. ^{77}Se{^{1}H} NMR (C_6D_6): δ [ppm] = 2209 (s).

8.4 References

[1]   a) W. Hieber, J. Gruber, *Z. Anorg. Allg. Chem.* **1958**, *296*, 91-103. b) C. H. Wei, L. F. Dahl, *Inorg. Chem.* **1965**, *4*, 1-11. c) C. Giannotti, A. M. Ducourant, H. Chanaud, A. Chiaroni, D. Riche, *J. Organomet. Chem.* **1977**, *140*, 289-295. d) H. Brunner, N. Janietz, W. Meier, G. Sergeson, J. Wachter, T. Zahn, M. L. Ziegler, *Angew. Chem., Int. Ed.* **1985**, *24*, 1060-1061.

[2]   a) M. Yuki, K. Kuge, M. Okazaki, T. Mitsui, S. Inomata, H. Tobita, H. Ogino, *Inorg. Chim. Acta* **1999**, *291*, 395-402. b) M. Okazaki, A. Sakuma, H. Tobita, H. Ogino, *Chem. Lett.* **2004**, *33*, 1130-1131.

[3]   a) D. M. Giolando, T. B. Rauchfuss, A. L. Rheingold, S. R. Wilson, *Organometallics* **1987**, *6*, 667-675. b) D. M. Giolando, M. Papavassiliou, J. Pickardt, T. B. Rauchfuss, R. Steudel, *Inorg. Chem.* **1988**, *27*, 2596-2600.

[4]   a) J. Wallick, C. G. Riordan, G. P. A. Yap, *J. Am. Chem. Soc.* **2013**, *135*, 14972-14974. b) J. Wallick, C. G. Riordan, G. P. A. Yap, *J. Am. Chem. Soc.* **2013**, *135*, 14972-14974. c) M. Rakowski DuBois, B. R. Jagirdar, S. Dietz, B. C. Noll, *Organometallics* **1997**, *16*, 294-296.

[5]   a) R. L. Richards, *Pure Appl. Chem.* **1996**, *68*, 1521-1526. b) J. C. Fontecilla-Camps, A. Volbeda, C. Cavazza, Y. Nicolet, *Chem. Rev.* **2007**, *107*, 4273-4303. c) I. Dance, *Dalton Trans.* **2010**, *39*, 2972-2983. d) E. Bill, *Hyperfine Interact.* **2012**, *205*, 139-147. e) P. A. Frey, G. H. Reed, *ACS Chem. Biol.* **2012**, *7*, 1477-1481.

[6]   a) S. Yao, M. Driess, *Acc. Chem. Res.* **2011**, *45*, 276-287. b) J. T. York, E. C. Brown, W. B. Tolman, *Angew. Chem., Int. Ed.* **2005**, *44*, 7745-7748. c) L. Y. Goh, T. W. Hambley, G. B. Robertson, *Organometallics* **1987**, *6*, 1051-1057.

[7]   a) R. Weberg, R. C. Haltiwanger, M. Rakowski DuBois, *Organometallics* **1985**, *4*, 1315-1318. b) M. Yamada, H. Tobita, S. Inomata, H. Ogino, *Bull. Chem. Soc. Jpn.* **1996**, *69*, 861-867. c) S. Inomata, T. Hiruma, H. Ogino, *Chem. Lett.* **1998**, *27*, 309-310.

[8]   a) I. Kuksis, M. C. Baird, *Organometallics* **1994**, *13*, 1551-1553. b) I. Kuksis, M. C. Baird, *Organometallics* **1996**, *15*, 4755-4762.

[9]   S. Heinl, G. Balázs, M. Scheer, *Phosphorus, Sulfur Silicon Relat. Elem.* **2014**, DOI: 10.1080/10426507.2014.903489.

[10]   For detailed information on X-ray and NMR data, selected bond lengths/angles and complete molecular structures see Supplementary Information. Also pictures of disordered core structures of compounds **3** and **4** are given.

[11]   a) S. Heinl, E. V. Peresypkina, A. Y. Timoshkin, P. Mastrorilli, V. Gallo, M. Scheer,

Angew. Chem., Int. Ed. **2013**, *52*, 10887-10891. b) S. Heinl, E. V. Peresypkina, A. Y. Timoshkin, P. Mastrorilli, V. Gallo, M. Scheer, *Angew. Chem.* **2013**, *125*, 11087-11091.

8.5 Supplementary Information

NMR Investigations:
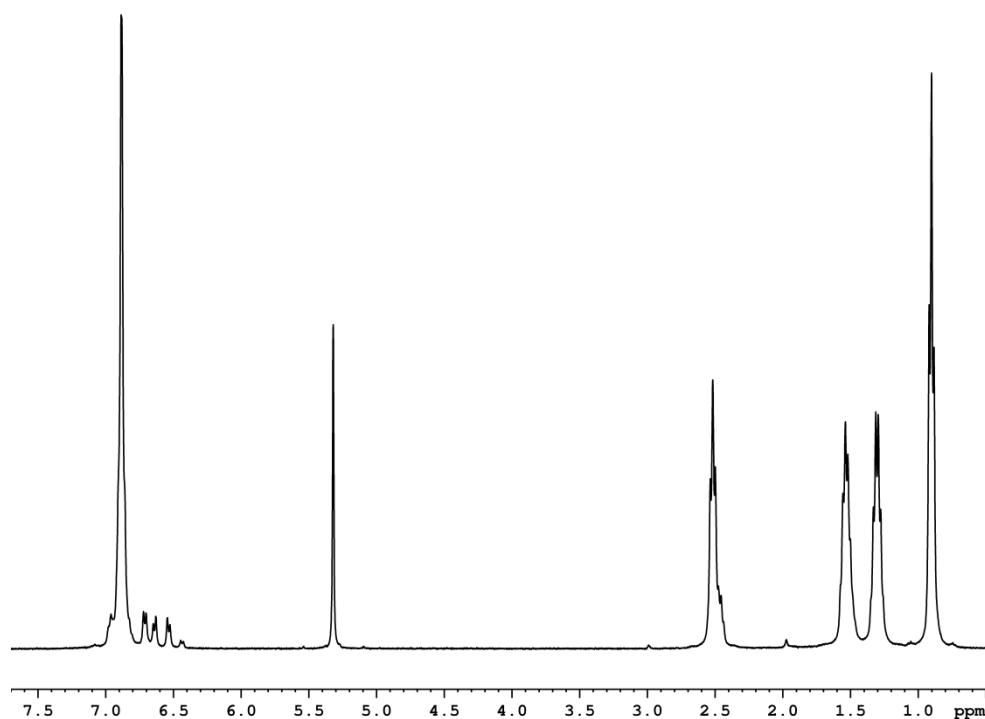
Figure S8.1. ^{1}H NMR spectrum of **2a** in CD$_2$Cl$_2$ at 298 K.
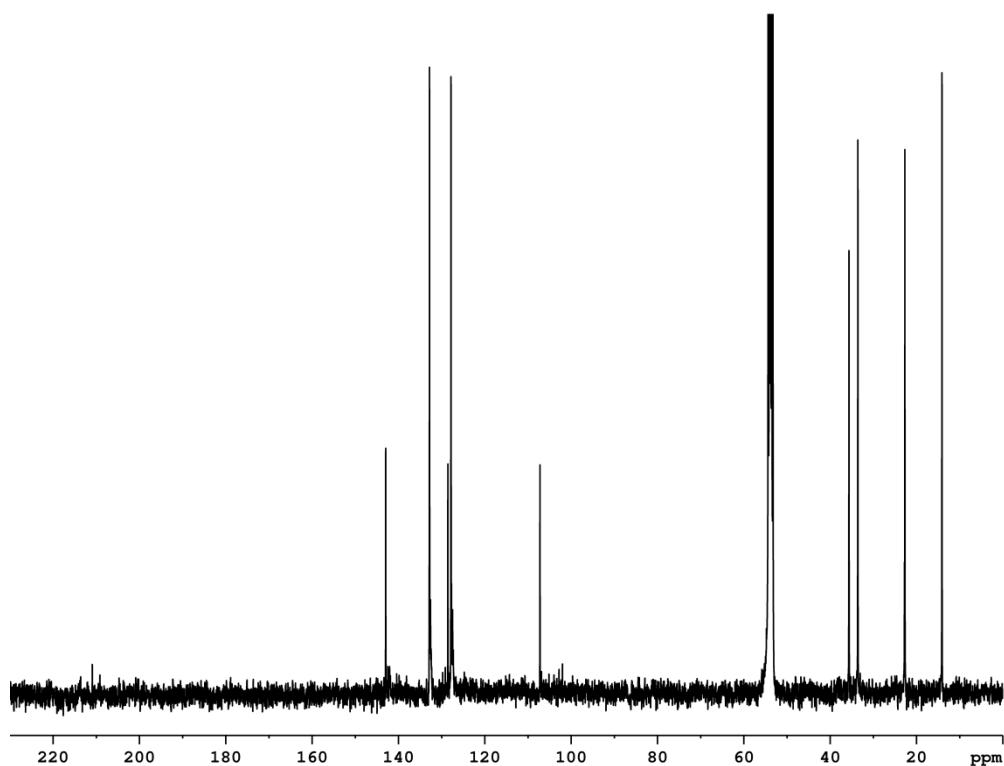
Figure S8.2. ^{13}C{^{1}H} NMR spectrum of **2a** in CD$_2$Cl$_2$ at 298 K.
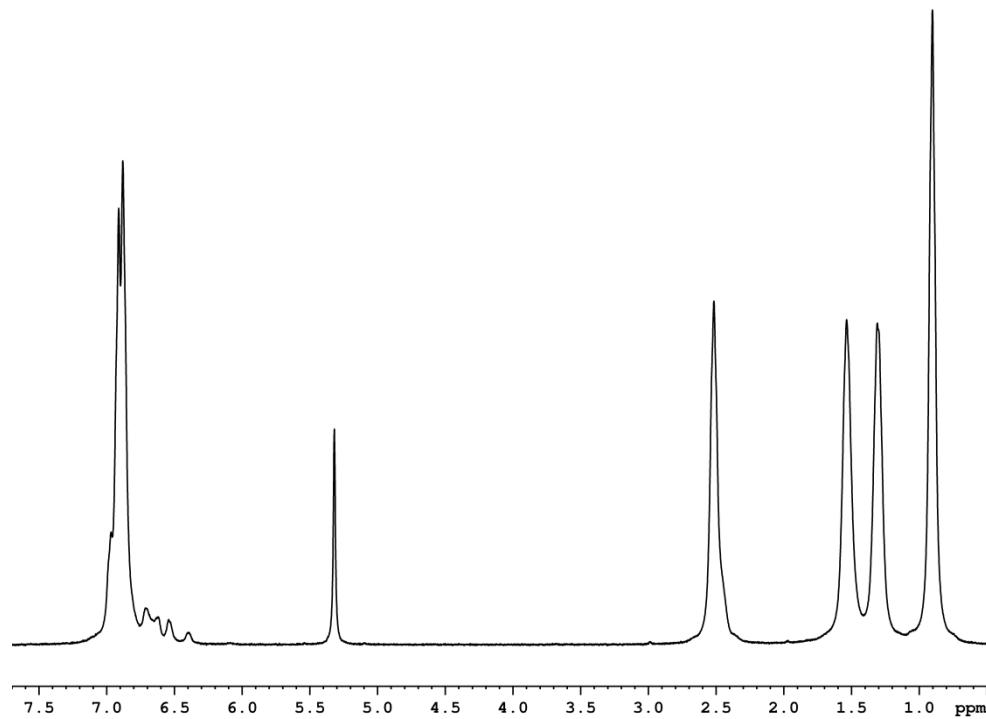
Figure S8.3. ^1H NMR spectrum of **2b** in CD_2Cl_2 at 298 K.
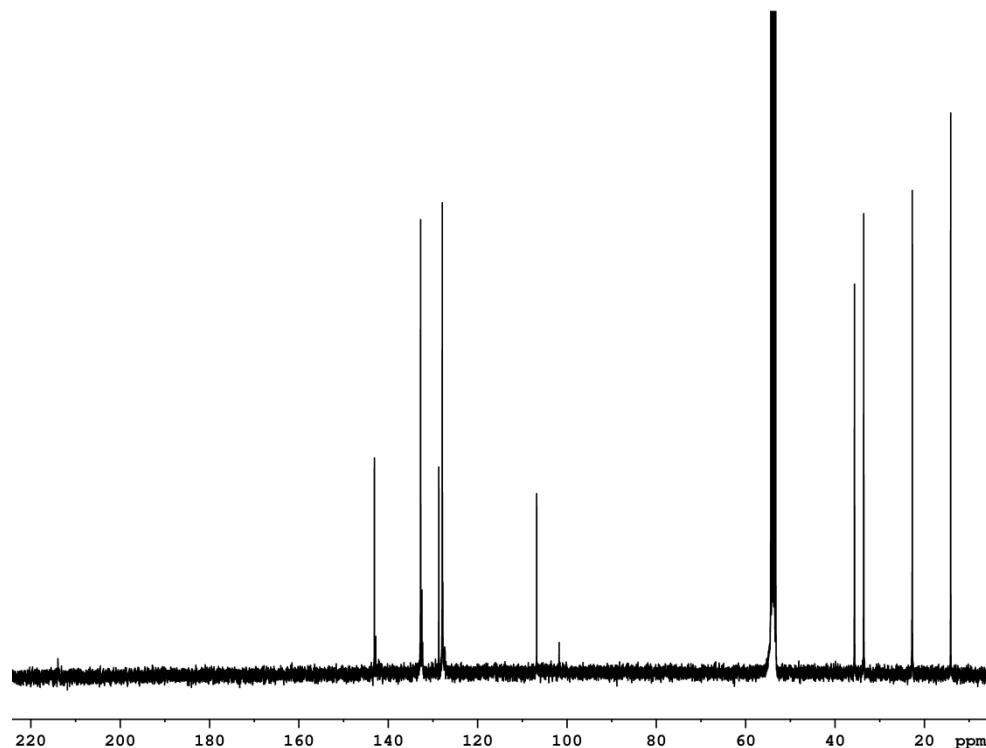
Figure S8.4. $^{13}C\{^1H\}$ NMR spectrum of **2b** in CD_2Cl_2 at 298 K.
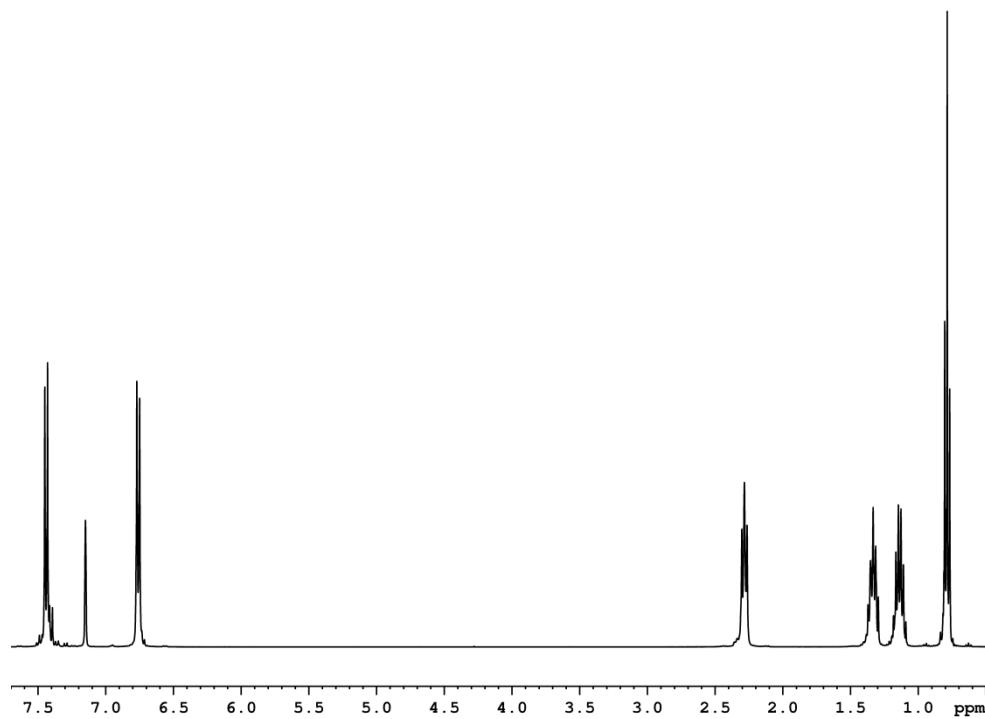
Figure S8.5. ^1H NMR spectrum of **3** in C_6D_6 at 298 K.
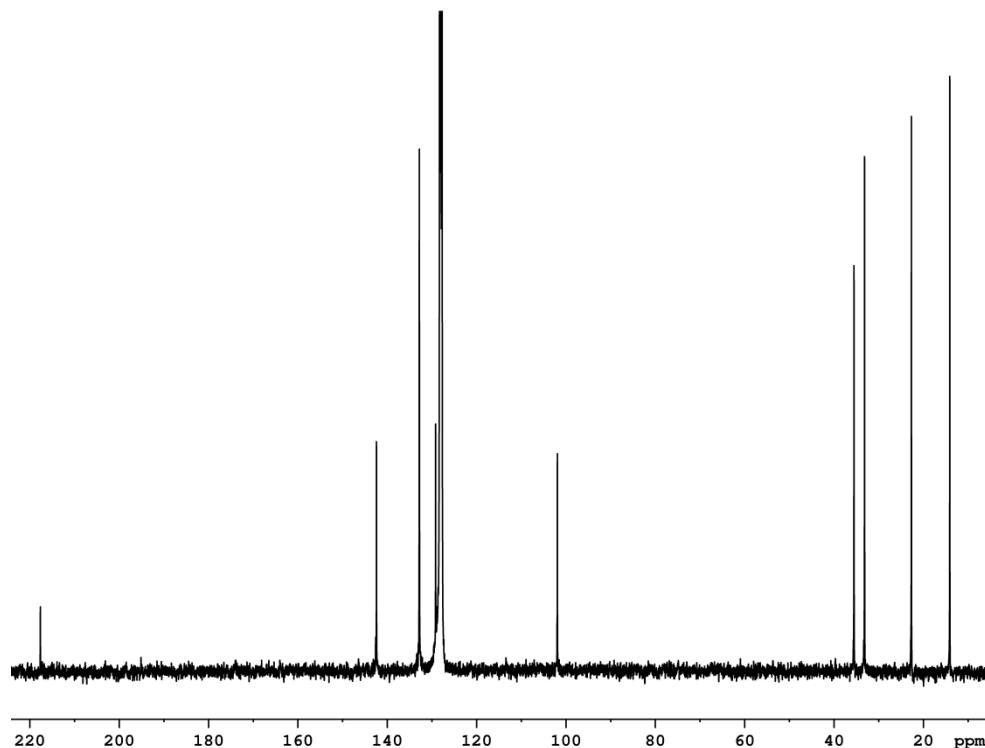
Figure S 8.6. $^{13}C\{^1H\}$ NMR spectrum of **3** in C_6D_6 at 298 K.
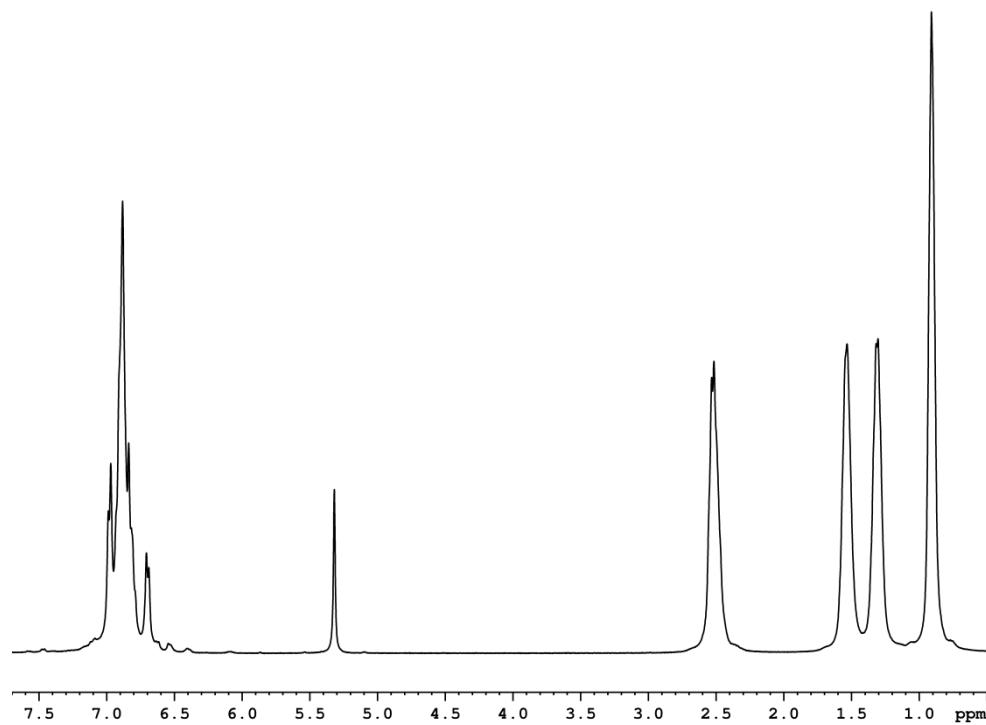
Figure S 8.7. ^{1}H NMR spectrum of **4** in CD_2Cl_2 at 298 K.
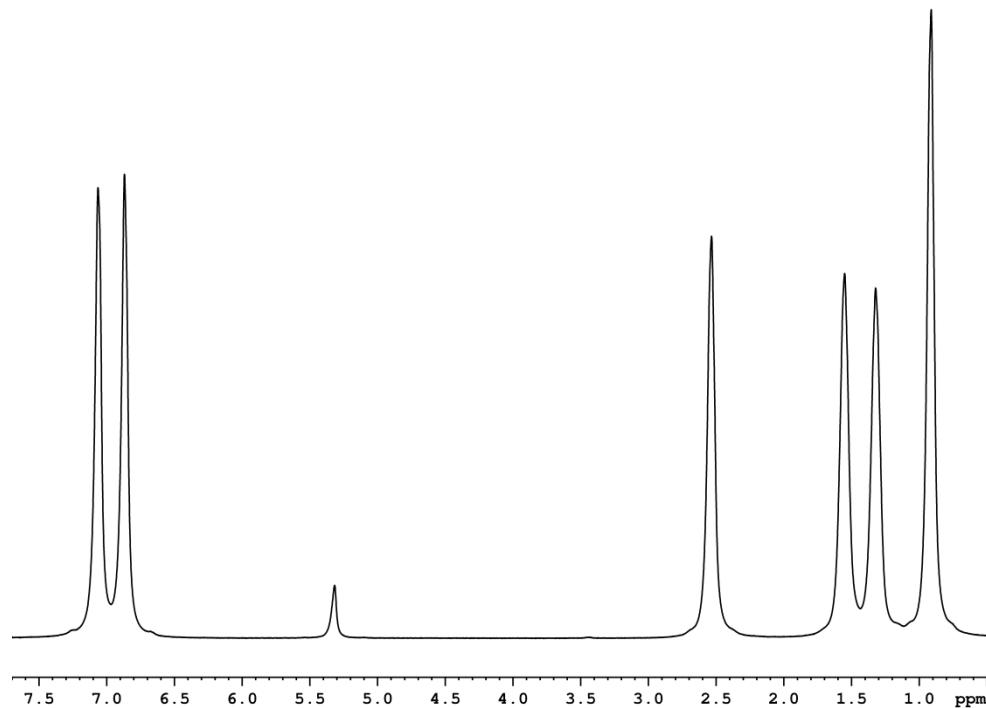
Figure S8.8. ^{1}H NMR spectrum of **5** in CD_2Cl_2 at 298 K.
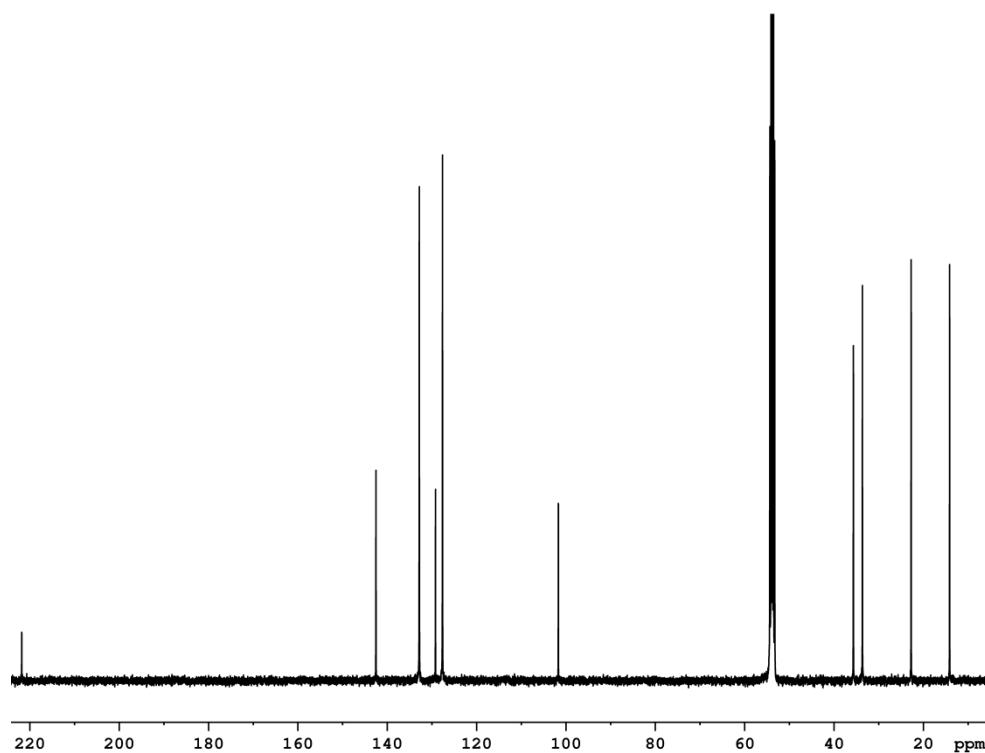
Figure S8.9. $^{13}C\{^1H\}$ NMR spectrum of **5** in CD_2Cl_2 at 298 K.
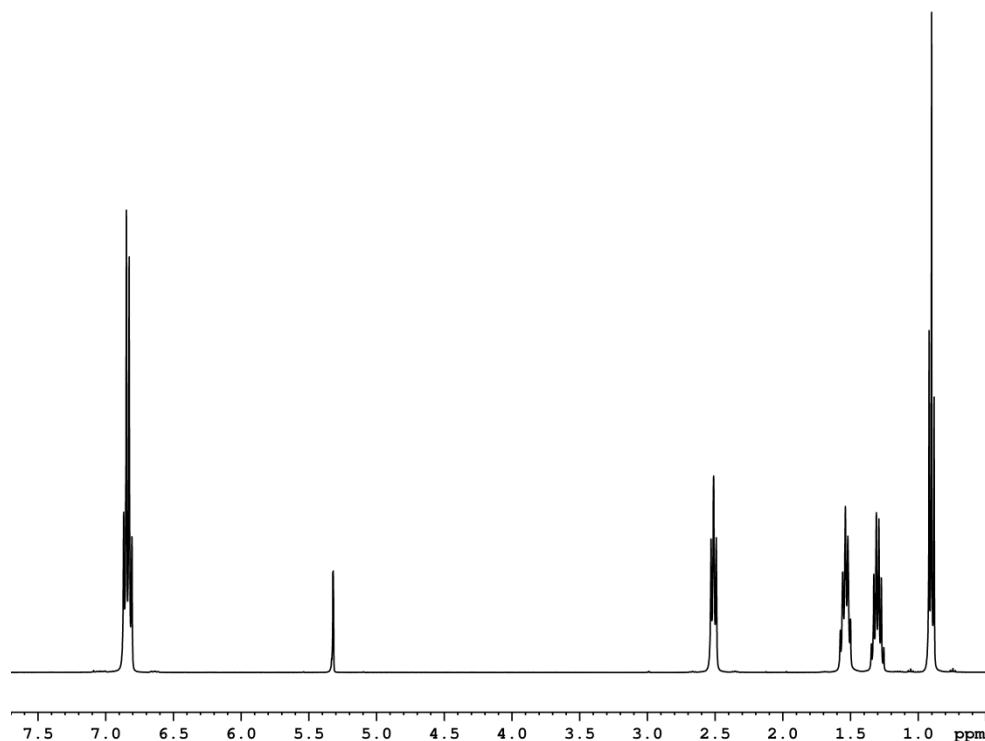
Figure S8.10. ^1H NMR spectrum of **6a** in CD_2Cl_2 at 298 K.
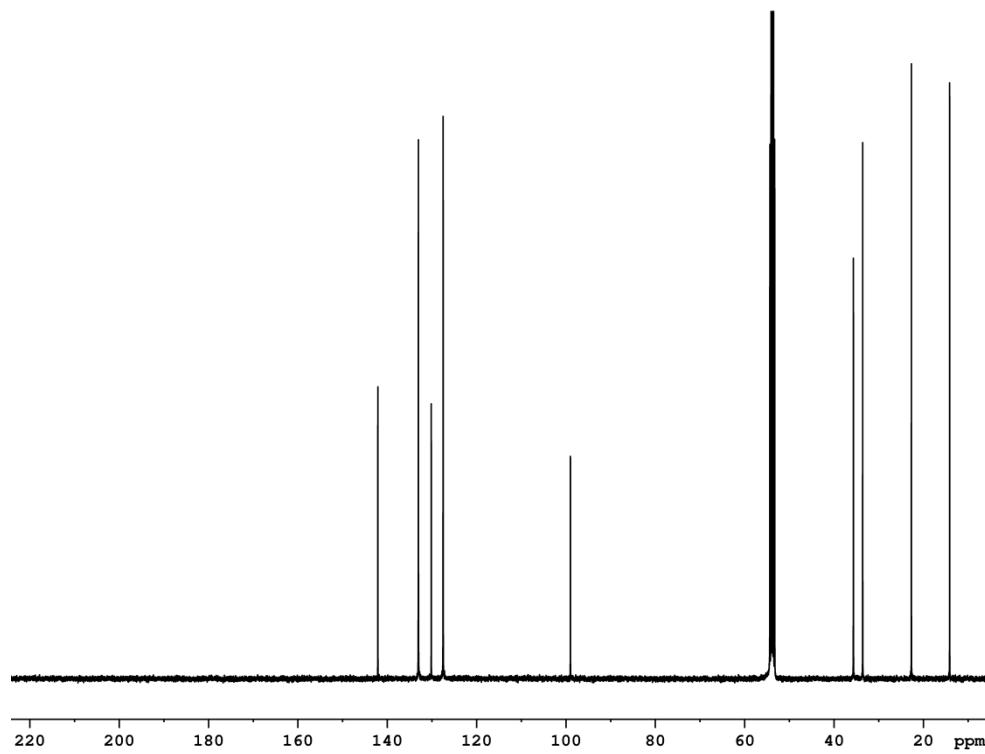
Figure S8.11. $^{13}C\{^1H\}$ NMR spectrum of **6a** in CD_2Cl_2 at 298 K.
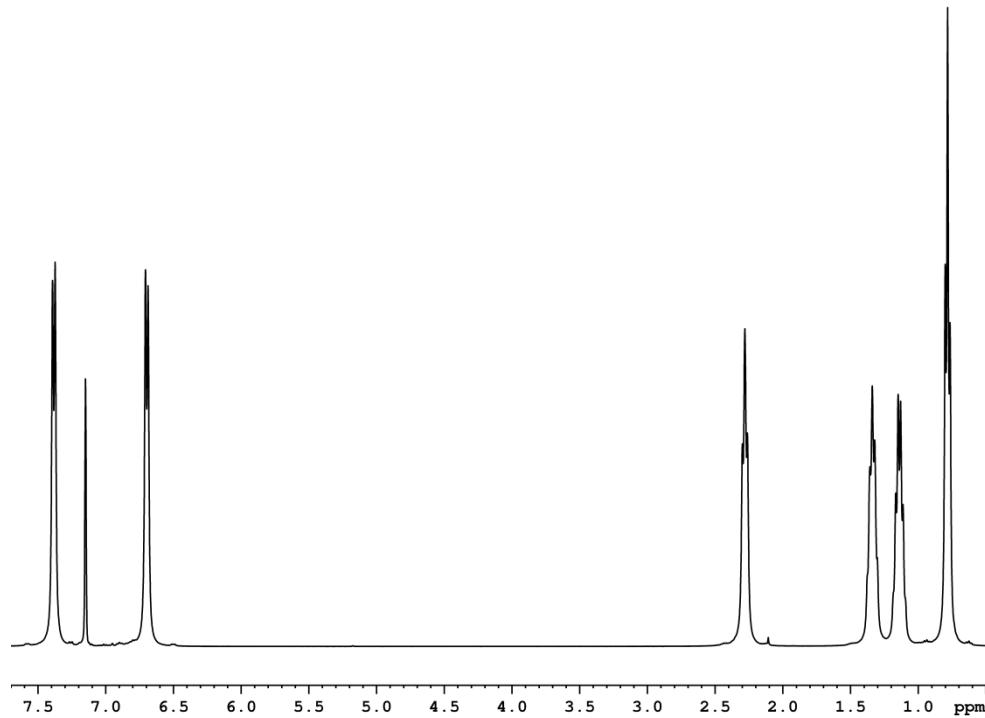
Figure S8.12. ^1H NMR spectrum of **6b** in C_6D_6 at 298 K.
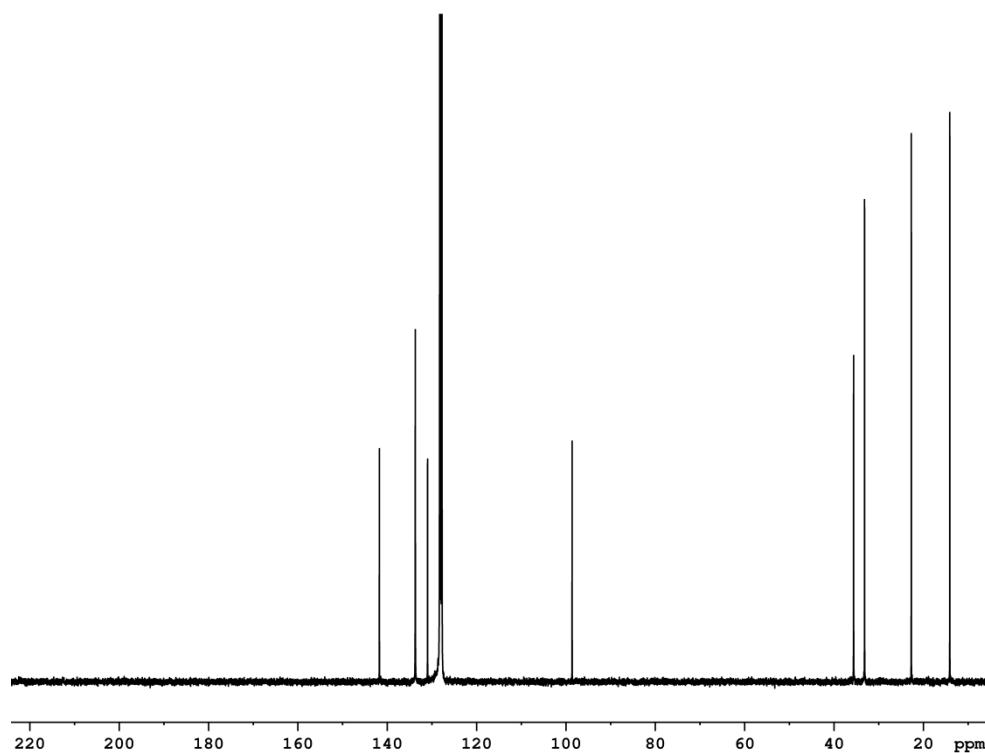
Figure S8.13. $^{13}C\{^1H\}$ NMR spectrum of **6b** in C_6D_6 at 298 K.

Crystallographic Details:

The crystal structure analyses were performed either on an Oxford Diffraction Gemini R Ultra CCD diffractometer (**2a, 2b, 3, 4, 5, 6a**) or an Oxford Diffraction SuperNova diffractometer (**6b**). For all compounds an analytical absorption correction was carried out.[1] The structures were solved by direct methods either of the program SIR-92[2] or SUPERFLIP[3] and refined with the least square method on F^2 employing SHELXL-97[4] with anisotropic displacements for non-H atoms. Hydrogen atoms were located in idealized positions and refined isotropically according to the riding model.

With the aid of PLATON,[5] three solvent accessible areas were found in the crystal structure of **6b**, but it was impossible to refine any reasonable molecules from difference Fourier peaks. Therefore the midpoints, the sizes and the numbers of electrons in the voids were refined and the contribution to the calculated structure factors of the disordered solvent is taken into account by back-Fourier transformation with the program SQUEEZE[6] (Sluis and Spek, 1990). The voids are found around (0.365 0.335 0.910), (0.500 0.000 0.000) and (0.635 0.665 0.089) and the sizes are 91, 117 and 91 $\mathring{A}^3$, and 23, 30 and 23 e⁻ respectively were detected (whole cell). The number of electrons corresponds to roughly three acetonitrile molecules.

CCDC-996971 (**2a**), CCDC-996972 (**2b**) and CCDC-996973 (**3**), CCDC-996974 (**4**), CCDC-996975 (**5**), CCDC-996976 (**6a**) and CCDC-996977 (**6b**) contain the supplementary crystallographic data for this paper. These data can be obtained free of charge at www.ccdc.cam.ac.uk/conts/retrieving.html (or from the Cambridge Crystallographic Data Centre, 12 Union Road, Cambridge CB2 1EZ, UK; Fax: + 44-1223-336-033; e-mail: deposit@ccdc.cam.ac.uk).

Crystal data for [($Cp^{BIG}FeCO)_2(\mu$-$S_2)_2$] (**2a**): $C_{112}H_{130}Fe_2O_2S_4$, M = 1748.14 g/mol, space group $P2_1/c$ (no.14), a = 13.5054(3) Å, b = 28.7294(5) Å, c = 13.3073(3) Å, $β$ = 114.321(3)°, V = 4705.0(2) Å^3, Z = 2, μ = 3.683 mm^{-1}, $F(000)$ = 1868, T = 123 K, 26963 reflections measured, 8085 unique (R_{int} = 0.0341), R_1 = 0.0518, wR_2 = 0.0934 for I > 2σ(I). CCDC-996971
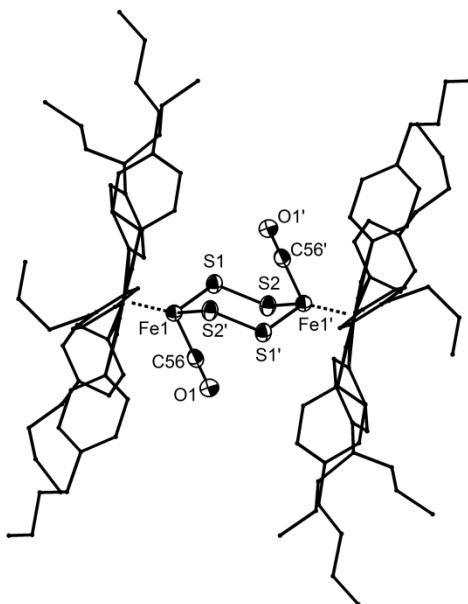

Figure S8.14. Molecular structure of **2a** in the crystal. For clarity reasons H atoms are omitted and in case of disorder only the main part is shown. Thermal ellipsoids are drawn with 50% probability level.

Crystal data for [($Cp^{BIG}FeCO)_2(\mu$-$Se_2)_2$] (**2b**): $C_{112}H_{130}Fe_2O_2Se_4$, M = 1935.70 g/mol, space group $P2_1/c$ (no.14), a = 13.4614(1) Å, b = 28.5802(2) Å, c = 13.7406(1) Å, $β$ = 114.394(1)°, V = 4814.48(7) Å^3, Z = 2, μ = 4.518 mm^{-1}, $F(000)$ = 2012, T = 123 K, 20789 reflections measured, 8255 unique (R_{int} = 0.0224), R_1 = 0.0556, wR_2 = 0.1475 for I > 2σ(I). CCDC-996972
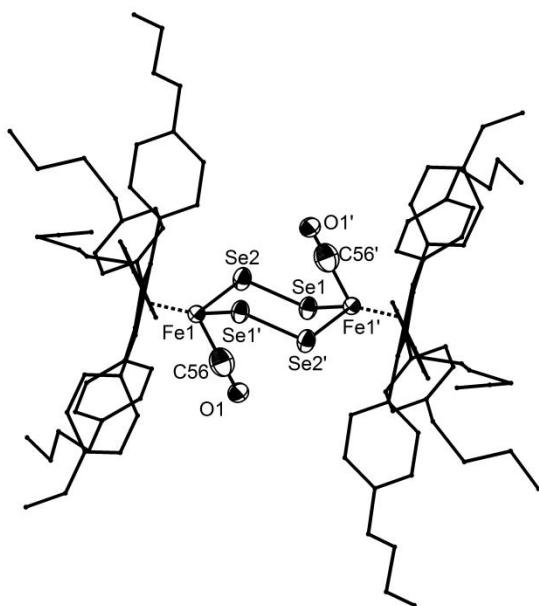
Figure S8.15. Molecular structure of **2b** in the crystal. For clarity reasons H atoms are omitted and in case of disorder only the main part is shown.

Crystal data for [{$Cp^{BIG}Fe(CO)_2$}$_2$(μ-Se_2)] (**3**): $C_{114}H_{130}Fe_2O_4Se_2$, M = 1833.80 g/mol, space group $P\bar{1}$ (no.2), a = 13.7339(4) Å, b = 14.0008(4) Å, c = 14.5709(4) Å, $α$ = 105.226(3)°, $β$ = 92.080(2)°, $γ$ = 114.452(3)°, V = 2427.2(2) Å^3, Z = 1, $μ$ = 3.648 mm^{-1}, $F(000)$ = 966, T = 123 K, 15903 reflections measured, 8357 unique (R_{int} = 0.0207), R_1 = 0.0919, wR_2 = 0.2423 for I > 2σ(I). CCDC-996973
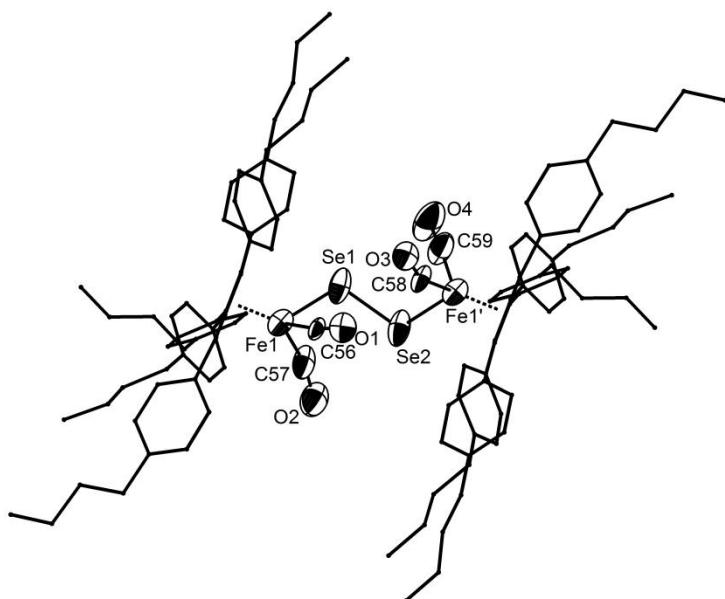
Figure S8.16. Molecular structure of **3** in the crystal. For clarity reasons H atoms are omitted and in case of disorder only the main part is shown. Thermal ellipsoids are drawn with 50% probability level.
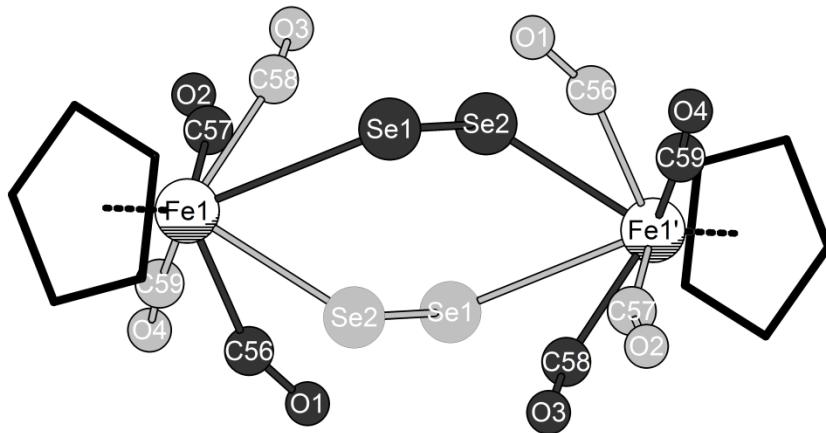
Figure S8.17. Disordered central structure of **3** in the crystal. Part 1 and 2 are colored differently.

Crystal data for $[\{Cp^{BIG}FeCO\}\{Cp^{BIG}Fe(CO)_2\}(\mu,\eta^{2:1}\text{-}Se_2)]$ * 0.5 CH_2Cl_2 * 0.5 CH_3CN (**4**): $C_{114.5}H_{132.5}ClFe_2NO_3Se_2$, M = 1868.79 g/mol, space group $P\bar{1}$ (no.2), a = 14.1706(4) Å, b = 19.5430(6) Å, c = 19.6307(5) Å, α = 74.040(3)°, β = 82.507(2)°, γ = 75.027(3)°, V = 5039.1(3) Å^3, Z = 2, μ = 3.755 mm^{-1}, $F(000)$ = 1968, T = 123 K, 38843 reflections measured, 17180 unique (R_{int} = 0.0318), R_1 = 0.0714, wR_2 = 0.1634 for I > 2σ(I). CCDC-996974
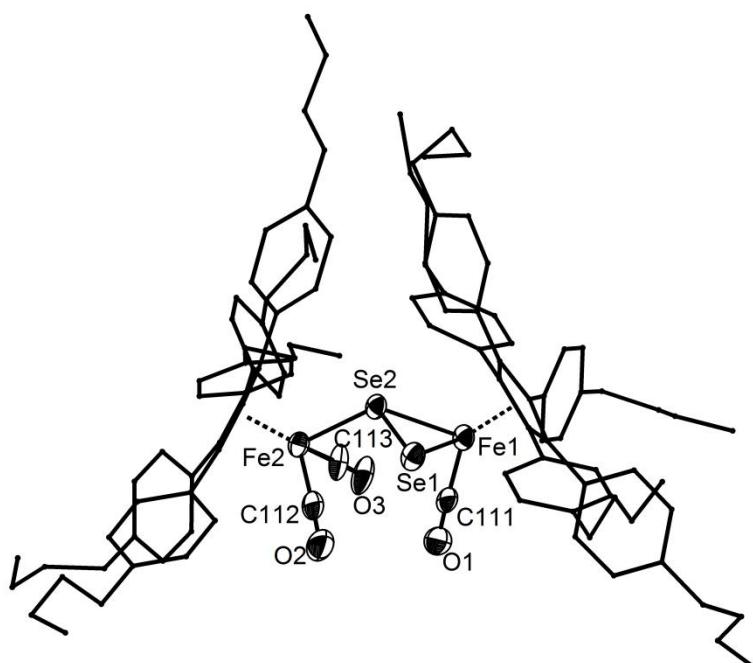

Figure S8.18. Molecular structure of **4** in the crystal. For clarity reasons H atoms are omitted and in case of disorder only the main part is shown. Thermal ellipsoids are drawn with 50% probability level.
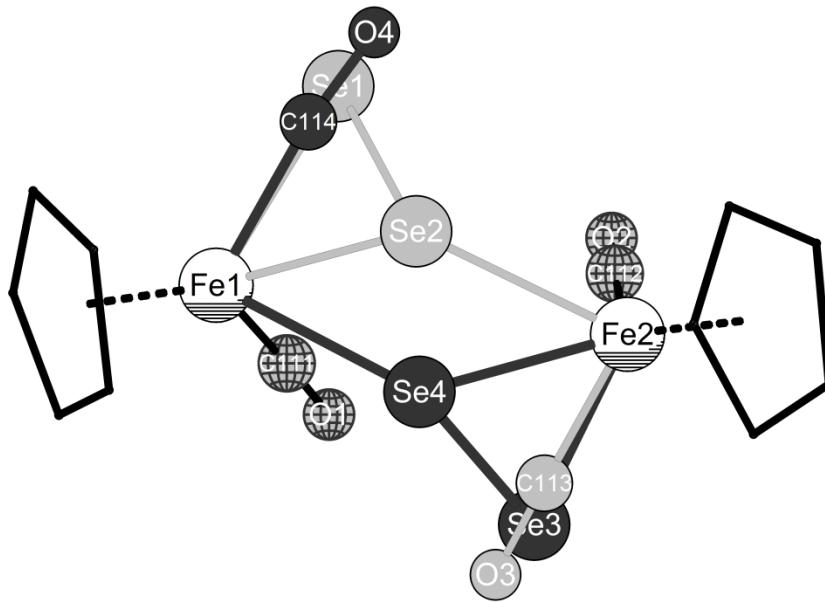
Figure S8.19. Disordered central structure of **4** in the crystal. Part 1 and 2 are colored differently. The hatched globes belong to both parts.

Crystal data for [{Cp^{BIG}Fe(CO)$_2$}$_2$(μ-Te)] * 0.5 CH$_2$Cl$_2$ (**5**): C$_{114.5}$H$_{131}$ClFe$_2$O$_4$Te, M = 1845.95 g/mol, space group $Pca2_1$ (no.29), a = 25.3317(2) Å, b = 27.1293(2) Å, c = 28.8386(2) Å, V = 19818.8(3) Å^3, Z = 8, μ = 5.261 mm^{-1}, $F(000)$ = 7768, T = 123 K, 107769 reflections measured, 35108 unique (R_{int} = 0.0368), R_1 = 0.0534, wR_2 = 0.1279 for I > 2σ(I). CCDC-996975

Crystal data for [(Cp^{BIG}Fe)$_2$(μ,η$^{1:1}$-S$_2$)(μ,η$^{2:2}$-S$_2$)] (**6a**): C$_{110}$H$_{130}$Fe$_2$S$_4$, M = 1692.13 g/mol, space group $P\bar{1}$ (no.2), a = 14.1813(1) Å, b = 15.5102(1) Å, c = 23.3895 (1) Å, a = 107.255(1)°, $β$ = 101.438(1)°, $γ$ = 95.228(1)°, V = 4753.33(6) Å^3, Z = 2, μ = 3.612 mm^{-1}, $F(000)$ = 1812, T = 123 K, 66247 reflections measured, 16722 unique (R_{int} = 0.0295), R_1 = 0.0335, wR_2 = 0.0784 for I > 2σ(I). CCDC-996976

Crystal data for [(Cp^{BIG}Fe)$_2$(μ,η$^{1:1}$-Se$_2$)(μ,η$^{2:2}$-Se$_2$)] * 2 CH$_2$Cl$_2$ * 0.75 CH$_3$CN (**6b**): C$_{113.5}$H$_{136.25}$Cl$_4$Fe$_2$N$_{0.75}$Se$_4$, M = 2049.54 g/mol, space group $P\bar{1}$ (no.2), a = 22.1190(4) Å, b = 22.2233(5) Å, c = 23.0616(3) Å, a = 90.382(1)°, $β$ = 92.790(1)°, $γ$ = 112.446(2)°, V = 10460.9(4) Å^3, Z = 4, μ = 5.090 mm^{-1}, $F(000)$ = 4248, T = 128 K, 38150 reflections measured, 14553 unique (R_{int} is not given because SQUEEZE was used. Otherwise it would be 0.0383), R_1 = 0.0751, wR_2 = 0.1615 for I > 2σ(I). CCDC-996977
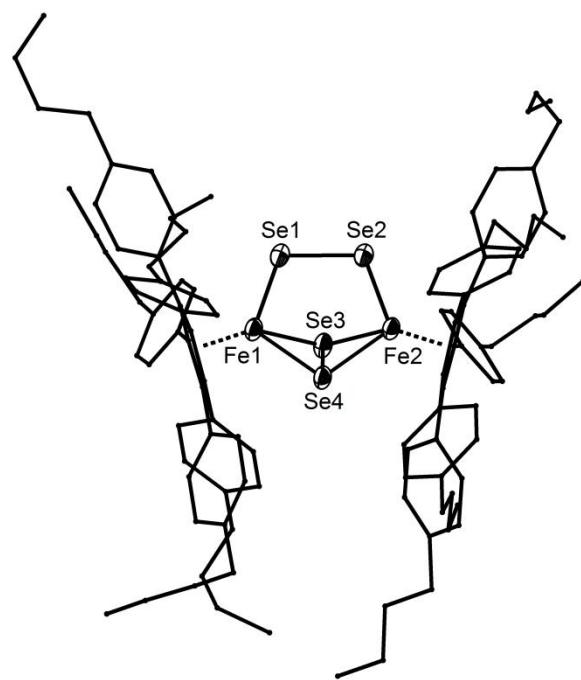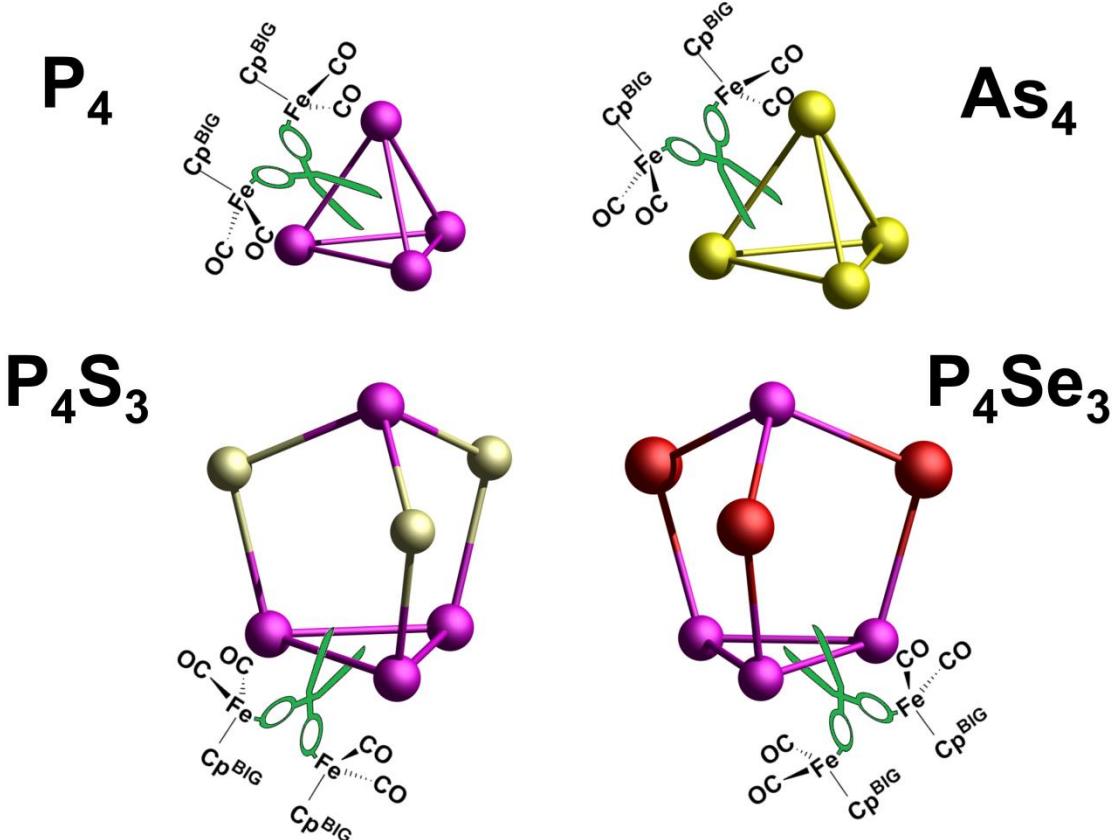
Figure S8.20. Molecular structure of **6b** in the crystal. For clarity reasons H atoms are omitted and in case of disorder only the main part is shown. Thermal ellipsoids are drawn with 50% probability level.

References for Supplementary Information:

[1]   R. C. Clark, J. S. Reid, *Acta Cryst.* **1995**, A51, 887-897.

[2]   A. Altomare, M. C. Burla, M. Camalli, G.L. Cascarano, C. Giacovazzo, A. Guagliardi, A. G. G. Moliterni, G. Polidori, R. Spagna, *J. Appl. Cryst.* **1999**, 32, 115-119.

[3]   L. Palatinus, G. Chapuis, *J. Appl. Cryst.* **2007**, 40, 786-790.

[4]   G. M. Sheldrick, *Acta Cryst.* **2008**, A64, 112-122.

[5]   Spek, A.L. *J. Appl. Cryst.* **2003**, 36, 7-13.

[6]   Sluis, P. van der & Spek, A.L. *Acta Cryst.* **1990**, A46, 194-201.

9. Activation of Group 15 Based Cage Compounds by [Cp^{BIG}Fe(CO)$_2$] Radicals
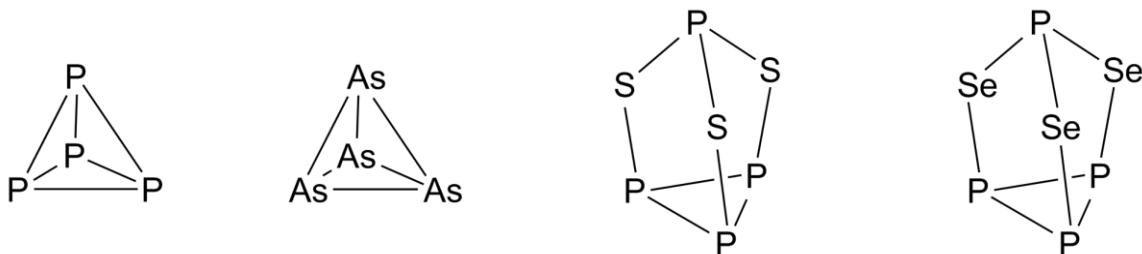
Sebastian Heinl and Manfred Scheer

❖ **All syntheses and characterizations were performed by Sebastian Heinl**

❖ **Manuscript was written by Sebastian Heinl**

❖ **Figures were made by Sebastian Heinl**

❖ **X-ray structure analyses and refinement were performed by Sebastian Heinl; Dr. Eugenia Perisypkina helped by recording crystal structures of 2c and 2d**

9.1 Introduction

The activation of white phosphorus with transition metal complexes[1] and main group elements[2] is of current research interest. During the last decades a large variety of transition metal complexes with P$_n$ units have been synthesized. In general, the reactions are thermolytically or photolytically induced to generate reactive complex fragments. Under these rather severe conditions typically a substantial fragmentation and reaggregation of the P$_4$ tetrahedron is found, which often is accompanied with mixtures of products. Exemplifying the situation for P$_4$, Scherer et al. reacted [Cp'''Fe(CO)$_2$]$_2$ with white phosphorus in a short time thermolysis (5 min) in toluene[3] and detected the butterfly complex [{Cp'''Fe(CO)$_2$}$_2$(μ,$\eta^{1:1}$-P$_4$)] as the main product. However, due to the high reaction temperatures further decarbonylation takes place leading to by-products, which had to be removed by low temperature column chromatography and led to reduced isolated yields.

The situation for the mixed cage compounds P$_4$S$_3$ and P$_4$Se$_3$, is even more intricate.[4] The presence of two different types of atoms complicated the separation and characterization of the obtained products. Thus, e.g. Wachter et al. described the reaction of P$_4$S$_3$ with [C$_5$Me$_5$Mo(CO)$_2$]$_2$ in boiling toluene to give triple-decker sandwich complexes with five-membered rings as middle deck. Both products [(C$_5$Me$_5$Mo)$_2$(P$_2$S$_3$)] and [(C$_5$Me$_5$Mo)$_2$(P$_4$S)] have almost the same molecular structure, only the middle decks are different (P$_4$S vs. P$_2$S$_3$).[5] The separation was only possible after the coordination of M(CO)$_5$ fragments (M = Cr, W) to these products.
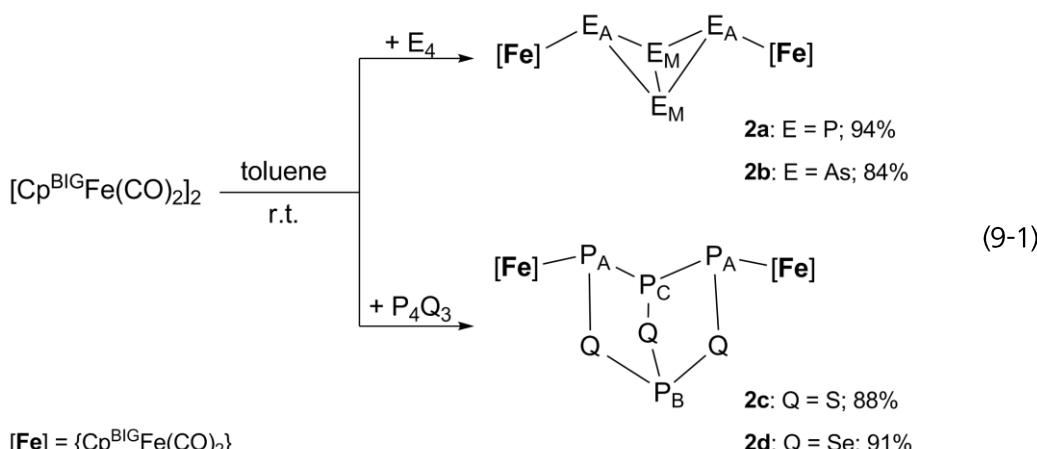

To avoid high temperatures or UV irradiation for triggering a reaction, stable complexes with reactive metal centers are needed. The dimeric compounds [(Cp^{Aryl})Fe(CO)$_2$]$_2$ (Cp^{Aryl} = C$_5$Ph$_5$, C$_5$Ph$_4$(p-tolyl)) readily dissociate in solution into two 17 VE radical fragments at room temperature, and therefore should be capable for this mission.[6] However, theire low solubility is a disadvantage for the reactivity studies. Therefore we synthesized the analogue complex [Cp^{BIG}Fe(CO)$_2$]$_2$ (**1**) (Cp^{BIG} = pentakis(4-n-butylphenyl)cyclopentadienyl),[7] whose additional n-butyl groups generate a good solubility.

In the following we report on the room temperature activation of P$_4$, As$_4$, P$_4$S$_3$ or P$_4$Se$_3$ by [Cp^{BIG}Fe(CO)$_2$]$_2$ (**1**) resulting in a selective E-E bond cleavage to give exclusively the

corresponding cage complexes in high yields. In addition, this complex is also capable to transform a small organic molecule like CS_2.

9.2 Results and Discussion

Addition of **1** to toluene solutions of P_4, As_4, P_4S_3 or P_4Se_3, respectively, results in an immediate change of color to intensive orange (P_4, As_4), or pink (P_4S_3, P_4Se_3) respectively. The IR spectra indicate a complete conversion of the starting material by showing two new CO stretching frequencies (Table 9.1, four CO bands for **1**). Also the NMR spectra of the reaction mixtures illustrate a clean and complete reaction. The products [{Cp^{BIG}Fe(CO)$_2$}$_2$(μ,$\eta^{1:1}$-**cage**)] (**cage** = P_4 (**2a**), As_4 (**2b**), P_4S_3 (**2c**), P_4Se_3 (**2d**)) are isolated in almost quantitative yields (Equation 9-1) and reveal that selectively only one E–E bond was homolytically cleaved.

(9-1)

Compounds **2a-d** are very good soluble in CH_2Cl_2, toluene, thf and hexane but insoluble in CH_3CN. The ESI mass spectra of **2a** and **2b** show the molecular ion peaks. In case of **2c** and **2d** characteristic fragments could be detected. The $^{31}P\{^1H\}$ NMR spectrum of **2a** shows two triplets at δ = -54.0 ppm and δ = -317.1 ppm ($^1J_{PP}$ = 187 Hz), which is typical for P_4 butterfly complexes.[8] For **2c** and **2d** the $^{31}P\{^1H\}$ NMR spectra show A$_2$BC spin systems (Table 9.1),

Table 9.1. $^{31}P\{^1H\}$ NMR features of **2a**, **2c** in C_6D_6, **2d** in CD_2Cl_2 and ν_{CO} in toluene of **2a-d**. For P labelling see scheme above. (δ in ppm, J_{PP} in Hz, ν_{CO} in cm^{-1})

| Complex	δ (P$_A$)	δ (P$_{M/B}$)	δ (P$_C$)	J_{PP}	ν_{CO}
2a	-53.9	-317.1	-	187 (P$_A$P$_M$)	2002, 1955
2b	-	-	-	-	1993, 1948
2c	169.4	153.5	91.5	296 (P$_A$P$_C$), 63 (P$_B$P$_C$), 45 (P$_A$P$_B$)	2011, 1967
2d	181.3	123.5	101.8	305 (P$_A$P$_C$), 66 (P$_B$P$_C$), 45 (P$_A$P$_B$)	2011, 1967
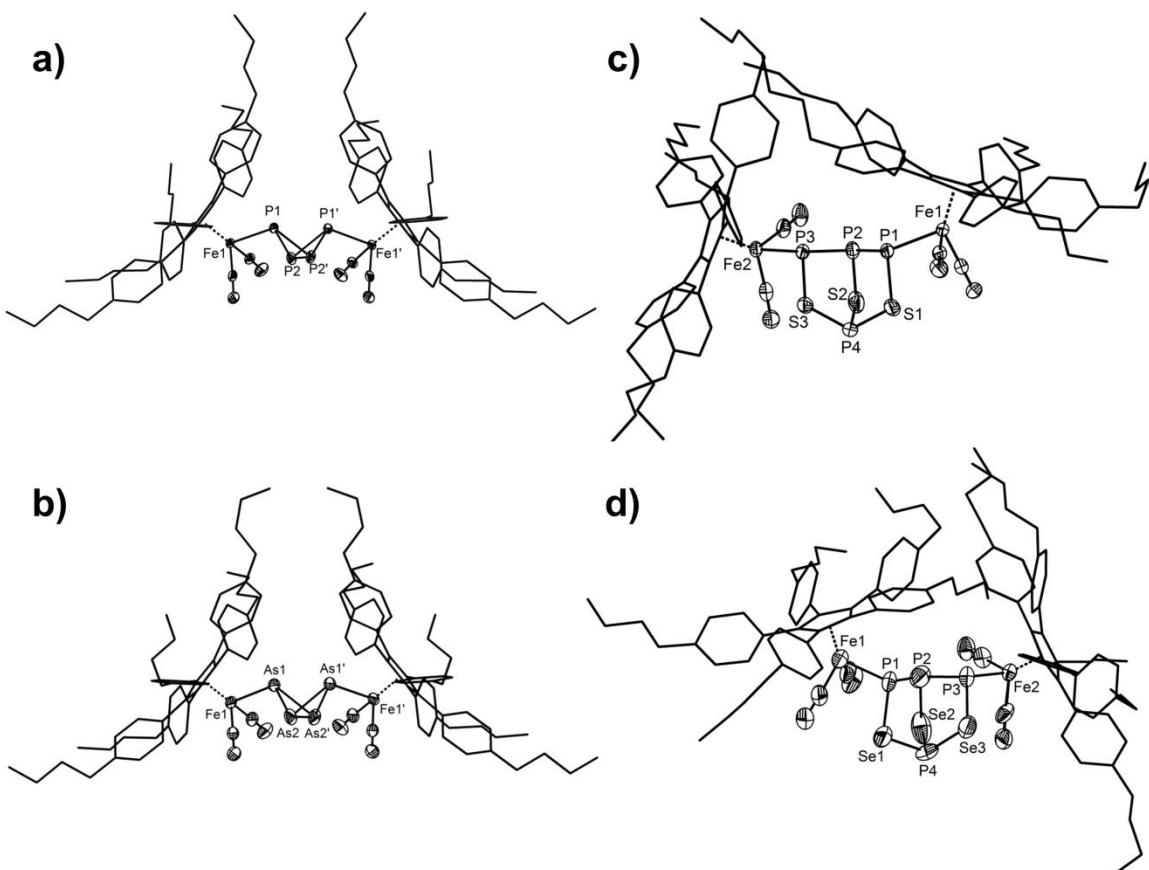
Figure 9.1. Molecular structures of **2a-d** in the crystal with selected labels (a: **2a**; b: **2b**; c: **2c**; d **2d**). Ellipsoids are drawn at 50% probability level. In case of **2c** only one of the two molecules in the asymmetric unit is depicted. In case of disorder only the main part is shown. For clarity reasons, H atoms and solvent molecules are omitted and Cp^{BIG} ligands are drawn in 'wire-or-stick' model. Selected atom distances [Å] and angles [°] in **2a**: P1-P2 2.2343(5), P1-P2' 2.2094(6), P1···P1' 2.7749(4), P2-P2' 2.1717(7), Fe1-P1 2.3397(4), P1-P2-P1' 77.28(2), P1-P2-P2' 60.17(2), P2-P2'-P1 61.32(2), P2-P1-P2' 58.51(2). Selected atom distances [Å] and angles [°] in **2b**: As1-As2 2.4639(6), As1-As2' 2.4357(7), As1···As1' 2.9958(4), As2-As2' 2.3976(9), Fe1-As1 2.4315(7), As1-As2-As1' 75.39(2), As1-As2-As2' 60.12(2), As2-As2'-As1 61.29(2), As2-As1-As2' 58.59(2). Selected atom distances [Å] and angles [°] in **2c** from both molecules in the asymmetric unit: P1-P2/P6-P7 2.227(2)/2.190(1), P2-P3/P5-P6 2.185(1)/2.194(1), P1···P3/P5···P7 3.268(1)/3.318(1), P1-S1/P7-S6 2.156(1)/2.172(1), P2-S2/P6-S5 2.108(2)/2.114(1), P3-S3/P5-S4 2.157(1)/2.161(1), P4-S1/P8-S6 2.074(2)/2.099(2), P4-S2/P8-S5 2.107(2)/2.100(1), P4-S3/P8-S4 2.097(2)/2.094(2), Fe1-P1/Fe4-P7 2.314(1)/2.313(1), Fe2-P3/Fe3-P5 2.309(1)/2.314(1), P1-P2-P3/P5-P6-P7 95.60(5)/98.38(5), P1-S1-P4/P7-S6-P8 105.34(6)/107.52(5), P2-S2-P4/P6-S5-P8 97.51(7)/97.46(5), P3-S3-P4/P5-S4-P8 108.02(6)/106.27(6). Selected atom distances [Å] and angles [°] in **2d** (in case of disordered atoms both values are given, signed by postfixes A and B): P1-P2A/P1-P2B 2.12(1)/2.247(8), P2A-P3/P2B-P3 2.18(1)/2.148(10), P1···P3 3.260(3), P1-Se1 2.299(2), P2A-Se2A/P2B-Se2B 2.32(2)/2.14(1), P3-Se3 2.304(2), P4A-Se1/P4B-Se1 2.25(2)/2.23(1), P4A-Se2A/P4B-Se2B 2.09(2)/2.36(2), P4A-Se3/P4B-Se3 2.30(1)/2.23(1), Fe1-P1 2.321(2), Fe2-P3 2.298(2), P1-P2A-P3/P1-P2B-P3 98.6(5)/95.7(3), P1-Se1-P4A/P1-Se1-P4B 96.1(3)/104.4(4), P2A-Se2A-P4A/P2B-Se2B-P4B 93.5(5)/97.1(5), P3-Se3-P4A/P3-Se3-P4B 98.9(3)/110.0(4).

which clearly indicate the suggested molecular structures.
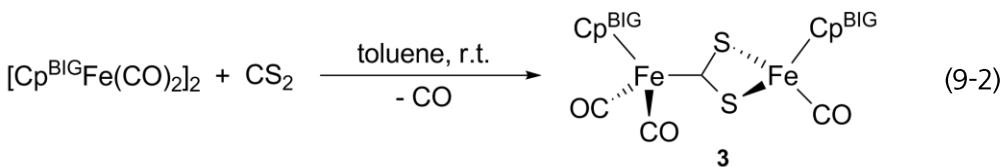
Single crystal X-ray structure analyses of **2a-d** (Figure 9.1) reveal the selective cleavage of one single E–E bond (E = P, As) and two {Cp^{BIG}Fe(CO)$_2$} fragments are now coordinated to these atoms. Compounds **2a** and **2b** show a central tetraphospha/tetraarsa-*bicyclo*[1.1.0]

butane (butterfly) structural motif, whereas for **2c** and **2d** a tetraphospha-trithio/triseleno-*bicyclo*[2.2.1]heptane core is found. The P$_4$ butterfly complex **2a** follow the same trend for P–P bond lengths like other derivatives, e.g. [{Cp'''Fe(CO)$_2$}$_2$(µ,η$^{1:1}$-P$_4$)].[3] The bond between P1 and P2/P2' (2.2094(6) Å and 2.2343(5) Å) are similar to a single bond like in P$_4$ (2.21 Å)[2a,9], however the bond P2-P2' is slightly shortened (2.1717(7) Å).

While for P$_4$ ligands the butterfly structural motif is known, it is particularly rare for As$_4$ ligands. The only structurally characterized compound in literature is [Cp*Co(CO)(η$^{1:1}$-As$_4$)] in which the As$_4$ unit is bound to only one metal atom.[10] Recently in our group two other arsenic butterfly complexes with arsenic were obtained, [{Cp'''Fe(CO)$_2$}$_2$(µ,η$^{1:1}$-As$_4$)] and [{Cp*Cr(CO)$_3$}$_2$(µ,η$^{1:1}$-As$_4$)].[11] In **2b** the bonds between the coordinating atom As1 and the non-coordinating As2 are also longer (2.4357(7) Å and 2.4639(6) Å) than the bridgehead bond As2–As2' (2.3976(9) Å) and agree well with the above mentioned examples. In addition, **2b** shows the same tendency of distortion after conversion in comparison with As$_4$ (As–As 2.44 Å)[12] like **2a** with P$_4$.

For the cleavage of one P–P bond of the P$_3$ ring in P$_4$S$_3$ only three examples are known. They all reveal an oligomeric metal bridged structure; dimeric for the iridium complexes *cis/trans*-[Ir(µ-P$_4$S$_3$)(PPh$_3$)Cl(CO)]$_2$[13] and trimeric for [Pt(µ-P$_4$S$_3$)(PPh$_3$)]$_3$.[14] In contrast, for **2c-d** a monomeric structural motif is observed without oligomerization because of steric protection of the {Cp^{BIG}Fe(CO)$_2$} fragments compared to PPh$_3$ ligands in the complexes mentioned above. Despite the different structure, the distances in the P$_4$S$_3$ core in **2c** are similar expect of the average P–P bond length of 2.20 Å, which is about 0.05-0.10 Å shorter than in the Ir and Pt complexes, respectively. Compound **2d** represents the unprecedented example, in which the first step of the degradation of the P$_4$Se$_3$ cage is observed. The P–P bond lengths (average 2.17 Å) are shorter than in the P$_4$Se$_3$ molecule (2.22 Å – 2.26 Å),[15] while the other bonds within the cage are rather unaffected.

The activation of a second bond in **2a-d** by **1** has never been observed regardless of used stoichiometry and applied reaction times. However, if solutions of **2a** are heated up the formation of [Cp^{BIG}Fe(η^5-P$_5$)] and [(Cp^{BIG}Fe)$_2$(µ,η$^{4:4}$-P$_4$)] is observed. We recently reported on the co-thermolysis of **1** with P$_4$ resulting in complete degradation of the tetrahedral structure of P4 forming the two products of [Cp^{BIG}Fe(η^5-P$_5$)] and [(Cp^{BIG}Fe)$_2$(µ,η$^{4:4}$-P$_4$)].[7] Furthermore, if white phosphorus is added to **2a** before heating, the same ratio of products and yields are obtained as was found before. This indicates **2a** to be the initial activation step for the complete conversion of P$_4$ by Cp^{R}Fe fragments. A higher grade of degradation at elevate temperatures can also be assumed for **2b-d**, which will be in focus of future reactivity studies.

$$[Cp^{BIG}Fe(CO)_2]_2 \;+\; CS_2 \quad \xrightarrow[- \, CO]{\text{toluene, r.t.}} \quad \text{(9-2)}$$

In addition, the reaction of **1** with an excess of CS$_2$ at ambient temperature results in the quantitative formation of the binuclear complex [{Cp^{BIG}Fe(CO)$_2$}{Cp^{BIG}FeCO}(µ,η$^{1:2}$-CS$_2$)] **(3)** accompanied by instant change of color from green to brown (Equation 9-2). The CO stretching bands of **1** have completely vanished. Three new CO absorption bands for **3** are observed in both, solution (DCM: 2023 cm^{-1}, 1979 cm^{-1}, 1928 cm^{-1}) and solid state (KBr: 2022 cm^{-1}, 1979 cm^{-1}, 1936 cm^{-1}). The ^{1}H NMR and ^{13}C{^{1}H} spectra of **3** in CH$_2$Cl$_2$ show multiple
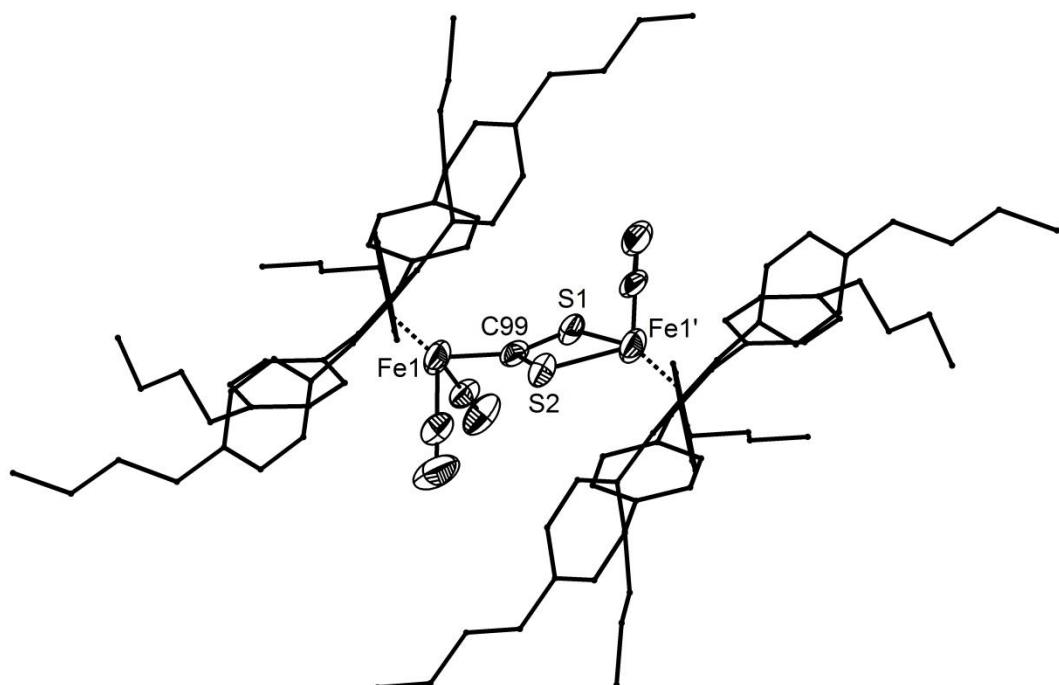

Figure 9.2. Molecular structure of **3** in the crystal with selected labels. Ellipsoids are drawn at 50% probability level. In case of disorder only the main part is shown. For clarity reasons, H atoms are omitted and Cp^{BIG} ligands are drawn in 'wire-or-stick' model. Selected atom distances [Å] and angles [°] in **3**: Fe1-C99 1.893(5), C99-S1 1.762(6), C99-S2 1.660(6), S1-Fe1' 2.396(2), S2-Fe1' 2.302(2), S1-C99-S2 104.9(3), Fe1'-S1-C99 89.4(2), Fe1'-S2-C99 95.3(3), S1-Fe1'-S2 70.51(5).

signals, indicating magnetic different Cp^{BIG} ligands which in addition might not freely rotate.[16] The X-ray structure analysis of **3** (Figure 9.2) shows two different iron fragments which are bridged by a CS$_2$ ligand. The molecule can be described as a ferradithiocarboxylate [Cp^{BIG}(CO)$_2$Fe-CS$_2$]$^-$ coordinating as a chelate to a {Cp^{BIG}FeCO}$^+$ fragment.

Unfortunately, because of high solubility a quantitative crystallization was not possible. Hence, crystalline samples of **3** could only be isolated in very low yields of 5%.

A possible reaction pathway starts from the addition of two {Cp^BIGFe(CO)$_2$} units onto a CS$_2$ molecule, one on the carbon atom and the other on one S atom. The not to iron bound S atom than attacks the iron fragment bound to sulfur under CO elimination and formation of **3**.

The spontaneous formation of metal centred radicals from the sterically encumbered complex **1** enables the selective cleavage of a single E–E bond (E = P, As) in the cage molecules P$_4$, As$_4$, P$_4$S$_3$ and P$_4$Se$_3$, respectively, already at room temperature. The products [{Cp^BIGFe(CO)$_2$}$_2$(μ,$\eta^{1:1}$-**cage**)] (**cage** = P$_4$ (**2a**), As$_4$ (**2b**), P$_4$S$_3$ (**2c**), P$_4$Se$_3$ (**2d**)) exhibit bicyclic structural motifs. Regardless of stoichiometry and reaction time applied, no further degradation of the molecules could be observed. Thermolysis of **2a** leads to *cyclo*-P$_5$ and P$_4$-butadiene containing products, which are also formed by the direct reaction of **1** with P$_4$ under elevate temperatures. Furthermore we have shown that **1** readily reacts with CS$_2$ to form a binuclear complex with a dithiocarboxylate ligand. Further studies will focus on the use of the dimeric complex **1** to activate other small (organic) molecules, also in a catalytically manner.

9.3 Experimental Part

General Remarks:

All experiments were carried out under an atmosphere of dry argon or nitrogen using glovebox and schlenk techniques. Solvents were purified, dried and degassed prior to use. P$_4$, P$_4$S$_3$ and P$_4$Se$_3$ were available and solutions of As$_4$[17] and [Cp^BIGFe(CO)$_2$]$_2$ (**1**)[7] were prepared according to literature procedures. The NMR spectra were measured on a Bruker Avance 300, 400 or 600 spectrometer. ESI-MS spectra were measured on a ThermoQuest Finnigan TSG 7000 mass spectrometer and FD-MS spectra on a Finnigan MAT 95 mass spectrometer. The elemental analyses were determined on a Vario EL III apparatus. The IR spectra were measured on a VARIAN FTS-800 FT-IR spectrometer.

Preparation of [{Cp^BIGFe(CO)$_2$}$_2$(μ,$\eta^{1:1}$-P$_4$)] (2a):

A solution of [Cp^BIGFe(CO)$_2$]$_2$ (**1**) (1.3 g, 0.78 mmol) in 100 mL toluene is added to a solution of P$_4$ (96 mg, 0.78 mmol) in 50 mL toluene. The orange solution is stirred for 30 min and the solvent is removed in vacuum. The residue is dissolved in ca. 15 mL CH$_2$Cl$_2$, transferred into a Schlenk-tube and layered with 50 mL CH$_3$CN. After complete diffusion, red crystals of **2a** are obtained (1.30 g, 94%).

2a: [C$_{114}$H$_{130}$Fe$_2$O$_4$P$_4$] calc.: C, 76.08; H, 7.28. found: C, 75.82; H, 7.13. ESI-MS (toluene/CH$_3$CN/CH$_2$Cl$_2$, cation): *m/z* (%) = 1884.7 (65%, [M+CH$_2$Cl$_2$]$^+$), 1718.7 (20%,

[Cp$^{BIG}_2$Fe$_2$P$_5$]$^+$), 1508.3 (20%, [Cp$^{BIG}_2$Fe$_2$]$^+$), 1718.7 (100%, [Cp^{BIG}Fe(toluene)]$^+$), 741.5 (80%, [Cp^{BIG}OH]$^+$). IR (toluene): v_{CO} [cm^{-1}] = 2002 (s), 1955 (s). ^{1}H NMR (C$_6$D$_6$): δ [ppm] = 0.81 (t, $^3J_{HH}$ = 7.3 Hz, 30H, CH$_3$), 1.16 (m, 10H, CH$_2$), 1.35 (m, 10H, CH$_2$), 2.29 (t, $^3J_{HH}$ = 7.7 Hz, 10H, CH$_2$), 6.73 (d, $^3J_{HH}$ = 7.9 Hz, 10H, C$_6$H$_4$), 7.34 (d, $^3J_{HH}$ = 7.9 Hz, 10H, C$_6$H$_4$). ^{31}P{^{1}H} NMR (C$_6$D$_6$): δ - 317.1 (t, $^1J_{PP}$ = 187 Hz, 2P, P$_M$), -53.9 (t, $^1J_{PP}$ = 187 Hz, 2P, P$_A$).

Preparation of [{Cp^{BIG}Fe(CO)$_2$}$_2$(μ,η$^{1:1}$-As$_4$)] (2b):

A solution of [Cp^{BIG}Fe(CO)$_2$]$_2$ (**1**) (0.75 g, 0.44 mmol) in 50 mL toluene is added at room temperature to a freshly prepared solution of As$_4$ (from 5 g As$_{gray}$ in 300 mL toluene). The orange solution is stirred for 30 min and the solvent is removed in vacuum. The residue is solved in ca. 10 mL CH$_2$Cl$_2$, filtered into a Schlenk-tube and layered with 30 mL CH$_3$CN. After complete diffusion, red crystals of **2b** are obtained (0.73 g, 84%).

2b: [C$_{114}$H$_{130}$Fe$_2$O$_4$As$_4$*CH$_2$Cl$_2$] calc.: C, 67.03; H, 6.46. found: C, 66.64; H, 6.44. ESI-MS (CH$_2$Cl$_2$, cation): m/z (%) = 1976.2 (100%, [M]$^+$). IR (toluene): v_{CO} [cm^{-1}] = 1993 (s), 1948 (s). ^{1}H NMR (C$_6$D$_6$): δ [ppm] = 0.80 (t, $^3J_{HH}$ = 7.2 Hz, 30H, CH$_3$), 1.16 (m, 10H, CH$_2$), 1.34 (m, 10H, CH$_2$), 2.27 (t, $^3J_{HH}$ = 7.6 Hz, 10H, CH$_2$), 6.72 (d, $^3J_{HH}$ = 8.0 Hz, 10H, C$_6$H$_4$), 7.34 (d, $^3J_{HH}$ = 8.0 Hz, 10H, C$_6$H$_4$).

Preparation of [{Cp^{BIG}Fe(CO)$_2$}$_2$(μ,η$^{1:1}$-P$_4$S$_3$)] (2c) and [{Cp^{BIG}Fe(CO)$_2$}$_2$(μ,η$^{1:1}$-P$_4$Se$_3$)] (2d):

A solution of [Cp^{BIG}Fe(CO)$_2$]$_2$ (**1**) (0.20 g, 0.11 mmol) in 5 mL toluene is added to a solution of P$_4$Q$_3$ (P$_4$S$_3$: 25 mg, 0.11 mmol; P$_4$Se$_3$: 40 mg, 0.11 mmol) in 5 mL toluene. The pink solution is stirred for 30 min, filtered via cannula and the solvent is removed in vacuum. The obtained solids are almost pure as indicated by NMR spectroscopy. Yield: 100 mg (88%) of **2c**; 110 mg (91%) of **2d**.

2c: An analytically pure crystalline sample can be obtained by the diffusion of CH$_3$CN in CH$_2$Cl$_2$ solutions of **2c**. Crystalline yield: 99 mg (47%). [C$_{114}$H$_{130}$Fe$_2$O$_4$P$_4$S$_3$*CH$_2$Cl$_2$] calc.: C, 69.73; H, 6.72; S, 4.86. found: C, 70.03; H, 6.54; S, 4.86. ESI-MS (toluene/CH$_3$OH, cation): m/z (%) = 1839.1 (100%, [M-2CO]$^+$). IR (toluene): v_{CO} [cm^{-1}] = 2011 (s), 1967 (s). ^{1}H NMR (C$_6$D$_6$): δ [ppm] = 0.82 (t, $^3J_{HH}$ = 7.3 Hz, 30H, CH$_3$), 1.18 (m, 10H, CH$_2$), 1.38 (m, 10H, CH$_2$), 2.32 (t, $^3J_{HH}$ = 7.8 Hz, 10H, CH$_2$), 6.75 (d, $^3J_{HH}$ = 8.2 Hz, 10H, C$_6$H$_4$), 7.30 (d, $^3J_{HH}$ = 8.2 Hz, 10H, C$_6$H$_4$). ^{31}P{^{1}H} NMR (C$_6$D$_6$): δ [ppm] = 91.5 (td, ^1J(P$_A$P$_C$) = 296 Hz, ^2J(P$_B$P$_C$) = 63 Hz, 1P, P$_C$), 153.5 (dt, ^2J(P$_B$P$_C$) = 63 Hz, ^2J(P$_A$P$_B$) = 45 Hz, 1P, P$_B$), 169.4 (dd, ^2J(P$_A$P$_B$) = 45 Hz, ^1J(P$_A$P$_C$) = 296 Hz, 2P, P$_A$). ^{13}C{^{1}H} NMR (C$_6$D$_6$): δ [ppm] = 14.1 (CH$_3$), 22.7 (CH$_2$), 33.1 (CH$_2$), 35.5 (CH$_2$), 103.5 (Cp), 128.4 (C$_6$H$_4$), 133.1 (C$_6$H$_4$), 142.6 (C$_6$H$_4$), 215.0 (CO), one Ph C atom is obscured by solvent signal.

2d: [C$_{114}$H$_{130}$Fe$_2$O$_4$P$_4$S$_3$*CH$_2$Cl$_2$] calc.: C, 67.23; H, 6.43. found: C, 66.06; H, 6.47. FD-MS (toluene): m/z (%) = 1786.1 (100%, [M-P$_3$Se$_2$]$^+$). IR (toluene): v_{CO} [cm^{-1}] = 2011 (s), 1967 (s). ^{1}H NMR (CD$_2$Cl$_2$): δ [ppm] = 0.91 (t, $^3J_{HH}$ = 7.2 Hz, 30H, CH$_3$), 1.30 (m, 10H, CH$_2$), 1.53 (m, 10H, CH$_2$), 2.49 (t, $^3J_{HH}$ = 7.2 Hz, 10H, CH$_2$), 6.84 (d, $^3J_{HH}$ = 7.7 Hz, 10H, C$_6$H$_4$), 6.92 (d, $^3J_{HH}$ = 7.7 Hz, 10H, C$_6$H$_4$). ^{31}P{^{1}H} NMR (CD$_2$Cl$_2$): δ [ppm] = 101.8 (td, ^1J(P$_A$P$_C$) = 305 Hz, ^2J(P$_B$P$_C$) = 66 Hz, 1P, P$_C$), 123.5 (dt, ^2J(P$_B$P$_C$) = 66 Hz, ^2J(P$_A$P$_B$) = 45 Hz, 1P, P$_B$), 181.3 (dd, ^2J(P$_A$P$_B$) = 45 Hz, ^1J(P$_A$P$_C$) = 305 Hz, 2P, P$_A$). ^{13}C{^{1}H} NMR (CD$_2$Cl$_2$): δ [ppm] = 14.1 (CH$_3$), 22.7 (CH$_2$), 33.5 (CH$_2$), 35.6 (CH$_2$), 103.4 (Cp), 127.9 (C$_6$H$_4$), 127.9 (C$_6$H$_4$), 132.8 (C$_6$H$_4$), 143.0 (C$_6$H$_4$), 215.4 (CO).

Preparation of [{Cp^{BIG}Fe(CO)$_2$}{Cp^{BIG}Fe(CO)}(μ,η$^{1:2}$-CS$_2$)] (3):

To a solution of [Cp^{BIG}Fe(CO)$_2$]$_2$ (**1**) (100 mg, 0.06 mmol) in 5 mL toluene 1 mL CS$_2$ is added. The solution immediately becomes brown. The reaction mixture is stirred for 30 min, filtered and the solvent is removed in vacuum. **3** is obtained as brown powder. Yield: 93 mg (91%)

To obtain crystals, the residue is dissolved in ca. 5 mL CH$_2$Cl$_2$, transferred into a Schlenk-tube and 10 mL CH$_3$CN is layered over it. After complete diffusion, red needle shaped crystals of **2a** are obtained.

3: FD-MS (toluene): m/z (%) = 1724.0 (45%, [M]$^+$), 1696.1 (100%, [M - CO]$^+$), 1640.2 (55%, [M - 3CO]$^+$). IR (toluene): v_{CO} [cm^{-1}] = 2023 (s), 1979 (s), 1928 (s). IR (KBr): v_{CO} [cm^{-1}] = 2022 (s), 1979 (s), 1936 (s). ^{1}H NMR (CD$_2$Cl$_2$): δ [ppm] = 0.91 (m, 30H, CH$_3$), 1.32 (m, 20H, CH$_2$), 1.53 (m, 20H, CH$_2$), 2.52 (m, 20H, CH$_2$), 6.7 − 7.0 (m, 40H, C$_6$H$_4$). ^{13}C{^{1}H} NMR (CD$_2$Cl$_2$): 14.14, 14.17, 22.70, 22.76, 22.80, 22.84, 33.56, 33.59, 33.61, 33.72, 33.78, 35.68, 96.29, 98.27, 102.00, 102.50, 103.49, 103.60, 127.24, 127.44, 127.49, 127.58, 127.88, 127.96, 128.08, 128.12, 128.20, 128.24, 129.0, 131.69, 132.23, 132.43, 132.55, 132.92, 141.14, 141.64, 142.21, 142.91, 142.97, 143.59, 214.87, 216.10.

9.4 References

[1]   a) B. M. Cossairt, N. A. Piro, C. C. Cummins, *Chem. Rev.* **2010**, *110*, 4164-4177; b) M. Caporali, L. Gonsalvi, A. Rossin, M. Peruzzini, *Chem. Rev.* **2010**, *110*, 4178-4235.

[2]   a) M. Scheer, G. Balázs, A. Seitz, *Chem. Rev.* **2010**, *110*, 4236-4256. b) N. A. Giffin, J. D. Masuda, *Coord. Chem. Rev.* **2011**, *255*, 1342-1359.

[3]   O. J. Scherer, T. Hilt, G. Wolmershäuser, *Organometallics* **1998**, *17*, 4110-4112.

[4]   a) J. Wachter, *Angew. Chem., Int. Ed.* **1998**, *37*, 751-768. b) M. Di Vaira, P. Stoppioni, *Coord. Chem. Rev.* **1992**, *120*, 259-279.

[5]   H. Brunner, U. Klement, W. Meier, J. Wachter, O. Serhadle, M. L. Ziegler, *J. Organomet. Chem.* **1987**, *335*, 339-352.

[6]   a) I. Kuksis, M. C. Baird, *Organometallics* **1994**, *13*, 1551-1553. b) I. Kuksis, M. C. Baird, *Organometallics* **1996**, *15*, 4755-4762.

[7]   S. Heinl, G. Balázs, M. Scheer, *Phosphorus, Sulfur Silicon Relat. Elem.* **2014**, DOI: 10.1080/10426507.2014.903489.

[8]   S. Heinl, S. Reisinger, C. Schwarzmaier, M. Bodensteiner, M. Scheer, *Angew. Chem. Int. Ed.*, 2014, **53,** accepted. http://dx.do.org/10.1002/anie.201403295.

[9]   a) L. R. Maxwell, S. B. Hendricks, V. M. Mosley, *J. Chem. Phys.* **1935**, *3*, 699-709. b) N. J. Brassington, H. G. M. Edwards, D. A. Long, *J. Raman Spectrosc.* **1981**, *11*, 346-348. c) A. Simon, H. Borrmann, H. Craubner, *Phosphorus, Sulfur Silicon Relat. Elem.* **1987**, *30*, 507-510. d) B. M. Cossairt, C. C. Cummins, A. R. Head, D. L. Lichtenberger, R. J. F. Berger, S. A. Hayes, N. W. Mitzel, G. Wu, *J. Am. Chem. Soc.* **2010**, *132*, 8459-8465.

[10]   O. J. Scherer, K. Pfeiffer, G. Wolmershäuser, *Chem. Ber.* **1992**, *125*, 2367-2372.

[11]   C. Schwarzmaier, PhD Thesis, University of Regensburg (Regensburg, Germany), 2012.

[12]   a) Y. Morino, T. Ukaji, T. Ito, *Bull. Chem. Soc. Jpn.* **1966**, *39*, 64-71. b) H. A. Spinney, N. A. Piro, C. C. Cummins, *J. Am. Chem. Soc.* **2009**, *131*, 16233-16243.

[13]   a) C. A. Ghilardi, S. Midollini, A. Orlandini, *Angew. Chem., Int. Ed.* **1983**, *22*, 790-791. b) E. Kuwabara, R. Bau, *Acta Crystallogr., Sect. C: Cryst. Struct. Commun.* **1994**, *50*, 64-67.

[14]   M. Di Vaira, M. Peruzzini, P. Stoppioni, *J. Chem. Soc., Dalton Trans.* **1985**, 291-295.

[15]   E. Keulen, A. Vos, *Acta Crystallogr.* **1959**, *12*, 323-329.

[16]   a) S. Heinl, E. V. Peresypkina, A. Y. Timoshkin, P. Mastrorilli, V. Gallo, M. Scheer, *Angew. Chem., Int. Ed.* **2013**, *52*, 10887-10891. b) S. Heinl, E. V. Peresypkina, A. Y. Timoshkin, P. Mastrorilli, V. Gallo, M. Scheer, *Angew. Chem.* **2013**, *125*, 11087-11091.

[17]   O. J. Scherer, H. Sitzmann, G. Wolmershäuser, *J. Organomet. Chem.* **1986**, *309*, 77-86.

## 9.5 Supplementary Information

NMR Investigations:
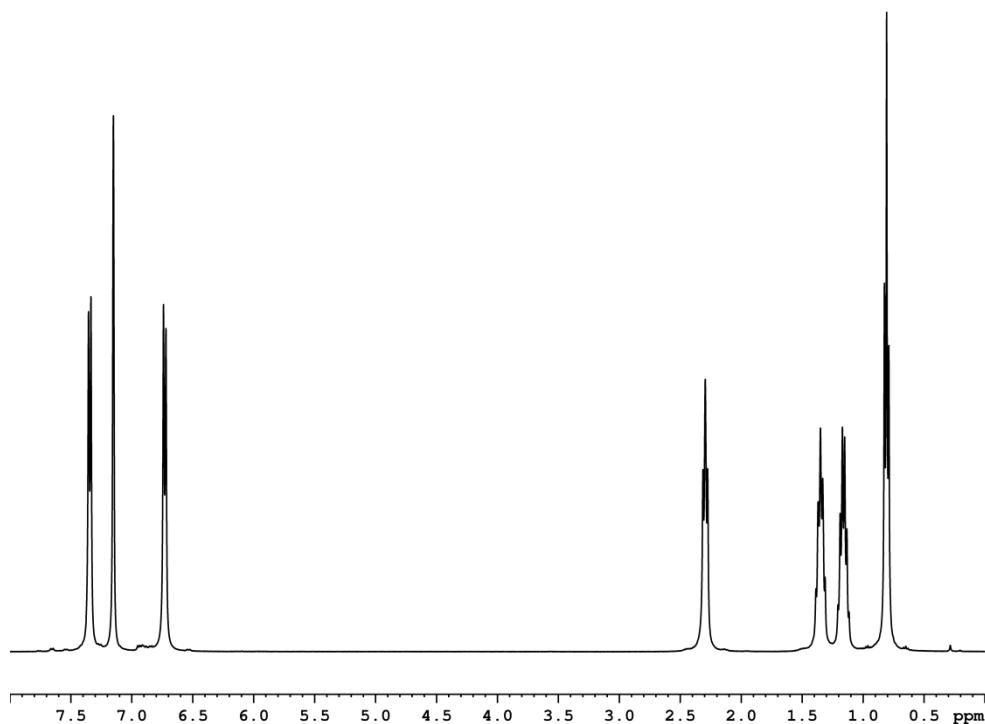
**Figure S9.1.** ^{1}H NMR spectrum of **2a** in C$_6$D$_6$ at 298 K.
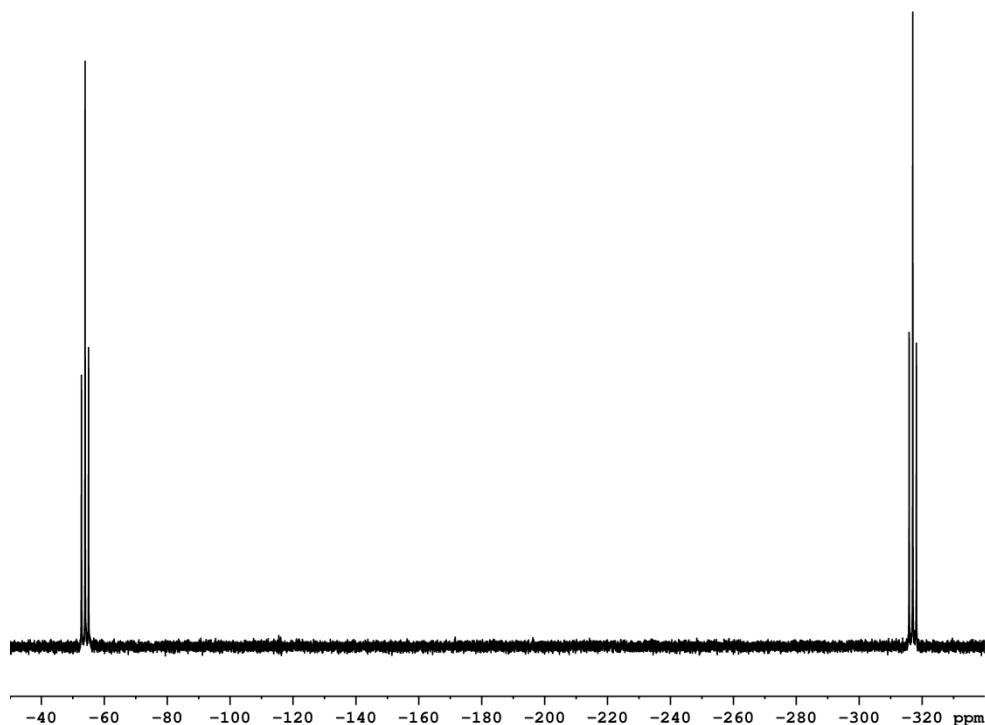
Figure S9.2. ^{31}P{^{1}H} NMR spectrum of **2a** in C$_6$D$_6$ at 298 K.
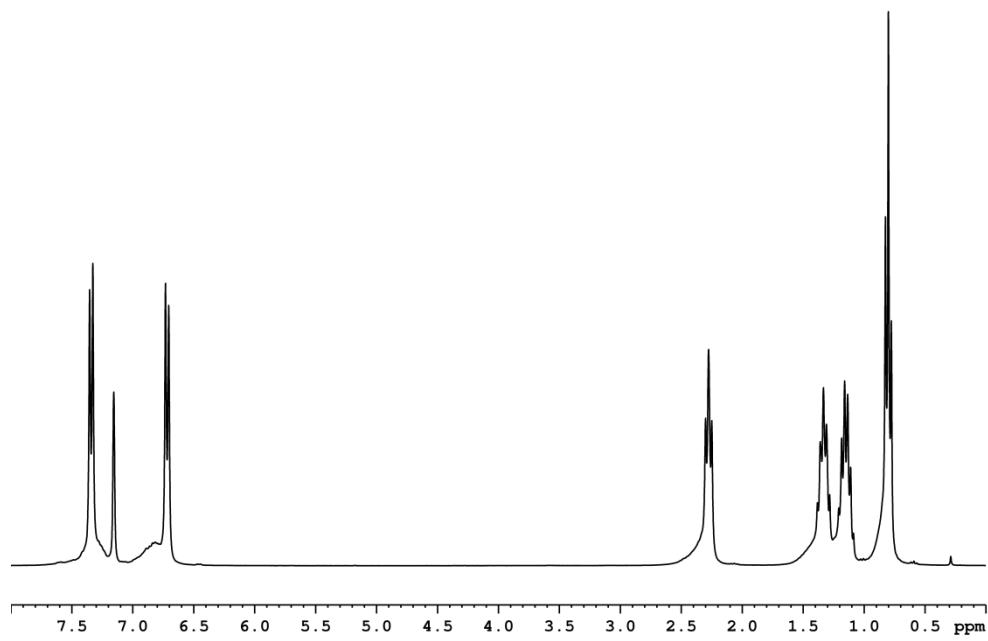
**Figure S9.3.** ^{1}H NMR spectrum of **2b** in C$_6$D$_6$ at 298 K.
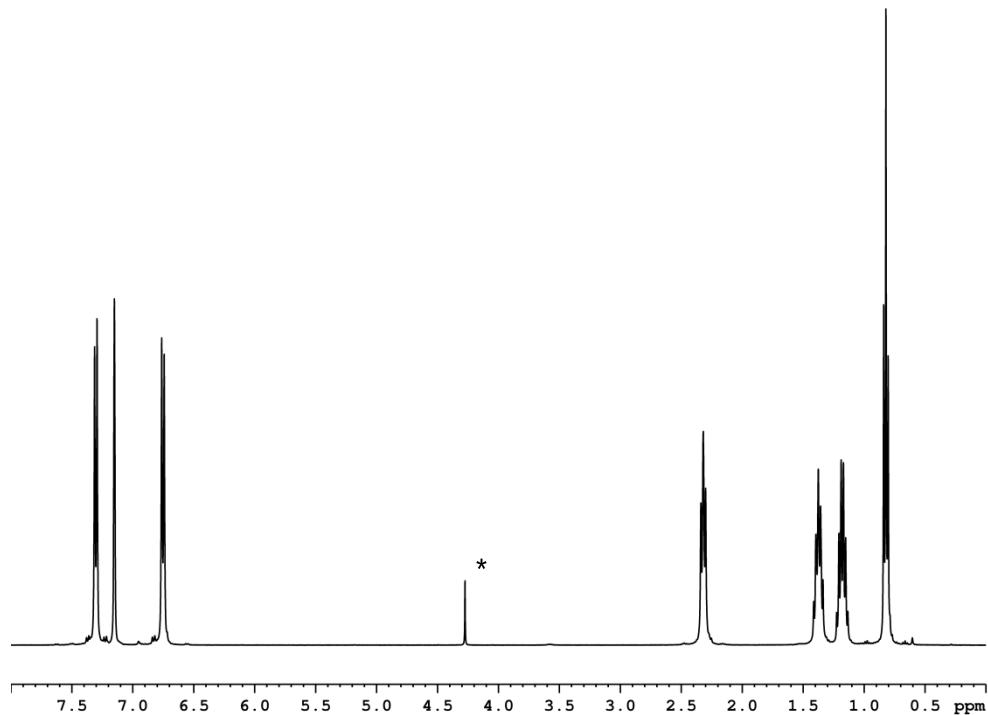
**Figure S9.4.** ^{1}H NMR spectrum of **2c** in C$_6$D$_6$ at 298 K. Signal marked with an asterisk is due to CH$_2$Cl$_2$.
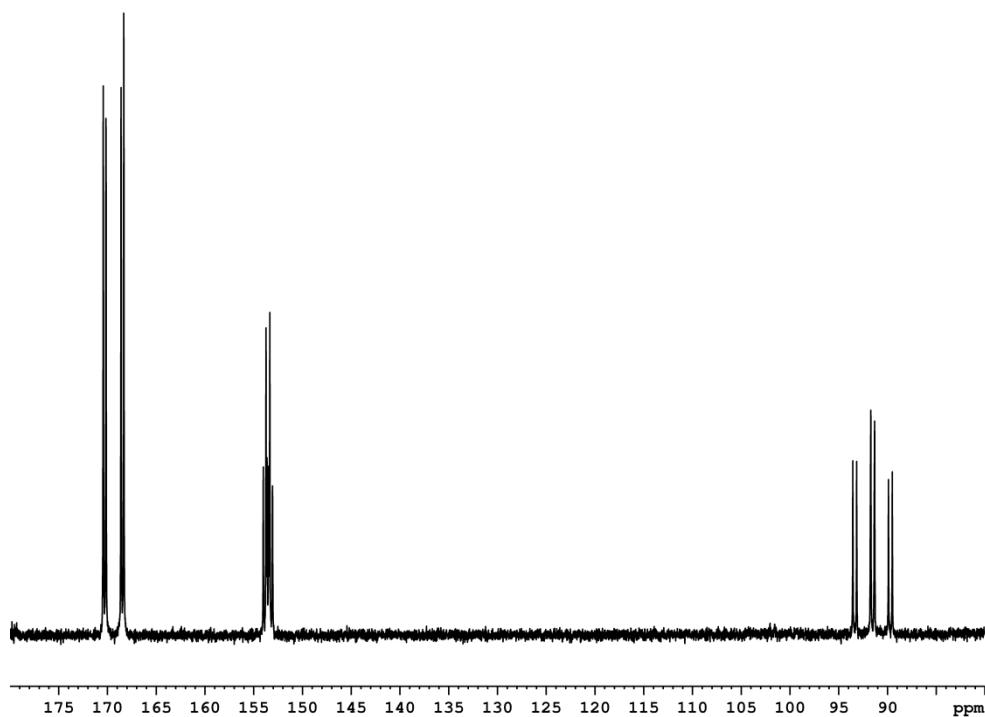
**Figure S9.5.** ^{31}P{^{1}H} NMR spectrum of **2c** in C$_6$D$_6$ at 298 K.
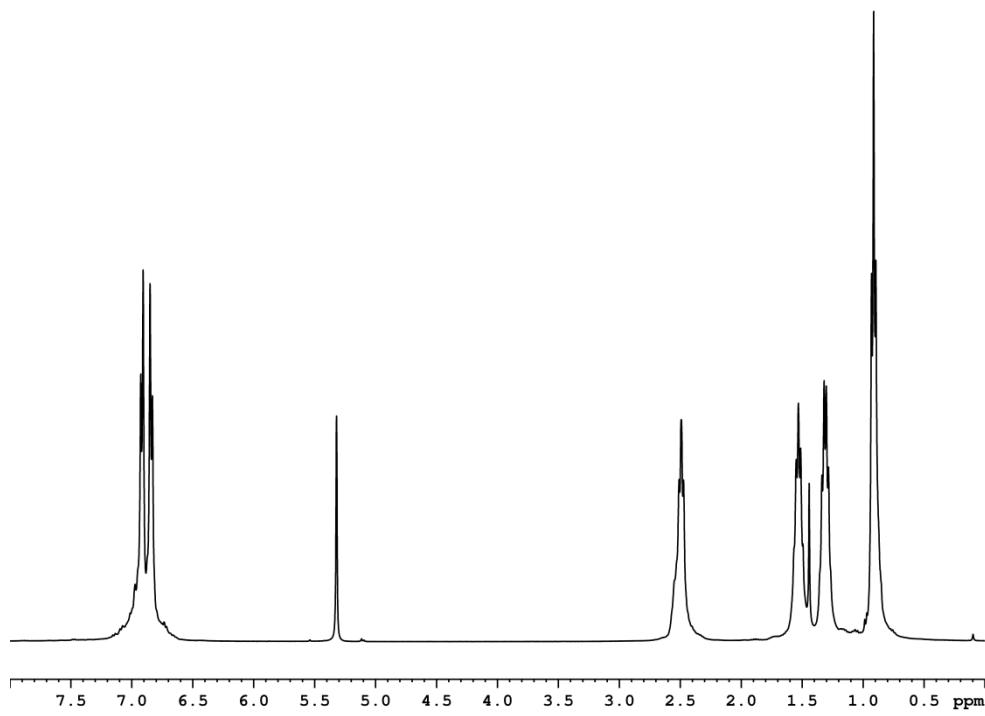
**Figure S9.6.** ^{1}H NMR spectrum of **2d** in CD$_2$Cl$_2$ at 298 K.
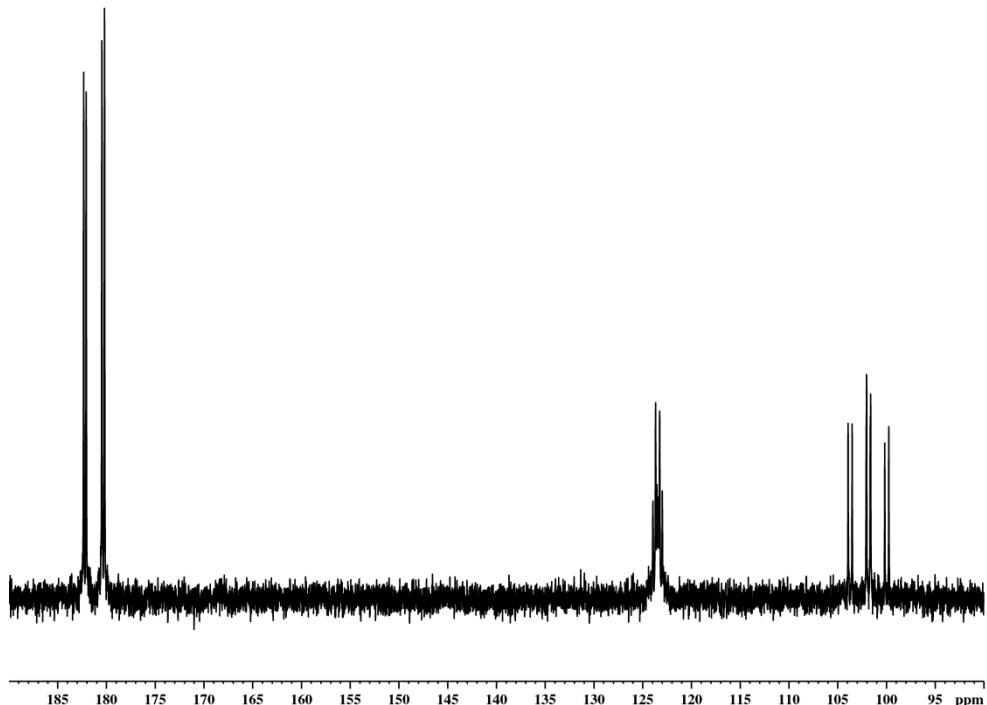
Figure S9.7. ^{31}P{^{1}H} NMR spectrum of **2d** in CD$_2$Cl$_2$ at 298 K.
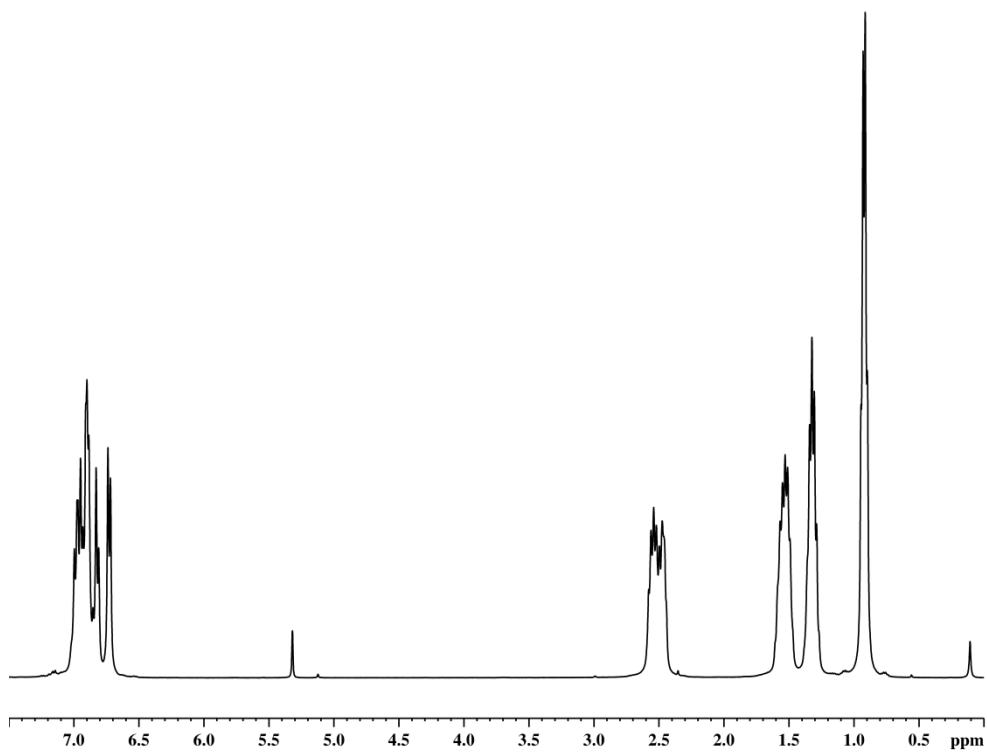
**Figure S9.8.** ^{1}H NMR spectrum of **3** in CD$_2$Cl$_2$ at 298 K.
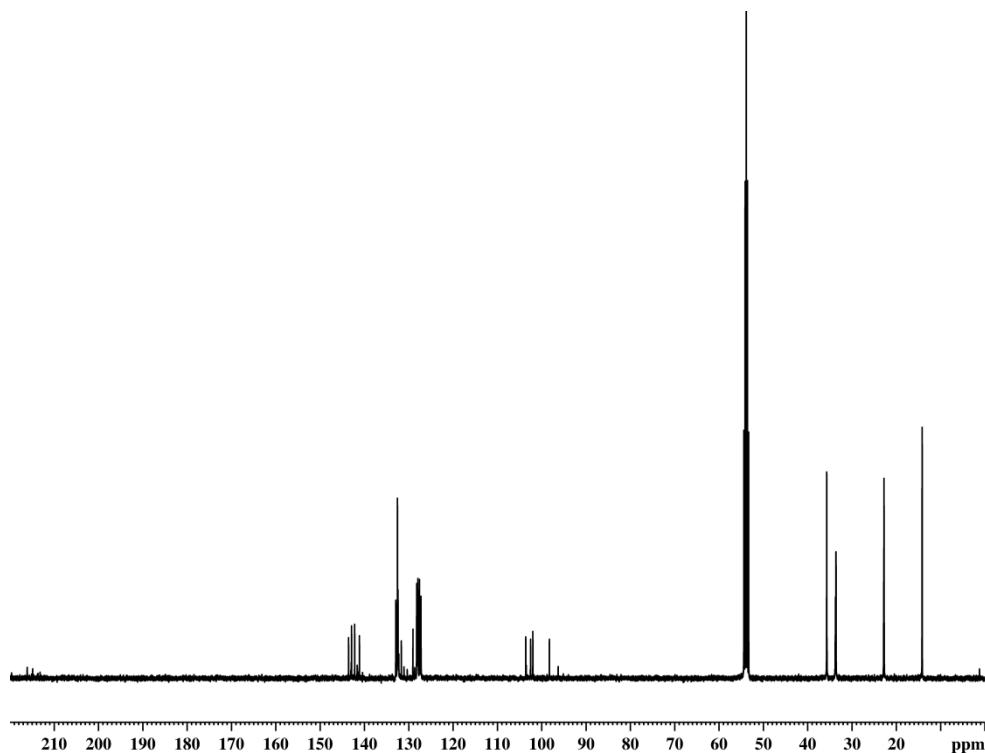
Figure S9.9. ^{13}C{^{1}H} NMR spectrum of **3** in CD$_2$Cl$_2$ at 298 K.

Crystallographic Details:

The crystal structure analyses were performed on an Oxford Diffraction SuperNova diffractometer (**2a-d, 3**). Absorption corrections for **2a** and **2b** are based on multi-scan, for **2c** based on nummerical gaussian integration over a multifaceted crystal model and for **2d** and **3** an analytical absorption correction was carried out.[1] The structures were solved by direct methods of the program SIR-92[2] and refined with the least square method on F^2 employing SHELXL-97[3] with anisotropic displacements for non-H atoms. Hydrogen atoms were located in idealized positions and refined isotropically according to the riding model.

CCDC-997912 (**2a**), CCDC-997913 (**2b**), CCDC-997914 (**2c**), CCDC-997915 (**2d**) and CCDC-997916 (**3**) contain the supplementary crystallographic data for this paper. These data can be obtained free of charge at www.ccdc.cam.ac.uk/conts/retrieving.html (or from the Cambridge Crystallographic Data Centre, 12 Union Road, Cambridge CB2 1EZ, UK; Fax: + 44-1223-336-033; e-mail: deposit@ccdc.cam.ac.uk).

Crystal data for [{Cp^{BIG}Fe(CO)$_2$}$_2$(μ,η$^{1:1}$-P$_4$)]*2(CH$_2$Cl$_2$) (**2a**): C$_{116}$H$_{134}$Cl$_4$Fe$_2$O$_4$P$_4$, M = 1969.61 g/mol, space group $C2/c$ (no.15), a = 16.5044(2) Å, b = 23.0305(2) Å, c = 28.6494(3) Å, $β$ = 104.041(1)°, V = 10564.4(2) Å^3, Z = 4, $μ$ = 4.097 mm^{-1}, F(000) = 4168, T = 123 K, 60294 reflections measured, 10951 unique (R_{int} = 0.0321), R_1 = 0.0400, wR_2 = 0.1090 for I > 2σ(I). CCDC-997912

<u>Crystal data for [{Cp^{BIG}Fe(CO)$_2$}$_2$(μ,η$^{1:1}$-As$_4$)]*2(CH$_2$Cl$_2$)</u> **(2b)**:　C$_{116}$H$_{134}$Cl$_4$Fe$_2$O$_4$As$_4$, M = 2145.41 g/mol, space group $C2/c$ (no.15), a = 16.0862(4) Å, b = 23.1908(5) Å, c = 29.2063(6) Å, $β$ = 103.712(2)°, V = 10584.9(4) Å^3, Z = 4, $μ$ = 4.907 mm^{-1}, $F(000)$ = 4456, T = 123 K, 18697 reflections measured, 10673 unique (R_{int} = 0.0404), R_1 = 0.0851, wR_2 = 0.1630 for I > 2σ(I). CCDC-997913

<u>Crystal data for [{Cp^{BIG}Fe(CO)$_2$}$_2$(μ,η$^{1:1}$-P$_4$S$_3$)]*(CH$_2$Cl$_2$)*0.5(CH$_3$CN)</u> **(2c)**: C$_{232}$H$_{267}$Cl$_4$Fe$_4$NO$_8$P$_8$S$_6$, M = 4002.86 g/mol, space group $P\overline{1}$ (no.2), a = 18.6002(4) Å, b = 19.1311(2) Å, c = 30.2819(5) Å, $α$ = 89.890(1)°, $β$ = 88.546(2)°, $γ$ = 84.899(1)°, V = 10729.5(3) Å^3, Z = 2, $μ$ = 4.128 mm^{-1}, $F(000)$ = 4236, T = 123 K, 84816 reflections measured, 41413 unique (R_{int} = 0.0329), R_1 = 0.0820, wR_2 = 0.1845 for I > 2σ(I). CCDC-997914
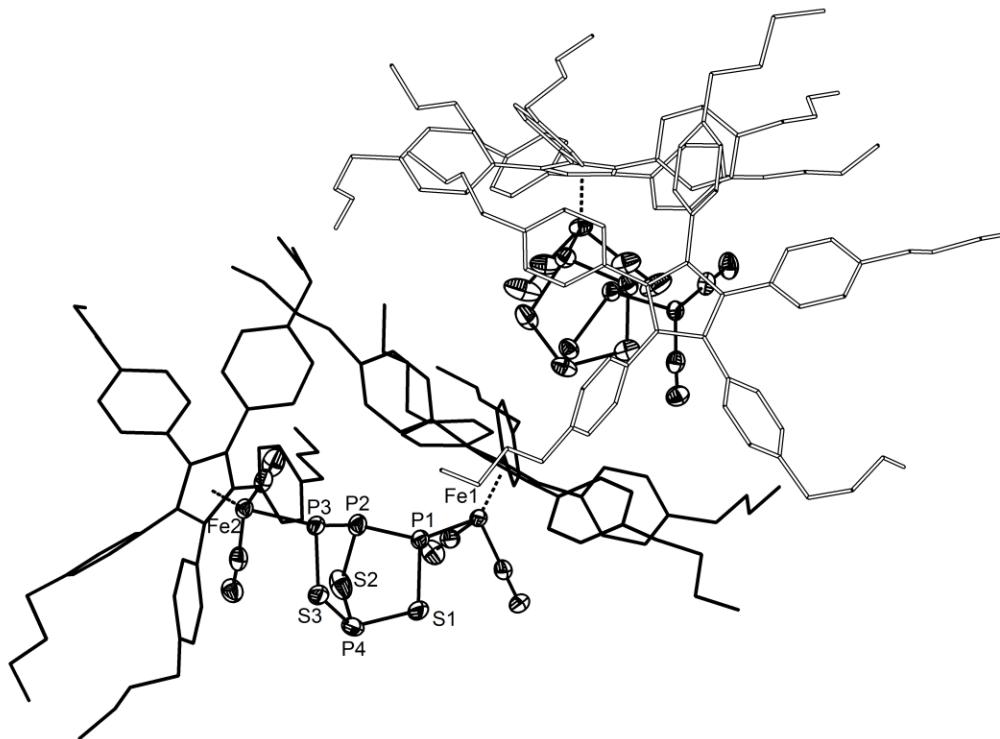

Figure S9.10. Molecular structures of **2c** in the crystal. For clarity reasons, H atoms and solvent molecules are omitted, Cp^{BIG} ligands are drawn in 'wire-or-stick' model and in case of disorder only the main part is shown. Thermal ellipsoids are drawn with 50% probability level.
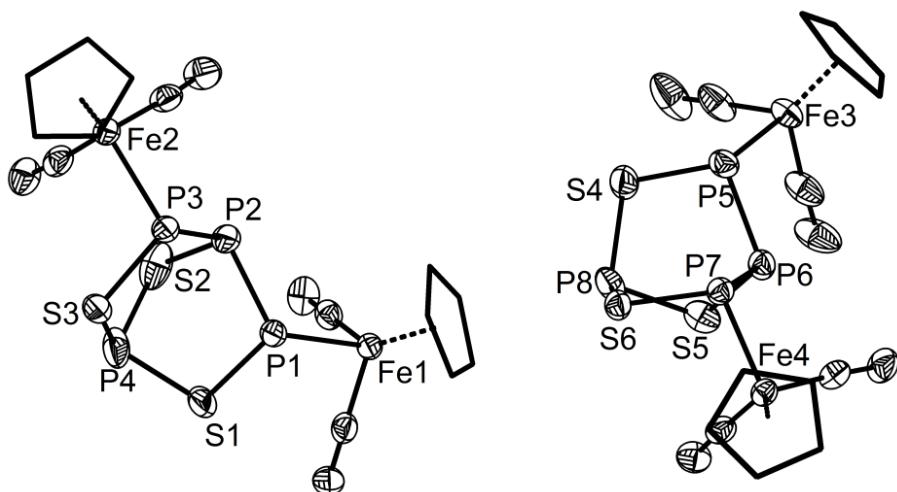
Figure S9.11. Central structures of **2c** in the crystal. For clarity reasons 4-nBuC$_6$H$_4$ groups of Cp^{BIG} lignads are omitted. Thermal ellipsoids are drawn with 50% probability level.

Crystal data for [{Cp^{BIG}Fe(CO)$_2$}$_2$(μ,η$^{1:1}$-P$_4$Se$_3$)] (**2d**): C$_{114}$H$_{130}$Fe$_2$O$_4$P$_4$Se$_3$, M = 2036.65 g/mol, space group $P\bar{1}$ (no.2), a = 13.6368(5) Å, b = 16.2697(5) Å, c = 23.7755(9) Å, a = 77.294(3)°, β = 86.087(3)°, γ = 85.081(3)°, V = 5120.9(3) Å^3, Z = 2, μ = 4.475 mm^{-1}, F(000) = 2120, T = 123 K, 27777 reflections measured, 15685 unique (R_{int} = 0.0893), R_1 = 0.1485, wR_2 = 0.1808 for I > 2σ(I). CCDC-997915
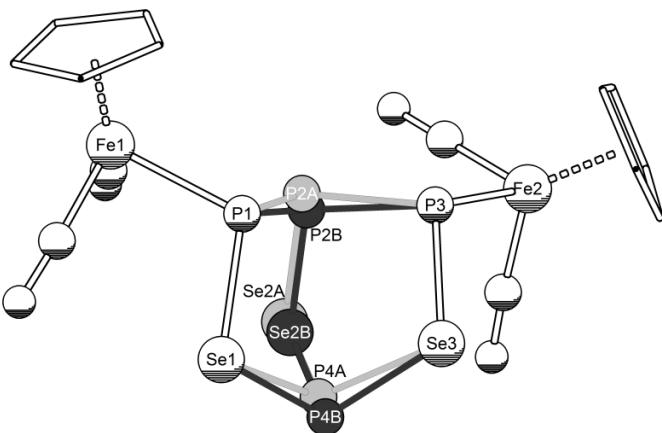

Figure S9.12. Disordered central structure of **2d** in the crystal. Different parts are colored differently. The hatched globes belong to both parts. For clarity reasons 4-nBuC$_6$H$_4$ groups of Cp^{BIG} ligands are omitted.

Crystal data for [{Cp^{BIG}Fe(CO)$_2$}{Cp^{BIG}FeCO}(μ,η$^{1:2}$-CS$_2$)] (**3**): C$_{114}$H$_{130}$Fe$_2$O$_3$S$_2$, M = 1724.02 g/mol, space group $P\bar{1}$ (no.2), a = 12.6885(2) Å, b = 13.6189(3) Å, c = 15.8914(3) Å, a = 103.957(2)°, β = 103.841(2)°, γ = 103.076(2)°, V = 2467.4(1) Å^3, Z = 1, μ = 3.128 mm^{-1}, F(000) = 922, T = 123 K, 22795 reflections measured, 9578 unique (R_{int} = 0.0184), R_1 = 0.0715, wR_2 = 0.1656 for I > 2σ(I). CCDC-997916
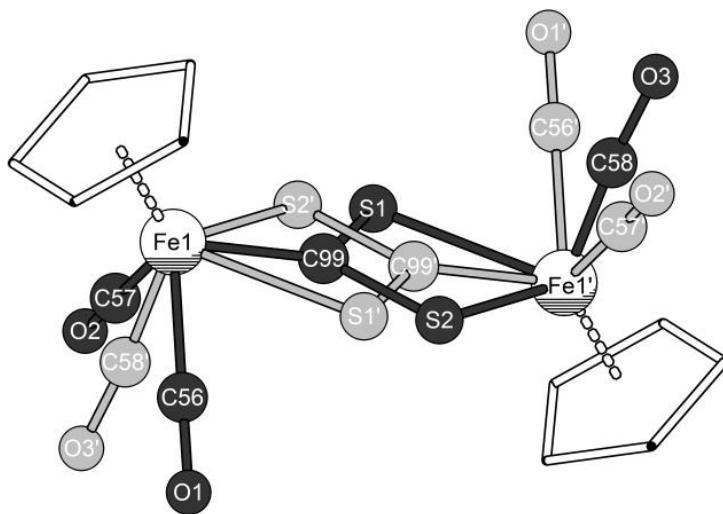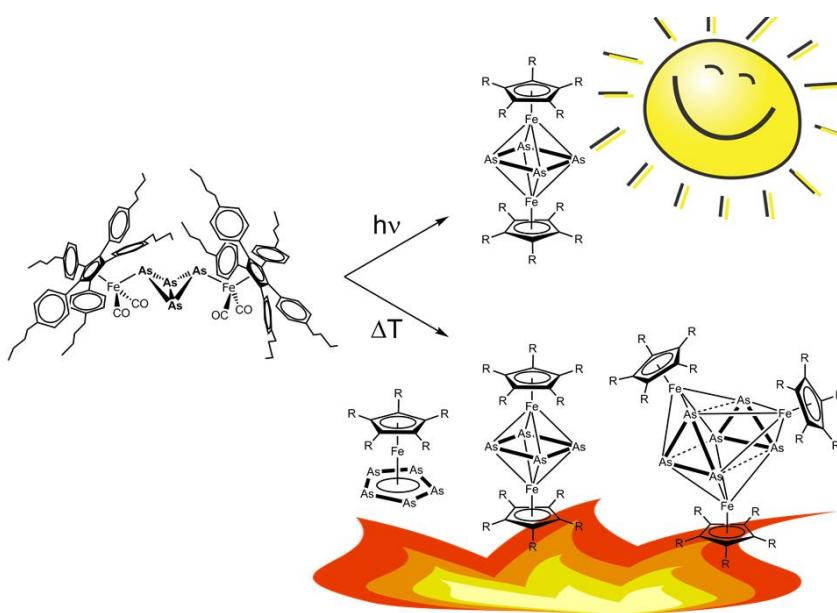
Figure S9.13. Disordered central structure of **2d** in the crystal. Part 1 and 2 are colored differently. The hatched globes belong to both parts. For clarity reasons 4-*n*BuC$_6$H$_4$ groups of Cp^{BIG} lignads are omitted.

References for Supplementary Information:

[1]   R. C. Clark, J. S. Reid, *Acta Cryst.* **1995**, *A51*, 887-897.

[2]   A. Altomare, M. C. Burla, M. Camalli, G.L. Cascarano, C. Giacovazzo, A. Guagliardi, A. G. G. Moliterni, G. Polidori, R. Spagna, *J. Appl. Cryst.* **1999**, *32*, 115-119.

[3]   G. M. Sheldrick, *Acta Cryst.* **2008**, *A64*, 112-122.

Differences in the Reaction Behavior of the Butterfly Complexes [{Cp^{BIG}Fe(CO)$_2$}(μ,η$^{1:1}$-E$_4$)] (E = P, As) – Irradiation and Thermolysis

161

10. Differences in the Reaction Behaviour of the Butterfly Complexes [{Cp^{BIG}Fe(CO)$_2$}$_2$(μ,η$^{1:1}$-E$_4$)] (E = P, As) – Irradiation and Thermolysis

Sebastian Heinl, Alexey Y. Timoshkin, Julian Müller and Manfred Scheer

unpublished results

❖ **All syntheses and characterizations were performed by Sebastian Heinl. The thermolysis reaction of 1b were done with the aid of Julian Müller within the scope of his Bachelor Thesis (2013, Referee: Manfred Scheer) with supervision of Sebastian Heinl**

❖ **Manuscript was written by Sebastian Heinl except DFT calculations (Alexey Y. Timoshkin)**

❖ **Figures were made by Sebastian Heinl**

❖ **DFT calculations were performed by Alexey Y. Timoshkin**

❖ **X-ray structure analyses and refinement were performed by Sebastian Heinl**

10.1   Introduction

Since the first As$_n$ ligand complex was discovered by Dahl et al.[1] in 1969 and the first P$_n$ ligand complex in 1971 by Lindsell and Ginsberg[2] respectively, this class of compounds moved into the focus of research. In the last four decades not only their synthesis was of interest, but also investigations on the coordination behavior and redox properties.[3] Synthetic routes mostly start from the tetrahedral molecules E$_4$ (E = P, As) which are activated and degraded in the presence of metal centers. Even though great efforts were done to shed light in this field of chemistry, the mechanism of the reactions are rather unknown. Scherer and co-workers investigated the reactivity of [{Cp″Fe(CO)$_2$}$_2$(μ,η$^{1:1}$-P$_4$)] (Cp″ = C$_5$H$_3$$tBu_2$) under thermolytic and photolytic conditions.[4] At elevate temperatures, total decarbonylation is observed leading to the formation of [(Cp^{R}Fe)$_2$(μ,η$^{4:4}$-P$_4$)]. However, the irradiation reaction enables the synthesis and characterization of each single decarbonylation product (loss of 1- 4 CO groups). Such reactivity studies was not possible for the As derivatives, since a synthetic route for isostructural As$_4$ butterfly complexes does not exist. Recently we have reported on the high yield synthesis of the two sterically crowded butterfly complexes [{Cp^{BIG}Fe(CO)$_2$}$_2$(μ,η$^{1:1}$-E$_4$)] (**1a**: E = P; **1b**: E = As; Cp^{BIG} = C$_5$(4-nBuC$_6$H$_4$)$_5$).[5] We have also demonstrated, that the reaction of **1a** under thermolytic conditions in toluene results in the formation of [{Cp^{BIG}Fe}$_2$(μ,η$^{4:4}$-P$_4$)] (**2a**) and [Cp^{BIG}Fe(η^5-P$_5$)].[5,6]

Herein we report on the thermolysis reaction of **1b** with an excess of As$_4$ and the photolysis of **1a** and **1b**.

10.2   Results and Discussion

After UV irradiation of **1a** in toluene for 30 min, the IR spectrum of the red solution does not show any CO stretching bands. The ^{31}P{^{1}H} NMR spectrum of the reaction mixture shows signals for the binuclear complex **2a** only (Figure 10.1). Diffusion of CH$_3$CN into a CH$_2$Cl$_2$ solution of the crude product affords crystals from **2a** in 59% yield. However, in one single experiment in a very small yield another brown product could be identified as [{Cp^{BIG}Fe}{Cp^{BIG}Fe(CO)$_2$}(μ,η$^{4:1}$-P$_4$)] (**3**) bearing a $cyclo$-P$_4$ ligand. The Cp″ analogue compound was also obtained by Scherer et al. in higher yields.[4] The ^{31}P{^{1}H} NMR spectrum of **3** in C$_6$D$_6$ shows three coupled signals for an AM$_2$X spin system at 29.9 ppm, 104.5 ppm and 173.6 ppm (^1J(P^{A}P^M) = 306 Hz, ^2J(P^{A}P^X) = 116 Hz, ^1J(P^{M}P^X) = 349 Hz). The IR spectrum in toluene shows two strong vibrational bands at 2024 cm^{-1} and 1984 cm^{-1}.

Differences in the Reaction Behavior of the Butterfly Complexes [{Cp^{BIG}Fe(CO)$_2$}(μ,η$^{1:1}$-E$_4$)] (E = P, As) – Irradiation and Thermolysis

163
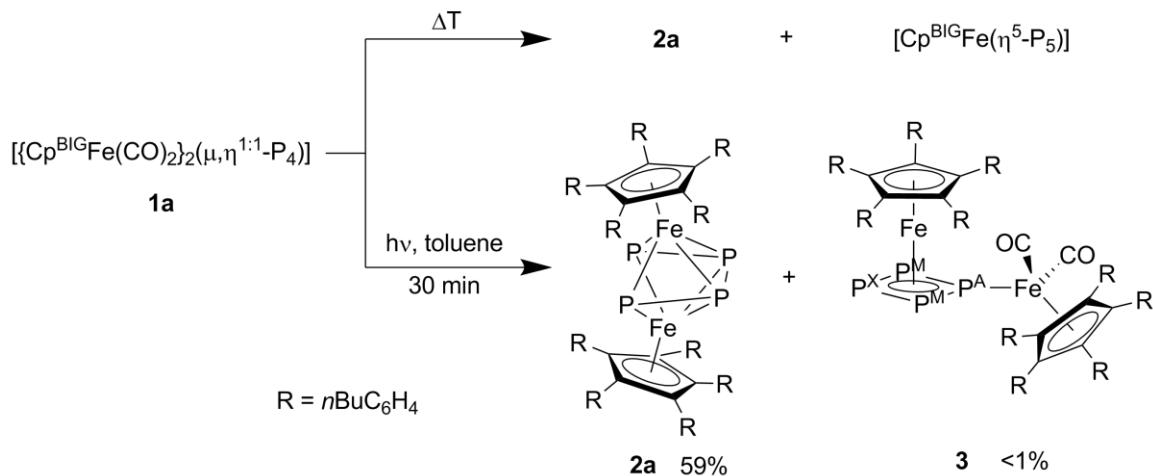
Figure 10.1. Reaction of **1a** under thermolytical conditions (top)[6] and UV irradiation (bottom).

X-Ray structure analysis proved the assumed binuclear structure of complex **3** with a bridging *cyclo*-P$_4$ ligand (Figure 10.2). The whole central core is disordered over two positions over the inversion center near the P1 atom (see supporting information). Compound **3** exhibits the same general tendencies in the structural parameters as the Cp'' derivative (values for the Cp'' substituted compound are given in brackets). However, there are some significant differences. The Cp^{BIG} ligand bound to Fe1 is 12.09(6)° (1.5°) tilted away from co-planarity with the *cyclo*-P$_4$ ligand and the angle P3-P1-Fe1' is with 159.48(4)° (174.1(1)°) much more deflected out of the P$_4$-plane. Due to the presence of an inversion center near the atom P1,
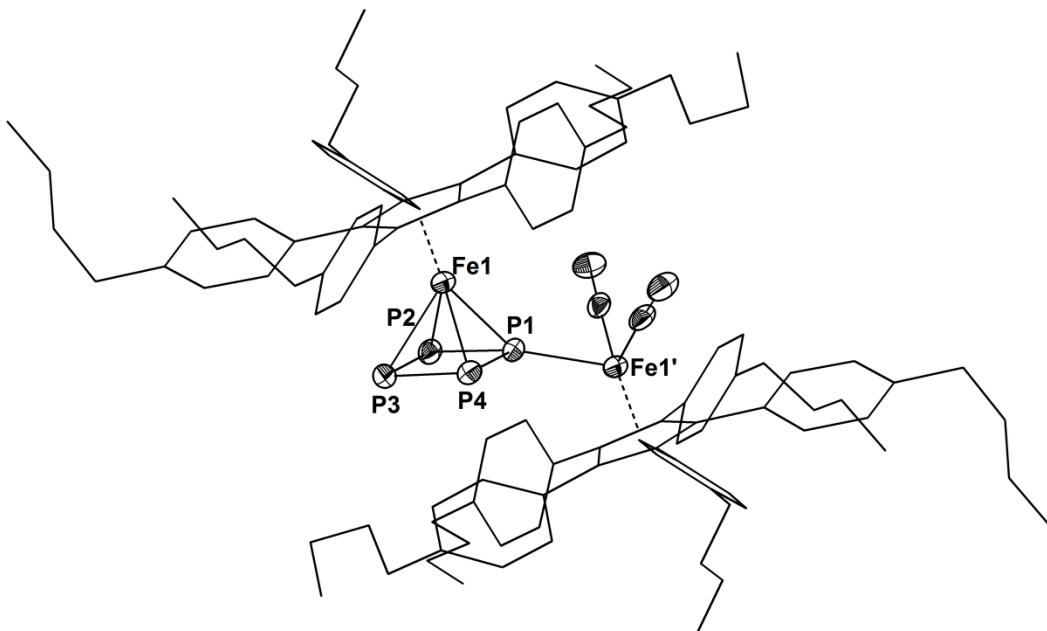
Figure 10.2. Molecular structure of **3** in the crystal with selected labels. Ellipsoids are drawn at 50% probability level. In case of disorder only the main part is shown. For clarity reasons the Cp^{BIG} ligands are drawn in 'wire-or-stick' model. Selected bond lengths [Å] and angles [°]: P1-P2 2.140(2), P2-P3 2.159(1), P3-P4 2.164(2), P1-P4 2.133(2), Fe1-P1 2.1756(8), Fe1-P2 2.344(2), Fe1-P3 2.3678(9), Fe1-P4 2.363(2), Fe1'-P1 2.3251(7), P2-P1-P4 96.03(6), P1-P2-P3 84.66(6), P2-P3-P4 94.60(7), P1-P4-P3 84.70(6), P3-P1-Fe1' 159.48(4), Cp$_{cent}$(Fe1)-Fe1-P$_{4,cent}$ 164.47(2), Cp$_{plane}$(Fe1)-P$_{4,plane}$ 12.09(6).

the Cp^{BIG} ligands are perfectly coplanar to each other (28.6(1)°). The observations in the molecular structure can easily be explained by steric repulsion between the Cp^{BIG} ligand bound to Fe1 and the two CO ligands on the Fe1′ atom.

The co-thermolysis of *in situ* generated butterfly complex **1b** with an excess of As$_4$ in high boiling solvents (*o*-xylene, 1,3-diisopropylbenzene) result in the formation of [{Cp^{BIG}Fe}$_2$(μ,η$^{4:4}$-As$_4$)] (**2b**), [(Cp^{BIG}Fe)$_3$(μ$_3$,η$^{4:4:4}$-As$_6$)] (**4**) and [Cp^{BIG}Fe(η^5-As$_5$)] (**5**) (Figure 10.3). Unfortunately, reaction conditions which guarantee the formation of **5** could not be figured out (the yield of compound **5** varies from 0% to 34%). It is possible to separate **5** from **2b** and **4** by column chromatography. The two clusters **2b** and **4** elute almost simultaneously from the column. However, a small fraction of almost pure **4** can be obtained by fractionating the band (**4** elutes slightly later). The compounds are highly soluble in CH$_2$Cl$_2$, toluene and THF, moderately soluble in hexane and insoluble in CH$_3$CN. The three complexes can be crystallized by diffusion of CH$_3$CN into CH$_2$Cl$_2$ solutions. From mixtures of **2b** and **4**, both compounds crystallize separately at the same time.

The pentaarsaferrocene **5** represents the second structurally characterized derivative of this class of compounds (Figure 10.4).[7] While the average As–As bond length with 2.32 Å is identical with that of the Cp* derivative, the average Fe–As distance of 2.52 Å is elongated compared to the Cp* derivative (2.50 Å in [Cp*Fe(η^5-As$_5$)]). This can be explained by the higher
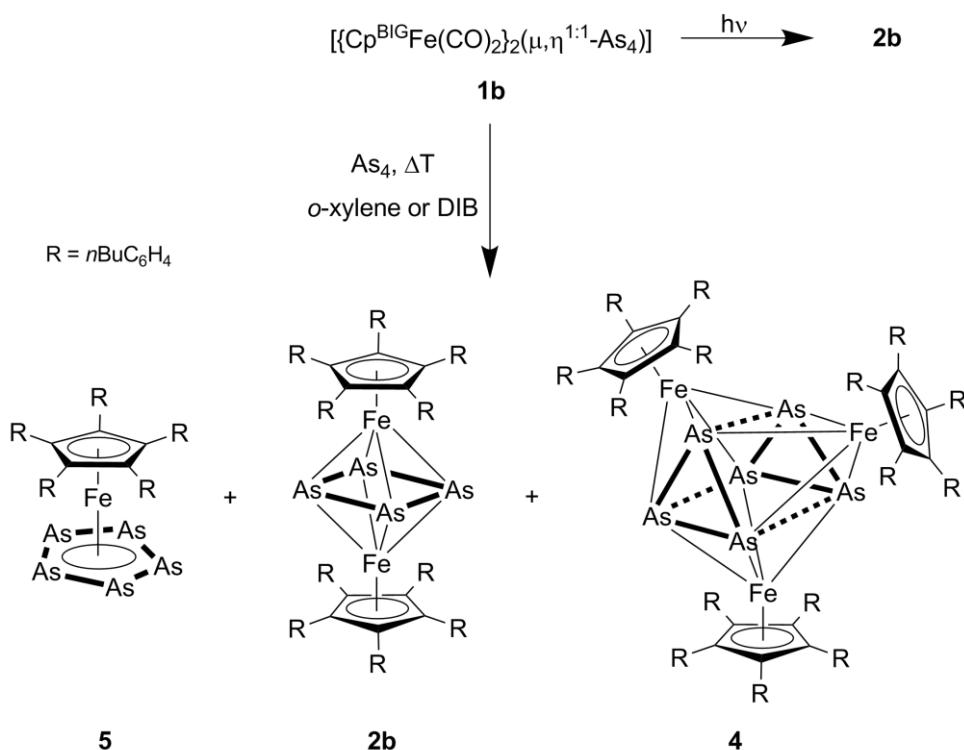
Figure 10.3. Synthesis of [Cp^{BIG}Fe(η^5-As$_5$)] (**5**), [(Cp^{BIG}Fe)$_2$(μ,η$^{4:4}$-As$_4$)] (**2b**) and [(Cp^{BIG}Fe)$_3$(μ$_3$,η$^{4:4:4}$-As$_6$)] (**4**) by co-thermolysis of **1a** with As$_4$.

Differences in the Reaction Behavior of the Butterfly Complexes [{Cp^{BIG}Fe(CO)$_2$}(μ,η$^{1:1}$-E$_4$)] (E = P, As) – Irradiation and Thermolysis

165
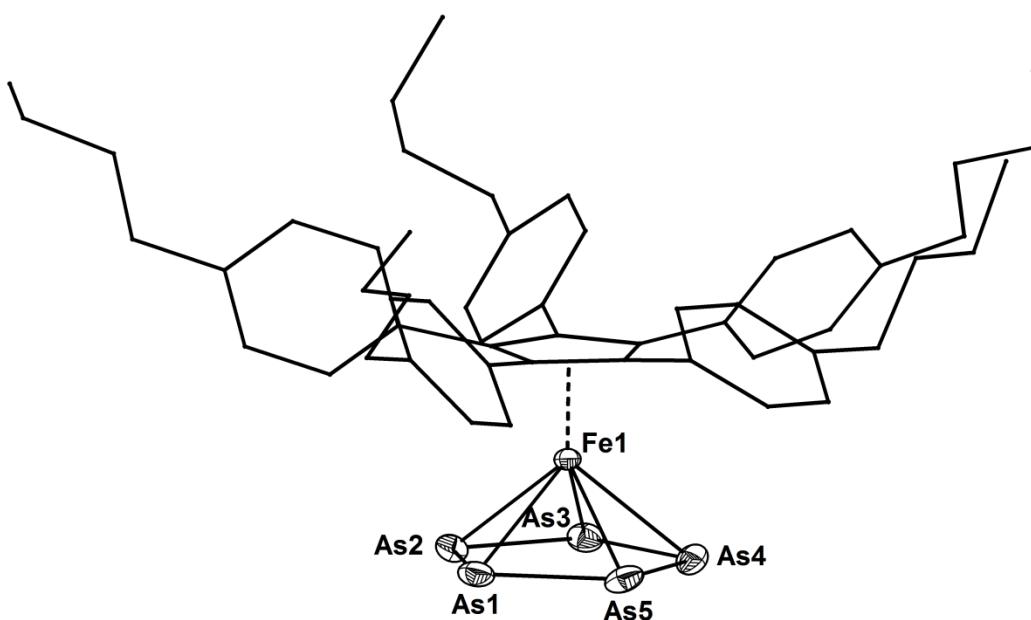
**Figure 10.4.** Molecular structure of **5** in the crystal with selected labels. Ellipsoids are drawn at 50% probability level. For clarity reasons the Cp^{BIG} ligand is drawn in 'wire-or-stick' model. Selected bond lengths [Å] and angles [°]: As1-As2 2.3165(4), As2-As3 2.3210(4), As3-As4 2.3202(5), As4-As5 2.3093(4), As1-As5 2.3177(5), Fe1-As1 2.5245(5), Fe1-As2 2.5293(4), Fe1-As3 2.5131(4), Fe1-As4 2.5419(6), Fe1-As5 2.5110(5), As2-As1-As5 107.94(2), As1-As2-As3 107.7082), As2-As3-As4 108.29(2), As3-As4-As5 107.61(2), As1-As5-As4 108.43(2), Cp$_{plane}$(Fe1)-As$_{5,plane}$ 0.75(7).

sterical demand of the Cp^{BIG} ligand compared to Cp*. The second difference in the molecular structures is the almost ecliptic conformation of the Cp ring and the *cyclo*-As$_5$ ring in complex **5** (17°). This results in a staggered conformation of the phenyl H atoms of the Cp^{BIG} ligand with the pentaarsalyl ligand. The same observations can be made with [Cp^{BIG}Fe(η^5-P$_5$)].[6]

Albeit **2a** and **2b** have the same formula [(Cp^{BIG}Fe)$_2$(μ,η$^{4:4}$-E$_4$)], the structural motif in the crystals is different. While in **2a** the P$_4$ ligand shows a *cisoid* arrangement, complex **2b** bears a *cyclo*-As$_4$ ligand (Figure 10.5). The As–As bond lengths range from 2.3905(8) Å to 2.4562(7) Å (Ø 2.43 Å) and the Fe–As bond lengths from 2.4156(8) Å to 2.5132(8) Å (Ø 2.47 Å). The complex core is well described by a Fe$_2$As$_4$ octahedron, as indicated by the uniform Fe–As and As–As bond lengths as well as the Fe–As–Fe and As–As–As angles (89.10(3)° - 93.62(3)°). The two Cp ligands and the As$_4$ plane are almost co-planar and the Cp^{BIG} ligands are about 24° twisted against each other.

Compounds with substituent-free planar *cyclo*-As$_4$ ligands are very rare. Only three complexes are known so far: the binuclear complexes [L$_2$Cr$_2$As$_4$][8] and [{(C$_5$Me$_4$tBu)Co}$_2$As$_4$]$^{2+}$,[9] and one mononuclear complex [Cp*Nb(CO)$_2$As$_4$].[10] Furthermore, Korber et al. succeeded in the preparation of alkaline metal salts with 'free' *cyclo*-As$_4^{2-}$ units.[11]

Compound **2b** can be described as a 30 VE triple-decker complex or as a *closo* cluster. An equilibrium between the *cisoid*-P$_4$ and the *cyclo*-P$_4$ conformation is found in solution for the
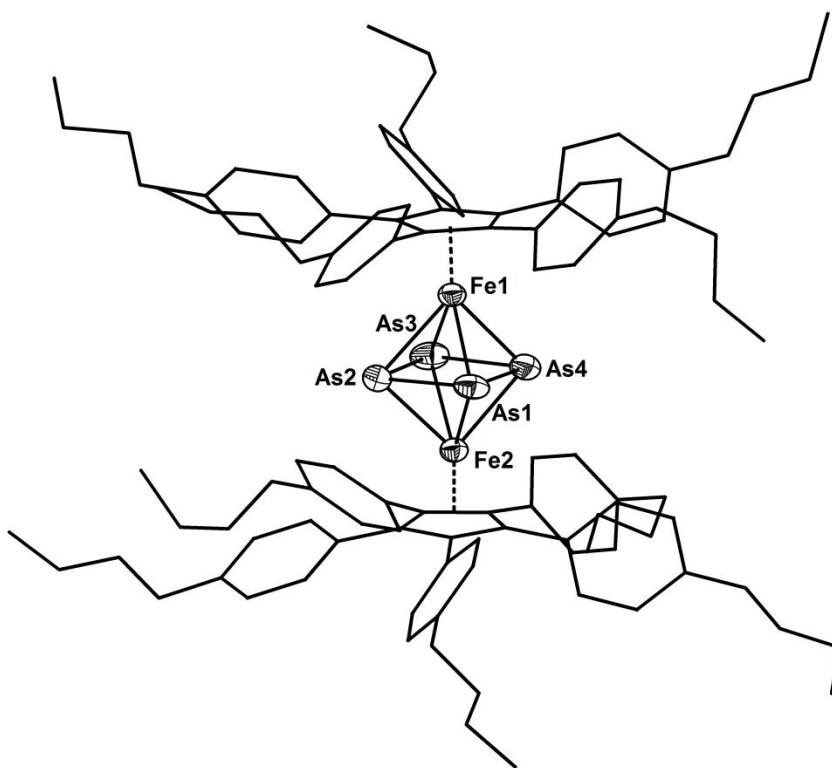
Figure 10.5. Molecular structure of **2b** in the crystal with selected labels. Ellipsoids are drawn at 50% probability level. In case of disorder only the main part is shown. For clarity reasons the Cp^{BIG} ligands are drawn in 'wire-or-stick' model and solvent molecules are omitted. Selected bond lengths [Å] and angles [°]: As1-As2 2.4335(7), As2-As3 2.3905(8), As3-As4 2.4217(8), As1-As4 2.4562(7), Fe1-As1 2.4156(8), Fs1-As2 2.5015(8), Fe1-As3 2.4911(8), Fe1-As4 2.4635(8), Fe2-As1 2.4438(8), Fe2-As2 2.4637(8), Fe2-As3 2.5132(8), Fe2-As4 2.4399(8), Fe1⋯Fe2 3.5431(10), As2-As1-As4 89.10(3), As1-As2-As3 90.59(3), As2-As3-As4 90.93(3), As1-As4-As3 89.32(3), Fe1-As1-Fe2 93.62(3), Fe1-As2-Fe2 91.05(3), Fe1-As3-Fe2 90.15(3), Fe1-As4-Fe2 92.53(3), Cp$_{plane}$(Fe1)-As$_{4,plane}$ 0.6(1), Cp$_{plane}$(Fe2)-As$_{4,plane}$ 2.4(1), Cp$_{plane}$(Fe1)-Cp$_{plane}$(Fe2) 2.5(2).

phosphorus analogues.[4,6] However, in case of **2b** a similar dynamic behavior could not be proven, due to the lack of an appropriate NMR active nuclei.

In order to gain insight into the structural differences between **2a** and **2b**, DFT calculations at B3LYP/def2-SVP level of theory[12] were carried out. Geometries of both *cisoid* and *cyclo* isomers of **2a** and **2b** in singlet states were optimized (Figure 10.6). In both cases the *cyclo* isomer is predicted to be more stable in the gas phase (by 50 and 89 kJ/mol for **2a** and **2b**, respectively).

The calculated *cyclo*-**2a** isomer shows a planar configuration of the P$_4$ ligand. The discrepancy of the arrangement of **2a** in the crystal structure (*cisoid*) with the calculated minimum structure in the gas phase (*cyclo*) might be explained by packing effects. The computed energy difference between gaseous isomers of **2a** (50 kJ mol^{-1}) is not prohibitingly large for establishing an equilibrium between the two forms in solution, taking into account that the more polar *cisoid* isomer may be additionally stabilized by interactions with polar solvent molecules. Based on computational results and the experimentally observed dynamic

Differences in the Reaction Behavior of the Butterfly Complexes [{Cp^{BIG}Fe(CO)$_2$}(μ,$\eta^{1:1}$-E$_4$)] (E = P, As) − Irradiation and Thermolysis

167
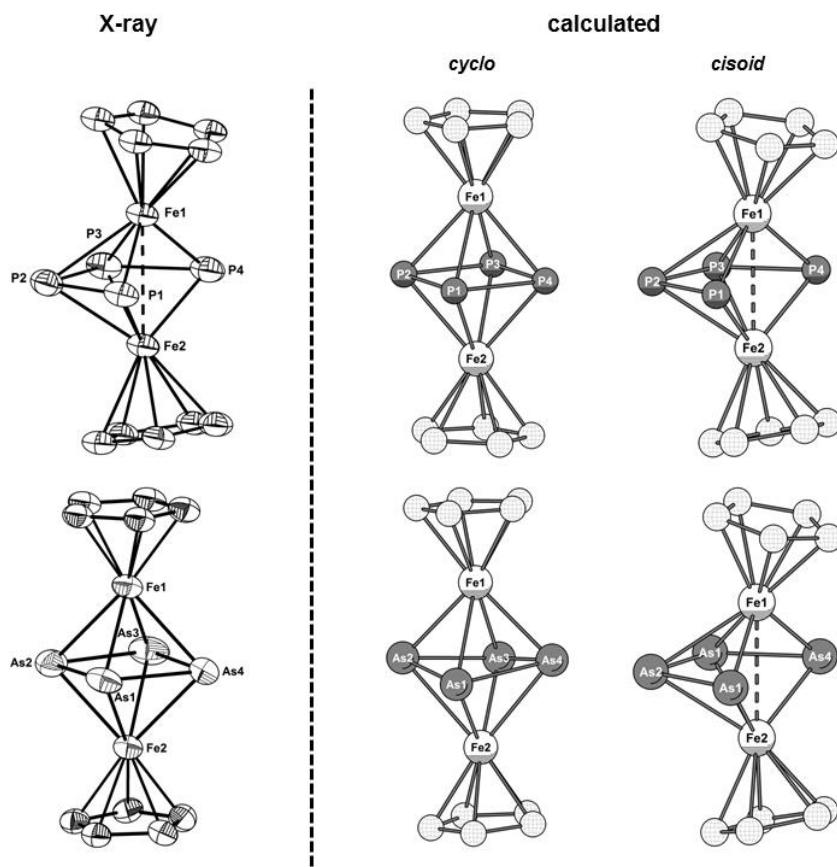
Figure 10.6. Left: Core structure of **2a**[6] and **2b** in the crystal. Right: calculated minima structures of **2a** and **2b** for a trapezoid and cyclic arrangement of the E$_4$ ligand (E = P, As; B3LYP/def2-SVP level of theory). 4-nBuC$_6$H$_4$ groups are omitted for clarity.

equilibrium in solution, it is expected, that crystallization of **2a** from a less polar solvent may afford the more stable *cyclo* isomer in the solid state. However, this could not be confirmed experimentally.

In contrast to the structure of the calculated *cyclo*-**2a** isomer, the As$_4$ moiety in the *cyclo*-**2b** isomer is distorted from planarity by a dihedral angle of about 13°. In case of **2b** the energy difference between the isomers is larger (89 kJ/mol), and the dynamic equilibrium in solution is less likely, although polar solvents are expected to favor the *cisoid* isomer, which could also not be confirmed by experiment so far.

The X-ray structure analysis of **4** exhibits an As$_6$ prism which quadrangular faces are all capped by a {Cp^{BIG}Fe} fragment (Figure 10.7). The As$_6$ prism shows shorter bonds in the triangular faces (Ø 2.57 Å) and higher distances between the two triangles (Ø 2.77 Å). In the literature some other compounds with the general formula [(LM)$_3$As$_6$] and similar structures can be found. Cluster **4** has 21 valence electrons and therefore falls in between the cationic 20 VE *closo* cluster [(Cp*Fe)$_3$As$_6$]$^+$,[13] and the 22 VE *nido*-type clusters [(Cp*Fe)$_2$(Cp*Co)As$_6$][14] and [(Cp^{R}Co)$_3$As$_6$]$^{2+}$,[15] (Cp^R = Cp*, C$_5$Me$_4t$Bu). The structure of **4** is more related to the *nido* clusters than to the *closo* cluster (one shorter Fe–Fe and one longer As–As distance).
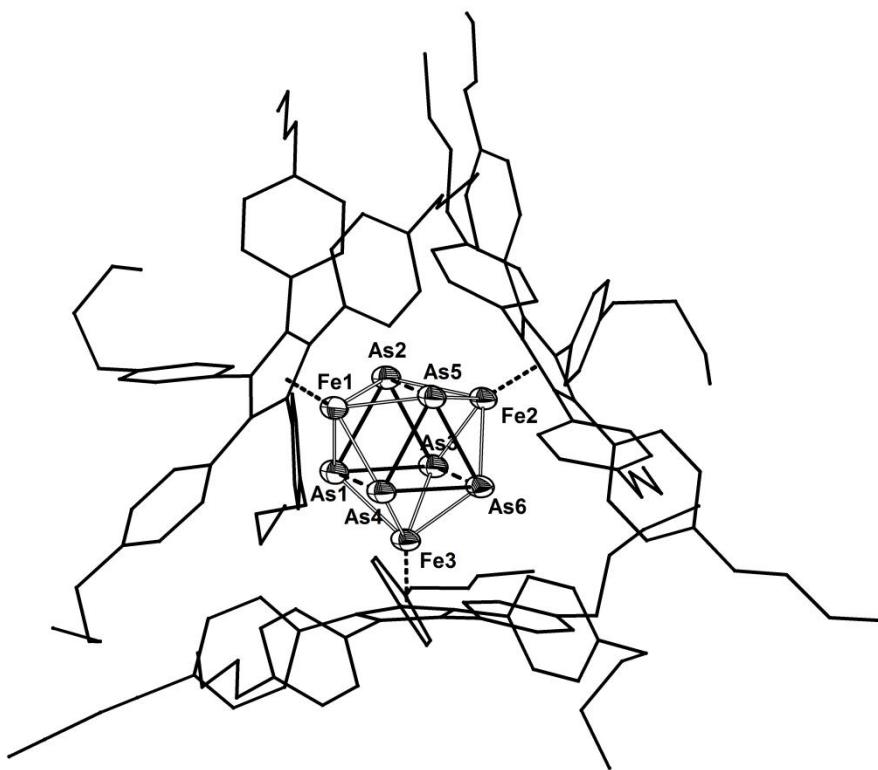
Figure 10.7. Molecular structure of **4** in the crystal with selected labels. Ellipsoids are drawn at 50% probability level. In case of disorder only the main part is shown. For clarity the Cp^{BIG} ligands are drawn in 'wire-or-stick' model and solvent molecules are omitted. Selected bond lengths [Å] and angles [°]: As1-As2 2.5782(7), As2-As3 2.5596(5) As1-As3 2.5761(7), As4-As5 2.5745(7), As5-As6 2.5823(5), As4-As6 2.5662(7), As1···As4 2.7878(10), As2···As5 2.7336(10), As3···As6 2.7813(10), Fe1-As1 2.3959(10), Fe1-As2 2.4231(10), Fe1-As4 2.3911(8), Fe1-As5 2.4001(11), Fe2-As2 2.4101(10), Fe2-As3 2.4099(11), Fe2-As5 2.376(1), Fe2-As6 2.4114(9), Fe3-As1 2.4032, Fe3-As3 2.4084(10), Fe3-As4 2.3943(9), Fe3-As6 2.3993(11) As2-As1-As3 59.55(2), As1-As2-As3 60.18(2), As1-As3-As2 60.27(2), As5-As4-As6 60.31(2), As4-As5-As6 59.69(2), As4-As6-As5 60.01(2), As4-As1-As2 89.57(3), As1-As2-As5 90.33(3), As2-As5-As4 90.86(3), As1-As4-As5 89.22(3), As3-As2-As5 90.18(2), As2-As3-As6 90.28(2), As3-As6-As5 88.67(2), As2-As5-As6 90.87(2), As3-As1-As4 89.57(2), As1-As3-As6 90.22(2), As3-As6-As4 89.92(2), As1-As4-As6 90.28(2).

Accordingly, the formation of [(Cp^{BIG}Fe)$_3$P$_6$] could not be observed in reactions of P$_4$ with [Cp^{BIG}Fe(CO)$_2$]$_2$. This might be explained by the smaller size of P atoms compared to As atoms. The resulting P$_6$ prism would lead to a higher steric repulsion between the Cp^{BIG} ligands due to its smaller size.

The results of the thermolysis of the arsenic butterfly complex **1b** motivated us to investigate its behavior during UV light exposure. Irradiation of orange solutions of **1b** in toluene for 30 min results in a change of color to brown. The reaction mixture does not show CO stretching bands in the IR spectrum. Diffusion of CH$_3$CN into CH$_2$Cl$_2$ solution of the crude product only affords crystals of the completely decarbonylated product **2b** in 54% yield. This observation is consistent with the reaction of **1a** forming **2a**. No fragmentation of the As$_4$ unit is observed (both with respect to formation of smaller As units or reaggregation to larger

Differences in the Reaction Behavior of the Butterfly Complexes [{Cp^{BIG}Fe(CO)$_2$}(μ,η$^{1:1}$-E$_4$)] (E = P, As) – Irradiation and Thermolysis

169

ones). Because of the selective reaction, **2b** can now be obtained in pure form (see above). In addition, column chromatography is not needed for purification.

We have shown the reactivity of **1a** and **1b** under thermolytical and photolytical conditions, respectively. While thermolysis results inter alia in fragmentation and reaggregation of the E$_4$ unit (E = P;[6] E = As: **4**, **5**), with UV irradiation only decarbonylation can be observed (E = P: **2a**,[6] **3**; E = As: **2b**). The obtained arsenic complexes exhibit rare structural motifs. An interesting structural difference between the compounds **2a** and **2b** is found in the solid state. The P$_4$ ligand in **2a** shows a trapezoid arrangement. In contrast, a *cyclo*-As$_4$ ligand is observed in **2b**. DFT calculations in the gas phase however predict a closed E$_4$ cycle in both cases.

10.3 Experimental Part

General Remarks:

All experiments were carried out under an atmosphere of dry argon or nitrogen using glovebox and schlenk techniques. Solvents were purified, dried and degassed prior to use. P$_4$ was available and sublimed before use. [Cp^{BIG}Fe(CO)$_2$]$_2$,[6] [{Cp^{BIG}Fe(CO)$_2$}$_2$(μ,η$^{1:1}$-P$_4$)], [{Cp^{BIG}Fe(CO)$_2$}$_2$(μ,η$^{1:1}$-As$_4$)]$^{[5]}$ and As$_4$ solutions[16] were prepared according to literature procedures. The NMR spectra were measured on a Bruker Avance 300, 400 or 600 spectrometer. FD-MS spectra were measured on a Finnigan MAT 95 mass spectrometer. The elemental analyses were determined on a Vario EL III apparatus. The IR spectra were measured on a VARIAN FTS-800 FT-IR spectrometer.

Synthesis of [(Cp^{BIG}Fe)$_2$(μ,η$^{4:4}$-P$_4$)] (2a) by UV irradiation:

A solution of **1a** (200 mg, 110 μmol) in 50 mL toluene is irradiated for 30 min. The red solution is dried in vacuum. The residue is dissolved in CH$_2$Cl$_2$ and layered with CH$_3$CN. Complex **2a** is obtained as red crystals after complete diffusion (110 mg, 59%). For analytical data of **2b** see reference 6. In one experiment a second very small fraction of crystals of **3** were obtained (yield < 1%).

3: IR (toluene): ν$_{CO}$ [cm^{-1}] = 2024 (s), 1984 (s). FD-MS (toluene): *m/z* (%) = 1744.5 (100%, [M]$^+$), 1688.6 (35%, [M - 2CO]$^+$). ^{31}P{^{1}H} NMR (CD$_2$Cl$_2$): δ [ppm] = 29.9 (td, 1P^X), 104.5 (dd, 2P^M), 173.6 (td, 1P^A); ^1J(P^{A}P^M) = 306 Hz, ^2J(P^{A}P^X) = 116 Hz, ^1J(P^{M}P^X) = 349 Hz.

Synthesis of [(Cp^{BIG}Fe)$_2$(μ,η$^{4:4}$-As$_4$)] (2b), [(Cp^{BIG}Fe)$_3$(μ^3,η$^{4:4:4}$-As$_6$)] (4) and [Cp^{BIG}Fe(η^5-As$_5$)] (5) by thermolysis:

To a freshly prepared solution of As$_4$ (from ~5 g As$_{grey}$) in 250 mL 1,3-diisopropylbenzene (DIB) or o-xylene a solution of [Cp^{BIG}Fe(CO)$_2$]$_2$ (500 mg, 149 μmol) in 10 mL DIB is added. An immediate change of color to orange is observed. The mixture is refluxed for 16 h. The brown solution is dried in vacuum. The residue is separated by column chromatography (20x3 cm, silica, hexane/toluene 5:1). The first band yields brown **5** followed by a broad band of a mixture of **2b** and **4**. Once it was possible to obtain an almost clean sample of **4** by fractionalizing the second band into several pieces. The compounds can be crystallized by diffusion of CH$_3$CN into CH$_2$Cl$_2$ solutions. Yield of **5**: 34 mg (6%). (Best yield from 50 mg [Cp^{BIG}Fe(CO)$_2$]$_2$: 20 mg (34%)). Yield of mixture of **2b** and **4**: 345 mg.

2b: [C$_{110}$H$_{130}$Fe$_2$As$_4$]*1/4CH$_2$Cl$_2$ (solvent molecules were found in the crystal structure) calc.: C, 70.26; H, 7.03. Found: C, 69.59; H, 7.04. FD-MS (toluene): m/z (%) = 1937.6 (30%, [Cp^{BIG}$_2$Fe$_2$As$_5$]$^+$), 1862.8 (100%, [M]$^+$), 1788.1 (20%, [Cp^{BIG}$_2$Fe$_2$As$_3$]$^+$), 725.7 (10%, [Cp^{BIG}]$^+$). ^{1}H NMR (CD$_2$Cl$_2$): δ [ppm] = 0.92 (t, ^{3}J$_{HH}$ = 7.3 Hz, 30H, ^{n}Bu), 1.33 (m, 20H, ^{n}Bu), 1.56 (m, 20H, ^{n}Bu), 2.52 (t, ^{3}J$_{HH}$ = 7.7 Hz, 20H, ^{n}Bu), 6.44 (d, ^{3}J$_{HH}$ = 8.4 Hz, 1H, Ph), 6.53 (d, ^{3}J$_{HH}$ = 7.7 Hz, 1H, Ph), 6.64 (d, ^{3}J$_{HH}$ = 7.7 Hz, 1H, Ph), 6.81 (d, ^{3}J$_{HH}$ = 8.1 Hz, 20H, Ph), 7.22 (d, ^{3}J$_{HH}$ = 8.1 Hz, 20H, Ph). ^{13}C{^{1}H} NMR (CD$_2$Cl$_2$): δ [ppm] = 14.1 (^{n}Bu), 22.7 (^{n}Bu), 33.6 (^{n}Bu), 35.6 (^{n}Bu), 88.8 (Cp), 127.3 (Ph), 132.8 (Ph), 133.8 (Ph), 141.5 (Ph).

Analytical data of **4**: FD-MS (toluene): m/z (%) = 2793.9 (100%, [M]$^+$), 726.9 (10%, [Cp^{BIG}H]$^+$). IR (toluene, cm^{-1}): ν$_{CO}$ 2020 (s), 1980 (s). ^{1}H NMR (C$_6$D$_6$): δ [ppm] = 0.74 (m, 45H, ^{n}Bu), 1.09 (m, 30H, ^{n}Bu), 1.22 (m, 30H, ^{n}Bu), 1.65 (m, 30H, ^{n}Bu), 5.71 (s, 30H, Ph), 7.74 (br-s, ω$_{1/2}$ = 39 Hz, 1H, Ph). ^{13}C{^{1}H} NMR (C$_6$D$_6$): δ [ppm] = 12.7 (^{n}Bu), 21.3 (^{n}Bu), 30.2 (^{n}Bu), 35.5 (^{n}Bu), 120.7 (Ph), 129.2 (Ph), 133.4 (Ph), , 143.0 (Ph). (Cp signal is not observed)

5: [C$_{55}$H$_{65}$FeAs$_5$] calc.: C, 57.62; H, 4.84. Found: C, 56.89; H, 5.58. FD-MS (toluene): m/z (%) = 1156.3 (100%, [M]$^+$); different settings: 726.7 (20%, [Cp^{BIG}H]$^+$), 299.9 (100%, [As$_4$]$^+$). ^{1}H NMR (CD$_2$Cl$_2$): δ [ppm] = 0.85 (m-br, 15H, ^{n}Bu), 1.21 (m-br, 10H, ^{n}Bu), 1.42 (m-br, 10H, ^{n}Bu), 2.35 (m-br, 10H, ^{n}Bu), 6.81 (d, ^{3}J$_{HH}$ = 8.3 Hz, 10H, Ph), 7.40 (s-br, 10H, Ph). ^{13}C{^{1}H} NMR (CD$_2$Cl$_2$): δ [ppm] = 14.1 (^{n}Bu), 22.6 (^{n}Bu), 33.1 (^{n}Bu), 35.5 (^{n}Bu), 89.8 (Cp), 127.4 (Ph), 130.5 (Ph), 134.7 (Ph), 142.2 (Ph).

Synthesis of [(Cp^{BIG}Fe)$_2$(μ,η$^{4:4}$-As$_4$)] (2b) by UV irradiation:

A solution of **1b** (210 mg, 110 μmol) in 50 mL toluene is irradiated for 30 min. The brown solution is dried in vacuum. The residue is dissolved in CH$_2$Cl$_2$ and CH$_3$CN is layered above. Complex **2b** is obtained as brown crystals after complete diffusion (110 mg, 54%).

Differences in the Reaction Behavior of the Butterfly Complexes [{Cp^{BIG}Fe(CO)$_2$}(μ,$\eta^{1:1}$-E$_4$)] (E = P, As) – Irradiation and Thermolysis

171

10.4 References

[1] a) A. S. Foust, M. S. Foster, L. F. Dahl, J. Am. Chem. Soc. 1969, 91, 5631-5633. b) A. S. Foust, M. S. Foster, L. F. Dahl, J. Am. Chem. Soc. 1969, 91, 5633-5635.

[2] A. P. Ginsberg, W. E. Lindsell, J. Amer. Chem. Soc. 1971, 93, 2082-2084.

[3] Some article reviewing this field of chemistry: a) B. M. Cossairt, N. A. Piro, C. C. Cummins, Chem. Rev., 2010, 110, 4164-4177; b) M. Caporali, L. Gonsalvi, A. Rossin, M. Peruzzini, Chem. Rev., 2010, 110, 4178-4235. a) M. Scheer, G. Balázs, A. Seitz, Chem. Rev., 2010, 110, 4236-4256. b) N. A. Giffin, J. D. Masuda, Coord. Chem. Rev., 2011, 255, 1342-1359.

[4] a) O. J. Scherer, G. Schwarz, G. Wolmershaeuser, Z. Anorg. Allg. Chem. 1996, 622, 951-957.

[5] See chapter 9

[6] S. Heinl, G. Balázs, M. Scheer, *Phosphorus, Sulfur Silicon Relat. Elem.* **2014**, DOI: 10.1080/10426507.2014.903489.

[7] O. J. Scherer, C. Blath, G. Wolmershäuser, *J. Organomet. Chem.* **1990**, *387*, C21-C24.

[8] L = (2,6-diisopropylphenyl)-[6-(2,6-dimethylphenyl)-pyridin-2-yl]-amine; C. Schwarzmaier, A. Noor, G. Glatz, M. Zabel, A. Y. Timoshkin, B. M. Cossairt, C. C. Cummins, R. Kempe, M. Scheer, *Angew. Chem., Int. Ed.* **2011**, *50*, 7283-7286.

[9] C. von Hänisch, D. Fenske, F. Weigend, R. Ahlrichs, R. Ahlrichs, F. Weigend, *Chem. Eur. J.* **1997**, *3*, 1494-1498.

[10] O. J. Scherer, J. Vondung, G. Wolmershäuser, *J. Organomet. Chem.* **1989**, *376*, C35-C38.

[11] a) F. Kraus, T. Hanauer, N. Korber, *Inorg. Chem.* **2005**, *45*, 1117-1123. b) T. Hanauer, F. Kraus, M. Reil, N. Korber, *Monatshefte für Chemie / Chemical Monthly* **2006**, *137*, 147-156.

[12] see SI for the details on computations.

[13] C. v. Hänisch, D. Fenske, *Z. Anorg. Allg. Chem.* **1998**, *624*, 367-369.

[14] G. Friedrich, O. J. Scherer, G. Wolmershäuser, *Z. Anorg. Allg. Chem.* **1996**, *622*, 1478-1486.

[15] C. von Hänisch, D. Fenske, F. Weigend, R. Ahlrichs, *Chem. Eur. J.* **1997**, *3*, 1494-1498.

[16] O. J. Scherer, H. Sitzmann, G. Wolmershäuser, *J. Organomet. Chem.*, 1986, **309**, 77-86.

10.5 Supplementary Information
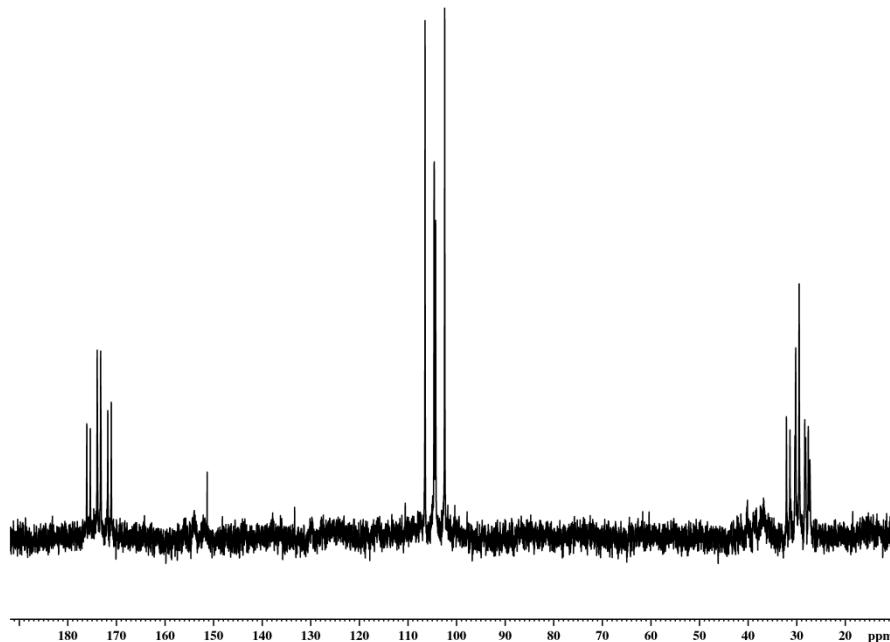
Figure S10.1. ^{31}P{^{1}H} NMR of [{Cp^{BIG}Fe}{Cp^{BIG}Fe(CO)$_2$}(μ,η$^{4:1}$-P$_4$)] (**3**) in C$_6$D$_6$ at 298 K.

Crystallographic Details:

The crystal structure analyses were performed either on an Oxford Diffraction Gemini R Ultra CCD diffractometer (**3**, **4**) or an Oxford Diffraction SuperNova diffractometer (**2b**, **5**). For all compounds an analytical absorption correction was carried out.[1] The structures were solved by direct methods either of the program SIR-92[2] or SUPERFLIP[3] and refined with the least square method on F^2 employing SHELXL-97[4] with anisotropic displacements for non-H atoms. Hydrogen atoms were located in idealized positions and refined isotropically according to the riding model.

Differences in the Reaction Behavior of the Butterfly Complexes [{Cp^{BIG}Fe(CO)$_2$}(μ,$\eta^{1:1}$-E$_4$)] (E = P, As) – Irradiation and Thermolysis

173

	Crystal Data for **2b***1/4CH$_2$Cl$_2$	Crystal Data for **3**
Empirical Formula	C$_{441}$H$_{522}$As$_{16}$Cl$_2$Fe$_8$	C$_{112}$H$_{130}$Fe$_2$O$_2$P$_4$
Formula Weight	7539.03	1743.74
Temperature [K]	123.0(1)	123.0(3)
Crystal System	orthorhombic	triclinic
Space Group	*Pbca*	*P$\bar{1}$*
a [Å]	26.8280(4)	12.4226(3)
b [Å]	24.5759(2)	13.5015(2)
c [Å]	28.7313(3)	16.1699(3)
α [°]	90	106.698(2)
β [°]	90	103.359(2)
γ [°]	90	101.267(2)
Volume [Å^3]	18943.2(4)	2425.67(10)
Z	2	1
ρ_{calc} [mg/mm^3]	1.322	1.194
μ [mm^{-1}]	4.488	3.392
F(000)	7876.0	930.0
Crystal Size [mm^3]	0.4514 × 0.2874 × 0.2159	0.3415 × 0.2184 × 0.1325
Radiation	Cu-K$_\alpha$ (λ = 1.54178)	Cu-K$_\alpha$ (λ = 1.54178)
2Θ Range	5.76 to 147.56°	7.12 to 133.28°
Index Ranges	-32 ≤ h ≤ 26	-14 ≤ h ≤ 14
	-30 ≤ k ≤ 30	-15 ≤ k ≤ 15
	-35 ≤ l ≤ 34	-16 ≤ l ≤ 19
Reflections Collected	134941	19295
Independent Reflections	18605	8313
	[R_{int} = 0.0371, R_{sigma} = 0.0216]	[R_{int} = 0.0185, R_{sigma} = 0.0270]
Data/Restraints/Parameters	18605/224/1180	8313/36/667
Goodness-of-Fit on *F^2*	1.054	1.072
Final *R* Indexes [I > 2σ(I)]	R_1 = 0.0625, wR_2 = 0.1827	R_1 = 0.0332, wR_2 = 0.0907
Final *R* Indexes [All Data]	R_1 = 0.0783, wR_2 = 0.1912	R_1 = 0.0366, wR_2 = 0.0920
Largest Diff. Peak/Hole [e·Å^{-3}]	1.10/-0.80	0.43/-0.23
Flack Parameter	-	-

	Crystal Data for **4***1/2CH$_3$CN	Crystal Data for **5**
Empirical Formula	C$_{332}$H$_{393}$As$_{12}$Fe$_6$N	C$_{55}$H$_{65}$As$_5$Fe
Formula Weight	5631.63	1156.52
Temperature [K]	122.9(5)	123.00(10)
Crystal System	triclinic	triclinic
Space Group	$P\bar{1}$	$P\bar{1}$
a [Å]	17.9595(3)	13.4626(4)
b [Å]	20.6559(4)	13.7448(3)
c [Å]	23.1766(3)	16.0091(4)
α [°]	98.922(1)	92.777(2)
β [°]	106.183(1)	114.468(3)
γ [°]	114.391(2)	107.131(2)
Volume [Å^3]	7152.4(3)	2526.71(14)
Z	1	2
ρ_{calc} [mg/mm^3]	1.308	1.520
μ [mm^{-1}]	4.331	6.288
F(000)	2944.0	1172.0
Crystal Size [mm^3]	0.4236 × 0.1792 × 0.0551	0.5106 × 0.3445 × 0.1791
Radiation	Cu-K$_\alpha$ (λ = 1.54178)	Cu-K$_\alpha$ (λ = 1.54178)
2Θ Range	5.84 to 133.3°	6.86 to 141.8°
Index Ranges	-20 ≤ h ≤ 21	-15 ≤ h ≤ 14
	-24 ≤ k ≤ 24	-16 ≤ k ≤ 16
	-27 ≤ l ≤ 27	-19 ≤ l ≤ 19
Reflections Collected	63536	34862
Independent Reflections	24577	9516
	[R_{int} = 0.0334, R_{sigma} = 0.0384]	[R_{int} = 0.0259, R_{sigma} = 0.0156]
Data/Restraints/Parameters	24577/331/1747	9516/0/550
Goodness-of-Fit on F^2	1.000	1.078
Final R Indexes [I > 2σ(I)]	R_1 = 0.0648, wR_2 = 0.1927	R_1 = 0.0292, wR_2 = 0.0786
Final R Indexes [All Data]	R_1 = 0.0776, wR_2 = 0.1995	R_1 = 0.0294, wR_2 = 0.0788
Largest Diff. Peak/Hole [e·Å^{-3}]	1.86/-0.78	1.03/-0.61
Flack Parameter	-	-
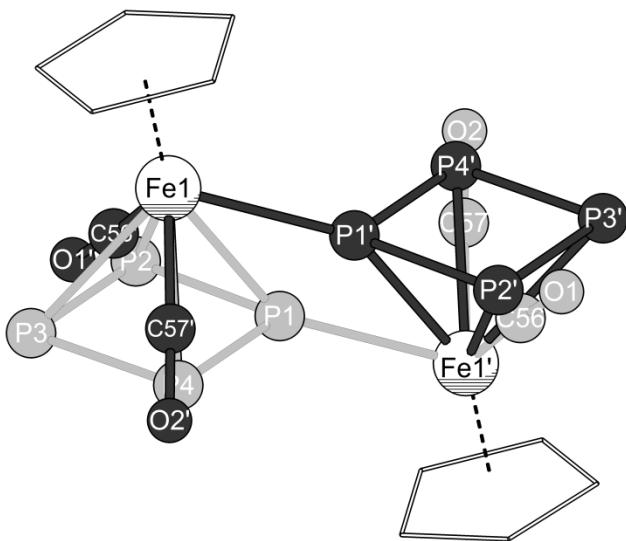
Figure S10.2. Disordered central structure of **3** in the crystal. Different parts are colored differently.

Details on DFT calculations

The DFT calculations have been performed by using the standard Gaussian 03 program suite.[5] B3LYP functional [6] has been used together with all electron def2-SVP [7] basis set. Full geometry optimization has been performed both for **2a** and **2b** (*cyclo* and *cisoid* isomers). Due to the large size of the studied molecules, vibrational analysis could not be performed. Both for **2a** and **2b** *cyclo* isomer is predicted to be more stable in the gas phase than *cisoid* isomer. The energy difference in case of the phosphorus analogue is by about 40 kJ mol^{-1} smaller than in the arsenic case (50 vs. 89 kJ mol^{-1}).

Table S10.1. Relative energies E$_{rel}$ [kJ mol^{-1}] of **2a** and **2b** in different conformations in the gas phase (B3LYP/def2-SVP level of theory).

Compound	E$_{rel}$	Compound	E$_{rel}$
2a (cyclo)	0	**2b** (cyclo)	0
2a (cisoid)	49.6	**2b** (cisoid)	89.4

176

Differences in the Reaction Behavior of the Butterfly Complexes [{Cp^BIG Fe(CO)₂}(μ,η^1:1-E₄)] (E = P, As) – Irradiation and Thermolysis

Table S10.2. Optimized geometries (xyz coordinates in Å) for studied compounds at the B3LYP/def2-SVP level of theory.

2a (*cisoid*)

Atom	x	y	z	Atom	x	y	z
Fe	-0.273698	-0.145189	1.312305	H	-4.96049	-2.107453	-3.465228
P	0.988469	1.520067	0.424853	C	-4.549771	-3.531574	-5.779502
P	-2.371122	0.372003	0.165207	H	-6.647993	-3.522229	4.847298
P	-0.987257	2.128039	0.758394	C	-5.95864	-5.514138	4.348442
C	-2.36527	-2.030827	3.111182	H	-6.827359	-3.940444	3.140058
C	-1.032786	-1.409577	2.872169	C	-7.27	-6.239164	4.664722
C	-0.594274	-0.152766	3.418087	H	-5.270715	-5.601466	5.208954
C	0.1685	-3.442976	1.735935	H	-5.450273	-6.0183	3.506691
C	-1.409323	0.745636	4.283012	H	-7.775188	-5.726727	5.503922
C	0.818155	-0.016306	3.151223	C	-7.081192	-7.7175	5.007949
C	1.70574	1.024999	3.74077	H	-7.954621	-6.144602	3.801994
C	1.249802	-1.187247	2.418621	H	-8.04248	-8.207808	5.230444
C	2.667634	-1.56729	2.159183	H	-6.431111	-7.844359	5.889972
C	0.108511	-2.046232	2.245608	H	-6.613111	-8.266303	4.173496
Fe	-0.41601	0.830547	-1.23592	H	-4.536848	3.782351	6.411578
C	-2.698611	2.293131	-3.12463	H	-3.145336	3.928577	7.489057
C	-1.343288	1.701776	-2.945477	C	-4.544149	2.39015	8.075641
C	-0.966463	0.340785	-3.248012	H	-4.985565	3.10206	8.796846
C	-0.066453	3.916401	-2.470581	H	-3.809407	1.79553	8.648715
C	-1.870356	-0.687201	-3.835502	C	-5.644783	1.464948	7.548514
C	0.469159	0.232495	-3.102719	H	-6.380378	2.065337	6.982086
C	1.301486	-0.919001	-3.553761	C	-6.362253	0.689933	8.654911
C	0.974438	1.524613	-2.721487	H	-5.213498	0.754886	6.821692
C	2.416233	1.88969	-2.676048	H	-6.838016	1.370462	9.381422
C	-0.147186	2.437831	-2.633019	H	-5.659773	0.050768	9.216159
C	-4.848264	-3.312405	3.69171	H	-7.150533	0.03747	8.246231
C	-2.876338	-2.075734	4.422754	H	3.709578	4.842741	5.978823
C	-3.120842	-2.647663	2.099096	C	5.40266	4.471302	4.680021
C	-4.33563	-3.271239	2.386336	H	4.775346	3.548276	6.536791
C	-4.090367	-2.70389	4.703915	H	4.930209	4.892853	3.774472
H	-2.3126	-1.618943	5.237388	H	5.993952	3.604871	4.332565
H	-2.760562	-2.63773	1.070292	C	6.336228	5.512567	5.304596
H	-4.9012	-3.731663	1.570671	H	5.738139	6.374573	5.652837
H	-4.457058	-2.71777	5.734822	C	7.428654	5.999865	4.35169
C	-6.144842	-4.025315	4.003383	H	6.801202	5.085889	6.212274
C	-2.971498	2.357596	6.041336	H	6.996403	6.467537	3.451203
C	-2.65579	1.255345	3.885214	H	8.066797	5.165942	4.013907
C	-0.960306	1.054143	5.580939	H	8.082662	6.745185	4.832063
C	-1.726611	1.843266	6.438938	H	7.202282	-3.184621	2.711989
C	-3.416774	2.04624	4.748223	H	7.492578	-1.743622	1.733238
H	-3.036209	1.034595	2.887663	C	7.184898	-3.550483	0.579753
H	0.001659	0.668937	5.924232	H	6.565746	-4.464108	0.636105
H	-1.343839	2.068911	7.43902	C	8.662683	-3.93763	0.468481
H	-4.378795	2.435276	4.402514	H	6.865998	-3.029257	-0.340879
C	-3.802199	3.196087	6.989637	H	8.974548	-4.447625	1.398375
C	3.382967	2.950827	5.012204	H	9.275138	-3.018998	0.413052
C	1.405196	2.398125	3.691872	C	8.972878	-4.831453	-0.732708
C	2.853279	0.635095	4.456129	H	8.406263	-5.776761	-0.68586
C	3.6719	1.579541	5.077416	H	10.043205	-5.088537	-0.780698
C	2.229931	3.336952	4.311784	H	8.70678	-4.33648	-1.68143
H	0.513015	2.740261	3.167944	H	-0.338459	-8.174211	0.798972
H	3.104276	-0.423031	4.539961	C	1.822613	-8.262603	0.902538
H	4.553358	1.239509	5.629415	H	0.475892	-7.639875	-0.674307
H	1.96637	4.397134	4.251154	H	1.876226	-8.207404	2.00493
C	4.302044	3.976653	5.636163	C	2.686138	-7.681424	0.531376
C	5.421706	-2.276996	1.92768	C	1.954116	-9.721189	0.454577
C	3.581616	-0.727768	1.501965	H	1.086013	-10.29481	0.827781
C	3.159837	-2.772953	2.695261	C	3.247846	-10.38921	0.922523
C	4.506989	-3.11748	2.581188	H	1.891254	-9.769265	-0.648056
C	4.927939	-1.079932	1.388156	H	3.322452	-10.39205	2.022995
H	3.24161	0.223181	1.090552	H	4.134846	-9.860448	0.534862
H	2.481649	-3.441277	3.228539	H	3.309781	-11.43548	0.582704
H	4.85703	-4.054975	3.023992	C	7.044433	3.861859	-1.600627
H	5.61461	-0.394313	0.882712	H	6.926313	3.366557	-3.705817
C	6.878905	-2.658931	1.796466	H	7.268802	1.985015	-2.65897
C	0.382416	-6.151873	0.872861	H	6.767355	3.40365	-0.634108

Differences in the Reaction Behavior of the Butterfly Complexes [{Cp^{BIG}Fe(CO)$_2$}(μ,η$^{1:1}$-E$_4$)] (E = P, As) – Irradiation and Thermolysis

177

C	0.829231	-3.775395	0.540366	H	6.434553	4.779765	-1.681127
C	-0.372456	-4.494419	2.49707	C	8.530442	4.231935	-1.586956
C	-0.266939	-5.820061	2.070959	C	8.908901	5.190931	-0.457253
C	0.931849	-5.101254	0.120826	H	8.80204	4.68147	-2.559703
H	1.268441	-2.985519	-0.069893	H	9.133771	3.309092	-1.50615
H	-0.877914	-4.2764	3.438962	H	8.680677	4.756924	0.530726
H	-0.704599	-6.61339	2.684372	H	8.352533	6.140175	-0.534321
H	1.448008	-5.323021	-0.818023	H	9.983597	5.433327	-0.474055
C	0.521471	-7.590395	0.427647	H	3.054256	-5.175066	-5.079075
C	-5.23481	3.507411	-3.587348	C	5.006676	-4.381873	-4.576406
C	-3.318097	3.078093	-2.137662	H	3.730751	-4.092056	-6.299112
C	-3.367827	2.135904	-4.352159	H	4.895911	-4.520458	-3.485802
C	-4.610047	2.731997	-4.575974	H	5.564533	-3.436428	-4.702885
C	-4.560912	3.669138	-2.36692	C	5.819927	-5.539279	-5.163933
H	-2.820299	3.231042	-1.179829	H	5.258732	-6.482124	-5.029504
H	-2.905912	1.547245	-5.146945	C	7.213103	-5.681427	-4.549754
H	-5.101459	2.594848	-5.544027	H	5.910975	-5.400076	-6.25684
H	-5.015179	4.274845	-1.577088	H	7.157145	-5.857042	-3.462622
C	-6.60148	4.113853	-3.813124	H	7.813736	-4.769213	-4.704033
C	0.149798	6.758304	-2.327796	H	7.767901	-6.523084	-4.994484
C	0.667097	4.540551	-1.446848	C	-5.466338	-2.85289	-6.816494
C	-0.680881	4.745943	-3.428474	H	-5.164229	-4.041292	-5.019222
C	-0.572797	6.135231	-3.35681	H	-3.96268	-4.318115	-6.285318
C	0.768548	5.930493	-1.378998	C	-6.386832	-3.812013	-7.584282
H	1.169061	3.935075	-0.691891	H	-4.832757	-2.307613	-7.537382
H	-1.240006	4.297639	-4.251062	H	-6.07444	-2.082262	-6.308571
H	-1.057956	6.747686	-4.122883	H	-6.888472	-3.243839	-8.387267
H	1.347679	6.380938	-0.567264	C	-7.449948	-4.509279	-6.731211
C	0.223988	8.264716	-2.221407	H	-5.769725	-4.572849	-8.096942
C	5.192806	2.53245	-2.746858	H	-8.107425	-5.139566	-7.351387
C	3.362763	1.101504	-1.998793	H	-8.088908	-3.775506	-6.210915
C	2.888255	2.999917	-3.40051	H	-7.003926	-5.161806	-5.963428
C	4.24873	3.311764	-3.431961	C	-7.759695	3.198612	-3.375959
C	4.720205	1.418739	-2.034929	H	-6.723195	4.359674	-4.882416
H	3.03297	0.223189	-1.442818	H	-6.674333	5.069158	-3.264767
H	2.186062	3.619106	-3.959539	C	-9.143701	3.815824	-3.597983
H	4.582782	4.179277	-4.009141	H	-7.634363	2.943857	-2.308099
H	5.429927	0.779811	-1.501229	H	-7.688564	2.240609	-3.922135
C	6.659048	2.901657	-2.74087	C	-10.29378	2.906452	-3.162871
C	2.802474	-3.087119	-4.643502	H	-9.259711	4.072615	-4.666961
C	1.107174	-2.234702	-3.104888	H	-9.204504	4.77531	-3.052429
C	2.26418	-0.709304	-4.560224	H	-11.27326	3.380085	-3.337049
C	2.995868	-1.770946	-5.092178	H	-10.22799	2.662977	-2.089143
C	1.846384	-3.292953	-3.638125	H	-10.28216	1.952643	-3.716715
H	0.356876	-2.437366	-2.340025	C	-0.923958	8.878474	-1.399195
H	2.428358	0.298304	-4.946154	H	0.216091	8.706757	-3.233001
H	3.725588	-1.571948	-5.883018	H	1.18609	8.553689	-1.763798
H	1.660168	-4.307325	-3.272943	H	-0.924608	8.428246	-0.390131
C	3.612073	-4.231944	-5.210079	H	-1.888391	8.590732	-1.855363
C	-3.611302	-2.565068	-5.092404	C	-0.845915	10.403423	-1.281528
C	-3.137823	-0.977922	-3.299339	C	-1.988258	11.010482	-0.465683
C	-1.497591	-1.34807	-5.020784	H	-0.839335	10.846524	-2.294313
C	-2.351811	-2.266246	-5.633351	H	0.122127	10.683516	-0.827133
C	-3.985212	-1.899043	-3.915244	H	-1.999869	10.614834	0.56382
H	-3.468733	-0.47817	-2.389244	H	-2.968506	10.781017	-0.916265
H	-0.529582	-1.136858	-5.476517	H	-1.901182	12.106889	-0.399704
H	-2.027681	-2.7642	-6.552224	P	-1.156718	-1.191747	-0.514789

2a (cyclo)

Atom	x	y	z	Atom	x	y	z
Fe	-0.170364	0.694277	-1.457755	H	-4.184122	1.525944	4.111474
P	1.592538	0.119524	0.011613	C	-3.921821	2.382139	6.706134
P	-1.531911	-0.416368	0.201347	H	-7.936969	1.438133	-2.913377
P	0.200343	-1.528164	-0.6674	C	-7.84943	3.579943	-2.601253
P	-0.174692	1.216825	0.884506	H	-7.750313	1.912641	-1.221634
C	-3.097311	1.616319	-2.570493	C	-9.360196	3.807573	-2.495721
C	-1.623293	1.509678	-2.730978	H	-7.509928	3.815905	-3.626143
C	-0.910116	0.428775	-3.373583	H	-7.320573	4.290346	-1.94041
C	-0.984741	3.874876	-1.83087	H	-9.88263	3.089666	-3.154263
C	-1.529654	-0.764148	-4.010847	C	-9.787702	5.232245	-2.851477
C	0.490424	0.788409	-3.423745	H	-9.692917	3.567562	-1.469196

Atom	X	Y	Z	Atom	X	Y	Z
C	1.559973	0.049338	-4.149553	H	-10.87842	5.361651	-2.764419
C	0.638367	2.086335	-2.807283	H	-9.503736	5.489807	-3.885701
C	1.879538	2.908703	-2.798285	H	-9.310891	5.971814	-2.186427
C	-0.667131	2.530211	-2.381829	H	-3.827579	-4.841028	-5.287848
Fe	0.305447	-1.003411	1.656327	H	-2.691993	-4.667997	-6.629242
C	-1.986874	-2.884369	3.009254	C	-4.599632	-3.713763	-6.973321
C	-0.631188	-2.274444	3.032623	H	-4.921744	-4.605571	-7.541297
C	-0.272679	-1.014615	3.644495	H	-4.217007	-2.999066	-7.724911
C	0.687061	-4.263468	1.973181	C	-5.813777	-3.103795	-6.266936
C	-1.194563	-0.112841	4.386905	H	-6.197895	-3.824687	-5.521589
C	1.163281	-0.865493	3.543705	C	-6.938782	-2.714372	-7.227179
C	1.983297	0.195106	4.191665	H	-5.496827	-2.217255	-5.690836
C	1.684908	-2.029742	2.867795	H	-7.302781	-3.585931	-7.797301
C	3.124461	-2.374026	2.708652	H	-6.598433	-1.962666	-7.959263
C	0.576384	-2.897548	2.551694	H	-7.800084	-2.286868	-6.689091
C	-5.921401	1.930194	-2.350567	H	4.370441	-3.095136	-6.55388
C	-3.941671	1.39791	-3.674043	C	6.023579	-1.954856	-5.743254
C	-3.694314	1.994091	-1.355313	H	4.723422	-1.608151	-7.440599
C	-5.076745	2.146386	-1.250355	H	5.945512	-2.372297	-4.723103
C	-5.324715	1.552768	-3.563269	H	6.300288	-0.893217	-5.611172
H	-3.509366	1.108779	-4.633683	C	7.130212	-2.682451	-6.512308
H	-3.066189	2.171048	-0.481293	H	6.843943	-3.741928	-6.644966
H	-5.509987	2.435235	-0.288093	C	8.497597	-2.603922	-5.831773
H	-5.953737	1.374498	-4.44078	H	7.20015	-2.262471	-7.532499
C	-7.414546	2.146128	-2.246752	H	8.469429	-3.050708	-4.823682
C	-2.773452	-2.969358	-5.32333	H	8.829379	-1.558175	-5.71796
C	-2.426224	-1.603778	-3.329514	H	9.269539	-3.13659	-6.410026
C	-1.266959	-1.049582	-5.363695	H	5.430362	6.054142	-3.83631
C	-1.876526	-2.129569	-6.003048	H	6.367579	4.722831	-3.150088
C	-3.032864	-2.682822	-3.974581	C	5.704185	6.178444	-1.691176
H	-2.65472	-1.409305	-2.280426	H	4.820648	6.818096	-1.514021
H	-0.577334	-0.41478	-5.923145	C	6.967352	7.043653	-1.724319
H	-1.644927	-2.32577	-7.054494	H	5.750795	5.487675	-0.829893
H	-3.721538	-3.320545	-3.412926	H	6.913837	7.731946	-2.587727
C	-3.446215	-4.124265	-6.035001	H	7.844765	6.397841	-1.91174
C	3.553453	-1.319372	-5.66074	C	7.189614	7.847849	-0.442562
C	1.829433	-1.312451	-3.932198	H	6.345721	8.530319	-0.245765
C	2.30152	0.710427	-5.146254	H	8.104552	8.458994	-0.501007
C	3.276623	0.037826	-5.884472	H	7.287351	7.185732	0.434167
C	2.807096	-1.978892	-4.671855	H	-2.909872	8.153852	-0.589783
H	1.266224	-1.858234	-3.173778	C	-0.99373	8.982462	-1.166346
H	2.106317	1.764439	-5.352273	H	-1.655154	7.994211	0.643917
H	3.832099	0.580941	-6.655136	H	-1.175483	8.907452	-2.253844
H	2.991216	-3.039681	-4.476341	H	0.07671	8.747111	-1.025248
C	4.645412	-2.033801	-6.425012	C	-1.271453	10.413575	-0.697181
C	4.240137	4.503251	-2.943862	H	-2.344499	10.639663	-0.836562
C	3.114539	2.423604	-2.334673	C	-0.429185	11.465986	-1.419733
C	1.852421	4.205101	-3.345386	H	-1.091613	10.480463	0.391498
C	3.009111	4.983351	-3.415555	H	-0.613744	11.449924	-2.507058
C	4.266512	3.207769	-2.404493	H	0.649001	11.290196	-1.26729
H	3.17536	1.421309	-1.909824	H	-0.654312	12.482585	-1.059413
H	0.913948	4.606696	-3.731931	C	7.65741	-4.22398	1.128813
H	2.952888	5.984926	-3.852643	H	7.630503	-4.086888	3.289867
H	5.211241	2.798204	-2.034085	H	7.971663	-2.556399	2.475104
C	5.484138	5.362193	-2.977982	H	7.370572	-3.598232	0.264323
C	-1.563626	6.508649	-0.906333	H	7.016266	-5.122251	1.073244
C	-0.271047	4.443214	-0.761846	C	9.127452	-4.634146	1.001582
C	-1.990304	4.653943	-2.432506	C	9.437991	-5.394007	-0.288931
C	-2.271098	5.943461	-1.978135	H	9.407461	-5.255335	1.872113
C	-0.558613	5.731081	-0.309701	H	9.763418	-3.732001	1.062053
H	0.514207	3.866237	-0.272994	H	9.206354	-4.784705	-1.178717
H	-2.557586	4.246285	-3.271105	H	8.842925	-6.319867	-0.361132
H	-3.061538	6.521484	-2.466532	H	10.501343	-5.676618	-0.347308
H	0.008934	6.13931	0.531969	H	3.80606	4.122491	6.388832
C	-1.841091	7.92071	-0.441652	C	5.672427	3.547724	5.451087
C	-4.542871	-4.143924	3.043015	H	4.678777	2.845026	7.242596
C	-2.545937	-3.425555	1.838779	H	5.390681	3.895448	4.440767
C	-2.727838	-2.994231	4.199816	H	6.260926	2.625339	5.296297
C	-3.979206	-3.612734	4.213229	C	6.545493	4.605412	6.132937
C	-3.798059	-4.039788	1.857748	H	5.950673	5.524684	6.284991
H	-1.98931	-3.368285	0.902346	C	7.815867	4.941938	5.350734
H	-2.314225	-2.599375	5.129684	H	6.817012	4.254758	7.145551
H	-4.527411	-3.687719	5.157318	H	7.576993	5.33062	4.346501

Differences in the Reaction Behavior of the Butterfly Complexes [{Cp^{BIG}Fe(CO)$_2$}(μ,η$^{1:1}$-E$_4$)] (E = P, As) − Irradiation and Thermolysis

179

Atom	x	y	z	Atom	x	y	z
H	-4.205114	-4.450015	0.928747	H	8.450674	4.05024	5.215035
C	-5.921495	-4.765374	3.051435	H	8.420077	5.704814	5.86741
C	0.96956	-6.924468	0.989428	C	-4.971826	1.551696	7.470317
C	1.443063	-4.536234	0.820218	H	-4.430356	3.092669	6.033843
C	0.083338	-5.351382	2.630344	H	-3.35378	2.990962	7.431127
C	0.224367	-6.653148	2.1472	C	-5.940087	2.37763	8.329186
C	1.576631	-5.838836	0.339318	H	-4.442912	0.828982	8.115575
H	1.931979	-3.717411	0.291817	H	-5.545105	0.943926	6.746537
H	-0.494362	-5.177693	3.539943	H	-6.544832	1.682201	8.937328
H	-0.252184	-7.477081	2.687111	C	-6.879743	3.29411	7.541422
H	2.171676	-6.015641	-0.561669	H	-5.35943	2.979902	9.052213
C	1.080928	-8.3293	0.441264	H	-7.581253	3.816113	8.211859
C	5.885595	-3.069704	2.556177	H	-7.480246	2.720601	6.814782
C	4.063755	-1.498048	2.139084	H	-6.331269	4.067017	6.979368
C	3.597059	-3.600877	3.211548	C	-7.055034	-3.743819	2.845947
C	4.948778	-3.938686	3.13635	H	-6.083042	-5.290371	4.00914
C	5.413925	-1.843419	2.063141	H	-5.984197	-5.533937	2.261753
H	3.733492	-0.537725	1.742582	C	-8.452863	-4.36955	2.854367
H	2.896391	-4.296772	3.676618	H	-6.892462	-3.211875	1.891224
H	5.28267	-4.898457	3.542327	H	-6.990371	-2.971261	3.633323
H	6.118563	-1.138784	1.611038	C	-9.576626	-3.350725	2.658018
C	7.340633	-3.460851	2.427993	H	-8.604344	-4.907582	3.808136
C	3.535531	2.159463	5.556021	H	-8.51074	-5.140619	2.064375
C	1.759315	1.567149	3.9888	H	-10.56742	-3.832626	2.668796
C	2.992957	-0.17456	5.09979	H	-9.474094	-2.821643	1.6957
C	3.750796	0.788967	5.766887	H	-9.568787	-2.587839	3.454545
C	2.52277	2.525913	4.656414	C	-0.069415	-8.712354	-0.507546
H	0.977438	1.88977	3.299585	H	1.108888	-9.049364	1.277795
H	3.181462	-1.232302	5.293163	H	2.039424	-8.439827	-0.094823
H	4.525373	0.466826	6.46957	H	-0.105177	-7.988627	-1.34182
H	2.32306	3.586306	4.474613	H	-1.030024	-8.600029	0.027027
C	4.394803	3.201241	6.236946	C	0.045172	-10.13428	-1.064781
C	-2.964036	1.535965	5.897363	C	-1.103139	-10.51736	-1.999405
C	-2.39698	0.361232	3.833858	H	0.092175	-10.85093	-0.224368
C	-0.897974	0.251402	5.712826	H	1.007084	-10.23826	-1.599513
C	-1.766378	1.058523	6.450332	H	-1.154412	-9.841612	-2.869661
C	-3.260107	1.167795	4.575384	H	-2.076033	-10.46119	-1.482774
H	-2.660639	0.097156	2.808522	H	-0.988864	-11.54423	-2.382182
H	0.025013	-0.103669	6.174753	H	-1.502203	1.327051	7.477714

2b (cisoid)

Atom	x	y	z	Atom	x	y	z
Fe	0.396314	0.28034	1.296934	H	4.474629	1.05782	-4.37446
As	-1.453157	-1.125584	0.728158	C	3.833034	2.515563	-6.613874
As	2.311419	-0.892602	0.000867	H	7.709534	1.748413	4.30935
As	0.519643	-2.3033	1.005497	C	7.670689	3.791374	3.590887
C	3.083651	1.553591	2.840065	H	7.917477	1.902012	2.56173
C	1.610877	1.380633	2.692704	C	9.161851	4.076951	3.791979
C	0.810693	0.405402	3.385968	H	7.098441	4.18912	4.448547
C	1.076463	3.605556	1.411164	H	7.304202	4.341684	2.705487
C	1.335901	-0.586158	4.366865	H	9.522298	3.519889	4.676149
C	-0.58347	0.712273	3.149731	C	9.480653	5.563379	3.959193
C	-1.733093	0.087576	3.863675	H	9.727732	3.671874	2.933138
C	-0.637142	1.869661	2.282676	H	10.560122	5.732999	4.100481
C	-1.84385	2.689274	1.966342	H	8.959816	5.989393	4.833213
C	0.713784	2.293848	2.017398	H	9.165675	6.142695	3.075016
Fe	-0.003704	-1.016986	-1.182554	H	3.43713	-4.142117	6.909409
C	1.789813	-2.900935	-3.251919	H	2.111242	-3.700743	7.989103
C	0.562181	-2.126083	-2.915723	C	3.943328	-2.621729	8.371864
C	0.289765	-0.754494	-3.287246	H	4.176332	-3.34253	9.176706
C	-0.855658	-4.134598	-2.058706	H	3.450858	-1.764839	8.867243
C	1.195939	0.115293	-4.090116	C	5.2502	-2.151225	7.726921
C	-1.08815	-0.472296	-2.944927	H	5.742872	-3.012663	7.239245
C	-1.879143	0.721861	-3.363791	C	6.216601	-1.507332	8.72247
C	-1.668775	-1.672468	-2.399478	H	5.02448	-1.436804	6.916308
C	-3.12929	-1.884339	-2.196292	H	6.49044	-2.207772	9.529645
C	-0.643339	-2.693097	-2.371099	H	5.768644	-0.618421	9.198038
C	5.875813	2.015022	3.220338	H	7.149261	-1.186317	8.231337
C	3.657146	1.554941	4.126237	H	-4.694651	-2.565111	6.6562
C	3.937593	1.801222	1.750487	C	-6.22535	-2.04342	5.216296
C	5.301994	2.02311	1.939847	H	-5.387731	-0.956852	6.892578

180

Differences in the Reaction Behavior of the Butterfly Complexes [{Cp^{BIG}Fe(CO)$_2$}(μ,η$^{1:1}$-E$_4$)] (E = P, As) – Irradiation and Thermolysis

Atom	X	Y	Z	Atom	X	Y	Z
C	5.022418	1.780953	4.309212	H	-5.874467	-2.741754	4.435146
H	3.025484	1.385435	4.999048	H	-6.571767	-1.142795	4.677847
H	3.534012	1.823549	0.738326	C	-7.397192	-2.670009	5.977684
H	5.936157	2.202135	1.066357	H	-7.041315	-3.566386	6.517952
H	5.432401	1.772374	5.323737	C	-8.575678	-3.049309	5.079725
C	7.34795	2.295532	3.421506	H	-7.740305	-1.967569	6.759377
C	2.385924	-2.35686	6.341964	H	-8.27548	-3.783187	4.31305
C	2.341691	-1.513277	4.0505	H	-8.97737	-2.168051	4.551871
C	0.873336	-0.553878	5.696322	H	-9.400501	-3.493576	5.659634
C	1.387469	-1.421681	6.659925	H	-5.614642	5.731635	2.18774
C	2.851057	-2.38086	5.018999	H	-6.197554	4.59021	0.971976
H	2.73333	-1.557382	3.034425	C	-5.087965	6.265194	0.158209
H	0.100108	0.162459	5.980199	H	-4.205607	6.872162	0.430518
H	0.998323	-1.373825	7.681624	C	-6.287379	7.186361	-0.083978
H	3.626874	-3.09764	4.734919	H	-4.818543	5.750334	-0.781829
C	2.94586	-3.284278	7.399586	H	-6.561537	7.681448	0.865525
C	-3.878094	-1.053364	5.366105	H	-7.164569	6.575144	-0.365443
C	-1.820684	-1.301974	4.076843	C	-6.036061	8.245725	-1.157939
C	-2.737664	0.892542	4.432428	H	-5.186575	8.895511	-0.888476
C	-3.78534	0.331398	5.165642	H	-6.916338	8.892131	-1.302975
C	-2.870025	-1.855512	4.809143	H	-5.800261	7.782804	-2.130856
H	-1.053924	-1.961414	3.671889	H	3.02521	7.859788	0.113364
H	-2.695188	1.975342	4.318633	C	1.03006	8.660216	0.379062
H	-4.543985	0.990665	5.598359	H	1.944033	7.569299	-1.253122
H	-2.902456	-2.939563	4.953659	H	1.074848	8.673509	1.483141
C	-5.038097	-1.663402	6.11985	H	-0.007214	8.37561	0.125458
C	-4.135599	4.325322	1.517821	C	1.325509	10.061259	-0.164143
C	-2.896284	2.253692	1.149805	H	2.365262	10.337633	0.089978
C	-1.958228	3.964114	2.554491	C	0.368915	11.132789	0.360966
C	-3.080888	4.761306	2.336704	H	1.284605	10.038192	-1.268562
C	-4.017729	3.058195	0.929394	H	0.413047	11.205389	1.460698
H	-2.836023	1.270566	0.682479	H	-0.675649	10.905818	0.088765
H	-1.156149	4.330066	3.199335	H	0.610204	12.127154	-0.047671
H	-3.14107	5.742548	2.817433	C	-7.813378	-3.296606	-0.58299
H	-4.820839	2.687207	0.285784	H	-7.824001	-3.012566	-2.729618
C	-5.331582	5.212866	1.254822	H	-7.957067	-1.513386	-1.803903
C	1.692075	6.195214	0.379312	H	-7.423735	-2.777182	0.310966
C	0.465178	4.090928	0.24137	H	-7.292807	-4.270808	-0.613357
C	1.98967	4.454011	2.063792	C	-9.320356	-3.523587	-0.430529
C	2.289312	5.719625	1.555996	C	-9.691979	-4.33385	0.812177
C	0.770761	5.354213	-0.263784	H	-9.703656	-4.034478	-1.332854
H	-0.264396	3.470876	-0.278988	H	-9.833713	-2.544954	-0.401274
H	2.469088	4.125969	2.986592	H	-9.354413	-3.831594	1.734249
H	3.008205	6.349799	2.088318	H	-9.22547	-5.333103	0.792726
H	0.284739	5.691266	-1.184269	H	-10.78152	-4.477319	0.891703
C	1.99061	7.579699	-0.150248	H	-3.665524	5.037707	-4.677531
C	4.03542	-4.485494	-4.012224	C	-5.600611	4.210587	-4.158177
C	2.461117	-3.706525	-2.316453	H	-4.368174	4.001699	-5.923696
C	2.256693	-2.915109	-4.579163	H	-5.460012	4.320512	-3.067545
C	3.357208	-3.690404	-4.948474	H	-6.148729	3.260995	-4.295203
C	3.561024	-4.478751	-2.691304	C	-6.447712	5.371035	-4.688411
H	2.113281	-3.735603	-1.283799	H	-5.898582	6.319191	-4.541207
H	1.744384	-2.319671	-5.337056	C	-7.825605	5.470149	-4.032153
H	3.690814	-3.681816	-5.990585	H	-6.566992	5.262628	-5.781994
H	4.059075	-5.095855	-1.937424	H	-7.740997	5.621293	-2.94289
C	5.253902	-5.291828	-4.40204	H	-8.412192	4.549907	-4.191827
C	-1.360604	-6.907287	-1.604929	H	-8.408867	6.311361	-4.439527
C	-1.501191	-4.576781	-0.890565	C	4.443421	1.704619	-7.773928
C	-0.480635	-5.110662	-3.001964	H	4.639993	2.944072	-5.996882
C	-0.728907	-6.465525	-2.777565	H	3.274244	3.370138	-7.034034
C	-1.743118	-5.933299	-0.670373	C	5.341563	2.515989	-8.718583
H	-1.826276	-3.852562	-0.143661	H	3.620393	1.254937	-8.356021
H	-0.001037	-4.805392	-3.932943	H	5.015566	0.855535	-7.357545
H	-0.429637	-7.194826	-3.536478	H	5.599174	1.881009	-9.584441
H	-2.247369	-6.239921	0.250953	C	6.63353	3.04173	-8.087525
C	-1.585804	-8.379034	-1.341404	H	4.761987	3.36268	-9.130563
C	-5.951646	-2.262222	-1.990054	H	7.253344	3.569317	-8.830226
C	-3.948284	-0.940089	-1.552303	H	7.240148	2.217546	-7.675062
C	-3.758617	-3.012909	-2.754038	H	6.436927	3.749769	-7.266361
C	-5.138503	-3.195379	-2.650435	C	6.580874	-4.535763	-4.207897
C	-5.326334	-1.128855	-1.448297	H	5.168624	-5.599933	-5.458583
H	-3.501065	-0.037468	-1.136425	H	5.283029	-6.222616	-3.809057
H	-3.165301	-3.753224	-3.291493	C	7.814411	-5.35565	-4.597577

Differences in the Reaction Behavior of the Butterfly Complexes [{Cp^{BIG}Fe(CO)$_2$}(μ,η$^{1:1}$-E$_4$)] (E = P, As) – Irradiation and Thermolysis

181

H	-5.592926	-4.082601	-3.101689	H	6.664919	-4.219175	-3.152594
H	-5.930414	-0.373292	-0.937173	H	6.554214	-3.602356	-4.79884
C	-7.438863	-2.487399	-1.838131	C	9.132246	-4.604364	-4.403137
C	-3.395054	2.933457	-4.33476	H	7.721636	-5.672399	-5.652643
C	-1.660108	2.018812	-2.879486	H	7.830943	-6.289476	-4.006171
C	-2.876674	0.550756	-4.343563	H	9.997495	-5.222344	-4.692097
C	-3.614581	1.633479	-4.81948	H	9.272452	-4.306951	-3.350347
C	-2.406573	3.100791	-3.35459	H	9.162776	-3.684307	-5.010725
H	-0.892019	2.183931	-2.123532	C	-0.403018	-9.06434	-0.632965
H	-3.067229	-0.446856	-4.745223	H	-1.780504	-8.89859	-2.29585
H	-4.374384	1.465315	-5.588739	H	-2.493989	-8.507432	-0.727249
H	-2.208474	4.099902	-2.955372	H	-0.200152	-8.540969	0.318767
C	-4.221871	4.097596	-4.833252	H	0.507926	-8.935437	-1.245053
C	2.916168	1.699796	-5.730421	C	-0.632765	-10.55397	-0.361208
C	2.574831	0.217489	-3.821691	C	0.543907	-11.23366	0.34062
C	0.702402	0.813325	-5.208184	H	-0.841675	-11.06962	-1.316497
C	1.546139	1.587104	-6.007678	H	-1.546587	-10.67484	0.248988
C	3.411038	0.993818	-4.623023	H	0.75459	-10.7632	1.315687
H	3.002297	-0.315578	-2.973161	H	1.464706	-11.16461	-0.262651
H	-0.35415	0.747531	-5.466445	H	0.345096	-12.30199	0.522753
H	1.124075	2.119679	-6.865417	As	1.252214	0.98882	-0.830314

2b (cyclo)

Atom	x	y	z	Atom	x	y	z
Fe	-0.050922	0.609581	-1.605981	H	-3.339562	1.003804	7.113986
As	1.70998	0.128732	0.015252	H	-5.236728	0.960502	3.245605
As	-1.713712	-0.31195	-0.097298	C	-5.672623	1.719523	5.850771
As	0.230375	-1.764075	-0.483434	H	-7.175163	3.849426	-2.896828
As	-0.219417	1.363991	0.908552	C	-6.399432	5.839775	-2.539263
C	-2.544318	2.41296	-2.665355	H	-6.814269	4.188303	-1.201209
C	-1.202133	1.800704	-2.864233	C	-7.755871	6.533009	-2.381396
C	-0.938984	0.528957	-3.498069	H	-6.025683	5.986865	-3.568816
C	0.260725	3.822133	-2.089839	H	-5.656598	6.323563	-1.879524
C	-1.950605	-0.367892	-4.124538	H	-8.494636	6.039109	-3.038878
C	0.493048	0.38806	-3.633055	C	-7.715331	8.03003	-2.691722
C	1.182784	-0.697536	-4.38305	H	-8.124046	6.379103	-1.350552
C	1.11567	1.573668	-3.097933	H	-8.705948	8.496631	-2.569276
C	2.561148	1.914088	-3.196631	H	-7.385951	8.2157	-3.727935
C	0.070063	2.441859	-2.611734	H	-7.013821	8.558776	-2.024704
Fe	0.015839	-0.891168	1.784366	H	-5.505025	-3.407184	-5.428837
C	-2.196694	-3.07932	2.741534	H	-4.420751	-3.549924	-6.815509
C	-0.981169	-2.257879	2.995405	C	-5.920718	-2.010924	-7.036979
C	-0.967248	-0.952453	3.620698	H	-6.533352	-2.721142	-7.621798
C	0.838881	-4.026973	2.36231	H	-5.349568	-1.422833	-7.778587
C	-2.157475	-0.226427	4.14514	C	-6.84732	-1.076219	-6.25452
C	0.409911	-0.575848	3.835642	H	-7.421125	-1.669318	-5.518506
C	0.878356	0.586852	4.639628	C	-7.814901	-0.29828	-7.14796
C	1.243926	-1.642935	3.335744	H	-6.241934	-0.368098	-5.662562
C	2.722533	-1.722683	3.486816	H	-8.461884	-0.976731	-7.729506
C	0.38828	-2.688091	2.828612	H	-7.272303	0.335876	-7.869365
C	-5.099696	3.647571	-2.376749	H	-8.471489	0.359874	-6.556435
C	-3.443374	2.489703	-3.744644	H	2.492889	-4.684364	-6.823508
C	-2.947306	2.975594	-1.441687	C	4.500846	-4.214273	-6.16161
C	-4.198116	3.577737	-1.303115	H	3.297298	-3.440768	-7.786858
C	-4.693693	3.094594	-3.600495	H	4.350591	-4.563782	-5.124109
H	-3.159376	2.07239	-4.712292	H	5.151808	-3.324504	-6.085919
H	-2.271688	2.942806	-0.585617	C	5.210585	-5.302289	-6.972721
H	-4.48234	3.997181	-0.333258	H	4.552847	-6.187745	-7.045808
H	-5.370308	3.132565	-4.459744	C	6.56164	-5.71574	-6.387197
C	-6.440082	4.332214	-2.229774	H	5.350469	-4.948306	-8.010592
C	-3.897303	-1.981646	-5.450994	H	6.451105	-6.108953	-5.362609
C	-3.057087	-0.88859	-3.435429	H	7.255372	-4.859697	-6.336934
C	-1.841104	-0.668166	-5.496417	H	7.043714	-6.499096	-6.993783
C	-2.792991	-1.457015	-6.141991	H	6.899077	3.632952	-4.543886
C	-4.006462	-1.680104	-4.085647	H	7.359135	2.039967	-3.934115
H	-3.18046	-0.67545	-2.372967	C	7.371901	3.598651	-2.43079
H	-0.997204	-0.275203	-6.066205	H	6.786847	4.502501	-2.18196
H	-2.670113	-1.674165	-7.207542	C	8.851126	3.968106	-2.57589
H	-4.850774	-2.075327	-3.513379	H	7.243657	2.914059	-1.572854
C	-4.934942	-2.819006	-6.168262	H	8.972525	4.649654	-3.43775
C	2.440385	-2.720919	-5.952349	H	9.428786	3.060443	-2.829917

C	0.931746	-2.060455	-4.149938	C	9.442796	4.616931	-1.323744
C	2.064988	-0.367721	-5.429168	H	8.910906	5.548006	-1.065366
C	2.678988	-1.359533	-6.195333	H	10.506456	4.869059	-1.461762
C	1.552083	-3.048046	-4.916251	H	9.37039	3.945108	-0.451959
H	0.242352	-2.353585	-3.357636	H	-0.045938	8.505693	-0.857329
H	2.264813	0.681372	-5.654173	C	1.997632	8.647922	-1.560001
H	3.354338	-1.066691	-7.005019	H	1.157423	7.94388	0.307945
H	1.333902	-4.099533	-4.706205	H	1.737218	8.630833	-2.633842
C	3.142462	-3.794699	-6.752667	H	2.937206	8.073187	-1.47082
C	5.314993	2.577421	-3.547168	C	2.235417	10.093378	-1.11271
C	3.580049	1.00766	-2.852823	H	1.290618	10.660338	-1.20116
C	2.951346	3.155074	-3.733338	C	3.334231	10.803667	-1.904528
C	4.299169	3.477065	-3.903139	H	2.489736	10.103318	-0.036964
C	4.925164	1.335421	-3.021852	H	3.091855	10.843378	-2.979838
H	3.317505	0.026813	-2.455292	H	4.301043	10.282137	-1.805087
H	2.189148	3.874462	-4.036722	H	3.478381	11.839577	-1.557981
H	4.565433	4.448959	-4.329652	C	7.753662	-2.648204	2.916624
H	5.69014	0.604183	-2.74377	H	7.250922	-2.572139	5.02162
C	6.774916	2.944439	-3.690077	H	7.45674	-0.985308	4.272014
C	0.655685	6.505025	-1.207154	H	7.531206	-2.073239	1.9995
C	1.187209	4.126772	-1.077389	H	7.329312	-3.654613	2.748857
C	-0.458707	4.889784	-2.656986	C	9.270306	-2.754722	3.101128
C	-0.263384	6.20217	-2.222915	C	9.9837	-3.408977	1.917039
C	1.377455	5.439523	-0.646233	H	9.484815	-3.325734	4.02308
H	1.768048	3.32408	-0.621646	H	9.6871	-1.745201	3.271933
H	-1.178844	4.690851	-3.45246	H	9.818776	-2.840884	0.986091
H	-0.843488	7.0082	-2.682471	H	9.61646	-4.434678	1.744908
H	2.099366	5.639438	0.151288	H	11.071505	-3.468661	2.08176
C	0.892071	7.931385	-0.763466	H	1.36143	4.624509	7.291761
C	-4.502182	-4.717169	2.36564	C	3.441753	4.569	6.693928
C	-2.451514	-3.706955	1.51042	H	2.351379	3.501997	8.230464
C	-3.114938	-3.298446	3.785237	H	3.260863	4.943995	5.670293
C	-4.241824	-4.100458	3.598955	H	4.24846	3.819667	6.600007
C	-3.580623	-4.50635	1.328438	C	3.911638	5.720144	7.587826
H	-1.75436	-3.572877	0.682292	H	3.09727	6.461578	7.683388
H	-2.9389	-2.840629	4.760252	C	5.176072	6.412697	7.077148
H	-4.932115	-4.252745	4.434277	H	4.087439	5.337146	8.609781
H	-3.747852	-4.978423	0.355623	H	5.020633	6.841261	6.072746
C	-5.752733	-5.539721	2.1509	H	6.019307	5.705311	7.004989
C	1.749478	-6.621074	1.601308	H	5.486666	7.233036	7.74397
C	1.891577	-4.190063	1.444065	C	-6.688772	0.704524	6.410764
C	0.256995	-5.190209	2.89794	H	-6.158003	2.344412	5.083232
C	0.704148	-6.458702	2.522536	H	-5.369279	2.402787	6.663429
C	2.334069	-5.459261	1.072464	C	-7.920885	1.332055	7.077752
H	2.377101	-3.309178	1.021941	H	-6.1711	0.061533	7.143593
H	-0.548884	-5.102096	3.628397	H	-7.010222	0.031151	5.595353
H	0.232753	-7.342218	2.963627	H	-8.501808	0.52711	7.561273
H	3.158155	-5.548272	0.35813	C	-8.841505	2.109918	6.133793
C	2.206167	-7.995241	1.166156	H	-7.589434	1.995646	7.897806
C	5.536311	-1.884706	3.923282	H	-9.731631	2.48387	6.66475
C	3.578599	-0.672669	3.113497	H	-9.193409	1.472749	5.304539
C	3.302446	-2.850522	4.09717	H	-8.337987	2.983112	5.688512
C	4.679724	-2.92696	4.309695	C	-6.971192	-4.701004	1.723632
C	4.955181	-0.756057	3.324613	H	-6.000877	-6.082139	3.079988
H	3.16086	0.222003	2.651477	H	-5.560758	-6.309867	1.383945
H	2.664724	-3.675143	4.420461	C	-8.241186	-5.529862	1.510423
H	5.09645	-3.815998	4.79281	H	-6.724873	-4.153783	0.795748
H	5.592156	0.079864	3.02001	H	-7.159328	-3.924409	2.486905
C	7.033206	-1.991449	4.108324	C	-9.451783	-4.692894	1.094381
C	1.702295	2.731888	6.333316	H	-8.47506	-6.081179	2.43968
C	0.415739	1.897806	4.433927	H	-8.046131	-6.30397	0.745699
C	1.756092	0.37106	5.719234	H	-10.34709	-5.318651	0.949968
C	2.157603	1.421766	6.545326	H	-9.263468	-4.157862	0.14843
C	0.822594	2.945422	5.261002	H	-9.695201	-3.934496	1.857318
H	-0.277374	2.102685	3.61793	C	1.469652	-8.526187	-0.077277
H	2.118625	-0.637359	5.924896	H	2.06582	-8.708905	1.99655
H	2.834101	1.215094	7.380261	H	3.289922	-7.972852	0.956793
H	0.439055	3.952503	5.071289	H	1.603102	-7.810845	-0.908928
C	2.16727	3.874646	7.207762	H	0.384037	-8.547091	0.127675
C	-4.444749	1.067428	5.255206	C	1.937327	-9.917098	-0.515433
C	-3.272267	0.088632	3.350414	C	1.207135	-10.44554	-1.751015
C	-2.212932	0.114788	5.509471	H	1.804992	-10.62544	0.322873
C	-3.333164	0.747876	6.050025	H	3.024645	-9.888647	-0.712805

Differences in the Reaction Behavior of the Butterfly Complexes [{Cp^BIGFe(CO)$_2$}(μ,η$^{1:1}$-E$_4$)] (E = P, As) − Irradiation and Thermolysis

183
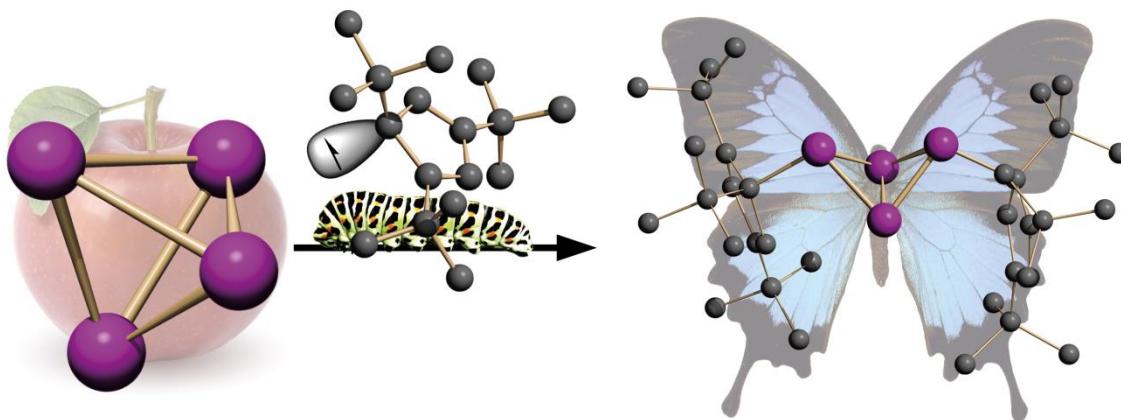
C	-4.389401	0.723025	3.895999	H	1.351101	-9.77845	-2.617531
H	-3.265549	-0.162666	2.288893	H	0.121314	-10.52215	-1.572957
H	-1.366432	-0.120009	6.157467	H	1.568216	-11.44613	-2.03819

References for Supplementary Information

[1]   R. C. Clark, J. S. Reid, *Acta Cryst.* **1995**, A51, 887-897.

[2]   A. Altomare, M. C. Burla, M. Camalli, G.L. Cascarano, C. Giacovazzo, A. Guagliardi, A. G. G. Moliterni, G. Polidori, R. Spagna, *J. Appl. Cryst.* **1999**, 32, 115-119.

[3]   L. Palatinus, G. Chapuis, *J. Appl. Cryst.* **2007**, 40, 786-790.

[4]   G. M. Sheldrick, *Acta Cryst.* **2008**, A64, 112-122.

[5]   M. J. Frisch, G. W. Trucks, H. B. Schlegel, G. E. Scuseria, M. A. Robb, J. R. Cheeseman, J. A. Montgomery, Jr., T. Vreven, K. N. Kudin, J. C. Burant, J. M. Millam, S. S. Iyengar, J. Tomasi, V. Barone, B. Mennucci, M. Cossi, G. Scalmani, N. Rega, G. A. Petersson, H. Nakatsuji, M. Hada, M. Ehara, K. Toyota, R. Fukuda, J. Hasegawa, M. Ishida, T. Nakajima, Y. Honda, O. Kitao, H. Nakai, M. Klene, X. Li, J. E. Knox, H. P. Hratchian, J. B. Cross, V. Bakken, C. Adamo, J. Jaramillo, R. Gomperts, R. E. Stratmann, O. Yazyev, A. J. Austin, R. Cammi, C. Pomelli, J. W. Ochterski, P. Y. Ayala, K. Morokuma, G. A. Voth, P. Salvador, J. J. Dannenberg, V. G. Zakrzewski, S. Dapprich, A. D. Daniels, M. C. Strain, O. Farkas, D. K. Malick, A. D. Rabuck, K. Raghavachari, J. B. Foresman, J. V. Ortiz, Q. Cui, A. G. Baboul, S. Clifford, J. Cioslowski, B. B. Stefanov, G. Liu, A. Liashenko, P. Piskorz, I. Komaromi, R. L. Martin, D. J. Fox, T. Keith, M. A. Al-Laham, C. Y. Peng, A. Nanayakkara, M. Challacombe, P. M. W. Gill, B. Johnson, W. Chen, M. W. Wong, C. Gonzalez, and J. A. Pople, Gaussian 03 (Revision D.01): Gaussian, Inc., Wallingford CT, 2004.

[6]   a) A. D. Becke, *J. Chem. Phys.*, **1993**, *98*, 5648; b) C. Lee, W. Yang, R. G. Parr, *Phys. Rev. B.*, **1988**, *37*, 785.

[7]   F. Weigend, R. Ahlrichs, *Phys.Chem.Chem.Phys.*, **2005**, *7*, 3297-3305.

11. Selective Functionalization of P$_4$ by Metal-Mediated C–P Bond Formation

Sebastian Heinl, Sabine Reisinger, Christoph Schwarzmaier, Michael Bodensteiner and Manfred Scheer
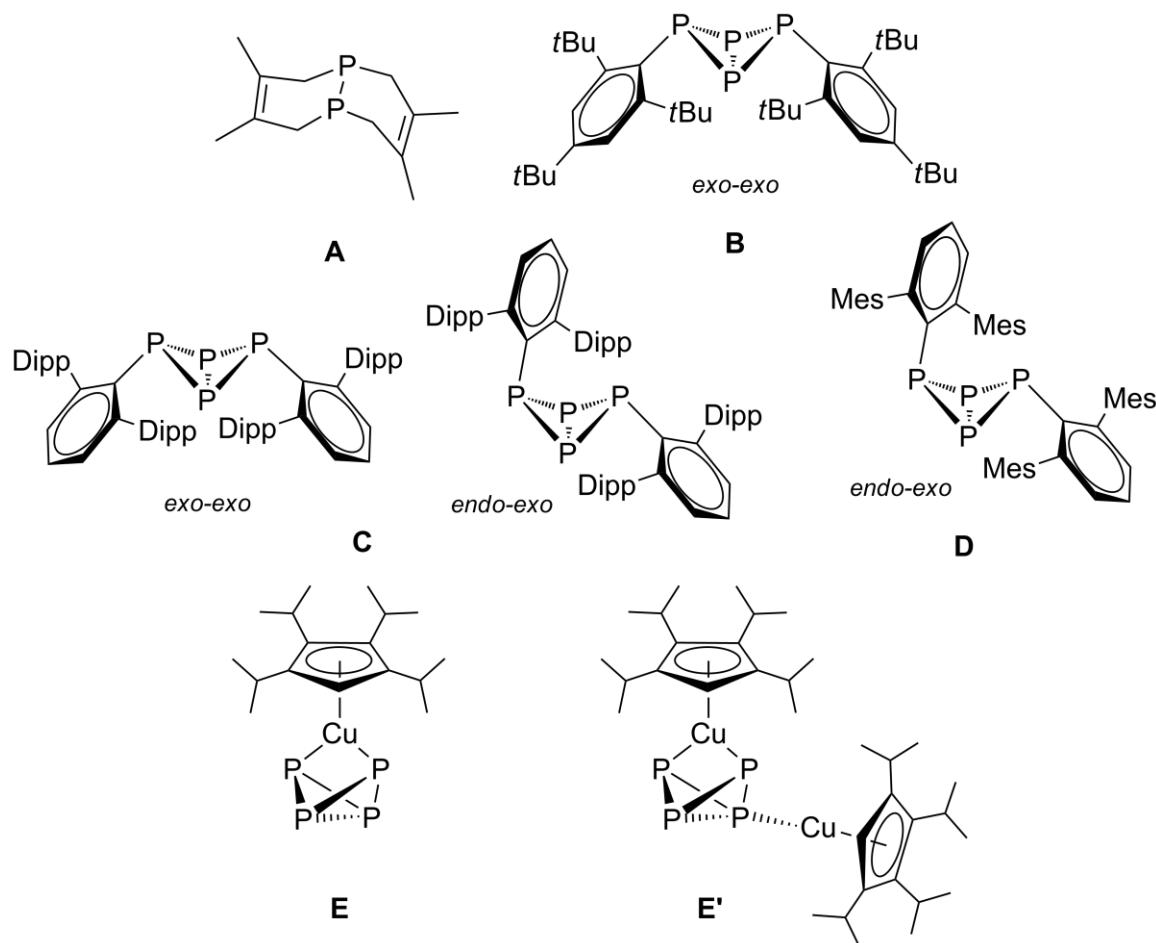
❖ **'Cu-route': all syntheses and characterizations were performed by Sebastian Heinl**

❖ **'Fe^{II}-route': all syntheses and characterizations were performed by Christoph Schwarzmaier (1b) and Sabine Reisinger (1a, 1c, 1d). These results are also subject of the PhD thesis of Christoph Schwarzmaier from 2012**

❖ **Fe^{III}-route': all syntheses and characterizations were performed by Sabine Reisinger. These results will be also subject of her PhD thesis in 2014**

❖ **Manuscript was written by Sebastian Heinl except Introduction (Christoph Schwarzmaier)**

❖ **ChemDraw figures were made by Sebastian Heinl, figures of crystal structures by Sabine Reisinger and graphical abstract by Christoph Schwarzmaier**

❖ **EPR measurements were performed by Sebastian Heinl with the aid of Ulrich Zenneck (University of Erlangen) and Michael Spörner (University of Regensburg)**

❖ **X-ray structure analyses and refinement were performed by Sebastian Heinl (1a), Christoph Schwarzmaier (1b), Sabine Reisinger (1c) and Michael Bodensteiner (1d)**

11.1   Introduction

As one of the essential elements phosphorus plays an important role in our daily life. Whereas the majority of phosphate minerals were consumed for fertilizers, only 10% are used to produce white phosphorus. This is the key compound for the production of inorganic and organic phosphorus derivatives. Such processes involve the use of hazardous reagents like chlorine gas, Grignard reagents or alkali metals to form C–P bonds by elimination of large amounts of salts. Hence, the search for atom efficient processes and milder activation ways of the P_4 tetrahedron is of central interest. Especially a catalytic process for the direct C–P bond formation with white phosphorus as the P source is a clear objective, but it is presently far from being achieved. In the last decade the activation of white phosphorus with transition metals[1] and main group elements[2] has become an active research area. However, to date only a few reactions are known in which carbon reagents react with P_4 selectively to yield organophosphorus compounds, among them a UV promoted degradation to P_2-containing organophosphorus derivatives, such as **A**.[3] Early results were achieved by the reaction of P_4 with organolithium or organomagnesium compounds to yield complex mixtures of pathway. The first step is the cleavage of one P–P bond, yielding a butterfly-like
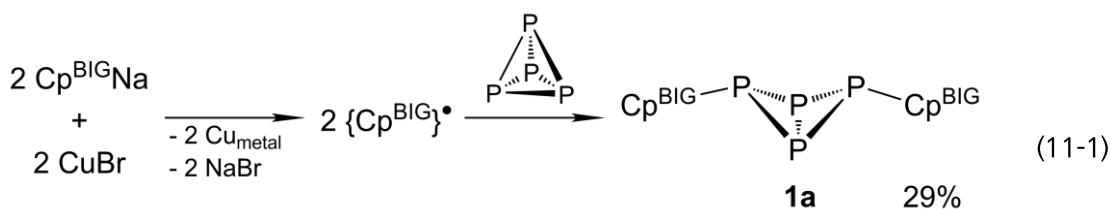
organophosphanides.[2a,4] The reactions are not selective and usually the degradation/reaggregation pathway of the P$_n$ fragments is not well understood. Recently, Bertrand et al. showed the potential of stable carbenes for the activation of white phosphorus.[5] However, in these cases the P$_4$ tetrahedron is fragmented or reaggregates to form extended polyphosphorus frameworks. In means of a targeted, carbon based activation of white phosphorus, it would be of great interest to understand every step of its degradation tetraphospha*bicyclo*-butane unit.[2b] To the best of our knowledge, only three examples of P$_4$ butterfly moieties with carbon substituents are known so far that are derived from white phosphorus. In the 1980s Fluck et al. presented the synthesis of [Mes*$_2$P$_4$] (**B**) (Mes* = 2,4,6-*t*Bu-(C$_6$H$_2$)) in 4% yield by the reaction of LiMes* with Mes*Br in the presence of P$_4$.[6] More recently Power et al. reported on the formation of [{Ar^{Dipp}}$_2$P$_4$] (**C**) (Ar^{Dipp} = C$_6$H$_3$-2,6-(C$_6$H$_3$-2,6-*i*Pr$_2$)$_2$) in a two-step synthesis in moderate yields.[7] While the formation of **B** and **C** involves a nucleophilic attack at the P$_4$ tetrahedron, Cummins et al. presented the formation of [Dmp$_2$P$_4$] (**D**) (Dmp = 2,6-Mes$_2$C$_6$H$_3$) via a radical reaction.[8] In this case the carbon radicals are generated *in situ* by treatment of DmpI with the Ti(III) complex [Ti(N(*t*Bu)Ar)$_3$] (Ar = 3,5-Me$_2$C$_6$H$_3$). However, all presented reactions use aromatics substituted with a sp^2 hybridized carbon atom as the reactive site.[9] Direct C–P bond formation reactions involving sp^3 hybridized carbon atoms and white phosphorus have not been reported so far.

Herein we report on the selective formation of Cp$^R_2$P$_4$ (Cp^R : Cp^{BIG} = C$_5$(4-^{n}BuC$_6$H$_4$)$_5$ (**1a**), Cp''' = C$_5$H$_2$^{t}Bu$_3$ (**1b**), Cp* = C$_5$Me$_5$ (**1c**), Cp^{4iPr} = C$_5$H^{i}Pr$_4$ (**1d**)) with P$_4$ as the phosphorus source. The metal-mediated selective conversions leading to **1a**-**1d** feature radical reactions.

11.2   Results and Discussion

Initially, we were interested in the synthesis of copper complexes with unsubstituted P$_n$ ligands, a class of compounds for which Scherer et al. reported the complex **E** and **E'** obtained by the reaction of [Cp^{4iPr}Cu(CO)] with white phosphorus.[10] However, the products were only characterized by ^{31}P NMR spectroscopy. In order to enhance the stability of such complexes, we used the sterically more demanding Cp^{BIG} ligand. In a first attempt, we tried to generate [Cp^{BIG}Cu(CO)] *in situ* by adding a solution of Cp^{BIG}Na in THF to a CuBr suspension in THF and subsequently discharging CO gas into the solution. However, already with the first drop of the Cp^{BIG}Na solution, the mixture turns into dark blue and metallic Cu precipitates. The intense color indicates the initial formation of {Cp^{BIG}}• radicals which was confirmed by EPR spectroscopy. The characteristic color together with the obtained EPR data fit well with the known {C$_5$Ph$_5$}• radical.[11] Upon discharging CO gas into the solution, the color does not

$$2\ Cp^{BIG}Na + 2\ CuBr \xrightarrow[{-2\ NaBr}]{-2\ Cu_{metal}} 2\ \{Cp^{BIG}\}^{\bullet} \longrightarrow Cp^{BIG}-P \cdots P \cdots P - Cp^{BIG} \tag{11-1}$$

1a   29%

change, a hint that the desired complex [$Cp^{BIG}Cu(CO)$] is not formed. However, following the synthetic protocol for [$Cp^{4iPr}Cu(\eta^2\text{-}P_4)$],[10] white phosphorus was added. After columnchromatographic work-up, yellow cube-shaped crystals were obtained. The X-ray structure analysis did not show the desired copper complex [$Cp^{BIG}Cu(\eta^2\text{-}P_4)$], but the metal-free compound **1a**, exhibiting two newly formed C–P bonds. In order to exclude [$Cp^{BIG}Cu(CO)$] as potential intermediate, the reaction was repeated without the CO discharge step, again leading to **1a** as the only reaction product. Hence, based on the EPR measurements, a radical mechanism including the formation of $\{Cp^{BIG}\}^{\bullet}$ radicals together with elemental copper has to be suggested. These radicals react with P_4 to afford the butterfly compound **1a** in moderate isolated yields (Equation 11-1).

In the $^{31}P\{^1H\}$ NMR spectrum of **1a** two coupled triplets of an A_2M_2 spin system are observed at d = -181.0 ppm ('wing-tip') and d = -308.2 ppm (bridgehead) ($^1J_{PP}$ = 192 Hz), which is characteristic for a P_4 butterfly structural motif. The ^1H and $^{13}C\{^1H\}$ NMR spectra show several superimposed signals because of the nonequivalent 4-nBuC$_6$H$_4$ moieties of the Cp^{BIG} ligands in **1a**. The FD mass spectrometry exclusively reveals the molecular ion peak at m/z =
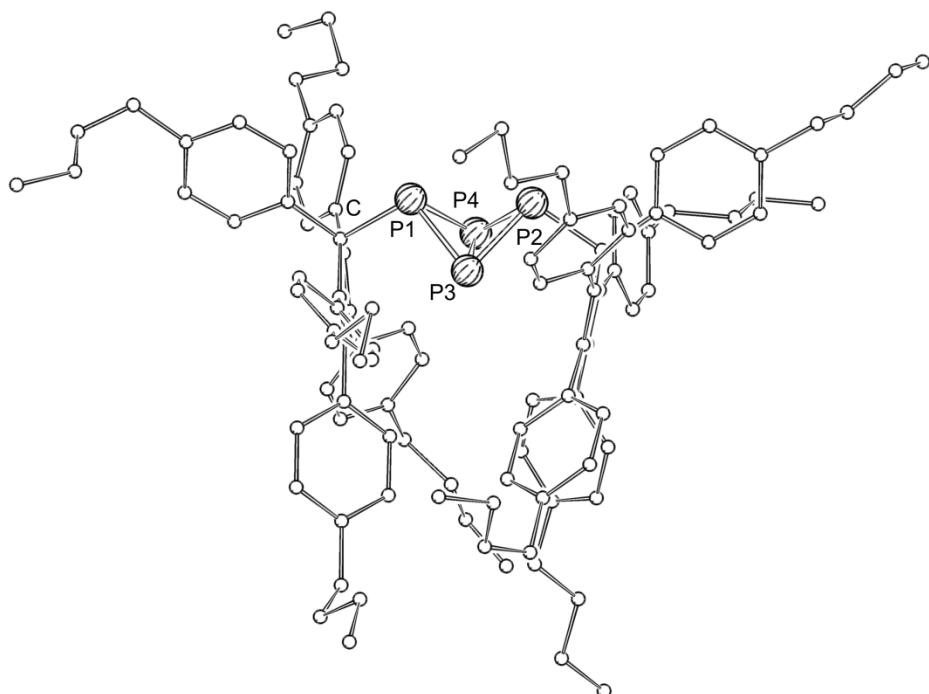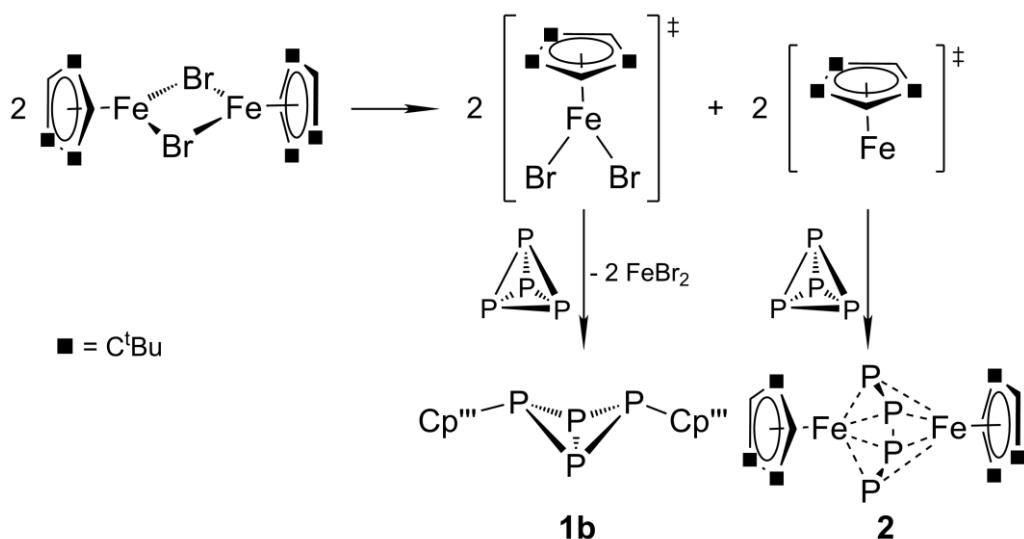
Figure 11.1. Molecular structure of **1a** in the crystal. For clarity only one of the three molecules in the asymmetric unit is depicted, H atoms are omitted.

1576.2. As inter alia for **B**, but in contrast to **C**, the X-ray structure of **1a** (Figure 1) shows only the *exo-exo*-configuration of the organic substituents in the solid state. The P–P and P–C distances of 2.1814(8) - 2.2279(8) Å and 1.935(2) − 1.954(2) Å, respectively, are in a comparable range with similar P_4 butterfly compounds such as **B** and **C**.[12]

To verify the possible generality of this method, reaction (Equation 11-1) was repeated with other CpR salts including CpNa, Cp*Na, Cp'''Na as well as Cp$^{4/Pr}$Na. However, no formation of Cp$^R_2$P$_4$ could be observed at all. A reason for this might be the lower {Cp^R}$^{\bullet}$ radical stability compared to the aryl substituted {Cp^{BIG}}$^{\bullet}$. For the latter, its high steric demand and the possible mesomeric stabilization lead to a less reactive radical species and a hindered radical coupling, allowing the reaction with the P_4 molecule. In case of the smaller and more reactive {Cp^R}$^{\bullet}$ derivatives, the radical decomposition (e.g. Cp^{R}H formation) seems to be faster than the reaction with white phosphorus and therefore the formation of the desired P_4 butterfly molecules does not proceed.

Since the key step in the formation of **1a** is the oxidation of {Cp^{BIG}}$^-$ to {Cp^{BIG}}$^{\bullet}$ by Cu$^+$ (together with the formation of Cu), a possibility of avoiding the formation of long-lived stable {Cp^R}$^{\bullet}$ radicals would be the use of a more flexible redox system with a broader variety of oxidation states. Thus, we chose the system Fe(II)/Fe(III) since Sitzmann et al. reported on the synthesis of a {Cp$^{5/Pr}$}$^{\bullet}$ radical from the reaction of the corresponding sodium salt and FeCl$_2$.[13] Thus, the dimeric iron(II) complex [Cp$^{5/Pr}$Fe(μ-Cl)]$_2$ might be a potential intermediate during this reaction, and the two derivatives [Cp'''Fe(μ-Br)]$_2$ and [Cp$^{4/Pr}$Fe(μ-Br)]$_2$ are already known and crystallographically characterized.[14] Since these 16 VE species are coordinatively unsaturated, we proposed that they could be able to interact with P_4 molecules allowing a direct C–P bond formation in the coordination sphere of the iron centers. Moreover, iron is a

Scheme 11.1. Proposed reaction pathway for the formation of **1b** and **2** from [Cp'''Fe(μ-Br)]$_2$ and P_4.

rather cheap and a non-toxic metal which would be beneficial in a further application of this method.

The reaction of [Cp'''Fe(µ-Br)]$_2$ with one equivalent of P_4 in toluene at room temperature leads to the formation of [{Cp'''Fe}$_2$(µ,η$^{4:4}$-P$_4$)][15] (**2**) as well as the carbon-substituted butterfly compound **1b** (Scheme 11.1) together with a brownish precipitate of FeBr$_2$. The ^{31}P{^{1}H} NMR spectrum of the reaction mixture shows a total conversion of P_4 into the two products in a 1:1 ratio. However, after chromatographic work-up, **1b** is obtained as pure material only in 14% yield. The ^{31}P{^{1}H} NMR spectra of **1b** show some coupled sets of signals. This can be explained by the presence of four different constitutional isomers (Figure 11.2). By ^{31}P{^{1}H}–^{31}P{^{1}H} COSY NMR spectroscopy, all signals could be assigned to the four isomers **1b-A**, **1b-B**, **1b-C** and **1b-D** showing a ratio of ca. 4:1:7:7.[12]
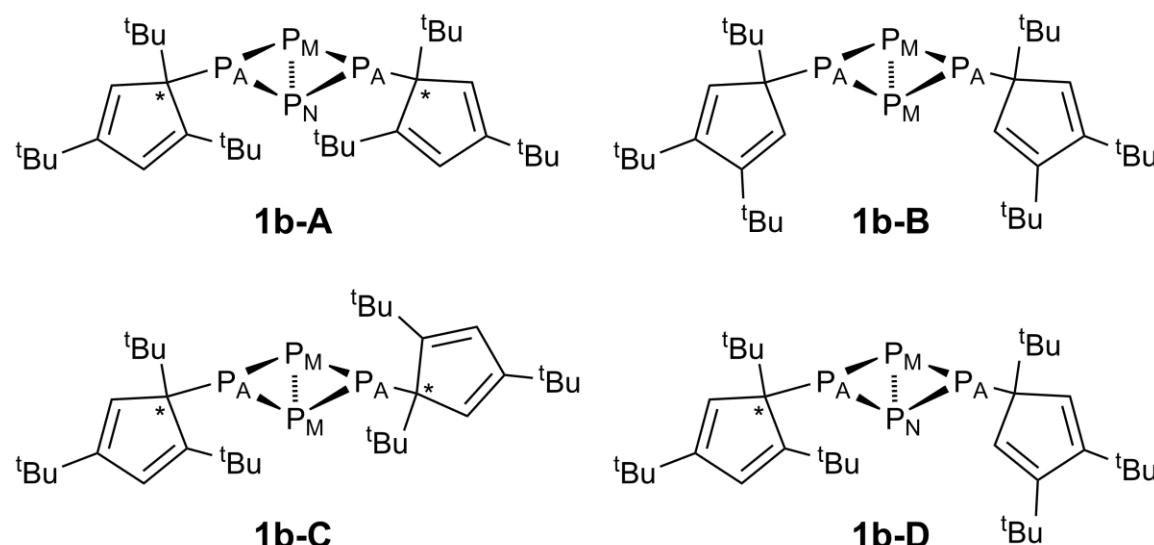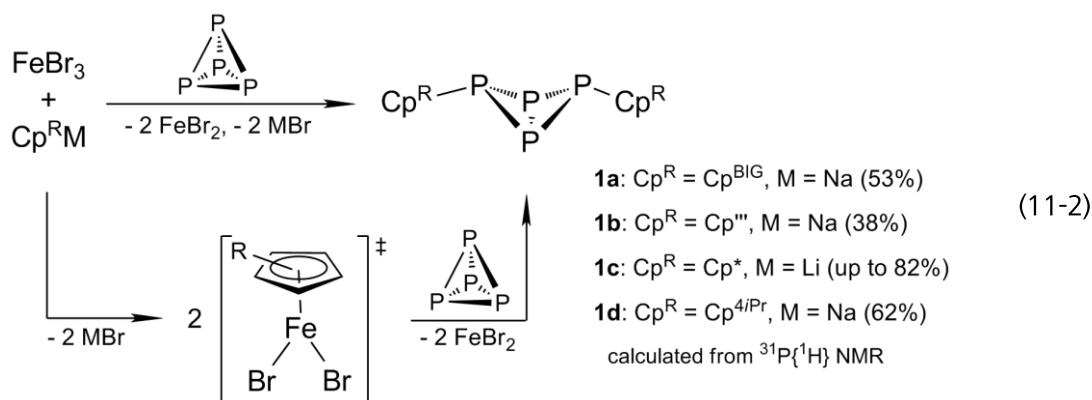
Figure 11.2. Isomers of **1b** monitored by ^{31}P{^{1}H} NMR spectroscopy. P atoms are assigned to the corresponding spin system. Isomers **1b-A** and **1b-C** are diasteriomeric, and **1b-A** represents the meso compound.

The respective chemical shifts and coupling constants clearly indicate the formation of butterfly compounds, in which the "wing-tip" P atoms of the *bicyclic* P_4 framework are only bound to tertiary P atoms. This gives a first hint on the underlying reaction mechanism involving Cp''' moieties. For the {Cp'''}$^•$ radical, several mesomers are possible in which the single electron is either located on a tertiary or on a secondary carbon atom of the ring. As the stability of tertiary radicals is higher than that of the secondary ones, their formation is favored, leading to the formation of the observed isomers. In contrast, an ionic mechanism requires the formation of an aromatic cyclopentadienyl anion with a delocalized 6π-electron system. Hence, the tertiary carbon atoms are no longer preferred reaction sites and the

formation of C–P bonds to secondary carbon atoms should be formed to a certain extent. Since that is not observed experimentally, a mechanism with radicals is most likely.

The 1:1 ratio of the two products **1b** and **2** in combination with the formation of a brownish precipitate of $FeBr_2$ gives further indication for the reaction pathway (Scheme 11.1). In solution a disproportionation of $[Cp'''Fe(\mu\text{-}Br)]_2$ into the two complex fragments $[Cp'''Fe^I]$ and $[Cp'''Fe^{III}Br_2]$ is most likely. Two of the $[Cp'''Fe^I]$ fragments react with one equivalent of P_4 to form compound **2** with a *cisoid*-P_4^{2-} ligand. The remaining two 16 VE $[Cp'''Fe^{III}Br_2]$ complex fragments are able to interact with white phosphorus. The coordination of a P_4 molecule to iron enables a transfer of a radical $\{Cp'''\}^\bullet$ onto the P_4 tetrahedron to give **1b**. As a consequence the reduced Fe(III) species precipitates as brownish $FeBr_2$ from the reaction mixture.

In order to verify whether $[Cp'''FeBr_2]$ is the key intermediate on the way to **1b**, we studied the reaction of the *insitu* generated $[Cp'''FeBr_2]$ (from $Cp'''Na$ and $FeBr_3$) with white phosphorus (Equation 11-2). In fact, the Cp''' substituted compound **1b** is obtained with an identical isomer distribution as observed before. Moreover, the intrinsic loss of 50% of the material by the formation of **2** is also avoided. In addition, a column chromatographic workup is not necessary for purification and the isolated yields are therefore increased.

1a: $Cp^R = Cp^{BIG}$, M = Na (53%)
1b: $Cp^R = Cp'''$, M = Na (38%)
1c: $Cp^R = Cp^*$, M = Li (up to 82%)
1d: $Cp^R = Cp^{4/iPr}$, M = Na (62%)
calculated from $^{31}P\{^1H\}$ NMR

(11-2)

By applying this synthetic protocol to other Cp^R ligands ($Cp^R = Cp$, Cp^{BIG}, Cp^*, $Cp^{4/iPr}$), it was also possible to synthesize the compounds $Cp^{BIG}_2P_4$ (**1a**), $Cp^*_2P_4$ (**1c**) and $Cp^{4/iPr}_2P_4$ (**1d**) in good yields. Unfortunately, the parent compound Cp_2P_4 was still not accessible. The reason for this might be the minimized stabilizing effects of the small Cp ring for the reaction intermediates as well as for the potential product.

However, this metal-mediated mechanism seems to be different to the above mentioned formation of $Cp^{BIG}_2P_4$ (**1a**) via the 'copper route', in which a free and stable radical has to be formed to successfully attack P_4. This explains why this method succeeded for Cp^{BIG} but not for Cp^*, Cp''' or $Cp^{4/iPr}$. The similar complex fragment $[Cp^RFe^{III}Br_2]$ might provide enough stability to transfer $\{Cp^R\}^\bullet$ radicals to P_4, which were indeed detected by EPR spectroscopy.[12]

The fact that the 'copper route' is only suitable for Cp^{BIG} for the reaction with P$_4$ but with iron halides also other Cp^R moieties can be transferred, is an indication that in the latter case a metal mediated process takes place. However, also for the 'Cu route' the radical formation proceeds via a metal, but the stability of the radical is much higher in the case of Cp^{BIG}. The presented new Fe mediated method allows the fast and clean conversion of white phosphorus into the carbon substituted butterfly compounds in only one step in good isolated yields.

As already observed for **1a**, compounds **1b-d** show two characteristic groups of signals in the ^{31}P{^{1}H} NMR spectrum at δ ≈ 134 ppm – -163 ppm ('wing-tip') and δ ≈ -307 ppm – -367 ppm (bridgehead). In case of the pentasubstituted Cp* moiety and its isomers with high molecular symmetry (e.g. **1b-B** and **1b-C**), two triplets of an A$_2$M$_2$ spin system with $^1J_{PP}$ coupling constants of 173 Hz – 193 Hz are observed.[12] However, if Cp^R is tri- or tetra-substituted (Cp^R = Cp''', Cp^{4iPr}), isomers with low molecular symmetry (Cp^R ligands are non-equivalent; see Figure 11.2) are also formed, leading to more complicated ^{31}P{^{1}H} NMR spectra with A$_2$MN or ABMN spin systems in a 1:1 ratio.[12] In the case of **1d**, even though several isomers are possible, only two of them are observed in the ^{31}P{^{1}H} NMR spectrum with an A$_2$M$_2$ and A$_2$MN spin system, respectively. The reason could be a random superimposition of signals of different isomers or the steric hindrance might lead exclusively to the formation of selected isomers.
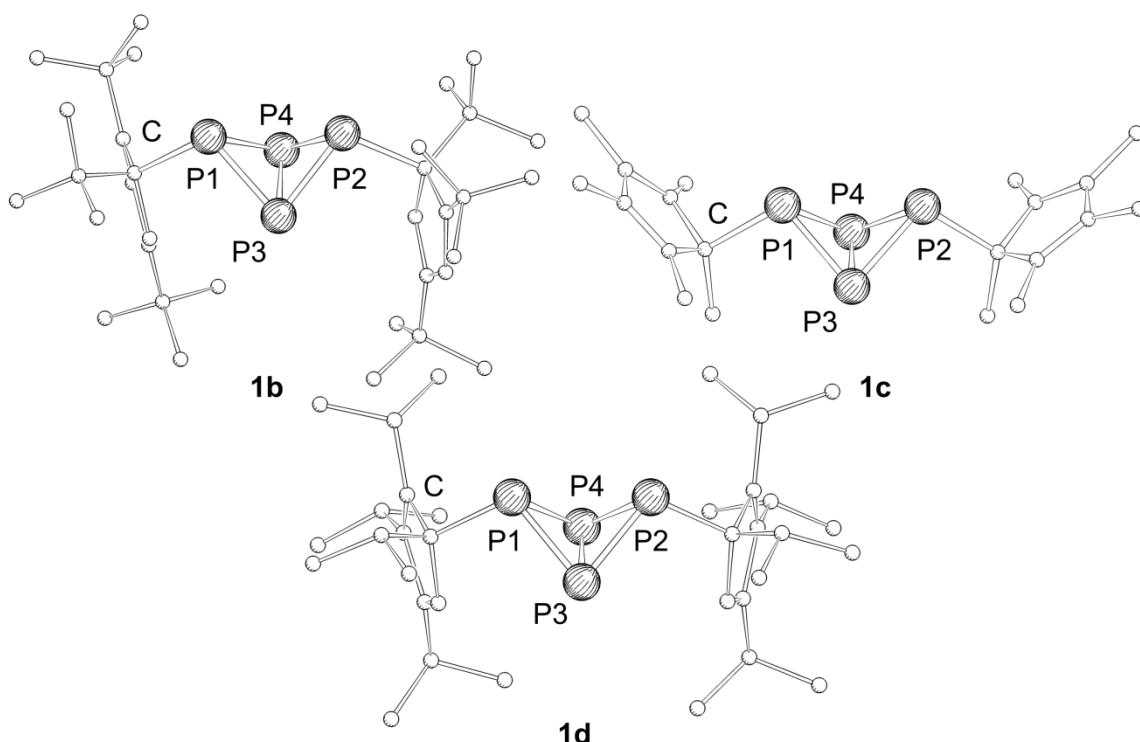
Figure 11.3. Molecular structures of **1b** (left), **1c** (right) and **1d** (bottom) in the crystal. For clarity only one molecule of the asymmetric unit (if more than one is present) is depicted and H atoms are omitted.

The hitherto unknown molecular structures of **1b-d** were examined by single crystal X-ray structure analysis (Figure 11.3). The P–P bond lengths vary in the range of 2.178(6) and 2.244(7) Å, the C–P bond lengths from 1.884(4) to 1.911(8) Å. The structural parameters compare well with those of known R_2P_4 butterfly compounds.[12] All of the four derivatives **1a-d** show a *exo*-exo configuration. Interestingly, in **1c**, the two Cp* substituents are pointing upwards, which is different to compounds **1a**, **1b** and **1d**, which is most likely due to packing effects.

The chemical shifts and coupling constants of the two isomers of **1d** are nearly identical to those published by Scherer et al. for the proposed copper complexes [Cp$^{4/Pr}$Cu(η^2-P_4)] **E** and [{Cp$^{4/Pr}$Cu}$_2$($\mu,\eta^{2:1}$-P_4)] **E'**.[10] In addition, in the FD mass spectrum of the corresponding crude reaction mixture (Equation 11-2) the molecular ion peak of **1d** (45%) was detected beside some P free Cp$^{4/Pr}$Fe complex fragments. Since our preparation of **1d** was performed without using copper, we assume that in reference [10] the NMR data were misinterpreted, and that they obtained Cp$^{4/Pr}_2P_4$ (**1d**) accidentally and unfortunately did not recognize their discovery. The crystal structure of **1d** considerably supports this fact. Thus, the quest for copper complexes of the type [LCu(η^2-P_4)] is still open.

In conclusion, we have shown that stable {Cp^{BIG}}$^•$ radicals are suitable to selectively activate one P–P bond of the P_4 tetrahedron to form the *bicyclic* butterfly compound **1a**. Further attempts to transfer the synthetic protocol to other Cp^R derivatives like Cp''', Cp* or Cp$^{4/Pr}$ failed. Therefore, a new synthesis was developed that uses the generation of {Cp^R}$^•$ radicals in the coordination sphere of Fe^{III} complexes. This unique, metal mediated transfer of carbon centered radicals to the P_4 tetrahedron allows a simple and selective synthesis of novel Cp$^R_2P_4$ compounds (**1a-d**). These unprecedented butterfly molecules exhibit a bond between sp^3 hybridized carbon atoms and phosphorus, which could so far not be realized by using white phosphorus as a P source in other systems.[9] Since the synthetic protocol works with different Cp^R derivatives, independently from their steric demand, it provides a general access to this fascinating class of compounds and reveals the first step of the P_4 activation process. Future studies will aim on the properties and reactivity of the carbon substituted butterfly compounds. Moreover, the further carbon based fragmentation of the P_4 tetrahedron will be investigated which might open the way to catalytic phosphorus activation.

11.3   Experimental Part

General Remarks:

All experiments were carried out under an atmosphere of dry argon or nitrogen using glovebox and schlenk techniques. Solvents were purified, dried and degassed prior to use. P_4, CuBr, $FeBr_3$ and Cp*Li were available, $Cp^{BIG}Na$,[16] $FeBr_2$*dme,[17] and Cp'''Na[17] were prepared according to literature procedure and $Cp^{4/Pr}Na$ was used as obtained from Prof. Dr. Helmut Sitzmann (TU Kaiserslautern). The NMR spectra were measured on a Bruker Avance 300, 400 or 600 spectrometer. EI-MS spectra were measured on a Finnigan MAT SSQ 710A mass spectrometer and FD-MS spectra on a Finnigan MAT 95 mass spectrometer. The elemental analyses were determined on a Vario EL III apparatus. The EPR spectrum was measured on a JEOL JES-FA200 CW X-Band ESR-Spectrometer or on a Bruker EMX-Plus-A-R X-Band ESR-Spectrometer.

Method 1 (Cu-route): Synthesis of $Cp^{BIG}_2P_4$ (1a) with CuBr

A solution of $Cp^{BIG}Na$ (900 mg, 1.2 mmol) in 10 mL THF is added to a suspension of CuBr (171 mg, 1.2 mmol) in 10 mL THF. The mixture turns into dark blue/purple and a dark precipitate forms. To the reaction mixture a solution of P_4 (150 mg, 1.2 mmol) in 20 mL THF is added dropwise and stirred for 30 min. After removal of the solvent in vacuum, 5 mL toluene is added and the precipitate is filtered off. The solvent is again removed and the residue is dissolved in 5 mL CH_2Cl_2. In a thin Schlenk-tube 5 mL CH_3CN is layered over the solution. After full diffusion the product crystalizes in yellow blocks/cubes. Yield: 283 mg (29%).

Method 2 (Fe^{II}-route): Synthesis of $Cp^R_2P_4$ (1a-d) with $FeBr_2$*dme

A suspension of Cp^RM in 5 mL THF is added to a suspension of $FeBr_2$*dme (153 mg, 0.5 mmol) in 5 mL THF. The mixture turns into yellow. To the reaction mixture a solution of P_4 (31 mg, 0.25 mmol) in 5 mL THF is added dropwise and stirred over night to form a brown reaction mixture. After removal of the solvent in vacuum, 1 mL benzene-d_6 is added and filtered into a NMR-tube.

Cp^RM = Cp'''Na (128 mg, 0.5 mmol), Yield: 14%; Cp*Li (71 mg, 0.5 mmol), Yield: 66% calculated from $^{31}P\{^1H\}$NMR.

Method 3 (Fe^{III}-route): Synthesis of $Cp^R_2P_4$ (1a-d) with $FeBr_3$

A suspension of Cp^RM in toluene is added to a solution of $FeBr_3$ (148 mg, 0.5 mmol) and P_4 (31 mg, 0.25 mmol) in toluene. Upon stirring over night the dark red solution turns brown and a brownish precipitate forms. After removal of the solvent in vacuum, 1 mL benzene-d_6 is added and filtered into a NMR-tube.

Cp^RM = $Cp^{BIG}Na$ (363 mg, 0.5 mmol), Yield: 53%; $Cp'''Na$ (128 mg, 0.5 mmol), Yield: 38%; $Cp*Li$ (71 mg, 0.5 mmol), Yield: 82%; $Cp^{4iPr}Na$ (128 mg, 0.5 mmol), Yield: 62%; Yields have been calculated from $^{31}P\{^1H\}NMR$.

An analytically pure sample of colorless **1b** can be obtained by column chromatography (hexane, silica gel, 50 x 4 cm) and crystallization from concentrated Et_2O solution at room temperature. Yield: 200 mg (14%). Some crystals for X-ray structure analysis of **1d** were grown from neat.

Analytical data for $Cp^{BIG}_2P_4$ (**1a**): [$C_{110}H_{130}P_4$] calc.: C, 83.83; H, 8.31. Found: C, 83.78; H, 8.12. FD-MS (toluene): m/z (%) = 1576.2 (100%, [M]$^+$). ^1H NMR (C_6D_6): δ [ppm] = 0.69 – 0.83 (m, 18H,^{n}Bu), 0.90 (t, $^3J_{HH}$ = 7.7 Hz, 12H, ^{n}Bu), 1.03 – 1.20 (m, 12H, ^{n}Bu), 1.20 – 1.40 (m, 20H, ^{n}Bu), 1.54 (q, $^3J_{HH}$ = 7.5 Hz, 8H, ^{n}Bu), 2.19 – 2.33 (m, 12H, ^{n}Bu), 2.48 (t, $^3J_{HH}$ = 7.7 Hz, 8H, ^{n}Bu), 6.76 (d, $^3J_{HH}$ = 7.7 Hz, 8H, Ph), 6.86 (d, $^3J_{HH}$ = 7.7 Hz, 8H, Ph), 6.93 (d, $^3J_{HH}$ = 7.3 Hz, 4H, Ph), 7.32 – 7.43 (m, 16H, Ph), 7.79 (s-br, ω$_{1/2}$ = 20.5 Hz, 4H, Ph). $^{31}P\{^1H\}$ NMR (C_6D_6): δ [ppm] = - 308.2 (t, $^1J_{PP}$ = 192 Hz, 2P, P-P-Cp^{BIG}), -181.0 (t, $^1J_{PP}$ = 192 Hz, 2P, P-Cp^{BIG}). $^{13}C\{^1H\}$ NMR (C_6D_6): δ [ppm] = 14.0, 14.2, 22.5, 22.7, 22.8, 33.2, 33.4, 33.8, 35.3, 35.5, 35.8, 128.6, 129.6, 131.4, 131.7, 132.7, 134.3, 141.2, 141.2, 141.5, 144.0, 148.2.

Analytical data for Cp'''_2P_4 (**1b**): [$C_{34}H_{58}P_4$] calc.: C, 69.13; H, 9.90. Found: C, 69.19; H, 9.68. ESI-MS (toluene): m/z (%) = 590.4 (5%, [M]$^+$), 533.3 (10%, [M - ^{t}Bu]$^+$), 466.3 (60%, [$Cp'''P_4(C_8H_{13})$]$^+$), 357.1 (20%, [$Cp'''P_4$]$^+$), 301.1 (17%, [M - ^{t}Bu – Cp''']$^+$). ^1H NMR (C_6D_6): δ [ppm] = 1.03 (s, ^{t}Bu), 1.15 – 1.26 (mult. s, ^{t}Bu), 1.35 – 1.45 (mult. s, ^{t}Bu), 1.55 (s, ^{t}Bu), 5.59 (br s, 2H, $C_5H_2(^tBu)_3$ isomer **C/D**), 6.02 (br s, 1.2H, $C_5H_2(^tBu)_3$ isomer **A** and **B**), 6.29 (mult s, 2H, $C_5H_2(^tBu)_3$ isomer **C/D**). $^{13}C\{^1H\}$ NMR (C_6D_6): δ [ppm] = 30.7 – 37.4 (mult. s, -C(CH_3)_3), 32.1 – 37.6 (mult. s, -C(CH_3)_3), 131.3 (d, $^1J_{CP}$ = 20 Hz, C_P), 131.4 (d, $^1J_{CP}$ = 28 Hz, C_P), 136.9 (s), 151.5 (d, $^1J_{CP}$ = 27 Hz, C_P), 154.1 (d, $^1J_{CP}$ = 27 Hz, C_P), 154.2 (s), 160.2 (d, $^1J_{CP}$ = 21 Hz, C_P), 160.8 (s). $^{31}P\{^1H\}$ NMR (C_6D_6) **A** δ [ppm] = -162.4 (t, 2P, $^1J_{AM}$ = $^1J_{AN}$ = $^1J_{A'M}$ = $^1J_{A'N}$ = 181 Hz, $P_AP_{A'}$), -307.3 (dt, 1P, $^1J_{AM}$ = $^1J_{A'M}$ = 181 Hz, $^1J_{MN}$ = 181 Hz, P_M), -366.0 (dt, 1P, $^1J_{AN}$ = $^1J_{A'N}$ = 181 Hz, $^1J_{MN}$ = 181 Hz, P_N).

^{31}P{^{1}H} NMR (C₆D₆) **B** δ [ppm] = -154.9 (t, 2P, $^1J_{AM}$ = 181 Hz, P$_A$), -341.6 (t, 2P, $^1J_{AM}$ = 181 Hz, P$_M$).

^{31}P{^{1}H} NMR (C₆D₆) **C** δ [ppm] = -157.9 (t, 2P, $^1J_{AM}$ = 183 Hz, P$_A$), -334.8 (t, 2P, $^1J_{AM}$ = 183 Hz, P$_M$).

^{31}P{^{1}H} NMR (C₆D₆) **D** δ [ppm] = -154.6 (ddd, 1P, $^1J_{AM}$ = 191 Hz, $^1J_{AN}$ = 175 Hz, $^1J_{AB}$ = 317 Hz, P$_A$), -162.5 (ddd, 1P, $^1J_{BM}$ = 175 Hz, $^1J_{BN}$ = 191 Hz, $^1J_{AB}$ = 317 Hz, P$_B$) , -324.8 (ddd, 1P, $^1J_{AM}$ = 191 Hz, $^1J_{BM}$ = 175 Hz, $^1J_{MN}$ = 173 Hz, P$_M$), -352.1 (ddd, 1P, $^1J_{AN}$ = 175 Hz, $^1J_{BN}$ = 191 Hz, $^1J_{MN}$ = 173 Hz, P$_N$).

Analytical data for Cp*₂P₄ (**1c**): [C₂₀H₃₀P₄] calc.: C, 60.91; H, 7.67. Found: C, 60.95; H, 7.65. FD-MS (toluene): m/z (%) = 394.2 (100%, [M]$^+$). ^{1}H NMR (C₆D₆): δ [ppm] = 1.02 (s, 3H, CH₃), 1.65 (s, 6H, CH₃), 1.89 (s, 6H, CH₃), ^{31}P{^{1}H} NMR (C₆D₆): δ [ppm] = -366.6 (t, $^1J_{PP}$ = 193 Hz, 2P, P̲-P-Cp*), -144.0 (t, $^1J_{PP}$ = 193 Hz, 2P, P̲-Cp*).

Analytical data for Cp^{4iPr}₂P₄ (**1d**): m/z (FD, toluene 590.4 (45%, [M]$^+$) 668.4 (100%, [Cp^{4iPr}₂Fe(Et₂O)O]$^+$) 710.5 (50%, [Cp^{4iPr}₂Fe(Et₂O)(CH₃CN)O]$^+$).

^{31}P{^{1}H} NMR (C₆D₆) **A** δ [ppm] = -134.2 (t, 2P, $^1J_{AM}$ = 180 Hz, P$_A$), -338.2 (t, 2P, $^1J_{AM}$ = 180 Hz, P$_M$).

^{31}P{^{1}H} NMR (C₆D₆) **B** δ [ppm] = -140.8 (t, 2P, ^1J = 179 Hz, P$_A$), -311.5 (*pseudo*-q, 1P, ^1J = 180 Hz, P$_M$), -365.1 (*pseudo*-q, 1P, ^1J = 176 Hz, P$_N$).

Unfortunately, the signals of isomer **B** in the ^{31}P{^{1}H} are not resolved properly to get exact coupling constants. However, a rough merit can be supported.

11.4   References

[1]   a) B. M. Cossairt, N. A. Piro, C. C. Cummins, *Chem. Rev.* **2010**, *110*, 4164-4177. b) M. Caporali, L. Gonsalvi, A. Rossin, M. Peruzzini, *Chem. Rev.* **2010**, *110*, 4178-4235.

[2]   a) M. Scheer, G. Balazs, A. Seitz, *Chem. Rev.* **2010**, *110*, 4236-4256. b) N. A. Giffin, J. D. Masuda, *Coord. Chem. Rev.* **2011**, *255*, 1342-1359. c) S. Khan, S. S. Sen, H. W. Roesky, *Chem. Commun.* **2012**, *48*, 2169-2179.

[3]   D. Tofan, C. C. Cummins, *Angew. Chem., Int. Ed.* **2010**, *49*, 7516-7518.

[4]   M. M. Rauhut, A. M. Semsel, *J. Org. Chem.* **1963**, *28*, 471-473.

[5]   a) O. Back, G. Kuchenbeiser, B. Donnadieu, G. Bertrand, *Angew. Chem., Int. Ed.* **2009**, *48*, 5530-5533. b) J. D. Masuda, W. W. Schoeller, B. Donnadieu, G. Bertrand, *Angew. Chem., Int. Ed.* **2007**, *46*, 7052-7055. c) J. D. Masuda, W. W. Schoeller, B. Donnadieu, G. Bertrand, *J. Am. Chem. Soc.* **2007**, *129*, 14180-14181. d) C. D. Martin, C. M. Weinstein, C. E. Moore, A. L. Rheingold, G. Bertrand, *Chem. Commun.* **2013**, *49*, 4486-4488. e) C. L. Dorsey, B. M. Squires, T. W. Hudnall, *Angew. Chem., Int. Ed.* **2013**, *52*, 4462-4465.

[6]   E. Fluck, R. Riedel, H. D. Hausen, G. Heckmann, *Z. Anorg. Allg. Chem.* **1987**, *551*, 85-94.

[7]   A. R. Fox, R. J. Wright, E. Rivard, P. P. Power, *Angew. Chem., Int. Ed.* **2005**, *44*, 7729-7733.

[8]   B. M. Cossairt, C. C. Cummins, *New J. Chem.* **2010**, *34*, 1533-1536.

[9]   If CyBr is used Cy$_3$P and Cy$_4$P$_2$ are obtained, as products of a complete P$_4$ degradation.

[10]   D. N. Akbayeva, O. J. Scherer, *Z. Anorg. Allg. Chem.* **2001**, *627*, 1429-1430.

[11]   For spectra of {Cp^R}$^•$ see supporting information. a) K. Ziegler, B. Schnell, *Justus Liebigs Ann. Chem.* **1925**, *445*, 266-282. b) W. Broser, P. Siegle, H. Kurreck, *Chem. Ber.* **1968**, *101*, 69-83. c) C. Janiak, R. Weimann, F. Görlitz, *Organometallics* **1997**, *16*, 4933-4936.

[12]   See supporting information for details of NMR spectroscopy and X-ray structural analysis, including the comparison of NMR parameters and atom distances (**1a-d**, **A**, **B**, **C** and **D**)

[13]   H. Sitzmann, R. Boese, *Angew. Chem., Int. Ed.* **1991**, *30*, 971-973.

[14]   a) H. Sitzmann, T. Dezember, W. Kaim, F. Baumann, D. Stalke, J. Kärcher, E. Dormann, H. Winter, C. Wachter, M. Kelemen, *Angew. Chem.* **1996**, *108*, 3013-3016. b) H. Sitzmann, T. Dezember, W. Kaim, F. Baumann, D. Stalke, J. Kärcher, E. Dormann, H. Winter, C. Wachter, M. Kelemen, *Angew. Chem., Int. Ed.* **1996**, *35*, 2872-2875. c) M.

Wallasch, G. Wolmershäuser, H. Sitzmann, *Angew. Chem., Int. Ed.* **2005**, *44*, 2597-2599.

[15]   O. J. Scherer, T. Hilt, G. Wolmershäuser, *Organometallics* **1998**, *17*, 4110-4112.

[16]   a) G. Dyker, J. Heiermann, M. Miura, J.I. Inoh, S. Pivsa-Art, T. Satoh, M. Nomura, *Chem. Eur. J.* **2000**,   *6*, 3426-3433. b) S. Harder, C. Ruspic, *J. Organomet. Chem.* **2009**, *694*, 1180-1184. c) R. Zhang, M. Tsutsui, D. E. Bergbreiter, *J.Organomet. Chem.* **1982**, *229*, 109-112.

[17]   S. Deng, Diploma thesis, University of Karlsruhe (Karlsruhe, Germany), **2002**.

11.5   Supplementary Information

NMR Investigations:

Table S11.1. Comparison of ^{31}P{^{1}H} NMR spectra in C$_6$D$_6$ of **1a-d**, **A**, **B** and **C**. If different isomers are present, the spinsystems are discussed separately.

Compound	R in R$_2$P$_4$	Spinsystem	δ [ppm] (multiplicity)	coupling constant
1a	Cp^{BIG}	A$_2$M$_2$	-181.0 (t) -308.2 (t)	$^1J_{AM}$ = 192 Hz
1b-A	Cp′″	A$_2$MN	-163.4 (t) -307.3 (dt) -364.0 (dt)	$^1J_{AM} = {}^1J_{AN} = {}^1J_{MN}$ = 181 Hz
1b-B	Cp′″	A$_2$M$_2$	-154.9 (t) -341.6 (t)	$^1J_{AM}$ = 181 Hz
1b-C	Cp′″	A$_2$M$_2$	-157.9 (t) -334.8 (t)	$^1J_{AM}$ = 182 Hz
1b-D	Cp′″	ABMN	-154.4 (ddd) -162.5 (ddd) -324.8 (dt) -352.1 (dt)	$^1J_{AM} = {}^1J_{BN}$ = 190 Hz $^1J_{AN} = {}^1J_{BM}$ = 175 Hz $^1J_{MN}$ = 173 Hz $^2J_{AB}$ = 317 Hz
1c	Cp*	A$_2$MN	-144.0 (t) -366.6 (t)	$^1J_{AM}$ = 193 Hz
1d-A	Cp^{4iPr}	A$_2$M$_2$	-134.2 (t) -338.2 (t)	$^1J_{AM}$ = 180 Hz
1d-B	Cp^{4iPr}	A$_2$MN	-140.8 (t) -311.5 (*pseudo*-q) -365.1 (*pseudo*-q)	^1J(P$_A$) = 179 Hz ^1J(P$_M$) = 180 Hz ^1J(P$_N$) = 176 Hz
A[1]	sMes	A$_2$M$_2$	-130 (t) -272 (t)	$^1J_{AM}$ = 176 Hz
B[2]	Ar^{Dipp}	A$_2$M$_2$	-163.0 (t) -331.8 (t)	$^1J_{AM}$ = 189 Hz
C[3]	Dmp	ABM$_2$	-104 (*pseudo*-q) -123 (*pseudo*-q) -318 (t)	^1J(P$_A$) = 193 Hz ^1J(P$_B$) = 191 Hz ^1J(P$_M$) = 190 Hz
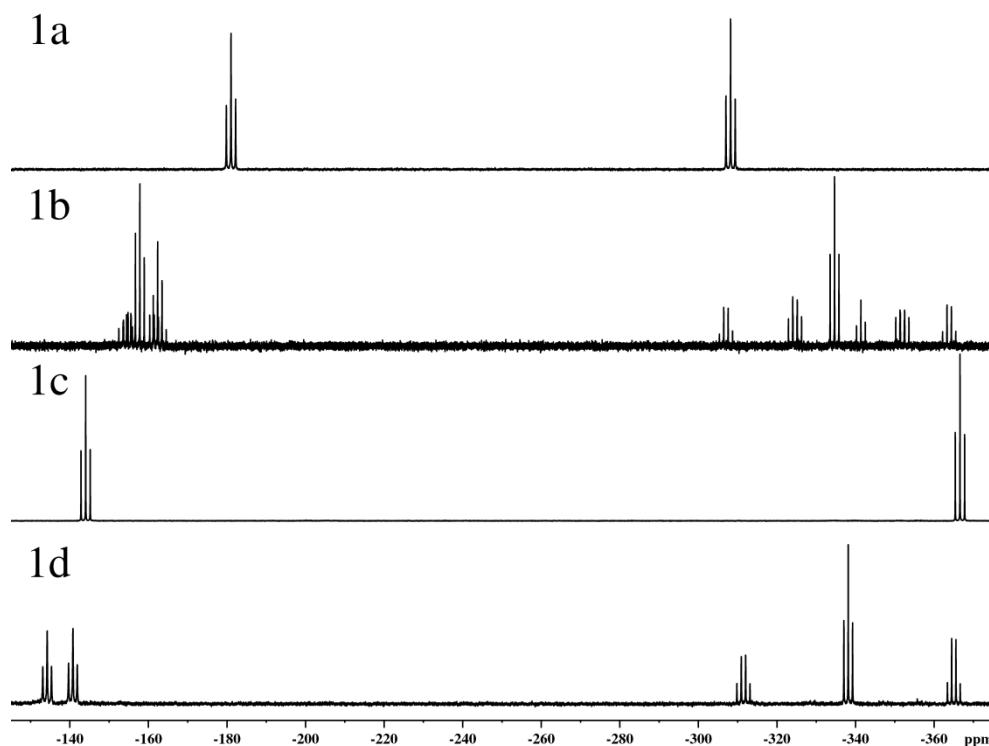
Figure S 11.1. $^{31}P\{^1H\}$ NMR spectra of **1a-d** in C_6D_6 at 298 K.

Crystallographic Details:

The crystal structure analyses were performed either on an Oxford Diffraction Gemini R Ultra CCD diffractometer (**1c**) or an Oxford Diffraction SuperNova diffractometer (**1a, 1b, 1d**). For all compounds an analytical absorption correction was carried out.[4] The structures were solved by direct methods either of the program SIR-92[5] or SUPERFLIP[6] and refined with the least square method on F^2 employing SHELXL-97[7] with anisotropic displacements for non-H atoms. Hydrogen atoms were located in idealized positions and refined isotropically according to the riding model.

Several tested crystals of **1d** were non-merohedrally twinned. For the refinement only the major component's reflections (blue in Figure S11.2) were used since the second component was much weaker. Hence, HKLF5 refinement results in a much worse model. Therefore the completeness is only 47.8%.

CCDC-990723 (**1a**), CCDC-990724 (**1b**), CCDC-990725 (**1c**) and CCDC-990919 (**1d**) contain the supplementary crystallographic data for this paper. These data can be obtained free of charge at www.ccdc.cam.ac.uk/conts/retrieving.html (or from the Cambridge Crystallographic Data Centre, 12 Union Road, Cambridge CB2 1EZ, UK; Fax: + 44-1223-336-033; e-mail: deposit@ccdc.cam.ac.uk).
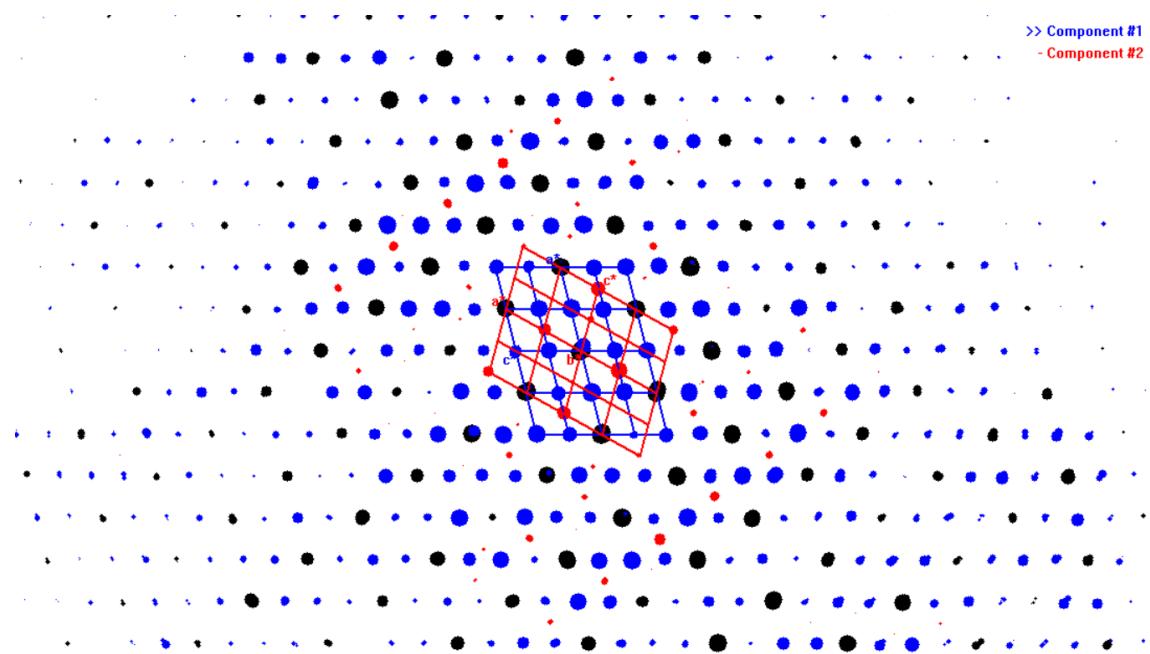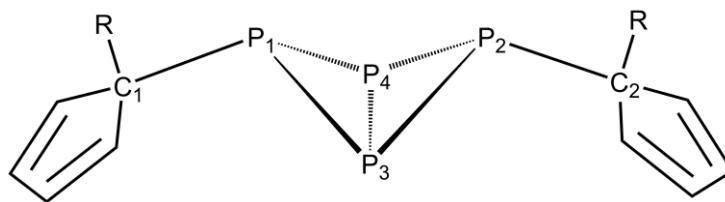
Figure S11.2. Reciprocal space view along the b* axis of compound **1d**. Reflections of component 1 in blue, component 2 in red and overlapping reflections in black.

Crystal data for $Cp^{BIG}_2P_4$ (**1a**): $C_{110}H_{130}P_4$, M = 1576.03 g/mol, space group $P\bar{1}$ (no.2), a = 20.1889(1) Å, b = 26,8192(2) Å, c = 27.8798(1) Å, α = 103.770(1)°, β = 94.363(1)°, γ = 106.814(1)°, V = 13863.3(2) Å^3, Z = 6, μ = 1.103 mm^{-1}, $F(000)$ = 5100, T = 105 K, 140650 reflections measured, 53336 unique (R_{int} = 0.0167), R_1 = 0.0654, wR_2 = 0.1726 for I > 2σ(I). CCDC-990723
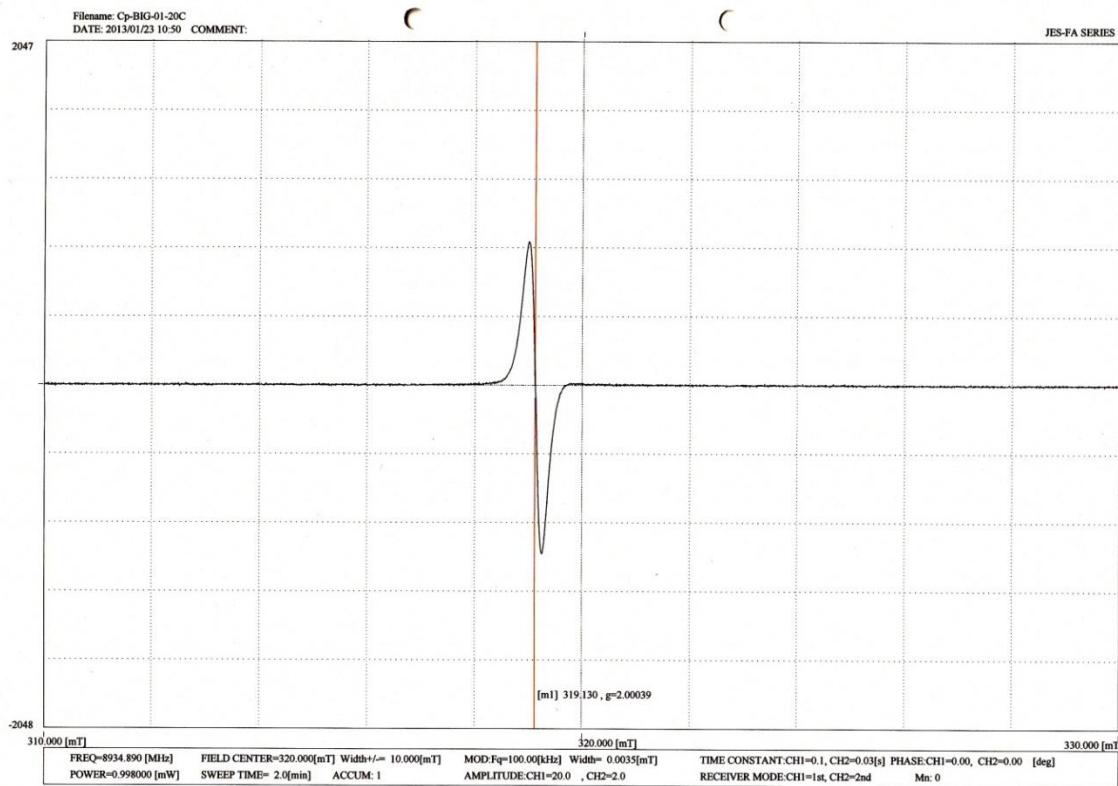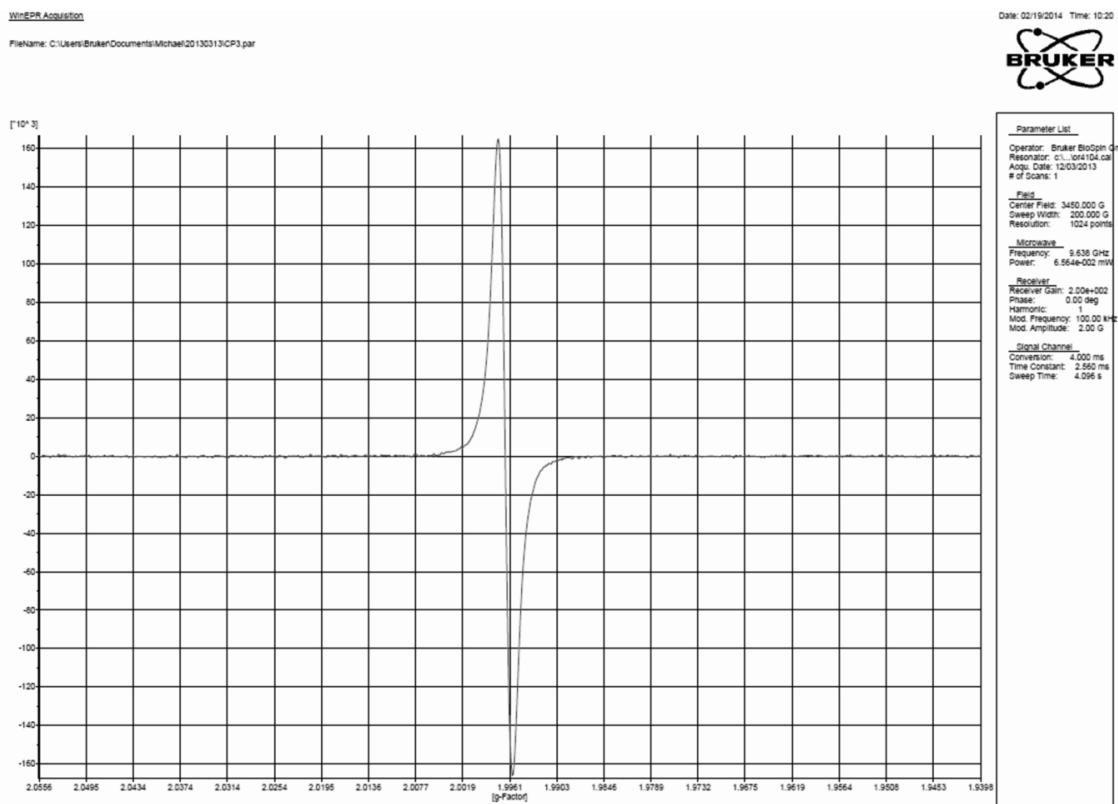
Crystal data for Cp'''_2P_4 (**1b**): $C_{34}H_{58}P_4$, M = 590.68 g/mol, space group Cc (no.9), a = 36.6533(3) Å, b = 10.3079(1) Å, c = 28.2745(2) Å, β = 96.283(1)°, V = 10618.5(2) Å^3, Z = 12, μ = 2.104 mm^{-1}, $F(000)$ = 3864, T = 123 K, 55596 reflections measured, 14553 unique (R_{int} = 0.0362), R_1 = 0.0505, wR_2 = 0.1087 for I > 2σ(I). CCDC-990724

Crystal data for $Cp^*_2P_4$ (**1c**): $C_{20}H_{30}P_4$, M = 394.32 g/mol, space group $P2_1/c$ (no.14), a = 14.4915(1) Å, b = 15.1964(1) Å, c = 9.7826(1) Å, β = 98.086(1)°, V = 2132.89(3) Å^3, Z = 4, μ = 3.251 mm^{-1}, $F(000)$ = 840, T = 123 K, 25054 reflections measured, 3758 unique (R_{int} = 0.0280), R_1 = 0.0282, wR_2 = 0.0721 for I > 2σ(I). CCDC-990725

Crystal data for $Cp^{4iPr}_2P_4$ (**1d**): $C_{34}H_{58}P_4$, M = 590.68 g/mol, space group $P\bar{1}$ (no.2), a = 13.3711(2) Å, b = 17.3342(3) Å, c = 17.7020(2) Å, α = 99.676(1)°, β = 103.804(1)°, γ = 108.923(1)°, V = 3632.1(1) Å^3, Z = 4, μ = 2.050 mm^{-1}, $F(000)$ = 1288, T = 123 K, 21561 reflections measured, 7013 unique (R_{int} = 0.0429), R_1 = 0.0501, wR_2 = 0.0963 for I > 2σ(I). CCDC-990919

Table S11.2. Comparison of P–P atom distances of compounds **1a-d**, **A** and **B** in Å. If the asymmetric unit consists of more than one molecule Cp$^R_2$P$_4$, a range for d$_{P-P}$ is given.

Compound	R in R$_2$P$_4$	P$_1$···P$_2$	P$_{1/2}$-P$_{3/4}$	P$_3$-P$_4$	P$_{1/2}$-C$_{1/2}$
1a	Cp^{BIG}	2.8207(8) — 2.8523(8)	2.1998(8) — 2.2279(8)	2.1814(8) — 2.1871(8)	1.935(2) — 1.954(2)
1b	Cp'''	2.787(4) — 2.836(4)	2.182(5) — 2.237(5)	2.155(3) — 2.172(5)	1.915(7) — 2.099(8)
1c	Cp*	2.8891(4)	2.2131(4) — 2.2237(4)	2.1924(4)	1.907(2) and 1.918(2)
1d	Cp^{4iPr}	2.774(3) — 2.7891(8)	2.206(5) — 2.244(7)	2.178(6) — 2.194(8)	1.884(4) — 1.911(8)
A[1]	sMes	2.88	2.222(3) — 2.236(9)	2.166(2)	1.885(<1) and 1.892(8)
cis-cis **B**[2]	Dmp	2.77	2.201(1) — 2.207(1)	2.203(2)	1.866(3) and 1.887(3)
cis-trans **B**[2]	Dmp	3.11	2.205(2) — 2.243(2)	2.219(2)	1.821(6) and 1.874(6)
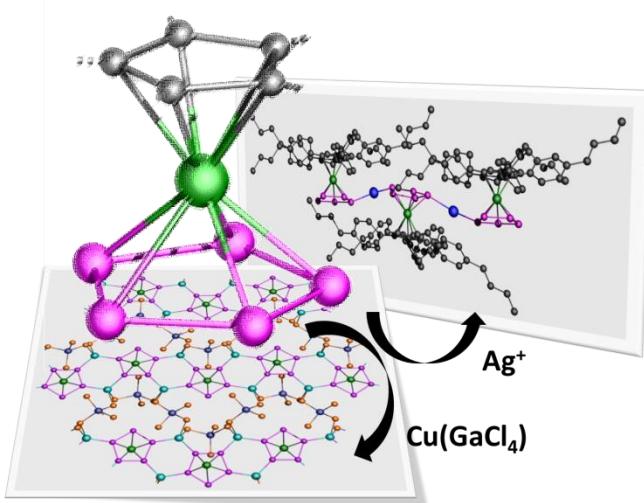
EPR Investigations:

Figure S11.3. EPR spectrum of {Cp^{BIG}}$^{\bullet}$ in THF at 20 °C.

Figure S11.4. EPR spectrum of {Cp$'''$}$^{\bullet}$ in THF at 20 °C.

References for Supplementary Information

[1]   E. Fluck, R. Riedel, H. D. Hausen, G. Heckmann, *Z. Anorg. Allg. Chem.* **1987**, *551*, 85-94.

[2]   A. R. Fox, R. J. Wright, E. Rivard, P. P. Power, *Angew. Chem. Int. Ed.* **2005**, *44*, 7729-7733.

[3]   B. M. Cossairt, C. C. Cummins, *New J. Chem.* **2010**, *34*, 1533-1536.

[4]   R. C. Clark, J. S. Reid, *Acta Cryst.* **1995**, A51, 887-897.

[5]   A. Altomare, M. C. Burla, M. Camalli, G. L. Cascarano, C. Giacovazzo, A. Guagliardi, A. G. G. Moliterni, G. Polidori, R. Spagna, *J. Appl. Cryst.* **1999**, 32, 115-119.

[6]   L. Palatinus, G. Chapuis, *J. Appl. Cryst.* **2007**, 40, 786-790.

[7]   G. M. Sheldrick, *Acta Cryst.* **2008**, A64, 112-122.

12. Novel Polymeric Aggregates of Pentaphosphaferrocenes and Monocationic Coinage Metal Salts – Synthesis of [{Cp^{BIG}Fe(η^5-P$_5$)}Ag]$_n$[Al(OC(CF$_3$)$_3$)$_4$]$_n$ and [{Cp*Fe(η^5-P$_5$)}{Cu(GaCl$_4$)}$_2$]$_n$

Claudia Heindl, Sebastian Heinl, David Lüdeker, Gunther Brunklaus, Werner Kremer and Manfred Scheer

❖ **All syntheses and characterizations of compound 2 were performed by Claudia Heindl and of compound 3 by Sebastian Heinl, unless subsequently noted otherwise**

❖ **Introduction, discussion of compound 2 and conclusion was written by Claudia Heindl**

❖ **Discussion of compound 3 was written by Sebastian Heinl**

❖ **Figures of crystal structures, graphical abstract and ChemDraw were made by Claudia Heindl, NMR picture of 3 by Sebastian Heinl**

❖ **MAS NMR of 2 were performed by David Lüdeker and Gunther Brunklaus**

❖ **MAS NMR of 3 were measured and interpreted by Werner Kremer**

❖ **X-ray structure analysis and refinement of compound 3 was performed by Sebastian Heinl and of compound 2 by Claudia Heindl**

Novel Polymeric Aggregates of Pentaphosphaferrocenes and Monocationic Coinage Metal Salts
— Synthesis of [{Cp^{BIG}Fe(η^5-P$_5$)}Ag]$_n$[Al(OC(CF$_3$)$_3$)$_4$]$_n$ and [{Cp*Fe(η^5-P$_5$)}{Cu(GaCl$_4$)}$_2$]$_n$

205

12.1 Introduction

The isolobal analogy between phosphorus atoms and methine groups opened up an interesting class of organometallic compounds: the phosphaferrocenes. The most exciting representative is probably pentaphosphaferrocene [Cp*Fe(η^5-P$_5$)] (Cp* = C$_5$Me$_5$) (**1a**) exhibiting a *cyclo*-P$_5$-ring.[1] In contrast to ferrocenes [Cp$^R_2$Fe], the lone pairs of the P atoms in **1a** turns them into excellent building blocks for coordination and supramolecular chemistry. This field was so far dominated by N- and O-donor ligands as bridging units between metal centres.[2] However, our group showed, that bare phosphorus ligands are in no way inferior.[3] Especially in combination with monocationic coinage metal salts, the versatile coordination behaviour of **1a** is demonstrated.[4] The products of its self-assembly processes with CuX (X = Cl, Br, I) range from 1D and 2D polymers[4c,h,j] to spherical supramolecules with fullerene-like topology.[4a,b,d-g,i]

Changing from CuX, containing a coordinated halogen ligand, to Ag[Al{OC(CF$_3$)$_3$}$_4$], bearing a weakly coordinating anion, a novel coordination motif and dynamic behaviour in solution of the resulting polymers were obtained.[4h] These findings demonstrate the influence of the used counter anion. Hence we were interested in the coordination chemistry of **1a** towards Cu(GaCl$_4$), whose tetrachlorogallate anion can form both: ion-contacted[5] as well as ion-separated[6] complexes.

Although the self-assembly process of the pentaphosphaferrocene proved to be versatile and very sensitive to all supposable parameters, the study of the steric influence of the Cp^R ring was neglected so far. Thus, we introduced the sterically much more demanding Cp^{BIG} (Cp^{BIG} = C$_5$(4-^{n}BuC$_6$H$_4$)) ligand and examined the coordination behaviour of [Cp^{BIG}Fe(η^5-P$_5$)][7] (**1b**) towards Ag[Al{OC(CF$_3$)$_3$}$_4$].

Herein we report on the synthesis of two new polymeric coordination compounds with monocationic coinage metal salts: [{Cp*Fe(η^5-P$_5$)}{Cu(GaCl$_4$)}$_2$]$_n$ (**2**) and [{Cp^{BIG}Fe(η^5-P$_5$)}Ag]$_n$[Al{OC(CF$_3$)$_3$}$_4$]$_n$ (**3**).

12.2 Results and Discussion

Upon diffusion of a toluene solution of **1a** into a CH$_2$Cl$_2$ solution of Cu[GaCl$_4$] the formation of the two-dimensional coordination network [{Cp*Fe(η^5-P$_5$)}{Cu(GaCl$_4$)}$_2$]$_n$ (**2**) can be obtained in quantitative yield (Figure 12.1).

The repeating unit of **2** contains **1a** and Cu(GaCl$_4$) in a 1:2 molar ratio, in which the tetrachlorogallate anion is part of the polymeric framework and coordinates to Cu, resulting in a neutral coordination compound.
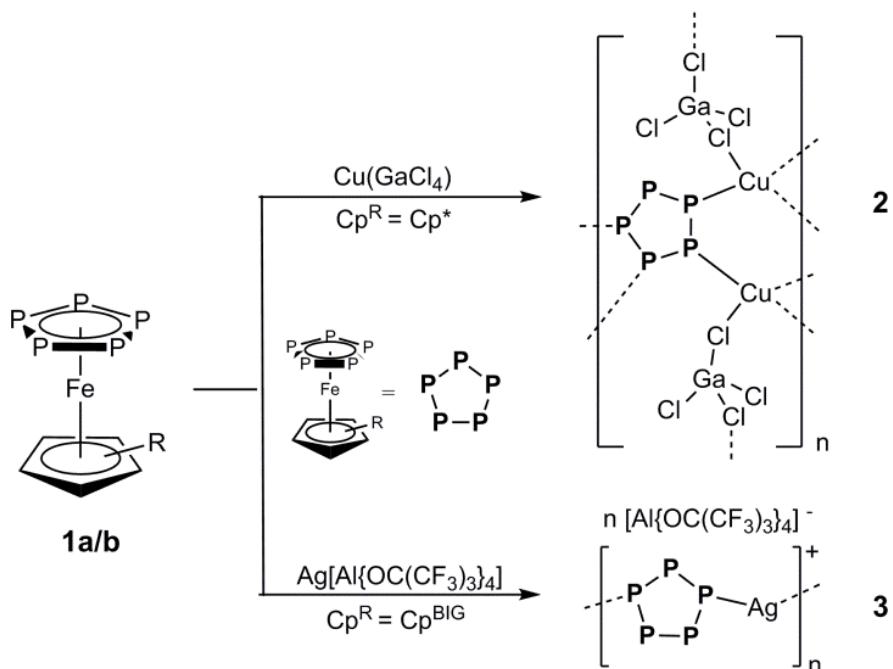
Figure 12.1. Reaction of $[Cp^RFe(\eta^5-P_5)]$ (**1a**: $Cp^R = Cp^*$; **1b**: $Cp^R = Cp^{BIG}$) with $Cu(GaCl_4)$ and $Ag[Al\{OC(CF_3)_3\}_4]$, respectively. The polymeric compounds are described by their repeating units.

The structure of **2** was elucidated by X-Ray structure analysis (Figure 12.2). It reveals an unusual 1,2,3,4 coordination mode of each P_5 ring, which was only observed once in a CuI-containing polymer.[4c] The Cu^I cations show a distorted tetrahedral environment with angles ranging from 87.72(3)° to 116.94(3)°, which is typical for copper in the oxidation state +1.[8] They are coordinated by two P atoms and two Cl atoms from $GaCl_4$ and form six-membered Cu_2P_4 rings between the *cyclo*-P_5 units. In contrast, the Cl atoms occur in two coordination modes: half of them are only coordinated to Ga and therefore terminal, the other two bridge Ga and Cu yielding seven-membered $P_2Cu_2Cl_2Ga$ rings, where the Cl-Ga distances for μ_2-Cl atoms (2.39 Å) are longer than the corresponding ones for terminal halides (2.14 Å).

The network can be described as a 2D sheet structure, whose single layers are limited by the terminal Cl and the Cp* ligands from **1a**. They in turn are orientated alternating upwards and downwards the layer (Figure 12.3).The shortest gap between the layers is the distance between terminal Cl ligands and H atoms from the Cp* units. It constitutes 2.780(1) Å and therefore goes below the sum of the van-der-Waals-radii of Cl and H (2.95 Å),[9] indicating the presence of hydrogen bonds.

Most likely due to formation of the 2D network, compound **2** is rather insoluble in common solvents though slight solubility in CH_3CN accompanied by fragmentation was observed. Hence, the corresponding $^{31}P\{^1H\}$ and ^1H NMR spectra of **2** in CD_3CN merely exhibit one sharp singlet at 143.4 ppm and 1.45 ppm, respectively, reflecting **1a** in a loose coordination

Novel Polymeric Aggregates of Pentaphosphaferrocenes and Monocationic Coinage Metal Salts
– Synthesis of [{Cp^{BIG}Fe(η^5-P$_5$)}Ag]$_n$[Al(OC(CF$_3$)$_3$)$_4$]$_n$ and [{Cp*Fe(η^5-P$_5$)}{Cu(GaCl$_4$)}$_2$]$_n$

207
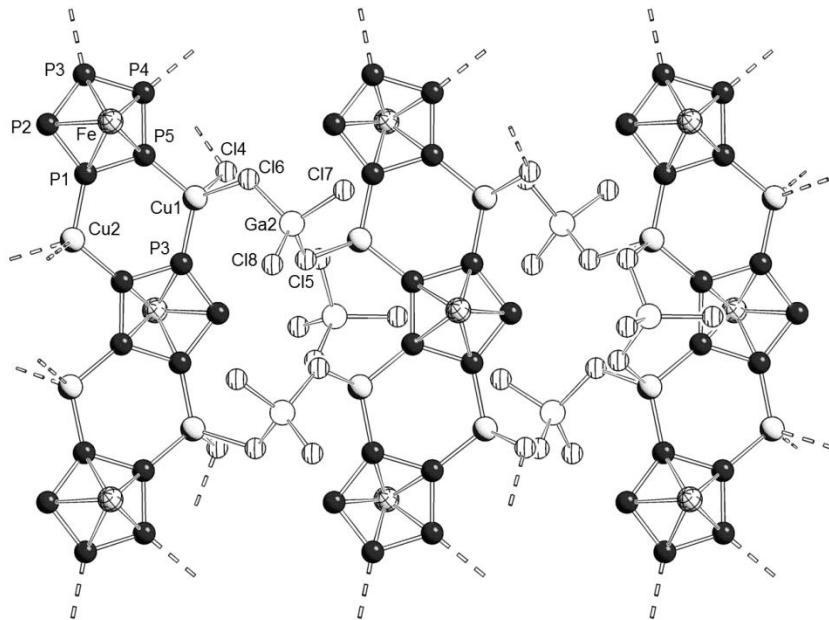
Figure 12.2. Section of the polymer network of [{Cp*Fe(η^5-P$_5$)}{Cu(GaCl$_4$)}$_2$]$_n$ (**2**) in the crystal. For clarity reasons the C and H atoms are omitted. In case of disorder only the main part is shown. Selected bond lengths [Å] and angles [°]: P1-P2 2.1145(11), P2-P3 2.1120(11), P3-P4 2.0996(11), P4-P5 2.1028(11), P1-P5 2.1019(11), P1-Cu2 2.2611(9), P5-Cu1 2.2777(9), Cu1-Cl4 2.4055(9), Cu1-Cl6 2.3687(9), Ga2-Cl5 2.2049(10), Ga2-Cl6 2.2149(9), Ga2-Cl7 2.118(4), Ga2-Cl8 2.1494(10), P1-P2-P3 104.14(4), P2-P3-P4 110.64(5), P3-P4-P5 107.21(5), P1-P5-P4 106.86(5), P2-P1-P5 110.743(5), P4-P5-Cu1 128.55(4), P1-P5-Cu1 123.89(4), P5-P1-Cu2 117.98(4), P5-Cu1-Cl4 110.35(3), P3-Cu1-Cl4 110.82(3), P5-Cu1-P3 116.94(3), Cl6-Cu1-Cl4 87.72(3), Cl6-Cu1-P3 115.51(3), Cl6-Cu1-P5 111.75(3), Ga2-Cl6-Cu1 119.06(4), Cl8-Ga2-Cl5 105.58(4), Cl5-Ga2-Cl7 117.5(1), Cl7-Ga2-Cl6 106.2(1), Cl7-Ga2-Cl8 113.8(1), Cl6-Ga2-Cl8 109.31(4), Cl6-Ga2-Cl5 103.92(3).

environment. The positive ion ESI mass spectrum of **2** also displays signals corresponding to small complex fragments up to the cation [(Cp*FeP$_5$)$_2$Cu$_3$Cl$_2$]$^+$ while the single peak in the negative ion ESI mass spectrum corresponds to (GaCl$_4$)$^-$.

In addition, compound **2** was further examined by multinuclear solid state NMR spectroscopy. The major peak at 1.98 ppm in its ^{1}H magic-angle spinning (MAS) NMR spectrum represents the methyl groups of Cp* units that are partially involved in hydrogen-bonding to Cl ligands while a peak at 7.18 ppm (area 4.5%) can be attributed to residual
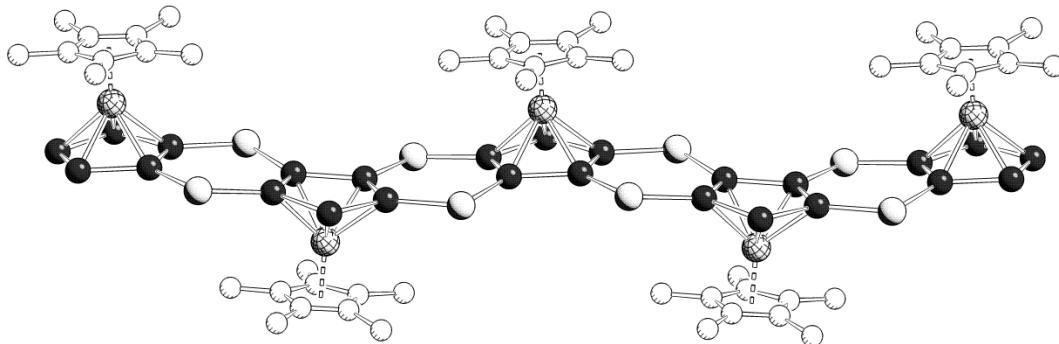
Figure 12.3. Section of **2** illustrating the alternating orientation of the Cp* ligands. For clarity reasons the Ga, Cl and H atoms are omitted.
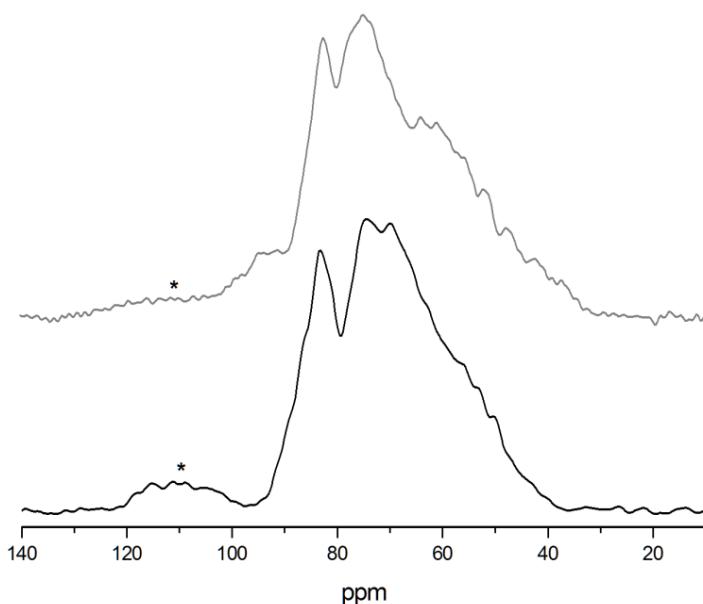
Figure 12.4. ^{31}P{^{1}H} MAS NMR spectra of **2** at 298 K at 7.0 T (top) and 11.7 T (bottom), each acquired at 30 kHz MAS. The presence of rather strong ^{31}P-^{63,65}Cu interactions is revealed by a spread of intensities and signal broadening at the lower magnetic field. The signal marked with an asterisk arises from an impurity.

toluene from the solvent diffusion reaction. Note that the ^{13}C{^{1}H} cross-polarization MAS NMR spectrum of **2** shows two main resonances at 15.3 ppm (methyl groups) and 100.2 ppm (Cp* ring) irrespective of the alternating arrangement, as expected in the likely presence of molecular (rotational) dynamics, though the two minor peaks at 11.2 ppm and 12.9 ppm, respectively, could be either indicative of hydrogen-bonding or of impurities. In contrast, the ^{31}P{^{1}H} MAS NMR spectra of **2** recorded at two different magnetic fields (7.0 T & 11.7 T) are rather crowded reflecting the presence of line-broadening effects such as residual dipolar couplings[10] due to significant ^{63,65}Cu and ^{35,37}Cl quadrupolar interactions imposed by a distorted tetrahedral coordination of both the Cu^I cations and tetra-chlorogallate anions (Figure 12.4). Unlike a more favorable case[11], the expected multiplet fine structure from either ^{31}P-^{31}P and/or ^{31}P-^{63,65}Cu indirect spin-spin couplings is obscured and compared to the 1D polymer of [CuCl{Cp*Fe(η^5:η^1:η^1-P$_5$)}]$_\infty$, all peaks are shifted to lower ppm values, rendering peak assignment difficult. Nevertheless, it appears reasonable to attribute the signal at 83 ppm to the crystallographic P2 site that solely is not coordinated to Cu^I cations (reminiscent of [CuBr{Cp*Fe(η^5:η^1:η^1-P$_5$)}]$_\infty$). The rather similar sites P1 and P5 are tentatively assigned to the signal centered at about 70 ppm while P3 and P4 are estimated at less than 60 ppm, which is in agreement with a preliminary DFT ^{31}P chemical shift computation of the *cyclo*-P$_5$ ring moiety.
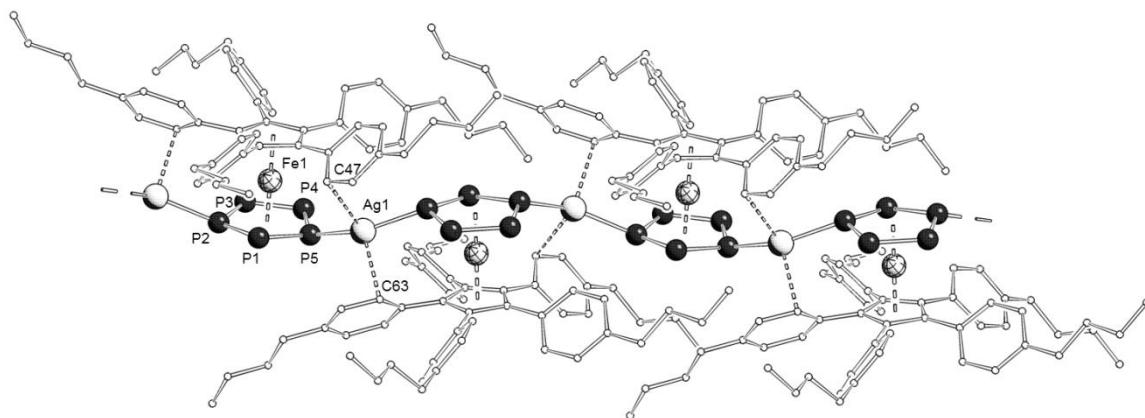
Figure 12.5. Section of the polymer chain [{(Cp^{BIG}Fe(η^5-P$_5$)}Ag]$_n^{n+}$ in **3** in the crystal. For clarity reasons the C atoms are shown in 'wire-or-stick' model and H atoms and [Al{OC(CF$_3$)$_3$}$_4$] counter anions are omitted. Selected bond lengths [Å] and angles [°]: P1-P2 2.101(3), P2-P3 2.117(3), P3-P4 2.101(3), P4-P5 2.102(3), P1-P5 2.107(3), Ag1-P2 2.443(2), Ag1-P5 2.454(2), Ag1-C47 2.618(8), Ag1-C63 2.730(9), Ag1-P$_{5,plane}$ 0.8032(6), P1-P2-P3 111.6(1), P2-P3-P4 105.9(1), P3-P4-P5 107.0(1), P1-P5-P4 111.4(1), P2-P1-P5 103.1(1), P2-Ag1-P5 149.78(7), P2-Ag1-C47 108.8(2), P2-Ag1-C63 93.6(2), P5-Ag1-C47 91.3(2), P5-Ag1-C63 95.4(2), C47-Ag1-C63 120.1(3), Ag1-P2-P1 111.0(1), Ag1-P2-P3 129.0(1), Ag1-P5-P1 125.0(1), Ag1-P5-P4 115.5(1), Ag1-P5-P$_{5-plane}$ 20.72(6).

The diffusion of [Cp^{BIG}Fe(η^5-P$_5$)] (**1b**) solutions (hexane/CH$_2$Cl$_2$) into CH$_2$Cl$_2$ solutions of [{Ag(CH$_2$Cl$_2$)}Al{OC(CF$_3$)$_3$}$_4$] results in the formation and crystallization of the one-dimensional polymer [{Cp^{BIG}Fe(η^5-P$_5$)}Ag]$_n$[Al{OC(CF$_3$)$_3$}$_4$]$_n$ (**3**). Notably, the repeating unit can be described as 1:1 adduct of the two starting materials, but with CH$_2$Cl$_2$ elimination from the silver salt (Figure 12.5). The less sterically demanding pentaphosphaferrocene moiety **1a** forms a 1D polymer [{Cp*Fe(η^5-P$_5$)}$_2$Ag]$_n$[Al{OC(CF$_3$)$_3$}$_4$]$_n$ (**4**) containing a 2:1 ratio of **1a** and Ag$^+$.[4h] A similar arrangement of four molecules **1b** around silver cations is prevented by the bulkiness of the Cp^{BIG} ligand.

The bright green needle shaped crystals were analyzed by X-ray diffraction. The Ag^I cations are coordinated by two molecules **1b** and in return each cyclo-P$_5$ ligand coordinates in a 1,3-coordination mode to two Ag ions. Each Ag$^+$ is additionally coordinated by two ortho-C atoms from the phenyl groups from the Cp^{BIG} ligands with Ag–C distances of 2.618(8) Å and 2.730(9) Å. Compared to already known compounds with Ag-π interactions with phenyl groups the contacts in **3** are in the upper region of distance.[12] The coordination of two P and two C atoms results in heavily distorted tetrahedral environment for the Ag atoms. The angles on the Ag centers range from 91.3(2)° to 149.78(7)°, illustrating the distortion from an ideal tetrahedron (109.5°). Alternatively it can be seen as linear complex where the Ag$^+$ is deflected from linearity due to Ag-π interactions. The Ag atom is moved out of the P$_{5-plane}$ by 0.8032(6) Å (Ag1-P5-P$_{5-plane}$ 20.72(6)°) while the counterions are located in the dimples formed by the Cp^{BIG} ligands on the opposite site to the iron atoms.
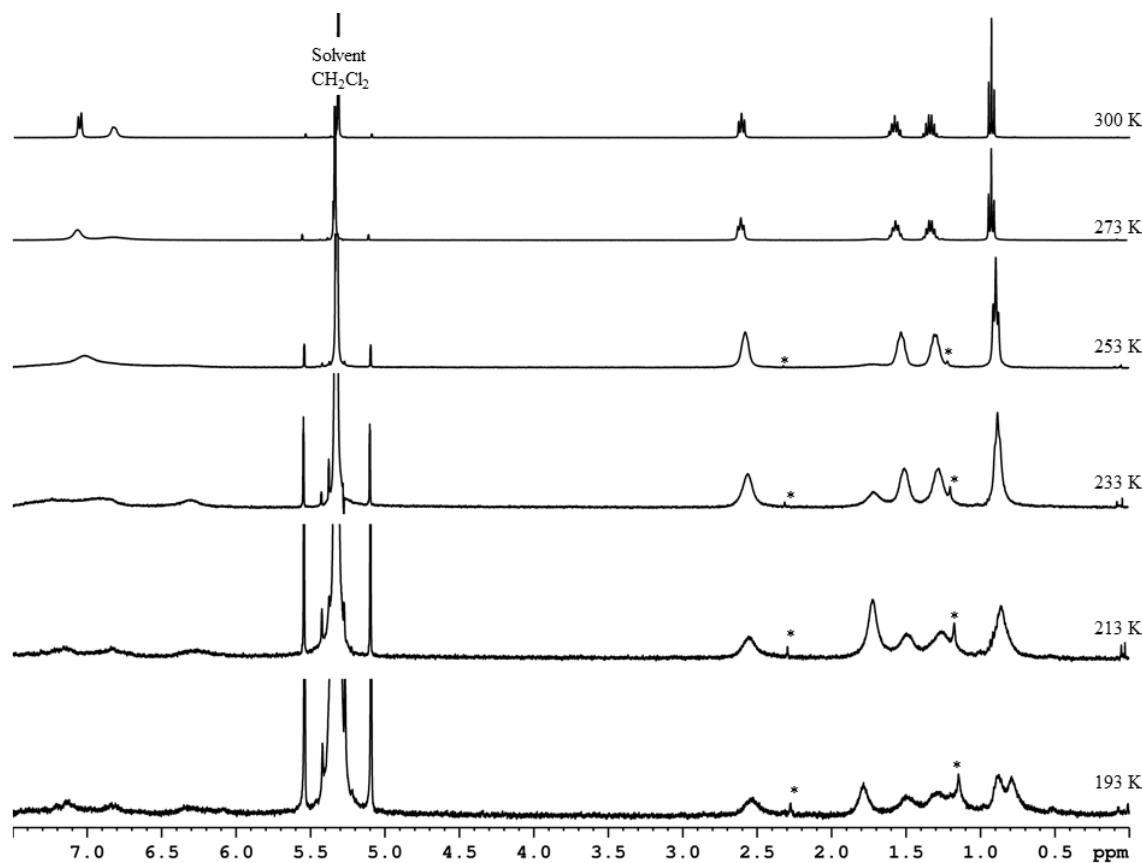
Figure 12.6. ^{1}H NMR spectra of **3** in CH$_2$Cl$_2$ at various temperatures. Intensities drop down at lower T why a higher magnification is used. Signal marked with an asterisk arise from small impurities.

Compound **3** is good soluble in CH$_2$Cl$_2$ and THF but insoluble in hexane. The ^{31}P{^{1}H} NMR spectrum of **3** in CH$_2$Cl$_2$ shows only one very broad signal at 135 ppm ($\omega_{1/2} \approx$ 4000 Hz). NMR investigations at various temperatures were carried out. Cooling the sample leads to an additional broadening of the signal and at 253 K even no signal can be detected. Further cooling does not lead to observable changes. A highly fluxional behavior in solution is also described for **4**.[4h] However, the dynamic processes of **3** are much slower, which is the reason, that at r.t. no sharp singlet is observed like in case of **4**. This can be explained by the coordination of one P and one C atom to Ag$^+$, which effectively results in a chelate-like ligand.

The ^{1}H NMR spectrum of **3** at r.t. shows one set of signals for a Cp^{BIG} ligand (Figure 12.6). Four sharp signals with the appropriate multiplicity in the aliphatic region for the *n*Bu groups are found (δ [ppm] = 0.93, 1.34, 1.58, 2.61). Two further signals are observed in the aromatic region for the phenyl groups, one broaden singlet at 6.83 ppm and one doublet at 7.06 ppm ($^3J_{HH}$ = 8.4 Hz). The observation of only one distinct set of signals is an indication for the fragmentation of the polymeric chain in solution as well as for an almost free rotation of the Cp^{BIG} ligand. The broadened signal at 6.83 ppm most likely reflects interactions between the Ag$^+$ ions and the π-systems of the phenyl groups, thus indicating that **1b** remains coordinated

Novel Polymeric Aggregates of Pentaphosphaferrocenes and Monocationic Coinage Metal Salts
– Synthesis of [{Cp^{BIG}Fe(η^5-P$_5$)}Ag]$_n$[Al(OC(CF$_3$)$_3$)$_4$]$_n$ and [{Cp*Fe(η^5-P$_5$)}{Cu(GaCl$_4$)}$_2$]$_n$

211

to silver even in solution. This is indeed evident from the ESI mass spectrum (CH$_2$Cl$_2$/CH$_3$CN) with the three major peaks attributed to either [(Cp^{BIG}FeP$_5$)$_2$Ag]$^+$, [(Cp^{BIG}FeP$_5$)Ag(CH$_3$CN)]$^+$or [(Cp^{BIG}FeP$_5$)Ag]$^+$. As anticipated, all signals in the ^{1}H NMR spectra get broader upon cooling, combined with an intensity decrease. At 253 K the signal at 6.83 ppm is not observed anymore and two new signals at 1.71 ppm and 6.30 ppm arise. When reaching 233 K, the signal at 7.06 ppm splits into two signals at 6.9 ppm and 7.2 ppm, respectively, while even the signal of the methyl groups at 0.93 ppm splits into two at 193 K. The relative integral ratio of the signal at 1.71 ppm and 2.61 ppm changes in favor of the signal at 1.71 ppm (at 193K 1.15:1). These observations suggest a rather hindered Cp^{BIG} rotation at low temperatures, even though pronounced aggregation/polymerization or intensity losses due to precipitation could also occur. Hence, the effective concentration of **3** in solution is lowered.

The ^{31}P{^{1}H} MAS NMR spectrum of **3** shows four multiplets at 73.4 ppm, 98.8 ppm, 129.3 ppm and 157.6 ppm, respectively, in a 1:1:2:1 integral ratio, reflecting the *cyclo*-P$_5$ moiety. Though an absolute assignment of the signals is not possible at this stage, it appears reasonable to attribute the two Ag$^+$ coordinated sites P2 and P5 to the peak at 129.3 ppm.

In summary, we presented the synthesis and characterization of two novel polymeric coordination compounds with mono-cationic coinage metal salts: [{Cp*Fe(η^5-P$_5$)}{Cu(GaCl$_4$)}$_2$]$_n$ (**2**) and [{Cp^{BIG}Fe(η^5-P$_5$)}Ag]$_n$[Al{OC(CF$_3$)$_3$}$_4$]$_n$ (**3**), where the 1,2,3,4- and 1,3- coordination modes of both P$_5$ ligands is rather uncommon. In combination with pentaphosphaferrocene **1a** the versatile counterion (GaCl$_4$)$^-$ prefers coordination to Cu and a 2D network with sheet-like structure is formed. Using the sterically much more demanding Cp^{BIG} structure motifs, which were realized with Cp*, cannot be formed due to the space requirements of **1b**. Hence, the formation of a hitherto unknown 1D polymer is observed. Its positive charges are balanced by rather weakly coordinating anions [Al{OC(CF$_3$)$_3$}$_4$], which separate the strands from each other. Since in both cases at least partial depolymerization was found in solution, the compounds were additionally characterized by solid state NMR spectroscopy.

12.3   Experimental Part

General Remarks:

All experiments were carried out under an atmosphere of dry argon or nitrogen using glovebox and Schlenk techniques. Solvents were purified, dried and degassed prior to use. [Cp*Fe(η^5-P$_5$)],[1] Cu(GaCl$_4$),[5b] [{Ag(CH$_2$Cl$_2$)}Al{OC(CF$_3$)$_3$}$_4$][13] and [Cp^{BIG}Fe(η^5-P$_5$)][7] were prepared according to literature procedure. The NMR spectra were measured on a Bruker Avance 300, 400 or 600 spectrometer. The solid state NMR spectra of **3** were measured on a Bruker Avance 300. The solid state NMR spectra of **2** were measured on a Bruker Avance III 300 and

Avance 500 spectrometer. ESI-MS spectra were measured on a ThermoQuest Finnigan MAT TSQ 7000 mass spectrometer. The elemental analyses were determined on a Vario EL III apparatus.

Synthesis of [{Cp*Fe(η^5-P$_5$)}{Cu(GaCl$_4$)}$_2$]$_n$ (2):

A turbid colorless solution of Cu(GaCl$_4$) (80 mg, 290 μmol) in 12 mL CH$_2$Cl$_2$ is layered with a green solution of [Cp*Fe(η^5-P$_5$)] (1a) (50 mg, 145 μmol) in 10 mL toluene in a long thin Schlenk tube. The phase boundary colors yellow, the turbid solution turns clear and crystal growth can be obtained within one day. After complete diffusion the yellow-golden needles are decanted, washed with hexane and CH$_2$Cl$_2$ and dried in vacuum (119 mg, 92%)

2: [C$_{10}$H$_{15}$Cl$_8$Cu$_2$FeGa$_2$P$_5$] calc. (%): C 13.40; H 1.69. found (%): C 13.61; H 2.19. ESI-MS (CH$_3$CN, cation): m/z (%) = 952.6 (1%, [(Cp*FeP$_5$)$_2$Cu$_3$Cl$_2$]$^+$), 854.7 (4%, [(Cp*FeP$_5$)$_2$Cu$_2$Cl]$^+$), 754.8 (100%, [(Cp*FeP$_5$)$_2$Cu]$^+$), 449.9 (52%, [(Cp*FeP$_5$)Cu(CH$_3$CN)]$^+$), 408.9 (5%, [(Cp*FeP$_5$)Cu]$^+$). ESI-MS (CH$_3$CN, anion): m/z (%) = 210.8 (100%, [GaCl$_4$]$^-$). ^{1}H NMR (CD$_3$CN): δ [ppm] = 1.45 (s, Cp*). ^{31}P{^{1}H} NMR (CD$_3$CN): δ [ppm] = 143.4 (s, P$_5$).

Synthesis of [{Cp^{BIG}Fe(η^5-P$_5$)}Ag]$_n$[Al{OC(CF$_3$)$_3$}$_4$]$_n$ (3):

A solution of [{Ag(CH$_2$Cl$_2$)}Al{OC(CF$_3$)$_3$}$_4$] (163 mg, 140 μmol) in 2 mL CH$_2$Cl$_2$ is layered with a solution of [Cp^{BIG}Fe(η^5-P$_5$)] (60 mg, 64 μmol) in a mixture of 3 mL hexane and 1 mL CH$_2$Cl$_2$. After complete diffusion bright green needle shaped crystals are obtained. The crystals are decanted, washed with hexane and dried in vacuum. The crystals are covered with a brownish amorphous substance, which could not be removed even not by recrystallization (56 mg, 43%).

3: [C$_{71}$H$_{65}$AgAlF$_{36}$FeO$_4$P$_5$] calc.: C, 42.39; H, 3.26. found: C, 40.48; H, 3.17. ESI-MS (CH$_3$CN/CH$_2$Cl$_2$, cation): m/z (%) = 1981.5 (40%, [(Cp^{BIG}FeP$_5$)$_2$Ag]$^+$), 1084.4 (100%, [(Cp^{BIG}FeP$_5$)Ag(CH$_3$CN)]$^+$), 1043.4 (38%, [(Cp^{BIG}FeP$_5$)Ag]$^+$). ESI-MS (CH$_3$CN/CH$_2$Cl$_2$, anion): m/z (%) = 967.1 (100%, [Al{OC(CF$_3$)$_3$}$_4$]$^-$).). ^{1}H NMR (CD$_2$Cl$_2$): δ [ppm] = 0.93 (t, $^3J_{HH}$ = 7.4 Hz, 15H, ^{n}Bu), 1.34 (sext, $^3J_{HH}$ = 7.4 Hz, 10H, ^{n}Bu), 1.58 (m, 10H, ^{n}Bu), 2.61 (t, $^3J_{HH}$ = 7.8 Hz, 10H, ^{n}Bu), 6.83 (s-br, ω$_{1/2}$ = 18 Hz, 10H, Ph), 7.06 (d, $^3J_{HH}$ = 8.4 Hz, 10H, Ph). ^{31}P{^{1}H} NMR (CD$_2$Cl$_2$): δ [ppm] = 135 (very broad, ω$_{1/2}$ ≈ 4000 Hz). ^{31}P{^{1}H} MAS NMR δ [ppm] = 73.4 (m, 1P), 98.8 (m, 1P), 129.3 (m, 2P), 157.6 (m, 1P). ^{19}F{^{1}H} NMR (CD$_2$Cl$_2$): δ [ppm] = -75.59 (s).

Novel Polymeric Aggregates of Pentaphosphaferrocenes and Monocationic Coinage Metal Salts
– Synthesis of [{Cp^{BIG}Fe(η^5-P$_5$)}Ag]$_n$[Al(OC(CF$_3$)$_3$)$_4$]$_n$ and [{Cp*Fe(η^5-P$_5$)}{Cu(GaCl$_4$)}$_2$]$_n$

213

12.4   References

[1]   O. J. Scherer, T. Brück, *Angew. Chem.* **1987**, *99*, 59-59.

[2]   a) E. C. Constable, C. E. Housecroft, *Chem. Soc. Rev.* **2013**, *42*, 1429-1439. b) P. J. Lusby, *Annu. Rep. Prog. Chem., Sect. A: Inorg. Chem.* **2013**, *109*, 254-276. c) Y. E. Alexeev, B. I. Kharisov, T. C. H. García, A. D. Garnovskii, *Coord. Chem. Rev.* **2010**, *254*, 794-831.

[3]   a) M. Scheer, *Dalton Trans.* **2008**, 4372-4386. b) E.-M. Rummel, M. Eckhardt, M. Bodensteiner, E. V. Peresypkina, W. Kremer, C. Groeger, M. Scheer, *Eur. J. Inorg. Chem.* **2013**, Ahead of Print. c) B. Attenberger, S. Welsch, M. Zabel, E. Peresypkina, M. Scheer, *Angew. Chem., Int. Ed.* **2011**, *50*, 11516-11519. d) L. J. Gregoriades, B. K. Wegley, M. Sierka, E. Brunner, C. Groeger, E. V. Peresypkina, A. V. Virovets, M. Zabel, M. Scheer, *Chem. Asian J.* **2009**, *4*, 1578-1587.

[4]   a) C. Schwarzmaier, A. Schindler, C. Heindl, S. Scheuermayer, E. V. Peresypkina, A. V. Virovets, M. Neumeier, R. Gschwind, M. Scheer, *Angew. Chem., Int. Ed.* **2013**, *52*, 10896-10899. b) A. Schindler, C. Heindl, G. Balazs, C. Groeger, A. V. Virovets, E. V. Peresypkina, M. Scheer, *Chem.Eur. J.* **2012**, *18*, 829-835. c) F. Dielmann, A. Schindler, S. Scheuermayer, J. Bai, R. Merkle, M. Zabel, A. V. Virovets, E. V. Peresypkina, G. Brunklaus, H. Eckert, M. Scheer, *Chem. Eur. J.* **2012**, *18*, 1168-1179. d) S. Welsch, C. Groeger, M. Sierka, M. Scheer, *Angew. Chem., Int. Ed.* **2011**, *50*, 1435-1438. e) M. Scheer, A. Schindler, J. Bai, B. P. Johnson, R. Merkle, R. Winter, A. V. Virovets, E. V. Peresypkina, V. A. Blatov, M. Sierka, H. Eckert, *Chem. Eur. J.* **2010**, *16*, 2092-2107. f) M. Scheer, A. Schindler, C. Gröger, A. V. Virovets, E. V. Peresypkina, *Angew. Chem., Int. Ed.* **2009**, *48*, 5046-5049. g) M. Scheer, A. Schindler, R. Merkle, B. P. Johnson, M. Linseis, R. Winter, C. E. Anson, A. V. Virovets, *J. Am. Chem. Soc.* **2007**, *129*, 13386-13387. h) M. Scheer, L. J. Gregoriades, A. V. Virovets, W. Kunz, R. Neueder, I. Krossing, *Angew. Chem., Int. Ed.* **2006**, *45*, 5689-5693. i) J. Bai, A. V. Virovets, M. Scheer, *Science* **2003**, *300*, 781-783. j) J. Bai, A. V. Virovets, M. Scheer, *Angew. Chem., Int. Ed.* **2002**, *41*, 1737-1740.

[5]   a) L. C. Forfar, T. J. Clark, M. Green, S. M. Mansell, C. A. Russell, R. A. Sanguramath, J. M. Slattery, *Chem. Commun.* **2012**, *48*, 1970-1972. b) H. Schmidbaur, W. Bublak, B. Huber, G. Reber, G. Müller, *Angew. Chem., Int. Ed.* **1986**, *25*, 1089-1090.

[6]   H. V. Ly, M. Parvez, R. Roesler, *Inorg. Chem.* **2006**, *45*, 345-351.

[7]   S. Heinl, G. Balázs, M. Scheer, *Phosphorus, Sulfur Silicon Relat. Elem.* **2014**, DOI: 10.1080/10426507.2014.903489.

[8]   R. Peng, M. Li, D. Li, *Coord. Chem. Rev.* **2010**, *254*, 1-18.

[9]   www.webelements.com (26.02.2014)

[10] a) S. E. Ashbrook, J. McManus, M. J. Thrippelton, S. Wimperis, *Prog. Nucl. Magn. Reson. Spec.* **2009**, *55*, 160-181. b) B. Thomas, S. Paasch, S. Steuernagel, K. Eichele, *Solid State Nucl. Magn. Reson.* **2001**, *20*, 108-117.

[11] G. Brunklaus, J. C. C. Chan, H. Eckert, S. Reiser, T. Nilges, A. Pfitzner, *Phys. Chem. Chem. Phys.* **2003**, *17*, 3768-3776.

[12] The Ag–C distances roughly range between 2.45 Å and 2.85 Å based on CCDC structural database search.

[13] I. Krossing, Chem. *Eur. J.* **2001**, *7*, 490-502.

Novel Polymeric Aggregates of Pentaphosphaferrocenes and Monocationic Coinage Metal Salts
– Synthesis of [{CpᴮᴵᴳFe(η⁵-P₅)}Ag]ₙ[Al(OC(CF₃)₃)₄]ₙ and [{Cp*Fe(η⁵-P₅)}{Cu(GaCl₄)}₂]ₙ

215

12.5 Supplementary Information

NMR Investigations:
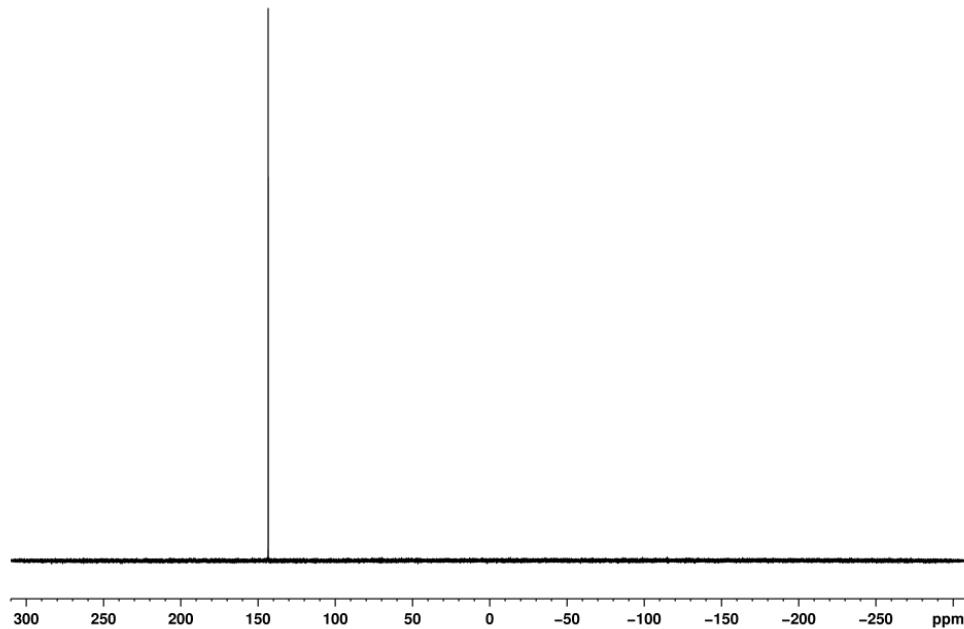
Figure S12.1. ^{31}P{^{1}H} NMR spectrum of **2** in CD$_3$CN at 298 K.
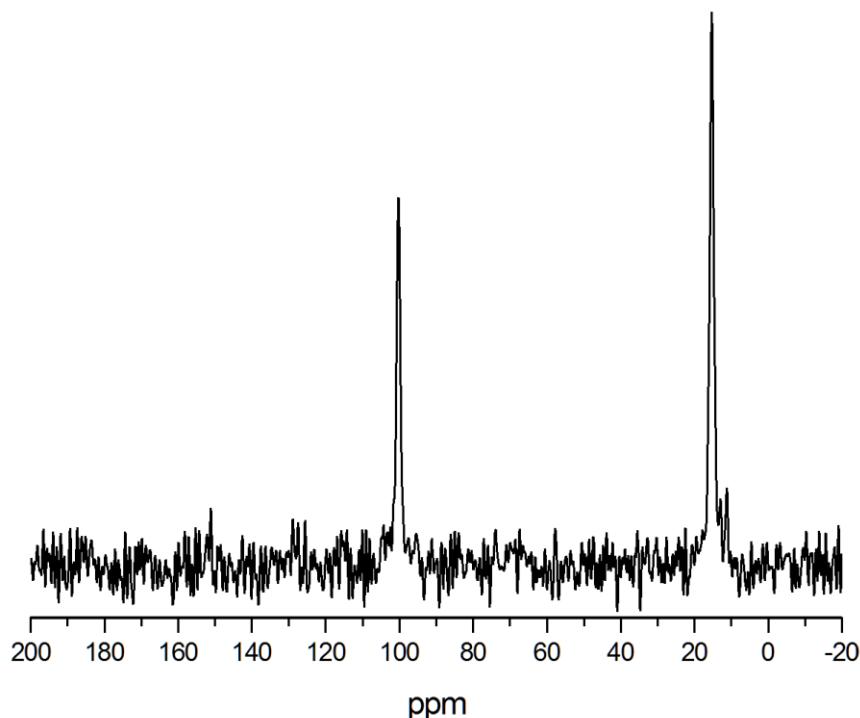
Figure S12.2. ^{31}C{^{1}H} CPMAS NMR spectrum of **2** at 298 K, recorded at 125.78 MHz (11.7 T) and 25 kHz MAS using a commercially available Bruker 2.5 mm HXY triple-resonance probe with a contact time of 4ms while accumulating 512 scans at a relaxation delay of 10s.
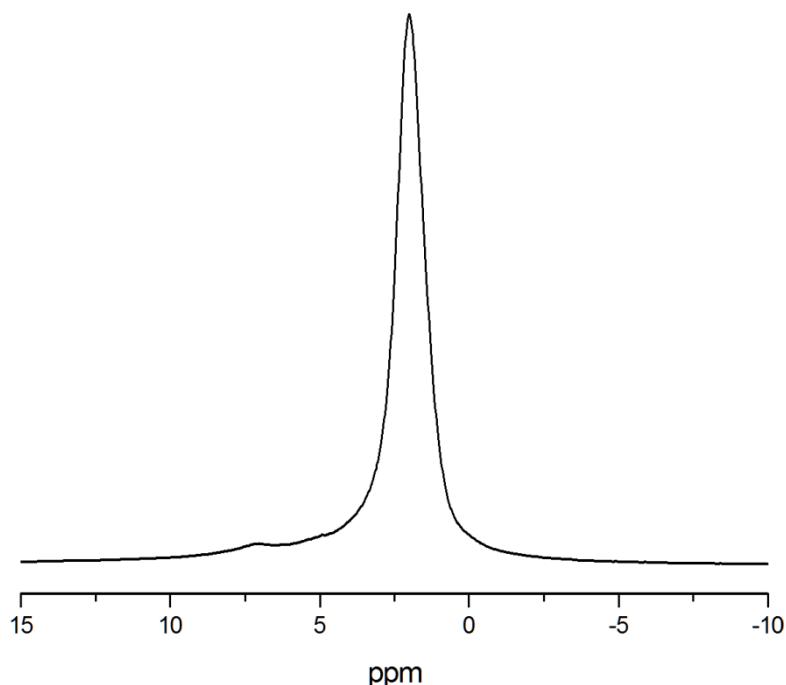
Figure S12.3. Rotor-synchronized ^{1}H MAS NMR spectrum of **2** at 298 K, acquired at 500.18 MHz (11.7 T) and 30 kHz MAS using a commercially available Bruker 2.5 mm HXY triple-resonance probe averaging 16 Scans a relaxation delay of 50s.
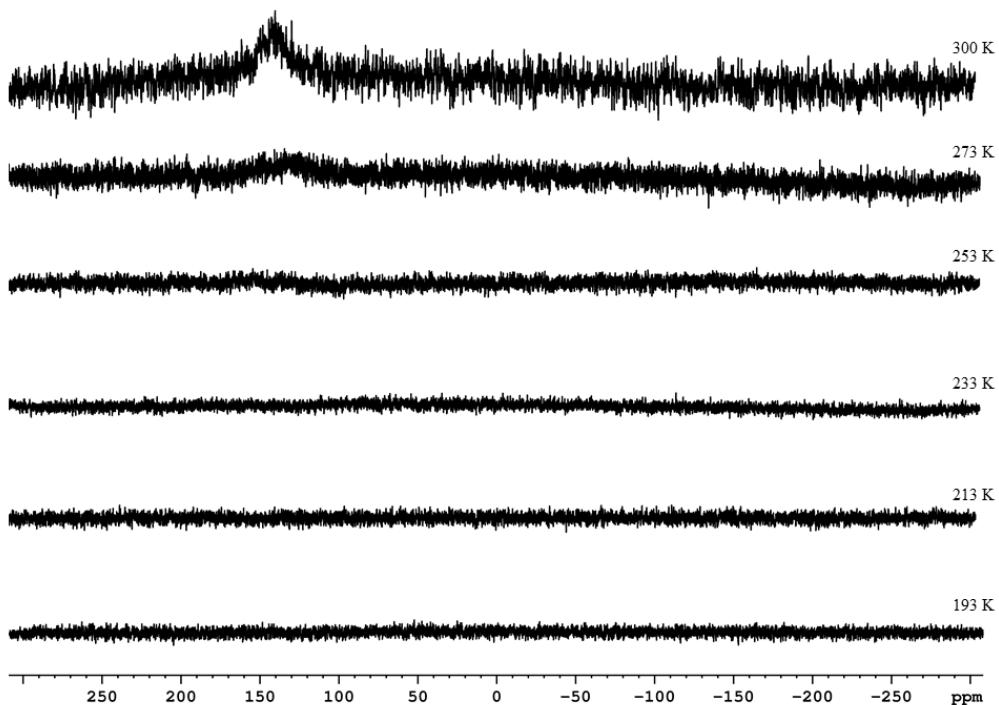
Figure S12.4. ^{31}P{^{1}H} NMR spectra of **3** in CH$_2$Cl$_2$ at various temperatures.

Novel Polymeric Aggregates of Pentaphosphaferrocenes and Monocationic Coinage Metal Salts — Synthesis of [{Cp^{BIG}Fe(η^5-P$_5$)}Ag]$_n$[Al(OC(CF$_3$)$_3$)$_4$]$_n$ and [{Cp*Fe(η^5-P$_5$)}{Cu(GaCl$_4$)}$_2$]$_n$

217
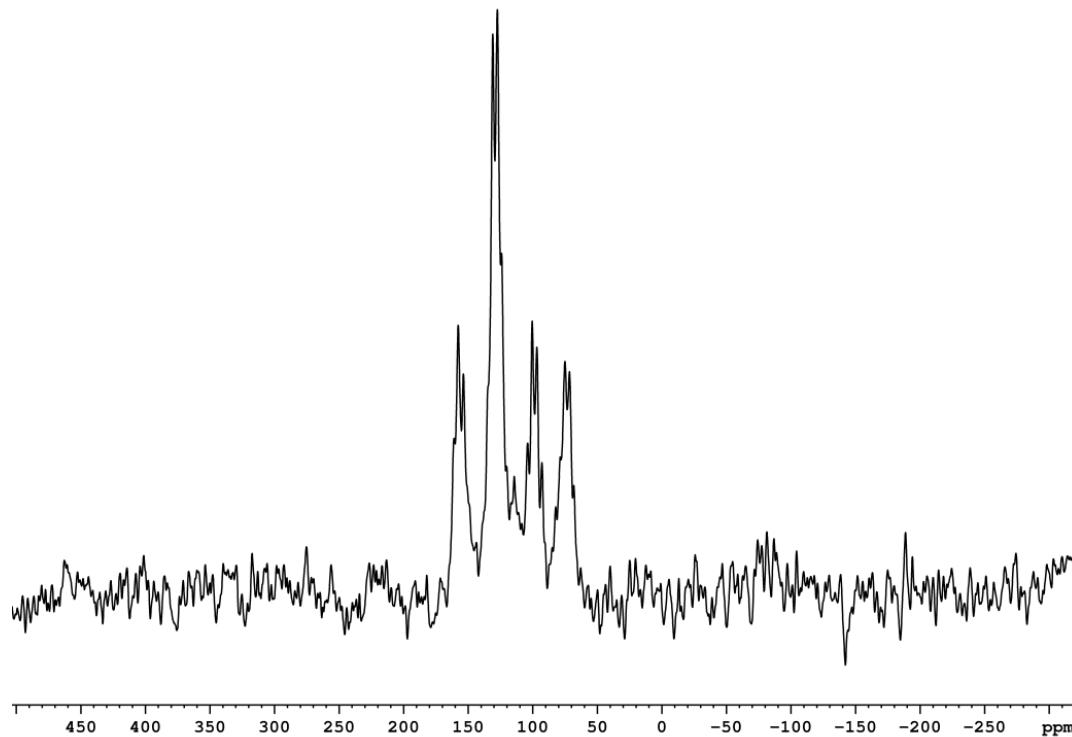
Figure S 12.5. ^{31}P{^{1}H} MAS NMR spectrum of **3** at 298 K.

Crystallographic Details:

The crystal structure analyses were performed on an Oxford Diffraction SuperNova diffractometer. For both compounds an analytical absorption correction was carried out.[1] The structures were solved by direct methods of the program SIR-92 (**2**)[2] or chargeflipping methods with the program Superflip (**3**)[3] and refined with the least square method on F^2 employing SHELXL-97[4] with anisotropic displacements for non-H atoms. Hydrogen atoms were located in idealized positions and refined isotropically according to the riding model. For compound **3** twin refinement for inversion twinning was necessary (Flack parameter 0.273(7)).[5]

CCDC-993425 (**2**) and CCDC-993426 (**3**) contain the supplementary crystallographic data for this paper. These data can be obtained free of charge at www.ccdc.cam.ac.uk/conts/retrieving.html (or from the Cambridge Crystallographic Data Centre, 12 Union Road, Cambridge CB2 1EZ, UK; Fax: + 44-1223-336-033; e-mail: deposit@ccdc.cam.ac.uk).

Crystal data for [{Cp*Fe(η^5-P$_5$)}{Cu(GaCl$_4$)}$_2$]$_n$ (**2**): C$_{10}$H$_{15}$Cl$_8$Cu$_2$FeGa$_2$P$_5$, M = 2011.78 g/mol, space group $Pbca$ (no.61), a = 19.6453(2) Å, b = 12.6984(1) Å, c = 21.3504(3) Å, V = 5326.15(10) Å^3, Z = 8, μ = 18.556 mm^{-1}, F(000) = 3456, T = 123 K, 28148 reflections measured, 5253 unique (R_{int} = 0.0517), R_1 = 0.0352, wR_2 = 0.0833 for I > 2σ(I). CCDC-993425
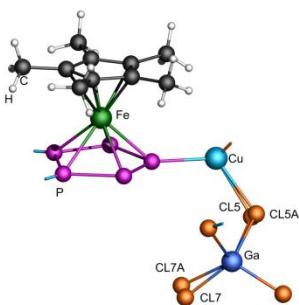
Figure S12.6. Section of **2** showing the disorder of Cl5 and Cl7. The occupation of Cl5 and Cl5A was refined to 0.5 each; the occupation of Cl7 and Cl7A was refined to 0.6 and 0.4, respectively.
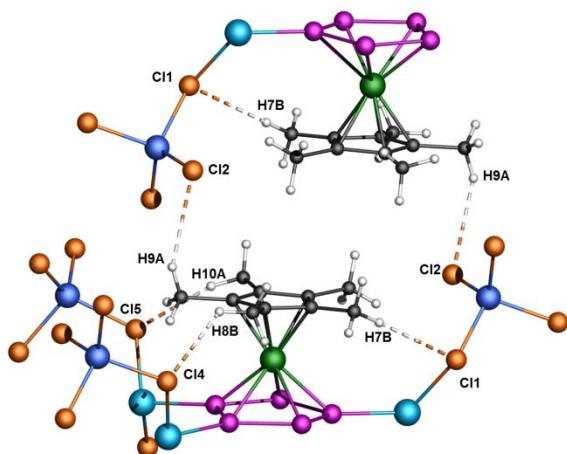
Figure S12.7. Section of **2** showing short Cl–H distances. Selected bond lengths [Å]: H9A-Cl2 2.8609(8), H7B-Cl1 2.7986(8), H8B-Cl4 2.6998(8), H10A-Cl5 2.6219(15).

Crystal data for [{Cp^{BIG}Fe(η^5-P$_5$)}Ag]$_n$[Al(OC(CF$_3$)$_3$)$_4$]$_n$ (**3**): C$_{71}$H$_{65}$AgAlF$_{36}$FeO$_4$P$_5$, M = 2011.78 g/mol, space group $Pna2_1$ (no.33), a = 31.4504(5) Å, b = 17.9259(3) Å, c = 14.7931(2) Å, V = 8340.0(2) Å^3, Z = 4, μ = 5.438 mm^{-1}, F(000) = 4032, T = 123 K, 60877 reflections measured, 14463 unique (R_{int} = 0.0675), R_1 = 0.0818, wR_2 = 0.2021 for I > 2σ(I). CCDC-993426
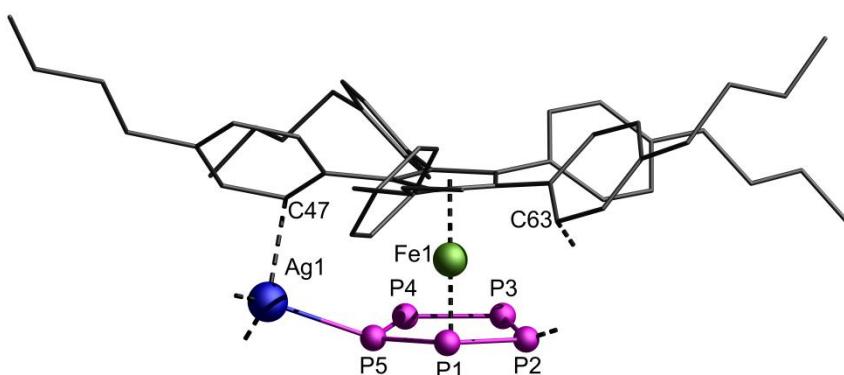
Figure S12.8. Repeating unit of the polymer chain [{Cp^{BIG}Fe(η^5-P$_5$)}Ag]$_n^{n+}$ in **3** in the crystal. For clarity reasons the C atoms are shown in 'wire-or-stick' model and H atoms and [Al(OC(CF$_3$)$_3$)$_4$] counter anions are omitted.
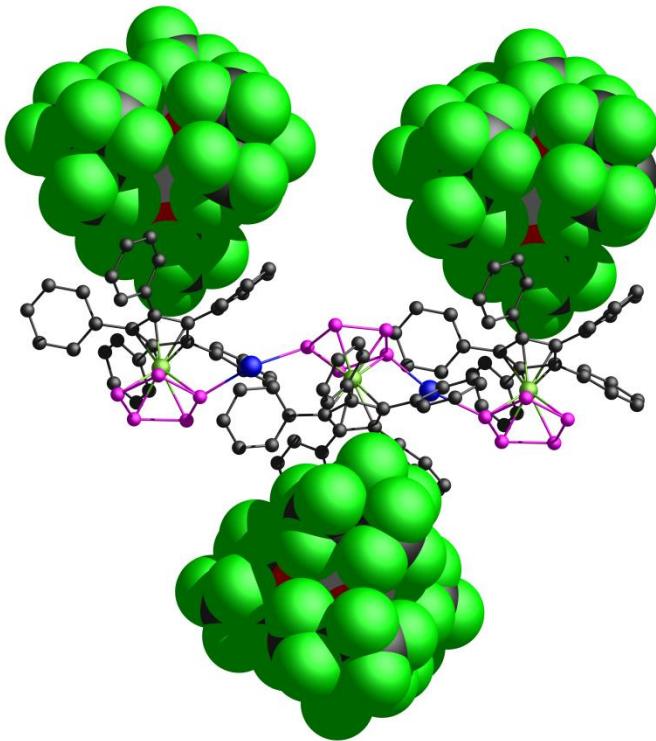
Figure S12.9. Section of polymer chain [{Cp^{BIG}Fe(η^5-P$_5$)}Ag]$_n$[Al(OC(CF$_3$)$_3$)$_4$]$_n$ displaying the location of the anions. For clarity reasons *n*butyl groups and H atoms are omitted. [Al(OC(CF$_3$)$_3$)$_4$] anions are depicted in space-filling model. F: green; C: grey; P: pink; Ag: blue; Fe: yellow; Al: white, O: red.
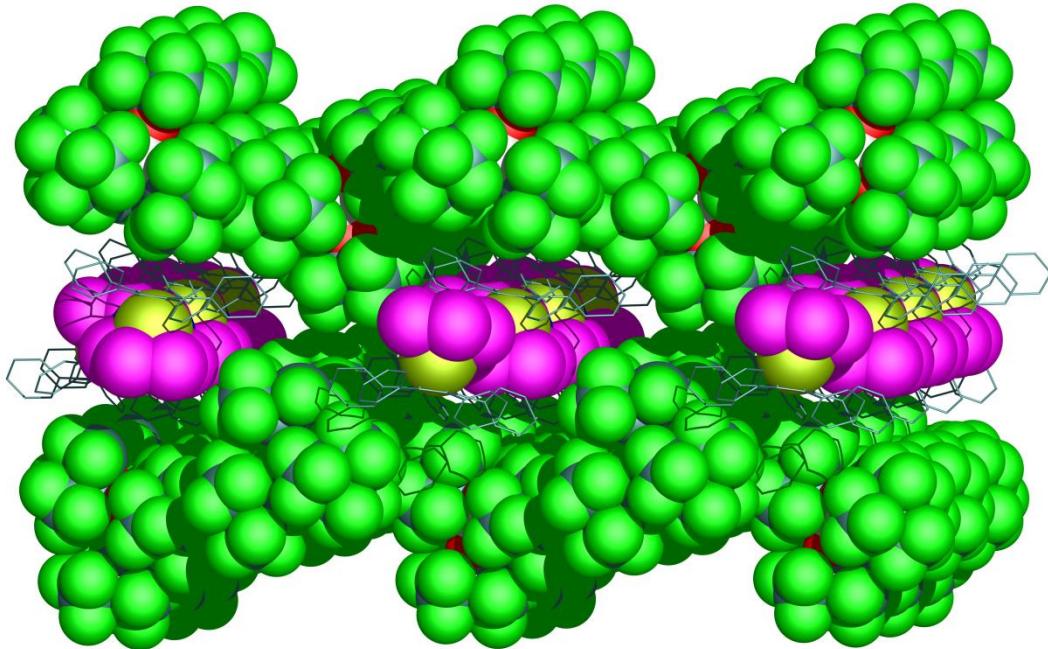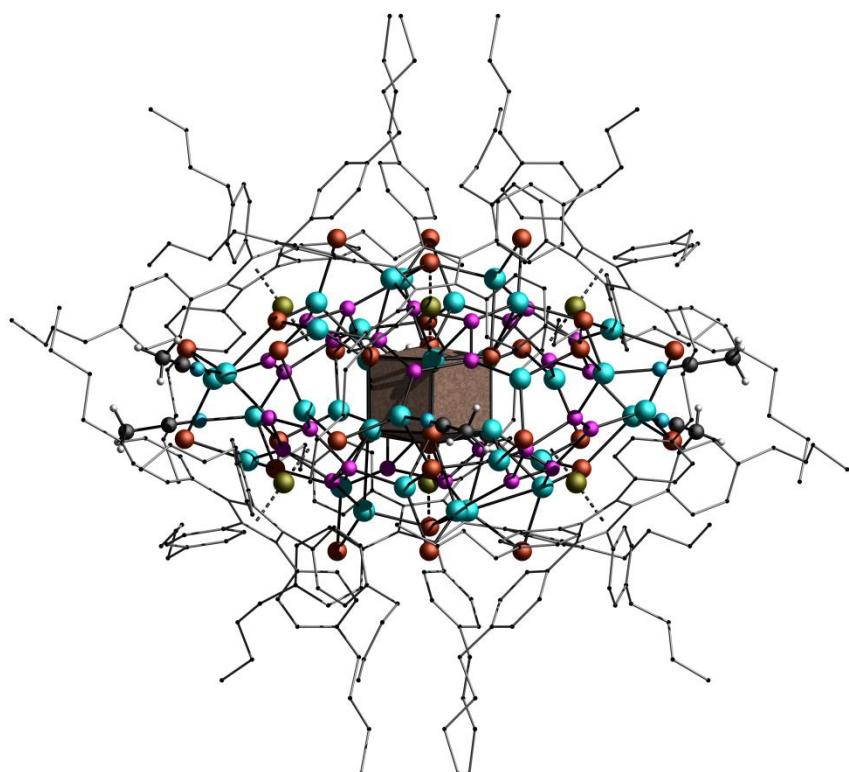
Figure S12.10. Packing scheme of compound [{Cp^{BIG}Fe(η^5-P$_5$)}Ag]$_n$[Al(OC(CF$_3$)$_3$)$_4$]$_n$ illustrating channels formed by the anions [Al(OC(CF$_3$)$_3$)$_4$] filled with cationic polymer chain [{Cp^{BIG}Fe(η^5-P$_5$)}Ag]$_n^{n+}$. F: green; C: grey; P: pink; Ag: blue; Fe: yellow; Al: white, O: red.

References for Supplementary Information

[1]   R. C. Clark, J. S. Reid, *Acta Cryst.* **1995**, A51, 887-897.

[2]   A. Altomare, M. C. Burla, M. Camalli, G.L. Cascarano, C. Giacovazzo, A. Guagliardi, A. G. G. Moliterni, G. Polidori, R. Spagna, *J. Appl. Cryst.* **1999**, 32, 115-119.

[3]   L. Palatinus, G. Chapuis, *J. Appl. Cryst.* **2007**, *40*, 786-790.

[4]   G. M. Sheldrick, *Acta Cryst.* **2008**, A64, 112-122.

[5]   Flack H.D. (1983), Acta Cryst. A39, 876-881.

The Superbulky Pentaphosphaferrocene [Cp^{BIG}Fe(η^5-P$_5$)] as Building Block for the Formation of Macromolecules with Lens-

221

13. The Superbulky Pentaphosphaferrocene [Cp^{BIG}Fe(η^5-P$_5$)] as Building Block for the Formation of Macromolecules with Lens-Shaped Scaffolds

Sebsatian Heinl, Eugenia Peresypkina, Alexander V. Virovets, Werner Kremer and Manfred Scheer

unpublished results

- ❖ **All syntheses and characterizations were performed by Sebastian Heinl, unless subsequently noted otherwise**
- ❖ **Manuscript was written by Sebastian Heinl**
- ❖ **Figures were made by Sebastian Heinl**
- ❖ **MAS NMR were measured by Werner Kremer**
- ❖ **X-ray structure analyses and refinement were jointly performed by Sebastian Heinl, Eugenia Peresypkina and Alexander V. Virovets. Eugenia Peresypkina and Alexander V. Virovets performed the recent refinement. Final refinements of the structures were not possible within the scope of this thesis**

13.1 Introduction

Since Kroto and coworkers provided the first experimental evidence for the C_{60} Buckminsterfullerene,[1] chemists realized the potential of five-fold symmetrical building blocks for the formation of macromolecules with fullerene-like topologies. However, only few examples are known which in fact are suitable for building spherical, ball-shaped clusters. In polyoxometalate chemistry the so called Keplerates[2] with the simplified formula $[\{(M^{VI})Mo^{VI}_5\}_{12}(linker)_{30}]$ (M = Mo, W) are well known.[3] Another more direct approach to obtain C_5-symmetric linking units is to substitute all H atoms of the cyclopentadienyl ligand by donor functions. Williams *et al.* synthesized the ferrocene complex $[(C_5H_4PO^tBu_2)Fe(C_5(4\text{-pyridyl})_5]$ and succeeded in the construction of spherical macromolecules with Cu(I) cations.[4] However, one of the most prominent class of compounds for the formation of fullerene-like supermolecules are the pentaphosphaferrocenes $[Cp^RFe(\eta^5-P_5)]$ (1). The first synthesized derivative $[Cp^*Fe(\eta^5-P_5)]$ (1a; $Cp^* = C_5Me_5$)[5] is well investigated regarding its physical[6] and coordination[7] properties. It has been shown that building block 1a in combination with Cu(I) halides is able to form spherical macromolecules with different topologies. In 2003, the first compound $[\{Cp^*Fe(\eta^{5:1:1:1:1:1}-P_5)\}_{12}\{CuCl\}_{10}\{Cu_2Cl_3\}_5\{Cu(CH_3CN)_2\}_5]$[8] was described, consisting of 90 non-carbon scaffold atoms. During the following decade different other geometries could be realized depending on Cu-halide, template and reaction conditions.[9] All compounds show low solubility in all solvents or are insoluble. By introducing $[Cp^{Bn}Fe(\eta^5-P_5)]$ (1b; $Cp^{Bn} = C_5(CH_2Ph)_5$),[10] the formation of similar fullerene-like aggregates was possible but the molecules show much higher solubility.[11] Recently we reported on the synthesis of the superbulky pentaphosphaferrocene $[Cp^{BIG}Fe(\eta^5-P_5)]$ (1c; $Cp^{BIG} = C_5(4\text{-}nBuC_6H_4)_5)$.[12] Because of the very high steric demand of the Cp^{BIG} ligand (r ≈ 9 Å) compared to Cp^* and Cp^{Bn} (r ≈ 3 Å),[13] new structural motifs become obligatory. In general, steric repulsion can be minimized either by moving the building blocks further apart or by arranging fewer units in a specific volume.

Herein, we report on the reaction of $[Cp^{BIG}Fe(\eta^5-P_5)]$ (1c) with CuX_2 (X = Cl, Br) forming well soluble lens-shaped macromolecules.

13.2 Results and Discussion

The addition of a CH_2Cl_2 solution of 1c to a CH_3CN solution of fivefold excess of CuX_2 (X = Cl, Br) results in a color change from green to dark red-brown within seconds. The dried crude product is extracted with CH_2Cl_2 and layered with toluene, affording black block-like crystals. X-Ray structural analyses show the molecular compositions $[\{Cp^{BIG}Fe(\eta^5-P_5)\}_6(CuBr)_{32}(CH_3CN)_6]$

(2a) and [{Cp^{BIG}Fe(η^4-P$_5$)}$_6$Cu$_{34}$Cl$_{28}$(CH$_3$CN)$_6$] (2b), respectively (for details see structure description below). Compound 2a and 2b contain only six pentaphosphaferrocene units, which is in contrast to the previously published clusters bearing twelve units.[8-11] The aggregate has an overall size of about 3.0x3.5 nm. Omitting the Cp^{BIG} ligands a lens-shaped scaffold is obtained instead of the approximate ball-shape of the macromolecules containing twelve 1a units. Irrespectively to stoichiometry, used solvents and reaction conditions, the formation of other spherical clusters or polymeric compounds could not be observed.

Similar cell parameters are obtained for 2a and 2b probably due to similar crystal packing and geometrical arrangements of the Cp^{BIG} ligands. Both compounds show a double-shell structure with identical outer shell connectivity. However, the inner parts reveal different compositions and arrangements of atoms. This can be explained by the different conformations of the cyclo-P$_5$ ligands. While in case of 2b the P$_5$ rings show an envelope conformation, in 2a a planar arrangement is observed.

The cluster 2a shows an idealized outer scaffold, where each P atom of the pentaphosphaferrocene coordinates to copper ion. The Cu atoms are further linked to Br atoms. The P$_5$ rings are surrounded by five P$_2$Cu$_3$Br$_2$ seven-membered folded cycles (Figure 13.1: c-Br, d-Br). The cycles on the flat top of the lens can also be specified as nearly planar P$_2$Cu$_3$Br six-membered rings, where the Cu-Cu edges are bridged by Br atoms. Considering the combination of five-membered and six-membered rings, the outer structure of 2a can therefore be described as two fused I-C$_{140}$ fullerene[14] caps. To afford a close linkage of the two half shells, some of the P$_2$Cu$_3$Br$_2$ seven-membered rings on the rim show approximate boat conformation. Six copper atoms on this conjunction line are coordinatively saturated by one acetonitrile ligands each. Two of the Cu sites are vacant, which are statistically distributed over 12 positions (Figure 13.1: c-Br). Therefore, two of the six [Cp^{BIG}Fe(η^5-P$_5$)] moieties show a 1,2,3,4 coordination mode and the remaining four a 1,2,3,4,5 coordination mode.

The inner core of 2a exhibits an adamantane-like framework (Figure 13.1: a-Br), which is disordered over two positions around the center of symmetry effectively resulting in a bicapped hexagonal prism (Figure 13.1: b-Br). Therefore, four of the eight possible (inner) positions of copper are occupied. All three Cu ions in the 'base' of the {Cu$_4$Br$_6$} adamantane-like cage are coordinated by one molecule [Cp^{BIG}Fe(η^5-P$_5$)] in a η^2-fashion each. The remaining three [Cp^{BIG}Fe(η^5-P$_5$)] units are not directly linked with the core, however are connected by an 'apical' Br ion which binds to the 'apical' Cu ion (elongated 2.91 Å) in the adamantane-like scaffold (Figure 13.1: a-Br). The displacement parameters of the 'apical' Cu atom are rather high but strictly required by charge balance, which can be explained in two ways. First, the observed Cu–Br distances of 2.48 Å are relatively long.[15] Therefore, the Cu ion might be disordered over three positions around $\bar{3}$ axis in a way that in every position it is coordinated

The Superbulky Pentaphosphaferrocene [Cp^{BIG}Fe(η^5-P$_5$)] as Building Block for the Formation of Macromolecules with Lens-Shaped Scaffolds
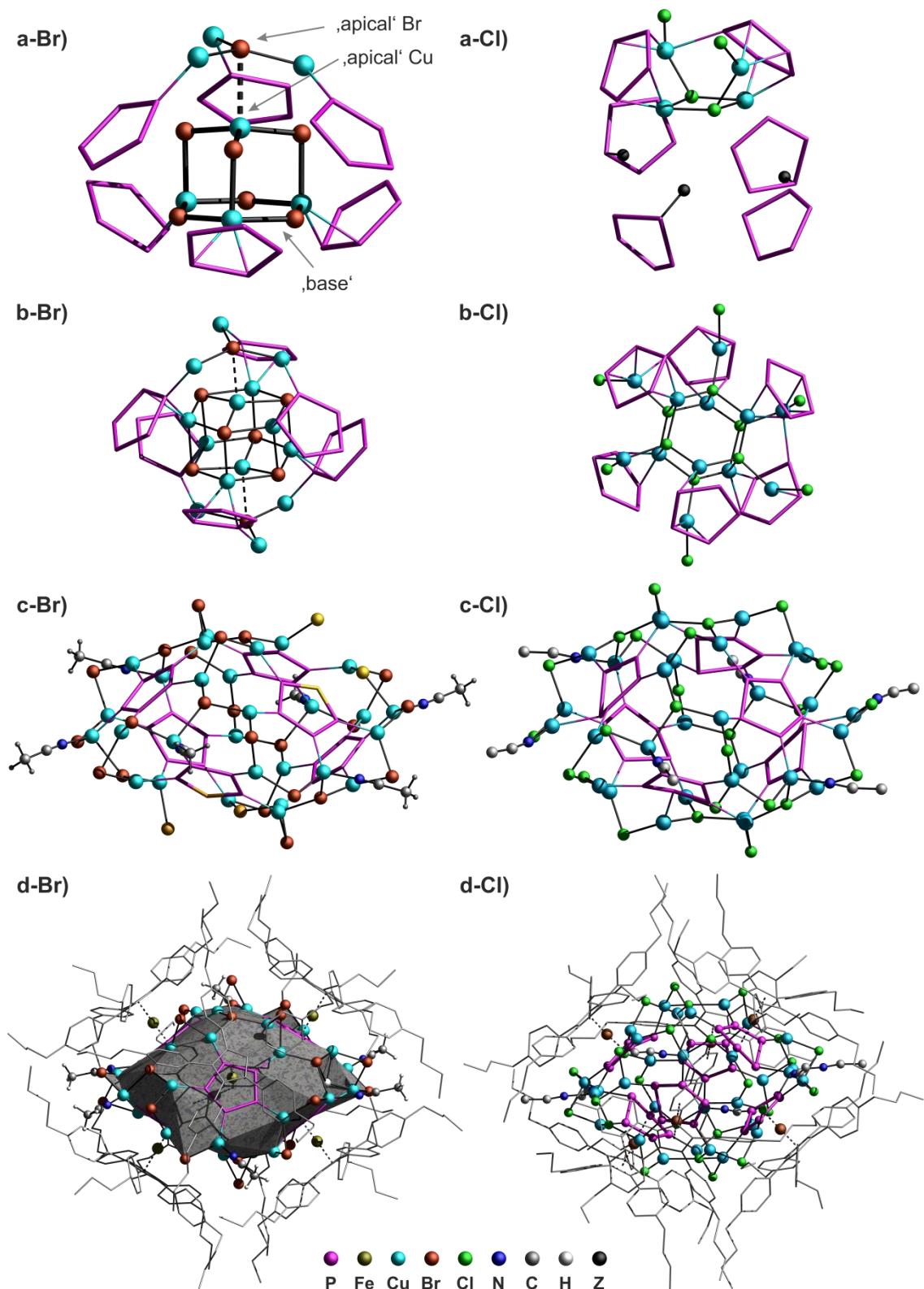
Figure 13.1. Stepwise buildup of the molecular structures of **2a** (left) and **2b** (right). a-Br: adamantane-like inner core of **2a** with linkage to *cyclo*-P$_5$ moieties. b-Br: disordered inner structure of **2a**. c-Br: outer shell of **2a** without core structure; P and Br neighboring atoms of two vacant Cu sites are marked by yellow and orange color, respectively. d-Br: whole molecular structure of **2a**; surface of the inorganic scaffold is colored. a-Cl: ordered view of inner cavity of **2b**. b-Cl: disorder of inner structure of **2b** forms hexagonal Cu$_6$Cl$_6$ prism; occupancy of each position of the prism is ⅓. c-Cl: inorganic scaffold of one possible isomer of **2a**. d-Cl: one possible isomer of macromolecule **2a**.

by only two of the three Br ions in the CuBr$_3$ plane. The second possibility to receive a neutral molecule is to assume mixed occupancies of Cu$^+$/Cu^{2+} that would lead to reduced occupancy of copper. If an equal occupancy of the atoms required by the charge balance is set, the total amount of copper in this position would be ⅓ instead of ½ and would result in reasonable displacement parameters. In that case the formula of **2a** could be written as [{Cp^{BIG}Fe(η^5-P$_5$)}$_6$(CuBr)$_{31.5}$(CH$_3$CN)$_6$]. However, we think that the first description is the more likely one from stereochemical point of view. The plane trigonal environment of the copper atom (additional contact of 2.91 Å can hardly be treated as coordination bond) is not usual for Cu(II). Applying all observations described above a final formula for **2a** can be given as [{Cp^{BIG}Fe($\eta^{5:1:1:1:1:1}$-P$_5$)}$_4${Cp^{BIG}Fe($\eta^{5:1:1:1:1}$-P$_5$)}$_2$(CuBr)$_{32}$(CH$_3$CN)$_6$].

As already mentioned above, the *cyclo*-P$_5$ rings in the macromolecule **2b** show an envelope conformation, in which one P atom is displaced out of plane.[16] The P$_5$ moieties are disordered over five orientations.[17] The bent P atoms bear a substituent group Z (Figure 13.1: a-Cl), which could not be definitely assigned because of unclear chemical origin and its low contribution to diffraction pattern.[16] If this is taken into account the formula [{Cp^{BIG}Fe(η^4-P$_5$)}$_6$Cu$_{34}$Cl$_{28}$(CH$_3$CN)$_6$(Z)$_6$] is obtained for **2b**. From residual electron density and distances P–Z (~1.65 Å)[18] the most reasonable atoms are O or N. However, the elemental analysis gives evidence for Z to be O or OH, otherwise a doubled value for nitrogen should be observed (see experimental part). The six pentaphosphaferrocenes bear a negative charge each and therefore the charge balance is achieved (34 Cu$^+$, 28 Cl$^-$, 6 **1c**$^-$).

Despite of the differences in the conformation of the P$_5$ units in **2a** and **2b**, the connectivity patterns of the outer surfaces are analogous to each other (Figure 13.1: c-Cl, d-Cl). However, **2b** does not show vacant sites for copper in the outer framework. Due to that all **1c** units show a 1,2,3,4,5 coordination mode. In contrast, the composition of the inner parts of **2a** and **2b** differ significantly. Instead of an adamantane-like cage like in **2a**, in compound **2b** a hexagonal Cu$_6$Cl$_6$ prism is observed with ⅓ occupancy for each atom (Figure 13.1: b-Cl). This core is linked to the P$_5$ rings via an η^2 coordination to Cu. The only way to get a reasonable, non-contradictory model of the disorder in the core is a Cu$_4$Cl$_2$ ring bridging two **1c** units (Figure 13.1: a-Cl). Two further Cu ions form additional linkage between the Cu$_2$Cl$_2$ dimer and the outer shell. The remaining four pentaphosphaferrocenes do not show an additional connection with the inner part. This inner structural motif in combination with disorder around the $\bar{3}$ axis results in the seeming hexagonal prism.

The ^{31}P{^{1}H} NMR spectrum of **2a** shows five separated *pseudo*-triplets for five non-equivalent P atoms with coupling constants of roughly 520 − 560 Hz in a 1:1:1:1:1 integral ratio. In contrast, the ^{31}P{^{1}H} NMR spectrum of **2b** is very broad and does not show satisfactory resolved signals in the same range of chemical shifts of **2a**. Not too surprising, the

^{1}H NMR spectra of **2a** and **2b** show a large number of superimposed signals, consistent with Cp^{BIG} ligands not freely rotating. ^{31}P{^{1}H} MAS NMR spectra of **2a** and **2b** show only one very broad anisotropic signal between -20 ppm and 100 ppm and between -70 ppm and 100 ppm, respectively.

The ESI mass spectra (CH$_2$Cl$_2$/CH$_3$CN) of the two compounds show only peaks for fragments with a composition of up to [(Cp^{BIG}FeP$_5$)$_2$Cu$_3$Cl$_2$]$^+$ and [(Cp^{BIG}FeP$_5$)$_2$Cu$_2$Br]$^+$, respectively. Interestingly, in the mass spectrum of **2b** no appropriate peak for **1c** with a Z (Z = O, OH, N, NH, NH$_2$) group is found (see structure description above). Therefore, the nature of Z remains unclear.

It is noteworthy that the reaction starts with Cu(II)-halides, but the identified products exhibit Cu(I)-halide units. Unfortunately, no corresponding oxidation product could be identified. However, Winter et al. and Scheer et al. reported on the oxidation of **1a** under P–P bond formation.[19] Therefore, an analogous reaction could also take place in case of **1c** forming **1c**$_2^{2+}$. The dication, however is not stable under the applied conditions and subsequently decomposes prohibiting its detection.

Summing up, we have shown that [Cp^{BIG}Fe(η^5-P$_5$)] (**1c**) in combination with Cu(II)-halides is capable of the formation of spherical macromolecules with sizes of 3.0x3.5 nm. The obtained clusters **2a** and **2b** show novel structural motifs, each contain six molecules of pentaphosphaferrocene **1c**. The outer shell of the molecules can be described as two fused fullerene caps (I-C$_{140}$), which is in case of **2a** partly vacant. Despite the similar outer scaffold, the inner parts essentially differ. While **2a** contains an adamantane-like cage as central core, **2b** only shows a Cu$_4$Cl$_2$ fragment. Furthermore, the P$_5$ rings in **2a** are planar but folded in case of **2b**, which has not been observed so far. Due to the *n*Bu groups of the Cp^{BIG} ligands, the supramolecules are well soluble in CH$_2$Cl$_2$ and can therefore be easily investigated in solution.

13.3 Experimental Part

General Remarks:

All experiments were carried out under an atmosphere of dry argon or nitrogen using glovebox and schlenk techniques. Solvents were purified, dried and degassed prior to use. CuCl$_2$ and CuBr$_2$ were used as obtained by commercial suppliers, [Cp^{BIG}Fe(η^5-P$_5$)][12] was prepared according to literature procedure. The NMR spectra in solution were measured on a Bruker Avance 300, 400 or 600 spectrometer. The MAS NMR spectra were recorded on a Bruker Advance 300 spectrometer by using a double resonance 2.5 mm MAS probe (^{31}P: 121.495 MHz). All spectra were acquired at MAS rotation frequencies up to 30 kHz with a

90° pulse length of about 2.3 µs and relaxation delays of 120 s (^{31}P). ESI-MS spectra were measured on a ThermoQuest Finnigan TSG 7000 mass spectrometer. The elemental analyses were determined on a Vario EL III apparatus or by external service (all elements) 'Lehrbereich Anorganische Chemie, TU Munich, Mikroanalytisches Labor, Tel.: (089)-289-13128'.

Synthesis of [{Cp^{BIG}Fe(η^5-P$_5$)}$_6$(CuBr)$_{32}$(CH$_3$CN)$_6$] (2a) and [{Cp^{BIG}Fe(η^4-P$_5$)}$_6$Cu$_{34}$Cl$_{28}$(CH$_3$CN)$_6$] (2b):

To a suspension of CuX$_2$ (1.33 mmol) in 5 mL CH$_3$CN a solution of [Cp^{BIG}Fe(η^5-P$_5$)] (250 mg, 0.267 mmol) in CH$_2$Cl$_2$ is added and stirred for 30 min resulting in a red-brown solution. After solvent is removed in vacuum the residue is triturated with 10 mL CH$_2$Cl$_2$ and filtered through cannula into a thin Schlenk tube. The reaction mixture is layered with 20 mL toluene. After complete diffusion black crystals of the product is obtained.

2a: [{Cp^{BIG}Fe(η^5-P$_5$)$_6$(CuBr)$_{32}$(CH$_3$CN)$_6$]: Yield: 285 mg (61%). [C$_{342}$H$_{408}$Br$_{32}$Cu$_{32}$Fe$_6$N$_6$P$_{30}$] * 6 CH$_2$Cl$_2$ calc. C, 39.28; H, 3.93; Br, 24.45; Cu, 19.44; Fe, 3.20; N, 0.80; P, 8.89. found: C, 36.18; H, 3.58; Br, 28.34; Cu, 19.1; Fe, 4.13; N, 0.77; P, 8.19. ESI-MS (CH$_3$CN/CH$_2$Cl$_2$, cation): m/z (%) = 2079.7 (30%, [(Cp^{BIG}FeP$_5$)$_2$Cu$_2$Br]$^+$), 1936.8 (100%, [(Cp^{BIG}FeP$_5$)$_2$Cu]$^+$), 1431.0 (10%, [(Cp^{BIG}FeP$_5$)Cu$_4$Br$_3$]$^+$), 1328.0 (12%, [(Cp^{BIG}FeP$_5$) Cu$_3$Br$_2$CH$_3$CN]$^+$), 1287.3 (18%, [(Cp^{BIG}FeP$_5$)Cu$_3$Br$_2$]$^+$), 1143.3 (40%, [(Cp^{BIG}FeP$_5$)Cu$_2$Br]$^+$), 1040.5 (70%, [(Cp^{BIG}FeP$_5$)CuCH$_3$CN]$^+$), 999.5 (10%, [(Cp^{BIG}FeP$_5$)Cu]$^+$), 726.4 (7%, [Cp^{BIG}]$^+$), 432.4 (20%, [Cu$_3$Br$_2$(CH$_3$CN)$_2$]$^+$). ^{31}P{^{1}H} NMR (CD$_2$Cl$_2$): δ [ppm] = 1.1 (*pseudo*-t, $^1J_{PP}$ ≈ 560 Hz, 1P), 16.4 (*pseudo*-t, $^1J_{PP}$ ≈ 520 Hz, 1P), 25.1 (*pseudo*-t, $^1J_{PP}$ ≈ 550 Hz, 1P), 37.0 (*pseudo*-t, $^1J_{PP}$ ≈ 550 Hz, 1P), 59.0 (*pseudo*-t, $^1J_{PP}$ ≈ 555 Hz, 1P). For NMR Spectra see supplementary Information.

2b: [{Cp^{BIG}Fe(η^4-P$_5$)}$_6$Cu$_{34}$Cl$_{28}$(CH$_3$CN)$_6$]: Yield: 193 mg (48%). [C$_{342}$H$_{408}$Cl$_{28}$Cu$_{34}$Fe$_6$N$_6$P$_{30}$] * 6 CH$_2$Cl$_2$ calc. C, 43.86; H, 4.44; Cl, 14.88; Cu, 22.67; Fe, 3.52; N, 0.88; P, 9.75. found (all elements): C, 42.66; H, 4.24; Cl, 14.87; Cu, 22.6; Fe, 4.98; N, 0.86; P, 9.61. ESI-MS (CH$_3$CN/CH$_2$Cl$_2$, cation): m/z (%) = 2135.8 (10%, [(Cp^{BIG}FeP$_5$)$_2$Cu$_3$Cl$_2$]$^+$), 2035.8 (30%, [(Cp^{BIG}FeP$_5$)$_2$Cu$_2$Cl]$^+$), 1937.0 (100%, [(Cp^{BIG}FeP$_5$)$_2$Cu]$^+$), 1297.0 (10%, [(Cp^{BIG}FeP$_5$)Cu$_4$Cl$_3$]$^+$), 1238.1 (10%, [(Cp^{BIG}FeP$_5$) Cu$_3$Cl$_2$CH$_3$CN]$^+$), 1197.1 (25%, [(Cp^{BIG}FeP$_5$)Cu$_3$Cl$_2$]$^+$), 1140.2 (5%, [(Cp^{BIG}FeP$_5$)Cu$_2$ClCH$_3$CN]$^+$), 1099.1 (35%, [(Cp^{BIG}FeP$_5$)Cu$_2$Cl]$^+$), 1040.3 (75%, [(Cp^{BIG}FeP$_5$)CuCH$_3$CN]$^+$), 999.3 (90%, [(Cp^{BIG}FeP$_5$)Cu]$^+$), 741.5 (10%, [Cp^{BIG}O]$^+$). For NMR Spectra see supplementary Information.

13.4 References
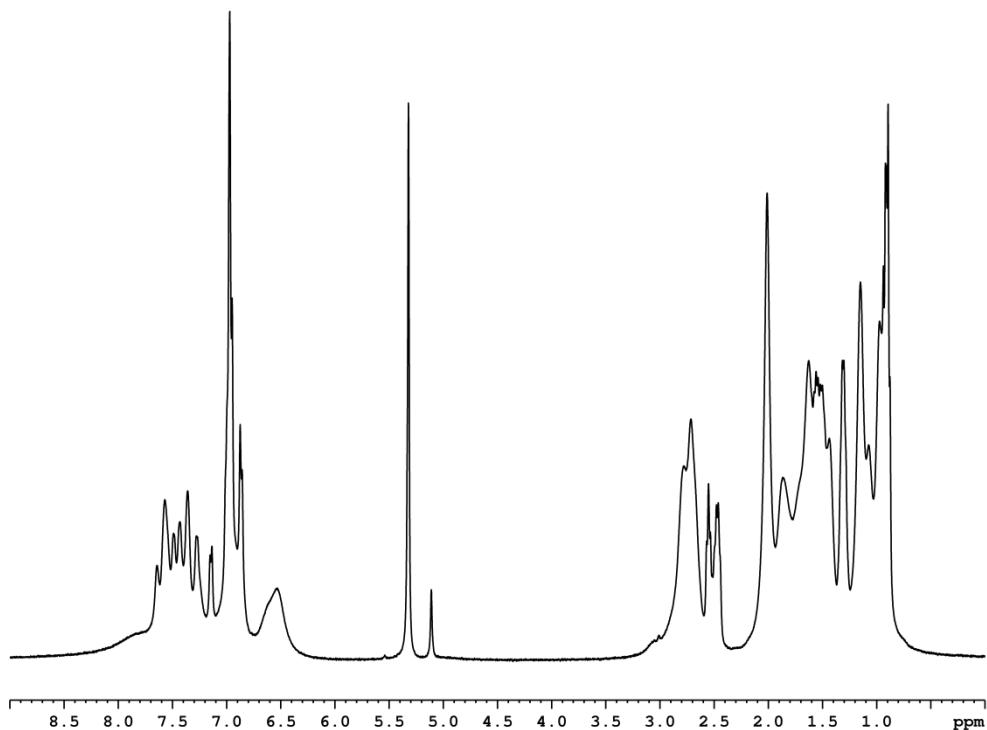
[1]   H. W. Kroto, J. R. Heath, S. C. O'Brien, R. F. Curl, R. E.Smalley, *Nature* **1985**, *318*, 162-163.

[2]   For the definition, see A. Müller, *Nature* **2007**, *447*, 1035.

[3]   a) A. Müller, E. Krickemeyer, H. Bögge, M. Schmidtmann, F. Peters, *Angew. Chem.* **1998**, *110*, 3567-3571. b) A. Müller, E. Krickemeyer, H. Bögge, M. Schmidtmann, F. Peters, *Angew. Chem., Int. Ed.* **1998**, *37*, 3359-3363. c) A. Müller, P. Kogerler, C. Kuhlmann, *Chem. Commun.* **1999**, 1347-1358. d) C. Schäffer, A. Merca, H. Bögge, A. M. Todea, M. L. Kistler, T. Liu, R. Thouvenot, P. Gouzerh, A. Müller, *Angew. Chem., Int. Ed.* **2009**, *48*, 149-153.

[4]   a) T. Jarrosson, O. Oms, G. Bernardinelli, A. F. Williams, *Chimia* **2007**, *61*, 184-185. b) O. Oms, T. Jarrosson, L. H. Tong, A. Vaccaro, G. Bernardinelli, A. F. Williams, *Chem. Eur. J.* **2009**, *15*, 5012-5022.

[5]   a) O. J. Scherer, T. Brück, *Angew. Chem.* **1987**, *99*, 59-59. b) O. J. Scherer, T. Brück, *Angew. Chem., Int. Ed.* **1987**, *26*, 59-59. c) O. J. Scherer, T. Brueck, G. Wolmershaeuser, *Chem. Ber.* **1988**, *121*, 935-938.

[6]   a) R. F. Winter, W. E. Geiger, *Organometallics* **1999**, *18*, 1827-1833. b) F. Li, K. Wu, *Mol. Phys.* **2008**, *106*, 1853-1866.

[7]   a) M. Detzel, G. Friedrich, O. J. Scherer, G. Wolmershäuser, *Angew. Chem., Int. Ed.* **1995**, *34*, 1321-1323. b) O. J. Scherer, S. Weigel, G. Wolmershäuser, *Chem. Eur. J.* **1998**, *4*, 1910-1916. c) F. Dielmann, A. Schindler, S. Scheuermayer, J. Bai, R. Merkle, M. Zabel, A. V. Virovets, E. V. Peresypkina, G. Brunklaus, H. Eckert, M. Scheer, *Chem. Eur. J.* **2012**, *18*, 1168-1179. d) O. J. Scherer, T. Brueck, G. Wolmershaeuser, *Chem. Ber.* **1989**, *122*, 2049-2054. e) M. Detzel, T. Mohr, O. J. Scherer, G. Wolmershaeuser, *Angew. Chem.* **1994**, *106*, 1142-1144. f) M. Scheer, L. J. Gregoriades, A. V. Virovets, W. Kunz, R. Neueder, I. Krossing, *Angew. Chem., Int. Ed.* **2006**, *45*, 5689-5693.

[8]   J. Bai, A. V. Virovets, M. Scheer, *Science* **2003**, *300*, 781-783.

[9]   a) M. Scheer, A. Schindler, R. Merkle, B. P. Johnson, M. Linseis, R. Winter, C. E. Anson, A. V. Virovets, *J. Am. Chem. Soc.* **2007**, *129*, 13386-13387. b) M. Scheer, A. Schindler, C. Groeger, A. V. Virovets, E. V. Peresypkina, *Angew. Chem., Int. Ed.* **2009**, *48*, 5046-5049. c) M. Scheer, A. Schindler, J. Bai, B. P. Johnson, R. Merkle, R. Winter, A. V. Virovets, E. V. Peresypkina, V. A. Blatov, M. Sierka, H. Eckert, *Chem. Eur. J.* **2010**, *16*, 2092-2107. d) C. Schwarzmaier, A. Schindler, C. Heindl, S. Scheuermayer, E. V. Peresypkina, A. V. Virovets, M. Neumeier, R. Gschwind, M. Scheer, *Angew. Chem., Int.*

Ed. **2013**, *52*, 10896-10899.

[10]   F. Dielmann, R. Merkle, S. Heinl, M. Scheer, *Z. Naturforsch., B* **2009**, *64*, 3-10.

[11]   Fabian Dielmann, Claudia Heindl, Matthias Fleischmann, Eugenia V. Peresypkina, Alexander V. Virovets, Ruth M. Gschwind, M. Scheer, Manuscript in Preparation. See also: a) F. Dielmann, PhD Thesis, University of Regensburg (Regensburg, Germany), **2011**. b) M. Fleischmann, PhD Thesis, University of Regensburg (Regensburg, Germany), **2011**.

[12]   S. Heinl, G. Balázs, M. Scheer, *Phosphorus, Sulfur Silicon Relat. Elem.* **2014**, DOI: 10.1080/10426507.2014.903489.

[13]   Radii are measured from Cp-centroid to outer C atoms of the substituents in plane of the Cp ring. Only rough estimations were conducted.

[14]   *I*-C$_{140}$ fullerene is not known so far. See Supplementary Information and Figure 14.1 on page 218.

[15]   Isolated CuBr$_3^{2-}$ ion show Cu–Br bond length of about 2.36 Å. C.f.: a) S. Andersson, S. Jagner, *Acta Chem. Scand., Ser. A* **1987**, *A41*, 230-236. b) G. A. Bowmaker, A. Camus, B. W. Skelton, A. H. White, *J. Chem. Soc., Dalton Trans.* **1990**, 727-731.

[16]   This phenomenon is not known in literature for supramolecules based on pentaphosphaferrocenes. However, this is sometimes observed in our own working group, c.f. reference 11a.

[17]   Occupancy factors of the disordered P atoms: 0.85/0.15, 0.667/0.333, 0.78/0.22, 0.78/0.22, 0.92/0.08.

[18]   For comparison see: E. Mädl, M. V. Butovskiy, G. Balázs, E. V. Peresypkina, A. V. Virovets, M. Seidl, M. Scheer, *Angew. Chem. Int. Ed.* **2014**, accepted. DOI: 10.1002/anie.201403581 and 10.1002/ange.201403581

[19]   a) R. F. Winter, W. E. Geiger, *Organometallics* **1999**, *18*, 1827-1833. b) M. V. Butovskiy, G. Balázs, M. Bodensteiner, E. V. Peresypkina, A. V. Virovets, J. Sutter, M. Scheer, *Angew. Chem.* **2013**, *125*, 3045-3049.

13.5   Supplementary Information

NMR Investigations:

FigureS 13.1. ^{1}H NMR spectrum of **2a** in CD$_2$Cl$_2$ at 298 K.
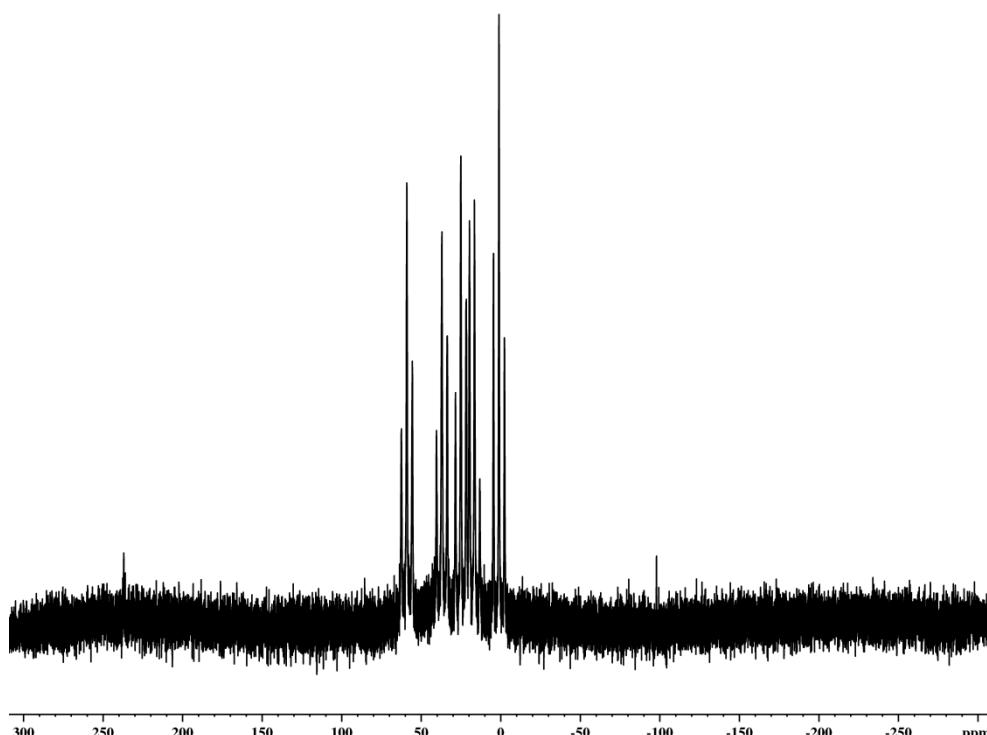
Figure S13.2. ^{31}P{^{1}H} NMR spectrum of **2a** in CD$_2$Cl$_2$ at 298 K.
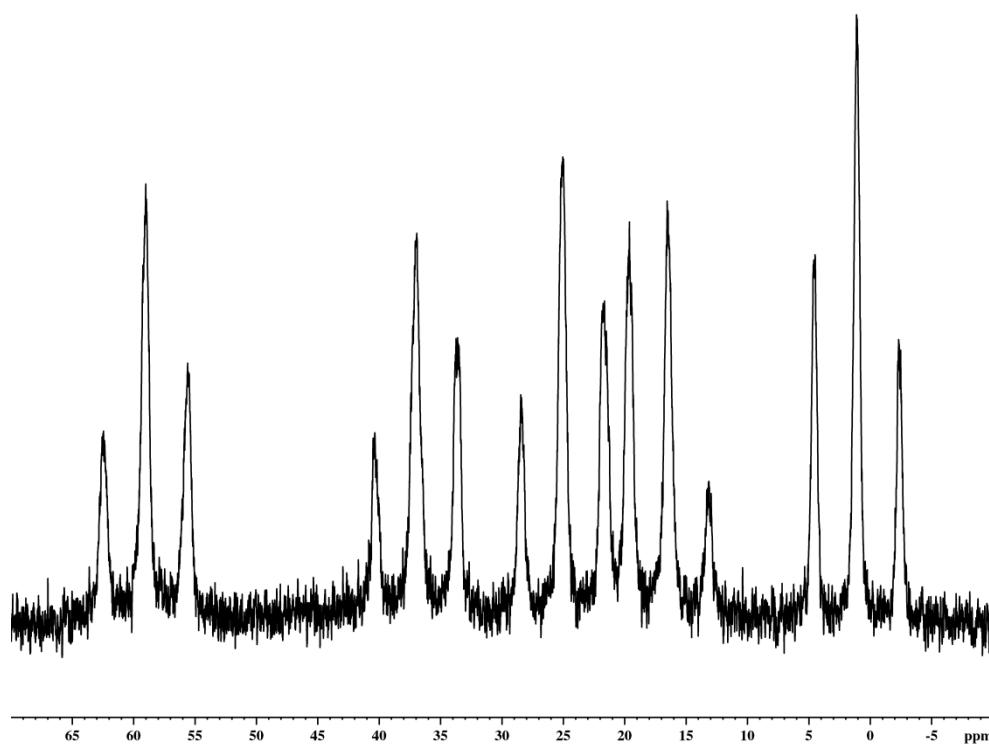
Figure S13.3. Zoomed section of the ^{31}P{^{1}H} NMR spectrum of **2a** in CD$_2$Cl$_2$ at 298 K.
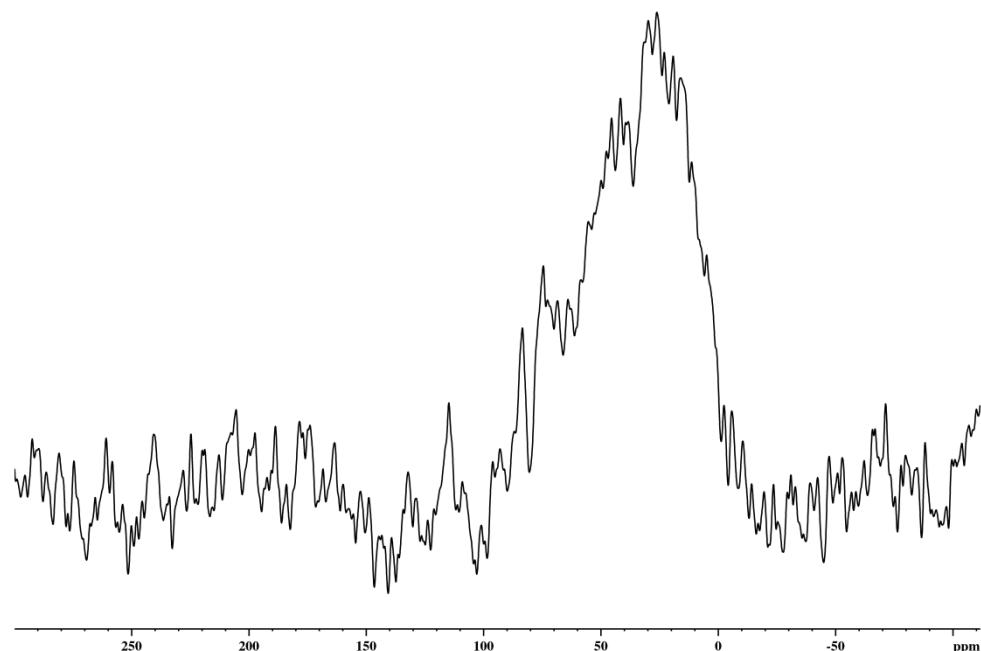
Figure S13.4. ^{31}P{^{1}H} MAS NMR spectrum of **2a** at 298 K.
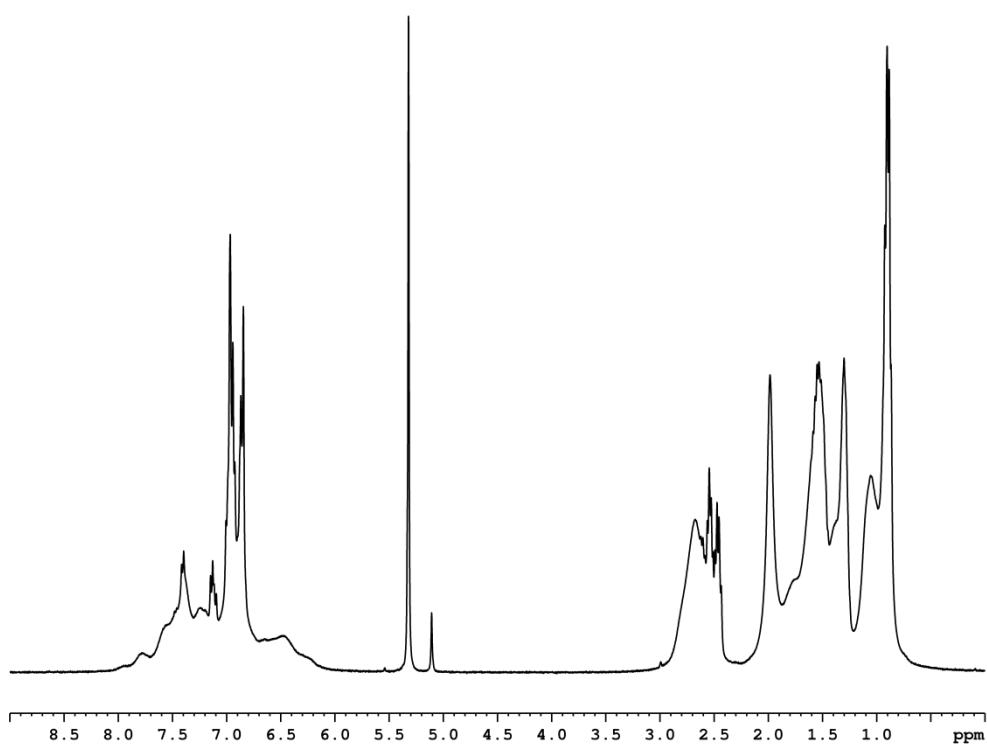
Figure S13.5. ^{1}H NMR spectrum of **2b** in CD$_2$Cl$_2$ at 298 K.
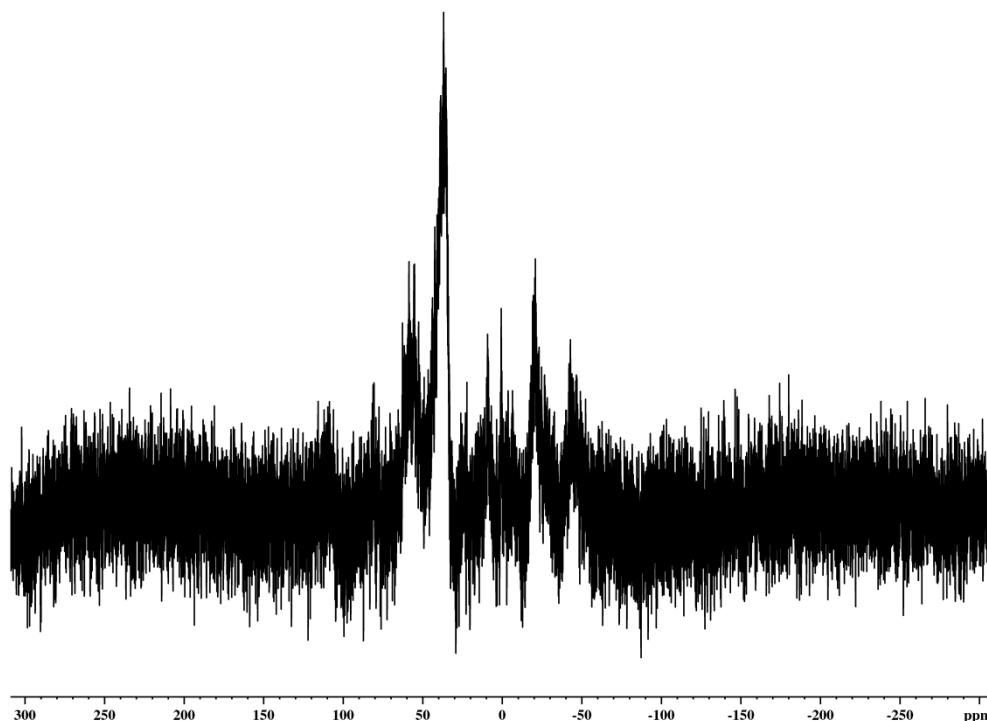
Figure S13.6. ^{31}P{^{1}H} NMR spectrum of **2b** in CD$_2$Cl$_2$ at 298 K.

The Superbulky Pentaphosphaferrocene [Cp^{BIG}Fe(η^5-P$_5$)] as Building Block for the Formation of Macromolecules with Lens-

233
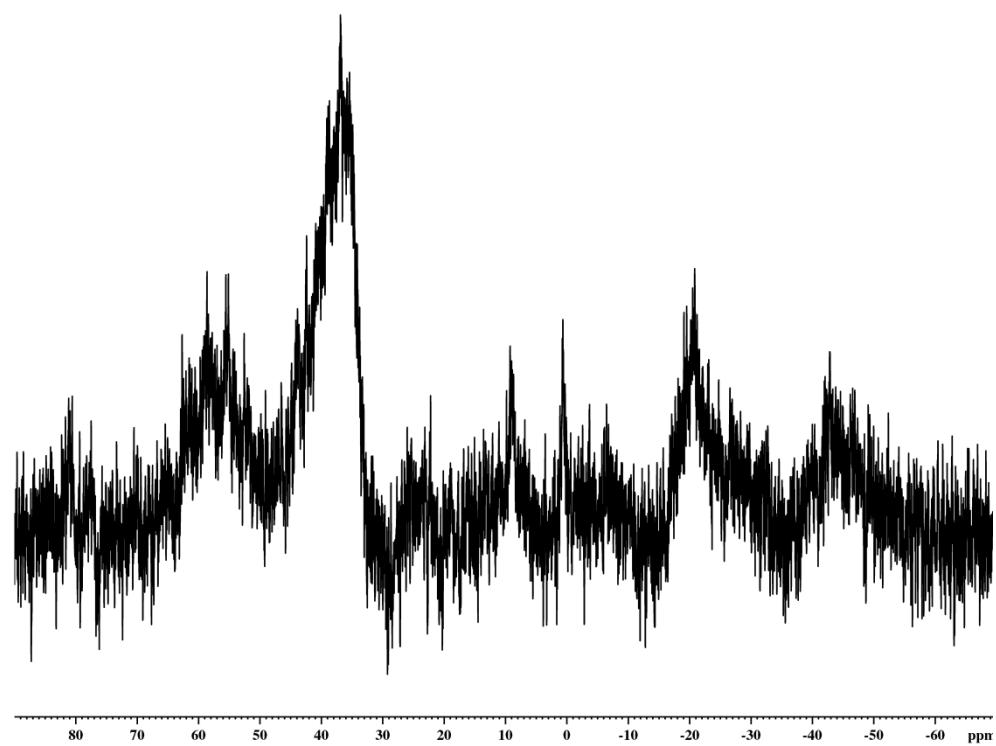
Figure S13.7. Zoomed section of the ^{31}P{^{1}H} NMR spectrum of **2b** in CD$_2$Cl$_2$ at 298 K.
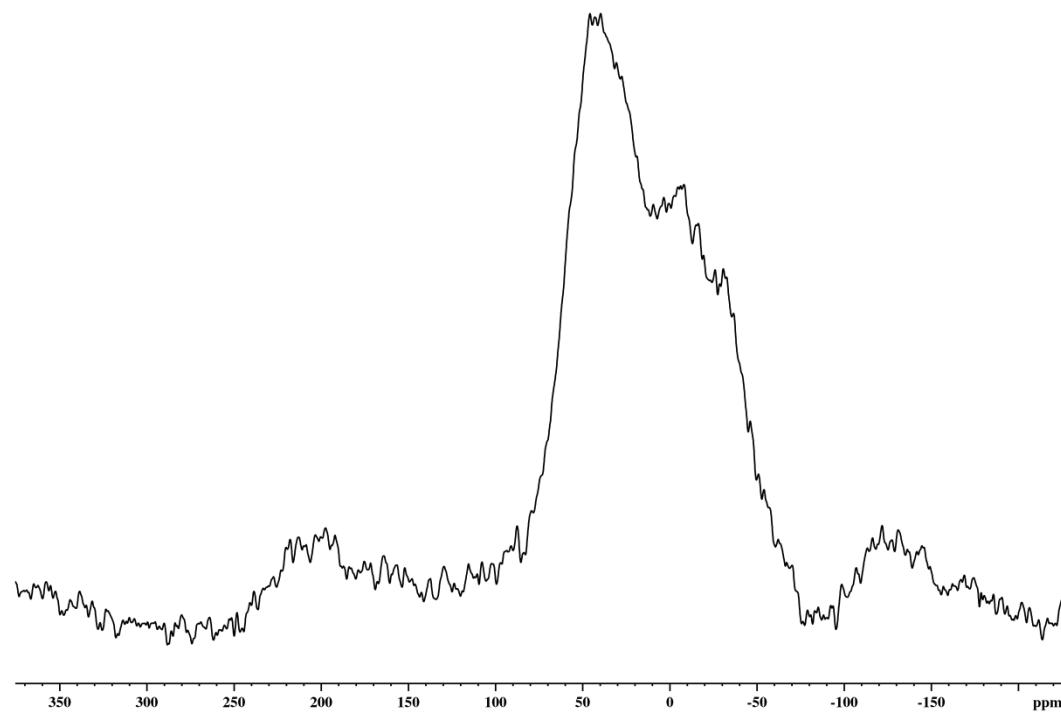
Figure S13.8. ^{31}P{^{1}H} MAS NMR spectrum of **2b** at 298 K.

The Superbulky Pentaphosphaferrocene [Cp^{BIG}Fe(η^5-P$_5$)] as Building Block for the Formation of Macromolecules with Lens-Shaped Scaffolds

Crystallographic Details:

The crystal structure analyses were performed on an Oxford Diffraction SuperNova diffractometer (**2a**, **2b**). For both compounds an analytical absorption correction was carried out.[1] The structures were solved by direct methods either of the program SIR-92[2] or SUPERFLIP[3] and refined with the least square method on F^2 employing SHELXL-97[4] with anisotropic displacements for non-H atoms. Hydrogen atoms were located in idealized positions and refined isotropically according to the riding model.
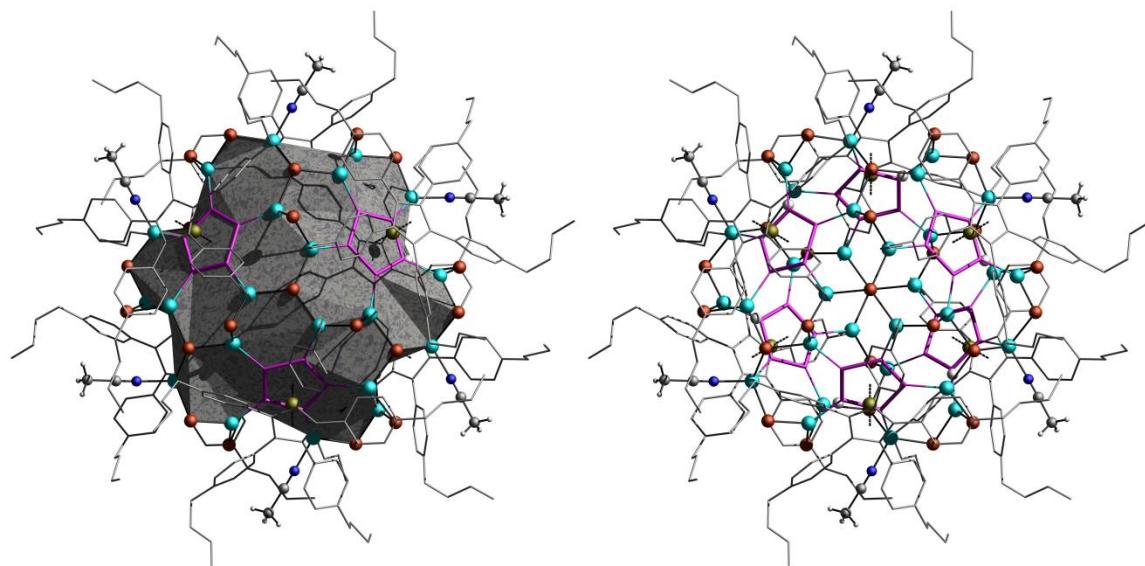
Figure S13.9. Top view of molecular structure of **2a**. Left: **2a** with colored surface of outer inorganic framework. Right: **2a** without core structure.
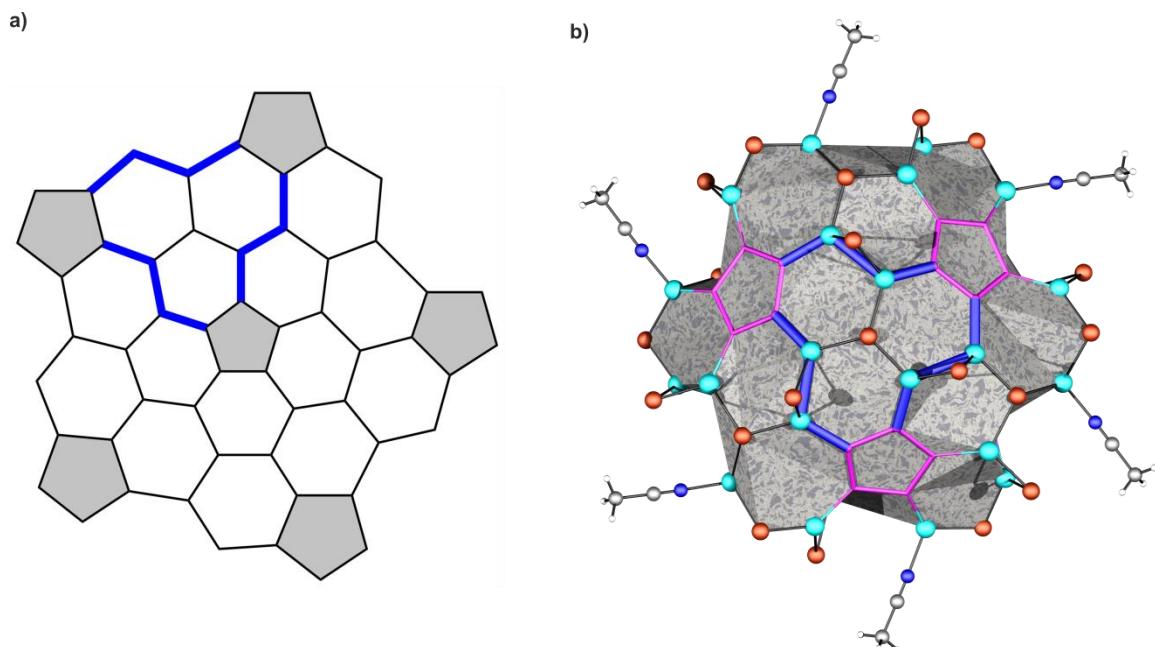
Figure S13.10. a) 2D projection of a section of *I*-C$_{140}$ fullerene. b) Top view of the inorganic scaffold of **2a**. In both pictures some bonds are marked in blue, showing the similarity to each other.

Preliminary Data	Crystal Data for **2a**	Crystal Data for **2b**
Empirical Formula	$C_{342}H_{408}Br_{33}Cu_{33}Fe_6N_6P_{30}$	$C_{342}H_{408}Cl_{26.67}Cu_{26.67}Fe_6N_6P_{30}$
Formula Weight	10648.04	9765.00
Temperature [K]	123(2)	123(2)
Crystal System	trigonal	trigonal
Space Group	$R\bar{3}$	$R\bar{3}$
a [Å]	30.0348(4)	29.61240(10)
b [Å]	30.0348(4)	29.61240(10)
c [Å]	38.1116(9)	38.3988(3)
α [°]	90	90.00
β [°]	90	90.00
γ [°]	120	120.00
Volume [Å³]	29774.0(11)	29160.5(3)
Z	3	3
ρ_{calc} [mg/mm³]	1.782	1.668
μ [mm⁻¹]	9.015	7.500
F(000)	15728.0	15051.0
Crystal Size [mm³]	0.1130 × 0.0677 × 0.0566	0.1255 × 0.0987 × 0.437
Radiation	Cu-K$_\alpha$ (λ = 1.54178)	Cu-K$_\alpha$ (λ = 1.54178)
2Θ Range	5.884 to 134.976°	6.9 to 135°
Index Ranges	-35 ≤ h ≤ 29	-33 ≤ h ≤ 35
	-35 ≤ k ≤ 32	-35 ≤ k ≤ 23
	-45 ≤ l ≤ 45	-45 ≤ l ≤ 43
Reflections Collected	71563	69509
Independent Reflections	11916	11706
	[R_{int} = 0.0359, R_{sigma} = 0.0200]	[R_{int} = 0.0311, R_{sigma} = 0.0205]
Data/Restraints/Parameters	11916/3/750	11706/0/797
Goodness-of-Fit on F^2	1.143	1.048
Final R Indexes [I > 2σ(I)]	R_1 = 0.0529, wR_2 = 0.1548	R_1 = 0.0526, wR_2 = 0.1637
Final R Indexes [All Data]	R_1 = 0.0591, wR_2 = 0.1572	R_1 = 0.0592, wR_2 = 0.1692
Largest Diff. Peak/Hole [e·Å⁻³]	1.24/-0.89	1.05/-1.06
Flack Parameter	-	-

A final refinement was not possible for **2a** and **2b** therefore all given values are preliminary.
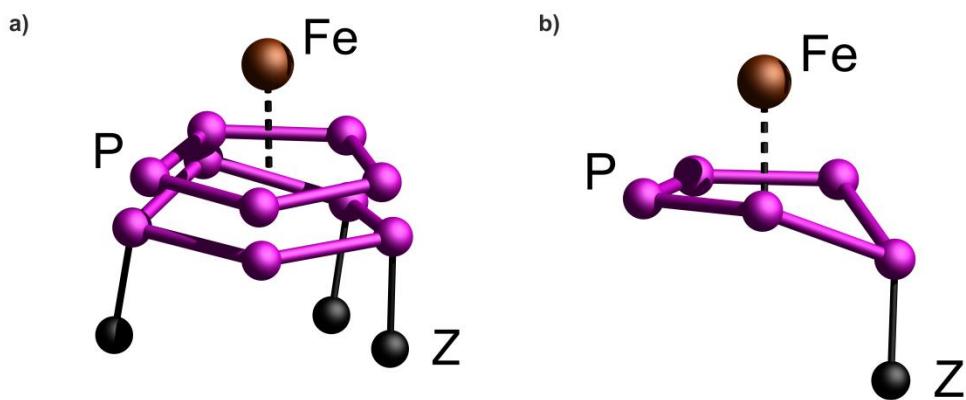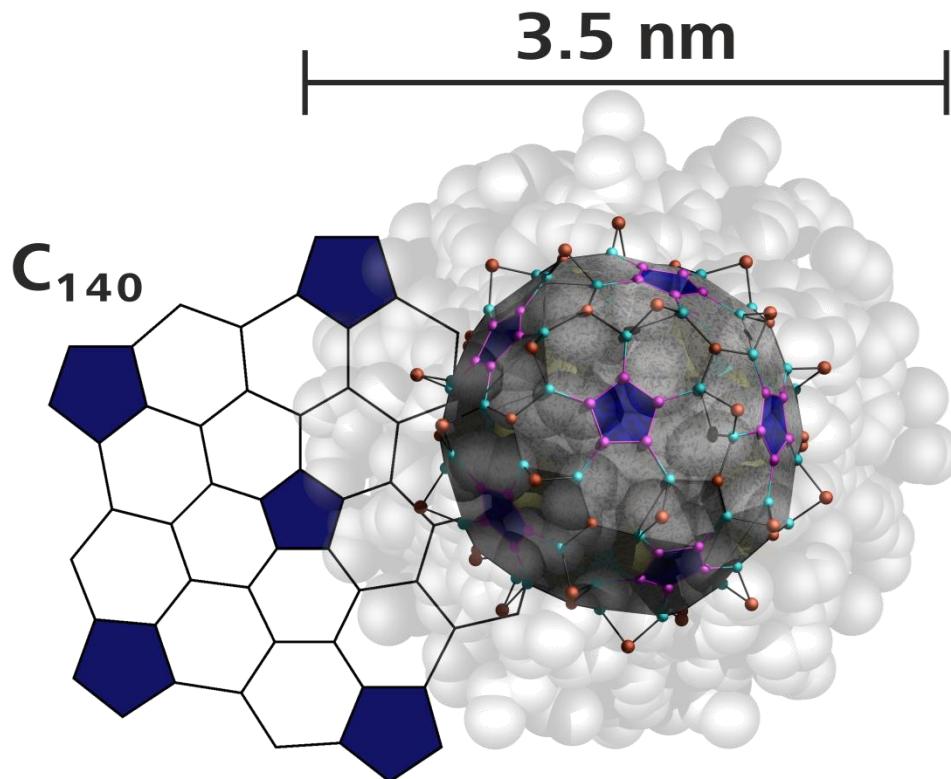
Figure S13.11. Sections of the structure of **2b**. a) Due to disorder almost co-planar P_5 rings with substituent Z. b) One distinct possibility of the disordered P_5 ring.

References for Supplementary Information

[1]   R. C. Clark, J. S. Reid, *Acta Cryst.* **1995**, A51, 887-897.

[2]   A. Altomare, M. C. Burla, M. Camalli, G.L. Cascarano, C. Giacovazzo, A. Guagliardi, A. G. G. Moliterni, G. Polidori, R. Spagna, *J. Appl. Cryst.* **1999**, 32, 115-119.

[3]   L. Palatinus, G. Chapuis, *J. Appl. Cryst.* **2007**, 40, 786-790.

[4]   G. M. Sheldrick, *Acta Cryst.* **2008**, A64, 112-122.

14. A Giant Spherical Cluster with *I*-C$_{140}$ Fullerene Topology

Sebastian Heinl, Eugenia Peresypkina, Alexander V. Virovets, Werner Kremer and Manfred Scheer

- ❖ **All syntheses and characterizations were performed by Sebastian Heinl, unless subsequently noted otherwise**
- ❖ **Manuscript was written by Sebastian Heinl**
- ❖ **Figures were made by Sebastian Heinl**
- ❖ **MAS NMR was measured by Werner Kremer**
- ❖ **X-ray structure analyses and refinement were jointly performed by Sebastian Heinl, Eugenia Peresypkina and Alexander V. Virovets, in which Eugenia Peresypkina and Alexander V. Virovets did the recent refinement. Final refinement of the structure was not possible within the scope of this thesis**

14.1   Introduction

Since the discovery of the C_{60} Buckminster-fullerene[1] in 1985 by Kroto et al., the synthesis of larger fullerenes is in focus of chemical research (Figure 14.1).[2] The largest structurally characterized examples are the endohedral fullerene $Sm_2@C_{104}$ from Balch et al.[3] as well as the chlorinated compounds $C_{104}Cl_{16}$ and $C_{104}Cl_{24}$, both reported by Yang et al.[4] However, also much larger fullerenes up to C_{418} are known as indicated by mass spectrometry.[5] But not only carbon is suitable for the formation of spherical macromolecules with fullerene topology. In polyoxometalate chemistry, Keplerates[6] with the simplified formula $[\{(M^{V})Mo^{VI}_5\}_{12}(linker)_{30}]$ (M = Mo, W) are well known.[7] In addition, pentasubstituted Cp^R derivatives can also form nano balls in combination with metal salts, Williams et al. for example, used $[(C_5H_4PO^tBu_2)Fe\{C_5(4\text{-pyridyl})_5\}]$ and Cu(I) cations.[8] Also using coordination compounds, Fujita et al. succeeded in the preparation of several spherical compounds by using oligopodal pyridine linkers and Pd(II) moieties, although none of them showed fullerene-like topology.[9] The pentaphosphaferrocenes $[Cp^RFe(\eta^5\text{-}P_5)]$ are also excellent building blocks for the formation of fullerene-like supramolecules. In 2003, Scheer et al. reported on the synthesis of $[\{Cp^*Fe(\eta^{5:1:1:1:1:1}\text{-}P_5)\}_{12}\{CuCl\}_{10}\{Cu_2Cl_3\}_5\{Cu(CH_3CN)_2\}_5]$[10] ($Cp^* = C_5Me_5$), built by 90 inorganic scaffold atoms. Depending on the Cu halide, template and reaction conditions, different structures could be obtained (e.g. scaffolds with I_h-C_{80} analogy).[11] With $[Cp^{bn}Fe(\eta^5\text{-}P_5)]$ ($Cp^{bn} = C_5(CH_2Ph)_5$)[12] as a linker, well soluble products were obtained.[13] Very recently we reported on the synthesis of the lens-shaped clusters $[\{Cp^{BIG}Fe(\eta^4\text{-}P_5)\}_6Cu_{34}Cl_{28}(CH_3CN)_6]$ and $[\{Cp^{BIG}Fe(\eta^5\text{-}P_5)\}_6(CuBr)_{32}(CH_3CN)_6]$, using the superbulky pentaphosphaferrocene $[Cp^{BIG}Fe(\eta^5\text{-}P_5)]$ (**1**; $Cp^{BIG} = C_5(4\text{-}n\text{BuC}_6H_4)_5)$.[14]

The radius of the Cp^{BIG} ligand (r $\approx$ 9 Å) is about three times larger than that of the Cp^* ligand (r $\approx$ 3 Å).[15] The increased steric demand compulsorily obviates the formation of structures which are comparable to those obtained with $[Cp^*Fe(\eta^5\text{-}P_5)]$.[10,11] The system can
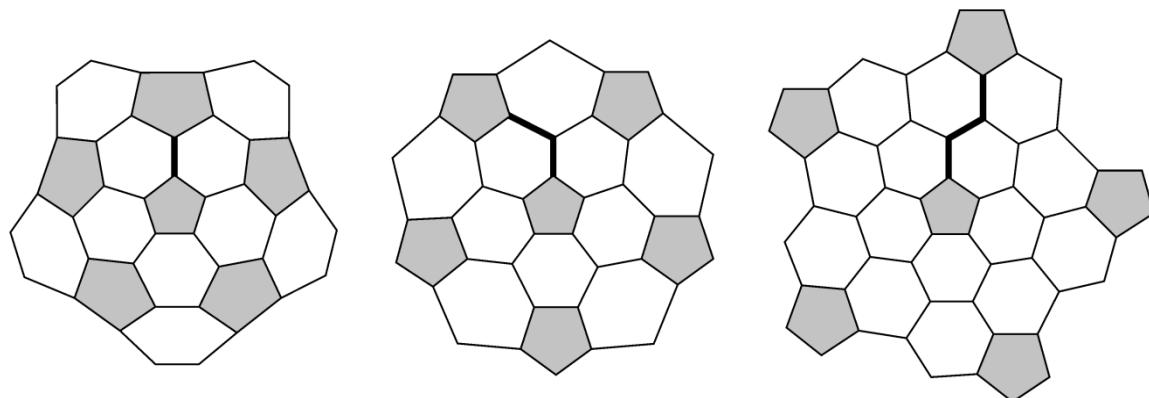
Figure 14.1. 2D projections of sections of the fullerene frameworks of C_{60} (left), I_h-C_{80} (middle) and I-C_{140} (right). The shortest connections between C_5 rings are highlighted.

avoid steric repulsion in two ways. The first possibility is to arrange fewer building blocks in a specific area, as it is observed in the lens-shaped compounds [{Cp^{BIG}Fe(η^4-P$_5$)}$_6$Cu$_{34}$Cl$_{28}$(CH$_3$CN)$_6$] and [{Cp^{BIG}Fe(η^5-P$_5$)}$_6$(CuBr)$_{32}$(CH$_3$CN)$_6$] (six pentaphosphaferrocene units instead of twelve). The alternative is moving the building blocks **1** further apart from each other. This results in an effective cluster expansion compared to the Cp* and Cp^{bn} derivatives.

Herein we report on the preparation and characterization of the 'expanded' cluster [{Cp^{BIG}Fe($\eta^{5:2:1:1:1:1:1}$-P$_5$)}$_{12}$(CuBr)$_{92}$] (**2**), which shows structural analogies to the theoretical *I*-C$_{140}$ fullerene.

14.2   Results and Discussion

Addition of a CH$_2$Cl$_2$ solution of **1** to a CH$_3$CN solution of CuBr results in the formation of the novel giant molecule [{Cp^{BIG}Fe($\eta^{5:2:1:1:1:1:1}$-P$_5$)}$_{12}$(CuBr)$_{92}$] (**2**) in low to moderate yields.[16] Compound **2** is poorly soluble in CH$_2$Cl$_2$. Furthermore, **2** is insoluble in hexane, toluene, CH$_3$CN and Et$_2$O. By diffusion of toluene into CH$_2$Cl$_2$ solutions, compound **2** crystallizes in the monoclinic space group *C2/c* as black cubes. Crystals could also be grown if hexane is used instead of toluene. However, they quickly lose crystallinity when they are removed from the mother liquor.

The idealized scaffold of **2** consists of 92 copper and 92 bromide positions as well as twelve units of **1** (see below). The macromolecule has an outer diameter of about 3.5 nm and shows a two-shell structure. This is in contrast to the compounds built by [Cp*Fe(η^5-P$_5$)], which exclusively show one-shell aggregates (filled by template or solvent molecules).[10,11,13] The 'space-filling' view of **2** exhibits a tight arrangement of the twelve Cp^{BIG} ligands forming a pentagonal dodecahedron (Figure 14.2a). The macromolecules are ordered in a slightly distorted cubic close packing (Figure S14.4).

All P atoms of the pentaphosphaferrocene units **1** are coordinated to a Cu ion resulting in a 1,2,3,4,5 coordination mode (Figure 14.2b,c,d). Each Cu ion of the outer shell additionally binds to three bromide ions: one pointing inwardly, one 'in plane' and one 'out of plane' (Figure 14.2c). These inwardly pointing Br ions represent one connection between the outer and the inner scaffold. Interestingly, with twelve five-membered P$_5$ rings and 60 six-membered P$_2$Cu$_3$Br rings ('in plane' Br), the idealized scaffold of **2** shows analogy to the theoretical structure of *I*-C$_{140}$ fullerene (Figure 14.2d). 30 'out of plane' Br atoms bridge the 30 Cu–Cu edges of the outer framework.

Inside the outer scaffold a second inner shell of a pentagon-dodecahedral shape is formed, whose edges and nodes are occupied by the 30 Br ions pointing inwards and 20 Cu ions,
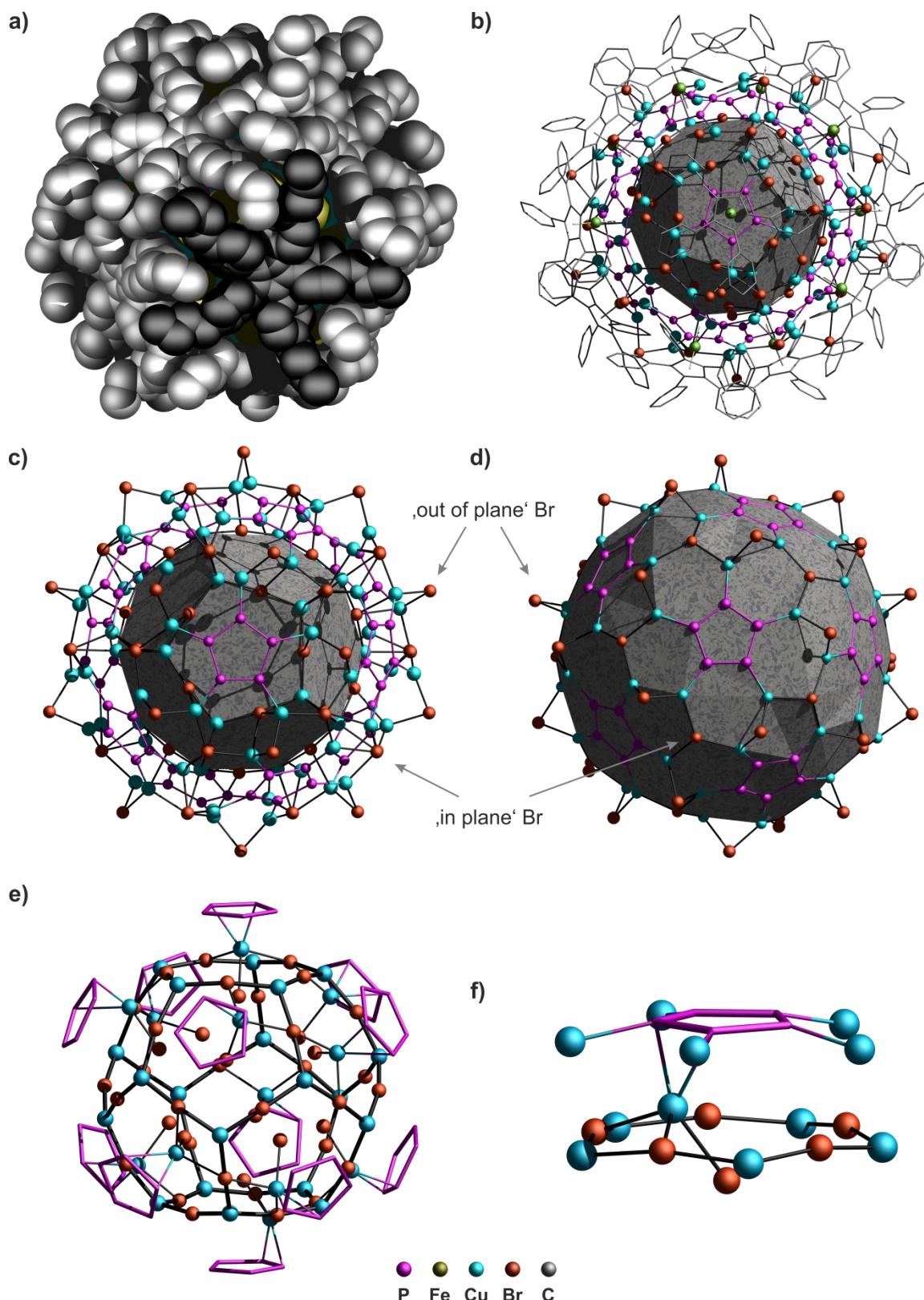
Figure 14.2. Stepwise buildup of the molecular structure of **2**. a) Complete aggregate in 'space-filling' model; one Cp^{BIG} ligand is highlighted in black and H atoms are omitted for clarity. b) Complete aggregate in 'ball-and-stick' model with inner Cu$_{20}$ dodecahedron; *n*Butyl groups are omitted for clarity. c) Inorganic scaffold of **2** with inner Cu$_{20}$ dodecahedron. d) Idealized inorganic scaffold of **2** representing *I*-C$_{140}$ analogy. e) Inner CuBr framework including all disordered positions of copper. f) Interconnection of the outer and inner shell via additional η^2-coordination of Cu ions to **1**.

respectively (d$_\emptyset \approx$ 14 Å). Twelve additional CuBr fragments coordinate to two adjusted Br ions in a way, that each pentagonal {Cu$_5$Br$_5$} cycle bears only one of it (Figure 14.2e). Every Cu ion of this additional CuBr unit coordinates one pentaphosphaferrocene **1** in a η^2-mode and therefore further connects the inner and outer shells (Figure 14.2f). The Br positions of these η^2 bound CuBr units form an icosahedron inside the dodecahedron.

Compound **2** is a solid solution of different isomers, which are related to each other by different amount and location of vacancies in the idealized molecular structure described above.[16] One of the isomers with non-contradictory molecular structure is shown in Figure S14.5b. The overall composition [{Cp^{BIG}FeP$_5$}$_{12}$Cu$_{70}$Br$_{83}$] is therefore seriously Cu-vacant and unsaturated with Cu and Br with respect to the idealized neutral composition [{Cp^{BIG}FeP$_5$}$_{12}$Cu$_{92}$Br$_{92}$]. The charge misbalance of 13 cannot be resolved within the current state of the structural investigation without an unreasonably increase of the displacement parameters of heavy copper atoms, resulting from an increase of their occupancies. Note that the objectively received difference between Cu and Br is close to 12 and therefore the lack of positive charges can also be attributed to one-electron oxidation of the pentaphosphaferrocenes **1**. The residual density and quality factors of the refinement are quite low and do not allow the interpretation of the 'incomplete model', where solvated copper counter cations are located in the interstitial space between the negatively-charged supramolecules. A series of X-ray structure analyses were carried out, always resulting in very similar results and charge misbalance.

The interior of the dodecahedron seems to be empty, though it is assumed that solvent molecules fill the cavity. Because of heavy disorder and no favored orientation, appropriate electron density peaks for the refinement of the solvent molecules could not be found from the difference Fourier map. The same observation can be made for the space between the macromolecules. With the aid of the program SQUEEZE,[17] solvent accessible voids were found with approximate volumes of 2200 Å^3, containing about 880 electrons.

The elemental analysis of **2** shows values, in between those for the idealized composition [{Cp^{BIG}FeP$_5$}$_{12}$Cu$_{92}$Br$_{92}$] and the crystallographically assumed formula [{Cp^{BIG}FeP$_5$}$_{12}$Cu$_{70}$Br$_{83}$] and fits best for the (equimolar Cu and Br) composition [{Cp^{BIG}FeP$_5$}$_{12}$Cu$_{81}$Br$_{81}$] (see experimental part).

It was not possible to detect the molecular ion peak of **2** by mass spectrometry, which is usually the case for such clusters.[10,11,13] The ESI mass spectrum (CH$_2$Cl$_2$/CH$_3$CN) of **2** shows peaks at *m/z* = 2082.0 and 1937.4 for [(Cp^{BIG}FeP$_5$)$_2$Cu$_2$Br]$^+$ and [(Cp^{BIG}FeP$_5$)$_2$Cu]$^+$, respectively, with low intensities. The base peak corresponds to [Cu(CH$_3$CN)(CH$_2$Cl$_2$)]$^+$.

The ^{31}P{^{1}H} NMR spectrum of **2** shows one very broad signal at about δ = 30 ppm. The signal is not well resolved, which on the one hand can be explained by the non-equivalent P

atoms and on the other hand by the low solubility. Similar to the previously obtained clusters derived from **1** (Chapter 13), the ^{1}H NMR spectrum of **2** shows several superimposed sets of signals, which is consistent with not freely rotating Cp^{BIG} ligands. The ^{31}P{^{1}H} MAS NMR spectrum shows one very broad, but symmetric signal at 30 ppm with $\omega_{1/2}$ = 5800 Hz.

In summary, we have shown the synthesis of the giant spherical molecule **2** with a diameter of about 3.5 nm. The aggregate exhibits structural analogy to the so far unknown *I*-C$_{140}$ fullerene. In contrast to the supramolecules obtained by [Cp*Fe(η^5-P$_5$)], but in agreement with that derived from **1**, compound **2** shows a CuBr framework inside the inorganic shell. The cluster shows rare solubility, but it could be characterized by NMR spectroscopy and mass spectrometry in solution. Due to its hollow structure the question arises, if **2** might be capable for acting as host for appropriate template molecules.

14.3   Experimental Part

General Remarks:

All experiments were carried out under an atmosphere of dry argon or nitrogen using glovebox and schlenk techniques. Solvents were purified, dried and degassed prior to use. CuBr was used as obtained by commercial suppliers, [Cp^{BIG}Fe(η^5-P$_5$)][18] was prepared according to literature procedure. The NMR spectra in solution were measured on a Bruker Avance 300, 400 or 600 spectrometer. The MAS NMR spectrum was recorded on a Bruker Advance 300 spectrometer by using a double resonance 2.5 mm MAS probe (^{31}P: 121.495 MHz). Spectrum was acquired at MAS rotation frequencies up to 20 kHz with a 90° pulse length of about 2.3 µs and relaxation delays of 120 s (^{31}P). ESI-MS spectra were measured on a ThermoQuest Finnigan TSG 7000 mass spectrometer. The elemental analyses were determined on a Vario EL III apparatus.

Synthesis of [{Cp^{BIG}Fe($\eta^{5:2:1:1:1:1:1}$-P$_5$)}$_{12}$(CuBr)$_{92}$] (2):

To a solution of CuBr (100 mg, 6.7 mmol) in 5 mL CH$_3$CN a solution of [Cp^{BIG}Fe(η^5-P$_5$)] (60 mg, 64 µmol) in 5 mL CH$_2$Cl$_2$ is added and stirred for 30 min resulting in a brown solution. After the solvent is removed in vacuum the residue is triturated with 10 mL CH$_2$Cl$_2$ and filtered through cannula into a thin Schlenk tube. The reaction mixture is layered with 20 mL toluene. After complete diffusion black crystals of **2** are obtained (32 mg, 25% for idealized cluster).

2: [{Cp^{BIG}FeP$_5$}$_{12}$Cu$_{92}$Br$_{92}$] calc. C, 32.44; H, 3.22. [{Cp^{BIG}FeP$_5$}$_{12}$Cu$_{70}$Br$_{83}$] calc. C, 35.51; H, 3.52. [{Cp^{BIG}FeP$_5$}$_{12}$Cu$_{81}$Br$_{81}$] calc. C, 34.67; H, 3.44. found: C, 34.71; H, 3.46. ESI-MS (CH$_3$CN/CH$_2$Cl$_2$, cation): *m/z* (%) = 2082.0 (1%, [(Cp^{BIG}FeP$_5$)$_2$Cu$_2$Br]$^+$), 1937.4 (2%,

[(Cp^{BIG}FeP$_5$)$_2$Cu]$^+$), 189.8 (100%, [Cu(CH$_3$CN)(CH$_2$Cl$_2$)]$^+$), 144.9 (30%, [Cu(CH$_3$CN)$_2$]$^+$). For NMR Spectra see supplementary Information.

14.4   References

[1]   H. W. Kroto, J. R. Heath, S. C. O'Brien, R. F. Curl, R. E.Smalley, *Nature* **1985**, *318*, 162-163.

[2]   For general information on fullerenes, see: a) P. W. Fowler, D. E. Manolopoulos, *An Atlas of fullerenes*, Clarendon Press, **1995**. b) M. S. Dresselhaus, G. Dresselhaus, P. C. Eklund, *Science of Fullerenes and carbon Nanotubes*, Academic Press, **1996**.

[3]   B. Q. Mercado, A. Jiang, H. Yang, Z. Wang, H. Jin, Z. Liu, M. M. Olmstead, A. L. Balch, *Angew. Chem.* **2009**, *121*, 9278-9280.

[4]   S. Yang, T. Wei, E. Kemnitz, S. I. Troyanov, *Chem. Asian J.* **2014**, *9*, 79-82.

[5]   a) F. Beer, A. Gugel, K. Martin, J. Rader, K. Mullen, *J. Mater. Chem.* **1997**, *7*, 1327-1330. b) H. Shinohara, H. Sato, Y. Saito, M. Takayama, A. Izuoka, T. Sugawara, *J. Phys. Chem.* **1991**, *95*, 8449-8451.

[6]   For the definition, see: A. Müller, *Nature* **2007**, *447*, 1035.

[7]   a) A. Müller, E. Krickemeyer, H. Bögge, M. Schmidtmann, F. Peters, *Angew. Chem.* **1998**, *110*, 3567-3571. b) A. Müller, E. Krickemeyer, H. Bögge, M. Schmidtmann, F. Peters, *Angew. Chem., Int. Ed.* **1998**, *37*, 3359-3363. c) A. Müller, P. Kogerler, C. Kuhlmann, *Chem. Commun.* **1999**, 1347-1358. d) C. Schäffer, A. Merca, H. Bögge, A. M. Todea, M. L. Kistler, T. Liu, R. Thouvenot, P. Gouzerh, A. Müller, *Angew. Chem., Int. Ed.* **2009**, *48*, 149-153.

[8]   a) T. Jarrosson, O. Oms, G. Bernardinelli, A. F. Williams, *Chimia* **2007**, *61*, 184-185. b) O. Oms, T. Jarrosson, L. H. Tong, A. Vaccaro, G. Bernardinelli, A. F. Williams, *Chem. Eur. J.* **2009**, *15*, 5012-5022.

[9]   a) Y. Fang, T. Murase, S. Sato, M. Fujita, *J. Am. Chem. Soc.* **2013**, *135*, 613-615. b) S. Horiuchi, T. Murase, M. Fujita, *Angew. Chem., Int. Ed.* **2012**, *51*, 12029-12031. c) Q.-F. Sun, J. Iwasa, D. Ogawa, Y. Ishido, S. Sato, T. Ozeki, Y. Sei, K. Yamaguchi, M. Fujita, *Science* **2010**, *328*, 1144-1147. d) S. Sato, Y. Ishido, M. Fujita, *J. Am. Chem. Soc.* **2009**, *131*, 6064-6065.

[10] J. Bai, A. V. Virovets, M. Scheer, *Science* **2003**, *300*, 781-783.

[11] a) M. Scheer, A. Schindler, R. Merkle, B. P. Johnson, M. Linseis, R. Winter, C. E. Anson, A. V. Virovets, *J. Am. Chem. Soc.* **2007**, *129*, 13386-13387. b) M. Scheer, A. Schindler, C. Groeger, A. V. Virovets, E. V. Peresypkina, *Angew. Chem., Int. Ed.* **2009**, *48*, 5046-5049. c) M. Scheer, A. Schindler, J. Bai, B. P. Johnson, R. Merkle, R. Winter, A. V. Virovets, E. V. Peresypkina, V. A. Blatov, M. Sierka, H. Eckert, *Chem. Eur. J.* **2010**, *16*, 2092-2107. d) C. Schwarzmaier, A. Schindler, C. Heindl, S. Scheuermayer, E. V.

Peresypkina, A. V. Virovets, M. Neumeier, R. Gschwind, M. Scheer, *Angew. Chem., Int. Ed.* **2013**, *52*, 10896-10899.

[12]   F. Dielmann, R. Merkle, S. Heinl, M. Scheer, *Z. Naturforsch., B* **2009**, *64*, 3-10.

[13]   Fabian Dielmann, Claudia Heindl, Matthias Fleischmann, Eugenia V. Peresypkina, Alexander V. Virovets, Ruth M. Gschwind, M. Scheer, Manuscript in Preparation. See also: a) F. Dielmann, PhD Thesis, University of Regensburg (Regensburg, Germany), **2011**. b) M. Fleischmann, PhD Thesis, University of Regensburg (Regensburg, Germany), **2011**.

[14]   See chapter 13.

[15]   Radii are measured from Cp-centroid to outer C atoms of substituents. Only rough estimations were conducted.

[16]   Given sum formula is idealized. For closer information see description of X-ray structure and Supplementary Information.

[17]   Sluis, P. van der & Spek, A.L. *Acta Cryst.* **1990**, A46, 194-201.

[18]   S. Heinl, G. Balázs, M. Scheer, *Phosphorus, Sulfur Silicon Relat. Elem.* **2014**, DOI: 10.1080/10426507.2014.903489.

14.5   Supplementary Information

NMR Investigations:

CH₂Cl₂   CH₃CN
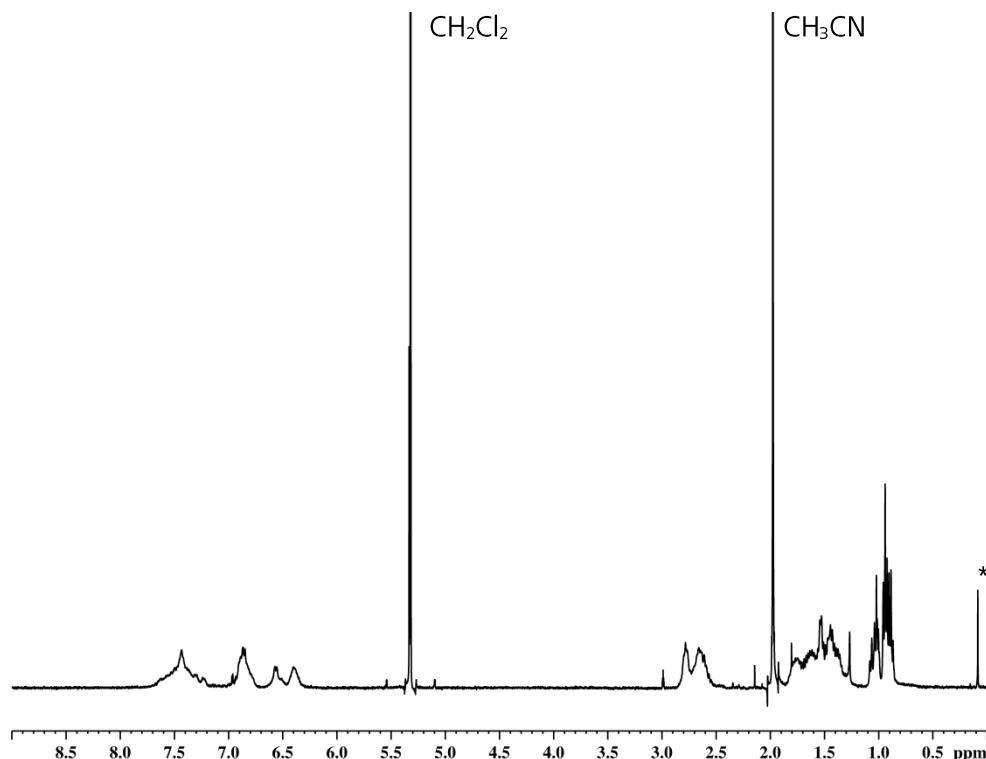
Figure S14.1. ¹H NMR spectrum of **2** in CD₂Cl₂ at 298 K. Signal marked with an asterisk is due to silicon grease impurities.
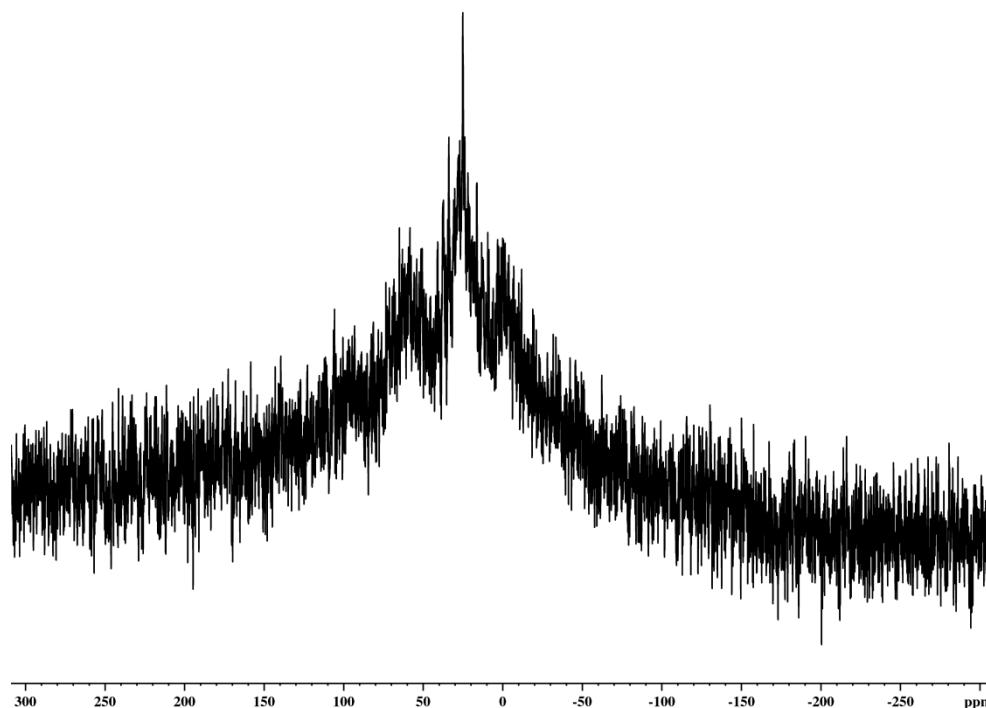
Figure S14.2. ³¹P{¹H} NMR spectrum of **2** in CD₂Cl₂ at 298 K.
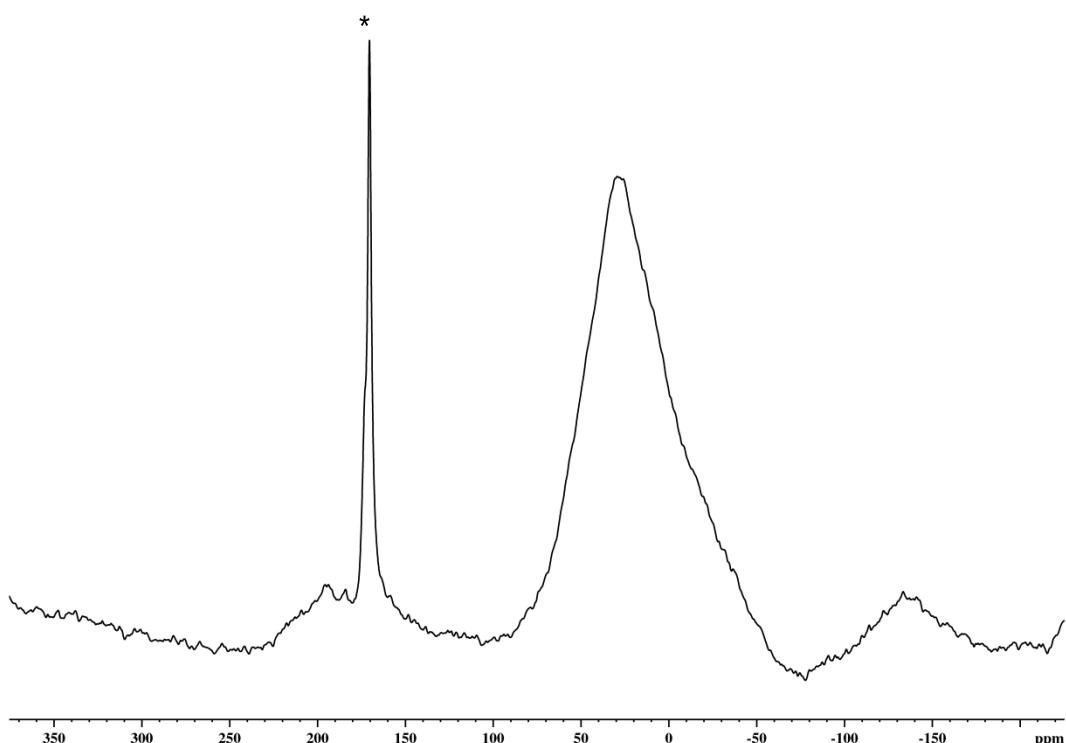
Figure S14.3. ^{31}P{^{1}H} MAS NMR spectrum of **2** at 298 K. Signal signed with asterisk arises from impurities of **1**.

Crystallographic Details:

The crystal structure analysis was performed on an Oxford Diffraction SuperNova diffractometer. An analytical absorption correction was carried out.[1] The structures were solved by direct methods either of the program SIR-92[2] or SUPERFLIP[3] and refined with the least square method on F^2 employing SHELXL-97[4] with anisotropic displacements for non-H atoms. Hydrogen atoms were located in idealized positions and refined isotropically according to the riding model.

In supramolecule **2**, some positions of Cu and Br are partly vacant indicated by larger displacement parameters. The occupancies for these positions were refined with an average isotropic U_{iso} of 0.05 typical for fully-occupied heavy atoms in this crystal structure. The constraints on the Cu and Br displacement parameters were then removed and an anisotropic approximation was used for the further refinement. The n-butyl groups of the pentaphosphaferrocene ligands are often disordered over two, sometimes three positions. The occupancies of the positions were refined with U_{iso} = 0.08, allowing higher displacements for light atoms and were then fixed in the obtained values. The carbon atoms with occupancies of less than 0.5 were refined isotropically.

According to X-ray diffraction data the idealized neutral molecular structure contains numerous vacancies in Cu and Br positions. In the outer shell all Br positions are fully occupied, while 8.5 Cu ions in total are statistically missing, every position with a different probability (0.0 − 0.3). In addition, every position of Cu is split into two close ones. In the icosahedral part of the inner shell (Figure 14.2e), only 7 Cu ions are disordered over 20 available positions, and all Br positions are fully occupied. The occupancies of atoms in the 'additional CuBr fragments' are much higher for Cu than for Br. Therefore, the 12 CuBr fragments which appear in idealized structure are reduced to 2 or 3 per supramolecule (2.7 in average) and 9 or 8 Cu ions with one vacant coordination site respectively. In total, only 11 of 12 pentaphosphaferrocenes are coordinated to the Cu ions in η^2-mode.

Analysis of crystal packing of supramolecules was performed with TOPOS 4.0 Professional software.[5] The supramolecules are arranged in a crystal following a slightly distorted motif of the face-centered cubic (f.c.c.) packing (Figure S14.4).
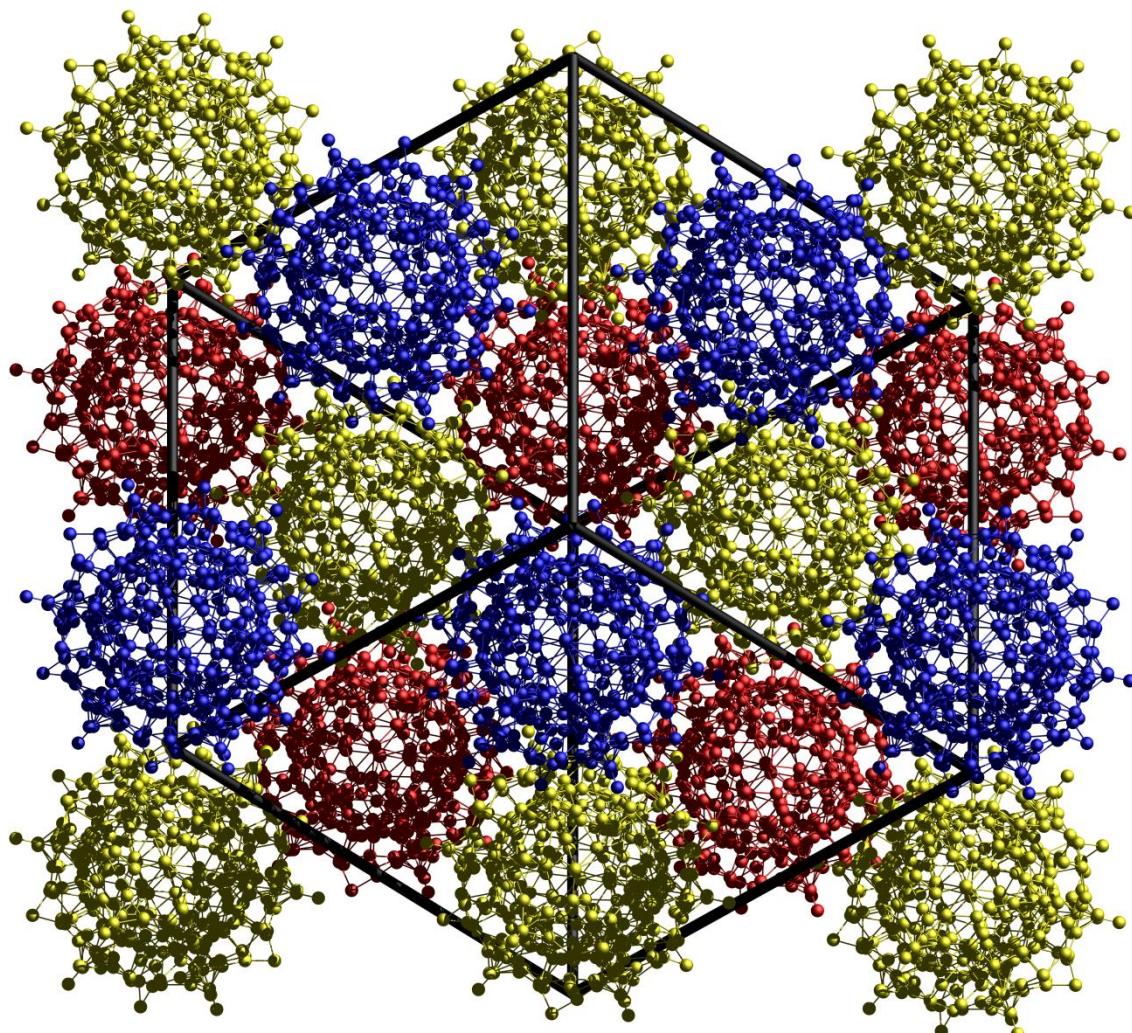
Figure S14.4. Three-layered face-centered cubic close packing of aggregates **2** in the crystal, view along the [111] direction. Each layer is drawn with a different color.

Preliminary Data	Crystal Data for **2**
Empirical Formula	C$_{660}$H$_{780}$Br$_{92-x}$Cu$_{92-x}$Fe$_{12}$P$_{60}$
Formula Weight	22269.78
Temperature [K]	123(2)
Crystal System	monoclinic
Space Group	*C2/c*
a [Å]	43.1169(3)
b [Å]	42.1302(2)
c [Å]	43.2800(2)
α [°]	90
β [°]	92.3100(10)
γ [°]	90
Volume [Å^3]	78555.2(8)
Z	4
ρ_{calc} [mg/mm^3]	1.883
μ [mm^{-1}]	10.109
F(000)	43455.0
Crystal Size [mm^3]	0.114 × 0.174 × 0.264
Radiation	Cu-K$_α$ (λ = 1.54178)
2*Θ* Range	6.16 to 150.646°
Index Ranges	-53 ≤ h ≤ 52
	-52 ≤ k ≤ 52
	-44 ≤ l ≤ 53
Reflections Collected	427909
Independent Reflections	79287
	[R_{int} = 0.0519, R_{sigma} = 0.0301]
Data/Restraints/Parameters	79287/0/4105
Goodness-of-Fit on *F^2*	1.067
Final *R* Indexes [I > 2σ(I)]	*R$_1$* = 0.0775, *wR$_2$* = 0.2525
Final *R* Indexes [All Data]	*R$_1$* = 0.1004, *wR$_2$* = 0.2678
Largest Diff. Peak/Hole [e·Å^{-3}]	3.31/-1.36
Flack Parameter	-

A final refinement was not possible for **2a** therefore all given values are preliminary.

a)

P Fe Cu Br

b)
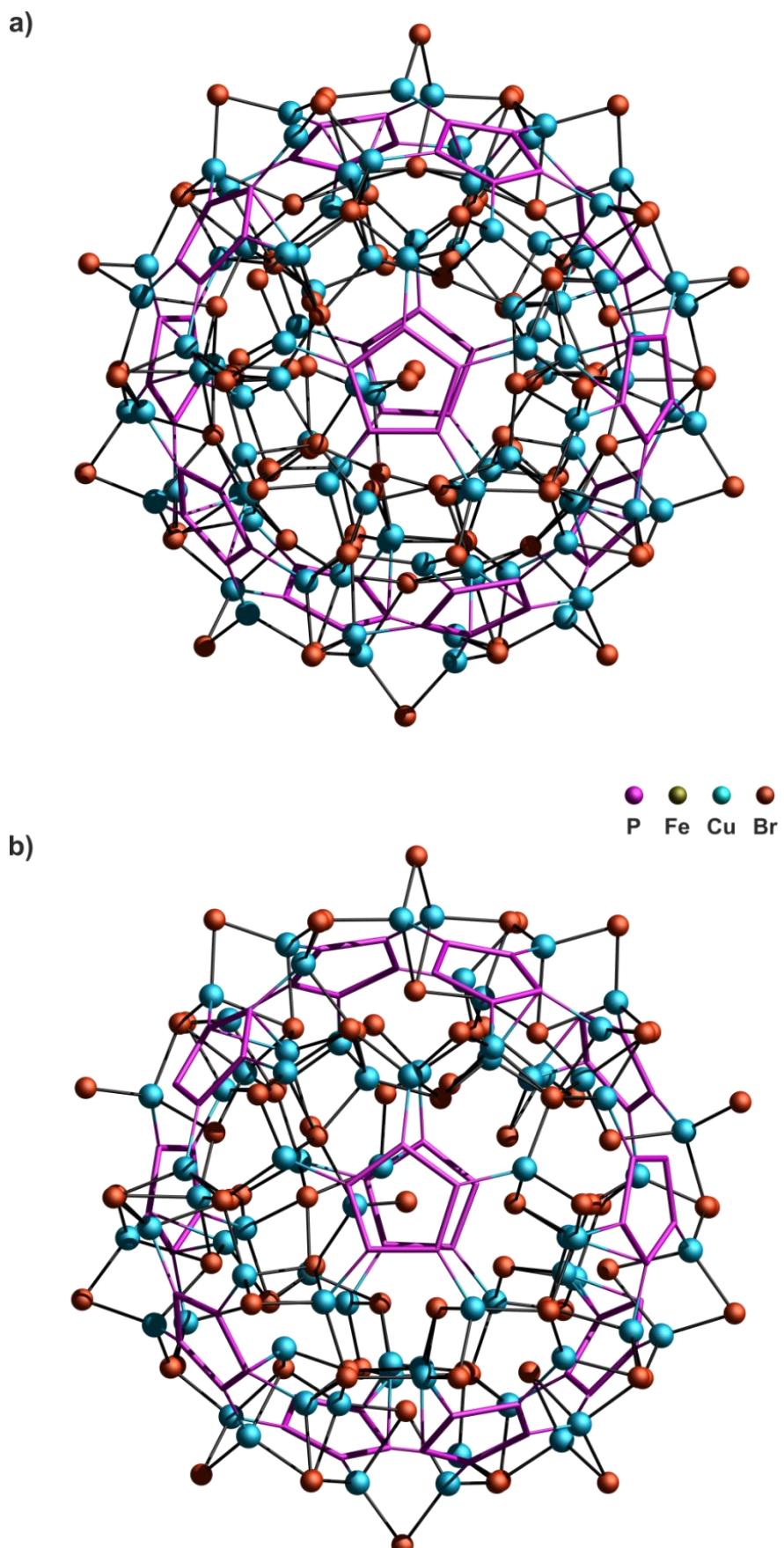
Figure S14.5. Inorganic scaffolds of **2**. a) Idealized aggregate with fully occupied atoms. b) Framework of one possible isomer with all partial occupancies taken into account.

References for Supplementary Information

[1]   R. C. Clark, J. S. Reid, *Acta Cryst.* **1995**, A51, 887-897.

[2]   A. Altomare, M. C. Burla, M. Camalli, G.L. Cascarano, C. Giacovazzo, A. Guagliardi, A. G. G. Moliterni, G. Polidori, R. Spagna, *J. Appl. Cryst.* **1999**, 32, 115-119.

[3]   L. Palatinus, G. Chapuis, *J. Appl. Cryst.* **2007**, 40, 786-790.

[4]   G. M. Sheldrick, *Acta Cryst.* **2008**, A64, 112-122.

[5]   V. A. Blatov. Newsletter Commission on Crystallographic Computing of International Union of Crystallography, **2006**, 4-38 (http://www.iucr.org/iucr-top/comm/ccom/newsletters/).

15. Conclusion
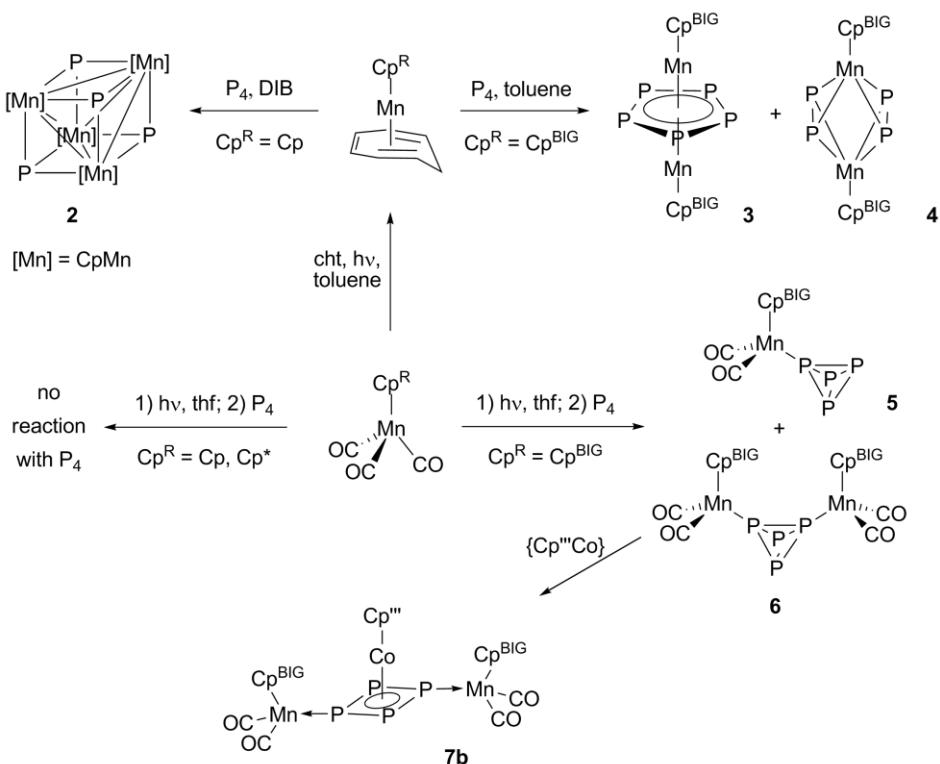
This work deals with the investigations of the highly sterically demanding Cp^{BIG} ligand ($Cp^{BIG} = C_5(4\text{-}n\text{BuC}_6\text{H}_4)_5$). After an introductory part (chapter 1) the research objectives are given (chapter 2), followed by a discussion of some general aspects of the Cp^{BIG} ligand (chapter 3).

Several complexes of manganese were prepared and their reactivity towards white phosphorus was studied. These results are described in the chapters 4, 5, 6 and 7. Furthermore, the reaction behavior of $[Cp^{BIG}Fe(CO)_2]_2$ (**1**) towards small molecules was examined in chapters 8, 9 and 10. Some of the obtained P_n ligand complexes were investigated in terms of their capability of forming supramolecular aggregates, which can be found in chapters 5, 12, 13 and 14. In addition, the reaction of $\{Cp^{BIG}\}^\bullet$ radicals with white phosphorus is reported in chapter 11. In the following, all executed topics are summarized. The results are discussed in a slightly different order than in the thesis itself.

15.1 Synthesis of P_n Ligand Complexes of Manganese

P_n ligand compounds are known for almost all transition metals and also for many main group elements. However, there are still some unexplored spots on the periodic table of elements. The lack of P_n ligand complexes of manganese for example motivated us to investigate the reactivity of Cp^{BIG} containing Mn precursors towards white phosphorus (Scheme 15.1).

To compare the reactivity of Cp^{BIG} derivatives with that of the stem compound bearing Cp, first [CpMn(cht)] (cht = cycloheptatriene) is reacted with P_4. No reaction is observed either in THF or toluene as solvents. In contrast, by using the high boiling solvent 1,3-diisopropylbenzene (dib), the heterocubane cluster $[Cp_4Mn_4P_4]$ (**2**) is formed. The very high temperature is most likely the reason that this conversion was not reported before. In order to check whether the lone pairs on the phosphorus atoms in **2** are generally available for further coordination, compound **2** is reacted with $[CpMn(CO)_2thf]$. In fact, the coordination of one upto four P atoms can be observed, forming $[\{Cp_4Mn_4P_4\}\{CpMn(CO)_2\}_n]$ (**2a**: n = 1; **2b**: n = 2; **2c**: n = 3; **2d**: n = 4). A reaction of $[Cp^{BIG}Mn(cht)]$ with white phosphorus could be achieved in the comparatively low boiling solvent toluene. In contrast to the reaction with the Cp derivative, here two manganese triple-decker complexes $[\{Cp^{BIG}Mn\}_2(\mu,\eta^{5:5}\text{-}P_5)]$ (**3**) and $[\{Cp^{BIG}Mn\}_2(\mu,\eta^{2:2}\text{-}P_2)_2]$ (**4**) were obtained. The EPR spectrum at 77 K of the mixture of **3** and **4**

Scheme 15.1. Synthesis of P_n ligand complexes of manganese.
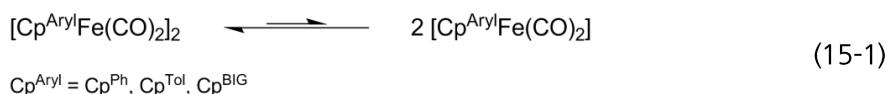
shows an anisotropic multiplet consistent with one unpaired electron coupling with two Mn nuclei ($I = 5/2$).

For the cymantrene complexes $[Cp^R Mn(CO)_3]$ the photolytic substitution of one carbonyl moiety by a solvent molecule is well known. The *in situ* generated solutions of $[Cp^R Mn(CO)_2 thf]$ ($Cp^R = Cp$, Cp^*, Cp^{BIG}) were added to white phosphorus. The Cp and Cp* derivatives did not show any observable reaction. However, in case of Cp^{BIG} the substitution of the thf ligand by P_4 occurred. Depending on the stoichiometry, either the mononuclear complex $[\{Cp^{BIG}Mn(CO)_2\}_2(\eta^1\text{-}P_4)]$ (**5**), the binuclear complex $[\{Cp^{BIG}Mn(CO)_2\}_2(\mu,\eta^{1:1}\text{-}P_4)]$ (**6**) or a mixture of both can be obtained. They exhibit intact P_4 tetrahedra as ligands and represent the first stable and soluble neutral complexes containing a $\eta^1\text{-}P_4$ ligand. Furthermore, for **5** an unusual Heteronuclear Overhauser Effect could be detected by HOESY NMR, indicating a coupling through space between the *ortho*-H atoms of the Cp^{BIG} ligand with the basal P atoms.
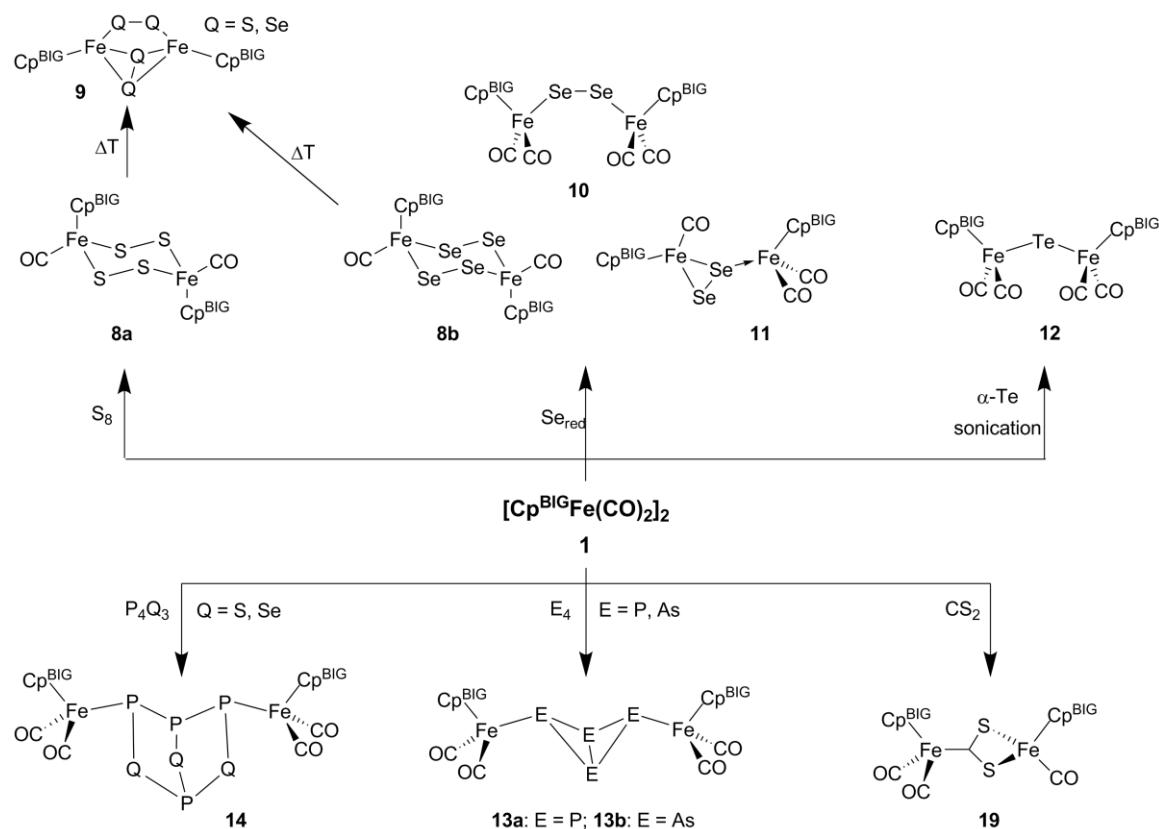
The two $\eta^1\text{-}P_4$ complexes $[\{CpRu(PPh_3)_2\}(\eta^1\text{-}P_4)][CF_3SO_3]$ and **6** were reacted with the triple-decker complex $[(Cp'''Co)_2 toluene]$. The two products $[\{CpRu(PPh_3)_2\}\{CoCp'''\}(\mu,\eta^{1:4}\text{-}P_4)][CF_3SO_3]$ (**7a**) and $[\{Cp^{BIG}Mn(CO)_2\}_2\{CoCp'''\}(\mu,\eta^{4:1:1}\text{-}P_4)]$ (**7b**) are stable at r.t. and show a *cyclo*-P_4 ligand. This stands in contrast to the reaction of $[(Cp'''Co)_2 toluene]$ and P_4, where $[CoCp'''(\eta^4\text{-}P_4)]$ can only be observed as an intermediate at this temperature. This is a good example for the observation that different reaction behavior occurs by pre-coordination of P_4.

15.2   Activation of Small Molecules with [Cp^{BIG}Fe(CO)$_2$]$_2$ and {Cp^{BIG}}$^{\bullet}$ Radicals

One reason for using of the highly sterically demanding Cp^{BIG} ligand is the kinetic stabilization of otherwise labile complexes. The preparation of the dimeric iron complex [Cp^{BIG}Fe(CO)$_2$]$_2$ (**1**) was achieved in my master thesis. As is already known for similar derivatives, **1** spontaneously dissociates in solution into two 17 VE {Cp^{BIG}Fe(CO)$_2$} fragments (Equation 15-1).

$$[Cp^{Aryl}Fe(CO)_2]_2 \quad \rightleftharpoons \quad 2\,[Cp^{Aryl}Fe(CO)_2]$$

$$Cp^{Aryl} = Cp^{Ph}, Cp^{Tol}, Cp^{BIG}$$

(15-1)
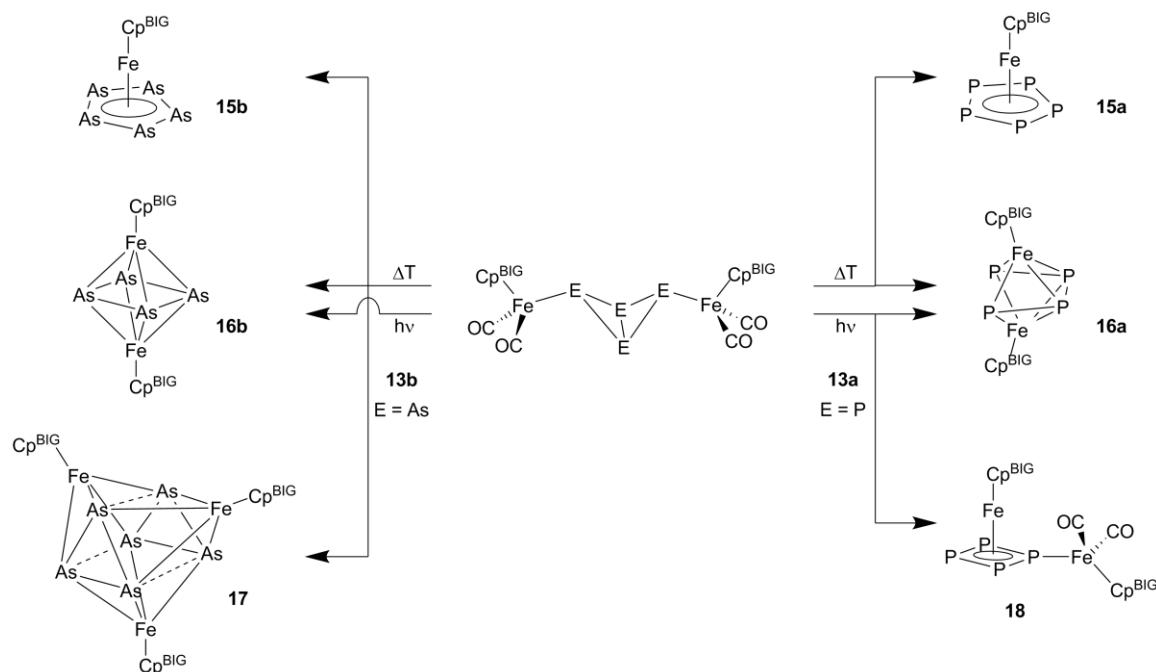
Preliminary experiments indicated the activation of P$_4$ at room temperature by **1**. For P$_4$ activations, usually high temperatures (boiling toluene, xylene etc.) are indispensable to generate the corresponding radicals/fragments. Since spontaneous dissociation of **1** in solution is observed, its reactivity at low temperatures has been investigated. The used substrates include elemental phases (P$_4$, As$_4$, S$_8$, Se$_{red}$, α-Te), main group cage compounds (P$_4$S$_3$, P$_4$Se$_3$) and the small organic molecule CS$_2$. In addition, reactions of **1** with P$_4$, As$_4$, S$_8$ and Se$_{red}$ at elevate temperatures were also carried out (Scheme 15.2).

Scheme 15.2. Activation of small molecules by **1**.

The reaction of **1** with elemental sulfur at r.t. leads to CO elimination and results in the fragmentation of the S_8 into S_2 units. The initial product could be identified as the binuclear complex [{Cp^{BIG}Fe(CO)}$_2$(μ-S$_2$)$_2$] (**8a**) with a central Fe_2S_4 six-membered ring. Compound **8a** loses its two CO groups at higher temperatures or on silica gel forming another binuclear product [(Cp^{BIG}Fe)$_2$(μ,η$^{1:1}$-S$_2$)(μ,η$^{2:2}$-S$_2$)] (**9a**) containing two perpendicularly orientated S_2^{2-} ligands. If Se$_{red}$ is chosen as substrate, not only [{Cp^{BIG}Fe(CO)}$_2$(μ-Se$_2$)$_2$] (**8b**) is formed, which is isostructural to **8a**, but also [{Cp^{BIG}Fe(CO)$_2$}$_2$(μ-Se$_2$)] (**10**) and [{Cp^{BIG}Fe(CO)}{Cp^{BIG}Fe(CO)$_2$}(μ,η$^{2:1}$-Se$_2$)] (**11**). Because of the different grade of carbonylation at the selenium complexes, it was possible to propose a reaction pathway. Thermolysis of **1** with Se$_{red}$ yields [(Cp^{BIG}Fe)$_2$(μ,η$^{1:1}$-Se$_2$)(μ,η$^{2:2}$-Se$_2$)] (**9b**), in analogy to the formation of **9a**. For the heavier homologue tellurium the metallic phase had to be used, due to the lack of a soluble molecular allotrope. However, a reaction could be triggered by sonication of **1** and α-Te resulting in the formation of [{Cp^{BIG}Fe(CO)$_2$}$_2$(μ-Te)] (**12**). In contrast to the sulfur and selenium containing complexes, **12** exhibits a mononuclear Te^{2-} ligand.

As mentioned above, the dimeric complex **1** reacts with white phosphorus at ambient temperature. Due to the notably mild reaction conditions only the selective cleavage of one single P–P bond is observed, regardless of stoichiometry of the reaction. The product could be identified as the butterfly complex [{Cp^{BIG}Fe(CO)$_2$}$_2$(μ,η$^{1:1}$-P$_4$)] (**13a**). The high yields and the smooth reaction in particular motivated us to also try yellow arsenic as starting material. And in fact, the isostructural arsenic containing butterfly compound [{Cp^{BIG}Fe(CO)$_2$}$_2$(μ,η$^{1:1}$-As$_4$)] (**13b**) was easily obtained in high yields. To check if the reaction can be generalized to
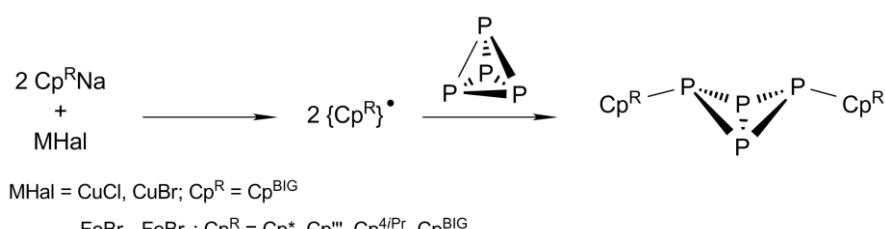
Scheme 15.3. Thermolysis and photolysis reaction of butterfly complexes **13a** and **13b**.

other cage compounds, the same experiments were carried out with P_4S_3 and P_4Se_3. Actually, these exceedingly stable molecules are also activated in a very selective manner. The two products [{Cp^{BIG}Fe(CO)$_2$}$_2$(μ,$\eta^{1:1}$-P$_4$S$_3$)] (**14a**) and [{Cp^{BIG}Fe(CO)$_2$}$_2$(μ,$\eta^{1:1}$-P$_4$Se$_3$)] (**14b**) show one broken P–P bond compared to the 'free' cages. The cleavage of a heteroatomic P–Q bond (Q = S, Se) could not be observed.

In addition, the thermolysis of **13a** and **13b** with an excess of P_4 and As_4, respectively, were studied (Scheme 15.3). In the case of the reaction with phosphorus the two complexes [Cp^{BIG}Fe(η^5-P$_5$)] (**15a**) and [(Cp^{BIG}Fe)$_2$(μ,$\eta^{4:4}$-P$_4$)] (**16a**) are obtained. The reaction with arsenic results in the formation of [(Cp^{BIG}Fe)$_2$(μ,$\eta^{4:4}$-As$_4$)] (**16b**), [(Cp^{BIG}Fe)$_3$(μ_3,$\eta^{4:4:4}$-As$_6$)] (**17**) and [Cp^{BIG}Fe(η^5-As$_5$)] (**15b**). Interestingly, despite of the equal composition of **16a** and **16b** the conformation of the middle deck is different. While in **16a** a trapezoidal shaped P_4 ligand is observed, in **16b** a *cyclo*-As$_4$ ligand is found. In contrast to the unselective thermolysis reaction, in the irradiation experiments of **13a** and **13b** exclusively **16a** and **16b**, respectively, can be identified from the reaction mixture. However, in an irradiation experiment of **13a** the partial decarbonylated complex [{Cp^{BIG}Fe}{Cp^{BIG}Fe(CO)$_2$}(μ,$\eta^{4:1}$-P$_4$)] (**18**) could be observed in very low yields.

As a model substance for small organic molecules, CS_2 was reacted with **1** at ambient temperature. The instant change of color form green to brown indicates the quantitative formation of [{Cp^{BIG}Fe(CO)$_2$}{Cp^{BIG}FeCO}(μ,$\eta^{1:2}$-CS$_2$)] (**19**). The binuclear complex shows a dithiocarboxylate ligand bridging two iron centers. This gives rise to the hope, that **1** could be able to activate other organic compounds, which could be the inition of catalytical processes to be studied in the future.

In the reaction of NaCp^{BIG} with CuX (X = Cl, Br), an intensive blue color is observed. The color could be traced back to the stable organic radical {Cp^{BIG}}$^\bullet$. We found that it is also capable to react with white phosphorus. Similar to the results mentioned above, here selectively one P–P bond is cleaved as well and the butterfly compound Cp$^{BIG}_2$P$_4$ (**20**) is formed (Scheme **15.4**). Within the scope of a cooperation with Sabine Reisinger and Christoph Schwarzmaier it was possible to extend this concept to a series of other {Cp^R}$^\bullet$ radicals (Cp^R = Cp*, Cp''', Cp^{4iPr}).

$$2\ Cp^R Na + MHal \longrightarrow 2\ \{Cp^R\}^\bullet \longrightarrow Cp^R\!-\!P \diagdown P \diagup P\!-\!Cp^R$$

MHal = CuCl, CuBr; Cp^R = Cp^{BIG}

FeBr$_2$, FeBr$_3$; Cp^R = Cp*, Cp''', Cp^{4iPr}, Cp^{BIG}

Scheme 15.4. Selective functionalization of P$_4$ by {Cp^R}$^\bullet$ radicals.
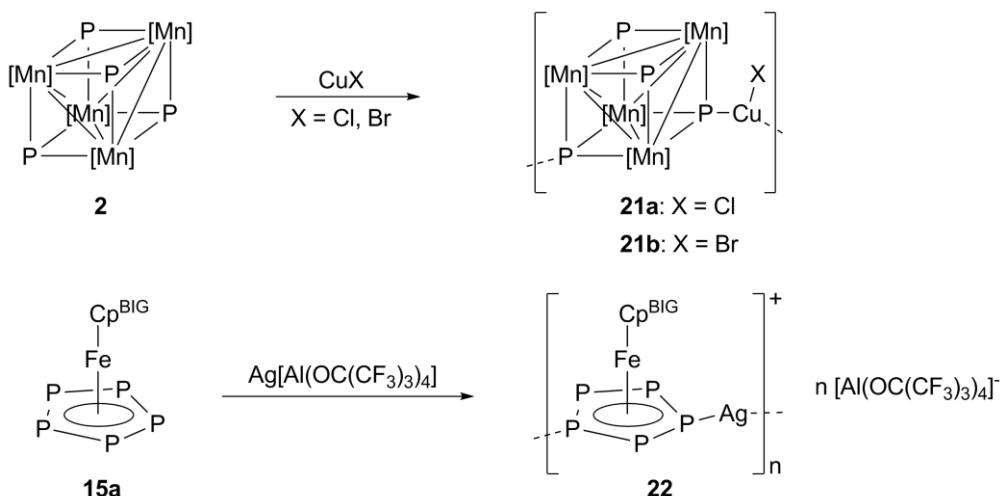
15.3 Formation of Supramolecular Assemblies using P_n Ligand Complexes and Coinage Metal Salts

Out of the pool of synthesized P_n ligand complexes, two derivatives were of special interest to investigate their coordination behavior towards monovalent coinage metal salts. The first one is the heterocubane cluster **2**, which might be able for the building of 3D scaffolds due to its tetrahedral symmetry. The second is the sterically demanding pentaphosphaferrocene **15a**, from which the formation of large spherical aggregates was expected.

It could be established that all P atoms in **2** can be addressed for further coordination (see above). Therefore also the reactions with CuX (X = Cl, Br) were studied (Scheme 15.5). Beside so far unidentified powder, black crystals are obtained. X-ray analysis showed 1D coordination polymers with the formula $[(CpMnP)_4(CuX)]_n$ (**21a**: X = Cl; **21b**: X = Br). The expected tetracoordination could not be observed yet with CuX.

The pentaphosphaferrocene **15a** in combination with $Ag[Al\{OC(CF_3)_3\}_4]$ forms the 1D coordination polymer $\{Cp^{BIG}Fe(\eta^5\text{-}P_5)\}Ag]_n[Al\{OC(CF_3)_3\}_4]_n$ (**22**) (Scheme 15.5). It shows a polycationic chain of molecules of **15a** coordinated in a 1,3-fashion to two Ag^+ ions. The strains are separated from each other by the weakly coordinating anions $[Al\{OC(CF_3)_3\}_4]$. Compound **22** is soluble in CH_2Cl_2, hence NMR investigations at various temperatures were carried out. Dynamic behavior was found, indicating a polymerization/depolymerization process. Despite this observation it was also identified that the Ag^+ cations remain coordinated in solution. Another feature of compound **22** is the interaction of two phenyl groups with a silver atom. This could be indicated by X-ray structure analysis as well as by NMR studies.
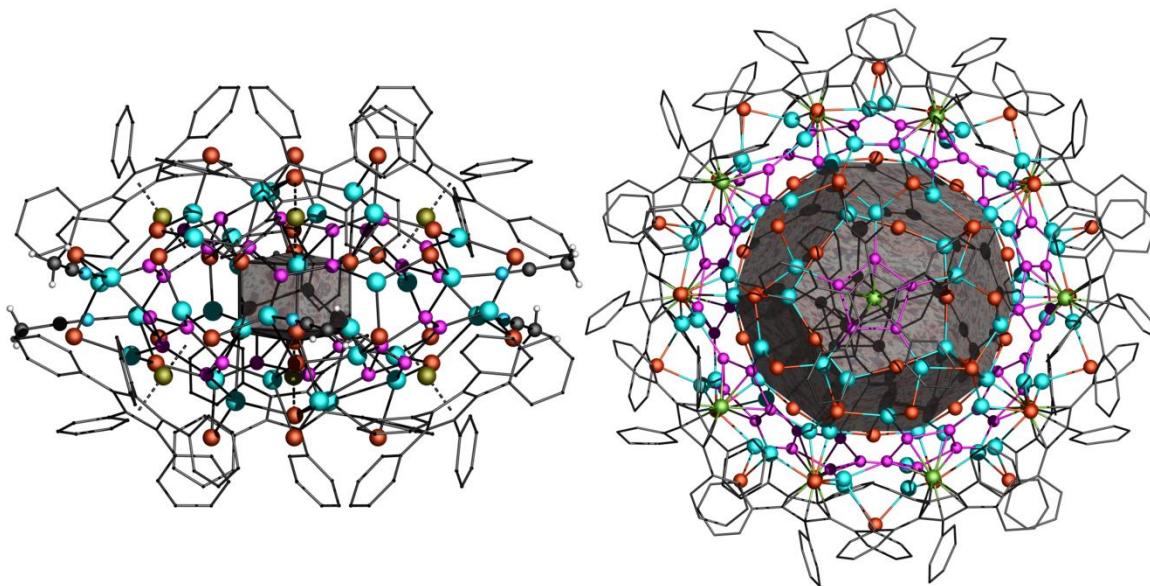
Complex **15a** was also reacted with copper halides. If CuX_2 (X = Cl, Br) is used, the formation of two lens-shaped double-shell clusters $[\{Cp^{BIG}Fe(\eta^4\text{-}P_5)\}_6Cu_{34}Cl_{28}(CH_3CN)_6]$ (**23**)

Scheme 15.5. Formation of 1D coordination polymers with P_n ligand complexes.

and $[\{Cp^{BIG}Fe(\eta^5\text{-}P_5)\}_6(CuBr)_{32}(CH_3CN)_6]$ (**24**) is observed. At first glance the supramolecules seem to be isostructural to each other however a closer look reveals remarkable differences. While in **24** the P_5 moieties are intact planaric cycles, they possess an envelope-like conformation in **23**. Furthermore, the inner core is also different in terms of its structural motifs. In spite of these differences the connectivity pattern of the outer shell is the same and shows partial analogy to $I\text{-}C_{140}$ fullerene. Due to the n-butyl groups of the Cp^{BIG} ligands the whole aggregate remains well soluble in CH_2Cl_2. Hence, it was possible to characterize **23** and **24** in solution by NMR spectroscopy and mass spectrometry. Both compounds exhibit a size of about 3.0x3.5 nm.

Finally, the reaction of **15a** with copper(I)-bromide leads to the formation of the totally different macromolecule $[\{Cp^{BIG}Fe(\eta^{5:2:1:1:1:1:1}\text{-}P_5)\}_{12}Cu_{92-x}Br_{92-y}]$ (**25**). In contrast to the lens-shaped clusters **23** and **24** a spherical ball-like structure is observed for **25**. The structure of the outer shell is most likely described as an analogue to the so far unknown $I\text{-}C_{140}$ fullerene. In contrast to the known hollow products formed with $[Cp^*Fe(\eta^5\text{-}P_5)]$, inside of the molecular structure of **25** a CuBr network is found. The inner part is formed by a formal Br_{12} icosahedron, surrounded by a $Br_{30}Cu_{20}$ pentagon-dodecahedron, which is connected to a fullerene-like scaffold of 60 P, 60 Cu and 50 Br atoms. The whole aggregate shows an outer diameter of 3.5 nm, which is three to four times larger than the C_{60} fullerene. Crystals of **25** are almost insoluble.

Scheme 15.6. Macromolecules based on $[Cp^{BIG}Fe(\eta^5\text{-}P_5)]$ (**15a**). Left: **24**; Right **25**. *n*-Butylgroups and H atoms are omitted for clarity.

16. Zusammenfassung

Diese Arbeit befasst sich mit Untersuchungen zur Chemie von Komplexen mit dem sterisch sehr anspruchsvollen Cp^{BIG}-Liganden ($Cp^{BIG} = C_5(4\text{-}n\text{BuC}_6H_4)_5$). Nach einem einleitenden Teil (Kapitel 1) sind die Ziele der Arbeit aufgelistet (Kapitel 2), gefolgt von einer Erörterung genereller Aspekte des Cp^{BIG}-Liganden (Kapitel 3).

Es wurden einige Komplexe des Mangans dargestellt und deren Reaktivität gegenüber weißem Phosphor untersucht. Diese Ergebnisse sind in den Kapiteln 4, 5, 6 und 7 thematisiert. Darüber hinaus wurde der Komplex $[Cp^{BIG}Fe(CO)_2]_2$ (**1**) mit kleinen Molekülen wie z.B. P_4, As_4 und CS_2 umgesetzt, dies wird in den Kapiteln 8, 9 und 10 diskutiert. Ausgewählte P_n-Ligandkomplexe wurden bezüglich ihrer Fähigkeit zum Aufbau supramolekularer Aggregate studiert, was in Kapitel 5, 12, 13 und 14 zusammengefasst ist. Zusätzlich wird die Reaktion von $\{Cp^{BIG}\}^\bullet$Radikalen mit weißem Phosphor in Kapitel 11 beschrieben. Im Folgenden werden alle bearbeiteten Themengebiete zusammengefasst, wobei die Ergebnisse hier teilweise in einer anderen Reihenfolge diskutiert werden.

16.1 Darstellung von P_n-Ligandkomplexen des Mangans

Verbindungen mit P_n-Liganden sind für annähernd alle Übergangsmetalle und einige Hauptgruppenelemente bekannt, jedoch gibt es immer noch unbekannte Kombinationen. Das Fehlen von P_n-Ligandkomplexen des Mangans motivierte uns die Reaktivität von entsprechenden Ausgangsverbindungen mit Cp^{BIG}-Liganden gegenüber weißem Phosphor zu untersuchen (Abbildung 16.1).

Um die Reaktionen der Cp^{BIG}-Verbindungen mit denen der entsprechenden Cp-Derivaten vergleichen zu können, wurde zunächst [CpMn(cht)] (cht = Cycloheptatrien) mit P_4 umgesetzt. Bei Reaktionsführung in siedendem THF bzw. Toluol konnte kein Umsatz beobachtet werden. Wird hingegen das hochsiedende 1,3-Diisopropylbenzol (DIB) verwendet, erhält man den Heterocubancluster $[Cp_4Mn_4P_4]$ (**2**). Die benötigten hohen Temperaturen sind vermutlich der Grund dafür, dass diese Reaktion nicht früher beschrieben wurde. Um zu untersuchen, ob die freien Elektronenpaare der Phosphoratome in **2** für eine Koordination zur Verfügung stehen, wurde Verbindung **2** mit $[CpMn(CO)_2thf]$ umgesetzt. In der Tat wird die Koordination von bis zu allen vier P-Atomen erhalten, wobei $[\{Cp_4Mn_4P_4\}\{CpMn(CO)_2\}_n]$ (**2a**: n = 1; **2b**: n = 2; **2c**: n = 3; **2d**: n = 4) gebildet werden. Für eine Reaktion von $[Cp^{BIG}Mn(cht)]$ mit weißem Phosphor war bereits das vergleichsweise niedrigsiedende Toluol ausreichend. Im Gegensatz zur
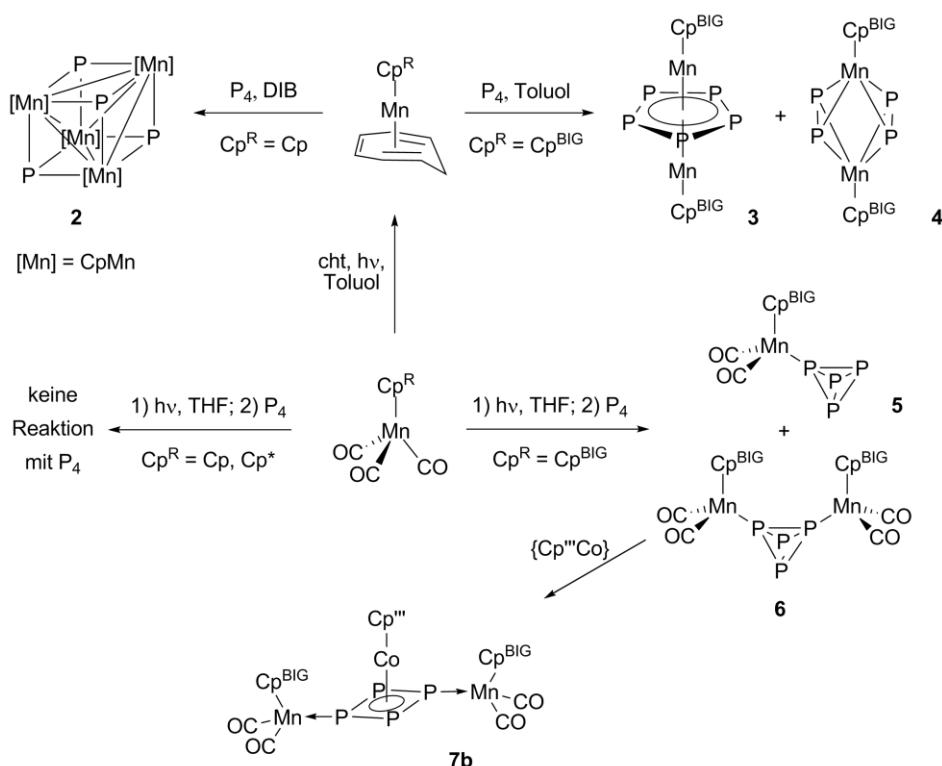
Abbildung 16.1. Synthese von P_n-Ligandkomplexen des Mangans.

Reaktion mit dem Cp-Derivat werden hier die beiden Tripeldecker-Komplexe $[\{Cp^{BIG}Mn\}_2(\mu,\eta^{5:5}\text{-}P_5)]$ (**3**) und $[\{Cp^{BIG}Mn\}_2(\mu,\eta^{2:2}\text{-}P_2)_2]$ (**4**) erhalten. Das ESR-Spektrum der Mischung aus **3** und **4** bei 77 K zeigt ein anisotropes Multiplett. Dies steht im Einklang mit einem ungepaarten Elektron in **3**, welches mit zwei Mn-Kernen koppelt ($I = 5/2$).
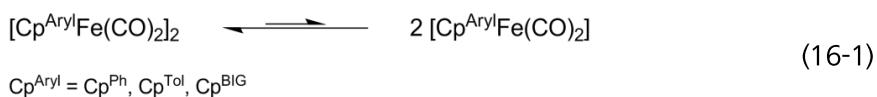
Bei Cymantren-Komplexen $[Cp^RMn(CO)_3]$ ist die photolytische Substitution einer Carbonylgruppe durch ein Lösungsmittelmolekül gut bekannt. *In situ* erzeugte Lösungen von $[Cp^RMn(CO)_2thf]$ (Cp^R = Cp, Cp*, Cp^{BIG}) wurden zu einer Lösung von weißem Phosphor gegeben. Dabei konnte im Fall der Cp- und Cp*-Derivate keine Reaktion beobachtet werden. Im Falle der Cp^{BIG} Verbindung erfolgt jedoch die Substitution des THF-Liganden durch P_4. Abhängig von der Stöchiometrie wird entweder der einkernige Komplex $[\{Cp^{BIG}Mn(CO)_2\}_2(\eta^1\text{-}P_4)]$ (**5**), der zweikernige Komplex $[\{Cp^{BIG}Mn(CO)_2\}_2(\mu,\eta^{1:1}\text{-}P_4)]$ (**6**) oder eine Mischung aus beiden erhalten. Sie weisen jeweils einen intakten P_4-Tetraeder als Liganden auf und repräsentieren somit die ersten stabilen und löslichen Neutralkomplexe mit einem η^1-P_4-Liganden. Bei **5** konnte der ungewöhnliche Heterokern-Overhauser-Effekt mittels HOESY NMR-Spektroskopie nachgewiesen werden, welcher eine Kopplung durch den Raum der *ortho*-H-Atome der Cp^{BIG}-Liganden mit den basalen P-Atomen zeigt.

Die beiden η^1-P_4 Komplexe $[\{CpRu(PPh_3)_2\}(\eta^1\text{-}P_4)][CF_3SO_3]$ und **6** wurden mit dem Tripeldecker-Komplex $[(Cp'''Co)_2Toluol]$ zur Reaktion gebracht. Die beiden bei Raumtemperatur stabilen Produkte $[\{CpRu(PPh_3)_2\}\{CoCp'''\}(\mu,\eta^{1:4}\text{-}P_4)][CF_3SO_3]$ (**7a**) und

[{Cp^{BIG}Mn(CO)$_2$}$_2${CoCp'''}(μ,η$^{4:1:1}$-P$_4$)] (**7b**) zeigen jeweils einen *cyclo*-P$_4$ Liganden. Das steht im Gegensatz zur Reaktion von [(Cp'''Co)$_2$Toluol] mit P$_4$ als Phosphorquelle, wobei der analoge Komplex [CoCp'''(η^4-P$_4$)] mit einem *cyclo*-P$_4$ Liganden nur intermediär bei tiefen Temperaturen gebildet wird. Dies zeigt, dass die Koordination von P$_4$ zu unterschiedlichem Reaktionsverhalten führen kann.

16.2   Aktivierung kleiner Moleküle mit [Cp^{BIG}Fe(CO)$_2$]$_2$ und {Cp^{BIG}}$^\bullet$ Radikalen

Ein wichtiger Vorteil des sterisch anspruchsvollen Cp^{BIG}-Liganden ist die kinetische Stabilisierung ansonsten labiler Komplexe. Über dar Darstellung der dimeren Eisenverbindung [Cp^{BIG}Fe(CO)$_2$]$_2$ (**1**) wurde bereits in meiner Masterarbeit berichtet. Wie bereits für ähnliche Komplexe bekannt, dissoziiert **1** spontan in Lösung zu zwei {Cp^{BIG}Fe(CO)$_2$} Komplexradikalen (Gleichung 16-1).

$$[Cp^{Aryl}Fe(CO)_2]_2 \rightleftharpoons 2\,[Cp^{Aryl}Fe(CO)_2]$$

$$Cp^{Aryl} = Cp^{Ph}, Cp^{Tol}, Cp^{BIG}$$

(16-1)

Voruntersuchungen haben gezeigt, dass **1** in der Lage ist, P$_4$ bei Raumtemperatur zu
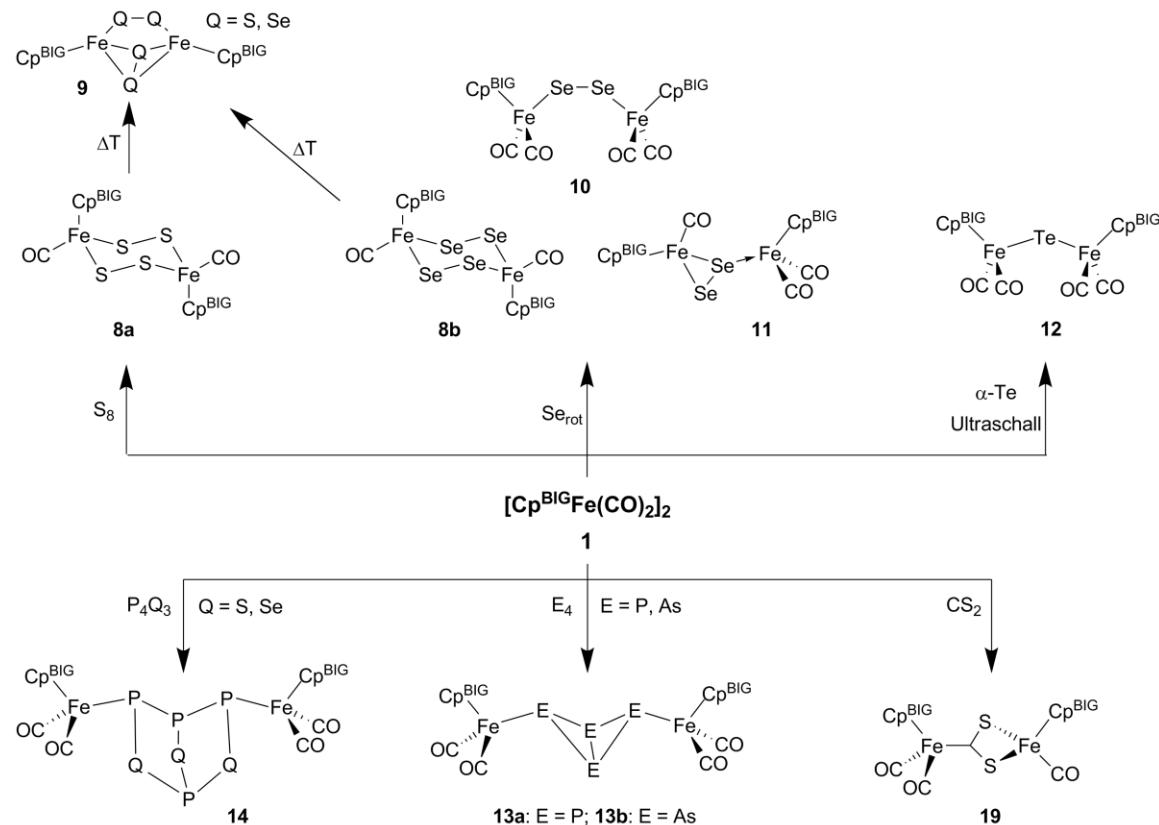
Abbildung 16.2. Aktivierung kleiner Moleküle mit **1**.

aktivieren. Üblicherweise sind für P_4-Aktivierungen höhere Temperaturen notwendig (siedendes Toluol, Xylol etc.), um die entsprechenden Radikale/Fragmente zu erzeugen. Da **1** in Lösung spontan dissoziiert, wurde seine Reaktivität bei tiefen Temperaturen untersucht. Die verwendeten Substrate umfassen die elementaren Phasen P_4, As_4, S_8, Se_{rot} und α-Te, Käfigverbindungen von Hauptgruppenelementen (P_4S_3, P_4Se_3) und das organische Molekül CS_2. Darüber hinaus wurden Reaktionen von **1** mit P_4, As_4, S_8 und Se_{rot} auch bei erhöhter Temperatur durchgeführt (Abbildung 16.2)

Die Reaktion von **1** mit elementarem Schwefel bei RT führt unter CO-Abspaltung zur Fragmentierung der S_8-Krone in S_2-Einheiten. Das zunächst erhaltene Produkt konnte als der Zweikernkomplex [{$Cp^{BIG}Fe(CO)$}$_2$(μ-S_2)$_2$] (**8a**) identifiziert werden, welcher einen zentralen Fe_2S_4-Sechsring enthält. Verbindung **8a** decarbonyliert bei höheren Temperaturen oder auf Kieselgel, wodurch ein weiterer zweikerniger Komplex [($Cp^{BIG}Fe$)$_2$($\mu,\eta^{1:1}$-S_2)($\mu,\eta^{2:2}$-S_2)] (**9a**) mit zwei zueinander senkrecht angeordneten S_2^{2-} Liganden erhalten wird. Wird rotes Selen als Substrat verwendet, so wird nicht nur der zu **8a** isostrukturelle Komplex [{$Cp^{BIG}Fe(CO)$}$_2$(μ-Se_2)$_2$] (**8b**) gebildet, sondern auch [{$Cp^{BIG}Fe(CO)_2$}$_2$(μ-Se_2)] (**10**) und [{$Cp^{BIG}Fe(CO)$}{$Cp^{BIG}Fe(CO)_2$}($\mu,\eta^{2:1}$-Se_2)] (**11**). Auf Grund des unterschiedlichen Carbonylierungsgrades in den Selenverbindungen war es darüber hinaus möglich, einen Vorschlag für den Bildungsweg zu geben. Die Thermolyse von **1** mit Se_{rot} führt in Analogie zu **9a** zur Bildung von [($Cp^{BIG}Fe$)$_2$($\mu,\eta^{1:1}$-Se_2)($\mu,\eta^{2:2}$-Se_2)] (**9b**). Für das schwerere Homolog Tellur musste mangels löslichem Allotrop die metallische Phase verwendet werden. Jedoch konnte auch hier unter Zuhilfenahme von Ultraschall-Behandlung von **1** und α-Te die Darstellung von [{$Cp^{BIG}Fe(CO)_2$}$_2$(μ-Te)] (**12**) erreicht werden. Im Gegensatz zu den Schwefel- und Selenkomplexen weist **12** einen monoatomaren Te^{2-} Liganden auf.

Wie bereits oben erwähnt, reagiert der dimere Komplex **1** mit weißem Phosphor bereits bei Raumtemperatur. Unabhängig von der Stöchiometrie wird der Bruch einer P–P- Bindung beobachtet. Das Produkt konnte als der *Bicyclo*[1.1.0]butankomplex [{$Cp^{BIG}Fe(CO)_2$}$_2$($\mu,\eta^{1:1}$-P_4)] (**13a**) identifiziert werden. Die hohen Ausbeuten und auch die Einfachheit der Reaktion ließen uns auch gelbes Arsen als Substrat untersuchen. Tatsächlich konnte die analoge Arsenverbindung [{$Cp^{BIG}Fe(CO)_2$}$_2$($\mu,\eta^{1:1}$-As_4)] (**13b**) isoliert werden. Um zu überprüfen, ob diese Reaktion im Allgemeinen auch auf andere Käfigverbindungen übertragen werden kann, wurden entsprechende Experimente mit P_4S_3 und P_4Se_3 durchgeführt. Auch hier erfolgte eine Aktivierung der ansonsten recht stabilen Moleküle. Die beiden Produkte [{$Cp^{BIG}Fe(CO)_2$}$_2$($\mu,\eta^{1:1}$-P_4S_3)] (**14a**) und [{$Cp^{BIG}Fe(CO)_2$}$_2$($\mu,\eta^{1:1}$-P_4Se_3)] (**14b**) weisen im Vergleich zu den ‚freien' Käfigen eine offenen P–P-Bindung auf, die Öffnung einer heteroatomeren P–Q- Bindung (Q = S, Se) konnte hingegen nicht beobachtet werden.
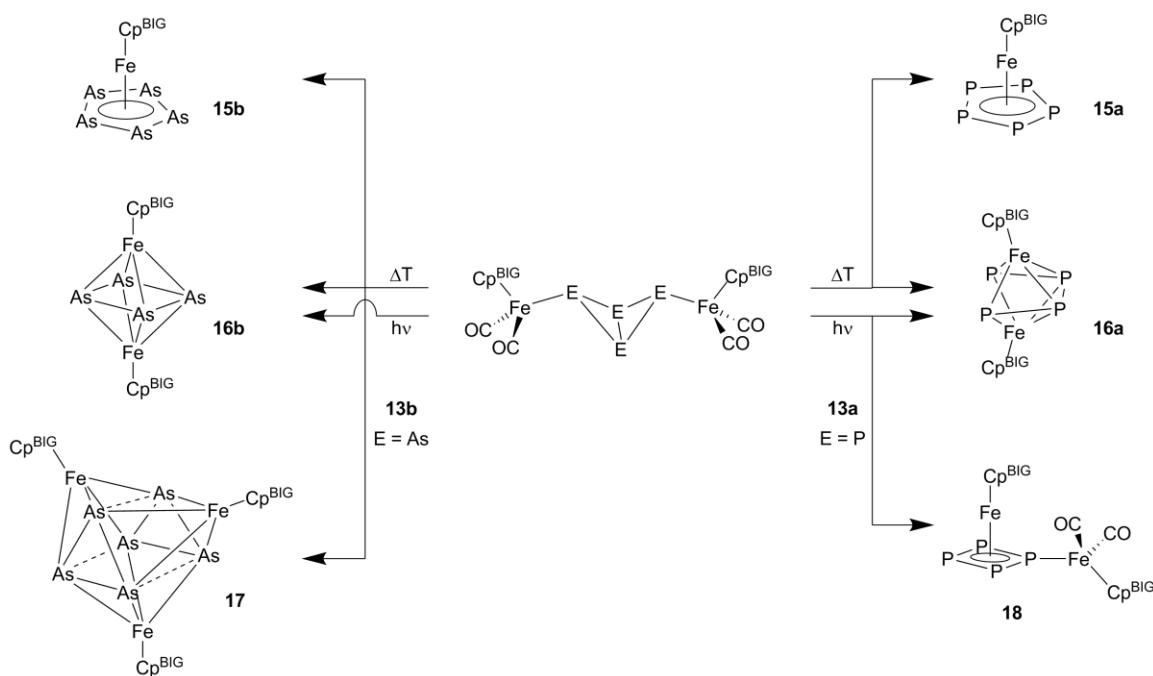
Abbildung 16.3. Thermolyse- und Photolysereaktion der Butterflykomplexe **13a** und **13b**.

Weiterhin wurden die Reaktionen von **13a** und **13b** mit P_4 bzw. As_4 unter thermolytischen Bedingungen untersucht. Im Fall der Reaktion mit Phosphor wurden die beiden Komplexe $[Cp^{BIG}Fe(\eta^5-P_5)]$ (**15a**) und $[(Cp^{BIG}Fe)_2(\mu,\eta^{4:4}-P_4)]$ (**16a**) erhalten. Bei der Reaktion mit Arsen wird die Bildung von $[(Cp^{BIG}Fe)_2(\mu,\eta^{4:4}-As_4)]$ (**16b**), $[(Cp^{BIG}Fe)_3(\mu_3,\eta^{4:4:4}-As_6)]$ (**17**) und $[Cp^{BIG}Fe(\eta^5-As_5)]$ (**15b**) beobachtet. Trotz der annähernd gleichen Zusammensetzung von **16a** und **16b** ist die Konformation der Mitteldecks interessanterweise verschieden. Während bei **16a** ein trapezoider P_4 Ligand beobachtet wird, liegt in **16b** ein *cyclo*-As_4-Ligand vor. Im Gegensatz zur Reaktion unter thermolytischen Bedingungen werden bei Bestrahlung von **13a** bzw. **13b** mit UV-Licht ausschließlich **16a** bzw. **16b** aus der Reaktionsmischung identifiziert. Zusätzlich wurde in einem einzelnen Bestrahlungsexperiment von **13a** der nur partiell decarbonylierte Komplexe $[\{Cp^{BIG}Fe\}\{Cp^{BIG}Fe(CO)_2\}(\mu,\eta^{4:1}-P_4)]$ (**18**) beobachtet.

Als Modellverbindung für ein kleines organisches Molekül wurde CS_2 mit **1** bei Raumtemperatur umgesetzt. Die sofortige Rotfärbung zeigt die Bildung von $[\{Cp^{BIG}Fe(CO)_2\}\{Cp^{BIG}FeCO\}(\mu,\eta^{1:2}-CS_2)]$ (**19**) an. Der Zweikernkomplex weist einen Dithiocarboxylat-Liganden auf, der zwei Eisenatome verbrückt. Dies lässt hoffen, dass **1** auch andere organische Verbindungen aktivieren kann, was Katalysen ermöglichen könnte.

Bei der Reaktion von $NaCp^{BIG}$ mit CuX ($X = Cl$, Br) wird eine intensive blaue Farbe beobachtet, die auf die Bildung des stabilen organischen Radikals $\{Cp^{BIG}\}^\bullet$ zurückgeführt werden kann. Untersuchungen haben gezeigt, dass $\{Cp^{BIG}\}^\bullet$ in der Lage ist, selektiv mit weißem Phosphor zu reagieren. Ähnlich zu den oben diskutierten Ergebnissen wird auch hier eine P–P-Bindung gespalten, wodurch die Schmetterlingsverbindung $Cp^{BIG}_2P_4$ (**20**) gebildet

wird (Abbildung 16.4). Im Zuge einer Kooperation mit Sabine Reisinger und Christoph Schwarzmaier war es möglich, dieses Konzept auf andere {Cp^R}$^\bullet$ Radikale (Cp^R = Cp*, Cp''', Cp^{4iPr}) zu erweitern.

MHal = CuCl, CuBr; Cp^R = Cp^{BIG}

FeBr$_2$, FeBr$_3$; Cp^R = Cp*, Cp''', Cp^{4iPr}, Cp^{BIG}
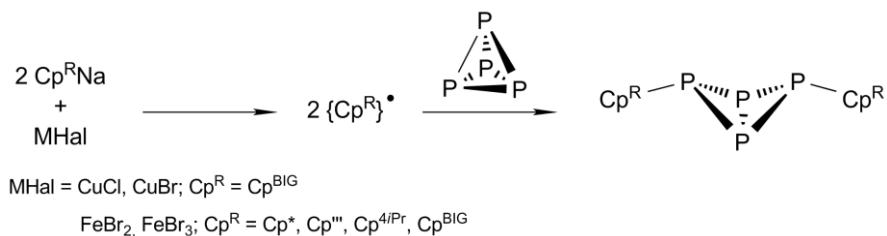
Abbildung 16.4. Selektive Funktionalisierung von P$_4$ durch {Cp^R}$^\bullet$ Radikale.

16.3 Bildung Supramolekularer Aggregate unter Verwendung von P$_n$-Ligandkomplexen und Münzmetallsalzen

Aus der Anzahl der synthetisierten P$_n$-Ligandkomplexe waren zwei Verbindungen von speziellem Interesse ihr Koordinationsverhalten zu untersuchen: Zum einen der Heterocubancluster **2**, welcher auf Grund seiner Tetraedergeometrie zum Aufbau dreidimensionaler Netzwerke fähig sein sollte, zum anderen das sterisch anspruchsvolle Pentaphosphaferrocen **15a**, bei der die Bildung von großen sphärischen Aggregaten erwartet wurde.

Es wurde gezeigt, dass alle P-Atome in **2** für eine weitere Koordination adressiert werden können (siehe oben), weshalb auch Reaktionen mit CuX (X = Cl, Br) durchgeführt wurden (Abbildung 16.5). Röntgenstrukturanalysen der erhaltenen schwarzen Kristalle zeigen die 1D-Koordinationspolymere [(CpMnP)$_4$(CuX)]$_n$ (**21a**: X = Cl; **21b**: X = Br). Die erwartete vierfache Koordination mit CuX konnte bislang nicht beobachtet werden.
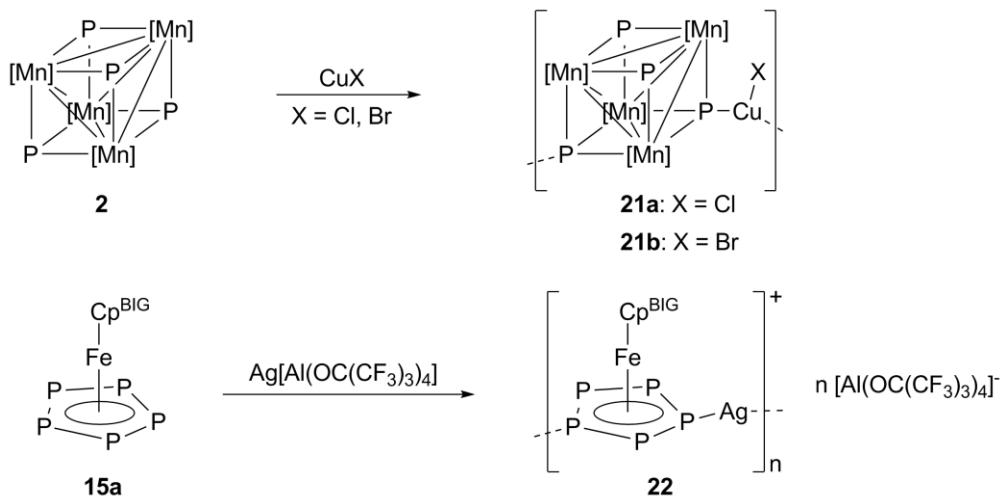
Abbildung 16.5. Darstellung eindimensionaler Polymere unter Verwendung von P$_n$-Ligandkomplexen.

Das Pentaphosphaferrocen **15a** reagiert mit [{Ag(CH$_2$Cl$_2$)}Al{OC(CF$_3$)$_3$}$_4$] unter Bildung von [{Cp^{BIG}Fe(η^5-P$_5$)}Ag]$_n$[Al{OC(CF$_3$)$_3$}$_4$]$_n$ (**22**; Abbildung 16.5), welche eine polykationische Kette aus **15a** Molekülen im 1,3-Koordinationsmodus und Ag$^+$-Ionen enthält. Die Polymerstränge sind voneinander durch die schwach koordinierenden Anionen [Al{OC(CF$_3$)$_3$}$_4$]$^-$ getrennt. Verbindung **22** ist löslich in CH$_2$Cl$_2$ und darin durchgeführte NMR-Untersuchungen bei verschiedenen Temperaturen zeigen ein dynamisches Verhalten, welches auf einen Polymerisations/Depolymerisations-Prozess hinweist. Zusätzlich ist ersichtlich, dass die Ag$^+$ Kationen in Lösung koordiniert bleiben. Eine weitere Eigenschaft von **22** sind Wechselwirkungen von je zwei Phenylgruppen mit einem Silberion. Dies konnte mittels Kristallstruktur als auch durch NMR-Studien belegt werden.

Komplex **15a** wurde ebenfalls mit Kupferhalogeniden umgesetzt. Bei Verwendung von CuX$_2$ (X = Cl, Br) wird die Bildung der linsenförmigen Cluster [{Cp^{BIG}Fe(η^4-P$_5$)}$_6$Cu$_{34}$Cl$_{28}$(CH$_3$CN)$_6$] (**23**) und [{Cp^{BIG}Fe(η^5-P$_5$)}$_6$(CuBr)$_{32}$(CH$_3$CN)$_6$] (**24**) beobachtet. Auf den ersten Blick scheinen die Supramoleküle strukturell ähnlich zu sein, jedoch werden bei einer genaueren Betrachtung erstaunliche Unterschiede deutlich. Während bei **24** die P$_5$-Einheiten intakte planare Zyklen bleiben, besitzen sie in **23** eine Envelope-Konformation. Darüber hinaus weisen die inneren Kerne unterschiedliche Strukturmotive auf. Unabhängig von diesen Unterschieden ist das Verknüpfungsmuster der äußeren Schale identisch und zeigt partielle Analogie zur Schale des *I*-C$_{140}$ Fulleren. Durch die *n*-Butylgruppen der Cp^{BIG}-Liganden bleiben die Aggregate gut löslich in CH$_2$Cl$_2$, wodurch eine Charakterisierung beider Verbindungen **23** und **24** in Lösung möglich wurde. Beide Verbindungen besitzen eine Größe von jeweils 3.0x3.5 nm.
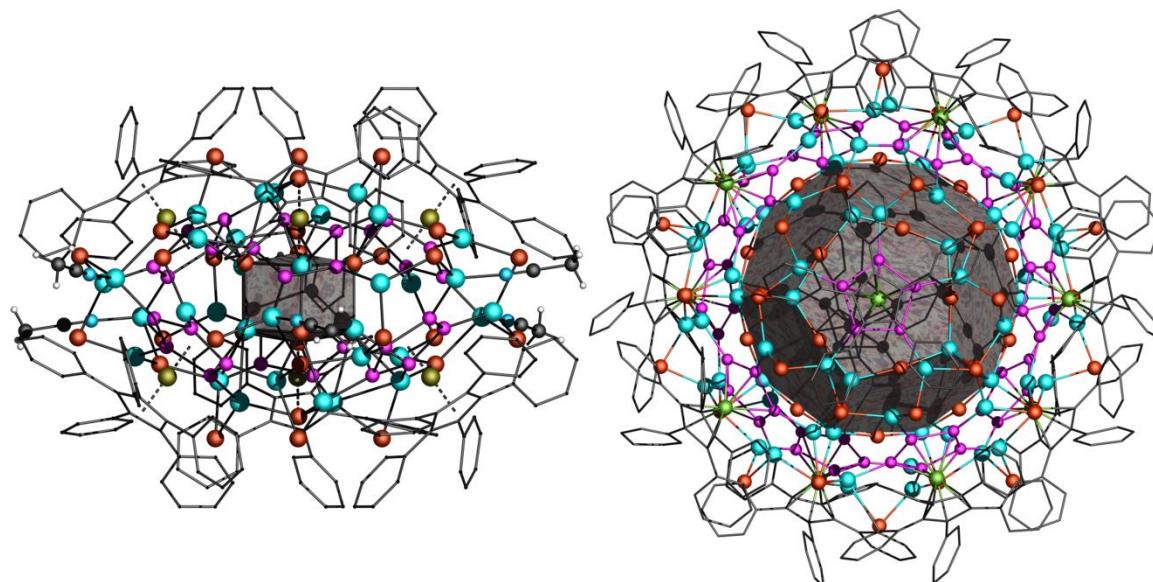

Abbildung 16.6. Makromoleküle basierend auf [Cp^{BIG}Fe(η^5-P$_5$)] (**15a**). Links: **24**; Rechts: **25**. *n*Butylgruppen und H-Atome sind aus Gründen der Übersichtlichkeit weggelassen.

Durch die Umsetzung von **15a** mit CuBr kann ein weiteres Makromolekül mit der Formel $[\{Cp^{BIG}Fe(\eta^{5:2:1:1:1:1}-P_5)\}_{12}Cu_{92-x}Br_{92-y}]$ (**25**) erhalten werden. Im Gegensatz zu den linsenförmigen Molekülen **23** und **24** weist **25** eine ballförmige Struktur auf. Die äußere Hülle zeigt Analogie zum nur aus Rechnungen bekannten I-C_{140} Fulleren auf. Im Gegensatz zu den hohlen Strukturen (gefüllt mit Templat- bzw. Solvensmolekülen) der Makromoleküle mit $[Cp^*Fe(\eta^5-P_5)]$ ist **25** mit einem mit der Hülle verbundenen CuBr-Gerüst gefüllt. Im Inneren befindet sich ein formaler Br_{12}-Ikosaeder, welcher von einem $Br_{30}Cu_{20}$-Dodekaeder umgeben ist. Dieser wiederum ist mit einem Fulleren-artigen Gerüst, bestehend aus 60 P, 60 Cu und 50 Br Atomen, verbunden. Das gesamte Aggregat besitzt einen Durchmesser von 3.5 nm, was dem drei- bis vierfachen Wert des C_{60}-Fullerens entspricht. Kristalle von **25** sind annähernd unlöslich.

17. Appendices

17.1 Alphabetic List of Abbreviations

Å	Angstroem, 1 Å = $1 \cdot 10^{-10}$ m
°C	degree Celsius
1D	one dimensional
2D	two dimensional
3D	three dimensional
Ar^{Dipp}	$-C_6H_3-2,6-(C_6H_3-2,6-^iPr_2)_2$
av.	average
butterfly	*bicyclo*[1.1.0]butane
br(NMR)	broad
COSY	correlation spectroscopy
Cp	cyclopentadienyl, C_5H_5
Cp″	1,3-di-*tert*-butylcyclopentadienyl, $C_5H_3tBu_2$
Cp‴	1,2,4-tris-*tert*-butylcyclopentadienyl, $C_5H_2tBu_3$
Cp*	pentametyhlcyclopentadienyl, C_5Me_5
Cp^{BIG}	pentakis-4-*n*butylphenylcyclopentadienyl, $C_5(4-nBuC_6H_4)_5$
Cp^{Bn}	penta-benzylcyclopentadienyl, $C_5(CH_2Ph)_5$
Cp^{Tol}	$C_5Ph_4(4-MeC_6H_4)$
Cp^{4iPr}	tetra-isopropylcyclopentadienyl, C_5HiPr_4
Cp^{5iPr}	penta-isopropylcyclopentadienyl, C_5iPr_5
Cp^R	substituted cyclopentadienyl ligand
CV	cyclovoltamography
d	distance
d(NMR)	doublet
E°$_0$	reaction energy
H°$_{298}$	standard reaction enthalpy
S°$_{298}$	standard reaction entropy
G°$_{298}$	standard gibbs reaction energy
δ	chemical shift
DFT	density functional theory
Dipp	2,6-diisopropylphenyl

dme	1,2-dimethoxyethane
dppe	$C_2H_4(PPh_2)_2$
dppm	$CH_2(PPh_2)_2$
E	heavier element of the 15th group, E = P, As, Sb
e[-]	electron
EI MS	electron impact mass spectrometry
ESI MS	electron spray ionization mass spectrometry
FD MS	field desorption ionization mass spectrometry
EXSY	exchange spectroscopy
HOESY	heteronuclear Overhauser enhancement and exchange spectroscopy
HOMO	highest occupied molecular orbital
Hz	Hertz
IR	infrared spectroscopy
J(NMR)	coupling constant
L	ligand (specified in text)
LUMO	lowest unoccupied molecular orbital
M	metal
m/z	mass to charge ratio
MAS	magic angle spinning
Mes	mesityl, 2,4,6-trimethylphenyl
MO	molecular orbital
NHC	N-heterocyclic carbene
NMR	nuclear magnetic resonance
nn_3	$(Me_3SiNCH_2CH_2)_3N$
NOESY	nuclear Overhauser enhancement and exchange spectroscopy
np_3	tris(2-diphenylphosphinoethyl)amine
v	frequency/wavenumber
$\omega_{1/2}$	half width
OTf[-]	triflate, $CF_3SO_3^-$
pftb	$[Al\{OC(CF_3)_3\}_4]$
ppm	parts per million
q(NMR)	quartett
R	organic substituent
r.t.	room temperature
s(IR)	strong
s(NMR)	singlet

sept(NMR)   septet

sh(IR)   shoulder

sMes   2,4,6-tri-tertbutylphenyl

t(NMR)   triplet

THF   tetrahydrofurane, C_4H_8O

tht   tetrahydrothiophene, C_4H_8S

TMS   tetramethylsilane, $Si(CH_3)_4$

triphos   1,1,1-tris(diphenylphosphanylmethyl)ethane, $CH_3C(CH_2PPh_2)_3$

vdW   van der Waals

VE   valence electron

VT   Various Temperature

w(IR)   weak

X   any halide, X = Cl, Br, I

17.2   List of Used Programs

MS Word2010   Text Components

MS PowerPoint2010   Graphical Abstracts

MS Excel2010   Tabular Analyses

CorelDrawX6   Araphical Abstracts and General Picture Work

ChemDrawUltra11   Drawings of Chemical Formula

Diamond3.0/POV-Ray   Colored Pictures and some Binary Images of Crystal Structures

SCHAKAL   Binary Images of Crystal Structures

TopSpin3.2   NMR Data Processing; NMR Pictures

CrysAlisPro   X-ray Data Processing (Integration, Refinalization)

SIR-92/SUPERFLIP   Structure Solving

WinGX/ORTEP   Structure Imaging during Refinement

SHELX97/SHELX2013   Structure Refinement

PLATON   CIF-File Generation

ConQuest1.15   CCDC Searches

SciFinderScholar   Literature Searches

EndNoteX6   Reference Management

17.3   Addresses of Cooperation Partners

Only partners, who are not members of the Chemical Department of the University of Regensburg are listed.

Prof. Dr. Alexey Y. Timoshkin

Institute of Chemistry, St. Petersburg State University, Universitetskii pr. 26, Old Peterhoff, 198504 St. Petersburg, Russia.

Prof. Dr. Alexander V. Virovets

Institute of Inorganic Chemistry SD RAS Ak. Lavrentiev prosp. 3, Novosibirsk 630090, Russia.

Dr. Eugenia Peresypkina

Institute of Inorganic Chemistry SD RAS Ak. Lavrentiev prosp. 3, Novosibirsk 630090, Russia.

Prof. Dr. Piero Mastrorilli

Dr. Vito Gallo

Dipartimento di Ingegneria Civile, Ambientale, del Territorio, Edile e di Chimica (DICATECh), Politecnico di Bari, via Orabona 4, I-70125 Bari, Italy.

Dr. Maurizio Peruzzini

Dr. Maria Caporali

Fuencisla Delgado

National Research Council, Institute of Chemistry of Organometallic Compounds, Florence(IT), Area di Ricerca del CNR di Firenze, Via Madonna del Piano 10, 50019 Sesto Fiorentino (Florence), Italy.

Prof. Dr. Werner Kremer

Institut für Biophysik und Physikalische Biochemie und Zentrum für Magnetische Resonanz in Chemie und Biomedizin, Universität Regensburg, Universitätsstraße 31, 93040 Regensburg, Germany.

PD. Dr. Gunther Brunklaus

David Lüdeker

Institut für Physikalische Chemie, Universität Münster, 48149 Münster, Germany.

17.4 Acknowledgments

This dissertation would not have been possible without the countless persons standing by in the background. Therefore, my particular gratefulness goes to